University of Nottingham

Institute of Engineering Surveying and Space Geodesy

The Performance of Hybrid GPS and GLONASS

by

D F Baker BA, MSc

Thesis submitted to the University of Nottingham

for the degree of Doctor of Philosophy

May 2001

Table of Contents

List of Figures

2 Global Satellite Navigation Systems

3 First Generation Hybrid Systems

4 Positioning Techniques

5 Practical Static

6 Practical Dynamic

7 Bob Skeleton

8 Trajectory and Parameter Extraction

9 Urban Tracking Performance Measures

List of Tables

2 Global Satellite Navigation Systems

3 First Generation Hybrid Systems

4 Positioning Techniques

5 Practical Static

6 Practical Dynamic

7 Bob Skeleton

8 Trajectory and Parameter Extraction

9 Urban Tracking Performance Measures

Abstract

In recent years, the market served by satellite positioning systems has expanded exponentially. It is stimulated by the needs of an ever increasing number and variety of scientific, business and leisure applications. The dominant system is the USA's GPS, or *Global Positioning System.* However, GPS is not a panacea for all positioning tasks, in any environmental situation. For example, two of the fastest growing applications, vehicle tracking and personal location, operate in an often harsh signal reception environment. This can be so severe that even with the current 29 working satellites, GPS may struggle to perform. In exceptional circumstances it can fail to provide a positioning service at all.

The simplest way to improve the situation when signal reception is poor, is to add similar signals from alternative satellite systems. This has already been achieved by combining GPS with the Russian satellite positioning system, Global'naya Navigatsionnaya Sputnikova Sistema, abbreviated to GLONASS. The combination of GPS with GLONASS is referred to here as Hybrid.

But how good is Hybrid relative to GPS, and how can performance be evaluated objectively? The research project presented here set out to answer this question, and to understand the situations in which Hybrid failed, and ask what solutions were then available to fulfil a positioning task. The problems

associated with integrating one satellite positioning system with another, their potential inconsistencies and their impact on positioning errors were also examined. This field of research is relevant to Hybrid as defined here, and also to other mixed systems, for example GPS with EGNOS, a European geostationary satellite system, and GPS with Galileo, a proposed global system controlled by the Europeans.

The issues were addressed from the viewpoint of practical usage of the positioning systems. Hence the many and varied experiments to quantify positioning performance using both static receivers, and a variety of platforms with wide ranging levels of vehicle dynamics. The capability of satellite positioning systems to work in the harshest environments, was tested in the proposed Olympic sport of bob skeleton. This involved the development of the acquisition system, and a number of programs. The latter were equally applicable to the ensuing work with road vehicles, and the quantitative assessment of positioning performance relative to a truth.

The processes established to manipulate, import, and merge satellite based vehicle tracking data with Ordnance Survey digital mapping products, have already been used in four other projects within the School of Civil Engineering. The software to regularise positioning interval, smoothing processes, and to compare tracking data with a truth, have been similarly provided. Without major funding the outlook for GLONASS and hence Hybrid looks bleak, and it is predicted that without replenishment the constellation may fall to six satellites by the end of 2001. However as mentioned above, the issues

identified, and ideas and software developed in this research, will be directly applicable to any future hybridisation of GPS with Galileo.

Acknowledgements

This research was carried at the Institute of Engineering Surveying and Space Geodesy, in the School of Civil Engineering, at the University of Nottingham. Funding was made available by the University, and in small part by QUEST Ltd., of Newcastle-upon-Tyne.

I would like to express my sincere thanks firstly to Professors Alan Dodson and Terry Moore for their guidance, encouragement, time, and effort. Thanks is also owed to all those who helped gather data, answered questions with many parts, and proof read chapters of this thesis – these include again Alan Dodson and Terry Moore, together with Dr Marcio Aquino, Dr Chris Hill, Dr Wu Chen, Dr Gethin Roberts, Dr Nigel Penna, Dr John Swann, Dr Dave Park, Dave Russell, and Kenny Gibson. I would also like to thank the Ordnance Survey of Great Britain for freely providing, the digital mapping tiles covering the Nottingham test area.

Finally, the lack of social life tolerated and support given, by my wife, Maureen, over the past six years of academic study, must be sincerely acknowledged, so she says.

Chapter 1

Introduction

1.1 Preface

Where am I? Where was I? Where have you been? Spatial needs for ourselves or for some other entity we are involved with, are often expressed in these ways. In a geographical sense, ever since emigration and trade across oceans began, the need for a globally available positioning system was paramount. The earliest of these used stellar and planetary observations, later with the help of magnetic compass, sextant and chronometer. The most exact results were obtained using stars with a sharp sea horizon, giving accuracy, even today, of at best, two to five kilometres. Modern day systems like GPS still employ objects in space. Only now, artificial satellites at sufficient altitude to be seen over a wide area on the ground are used. Though the technology has changed, with improvement in accuracy of between 3 and 7 orders of magnitude, *clocks* and *time* remain very important.

Since the 1980s civilians have been able to access the single globally-capable GPS. The exponential rise in the user population, and number and diversity of applications that can be served, have enabled economies of scale in receiver

production, that together with advances in micro-electronics, have driven down prices accordingly. The military imperative this system was designed to serve, now forms a small part of the capabilities realised in the last decade. As a result of global capability and plummeting cost of receivers, the cost-effectiveness of many terrestrial systems has been reduced, for example: Argo, Decca (RIP December 2000), Loran C, Maxiran, Omega (RIP September 1997), and Syledis. Some of these older systems remain in limited use, sometimes in another guise. For example the low frequency nature of Loran C can be harnessed in an integration with GPS, since it is less susceptible to signal blockage and reflection than the microwave frequencies of GPS.

However, no system is perfect, and GPS is no exception. There is a fundamental limitation on the system's ability to facilitate a positioning service: the receiver's antenna must have an open line of sight to a sufficient number of satellites. GPS functions at its best when there is a clear and unobstructed view of the sky. Such a reality is rarely the case, and is usually only contrived when the highest accuracy is required. What is far more interesting is how the performance of GPS is affected in less than ideal conditions. This is the everyday reality of an obscured skyview, that is experienced when travelling to work, or getting lost on a walk in the forest. Under the most difficult conditions GPS will become unreliable and eventually, incapable of operating. It is in these scenarios that other sources of positioning information are sought to integrate or *hybridise* with GPS. To make integration easier, the first choice of a system to combine with GPS to mitigate its deficiencies in hostile environments, would be a *similar* system.

The arms race in the late 20th century fuelled parallel developments in space technology in the former Soviet Union and the USA. The Soviet Union had GLONASS, and the USA had GPS. This competition, if first prototype launch is taken as the winning post, was won by GPS. However, whilst detail of GPS has been in the public domain for almost two decades, it was not until democratisation of the former USSR, that information on GLONASS was made freely available. GLONASS provided the only significant contemporary partner for GPS, to give the *Hybrid* system.

In response, several western companies such as Ashtech, MAN Technologie, 3S Navigation, and Trimble, built GLONASS capable hardware, and processing software.

However, the integration of *similar* systems implies some level of difficulty, and Hybrid is no exception. There are three main areas of difference between the two systems:

- The coordinate reference system
- The time reference system
- The frequency of the satellite signals

How effectively these disparities are addressed will impact on the net advantage gained through the larger Hybrid constellation. Potential advantages include:

- Improved coverage
- Better geometry, and thence accuracy
- Accelerated ambiguity resolution

- Rapid detection of unhealthy satellites, improving integrity
- Frequency diversity may protect against jamming and interference

1.2 Research aims and objectives

This research adopts the practical viewpoint of the Hybrid system user, who in essence, asks: *what are the quantifiable benefits and limitations of Hybrid relative to GPS?* Underpinning the answers, is the need to understand how system idiosyncrasies, and inaccuracy in the determination of system differences that are used in the integration process, propagate into positioning error. Hence the objectives of this work were to:

- Investigate the effects of between system difference and system peculiarities, to enable definitive figures on positioning accuracy to be derived
- Assess the relative capabilities of GPS and Hybrid with respect to positioning accuracy and continuity
- Establish the practical limitations of the Hybrid system

The main achievements were:

- Validation on a local basis, of the transformation between the GPS and GLONASS coordinate reference systems, with limited success
- The up-to-date quantitative evaluation of absolute positioning accuracy of GPS, Hybrid and GLONASS
- The quantification of the effect of receiver operating temperature on Hybrid and GLONASS relative positioning

- Realisation, using a vehicle tracking exercise with high dynamics, of the positioning limitations of both GPS and Hybrid

- The development of processes to give quantitative measures in order to analyse vehicle positioning performance by GPS and Hybrid

The experience and knowledge gained from this study of the hybridisation of GPS with GLONASS, should in the future, be useful in examining other potential satellite system combinations. These may include GPS with: the proposed Galileo system; EGNOS (see §3.1); and the Beidou (literal translation *Northern Dipper* - which refers to the Plough constellation that points to the Pole Star) Navigation System, of the People's Republic of China, now at the initial deployment and testing stage. This study will also find relevance to hybridisation of GPS with other positioning technology, such as that offered by cellular telephony.

1.3 Methodology and innovation

This research took the following broad chronological order, with areas of innovation identified in **bold** typeface:

1. A thorough investigation of the development and nature of GLONASS was made, and comparisons were drawn with GPS, in both construction and operation. **This provided the previously lacking comprehensive single source of reference for system comparison.**

2. Review of the transformation between the GPS and GLONASS coordinate reference frames (CRFs), **generating work to address local validation of global parameter values.**

3. Review of historic performance analyses of GPS, Hybrid and GLONASS, for all modes of operation, as available.

4. **This prompted an investigation into the effects of receiver operating temperature in the coordinate domain, and the updating of performance analyses of all modes of operation, plus new analyses of GPS and Hybrid without Selective Availability.**

5. **A novel field experiment to test GPS and Hybrid capabilities in the most difficult application of bob skeleton was designed and executed.**

6. **This identified the need for consideration of further systems' integration, prompting the design and testing of a land-based contraption to mimic skeleton dynamics. Also, the lack of methodology for obtaining a truth was highlighted, and this instigated the development of a way to evaluate vehicle tracking against a truth, and other performance measures. These were subsequently developed using road vehicle tracking.**

7. **Techniques to filter tracking data were also required and developed.**

1.4 Thesis Overview

Chapter 1 sets the background to the research, before introducing the aims and objectives, followed by a chronological methodology and sequential innovation.

Chapter 2 provides a developmental history to date, and comprehensive operating detail of firstly GPS and then GLONASS. This includes the

evolution of CRFs, space vehicles and infrastructure modernisation in general, together with operator and independent monitoring of the systems.

Chapter 3 considers the primary integration issues of first generation hybrid systems or GNSS-1 (Global Satellite Navigation System) i.e. GPS with GLONASS. The crucial differences of coordinate reference system, and time reference system are discussed, as are the efforts of IGEX (the Independent GLONASS EXperiment) to determine, amongst other things, an improved transformation between the two CRFs. Other sources and types of observation data suitable for hybridisation are identified, and finally some detail of GNSS-2, involving completely new constellations such as the proposed Galileo, are covered.

Satellite observables and the error budget that affects them, are covered in **Chapter 4**. These form the basic inputs to positioning techniques, which are developed for the pseudorange and carrier phase observables. The chapter closes with discussion of the multiple frequency nature of GLONASS, which gives rise to inconsistent on-receiver signal delays. These are examined by experiment in Chapter 5.

Chapter 5 explores positioning performance for static modes of operation. These are the absolute, differential C/A code, and carrier phase modes, which are examined for GPS, Hybrid and GLONASS. The investigation and analysis of relative positioning modes, was based on the observation of a zero baseline, to obviate any significant frequency dependent bias introduced by GLONASS.

This work was extended to investigate and quantify the effects of a difference between receiver operating temperatures on relative positioning. It is demonstrated that thermal offsets are below the solution noise threshold in absolute and differential C/A code modes, but in carrier phase mode significant baseline measurement errors can arise.

Chapter 6 continues this theme of rigorous examination of GPS and Hybrid performance, but now for dynamic applications. The vehicles used form a chronological sequence of increasing difficulty, in terms of fixed and dynamic multipath and sky view restriction. This culminated in the development of a package to attempt the tracking of a bob skeleton athlete, at a track in the French Alps. The objective was to define the track convolution parameters and vertical gradient. This application is discussed in detail in Chapter 7. In order to test the package locally, it was set up to track a road vehicle on a circuit between the University and Nottingham city centre. Performance is discussed in this chapter.

Chapter 7 covers all aspects of the bob skeleton exercise carried out at La Plagne in the French Alps. Positioning pack development, logistics and planning, execution, and track determination are all discussed. The primary method to define the track shape of tracking the skeleton failed, owing to the excessively arduous signal reception conditions. However, the back-up method of tracing one of the track walls with the road wheel mounted antenna, was successful. Preliminary results are presented in this chapter, and further developed in Chapter 8.

The extraction of trajectory and thence track convolution parameters from the La Plagne data are considered in **Chapter 8.** Treatments and routines were developed to clean the raw tracking data, and enable parameters of down-track distance, radius of curvature, vertical gradient, and directional indications, to be extracted. Though the primary skeleton tracking experiment failed, the contingency method led to useful numeric data for the competitor, to integrate with the pre-existing skeleton engineering models, where exactly none was available before. Further development of the skeleton tracking package is proposed, and the design and operation of a road-based skeleton simulator tested, with preliminary results given.

Chapter 9 builds on the work discussed in §6.6, developing measures of positioning performance, that could be used to quantitatively assess GPS and Hybrid in difficult signal reception conditions. A major issue was the determination of a truth, against which to assess vehicle positioning, on a digital mapping background.

Finally, **Chapter 10** summarises the main points of the complete work, draws a set of conclusions, and makes some recommendations for further work.

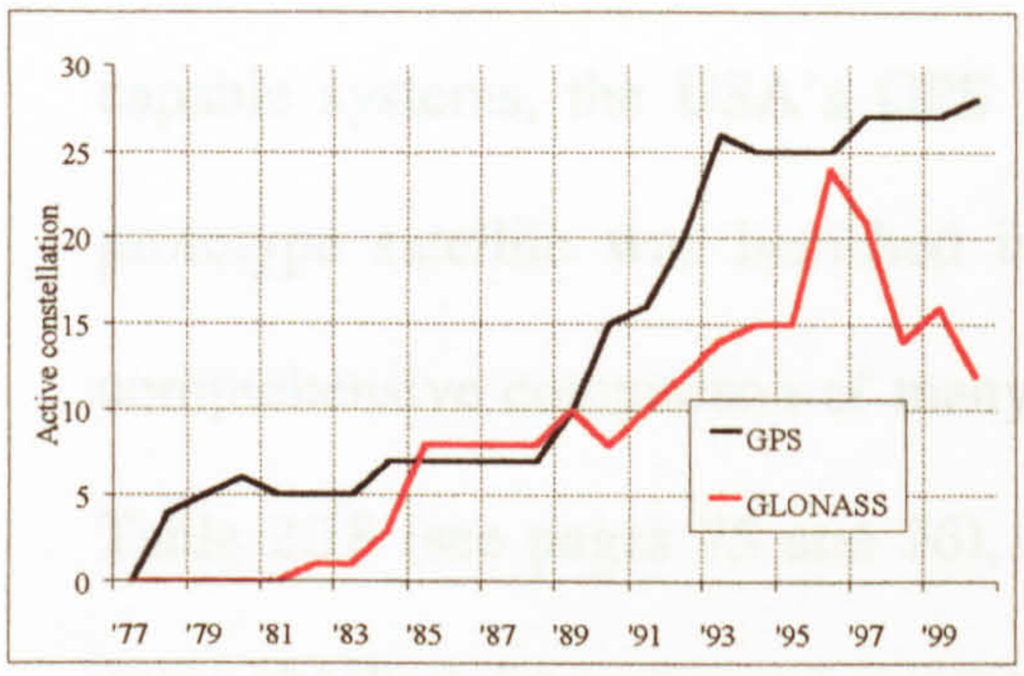

Chapter 2

Global Satellite Navigation Systems

2.1 Introduction

The military imperative of staying one step ahead of the opposition, was epitomised in the arms race between the Russians and Americans between the 1950s and 1970s. Inevitably the competition permeated land, sea, and air, and finally progressed into space with the launch of the first artificial satellite, Sputnik, by the Russians on 4th October 1957. The discovery that signals from satellites could be used in positioning at the Earth's surface, provided that the satellite's position was known, led to the early Doppler based navigation systems of the US Navy Navigation Satellite System (NNSS) also known as TRANSIT, operational in 1973, and the Russian Tsikada in 1965. Though globally capable, these systems were limited in constellation size, at 12 vehicles each, and hence could not provide a continuous positioning service.

The need for accurate munitions delivery world-wide, twenty-four hours a day, in all weather, drove the development of the second generation globally

capable systems, the USA's GPS and Russia's GLONASS. The first GPS prototype satellite was launched in 1978 and for GLONASS in 1982. A comprehensive comparison of many elements of these two systems is made in Table 2.18 (see pages 75 and 76), the information having been obtained and cross-checked from several sources. Though the investment in GPS was extremely high, there were benefits in a reduction in the proliferation of navigation systems in the military [Parkinson et al, 1996], and later as civilians took up the technology, major revenue flows returned to the US. The secrecy associated with GLONASS precluded external revenue benefits to the former Soviet Union, and though in recent years the West has become interested in GLONASS, its depleted state has kept major investment away.

2.2 GPS: History and Structure

It took just 17 years from the launch of the first prototype satellite, for GPS to reach full operational capability (FOC) in 1995, with a 24 satellite constellation. During this period, continuous slow refinement to all parts of the system were made. This process of modernisation continues today at a now accelerated rate, undoubtedly influenced by the emergence of a potential competitor – the proposed European civilian system, Galileo.

GPS was designed to provide two user groups, the civilian and military sectors, with a positioning service of different accuracy. Minimum performance levels have been specified for the two levels of service, which are the Standard Position Service (SPS) and Precise Positioning Service (PPS). The SPS is

available to all users, and was from 25th March 1990 until 1st May 2000 almost always, with a short break for the Gulf War, associated with an accuracy in plan of better than 100 metres 95% of the time. The main determinant of this accuracy level was intentional signal degradation termed Selective Availability (SA), a satellite-specific error with a rapidly changing time-dependent nature. On May 2nd 2000 SA was removed by the US authorities and accuracy in plan improved to about 7 metres 95% of the time, see Table 2.5 and Chapter 5. The official SPS 95% accuracy figures without SA have yet to be issued, and it has been verbally stated by Shaw [2000], that SA will not be switched on again. Some detail of the nature of SA is provided later (§ 2.2.4), as it contaminates research carried out between 1997 and 2000. The alternative PPS is for restricted use only, by the military and by specially authorised users. For these users the PPS was designed to provide an accuracy in plan of about 18 metres 95% of the time. The PPS is effectively insensitive to SA (see page 26).

Generic globally-capable positioning systems consist of three main components: the control, space and user segments. These are now comprehensively covered for GPS and then for GLONASS.

2.2.1 Control segment

The GPS Operational Control Segment (OCS) manages, supports, and controls the complete GPS system. The OCS is responsible for: the maintenance, control, and spatial configuration of the constellation; for the computation and

upload of navigation data to the satellites; and for monitoring the quality of the services.

In more detail, for a GPS receiver to be able to locate itself by the intersection of range spheres from a number of space based reference stations i.e. the *satellites*, their location must be accurately known at discrete points on some time scale, and be predictable in the short term. This requirement involves not only monitoring satellite positions (the ephemerides) from a terrestrial network of tracking stations, but also monitoring the behaviour of clocks at the various system components, since observations must be made in a common time frame.

Estimates of ephemeris and clock performance parameters are generated using raw data from the original USAF owned network of five autonomous GPS ground tracking stations. These are at Hawaii and Kwajalein Atoll in the Pacific Ocean, Diego Garcia in the Indian Ocean, Ascension Island in the Atlantic, and Colorado Springs on mainland USA. They are well dispersed longitudinally, and except for Colorado Springs, relatively close to the Equator, so that the complete 110° ground-track latitude band is covered with overlap between stations. A further tracking station is in the process of being set up at Cape Canaveral in Florida [USCG, 2000].

Shriever Air Force Base also at Colorado Springs has the role of Master Control Station (MCS) with a back-up MCS at Onizuka Air Force Base in California. The MCS acts as a central data collection point, command, communication and computing facility. All tracking data are streamed to the

MCS, here satellite ephemerides and clock errors are computed, for dissemination by upload link to all satellites via a common navigation message. The MCS also has responsibility as system performance monitor and satellite controller. There are three upload stations, at Ascension Island, Diego Garcia, and Kwajalein.

2.2.2 Space segment

The space segment comprises the satellites which emit signals that can be used in the positioning task. The constellation design was changed in its formative period, for cost and coverage considerations, from 18 to 24 satellites in three orbital planes, to 21 plus three active spares in six orbital planes. In recent years the population has been boosted until by year 2001 the constellation was at 29, populating then up to 5 slots per plane, including a number of active spare satellites.

The orbits are near circular, with an inclination of 55°, period of 11 hours 58 minutes, and altitude of 20200 km above the earth's surface. In-plane phasing is uneven (Figure 2.1), with separations of between 29.9° and 32.9°, and 92.38° to 131.98°. The original design was optimised to minimise the effects of a single vehicle's failure on system degradation as a whole [Parkinson et al, 1996], the increased plane population improves this further.

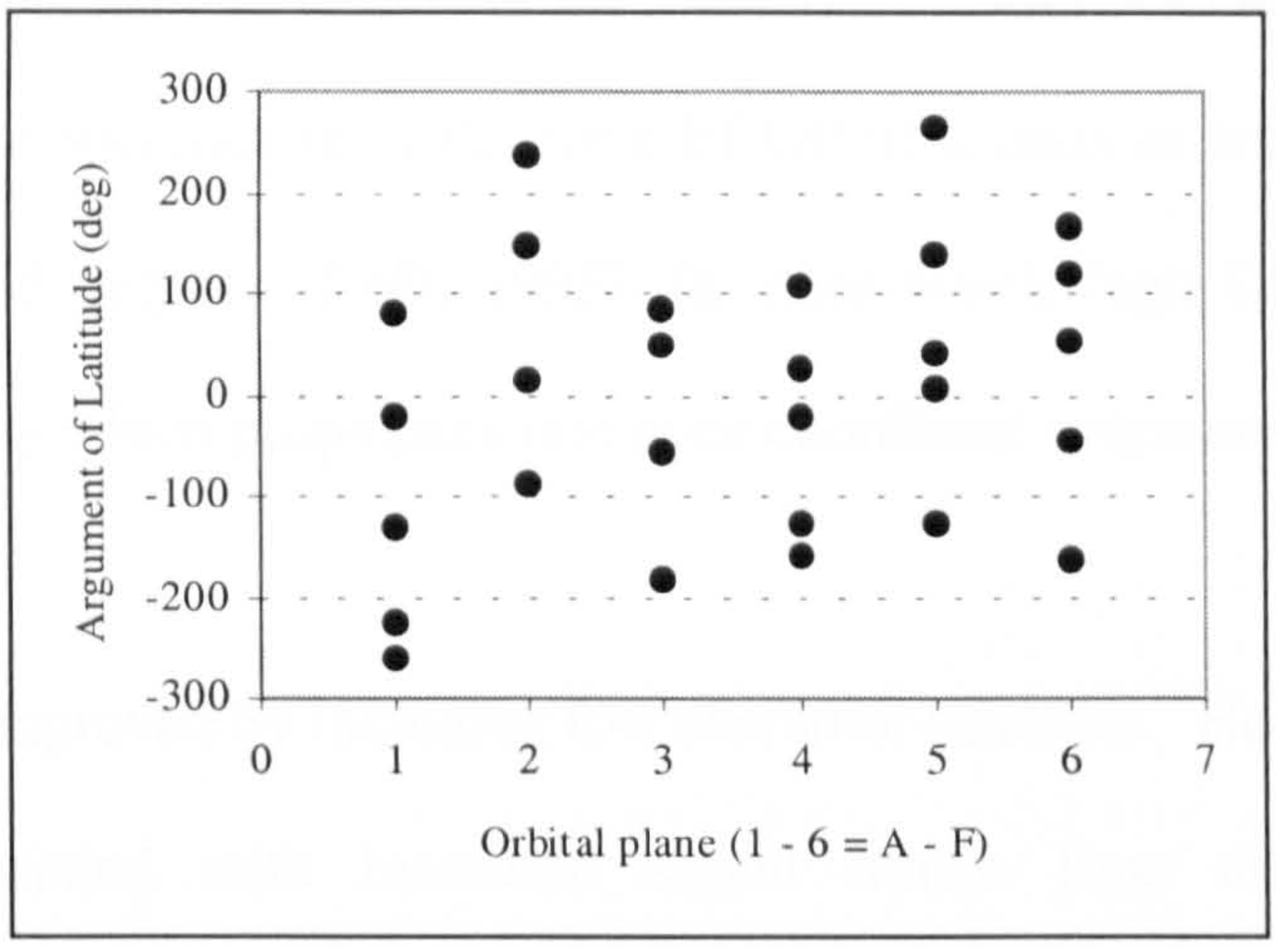

(Figure constructed from broadcast almanac data)
(Note: Argument of latitude = mean anomaly + argument of perigee)

Figure 2.1 GPS constellation at 23rd June 2000

Again the original design of GPS was intended to provide at least 99.9% global coverage with at least 4 satellites in view throughout the 24 hour period, with 4 satellites always providing a minimum level of geometric quality. The need for 4 satellites to be simultaneously in view stems from the number of unknowns to be solved for in a (non-redundant) 3-dimensional solution for a receiver's position: these are the (X, Y, Z) or (Latitude, Longitude, Ellipsoidal height), plus the possible offset between the highly stable GPS system time and the relatively unstable receiver clock time, based on relatively cheap low quality quartz crystal technology. Good geometry or *angles of cut* with any positioning system are associated with low levels of uncertainty or high precision, relative to that obtainable with poor geometry. Geometric quality of a GPS position fix is encapsulated in Dilution of Precision (DOP), a unitless variable that is related to the geometry between receiver and satellites. Low DOP values translate to good geometry. DOPs are also linear scalars of position precision i.e. if DOP trebles, position precision is degraded. PDOP

(Position DOP) is the geometric quality indicator for a 3-dimensional position, and the GPS design specification calls for a PDOP of 6 units or less, with an elevation mask of 5 degrees [DoD, 1995]. In other words high DOP values mean poor geometry which propagates into poor coordinate precision.

Geometry can be improved by including low elevation satellites. However low elevation is associated with increased signal transit time through the atmosphere which increases noise levels, but this can be addressed by applying an elevation dependent weighting regime [Hartinger et al, 1998].

GPS was declared at FOC in July 1995 with a constellation of 24 healthy Block II/IIA satellites. Satellites launched after this point were either IIA or Block IIR, or *R*eplacement, to take the place of malfunctioning II/IIA units. The launch program has been pretty uneventful compared with that of the Russians (see § 2.3.2). There were two failures at launching: on January 17 1997 a Delta II launch vehicle carrying the first replenishment (Block IIR) satellite exploded close after launch, with a similar occurrence in December 1981. Since 1981 there have been 31 successful launches, including 27 Block IIs, all by Delta II launch vehicle [GPS World, 1997a]. It had been intended that the Block IIs would be launched up to three at a time by the Space Shuttle, but the Challenger disaster caused a reversion to rocket launches [Langley, 1991a], which continues today (2001). An overview of the systematic improvement made over time with new and revised satellite series is given in Table 2.1.

Block	Status	Launching	Design life / actual	Comment / Improvements
I	All 11 withdrawn	1978-85	3 years / max 10 years	Orbital inclination = 63° for Arizona military operations coverage. No SA.
II	7 operating 2 failed	1989-90 SA introduced	7.5 years / ?	Can operate autonomously for up to 14 days. †
IIA	18 operating	1990-Nov 1997	7.5 years / life expectancy increased to 10.6 years [GPS World, 2000a]	A(dvanced) vehicles. Can operate autonomously for up to 180 days. Some carry retro-reflectors for laser tracking.
IIR	2 operating 1 launch fail	July 1997-?	7.8 years	R(eplacement) vehicles. Longer design life, and will operate autonomously for up to 180 days. Rubidium clocks. Inter satellite ranging introduced.
IIF-Light	Development stage	1st phase (6 sats) 2002-2002, 2nd phase (15 sats) 2004-2005	12.7 years	F(ollow on) vehicle in development, including:. Inertial navigation system. Civil signal at L2. New military signal. Third civil frequency.
IIF-Heavy	Development stage	After IIF-Light	?	Starts with 7th IIF launch. Military spotbeam fitted, which increases power over a limited area to overcome jamming
GPS III	Modernisation	-	?	Possible improvements based on Capstone Requirements Document

† Autonomous operation refers to the ability to meet range error specification for up to so many days since the last upload from the MCS.

Table 2.1 GPS development status at May 2001

In 1999, a significant number of satellites had surpassed their design life (Table 2.2). The forward launch schedule was changed in 2000 to reflect an accelerated modernisation program (Table 2.3).

Block - Number	PRN	Launch date	Plane	Age
II-2	02	10.06.89	B3	11.8
II-4	19	21.10.89	A5	11.5
II-5	17	11.12.89	D3	11.4
II-8	21	02.08.90	E2	10.7
II-9	15	01.10.90	D5	10.6
IIA-10	23	26.11.90	E4	10.5
IIA-11	24	04.07.91	D1	9.9
IIA-12	25	23.02.92	A2	9.3
IIA-14	26	07.07.92	F2	8.9
IIA-15	27	09.09.92	A4	8.8
IIA-16	01	22.11.92	F4	8.5
IIA-17	29	18.12.92	F1	8.4
IIA-18	22	03.02.93	B1	8.3
IIA-19	31	30.03.93	C3	8.2
IIA-20	07	13.05.93	C4	8.0
IIA-21	09	26.06.93	A1	7.9
IIA-22	05	30.08.93	B4	7.8
IIA-23	04	26.10.93	D4	7.6
IIA-24	06	10.03.94	C1	7.2
IIA-25	03	28.03.96	C2	5.2
IIA-26	10	16.07. 96	E3	4.8
IIA-27	30	12.09.96	B2	4.7
IIA-28	08	06.11.97	A3	3.6
IIR-1[1]	-	17.01.97	-	-
IIR-2	13	23.07.97	F5	3.8
IIR-3	11	07.10.99	D2	1.7
IIR-4	20	11.05.00	E1	1.0
IIR-5	28	16.07.00	B5	0.9
IIR-6	14	10.11.00	F1	0.5
IIR-7	18	30.01.01	E4	0.3

[1] Unsuccessful launch

Table 2.2 GPS satellite age at May 2001

Year | Launching	Launching	Comment
1999	IIR	1 launched
2000	IIR	3 launched
2001	IIR	1 launched
2002	IIR	
2003	IIR (f) = IIR with partial [†] upgrade to IIF	IOC 2008 FOC 2010
2005	IIF	IOC 2012 FOC 2015
2010	1st GPS III	IOC 2016 FOC 2018

[†] C/A on L2 and M-code added

Table 2.3 Forward GPS launch schedule / status at May 2001

2.2.3 User segment

This comprises the military and civilian sectors i.e. the users themselves and their receiver installations, the *user population.* A receiver installation comprises a receiver and antenna with inter-connecting cabling, a power supply, with associated integrated and/or post-process software. The civilian GPS receiver inventory outnumbers by far that of the military. The imbalance is driven by innovation in the civilian and scientific segments, which have stimulated enormous levels of interest in satellite positioning and hence an exponential rise in receiver demand.

Receivers come in all shapes, sizes, and capabilities, and costs vary accordingly. Handheld units the size of a small mobile telephone, with a built-in antenna, tracking screen and way-point / return to base functions, cost around £100, and give an accuracy in plan of about 20 to 30 metres (since May 2000). These units currently access the SPS C/A (Clear/Acquisition) code signal, with a wavelength of about 300 metres. For several thousand pounds more, the receiver can make use of the carrier phase onto which the C/A code signal is modulated, and it is possible with even more expensive receivers to access the PPS, without formal authorisation.

2.2.4 Signal structure and usage

GPS satellite signals are very complex. The signal received at an antenna is a composite comprising a continuous carrier wave on to which are modulated

coded signal(s) with certain repeat period(s), and a navigation message again with a repeat period. These components are at widely different frequencies, which when combined give a signal with a *spread spectrum* nature i.e. it occupies a significant bandwidth relative to each of its components. Bandwidth is an important defence against jamming, intentional or otherwise, since it is more difficult to cause interference over a range of frequencies.

Intentional jamming of positioning signals can be a real problem, for example the Air Force Guest Weekly Newsletter, [1997], which gives an account of the Russian company Aviaconversia's portable GPS and GLONASS jammer shown at the Moscow Air Show in 1997. This is a 4-watt system capable of jamming the civilian and military frequencies of GPS and GLONASS at ranges up to 200 kilometres. It is claimed to be capable of directional jamming whilst maintaining safe areas for friendly users receiving GPS and GLONASS. On the other hand it is asserted that intentional jamming, or otherwise, say from cross band leakage may be reduced to the level of thermal noise, using a Fourier technique to estimate the frequency of interferer(s) [Cooper et al, 1997].

EM spectrum is negotiated at World Radio Conferences (WRCs) held every three years. Major recent issues have been new allocation for GNSS, and retention of bandwidth for GPS. At WRC 2000, pressure from Mobile Satellite Services (MSS) to share the band 1559-1610 MHz, containing GPS L1, failed on the basis that sharing was infeasible. Furthermore the band 1164-1215

MHz was allocated to satellite based navigation including GNSS, which helps both GPS modernisation and Galileo programs.

GPS signals are in the microwave part of the electromagnetic spectrum, for the specific purpose of reducing the effect of the ionosphere, which delays radio signals, and has less effect at higher frequencies. GPS satellites transmit a dual frequency carrier wave regime at frequencies of 1575.42 MHz and 1227.60 MHz, these are known as Link 1 (L1) and Link 2 (L2) respectively. The mathematical combination of signals from such widely separated frequencies then allows the estimation and practical elimination of the absolute ionospheric delay, for users equipped with so called dual-frequency units. The frequency diversity of L1 and L2 serves also as a defence against interference and jamming.

The coded signals referred to above are known as Pseudo-Random Noise (PRN) codes, these codes are used not only as a measurement medium but also to uniquely identify each satellite's transmissions, and prevent interference. The term *pseudo-random* is descriptive of the character of the codes which though artificially generated have a random noise-like appearance. Unique identifying codes modulating a common carrier wave are an important characteristic both in terms of commonality in hardware, but also in positioning processing as will be demonstrated later (see Chapter 4). This concept is encapsulated in the term Code Division Multiple Access (CDMA). There are two code regimes, the C/A code already mentioned associated with the civilian SPS, and the Precise or P code associated with the military PPS level of

service. Both the C/A and P codes are modulated onto L1, but the P code is also modulated onto L2. From this it can be implied that the intention is for the military only to have access to measurements that are free of ionospheric delay. For a complete description of the nature of these codes and the processes used to generate them, see Spilker [1994].

To position a receiver, signals from at least four satellites must be available. The range between a satellite and an antenna is the signal flight time (SFT) factored by the speed of light. To establish SFT the time of signal transmission by the satellite and its time of reception at the receiver are needed, in a common time system. Also, in order to use more than one satellite, all satellites must operate on the same time system, and since the satellites are effectively reference stations in space, then their orbital location at the instant of signal transmission is also required again on the same time system. These needs imply the requirement for a highly stable time reference system, with continuous monitoring to provide information on satellite clock drift from a master clock. The co-ordinating time reference system, or GPS time, is a crucial element of GPS, and is realised using a large number of atomic quality clocks around the world and on board the satellites. The satellites carry four atomic clocks, which indicate time in the satellite time frame, and also provide the means to generate the fundamental signal frequency (f_o) of 10.23 MHz (with diurnal stability of around 10-13 Hz), of which other satellite signals are multiples:

$$f_{L1} = 154 * f_o = 1575.42\,\text{MHz} \qquad f_{L2} = 120 * f_o = 1227.60\,\text{MHz}$$

$$f_{C/A\,code} = f_o/10 = 1.023\,\text{MHz} \qquad f_{P\,code} = f_o = 0.23\,\text{MHz}$$

If the receiver was fitted with an atomic quality clock then it too could be synchronised with GPS time, and only three co-ordinate unknowns would exist in a solution for the antenna location, requiring signals from a minimum of just three satellites. However costs, portability, and safety dictate that in general, receivers are fitted with quartz technology clocks, which introduces the fourth unknown to a position solution, the time offset between the receiver time frame and GPS time. Hence the need for a minimum of four satellites.

The way that a receiver uses a satellite signal to perform code type positioning, is first to demodulate the code, and then to compare this with a locally generated version, the receiver then shifts the local version until it is aligned with the satellite signal, at this stage *receiver lock* with that satellite is said to have occurred. The distance between each satellite and the receiver's antenna is then a measure of how much the local code has to be shifted. However the satellite and receiver clocks are not aligned as explained above, so that the indicated range is contaminated by the clock error between them – hence the term *pseudo-range* for this type of measurement.

It is useful to summarise the synchronisation with GPS time of the three operating segments (Table 2.4):

Segment	Alignment with GPS time by?
Ground	Provides definitive GPS system time (and time tags ephemerides)
Space	Satellite clock time + error estimates = GPS system time (at the satellite)
User	GPS system time + solved offset between receiver clock and GPS system time = GPS system time (at the receiver)

Table 2.4 Segment alignment with GPS time

SPS and PPS levels are as said before, differentiated by access to different codes, and code measurement resolution is a function of wavelength. The C/A code has a frequency of 1.023 MHz, a wavelength of about 300 metres and a repeat period of 1 millisecond or 300 Km, allowing rapid receiver lock, whilst the P code has a frequency of 10.23 MHz, a wavelength of about 30 metres and a repeat period of 267 days. Code measurement resolution in geodetic quality receivers is around 0.1 % wavelength, or for C/A and P code measurements about 30 cms and 3 cms respectively. Each satellite is assigned a seven day segment of the P code. Access to the P code is restricted through combination with an encrypting W code resulting in a secure Y code. This practice is known as Anti-Spoofing (AS). AS status is either on or off, in contrast to SA's time-dependent nature. Innovative receiver design e.g. Ashtech Z12, Turbo Rogue and Trimble SSi models, has allowed satellite tracking to continue seamlessly on L1/L2 P code during periods of P code encryption, e.g. Trimble, [1994] or Gourevitch [1994]. But all techniques involved suffer from a loss in SNR, and perform less well than authorised PPS users in dynamic applications [GPS World, 1994].

Perhaps the most important advance in the use of GPS signals, was the realisation that the carrier waves themselves, L1 and L2, could be used to provide phase measurements at the millimetre or sub-millimetre level. The problem with such measurements was that they were highly *ambiguous*, with upwards of 100 million cycles between a satellite and surface user. This led to much research in the field of *ambiguity* resolution i.e. finding the integer number of carrier phase cycles between satellite and receiver to add to the

receiver's within-cycle measurement to give the total range. Furthermore non-military and academic research establishments have taken a major role in advancing receiver design and data processing methodologies.

It was noted above that SA was removed in May 2000, however its reintroduction could occur at any time expedient to the US authorities, so some detail of its nature is provided here. Shortly after the Block I satellites were launched in the 1970s, it was found that C/A code positioning plan accuracy was in practice around 20 – 30 metres instead of the predicted accuracy of no better than 100 metres [Georgiadou et al, 1990], see Table 2.5. This was regarded as military level accuracy, so artificial degradation, termed SA, was introduced into the next series, Block II, to restrict civilian capability. Degradation was initially set to achieve 500 metres plan accuracy 95% of the time, but this was changed to 100 metres (95%) in 1983. SA was achievable by directly dithering satellite clock output frequency (dither or δ-process) and / or altering ephemerides (epsilon or ε-process), uploaded in the navigation message from ground control. Dither is effectively an additional time variant satellite clock bias, which affects both C/A and P code and carrier phase observations, and is different for each satellite. Epsilon is effected by changing ephemeris terms so that accurate orbital positions cannot be derived, resulting in slowly varying user position errors with periods in the order of hours. To date however, this does not appear to have been applied.

	SA off		SA on	
95% level	PPS	SPS	PPS	SPS[†]
Plan	8 –10	5 - 8[‡†]	8 – 10	40 - 80
Height	15	10*	15	80 - 100

[†] Performance monitored at the IESSG between 1998 and 2000. [‡]Note the decrease in plan error with SPS off, from 20-30m in the 1970s, due to system and receiver improvements, and an increased number of satellites. *Sourced from Langley[2000]

Table 2.5 PPS and SPS performance (95%) with SA on and off (m)

The 100 metre (95%) level of SA was intended to supply a level of accuracy similar to that achieved for non-precision approach at airports, using VHF Omni-directional Ranging systems (VOR). This normally refers to a combined range and bearing system, with a VHF bearing component and a UHF ranging component.

Until recently, SA propagated into range errors with amplitudes of up to some 50 metres and periods in the order of minutes [Hoffman-Wellenhof et al, 1994]. For civilian users the effects of SA can be overcome by differential methods. The basis of such methods, is the comparison at a known point of the observed with computed ranges to satellites, to give pseudorange corrections. These are then transmitted to mobile receivers, where they are applied to give a differentially corrected solution. There are many differential services, some fee-paying e.g. Focus FM [1999], and some free to many users e.g. Trinity House [2000], financed by light dues on commercial shipping and other sources. For military and authorised users of the P codes and PPS, SA is eliminated through some secret process. Elimination might be enabled through a key decryption device allowing access to SA parameters encrypted in a navigation message sub-frame, or via a similar key but with built-in knowledge of the same parameters [Moore et al, 2000].

2.2.5 Navigation message

The L1 and L2 carrier waves are modulated not only by PRN codes, but also by a navigation message. This is an essential part of the GPS, conveying to the user the following:

- Time within the GPS week.
- Almanacs (a coarse form of ephemerides) and health flags for all satellites.
- Broadcast ephemeris parameters for the particular satellite transmission including perturbation and rate of change terms.
- Satellite clock drift parameters of bias, drift and drift rate.
- Ionospheric delay model parameters.
- HOW – Hand Over Word to enable rapid access to the P code.
- URA – User Range Accuracy, a satellite-specific statistical indicator of ranging accuracy, including errors from space and control segments, but not atmospheric or user errors.

Each satellite broadcasts self-specific information of ephemeris, clock offset from GPS time, health status, and expected measurement accuracy, together with generic information about all other satellites, including their health status, and a coarse version of their ephemerides, known as an *almanac, w*hich allows a receiver to find satellites and acquire lock quickly.

2.2.5.1 Broadcast ephemeris

For real-time positioning the receiver must know where the satellites are continuously, this information is contained in the satellites' ephemerides, which are conveyed as part of the navigation message. These real-time

ephemerides are collectively termed the Broadcast Ephemeris (BE), which is used by both the SPS and PPS. The BE is provided in terms of Keplerian type orbital parameters. BE accuracy has been improved over time as more ground tracking stations have been added to the official GPS global network, and data processing techniques have improved, see Table 2.6, but it is insufficiently accurate for the most exacting applications. Organisations and infrastructure have been set up to satisfy these needs, giving rise to a *precise ephemeris* e.g. see IGS [1999].

2.2.6 Precise ephemeris

Independent organisations have for many years worked in parallel with the GPS authorities, using tracking data from the GPS and 3rd party tracking networks, to provide precise ephemerides. Pre-eminent amongst these are the activities of the International GPS Service for Geodynamics (IGS), which since 1993, has amongst other things, coordinated the operation of a global precise tracking network, data collection, and processing centres.

The IGS generates several high quality GPS-derivative products, including GPS ephemerides with various lead-times and levels of accuracy, see Table 2.6, where L is baseline length in kilometres. For example a 100 km baseline determined using the BE, could be expected to be in error by up to 25 millimetres, or 0.25 parts per million (ppm), and if the IGS final issue is used, 0.0025 ppm.

Ephemeris source	Availability	Orbital error	Position error
Broadcast navigation message ‡	Real time	5 m	$2.5 * 10^{-7}$ L
IGS predicted (igp) †	0.5 hr before start of day	50 cm	$2.5 * 10^{-8}$ L
IGS rapid (igr) †	2 hour delay	10 cm	$5.0 * 10^{-9}$ L
IGS final (igs) †	14 day delay	5 cm	$2.5 * 10^{-9}$ L

(† Source: IGS (2000); ‡Barnes et al, 1998)

Table 2.6: Ephemeris accuracy at January 2000

The primary objective of the IGS is to provide a service to support, through the supply of GPS data products, both geodetic and geophysical research activities [IGS, 1996]. The IGS collects, archives and distributes GPS observation data sets of sufficient accuracy to satisfy the objectives of a wide range of applications and experimentation. These data sets are used by the IGS to generate amongst others, the following data products :

- High accuracy ephemerides.
- Medium accuracy short lead-time and predicted ephemerides.
- Coordinates and velocities of the IGS tracking stations.
- GPS satellite and tracking station clock information.
- Ionospheric information.
- Tropospheric information.

IGS orbit determination has been continually improved over time. In 1994 the best IGS orbit solutions were approaching the 10 cm level even under AS conditions, and by 1997 this had improved to 5 cms. Eighteen new network stations in areas of sparse coverage were added in 1995, making a total of 112 stations distributed world-wide. As well as the IGS network of high precision stations, there are others such as the 600-station Japanese Geographical Survey Institute GPS Earth Observation Network (GEONET), and the proposed 250-station Southern California Integrated GPS Network (SCIGN). Other countries

are also developing networks, for example Australia, Sweden, Norway, and the Earth Observation Science Initiative (EOSI) in the UK. EOSI is a network of about 50 Continuously Operating GPS Receivers (COGRs) in the UK, with data management and archival by the IESSG.

The relationship between the orbital system and terrestrial reference frames is achieved by collocation of GPS receivers at VLBI and SLR stations, with global networks of evenly dispersed stations rather than regional networks, resulting in the highest levels of accuracy and reliability [Rizos, 1997].

In point positioning mode using a single receiver, rather than relative positioning used in baseline determination, orbital accuracy requirements are far more stringent, since any error in ephemeris data propagates directly into an equivalent range error, or *User Equivalent Range Error* (UERE) or just URE. Other URE components come from residual satellite and receiver clock errors, ephemeris error, residual ionospheric delay, and tropospheric delay. The square root of the sum of the squares of these errors is the rms UERE. If the average rms UERE for all satellites in solution is taken, and multiplied by some measure of fix geometry, then the rms position error results (§4.1). It can be seen then, that any ephemeris error (radial error being the worst), once translated into URE terms, biases positioning in a systematic way [Wells, 1987].

2.2.7 Coordinate reference system and frame

A coordinate reference system (CRS) is defined by a set of global models and physical constants. A coordinate reference frame (CRF) is the realisation, or link between the abstract and reality, of a CRS, through the adoption of a set of point coordinates. These coordinates implicitly define model location in terms of origin position, scale, and axial orientation in space. A comprehensive definition of these terms is given by Mueller [1985].

GPS uses the World Geodetic System 1984 (WGS-84) CRS, and WGS-84(G873) CRF. The WGS-84 CRS is a Conventional Terrestrial Reference System (CTRS) which includes in its definition a geocentric coordinate system, a reference ellipsoid, a consistent set of fundamental constants, an earth gravitational model, and an associated global geoid [Malys et al, 1997]. (Conventional in the sense of a CTRS, means the origin is at the centre of the earth, the z-axis points towards the IERS Reference Pole, and the y-axis is in the direction of the IERS Reference Meridian). A vector in such a terrestrial reference system can be represented by coordinates in Cartesian (x, y, z) terms, often referred to as ECEF (Earth Centred Earth Fixed) coordinates, and by ellipsoidal (ϕ, λ, h) coordinates [Hoffman-Wellenhof et al, 1994].

At epoch 1997 [Malys et al, 1997], the values of the four defining parameters of the WGS-84, a, 1/f, GM and ω, were as quoted in Table 2.7. Other parameters are also listed [Seeber, 1993].

Parameter	Symbol	Unit	Value
Earth angular velocity	ω	radian.s^{-1}	7 292 115.0 * 10^{-11}
Earth angular velocity (for sat. applications)	ω (Sat)	radian.s^{-1}	7 292 115.146 7 * 10^{-11}
Universal gravitational constant	GM	m^{3}s^{-2}	3 986 004.418 * 10^8
Earth Gravitational Model	-	-	EGM96
Speed of light	c	ms^{-1}	299 792 458
Second zonal harmonic of the geopotential	C2,0	-	-484.166 85 * 10^{-6}
Semi-major axis	a	m	6 378 137.0
Inverse flattening	1/f	-	1 / 298.257 223 563

Table 2.7 Fundamental Parameters of WGS-84

The formal definition of the WGS-84(G873) CRF is:

- Origin is the centre of mass of the Earth.
- *z*-axis is parallel to the direction of the International Reference Pole (IRP), as defined by the International Earth Rotation Service (IERS).
- *x*-axis is the intersection of the WGS-84 Reference Meridian Plane and the plane of the IRP Equator, the reference meridian being parallel to the zero meridian defined by the IERS. The x-axis is defined implicitly by the coordinates of stations providing observational data to the BIPM for the determination of UT (Universal Time).
- *y*-axis completes the system as a right-handed geocentric cartesian co-ordinate system, measured in the plane of the IRP Equator, 90° of the x-axis.

The above definitions are also adopted as the x, y, and z axes, and geometrical centre, of the WGS-84 reference ellipsoid.

WGS-84 is the latest in a series of global CRFs [DMA, 1987; Malys et al, 1997; Slater et al 1997a], each of successively greater fidelity than the previous. In recent years WGS-84 has undergone successive refinement, until it is now aligned with the International Terrestrial Reference Frame (ITRF) 1994 at the 5 cm level, see Table 2.8 [Malys et al, 1997]. The ITRF is the highest accuracy global CRF, and is maintained by the Paris based International Earth Rotation Service (IERS). The development was as follows, being the result of leaps in positioning technology and improvements in the understanding of associated models e.g. surface gravity.

- WGS-60 – only satellite data use to determine ellipsoid flattening.
- WGS-66 – large amounts of Doppler and optical satellite tracking data, plus advances in computer science.
- WGS-72 - large amounts of Doppler and optical satellite tracking data, plus advances in computer science.
- WGS-84 – deficiencies in WGS-72 were addressed.

WGS-84 is practically independent from WGS-72 [Malys et al, 1997]. Initial realisation of the reference frame was based almost exclusively on a world-wide set of coordinates derived from TRANSIT Doppler positions in the NSWC 9Z-2 (Naval Systems Warfare Centre) reference frame [DMA, 1987]. Systematic translation, scale and rotation errors were identified in NSWC-9Z2, through collocation of TRANSIT with SLR and VLBI stations. With the latter implemented, absolute positions in WGS-84 had a 1-sigma accuracy of ± 1 metre in each horizontal dimension, and ± 2 metres in height [Slater et al, 1997a].

Refinements to WGS-84 (1984-1993):

- New surface gravity data.
- Improved computational techniques.
- Improved satellite data – Doppler, SLR, satellite radar altimetry, and using GPS, including observations made at IGS stations.
- New realisation of reference frame, designated WGS-84(G730). (G denotes coordinates were obtained through GPS techniques, 730 is the GPS week number of coordinate implementation).

Refinements to WGS-84 (1994-1996)

- Five globally dispersed permanent GPS monitor stations established to complement the USAF tracking stations, to provide GPS precise carrier phase observations.
- IERS GM value adopted.
- New gravity field and global geoid.
- New realisation of reference frame, designated WGS-84(G873), using data from 24 IGS and 10 DoD stations. Reference frame now in close alignment with ITRF (Table 2.8).

Parameter	Mean	St.Dev.
Origin shift in X (cms)	0.1	2.9
Origin shift in Y (cms)	-0.2	2.3
Origin shift in Z (cms)	0.1	1.4
Rotation about X-axis (mas)†	0.0	0.3
Rotation about Y-axis (mas)	0.4	0.2
Rotation about Z-axis (mas)	0.6	0.4
Scale factor (ppb)	-0.5	0.2

† milli arc seconds

Table 2.8 WGS-84 (G873) to ITRF94 transformation

2.2.8 System time

As mentioned earlier (§2.2.4), accurate timing is fundamental to the operation of any ranging system such as GPS. GPS has it's own time standard, *GPS*

time, which can be related to the international civil time standard, which is UTC (Universal Coordinated Time).

There are several UT (Universal Time) scales, these will be introduced briefly, and then GPS time brought into context relative to them.

UT0 is a mean solar time scale, and is non-uniform in nature.

UT1 is UT0 corrected for polar motion, this is the civilian time scale.

UT2 is UT1 corrected for seasonal variation.

UTC is an atomic time scale kept in approximate alignment with the earth's rotation (UT1) by introducing leap seconds (to UTC).

UTC (BIPM) is that coordinated at BIPM (The Bureau International des Poids et Mesures), in Sèvres, France.

UTC(USNO) is the US time standard, kept at the United States Naval Observatory.

UTC(SU) is the Russian time standard.

There are three UTCs which concern us here: UTC(USNO), UTC(BIPM) and UTC(SU). The first two will be discussed here, and UTC(SU) in §2.3.8.

The Time Service Department of the USNO provides the following explanation of UTC: "The World's Timing centres, including USNO, submit their atomic clock measurements to BIPM. These are used to compute an un-steered (free-

running) mean time scale, Echelle Atomique Libre (EAL). BIPM then applies frequency corrections (steering) to EAL, based on measurements from primary frequency standards and intended to keep the International System's (SI) basic unit of time, the second, constant." Thus another timescale is realised, International Atomic Time (TAI). Finally, the addition of leap seconds to TAI produces UTC(BIPM). See below for an explanation of leap seconds. The world's timing centres have agreed to keep their real-time timescales closely synchronised (or *coordinated*) with UTC(BIPM). Hence all these atomic timescales are called Coordinated Universal Time (UTC), of which USNO's version is UTC(USNO). UTC(USNO) and UTC(BIPM) are regularly coordinated by the common view GPS time transfer method. For an explanation of common view time transfer, visit the website of the USNO or see Dana et al [1990].

UTC(USNO) is derived from the largest ensemble of atomic clocks in the world, comprising 50 high quality caesium and 14 hydrogen maser units. This ensemble is the largest contributor to UTC(BIPM). GPS time is referenced to UTC(USNO), and kept within about 1 microsecond of UTC(USNO), ignoring leap seconds.

GPS time is coordinated by the control segment, using a set of high accuracy caesium beam atomic clocks at the central control site and the remote system monitor stations. Note that until June 1990, time was kept by a single atomic clock at one of the system monitor stations [Langley, 1998]. GPS time is for practical reasons a continuous time scale, unlike UTC(BIPM) and

UTC(USNO) into which leap seconds are occasionally introduced. This is not possible with GPS, as P-code receivers would lose lock, with disruption to users. GLONASS system time is UTC(SU), the Russian realisation of UTC and Russia's civil time, into which leap seconds are introduced. When this occurs there are short term operational difficulties for GLONASS and GLONASS users, see §2.3.8.

GPS time equalled UTC at 00:00 6th January 1980. Owing to the cumulative introduction of leap seconds to UTC, GPS time now (2001) leads UTC by 13 seconds, plus some varying fraction of a microsecond.

Leap seconds are introduced for the following reason: UT1 is the non-uniform time based on the Earth's rotation, this is civil time. If an analogy is drawn between the Earth's rate of rotation and the time keeping of a clock [NANU-001, 1997], then the Earth's rate of rotation is *running slow* by about 2ms per day, termed *excess length of day*. To keep UT1-UTC < 0.9s, a leap second is added to atomic time to maintain alignment between atomic and civil time i.e. instead of resetting the 'watch that is running slow' we reset that which is keeping uniform precise time.

GPS time is segmented into GPS weeks, with time scale origin at 00:00:00 UTC 6th January 1980. A GPS cycle is 1024 weeks, so that the first rollover occurred at 00:00:00 22nd August 1999. The start of each week is at 00:00 Sunday, counting up to 604800 seconds and then resetting to zero at the start of the next week. Hence an epoch in GPS time is ambiguous on a weekly basis.

To avoid this each week is given a unique number, starting at week 0 on January 6th 1980, and incrementing at the start of each subsequent week. An example illustrating the general arrangement of GPS time and its relationship to UTC and TAI is given below, at midday UTC(USNO) 11th December 1997:

- TAI - UTC = 31 seconds
- TAI - GPS = 19 seconds
- UTC (USNO) 12:00:00 Thursday December 11, 1997
- GPS 12:00:12 Thursday December 11, 1997

- GPS Time – UTC = 12 seconds
- GPS week 935
- GPS seconds 388812
- Day of year 345

2.2.9 GPS modernisation

The overt objective of the US State Department is to maintain GPS as the sole means to provide a global positioning capability, and so avoid a proliferation of positioning systems (Figure 2.2). This is a military-led aim. The main way to achieve this is to keep the service free of charge, thereby devaluing other fee-paying or less comprehensive systems. For example consider the costs of hiring and deploying an MF terrestrial ranging system in a remote coastal region for an offshore survey – even in the early days of GPS with relatively costly receivers, a significant cost advantage existed.

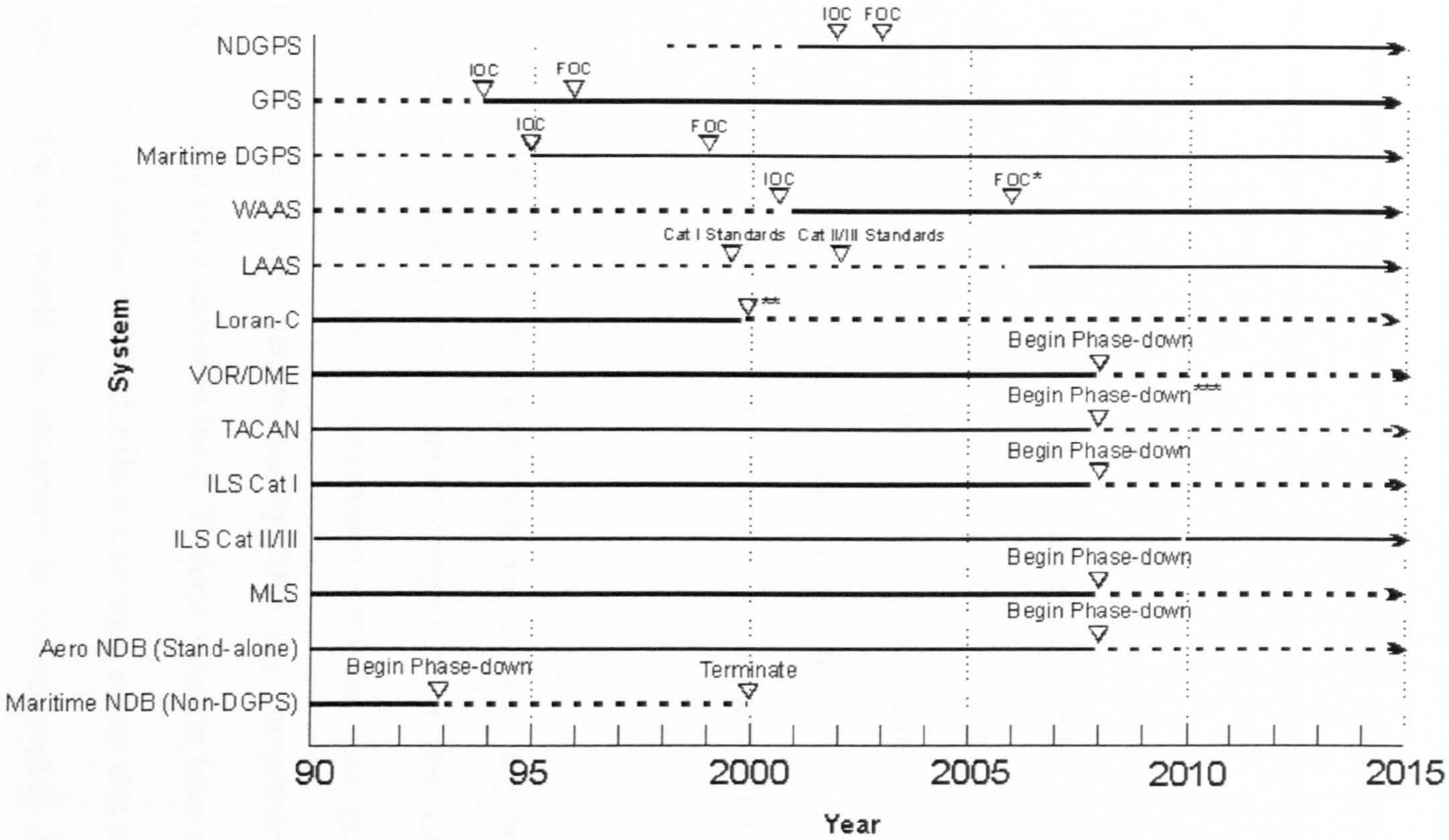

Figure 2.2 Radionavigation Systems Operating Plan 1999 [USDoT, 2000].

But GPS in its current state does not satisfy the needs of large segments of the civilian sector, for reasons as diverse as sovereignty, quality of service, and revenue. This civilian sector, in particular within the European region, has made proposals, and carried out research and feasibility studies into independent augmentations to GPS and completely new constellations, with the aim to eventually de-couple from the US military controlled system altogether.

The US government has attempted to eliminate such third party initiatives by announcing a program of GPS improvement, with the enhanced system remaining free of charge. Of course as the European contingent [Lechner,1997] pointed out, when referring to a perceived link between GPS improvement and European initiatives, the former would not have been presented if the latter had not occurred, since there is no progress without competition.

To be assured of gaining a significant market share, any proposed European satellite positioning system must compete with the GPS Improvement Programme (see below). Competition with the next generation of GPS satellites, Block IIF, dictates that by 2005 any competitor system must be operational at some advanced level. To fund a system from the drawing board to operational status with such a short lead-time, means that service and system upkeep charges would be necessary to recoup capital outlays. A new generation of receivers would also be needed. These factors are major barriers to market entry.

Of course the US do not need to charge for access to the GPS service, since vast wealth is generated by virtue of most GPS receivers being built in the US. This gives taxation benefits to the government and increased employment in the electronics and space industries. The size of the West European GPS market is predicted to grow by a factor of 16 in terms of receiver units, and revenue by $US 664 billion, between year 1998 and 2004 [Frost & Sullivan, 1998].

The US plan for GPS modernisation is contained within announcements by e.g. Armor [1997] and Shaw et al [2000], and summarised by Moore [1998].

The first concession by the US to civilian GPS users was given in 1997, after intense lobbying by the FAA and DoT: legal civilian access to the L2 carrier. However knowledge of the encrypting Y code remained restricted.

The next development was an accuracy improvement initiative also announced in 1997, to be implemented through enhancement of the OCS (Operational Control System) of ground tracking stations. The aim was to improve orbit computation, which should then eliminate discontinuities in ephemerides at change of IODE (Issue of data Ephemeris) in the navigation messages. Using the five original tracking stations a satellite was typically out of view of a tracking station for about 7% of the day. A sixth station in Florida, was planned for inclusion in 1999, but this was still under construction in 2001. The objective is for twenty tracking stations to provide the military with P code accuracy at the one metre level, instead of the prior 8-15 metres.

Furthermore, to placate concerns on GPS's vulnerability as a sole system, the USDoT called for continued availability of ground based Loran-C beyond the proposed termination date of December 31, 2000, and requested $20 million for Loran-C upgrades in 2001 [USDoT, 2000].

The first of the IIR, (R)eplacement, series was launched in 1999, to rejuvenate an ageing constellation - 12 Block IIAs were in 1998 at the end of their 7 year design life. The subsequent series is to be Block IIF, (F)ollow-on, a sustainment program totalling 33 satellites, although the operational constellation is still considered to be 24 units. Design life is set to 12.7 years, with mean time between failures of 10-11 years. Added flexibility has been built into the design, including for example inter-satellite ranging (Autonav) using a dedicated antenna and non-GPS type signals, this will provide a link between satellite clocks, provide improved orbit integrity, with less lead-time taken to determine and announce faults. The system is designed to operate autonomously, without ground control intervention for up to 180 days. In theory the broadcast ephemeris should be improved by inter-satellite ranging, which also provides higher system redundancy required by military users.

An opportunity for the GPS program to leapfrog the European GALILEO initiative, by the inadvertent disposal of the twenty remaining Block IIRs, opening the way for full scale IIF deployment, was missed when hurricane Floyd avoided Cape Canaveral, where twenty IIRs were in storage in a class 2 hurricane structure [Armor, 1999].

Even more into the future is GPS III, which does not follow from Phase or Block II. GPS III is a concept defining the future requirements of GPS, encapsulated graphically in the so-called Capstone Requirements Document (Figure 2.2a).

Figure 2.2a The Capstone Requirement

User groups were polled for their requirements, and the Capstone requirement represents the consensus from this. Main group needs were identified as:

Civilian

- Increase accuracy
- Increase availability
- Provide integrity

Military

- Maintain accuracy in electronic warfare environment through anti-jamming technology
- Deny use to adversaries

FAA (Federal Aviation Authority)

In conjunction with other flight instruments, the navigation system must in all circumstances provide information to the pilot and aircraft systems for performance of the following functions:

- Continuous track deviation guidance.
- Continuous determination of distance along track.
- Continuous determination of position of aircraft.
- Position reporting.
- Manual or automatic flight.

The pursuit of a new civilian frequency continues, possibly reusing the existing L1/L2 spectrum, and providing separate civilian and military signals.

The constellation design itself is also under consideration, with possibly 30 vehicles in 3 planes of 10, a similar planar arrangement to GLONASS.

In 1999, funding of the GPS Modernisation programme, along with WAAS, was deferred by the House Appropriations Committee amidst a larger budgetary and political battle between different appropriations sub-committees. This was overshadowed by the 2000 elections. The tranche of funding at stake was $17M, some earmarked for the establishment of new civil frequencies [GPS World, 1999a, 1999b]. Editorial comment [GPS World, 2000a] crystallised the American views and hopes on Galileo: "The second and third civil frequencies (L2 and L5) could impact the efficacy of Galileo, perhaps *eliminating the need* for that system, a rival system that could create national security concerns for the US". In 2000, as Galileo moves through the

definition phase and closer to realisation, the US will be under pressure to devalue its potential. So innovative routes to get ahead of Galileo and around the budget problems are proposed, for example, modernisation of five of the Block IIRs currently being launched (2000) would accelerate deployment of the new military M-code and civil C/A code on L2 [GPS World, 2000b]. Previously these changes were to be made some way into the next series, Block IIF.

The modernisation program has become a political issue both within the US administration and in the international context. It is therefore subject to many pressures that preclude definitive forward statements on satellite deployment. Reference should be made to web sites of US administration, State departments and organisations for latest information.

2.3 GLONASS: History & Structure

Early in the 1970s the Soviet Ministry of Defence instigated the development of a global satellite positioning system to supersede their earlier Tsikada navigation system [Langley, 1997]. The new system was known as the Global'naya Navigatsionnaya Sputnikova Sistema (GLONASS), also translating into Global Orbiting NAvigation Satellite System). To a large extent this system was similar to GPS. The first test vehicle was launched in 1984, and the 24 satellite system was declared FOC (Full Operational Capability) in January 1996, the development program having successfully negotiated a period of political and social upheaval as the Confederation of Russian States emerged from the former Soviet Union. This was a remarkable achievement, taking 13.5 years from prototype launch to FOC, compared with the US program which took 17.5 years. Unfortunately by mid year 2001 only eight satellites remained, and without further internal or external funding for more launches, it was predicted that only six satellites would remain by year end 2001. The ready availability of GPS signals and receivers, and lack of internal funding, means that GLONASS may now be regarded as an expendable duplication.

Until the 1990s there was little freely available information on GLONASS. Since then, with the end of the Cold War, there has been a new technological openness, and much of the system detail is in the public domain. Even before

that, pioneering civilian work accessing, decoding, and using GLONASS signals was being carried out at the University of Leeds, by Dr Peter Daly (now Professor), amongst others.

On September 24th 1993, by presidential decree [CSIC, 1993], the GLONASS program was put under the control of the Russian Military Space Forces (RMSF), [Langley, 1997]. At that time the constellation consisted of 12 satellites. The RMSF was given the remit of bringing the constellation up to 24 satellites, including launches, in-flight maintenance and certification of user equipment. Information was to be disseminated to the civilian user population by the Coordinational Scientific Information Centre (CSIC), a department of the RMSF.

A further decree [Chernomyrdin, 1995] was issued by the Chairman of the Government of the Russian Federation, Viktor Chernomyrdin, in March 1995. This outlined the departmental responsibilities for enabling: the use of GLONASS by national and foreign civil users; satellite receiver development and manufacture; provision of differential services; and dissemination of system information and status through Notice Advisory to GLONASS Users (NAGUs), the counterpart to GPS' Notice Advisory to NAVSTAR Users (NANUs). That same year civilian information access culminated in the issue of a GLONASS interface control document (ICD), [CSIC, 1995], and in July one year later the International Civil Aviation Organisation (ICAO) accepted the Russian offer of a GLONASS Channel of Standard Accuracy (CSA)

positioning service (Table 2.9), analogous to GPS's SPS. This service was to be provided free of charge for at least 15 years [Misra et al, 1996a].

Error / System	GLONASS / CSA	GPS / SPS (SA on)	GPS / SPS (SA off)
Horizontal	< 40 m	≤ 100 m	6 m [1]
Vertical	< 50 m	≤ 156 m	10 m [2]
Velocity	0.15 ms^{-1}	0.3 ms^{-1}	0.2 ms^{-1} ‡
Time transfer	1 μsec	300-400 nsec	40 ns [3]

[1] 48 hours data at 1 minute epoch interval at the IESSG, after SA switched off in May 2000
[2] 24 hour contemporaneous 3rd party sources (Size of values imply no broadcast ionospheric corrections applied).
[3] from USNO website.
‡Benhallam et al, 1996.

Table 2.9 Nominal civilian service accuracy (95%)

GLONASS in fact provides a two-tier PRN code service directly analogous to GPS's SPS and PPS: this comprises the CSA for civilian use, associated with an accuracy in plan of about 40 metres 95% of the time, and a CHA (Channel of High Accuracy) for authorised user groups [Misra et al, 1996a]. Authorised access to the P-code is predominantly military, with the potential to be encrypted, but access *might* be made available to well defined non-military groups [Stich et al, 1993]. The operators do not recommend unauthorised use of the P-code [CSIC, 1995], although it's structure is easily (and has been) determined.

A major difference between GPS and GLONASS is that the Russians do not apply intentional degradation to the civilian standard service (Tables 2.9), also see scatter plots in Chapter 5. Neither has any encryption been applied to the CHA (Table 2.10), so currently there is no need to resort to innovative receiver design that is necessary with GPS (§2.2.4).

Error / System	GLONASS / CHA	GPS / PPS	GPS / PPS (SA off)[1]
Horizontal (95%)	< 30	8-10 m	8.8
Vertical (95%)	?	15 m	19.8
Velocity	?	≤ 0.1 sec rms	?
Time	60-80 nsec	≤ 100 nsec 2drms	?

[1] Military P/Y code receivers made by Rockwell Collins, 8 hours at a 15 minute interval, courtesy of the Royal School of Military Survey (2000)

Table 2.10 Nominal restricted service accuracy

The quality of GLONASS code phase measurements has been found by extended analysis [Misra et al, 1996a] to be comparable to that of GPS with SA switched off, despite the fact that the GLONASS code chip length is twice that of GPS. The long term URE (User Range Error), which is essentially a Observed minus Computed pseudorange (O-C), was close to zero mean with a standard deviation, σ_{URE}, of 8 to 10 metres. The equivalent value for GPS with SA off is about 7 metres, the slightly worse GLONASS figure was attributed to uncorrected ionospheric delays. For GPS with SA on σ_{URE} is about 25 metres.

2.3.1 Control segment

The Russian ground infrastructure is contained completely within the borders of the former Soviet Union. The segment components are [Basker et al, 1997]:

- Master Control Centre (MCC) at Moscow.
- Command and Measurement Station (CMS).
- Satellite Ranging Station (SLR).
- Navigation Field Monitoring Equipment (NFME).
- System Central Synchroniser (SCS).
- Phase Control System (PCS).

The role of the MCC is similar to that of GPS: to coordinate and use tracking information to determine satellite clock offsets with respect to GLONASS system time, monitor satellite health, and compute ephemerides, for upload as a navigation message. Ephemerides are supplied as geocentric Cartesian coordinates along with derivatives of velocity and acceleration. No ionospheric parameters are provided in the navigation message, however accessibility to an unencrypted P-code on two sufficiently disparate frequencies, allows real time determination of ionospheric delay for dual frequency receivers.

CMSs provide the satellite tracking capability by 2-way radio ranging, and perform upload of control commands and navigation data. The satellite mounted radio transponders are periodically calibrated using SLR stations. These are the *Quantum Optical Tracking Stations* which track the small retro-reflectors fitted to each satellite.

Site / mode	Telemetry, Tracking & Command	Laser ranging	Monitoring
St.Petersburg	*		
Ternopol	*	*	*
Jenissejsk (Yeneseisk)	*		
Konsomol'sk-na-Amure	*	*	
Baklash		*	
Jevpatoria		*	
Kitala (Kitab)		*	

Table 2.11 GLONASS 1995 tracking station capabilities

In 1995 station roles were according to Table 2.11 [Janshe, 1995]. In 2001 only three remained on Russian Federation soil. Two of these stations are also used for laser tracking: Komsomol'sk sk-na-Amure, and Kitab in Uzbekistan [Moore, 1997]. Regular tracking stations were subsequently quoted [Mitrikas

et al, 1998] as Moscow, St. Petersburg, Yeneseisk (Siberia), and Konsomol'sk sk-na-Amure.

In practice very little tracking data are required, this is a direct consequence of the *non-resonant* nature of GLONASS orbits. Normally tracking for one minute at rise, zenith and set appears sufficient [Basker et al, 1997]. *Resonance* occurs when the period of a satellite orbit is an integer multiple of the Earth's Rotation Period (ERP). If a satellite follows the same repeated geographical track, then the effect of the earth's gravity components (that have a wavelength equal to the ERP) on the orbital track is amplified – the orbit is said to be resonant [Seeber, 1993]. GPS has a repeat period of one day, and so suffers from resonance with the Earth's rotation, and has to undergo regular manoeuvres to overcome these effects. The benefit of the GLONASS eight day repeat period is that, under normal conditions, the satellites do not need to be manoeuvred at all once they reach their orbital slot [Rooney, 2000].

This minimises time and cost overheads in orbit determination. The design of the GLONASS space segment resulted from the need to track all satellites from the Russian national tracking network alone. The elegant solution to this design is described in detail in § 2.3.2.

The SCS controls and comprises an ensemble of ten hydrogen maser clocks steered to UTC(SU), and the PCS uses the SCS output to predict satellite clock behaviour. NFMEs provide an integrity monitoring service within national boundaries. The results of system integrity monitoring are broadcast to users

as NAGUs. Rooney et al [1999] provide a summary of this NAGU efficiency, the main defects identified included: NAGUs are never released at weekends; it appears that the reporting procedure is at most daily; and issued NAGUs may not be promulgated.

2.3.2 Space segment

GLONASS satellites are known as *Uragan,* or in English *Hurricane.* The constellation design was 24 satellites providing at least four satellite visibility over 97% of the Earth's surface with a PDOP of better than 6 [CSIC, 1995]. Eight satellites, seven plus one spare, occupy each of 3 orbital planes, separated by 120° of longitude at the equator. In-plane separation was 45°, with phase stagger of 15° between satellites in adjacent planes. This results in a satellite crossing the equator either north or southbound at intervals of about 28 minutes. Each satellite is identified by its orbital plane and slot within that plane. The planes are numbered 1, 2 and 3, and the slots 1-8, 9-16, and 17-24 respectively, see Figure 2.3. A satellite is allowed to deviate by up to 5 degrees of arc in its orbital plane.

GLONASS orbits have an eight day repeat cycle. This character was achieved using specific orbital parameters: a mean altitude above the earth's surface of 19100 kilometres, an orbital period of nearly 676 minutes, and an inclination of 64.8°. This inclination gain of almost 10° over GPS, provides for improved coverage at higher latitudes.

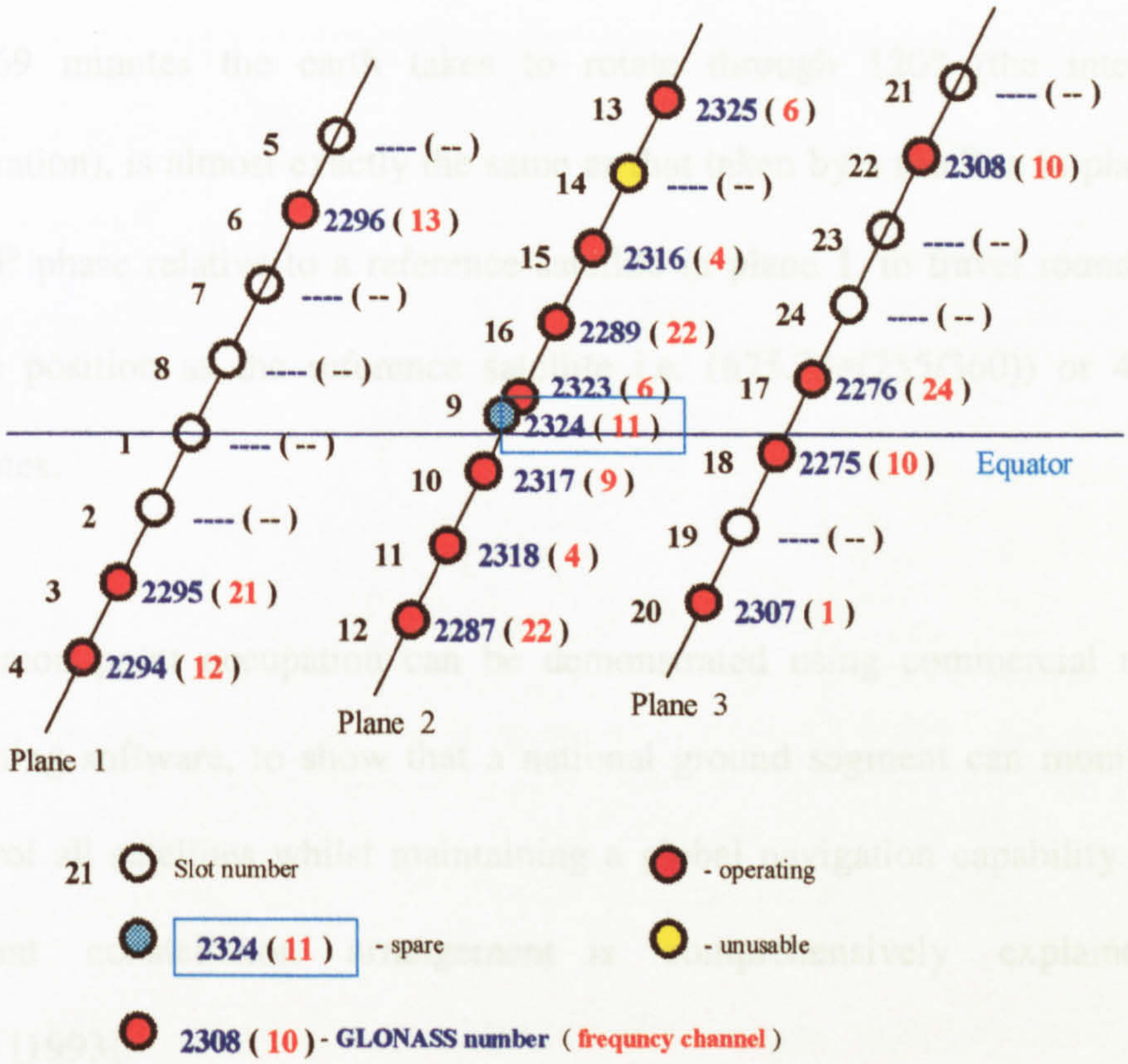

Figure 2.3 Constellation status and slot occupation at 19th March 1998
(adapted from graphic at CSIC website)

In a sidereal day each satellite completes 2.125 orbits, with a longitude change of 169.41°W each orbit. Considering a single plane only and the fact that satellites are phased by 45° (0.125 orbits) within a plane, then each day a successive satellite from that plane will occupy the same position in the sky at the same time, albeit earlier by about four minutes. Thus each satellite will occupy the same point in space and time every 8 days (8 * 45°) less 32.56 minutes.

This same point in the sky will be similarly occupied by satellites from the other two planes, however the common time of occupation will be different for each plane i.e. about ± 8 hours relative to plane 1. In a little more detail, the

478.69 minutes the earth takes to rotate through 120° (the inter-plane separation), is almost exactly the same as that taken by a satellite in plane 2 at +255° phase relative to a reference satellite in plane 1, to travel round to the same position as the reference satellite i.e. (675.73*(255/360)) or 478.642 minutes.

Common point occupation can be demonstrated using commercial mission planning software, to show that a national ground segment can monitor and control all satellites whilst maintaining a global navigation capability. This elegant constellation arrangement is comprehensively explained by Daly [1993].

Figure 2.10 shows the basic constellation design, and operating status at March 1998, caused by the inability of the Russians to make replenishments.

At mid-2001, a total of 71 GLONASS vehicles had been successfully launched, excluding 3 launches of 3 vehicles failing to reach final orbit at all. The Proton K Block-DM2 (also known as SL12) launcher was used for all launches. There are various configurations to this rocket, the largest launch vehicles ever realised, capable of lifting in the top configuration to MEO (Medium Earth Orbit), a payload of 10480 kgs. Compare this with the U.S. Delta II launcher with a payload capacity of 1665 kgs.

Block	Success	Launch	Design life / actual	Improvements
I	10	1982-85	1 year / 14 months average	-
IIa	6	1985-86	1 year / all averaged 17 months	Time and frequency
IIb	9	1987-88	2 years / 22 months average	Longevity
IIc	46	1988-??	3 years / max 50 months	Longevity
M	Nil	2002?	5 years	Time and frequency stability, C/A on L1 and L2, longevity, transmit time offset between GPS and GLONASS systems, ephemeris accuracy, reduce URE, detect satellite health problems within 10 seconds of failure
M2	-	?	?	Series in development

Table 2.12 GLONASS development at May 2001

GLONASS satellites have been improved over time, with advances in most areas over earlier series (Table 2.12). The latest in the line of satellite development and improvement, GLONASS-M, was announced for launching in 1995, but this remains unrealised at year 2001. This program covers improvements in both ground and space segments [Kazantsev, 1996]:

- Extension of designed operating life, 5 to 7 years.
- Transfer of frequency band in co-operation with ITU (International Telecommunications Union).
- Improve standards of onboard synchronisation.
- Improve accuracy of broadcast ephemerides.
- Civilian accuracy code positioning service on L1 and L2.
- Health status changed within 10 seconds of problem recognition.
- Computation and inclusion in navigation message of the time offset between the GPS and GLONASS time reference systems.

By May 2001 the healthy constellation had fallen to 7 satellites plus 1 spare, and operating problems existed with some of these. For example the satellite

in slot 18 showed periodic outages of six weeks every six months, which must be power related since they correlate with earth eclipse periods for that slot. Rooney et al [1999] report a possible link between short period satellite outage and lunar eclipse, suggesting that if there is an onboard problem then it may be so serious that the only solution is to switch the satellite off.

Constellation performance covering the years 1998 – 2000 is shown graphically in Figures 2.4 to 2.6, sourced from the web site of the German Aerospace Centre. These highlight the level of operational difficulty in maintaining the system, or perhaps that little, if any, remedial work is possible. Figures 2.8 and 2.9 give an alternative perspective of GLONASS health, with a resolution of one week. For comparison Figure 2.7 gives GPS performance for part of 1998. Note the use by independent monitoring organisations, of GPS week as time reference in all these figures.

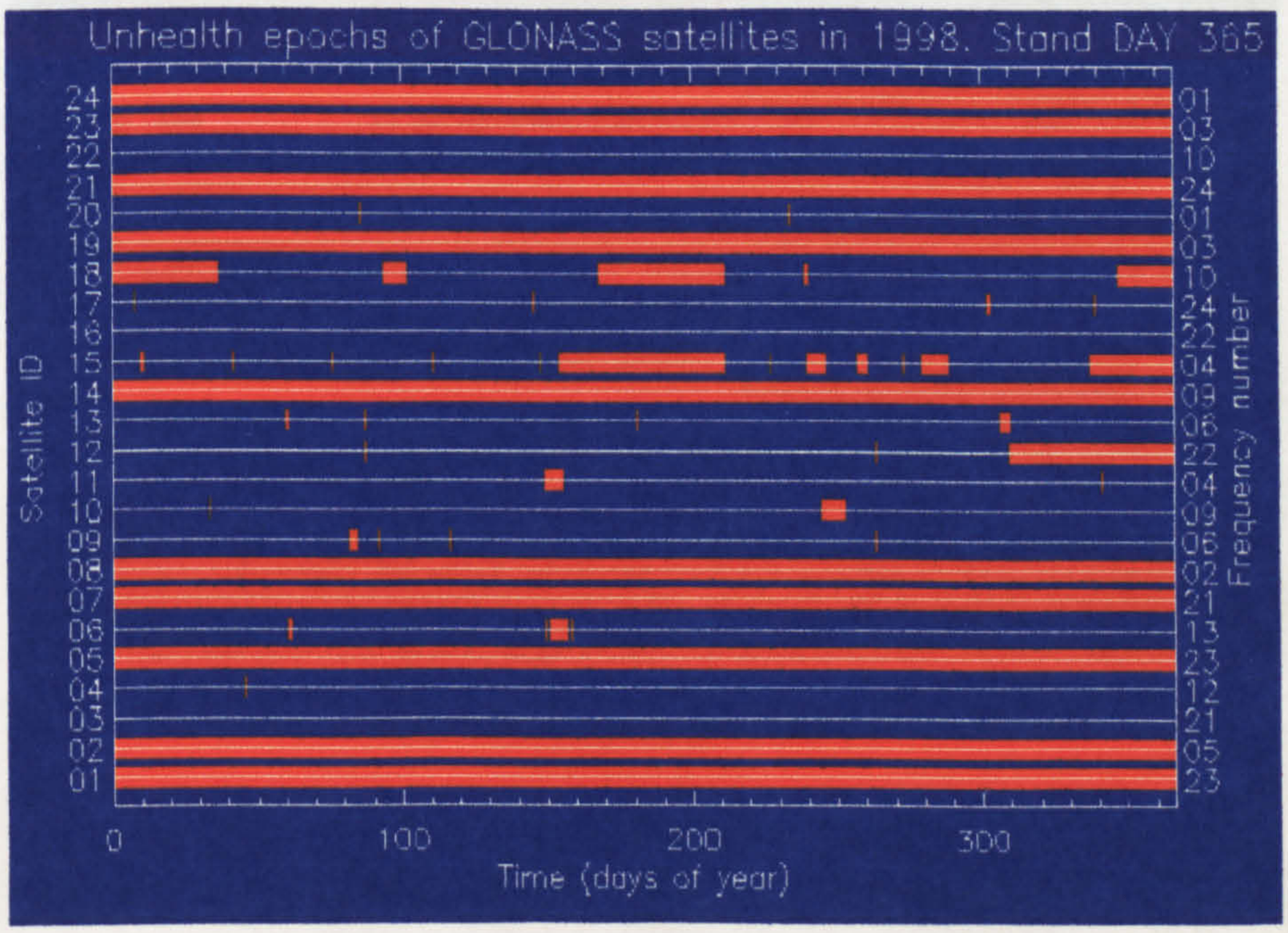

Key: Unhealthy/Withdrawn = Red

Figure 2.4 GLONASS Constellation performance 1998

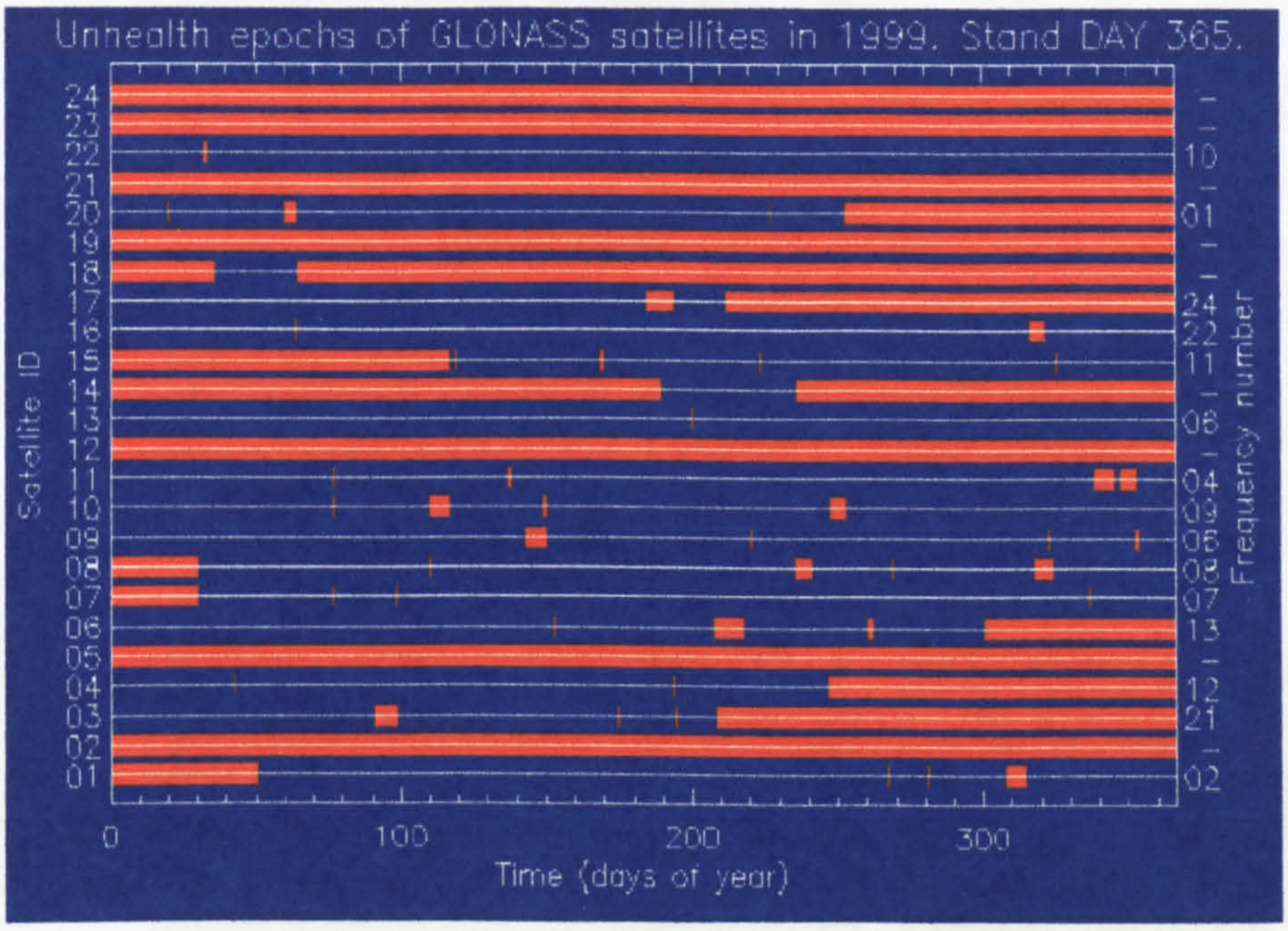

Key: Unhealthy/Withdrawn = Red

Figure 2.5 GLONASS Constellation performance 1999

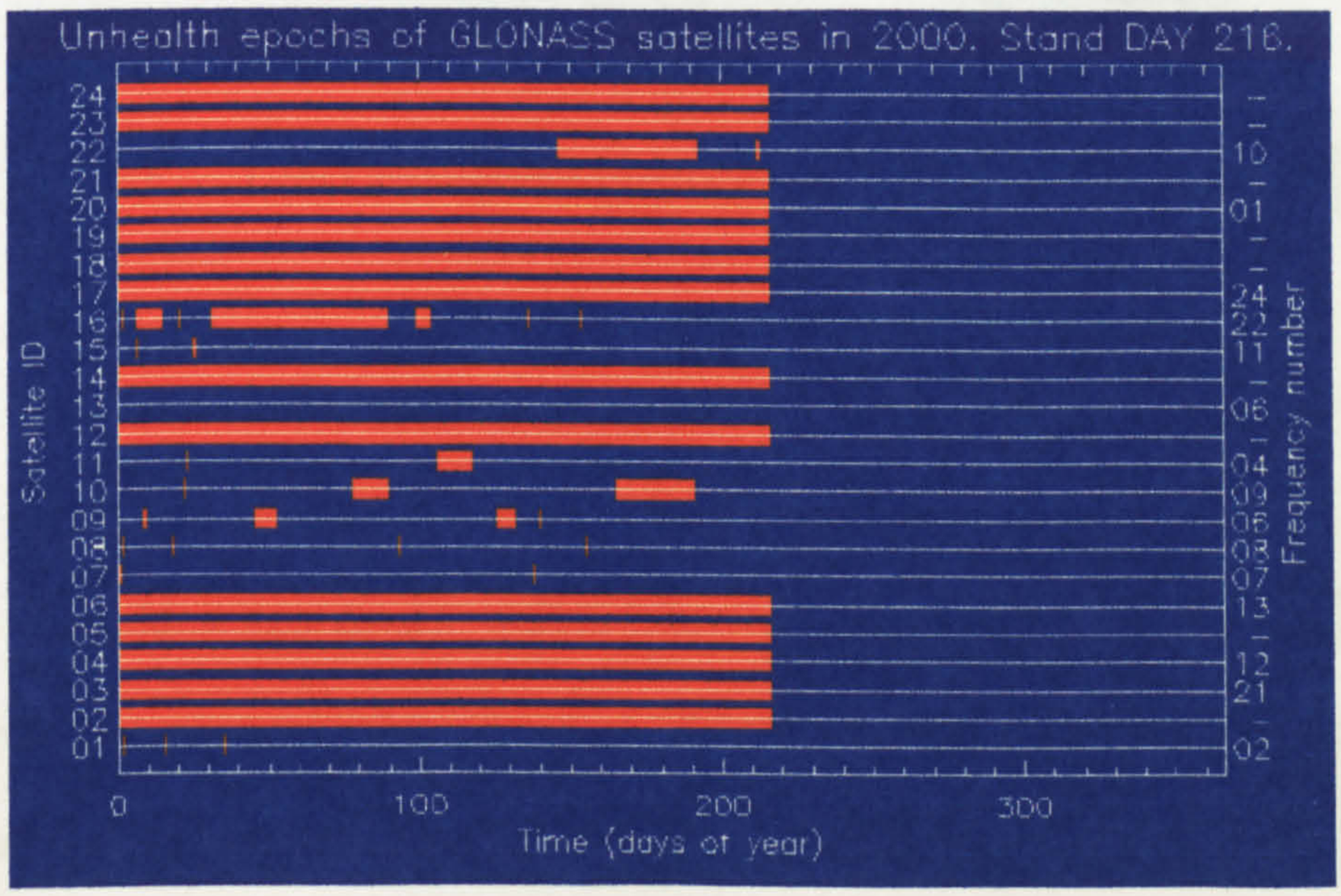

Key: Red = unhealthy / withdrawn

Figure 2.6 GLONASS constellation performance 2000
(Reporting service ceased in mid-2000)

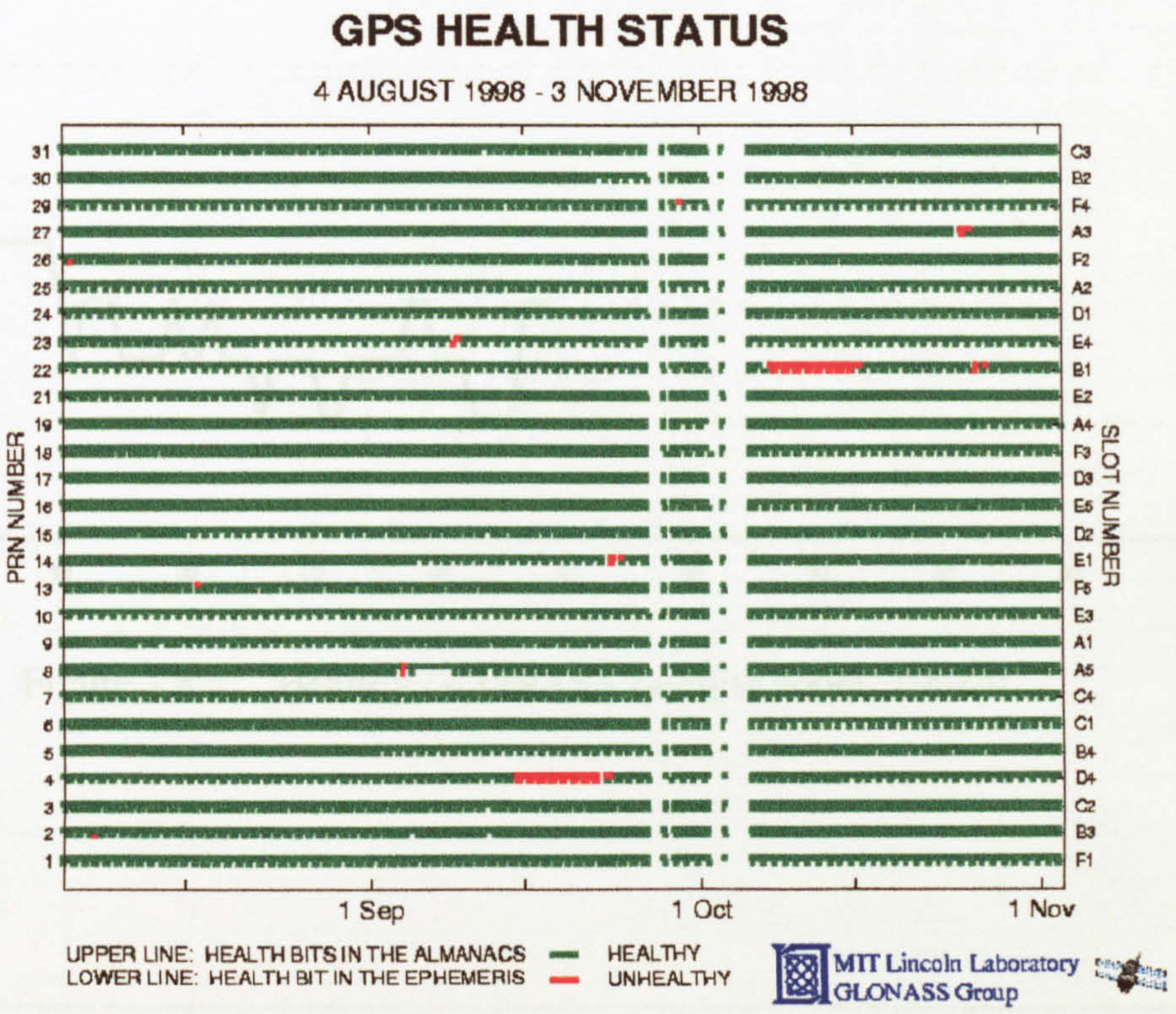

Figure 2.7 GPS Constellation performance, August to November 1998

The eldest GLONASS satellite still operational at year end 1997, was launched on 11th April 1994, and the youngest on 14th December 1995. At year end 1999 the eldest operational vehicle was 5.4 years old. A useful summary covering the period 1992-1998 was available at NASA's website, this has been edited, brought up to date, and reproduced here (Table 2.13).

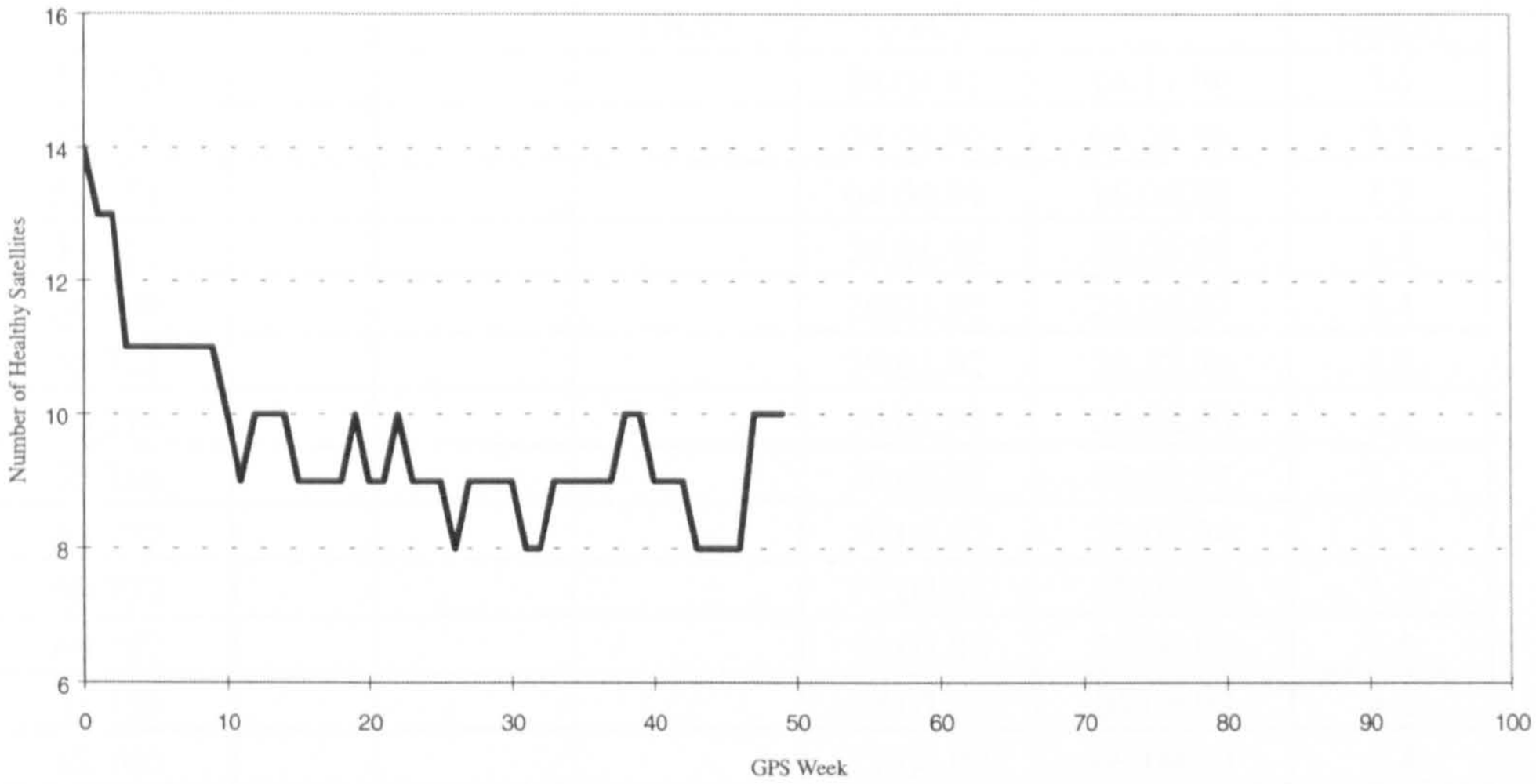

Figure 2.8 Healthy GLONASS satellite count, 1998/9

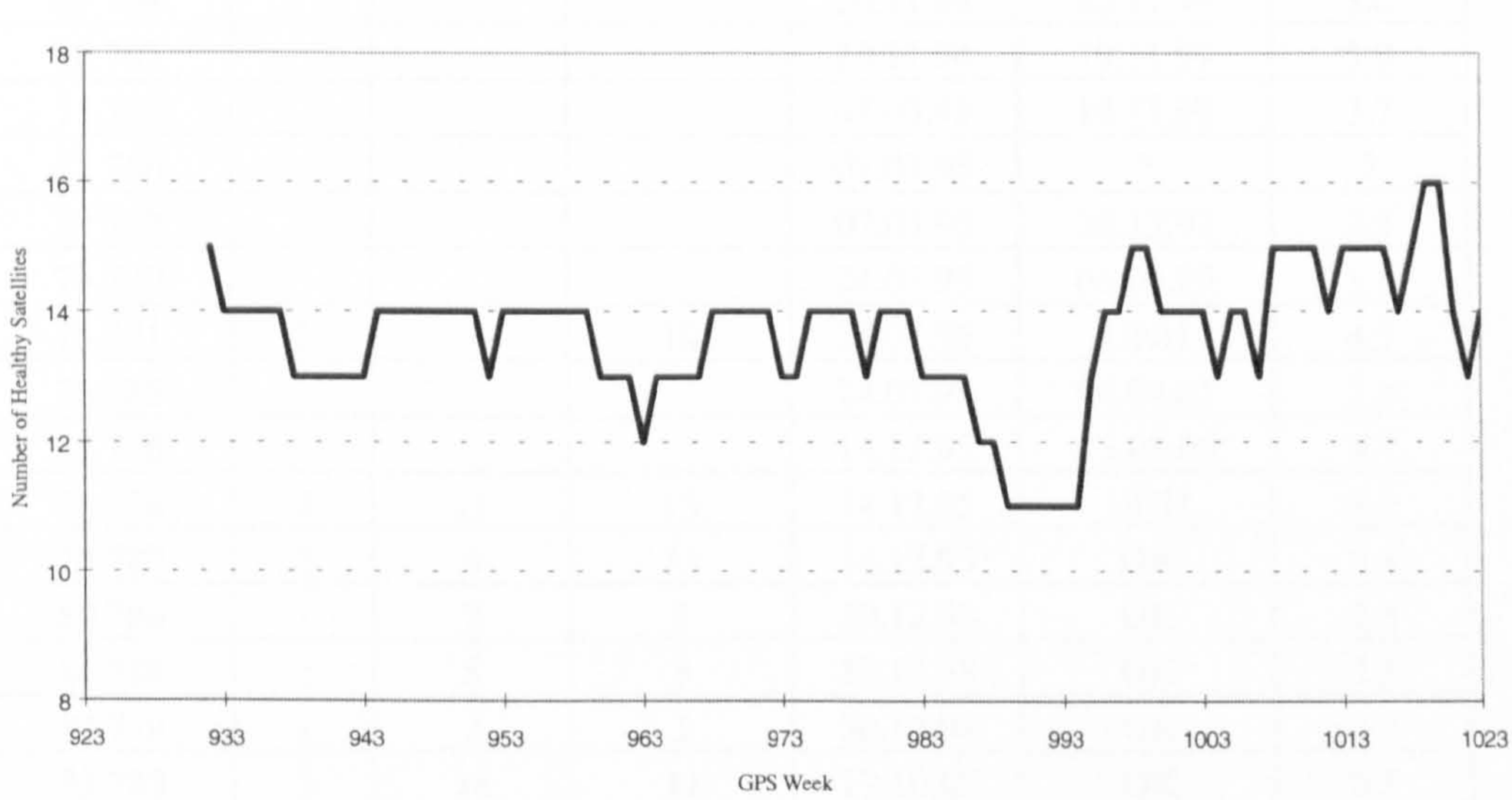

Figure 2.9 Healthy GLONASS satellite count, 1999/2000

GLONASS Numbers	Plane	Channel	Almanac Number (Slot)	Launch Date (UTC)	Status (Date withdrawn)	Life @ 01.05.01 (years)
50 750				04.04.91	14.11.94	3.6
51 753				04.04.91	04.06.93	2.2
52 754				04.04.91	16.06.92	1.2
53 768				29.01.92	29.06.93	1.4
54 769				29.01.92	25.06.97	5.4
55 771				29.01.92	21.12.96	3.9
56 774				30.07.92	26.08.96	4.1
57 756				30.07.92	04.08.97	5.1
58 772				30.07.92	27.08.94	2.1
59 773				17.02.93	17.08.94	1.5
60 757				17.02.93	23.08.97	4.5
61 759				17.02.93	04.08.97	4.5
62 760				11.04.94	09.09.99	5.4
63 761				11.04.94	29.08.97	3.3
64 758				11.04.94	15.01.00	5.8
65 767				11.08.94	03.02.99	4.5
66 775				11.08.94	13.08.00	6.0
67 770				11.08.94	15.01.00	5.4
68 763				20.11.94	05.10.99	4.9
69 764				20.11.94	30.11.99	5.0
70 762				20.11.94	19.11.99	5.0
71 765				07.03.95	19.11.99	3.7
72 766				07.03.95	?	?
73 777				07.03.95	26.12.97	2.8
74 780				24.07.95	06.04.99	3.8
75 781	2	9	10	24.07.95	UNH	4.5
76 785				24.07.95	06.04.01	5.4
77 776				14.12.95	13.08.00	4.7
78 778	2	11	15	14.12.95	UNH	4.2
79 782	2	6	13	14.12.95	OK	5.4
80 786	1	7	7	30.12.98	OK	2.3
81 784	1	8	8	30.12.98	OK	2.3
82 779	1	2	1	30.12.98	OK	2.3
83 783	3	18	11	13.10.00	OK	0.5
84 787	3	17	5	13.10.00	OK	0.5
85 788	3	24	3	13.10.00	OK	0.5

Table 2.13 GLONASS satellite performance at 1st May 2001
(Adapted from information at the NASA web site)

Since 1997 there have been many advance notifications of launches, but it was not until 30th December 1998, and subsequently 13th October 2000, that further

sets of three Block IIc satellites were despatched from Baikonur, situated at latitude 45.63°N and longitude 63.26°E [Shienok, 1999]. Reasons for delays to the launch schedule included: a large number of satellites were on the ground, but there was a problem with delivery of key components previously manufactured in former Soviet states, so new facilities had to be built; finance problems meant that the Proton launch vehicles were used for commercial launch programs such as Inmarsat, and Iridium LEO telecommunications satellites launched seven at a time (Serra, 1999); and a further financial hiccup and launch delay occurred because of imposition of launch fees in hard currency at Baikonur by the Khazaks. Other launch sites were investigated, such as Plesetsk Cosmodrome south of Archangel, however the 1998 and 2000 launches were still from Baikonur.

The forward plan at end 2000 was that two further launches of Block IIc vehicles were scheduled for 2002, including perhaps the first series-M satellite.

The Proton's capability could return the constellation to FOC rapidly, if funding was available, but despite the 1998 and 2000 launches, by May 2001 the healthy constellation had been reduced to seven, with three in plane 1, one in plane 2 (plus one unhealthy), and three in plane 3. In this run-down state GLONASS provided daily standalone coverage of three to four hours, hardly a global positioning capability.

Referring to Figure 2.10, which shows the relationship between launch epoch and life-span, it can be seen that with the inclusion of the 2000 launch, and allowing a five year life for those still active, then by year end 2001 just six satellites will remain. It seems even more unlikely that a second improved M series will appear, this is said to be under development, involving a total redesign of spacecraft and constellation, for proposed launch in 2002.

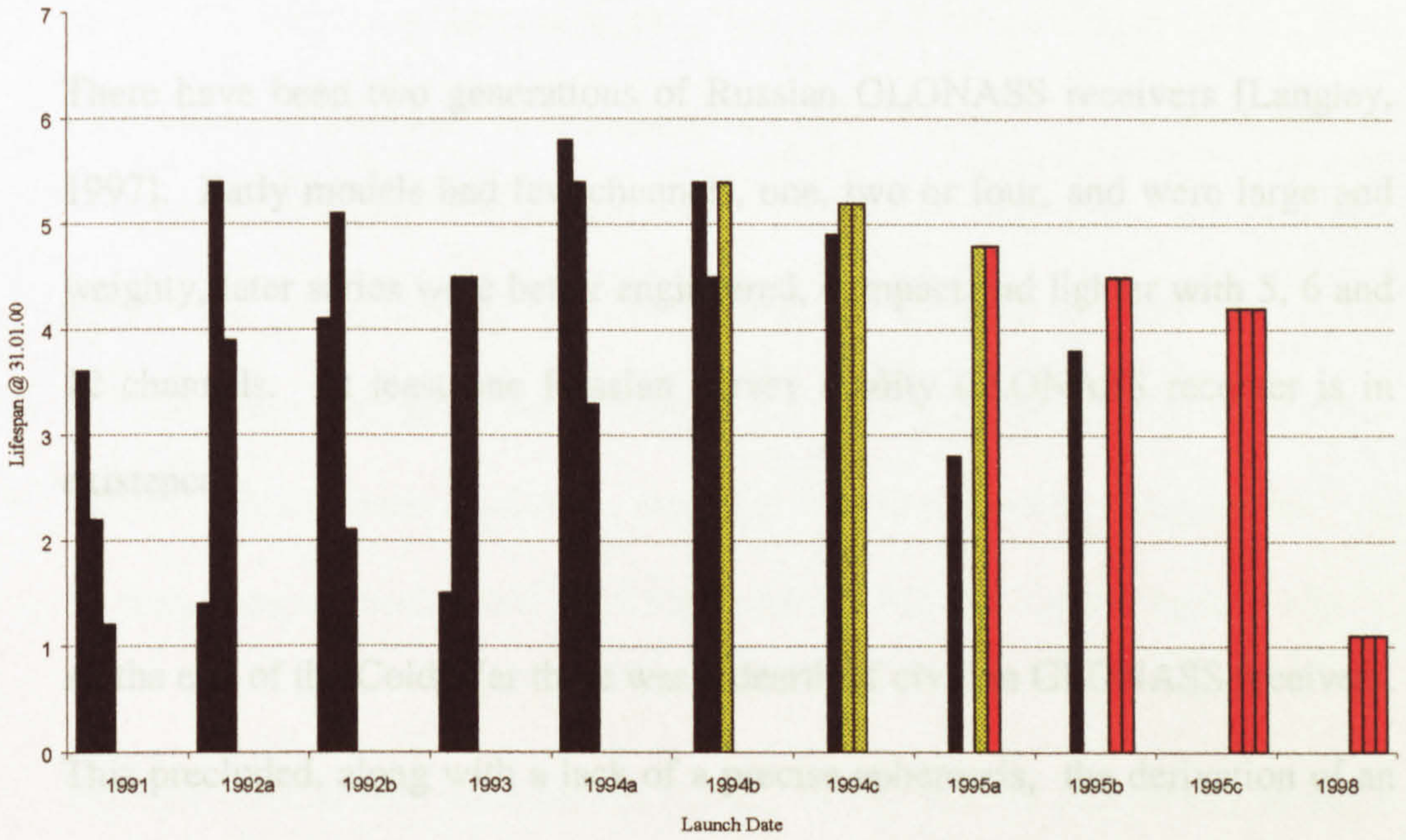

Key: Black = Withdrawn, Green = Unhealthy, Red = Operational

Figure 2.10 GLONASS life-spans at end January 2000

(constructed using data in Table 2.14)

2.3.3 User segment

GLONASS was originally designed for military use only, so there was no infrastructure in place to interface with a civilian user group, hence the development of civilian receivers was slow. By the mid-1990's only a few hundred civilian GLONASS receivers had been produced [Gouzhva et al, 1994]. The ratio of Russian military to civilian GLONASS receivers is the

complete opposite to that of GPS receiver availability. In the past, there has been little attention paid to civilian satellite positioning needs.

The signal frequency regime adopted by GLONASS, see §2.3.4, requires more complex receiver RF sections, and in a hybrid GPS + GLONASS receiver, the bandwidth must be much wider than a GPS-only receiver.

There have been two generations of Russian GLONASS receivers [Langley, 1997]. Early models had few channels, one, two or four, and were large and weighty, later series were better engineered, compact and lighter with 5, 6 and 12 channels. At least one Russian survey quality GLONASS receiver is in existence.

At the end of the Cold War there was a dearth of civilian GLONASS receivers. This precluded, along with a lack of a precise ephemeris, the derivation of an accurate global transformation between the WGS-84 and PE-90 CRFs. Since then Western companies such as 3S Navigation, Ashtech, Javad Positioing Systems (JPS), MAN Technologie, and academic institutions, for example the University of Leeds CAA Institute of Satellite Navigation, have developed their own Hybrid receivers.

Of the two GLONASS codes it is only the CSA code and navigation message modulated onto the L1 carrier wave which are officially available to the civilian sector, however as pointed out above, access to the CHA does not pose

a problem. The use of these signals by a satellite receiver to autonomously position itself as related for GPS (2.2.4), is equally applicable to GLONASS.

2.3.4 Signal structure and usage

GLONASS satellite transmissions in common with GPS occupy the microwave band, with frequency separation to give L1 and L2 (see Figure 2.11). Two PRN codes are also used to modulate the carrier waves, coarse and precise for civilian and military user respectively. However these codes are common across the constellation, so an alternative method of satellite signal differentiation was necessary. This is Frequency Division Multiple Access (FDMA), where each satellite is assigned unique L1 and L2 frequencies. At L1 frequency separation is 0.5625 MHz and at L2 0.4375 MHz (Table 2.15).

The C/A code is well documented [CSIC, 1998], and the complexity of the P code has been found to be not much greater than the GLONASS C/A code [Lennen, 1989].

The *initial design* entry in Table 2.14 lists the design frequency regime. Unfortunately one of the bands chosen, that for L1, 1602.0 – 1615.5 MHz, posed problems for two other user groups, who had been assigned parts of this band by the International Telecommunications Union (ITU), [Langley, 1997]. These are the fields of radio astronomy where very weak radio emissions are studied in the bands 1610.6 – 1613.8 (GLONASS channels 15-20) and 1660 –

1670 MHz, and 1610 – 1626.5 MHz assigned to the operators of Low Earth Orbit (LEO) mobile communications satellites.

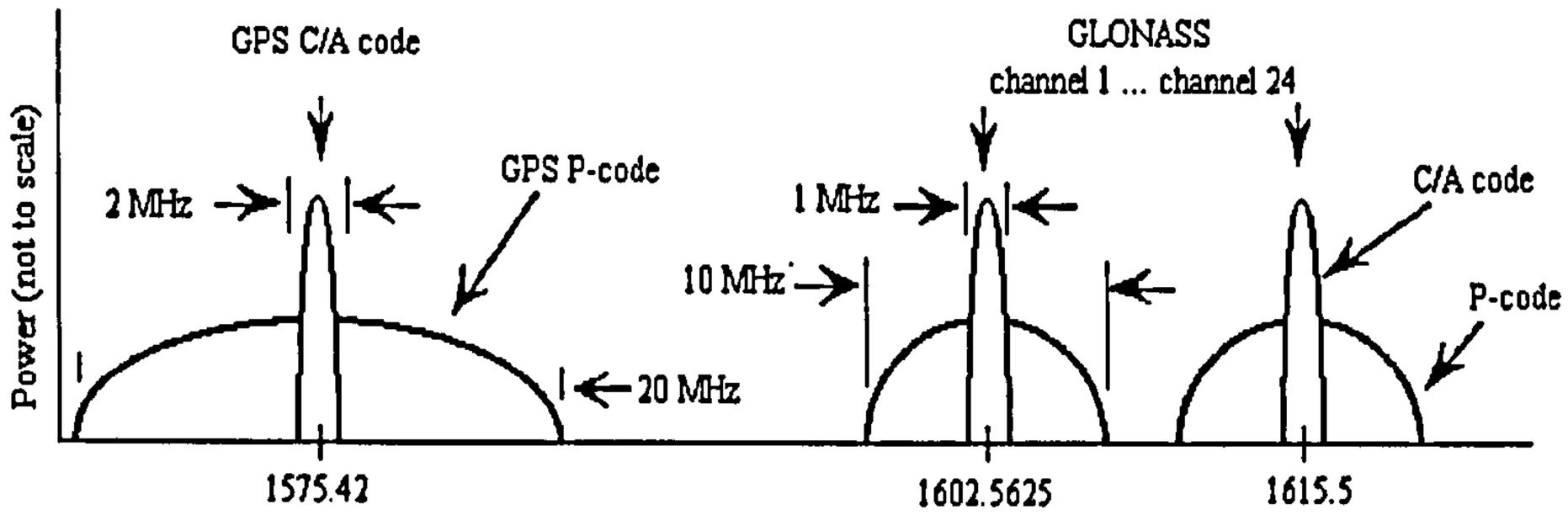

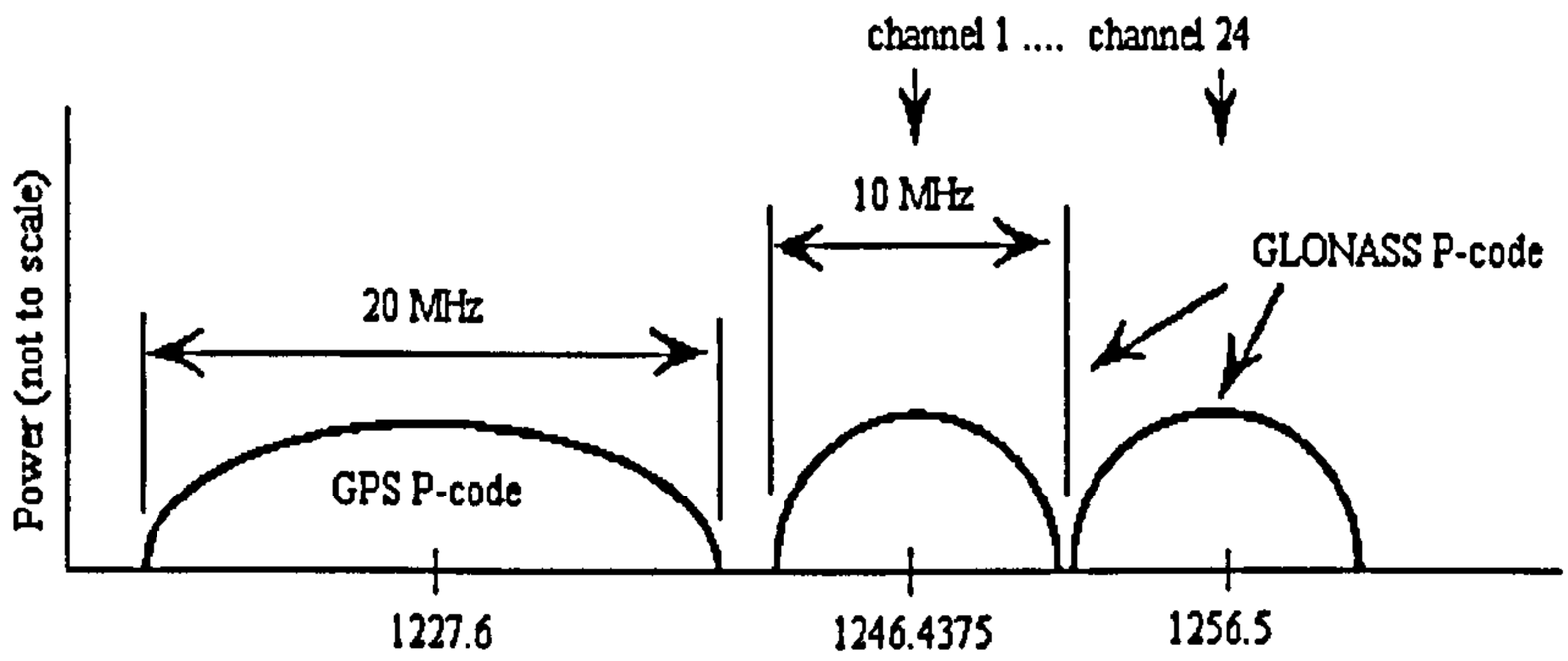

Figure 2.11 GPS and GLONASS frequency utilisation
(Reconstructed from a graphic by Beser et al, 1996)

Initial design	**L Bandwidth (MHz)**
f_{k1} = (1602 + k * 0.5625) MHz f_{k2} = (1246 + k * 0.4375) MHz where k = 0, 1, 2, ... 24 (where 0 is for testing only)	L1: 1602.0 - 1615.5 L2: 1246.0 - 1256.5
1997 – 1998	
k = 0 .. 12, 15, 22 ..24 normal use k = 13, 14, 21 exceptional use only k = 16 .. 20 not used New satellites might use k = -7 to -1	L1: 1602.0 - 1608.80, 1614.400 - 1615.5 L2: 1246.0 - 1251.25, 1255.625 - 1256.5
1998 – 2005	
k = -7, -6, ... 12 k = 13 exceptional use only	L1: 1602.0 - 1608.8 L2: 1246.0 - 1251.25
After 2005	
k = -7, -6, ... 6 (5, 6 are for testing only)	L1: 1598.0625 - 1605.375 L2: 1242.9375 - 1248.625

Table 2.14 Planned evolution of GLONASS bandwidth

The solution to this problem was an agreement with the RMSF to gradually change frequencies (downwards) and reduce bandwidths occupied by GLONASS, in particular those of L1, hence the evolution described in Table 2.15. Eventually the bandwidths will be shifted to 1598.0625 – 1604.25 and 1242.9375 – 1247.75 MHz. Given the required spacing between channels of 0.5625 and 0.4375 MHz for L1 and L2 respectively, there is obviously only space for 12 instead of the required 24 channels. This is resolved by assigning the same channels to antipodal satellites, making use of the practicality that a surface observer cannot simultaneously receive signals from two such satellites. On the other hand, a spacecraft borne receiver at an altitude as low as 193 kms, could receive Earth surface-grazing signals from a pair of antipodal satellites.

The reassignment process began in 1993 with the first batch of antipodal satellite frequency pairing. The status at January 2000 was that ten frequency pairings had been made, however Table 2.15 shows that several are now defunct because of satellite withdrawal.

Channel	Unhealthy	Working	Paired?	Spare
02	0	1	-	
03	0	1	Yes	
04	0	0	Yes	
05	0	1	Yes	
06	0	1	Yes	
07	0	1	-	
08	0	1	-	
09	1	0	Yes	
10	0	1	Yes	
11	1	0	-	

Table 2.15 Frequency pairing and status at May 2001

2.3.5 Navigation message

The navigation message broadcast by each satellite is updated on the half-hour, and contains various essential information for the user:

- Almanacs (Keplerian elements) and health flags for all satellites.
- Broadcast ephemeris parameters for the particular satellite transmission, generally uploaded once per day, updated each half-hour.
- Satellite clock offset from GLONASS time, uploaded twice per day, but there is no time tag or Issue of Data Clocks (IODC) number, parameters are updated each half-hour. The format is a bias and a single drift term.
- Relative difference between nominal and actual satellite carrier frequency health.
- Difference between GLONASS time and UTC (SU), uploaded once per day.

Note that there are no atmospheric parameters supplied to the user, in stand-alone mode this can be overcome by using a dual frequency receiver, and since SA is not applied to GLONASS, then better results can be obtained than with GPS (with SA enabled).

2.3.5.1 Broadcast ephemeris

GLONASS broadcast ephemerides (BE) are uploaded daily, and clock parameters twice daily. GLONASS BE are in terms of cartesian coordinates plus velocities and accelerations, whilst the almanac is in Keplerian terms. BE are updated half-hourly in the navigation message broadcast by each satellite. At each update the cartesian coordinate position of the satellite is specified at

the mid-point of the next half-hour interval, and velocity and acceleration parameters allow user computation of satellite position at any intervening instant.

The GLONASS Interface Control Document [CSIC, 1995] specifies BE rms component error in satellite position (Table 2.16). Independent analysis [Misra et al, 1996a] suggests the specified radial error is pessimistic, whilst along-track and across-track errors appear mainly as long wavelength biases with occasional excursions to 50 – 75 metres, that change slowly over days.

Component	Position (m)	Velocity vector ($cm.s^{-1}$)
Along track	20	0.05
Cross track	10	0.1
Radial	5	0.3

Table 2.16 GLONASS broadcast ephemeris, rms error [CSIC, 1995]

2.3.6 Precise ephemeris

The Russians have not until recently, participated nor benefited from involvement with the IGS (§2.2.6), and so without their own efforts, post-processed precise ephemerides (PE) were not available until the International GLONASS Experiment (IGEX) started work in 1998, though the Russians '*had the task in mind*' [Panyushin et al, 1996]. See §3.2.7 for details of the IGEX PE and IGEX itself.

2.3.7 Coordinate reference system and frame

GLONASS uses the PZ-90, or Parametry Zemli 1990, which translates to 'Parameters of the Earth', (PE-90), CRS and CRF. The evolution of PE-90 has been apparently less complex and shorter than that of GPS's WGS-84, though this assessment may be inaccurate from just a historical lack of information. PE-90's immediate predecessor was SGS-85 (Soviet Geodetic System) [Misra et al, 1994], used until 1993, and its transformation parameters to WGS-84 indicate that the definition of its CRS and CRF are probably quite similar to that of PE-90 (see the matrices below).

Further information on the parameters and realisation of SGS-85 were requested from the Russian authorities, but with no response. Coincidence between SGS-85 and WGS-84 CRFs is achieved primarily through a rotation about the Z-axis, with a further contribution gained by introducing a 4 metre shift along the Z-axis.

$$\begin{bmatrix} x \\ y \\ z \end{bmatrix}_{WGS-84} = \begin{bmatrix} 0 \\ 0 \\ 4 \end{bmatrix} + \begin{bmatrix} 1 & -3*10^{-6} & 0 \\ 3*10^{-6} & 1 & 0 \\ 0 & 0 & 1 \end{bmatrix} \begin{bmatrix} x \\ y \\ z \end{bmatrix}_{SGS-85}$$

N.B. Elements of the rotations matrix are in radians

The parameters of the PE-90 CRF are given in the GLONASS ICD [CSIC, 1995 and 1998]. Those from the 1998 document are given in Table 2.17.

Parameter	Value
Earth angular velocity	7 292 115.10 * 10^{-11} radian.s^{-1}
Universal gravitational constant	398 600.44 *10^{9} m^3s^{-2}
Atmosphere gravitational constant	0.35 * 10^{9} m^3s^{-2}
Speed of light	299 792 458 ms^{-1}
Semi-major axis	6 378 136 m
Inverse Flattening (1/f)	1 / 298.257 839 303
Equatorial acceleration of gravity	978 032.8 mgal
Normal potential	626 368 61.074 m^2s^{-2}
Second harmonic coefficient	-484 164.953 * 10^{-9}
Correction to acceleration of gravity at sea level, due to the atmosphere	-0.9 mgal

Table 2.17 Fundamental constants and parameters of PE-90

The formal definition of the PE-90 ECEF co-ordinate reference system is:

- Origin is the centre of mass of the earth.
- Z-axis is parallel to the direction of the North Pole at the mean epoch of 1900 – 1905 as defined by the IAU (International Astronomical Union) and IGA (International Geodetic Association).
- X-axis is directed to the point of intersection of the Earth's equatorial plane and the zero meridian as established by the IERS.
- Y-axis completes the system as a right-handed geocentric cartesian coordinate system.

These definitions are very similar to those of the WGS-84 system, however there are slight differences in the origin position and axial orientation. PE-90 was realised [Langley, 1997] by the adoption of reference station coordinates in continental Russia only, hence it's standing as a global datum will be degraded by the limited tracking network, and the small number of GLONASS receivers available at that time relative to the geographical extent of the former Soviet Union. The shortage of GLONASS receivers has historically precluded the accurate determination of the transformation between PE-90 and WGS-84. Efforts to remedy this inaccuracy have since been made during IGEX (§3.2.7).

2.3.8 System time

GLONASS is directly referenced to the Russian realisation of UTC, UTC(SU). UTC(SU) is derived from an ensemble of ten hydrogen maser clocks, and like UTC(BIPM) requires the occasional introduction of leap seconds to keep it in approximate alignment with civil time. Such direct alteration of the GLONASS time scale is problematic, as detailed below.

UTC(SU) and hence GLONASS time drifts relative to UTC(BIPM). GLONASS time roughly equals UTC plus 3 hours i.e. it is also related to Moscow Zone Time. An additional time shift exists relative to GPS time and UTC, which at midnight on 1st June 1997 was about –35 microseconds [Langley, 1997], therefore when:

UTC	= 00:00:00.000000
GPS time	= 00:00:11.000000
GLONASS time	= 00:02:59.9999650

That is, GLONASS time leads GPS time by 3 hours minus the number of leap seconds plus the sub-second time shift value, which was equal to 2:59:48.9999650 at midnight UTC 1st June 1997.

The operators corrected GLONASS time by 9 microseconds in 1996, and removed the 35 microsecond time shift along with the latest UTC leap second, at midnight on 1st July 1997. The introduction of such timing corrections and leap seconds to an online navigation system, has historically interfered with service continuity [Misra et al, 1996a]. Several of these have been spectacular:

in 1995, 1994 and 1993 the outage was about 3 minutes, whilst in 1992 the system was unusable for about an hour. The latest outage occurred on 1st January 1999, when a further leap second was introduced.

The 13th Meeting of the Consultative Committee on the Definition of the Second, in 1996, recommended that all satellite navigation systems synchronise their time reference systems as closely as possible to UTC. The Russian federation 'agreed to make improvements', as quoted in [Lewandowski et al, 1996].

2.3.9 GLONASS modernisation

Although the Russians have spoken of GLONASS modernisation, with the M and M2 class satellites, and improvements in the ground segment, it can be surmised that they are probably waiting for a partner to provide financial help. This is emphasised by their inability to significantly repopulate the constellation.

2.3.10 Independent Monitoring

In addition to the Russian system monitoring and reporting activities, several independent institutions have provided third party assessment of the operational efficiency of GLONASS e.g. Misra et al [1996a] at The Massachusetts Institute of Technology (MIT) Lincoln Laboratory, the University of Maine, and the UK CAA (Civil Aviation Authority) Institute of

Navigation. The Lincoln Laboratory operated an FAA (Federal Aviation Authority) sponsored program between 1989 and 1999 looking at independent performance appraisal, technical issues related to combining GPS with GLONASS measurements, and assessment of how well such a hybrid system matches the requirements of civil aviation. Monitoring and analysis was carried out on the C/A code on L1. Unfortunately this site ceased to operate in mid-1999, but as well as Maine and Leeds, there are several others institutions operating a similar service in Europe. These independents have reported a steady flow of GLONASS health anomalies, which are contrary to the operator set health flags. For the period 1996-1997, there were 21 such unreported instances. They were characterised by range errors from around one hundred out to about 30000 metres, lasting from minutes to hours. The causes were transmission of incorrect clock parameters, with on occasion clock parameters being uploaded to the wrong satellite, incorrect ephemerides (upload of an ephemeris to the wrong satellite has not yet been seen), or intermittent transmission problems. This does not imply that the operation of GPS is faultless. There have instances where unhealthy satellites have been marked healthy, and notification of forecast satellite outages by NANU has been historically less than prompt.

A GLONASS-GPS Interoperability Working Group was formed in 1996 under the guidance of the US National Imagery and Mapping Agency (NIMA) and the MIT Lincoln Laboratory. The working group sought to organise pooling of information and resources, and create international alliances for data collection, to produce precise ephemerides for instance. A web discussion area was also

set up at the ION (US Institute of Navigation). Issues considered included coordinate reference frames, time reference systems, and determination of GLONASS precise ephemerides. These were reported on at ION GPS-96 [Senus et al, 1996] and 1997 [Slater et al, 1997b]. Notable developments in 1997, were the Russians' agreement to steer UTC(SU) and GLONASS system time to within 1 microsecond of UTC, and an IGS proposal for a three month global network tracking exercise in late 1998, formalised as IGEX (the International Glonass EXperiment), see §3.2.7, to determine, amongst other things, accurate transformation parameters between PE-90 and ITRF/WGS-84. Fortunately GLONASS satellites are fitted with laser retro-reflectors, allowing independent and precise tracking by SLR (Satellite Laser Ranging).

2.4 Comparing GPS with GLONASS

This chapter has outlined the main features of GPS and GLONASS, and has drawn attention to some of the idiosyncrasies of each. A comprehensive comparative listing of the features of GPS and GLONASS rounds up this chapter, in Table 2.18.

Attribute / System	GPS	GLONASS
Orbital Parameters		
Inclination	55.0° (Block 1 - all defunct now, were at 63.0°)	64.8°
Orbital radius (altitude)	26 570 (20160) km	25 510 (19100) km
Orbital period and type	717.97 mins, near circular	675.73 mins, near circular
Ground track repeat, orbits	2	17
Ground track repeat period	1 day less 4.07 minutes	8 days less 32.56 minutes
Number of planes / separation at equator	6 (A to F) / 60°	3 (I to III) / 120°
Design constellation	21 + 3 spare	21 + 3 spare

Table 2.18 GPS and GLONASS compared

Attribute / System	GPS	GLONASS
Orbital Parameters (continued)		
Satellites per plane, nominal spacing	4, unevenly spaced 2 @ 30.0 to 32.1° 2 @ 92.38 to 130.98°	8, evenly spaced
Healthy constellation at 5/2001	29	7
Tracking stations at end 5/2001	6 Air Force, 6 NIMA, global	5, in the former USSR only
Signal parameters / performance		
Signal type, satellite identification by	Spread spectrum, CDMA	Spread spectrum, FDMA
Carrier modulated by	Navigation message, PRN code	Navigation message, PRN code
C/A code type	PRN code sequence (from the family of Gold codes)	PRN code sequence
P code type	PRN code sequence	PRN code sequence
Modulation	Binary Phase Shift Keying (BPSK)	BPSK
Satellites identified by	Unique PRN codes at a common frequency	Common PRN code at unique frequencies
Satellites referenced by	PRN	Slot number, frequency channel
Polarisation	Right hand circular	Right hand circular
C/A code on frequency	L1	L1
P code on frequency	L1 and L2	L1 and L2
Fundamental clock frequency	10.23 MHz	5.11 MHz
L1 carrier frequency, λ	1575.42 MHz, 19.04 cm	1602.0 – 1608.8 MHz, 18.73 – 18.65 cm
L2 carrier frequency, λ	1227.60 MHz, 24.44 cm	1246.00–1251.25 MHz, 24.08 – 23.98 cm
C/A code chipping rate	1.023 MHz / 293m	0.511 MHz / 587m
C/A code length	1023 chips	511 chips
SPS 2D accuracy (95%)	100 m 2drms	<30 m 2drms
P code chipping rate, λ	10.23 MHz , 29.3m	5.11 MHz, 58.7m
P code length	$2.3547 * 10^{14}$ chips	$5.11 * 10^{6}$ chips
P code repeat period	266.4 days	1 sec
C/A code bandwidth	2 MHz	2 * 1 MHz bands (minimum band separation 11.9375 MHz)
P code bandwidth	20 MHz	2 * 10 MHz bands (minimum band separation 2.9375 MHz)
Total code bandwidth	367.82 MHz	379.0625 MHz
Code phase noise factor	1	2 i.e. worse than GPS
Observables	Pseudorange, carrier phase, Doppler	Pseudorange, carrier phase, Doppler
Ranging precision	1	2 i.e. worse than GPS
Pseudorange observation	By code correlation	By code correlation
Reference System		
Reference ellipsoid	WGS-84 (GRS80)	PE-90
Global datum	WGS-84 (G873)	PE-90
Time scale	Seconds since 00:00 @ 6th January 1980, in the form GPS week number + seconds since 00:00 Sunday – the start of the GPS week. GPS time is kept within 1 μsec of UTC (USNO)	UTC (SU)
Accessibility		
C/A code Selective Availability	Applicable, discontinued at May 2000 (for ever?)	Not introduced
Horizontal accuracy (SPS)	100m 2drms	<30m 2drms
P code access	Restricted	Information not published, but access unrestricted
P code Anti-Spoofing (AS)	Switched on 31st January 1994	Not introduced, potential exists
Precise ephemerides	Several sources, various accuracy and lead-times	Available for period of IGEX, but not before, with 2 month delay

Table 2.18 GPS and GLONASS compared (continued)

Attribute / System	GPS	GLONASS
Messaging		
Navigation message rate	50 bps	50 bps
Nav. message repeat rate	12.5 mins	2.5 mins
Ephemeris and satellite clock offset repeat rate	30 secs	2.5 mins?
Ephemeris provided in .. see Figure 2.12	Modified Keplerian elements	Geocentric Cartesian coordinates, velocity and acceleration
Ephemeris update rate	1 hr	0.5 hr
Ephemeris upload interval	Daily	Daily
Clock data	Clock and clock frequency offsets, frequency rate (ageing)	Clock and clock frequency offsets
Clock parameter upload interval	Daily	Twice daily
Ionospheric model parameters?	8 spherical harmonic terms	None
Superframe duration	12.5 mins	2.5 mins
Superframe capacity	37500 bits	7500 bits
Superframe reserve	2700 bits (approx.)	620 bits (approx.)
Frame duration	30 secs	30 secs
Word duration	0.6 secs	2 secs
Word capacity	30 bits	100 bits
Words per frame	50	15
Sub-frames	5	5
Service History		
First prototype launch	22nd February 1978	12th October 1982
Launch vehicle	Delta II, Shuttle	Proton K Block-DM2
Maximum GNSS-type payload to date to MEO	1665 kgs (Delta II)	4245 kgs i.e. 3 GLONASS vehicles at once
Declared operational	27 April 1995	18th January 1996
Latest launch	PRN 20, 110500 Block IIR	Late 1995, then Dec. 1998
Next launch	See schedule (Table 2.3)	Mid-2000 ?
Next satellite series	Block IIF, 1st launch 2002?	GLONASS-M, then M2
Satellite vehicle mass	Block II 840 kgs Block IIA 930 kgs Block IIR 1130 kgs	1411 - 1415 kgs
Frequency dependent factors		
Multipath maximum code error factor	1	2†
Multipath maximum carrier phase error factor	1	minimum 0.975
Multipath signature repeat period	23h 56m	7d 23h 27.5m
C/A code SNR at 5° / 90° el. [Benhallam et al, 1996]	42.0 / 52.5	42.35 / 53.0

† In practice GPS and GLONASS code multipath have been found to be very similar.

Table 2.18 GPS and GLONASS compared (continued)

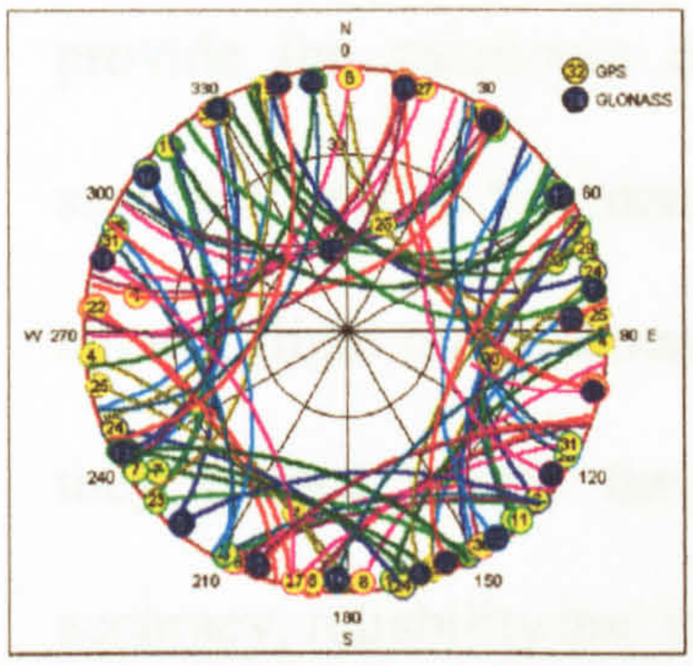

Chapter 3

First Generation Hybrid Systems

3.1 Introduction

As has been described in previous chapters, some users find that GPS in its current state is insufficient for their needs, requiring assistance from a third party system(s) whilst retaining GPS as the *core*. The term Global Navigation Satellite System (GNSS) is used to describe a core system with a global capability, together with any other systems with which it is combined or *hybridised*. Hybridisation can be achieved through the combination of satellite type positioning systems, or their augmentation, usually by some terrestrial system. There are currently two sequential categories of GNSS (ICAO, 1998): GNSS-1 which are being realised, and the proposed GNSS-2, involving completely new constellations.

The impetus for development beyond the existing core systems of GPS and GLONASS (a potential core), has been generated by several factors. Firstly, neither GPS nor GLONASS in their design capability, can in themselves

provide the minimum continuous globally accessible constellation of six satellites needed for many applications e.g. safety-critical operations such as aircraft flight management, which demand a high level of integrity. Secondly, they cannot satisfy the associate demands for extremely high levels of accuracy, reliability and integrity. And finally neither is under civilian control.

The design of GPS for instance was optimised to maximise the probability, that at least four satellites with good geometry above a 5° elevation mask, would always be visible to any terrestrial user [Bagley, 1992]. Even though the current operational GPS constellation is 29 vehicles, 5 more than the design specification, positioning may still, dependent on time and location, have zero redundancy or worse. To mitigate this and other shortcomings, extra data must be combined with that already available. GLONASS on the other hand, cannot in its current run down state (year 2001), be considered a core system, requiring major replenishment, and so ranks only in a supplementary role as a provider of additional observations to a core GPS.

Extra data can be sourced from many other sensor types, from ground, through air, to space based. Ground based systems include accelerometers, gyro compasses, inertial navigation systems (INS), differential services, and pseudolites. Examples of air based systems are aircraft altimetry and INS. Finally space based systems include differential service delivery based on ground reference stations, GPS-like ranging signals from geostationary communications satellites, and as discussed already GLONASS in a supporting role.

Currently, GNSS-1 uses GPS as the core, to which may be added any number of sources of extra data, a few of which have been listed above, also see §3.9.

A good example of a regional augmentation for GPS and GLONASS, has been in development in Europe since the late 1990s, to cover Europe, the Atlantic and Indian Oceans, South America, Africa, the Middle East and Central Asia [ESA, 1997]. This augmentation is called an *overlay*, and the programme the European Geostationary Navigation Overlay Service (EGNOS). EGNOS currently uses two INMARSAT III geostationary satellites as platforms from which to broadcast GPS-like ranging signals, together with integrity monitoring and wide area differential correction services. Signals have been available in space since February 2000. A third similarly equipped geostationary meteorological satellite, named Artemis, is also to be used. EGNOS is an example of an SBAS (Space Based Augmentation System), as opposed to a GBAS (Ground Based Augmentation System), such as Differential GPS (DGPS). Other major SBAS examples include the American WAAS and Japanese counterpart MSAS, see §3.2.8.2 for details of both.

Whilst GNSS-1 uses the military-controlled GPS as the core, the objective of GNSS-2 is to provide a civilian led and run system orientated to civilian needs. This concept involves a core provided by completely new satellite constellations, such as the European Galileo initiative in development since 1997/8 (see §3.3). Effort expended on EGNOS which is planned at Advanced Operational Capability (AOC) in 2003, will not be wasted, since it is to play a vanguard role to Galileo, into which it will eventually be absorbed. Funding to

launch Galileo was approved by the European Council of Transport Ministers on the 6th April 2001.

There is wide interest in the development of GNSS-1 and 2, with both practical and financial benefits to participants. Many applications require the services of an enhanced system, not least that of transport and in particular aviation, where airport and regional air space is a valuable commodity. Here advantages are to be gained in terms of the safe increase of aircraft density, replacement of old and expensive airport guidance infrastructure, a reduced proliferation of navigation and guidance systems, and the use of a pre-existing system of service charging that should help fund and maintain augmentations and ultimately GNSS-2.

How do the Americans regard civil aviation navigation? One view expressed by the FAA in GPS World [1998a], articulated reservations on the sole use of GPS for aviation because of the fear of interference and hostile jamming, advocating GPS in the primary role with some conventional system as backup. Systems in the latter group might be Loran-C or some reduced VOR (an aircraft guidance system providing bearing range and data). This still leaves the world outside the US with a system that is controlled by an unaccountable foreign military force. It seems inevitable therefore, that the Europeans will feel the need for their own system, be it civilian, military, or jointly controlled.

GNSS-1 in terms of Hybrid (GPS with GLONASS), is now covered in more detail, followed by GNSS-2.

3.2 GNSS-1

In the context of Hybrid, the prototypical realisation of a combined single measurement-type system, why hybridise? Because as will be demonstrated, adding more satellites gives an improvement in terms of the ability to satisfy the positioning needs of a multiplicity of applications. Shortcomings in either system that preclude all user population needs to be satisfied, are in three main areas: solution accuracy, availability, and integrity, and hence with safety, productivity and cost implications. GNSS receivers capable of receiving and processing signals from disparate systems, and outputting integrated solutions, can mitigate these deficiencies [3S Navigation, 1997]. Hybrid measurements can be combined in a code phase non-differential or differential weighted solution, or carrier phase solution. The benefits of hybridisation can be classified under several headings such as availability and accuracy, according to Hall et al [1997]. Issues under these and other headings are now detailed.

Availability

- A larger minimum constellation, providing a higher operational safety margin.

- An enlarged constellation which mitigates the effects of obstructions to line of sight, limited aperture or *blockage*, shadowing, and terrestrial multipath, which is essential for applications requiring continuous tracking. At a mask of 20°, 3-D GPS positioning at May 2000 was available for about 80% of the time, in Hybrid mode this rose to on average 99% (see Table 3.1).

- The availability of nearly forty satellites means that single frequency receivers may be sufficient for RTK mode, thus minimising cost overheads relative to dual frequency units. (This comparable

performance is related to the accurate location of the ambiguity search space and minimisation of the volume to be searched, ambiguity search is discussed in Chapter 4). With a 5° mask ten GPS satellites were available for just three hours a day in May 2000, in Hybrid mode the figure was over nineteen hours.

- Increased geographical coverage. The higher inclination of GLONASS orbits by about 10°, improves latitudinal coverage relative to GPS, and increases accuracy in high latitudes within a Hybrid solution. In particular GPS-only constellations at high latitude provide geometrically poor solutions (Figure 3.1). A Hybrid constellation at 1st May 2000 reduced the coverage hole over Mount Erebus by about 50%, (compare Figures 3.1 and 3.1a), should one wish to visit, but not by Air New Zealand DC10 (major air crash on this mountain in 1979), where with a brilliantly blue sky, the pilots were deceived into believing they were flying up the line of a glacier, but in fact flew straight into the rock face. Note that the GPS constellation stood at only four satellites in 1979, and GLONASS at zero.

Accuracy

- More satellites usually means better geometry, by typically 30% for Hybrid relative to GPS at 2000, see Figures 3.1b and 3.1c, this in turn improves precision of positioning. Geometry is improved from the combination of 6-plane GPS and 3-plane GLONASS with disparate inclinations and dispersion of satellites within each plane.

- Mitigation of GPS's SA, which was discontinued on 2nd May 2000.

- Bias modelling in either system.

- At high latitudes the maximum GLONASS elevation exceeds that of GPS, giving more choice of reference satellites in carrier phase work, which with higher elevation mitigates multipath.

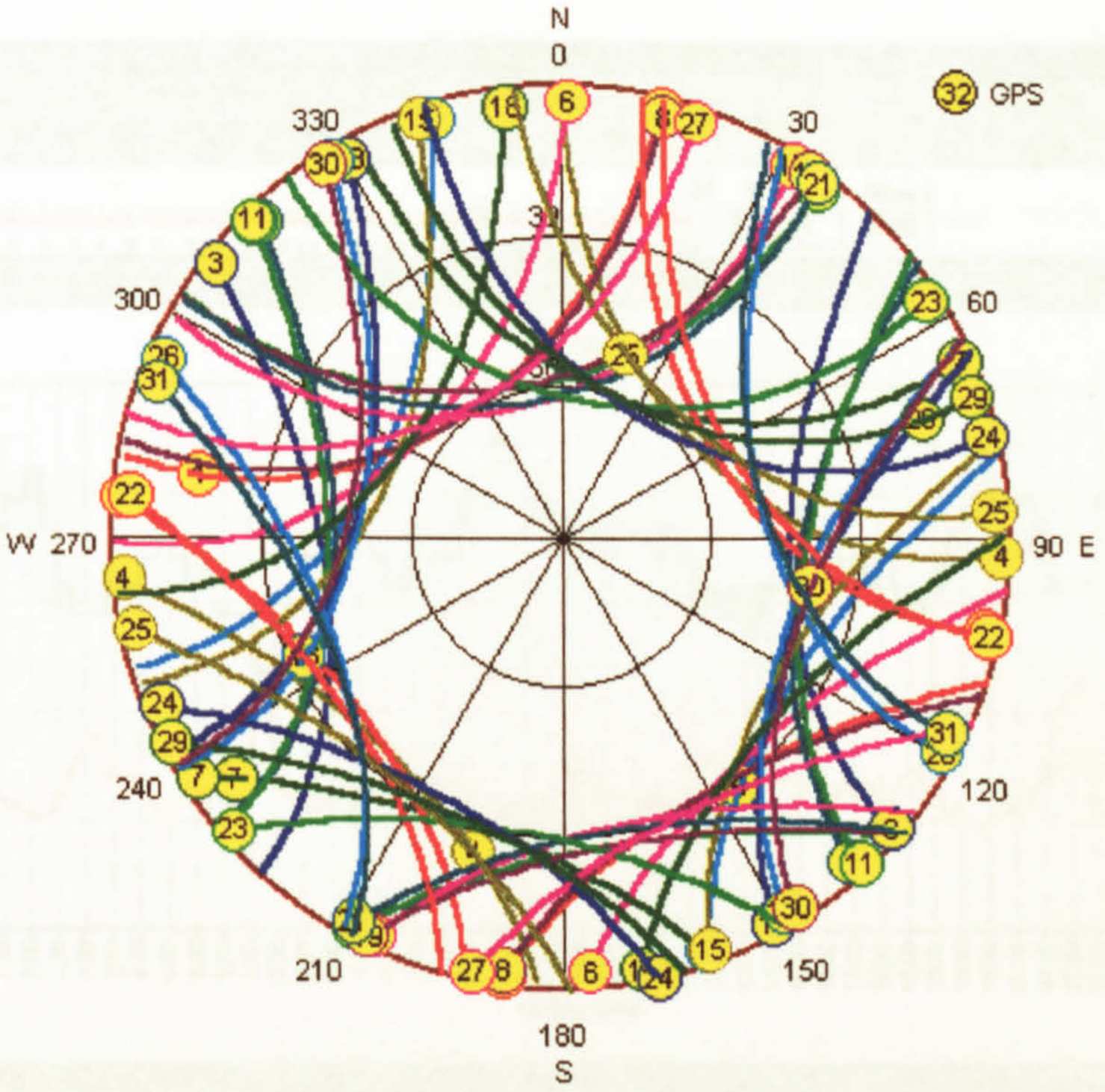

Figure 3.1 GPS skyplot at 10000 metres over Mount Erebus

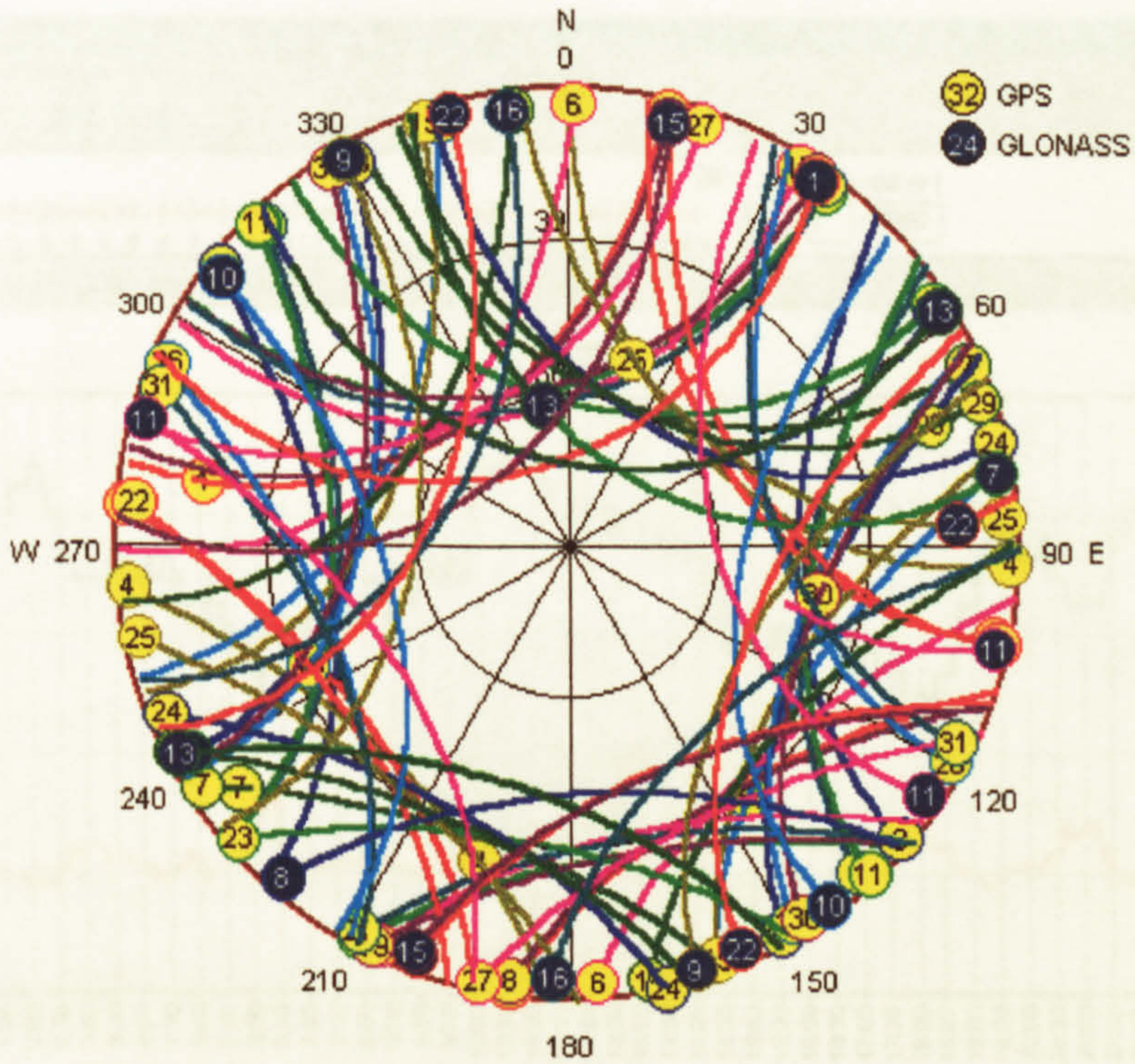

Figure 3.1a Hybrid skyplot at 10000 metres over Mount Erebus

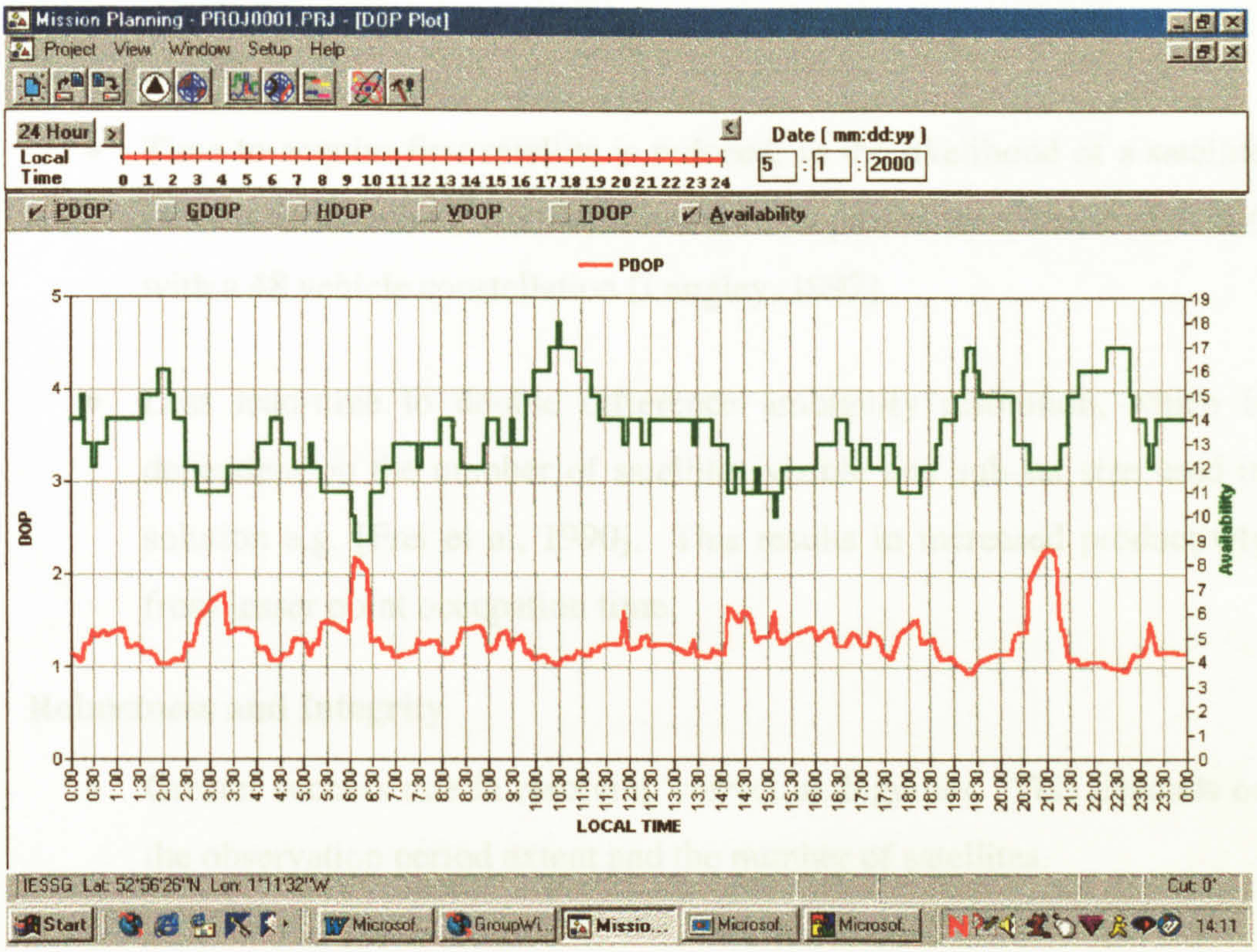

Figure 3.1b GPS constellation size and geometry at 1st May 2000

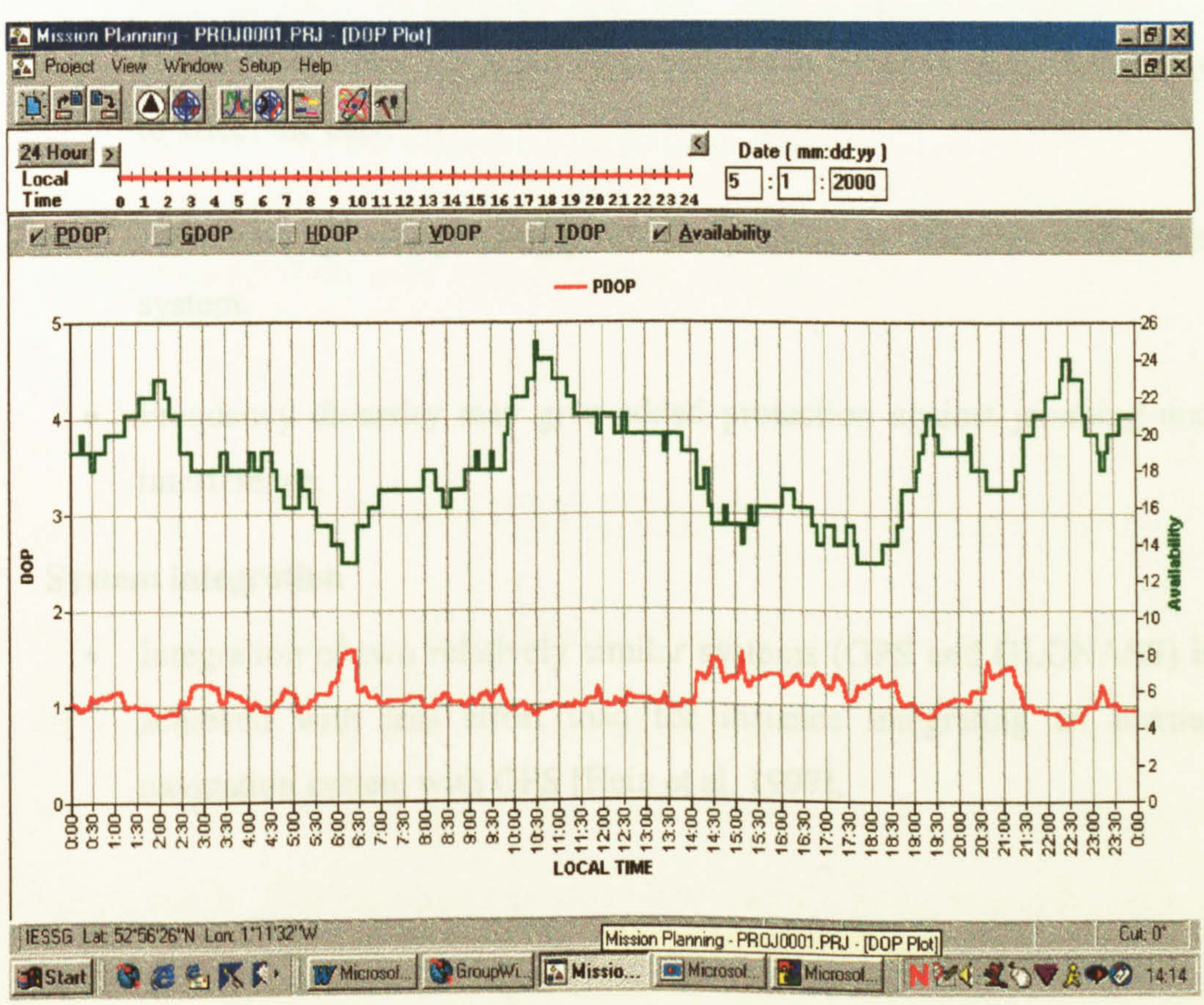

Figure 3.1c Hybrid constellation size and geometry at 1st May 2000

Receiver cold start

- Time to acquire first satellite is reduced, as the likelihood of a satellite in view is increased. Initialisation time improves by a factor of 3 to 6 with a 48 vehicle constellation [Langley, 1997].

- Less lead-time to double difference ambiguity resolution, which is dependent on the number of satellites visible and sub-set size used in solution e.g. [Frei et al, 1990]. This results in increased productivity from lesser point occupation time.

Robustness and Integrity

- Greater success rate in resolving correct ambiguities. This depends on the observation period extent and the number of satellites.

- Earlier, faster, and more certainty in detection of unhealthy satellite status, this is Receiver Autonomous Integrity Monitoring (RAIM).

- Greater robustness i.e. small abnormalities in either system are unlikely to affect the user.

- Protection against operating problems, political or technical, with either system.

- Frequency diversity may give added protection against jamming and interference.

System integration

- Integration of two relatively similar systems (GPS and GLONASS) is achieved with less effort than for instance integrating an inertial navigation system with GPS [Hein et al, 1997].

Mask	GPS	Hybrid (Days 1 to 8 of the GLONASS cycle)							
		1	2	3	4	5	6	7	8
5°	24	24	24	24	24	24	24	24	24
10°	24	24	24	24	24	24	24	24	24
20°	20	23	24	24	24	24	24	24	24
30°	8	19	23	24	24	24	24	24	23
40°	4	9	20	20	21	21	21	21	21

Table 3.1 GPS and Hybrid coverage with ≥ 5 satellites (hours)

(At 1st May 2000, with 9 healthy GLONASS and 27 healthy GPS satellites)

Several key differences between GPS and GLONASS must be addressed before their observations can be combined in a single solution:

- They operate on different coordinate reference frames.
- They use different time reference systems.
- The GPS constellation uses two discrete carrier frequencies for all transmissions, GLONASS uses two unique carrier frequencies per satellite.
- Ephemerides are supplied in different forms.

These issues are dealt with in the following sections.

3.2.1 Transformation

Cartesian coordinate reference frames, of which there are many, consist of three orthogonal axes, with Z pointing nominally to the pole, X to some reference meridian, such as the Greenwich Meridian, and Y at right angles to both X and Z. Consider also a second system with axes U, V, and W. Axial orientation and location of origin are often inconveniently different (Figure 3.2).

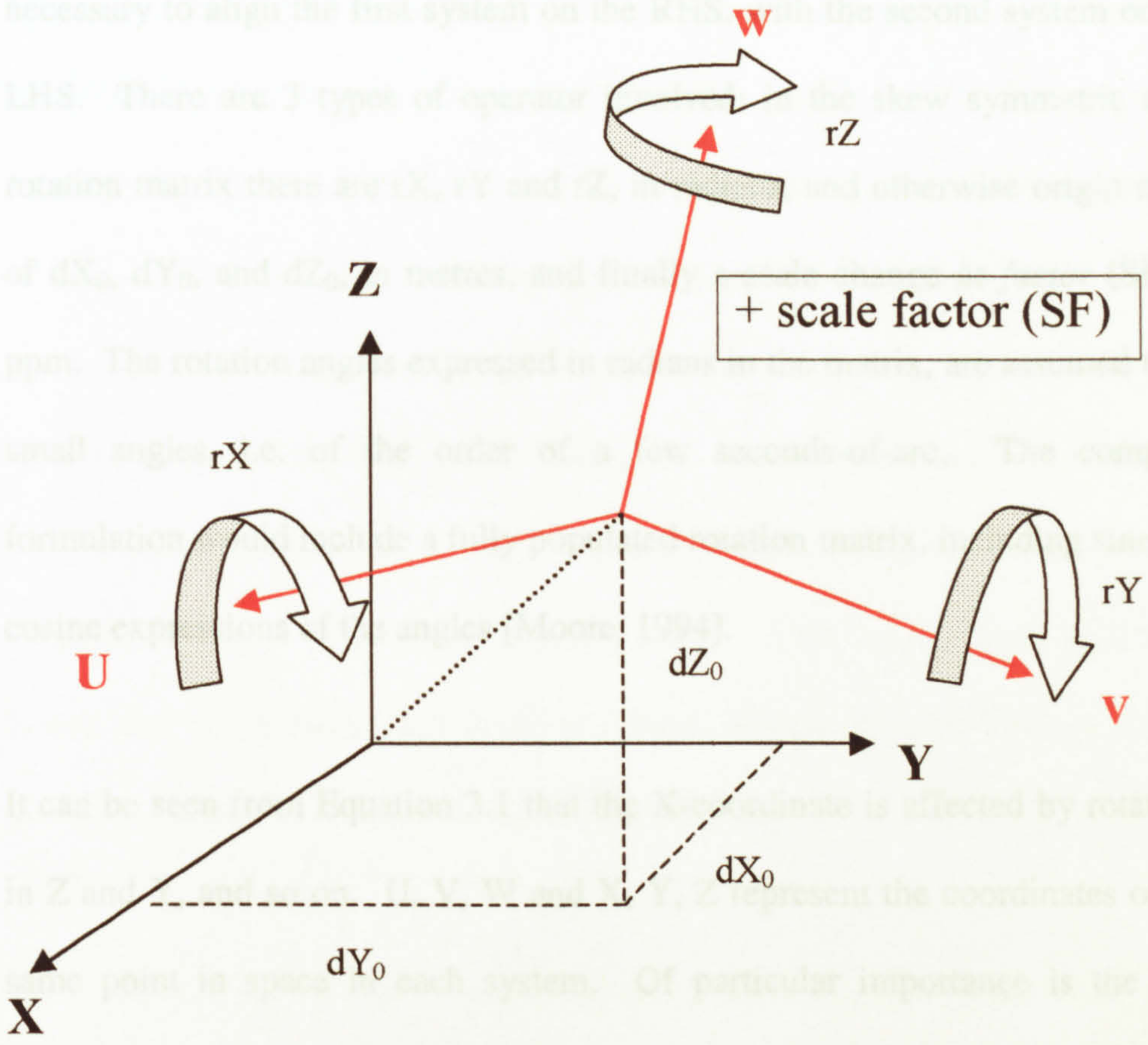

Figure 3.2 Transformation elements between two cartesian coordinate reference frames

GPS and GLONASS use different geocentric cartesian coordinate reference frames: GPS on WGS-84 and GLONASS on PE-90, so their ephemerides are initially inconsistent. The spatial relationship between WGS-84 and PE-90 at a global scale is expressed in a set of seven parameters, also known as the *Helmert transformation*, [Kennie et al, 1993] which in matrix form, is the so called *transformation model*:

$$\begin{bmatrix} X \\ Y \\ Z \end{bmatrix} = \begin{bmatrix} dX_o \\ dY_o \\ dZ_o \end{bmatrix} + (1+SF)\begin{bmatrix} 1 & -rZ & rY \\ rZ & 1 & -rX \\ -rY & rX & 1 \end{bmatrix}\begin{bmatrix} U \\ V \\ W \end{bmatrix} \qquad \text{Eqn.(3.1)}$$

The RHS (Right Hand Side) of Equation (3.1) expresses the operations necessary to align the first system on the RHS, with the second system on the LHS. There are 3 types of operator involved: in the skew symmetric axial rotation matrix there are rX, rY and rZ, in radians, and otherwise origin shifts of dX_0, dY_0, and dZ_0, in metres, and finally a scale change or *factor* (SF) in ppm. The rotation angles expressed in radians in the matrix, are assumed to be small angles, i.e. of the order of a few seconds-of-arc. The complete formulation would include a fully populated rotation matrix, including sine and cosine expressions of the angles [Moore, 1994].

It can be seen from Equation 3.1 that the X-coordinate is affected by rotations in Z and Y, and so on. U, V, W and X, Y, Z represent the coordinates of the same point in space in each system. Of particular importance is the sign convention adopted in the skew symmetric rotation matrix. Historically, use of an inappropriate sign convention with navigation software packages, has led to the costly misplacement of more than one drilling rig or seismic survey by up to several kilometres. To eliminate this risk specimen coordinates must be obtained with which to test software transformation routines. The *Bursa-Wolf* or *positive clockwise* sign convention is used throughout this chapter, which can be visualised as a clockwise rotation about an axis observed from the end of the axis (Figure 3.2), which corresponds with Equation 3.1.

To compute the 7-parameter transformation between two cartesian coordinate reference frames, a number of points with coordinates of ideally comparable accuracy on both frames must be available. A simultaneous mathematical

solution to these parameters requires one equation for each parameter, that is 7 equations. Each dual-coordinated point provides three coordinate differences, therefore at least 3 such points are needed to solve for the full set of 7-parameters. Three points give a surplus of information, or *redundancy*, which in this case is a redundancy of 2, (3 * 3 – 7 = 2). A surplus allows the quality of the derived parameters to be computed, by applying the least squares estimation (LSE) method. It is normal to supply as much redundancy as possible, as this improves parameter quality, by providing a system of cross-checking between solutions and observations. This allows poor quality or biased data to be eliminated or de-weighted, so that more confidence can be placed in the results – they will have higher integrity.

WGS-84 and PE-90 cartesian coordinate reference frames are not quite coincident, owing to a small disagreement in the implied location of the centre of the earth, and slightly different axial orientation in space. The maximum difference in coordinates of a point on the Earth's surface in WGS-84 and PE-90 terms, is less than 15 metres, predominantly in Longitude, and with a mean value of about 5 metres [Misra et al, 1996a].

Parameter	Value
Rotation about X-axis	0
Rotation about Y-axis	0
Rotation about Z-axis	+0.3919 arc sec
Origin shift in X	0
Origin shift in Y	+2.5 m
Origin shift in Z	0
Scale factor	0

Table 3.2 PE-90 to WGS-84 transformation
(Bursa-Wolf sign convention)

A consensus, albeit with slight variation, has given rise to a 7-parameter transformation, consisting of two significant non-zero elements, a rotation and a translation (Table 3.2). The rotation about the WGS-84 Z-axis, plays the major role in harmonising the two coordinate frames, and is equivalent to a longitude rotation of about 12 metres at the equator. The translation along the WGS-84 Y-axis is of a much lesser impact. This transformation, quoted as good to about one metre, is the default set into the Ashtech GG24 Hybrid receiver [Ashtech Inc, 1997], for real-time output of Hybrid positioning.

In matrix form using the basic transformation model, with angular measure in radians, this translates with the Bursa-Wolf sign convention, to [Ashtech Inc, 1997]:

$$\begin{bmatrix} x \\ y \\ z \end{bmatrix}_{WGS-84} = \begin{bmatrix} 0 \\ 2.5 \\ 0 \end{bmatrix} + (1+0) \begin{bmatrix} 1 & -1.9*10^{-6} & 0 \\ 1.9*10^{-6} & 1 & 0 \\ 0 & 0 & 1 \end{bmatrix} \begin{bmatrix} u \\ v \\ w \end{bmatrix}_{PE-90} \qquad \text{Eqn.(3.2)}$$

And in graphical form (Figure 3.2a):

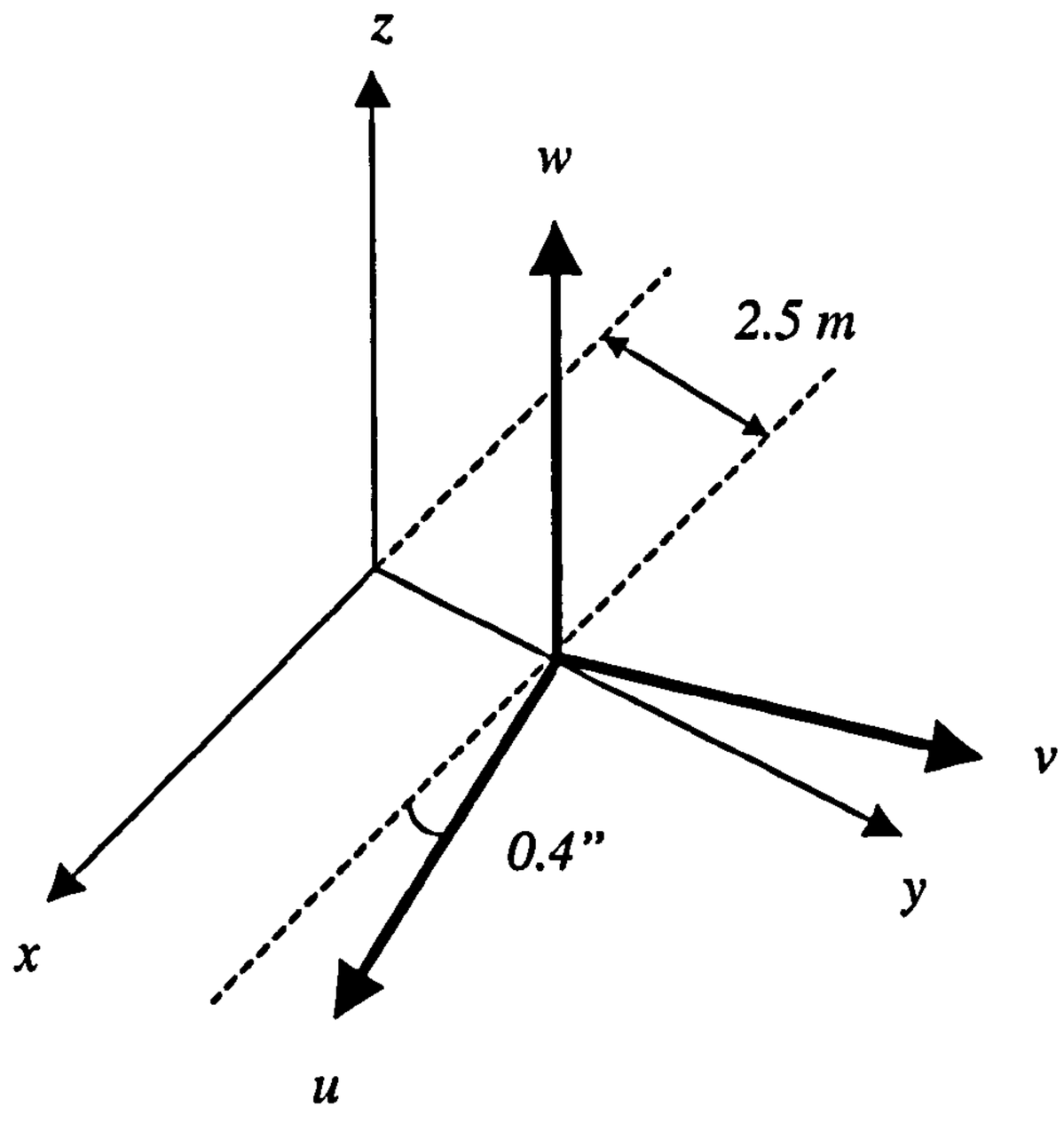

Figure 3.2a

The major elements in a PE-90 to WGS-84 transformation

More than one method has been adopted in deriving the transformation between WGS-84 and PE-90. Success has been governed to a large extent by the availability of GLONASS capable receivers. The two contemporary approaches are now discussed.

3.2.1.1 Orbital positions

In this approach the transformation is derived through the comparison of orbital positions in each cartesian coordinate reference frame. The GLONASS ICD estimates the BE accuracy at about 23 metres rms position error, whilst the GPS precise ephemeris is at about the 5 cm level. But the satellites are at orbital heights above the geocentre of about four earth radii, so the rms error associated with a transformation calculated for locations near the earth's surface will be about 25% of this value or about 5.7 metres. So the GLONASS BE is found to be more appropriate than might first appear – for this purpose anyway. If the alternative method of coordinate differences at the Earth's surface (see §3.2.2) was used, then the GLONASS BE would need to be of a much higher accuracy.

The orbital position method was used between 1995 and 1996 [Misra et al, 1996a], when two GLONASS satellites from different planes were tracked, GLONASS numbers 63 (now defunct) and 67 (Table 2.14). The paucity of GLONASS receivers at the time, was overcome by using the alternative satellite laser ranging (SLR) tracking network, de-coupling completely from GLONASS signals.

PE-90 orbital positions were used directly from the broadcast ephemeris, and in WGS-84 terms were provided via a global network of stations making laser, radar, and optical observations to the two satellites. Sites were located in: Australia, Austria, Finland, Germany, Hawaii, Japan, Latvia, the Marshall Islands, Russia, Ukraine, USA, and Uzbekistan. Tracking data were acquired between September 1995 and March 1996, and comprised 10 data sets of 9 days length each. About 150 satellite positions were derived for each 9 day session, these were used to estimate orbital parameters at the epochs of the GLONASS BE, which were provided at 30 minute intervals. The transformation found populates Table 3.1, that is:

- A rotation of the PE-90 Z-axis by 0.4 arc seconds
- A 2.5 metre translation of the origin along the Y-axis of WGS-84

The Russian system operators [Mitrikas et al, 1998] reported on a similar but extended international effort and results, using twenty months of global laser tracking data from more than twenty stations between November 1995 and July 1997, overlapping with the 1995/6 program data detailed above. Again, satellites 63 and 67 were targeted. But since the earlier campaign, PE-90 orbits had been improved, through the application of a higher accuracy solar radiation model, and a revised correction of laser reflector to centre of mass of the space vehicle. Two sets of results were produced (Table 3.3). The first, column A, was derived in the orbital domain, expressing the average orbital difference between PE-90 and WGS-84. The second (B) was in the coordinate domain (see §3.2.2), expressing the difference between the PE-90 cartesian coordinate

reference frame defined in part by the accepted coordinates of the GLONASS tracking stations, and by the equivalent WGS-84 coordinates by GPS measurement. Both sets of results are similar to the consensus reached by earlier shorter programs i.e. a rotation about the Z-axis of about 0.4 arc-second is the most significant transformation parameter. Accuracy of this parameter and the Z-translation, the next most significant parameter was estimated at 20-25 cms.

Parameter	A	B
Rotation about X-axis (arc sec)	-0.015 7	0.002 5
Rotation about Y-axis	-0.003 5	0.001 0
Rotation about Z-axis	0.356 4	0.356 4
Origin shift in X (m)	-0.47	-0.47
Origin shift in Y	-0.51	-0.51
Origin shift in Z	-1.56	-2.00
Scale factor	1.000 000 022	1.000 000 022

Table 3.3 PE-90 to WGS-84 transformation (II)

In terms of transforming plan ground coordinates, the difference between using A and B parameters translates to about 0.5 metre on the ground at Nottingham.

3.2.1.2 Point coordination

The determination of transformation parameters through point coordination involves just that: the direct coordination of a point at the earth's surface by both GPS and GLONASS observations within their own cartesian coordinate reference frames, and subsequent analysis of coordinate differences to provide a solution to the parameters.

A further example (in addition to that given in Table 3.2, column B) of this approach was carried out in 1996 [Rossbach et al, 1996a], when the GLONASS constellation was momentarily at FOC. GLONASS P-code and carrier phase were observed at selected International Terrestrial Reference Frame (ITRF) stations across Europe and Russia, so this was a hemispherical rather than global campaign. The transformation was then derived from measured positions and baselines, using a rearranged basic transformation model (as Equation 3.1):

$$\begin{bmatrix} X-U \\ Y-V \\ Z-W \end{bmatrix} = \begin{bmatrix} 1 & 0 & 0 & X & 0 & -Z & Y \\ 0 & 1 & 0 & Y & Z & 0 & -X \\ 0 & 0 & 1 & Z & -Y & X & 0 \end{bmatrix} \begin{bmatrix} dX_0 \\ dY_0 \\ dZ_0 \\ SF \\ rX \\ rY \\ rZ \end{bmatrix} \qquad \text{Eqn.(3.3)}$$

The final European-wide network comprised six ITRF sites: at Herstmonceaux (UK), Madrid (Spain), Maspalomas (Canary Is), Metsähovi (Finland), Wettzell (Germany), and Zwenigorod (Russia). All receivers were 3S Navigation R-100/R-101 GPS/GLONASS type, 20 channel dual frequency units, with explicit channel allocation as follows:

- 8 channels - GLONASS L1 C/A code, L1 P code, or L2 P code.
- 12 channels - GPS and GLONASS on L1 C/A code.

Precise PE-90 coordinates were not available/made available for any observing stations (including Zwenigorod in Russia), so the program was split into two threads at the processing stage. One route used GPS and GLONASS carrier

phase measurements in network baseline computations, allowing analysis of the relative shape and dimension of the two network realisations to extract three rotations and the scale factor.

The absence of absolute and precise station coordinates on PE-90, precluded a solution for the origin translations. So an alternative less accurate method was adopted to solve for all 7 transformation parameters, using relatively noisy (compared to carrier phase measurements) P code accumulated single point positioning based on the broadcast ephemeris. Solutions were computed for each day's observations over five days, and averaged in a final approximation to the transformation.

The 8 channels were set up to observe 4 GLONASS satellites' P code on L1 and L2 (and both carrier waves), so the ionospheric delay could be calibrated.

From the P code single point solutions, the most significant common element of a 7-parameter transformation was a rotation about the Z-axis of WGS-84. On the basis of this a 4-parameter solution comprising 3 translations and one rotation was modelled. Good agreement with counterparts in the 7-parameter code solution was found only with the Z-rotation. Therefore the Z-axis rotation was confirmed as the most significant element. Table 3.4 summarises these results.

Solution / Parameter number	Rotation about z-axis (arc sec)
Baseline 4 parameter	0.296
P code single point 7 parameter	0.318
P code single point 4 parameter	0.374
Program mean	0.330

Table 3.4 Comparative rotation about the Z-axis (PE-90 to WGS-84)
(Bursa-Wolf sign convention)

A subsequent coordinate based computation was reported by the Russians [Bazlov et al, 1999]. The eight stations involved with accurately known coordinates on PE-90, were all on Russian soil: Blagoveschensk, Irkutsk, Krasnoye Selo, Magadan, Moscow, Norilsk, Pulkovo and Ussuriysk. This network spanned some 20 degrees of Latitude and 120 degrees of Longitude. None of the main Russian GLONASS ground segment stations were involved. The Russian Low Earth Orbit (LEO) series Geo-IK (Geodetic Intercosmos) space geodetic complex, better known as the Tsikada Doppler type satellite system (similar to Transit), was used to coordinate these eight sites on PE-90, using Doppler transmitters, laser reflectors, radio ranging, light beacons, and radio altimeters.

These eight PE-90 sites were subsequently coordinated using dual frequency geodetic quality GPS receivers, collecting data over a period of about one month. With absolute coordinates of the eight sites known to the decimetre level in both WGS-84 and PE-90 terms, coordinate differences were used in a LSE to derive various transformation parameter sets.

Analysis showed that the most significant transformation element was a rotation of about the Z-axis of about 0.17 arc seconds (equivalent to about 5

metres longitude difference at the equator). This is less than half the Z-rotation value indicated by the European [Rossbach et al, 1996a] and global, e.g. [Mitrikas et al, 1998], campaigns. The transformation recommended by the Russians for use *within Russia and nearby areas*, is expressed with the Bursa-Wolf sign convention, in the matrix:

$$\begin{bmatrix} X \\ Y \\ Z \end{bmatrix}_{WGS-84} = \begin{bmatrix} -1.1 \\ -0.3 \\ -0.9 \end{bmatrix} + (1 - 0.12 * 10^{-6}) * \begin{bmatrix} 1 & -0.82 * 10^{-6} & 0 \\ 0.82 * 10^{-6} & 1 & 0 \\ 0 & 0 & 1 \end{bmatrix} \begin{bmatrix} U \\ V \\ W \end{bmatrix}_{PE-90}$$

Application of the above is associated with a quoted conversion accuracy of 1 metre at the 3-sigma level.

3.2.3 Time reference

GPS uses a uniform time scale that is completely independent of civil time systems, with an offset from UTC(USNO) expressed in a set of broadcast parameters contained in the navigation message. In contrast GLONASS uses UTC(SU), the Russian realisation of UTC, directly. This is a non-uniform time scale, since leap seconds are introduced to all realisations of UTC at intervals of one or two years, in recent times: July 01 1994, January 01 1996, July 01 1997, and January 01 1999.

So an offset exists between GPS and GLONASS system time, comprising the number of leap seconds introduced since the start of GPS time, plus a small slowly changing time dependent term of about 10 milliseconds, at year 1997 [Pratt et al, 1997]. This offset can be handled easily in a position solution by

including an additional unknown at the cost of a redundancy reduced by one, but this is mitigated by the enlarged Hybrid constellation.

GPS and GLONASS also use different satellite clock correction parameters, update rate and message time tagging. GPS uses a polynomial with 3 coefficients to describe the temporal drift between satellite and GPS time, whilst GLONASS uses a linear relationship described by two parameters in the navigation message. GLONASS clock parameters are uploaded twice daily, and may be noted by unscheduled changes in clock parameters [Misra et al, 1996b]. Because GLONASS clock uploads have no time tag, then in stand-alone mode, the effects of this will propagate into a poorer positioning performance than would otherwise be expected [Vieweg et al, 1995].

3.2.4 Orbital parameters

GPS and GLONASS almanac parameters are expressed in similar terms, but this is not the case with ephemerides. GPS uses Keplerian elements to describe the satellite orbits, with an effective hourly update rate. GLONASS on the other hand provides updates to satellite position in cartesian triplets, plus velocity and acceleration vectors, at a reference time, at thirty minute intervals. So GLONASS receivers and users must interpolate or extrapolate between the last data and the epoch required, by integrating the satellite's equations of motion, to give satellite location [Vieweg et al, 1995].

3.2.5 Antenna design

The range of frequencies over which a device is designed to operate is the bandwidth. This is a major determinant in the design of antennas, which are *bandwidth tuned*, so GLONASS and Hybrid reception called for new designs. For example the thickness of microstrip antennas for GPS, GLONASS and Hybrid reception are typically 5, 9, and 19 millimetres respectively. The increased thickness is due to the wider bandwidths necessary.

3.2.6 Receiver design

The use by GLONASS of multiple satellite-unique carrier frequencies means that receiver design is of greater complexity relative to that needed for GPS. This is particularly so in the synthesis of receiver reference frequencies, with GLONASS requiring a basic bandwidth of 3.5 MHz. Also natural interference in the GLONASS bandwidth means that a sophisticated signal filtering regime must be applied, increasing receiver complexity again [Gouzhva et al, 1994].

Signals with different frequencies incur different delays when transiting analogue RF components in the receiving antenna, antenna cabling and on-receiver. These signal delays are known as *Inter-Channel hardware Biases* (ICBs), which are discussed further in §4.5. The operating temperature of such RF components also affects these delays, a change in temperature resulting in a new set of ICBs. For the Ashtech GG-24, delays are receiver-unique, owing to

component variability at the point of manufacture. This means that ICBs do not cancel in some of the standard positioning methods, see Chapter 4.

3.2.7 IGEX

When considering future GNSSs, the interoperability and seamless use of several satellite constellations are important issues [Slater et al, 1999]. The International GLONASS Experiment (IGEX) provided a test-bed with which to investigate the interoperability issues between GPS and GLONASS.

The experiment was organised and managed by a representatives of the four major sponsoring organisations: the International Association of Geodesy (IAG) Commission VIII, International Coordination of Space Techniques and Geodynamics (CSTG); the International GPS Service for Geodynamics (IGS); the US Institute of Navigation (ION); and the International Earth Rotation Service (IERS). Experience gained with GPS campaigns and the existing IGS infrastructure meant that the IGEX program and supporting infrastructure were set up and mobilised relatively quickly.

The main objectives [Misra et al, 1998] of the program were to:

- Set up a global GLONASS observation network.
- Test GLONASS data processing software.
- Determine GLONASS orbits at the metre level in the ITRF.

- Gain an insight into GLONASS vehicle orbit modelling peculiarities, e.g. solar radiation pressure.
- Study common GPS/GLONASS processing strategies.
- Involve the Satellite Laser Ranging (SLR) community in the evaluation of determined GLONASS orbital accuracy.
- Determine transformation parameters between PE-90, the ITRF, and WGS-84.
- Connect the GPS and GLONASS time reference systems.
- Compare receiver equipment performance.
- Compare and contrast single and hybrid satellite systems on a global basis.
- Foster participation and cooperation between the Russian agencies and the above sponsoring organisations.

To achieve these objectives required the mobilisation of global networks of GLONASS sites and SLR observatories: during the first six months of IGEX, about 60 stations in over 25 countries logged GLONASS tracking data, whilst thirty SLR observatories in 15 countries were involved with tracking of laser reflectors on nine of the satellites, see Figure 3.3.

Other infrastructure and operational needs included setting up:

- Observation station operational and documentation requirements.
- A fast and economic communication system – IGEXMAIL.
- Data transmission archival and format requirements.
- Data archival facilities.

- An adapted RINEX format to handle GPS and/or GLONASS observations and ephemerides.

- GPS and SLR software modification to handle GLONASS data.

The program ran initially for a three month period from 19th October 1998 until 19th January 1999. Then, in early 1999, in view of the 30th December launch of three further GLONASS satellites, the late installation of IGEX program receivers, and a willingness by several participants to continue the program [Willis, 1999], it was decided to extend the program for another three months until April 1999.

The six month campaign that ended in April 1999 was hailed a great success, and since then the operation of IGEX continues, albeit with a reduced number of participants, giving support to continued tracking and orbit determination for a further four years.

A new organisation was set up in mid-2000 to coordinate these efforts: The International GLONASS Service – Pilot Project (IGLOS-PP), a pilot service run under the auspices of the IGS (see §2.2.6). The main work of IGLOS-PP is to track and analyse data from the GLONASS constellation, and in particular to facilitate a test-bed for users to experiment with as a prototype GNSS. The goals and objectives of IGLOS-PP can be summarised as:

- Establish and maintain a global GLONASS tracking network.

- Produce precise (10 cm level) orbits, satellite clock error estimates, and station coordinates.

- Monitor and assess GLONASS system performance.
- Improve atmospheric products for the IGS.
- Fully integrate GLONASS into IGS products, operations and programs.

The pilot service duration however was optimistic, as without major replenishment of the GLONASS constellation, there were likely to be only six operational satellites flying at the end of year 2001.

Preliminary IGEX results as reported at ION GPS-99, in Slater et al [1999], are now summarised for precise orbit determination (§3.2.7.1) and transformation (§3.2.7.2).

3.2.7.1 Precise orbit determination

Precise ITRF-96 ephemerides for all operational GLONASS satellites were computed for each day of IGEX. Data processing of GLONASS data was carried out by seven organisations, and a further four used the SLR data. Tracking sites were coordinated on ITRF-96. The accuracy of the GLONASS derived orbits can be evaluated by comparison with those derived by SLR methods. For example using the United Kingdom NERC SLR facility, agreement along-track and across-track was at the metre level and at about 20 cm radial. Repeatability of the GLONASS derived orbits was evaluated using orbit overlaps with preceding determinations, and in general over the entire campaign, solutions were found consistent at the 20 to 30 cm level [Slater et al, 1999].

3.2.7.2 Transformation

Most organisations used the orbit approach (§3.2.1), but with some variation in data source: SLR (ITRF-96) or GLONASS precise (ITRF-96), and broadcast orbits (PE-90). Nevertheless consensus was reached in that the most significant parameter was a rotation about the Z-axis of between 0.3 and 0.4 arc seconds.

Seven-parameter transformations between PE-90 and ITRF-96 (ITRF-96 and WGS-84 are consistent at the 0.1 metre level) were computed on a daily basis and promulgated in the public domain at weekly intervals, by IGEX until April 1999 and subsequently by IGLOS-PP. Results spanning IGEX and IGLOS-PP operation, from Julian day 248 to 365 of 1999, are given in Table 3.5 and Figures 3.4 to 4.7 as colour coded accumulated mean values. These accumulations show that the Z-rotation remains the most significant parameter by far, at a value of about 0.360 arc seconds.

Parameter	Mean	Std.Dev.
Rotation about X-axis (mas)	-28.560	9.924
Rotation about Y-axis (mas)	+1.955	8.509
Rotation about Z-axis (mas)	+359.420	25.147
Origin shift in X (cm)	5.872	47.625
Origin shift in Y (cm)	-29.316	70.854
Origin shift in Z (cm)	-45.631	67.700
Scale factor (ppb)	10.664	5.989

Table 3.5 118 day average IGEX parameters (PE-90 to ITRF-96)
(Bursa-Wolf sign convention)

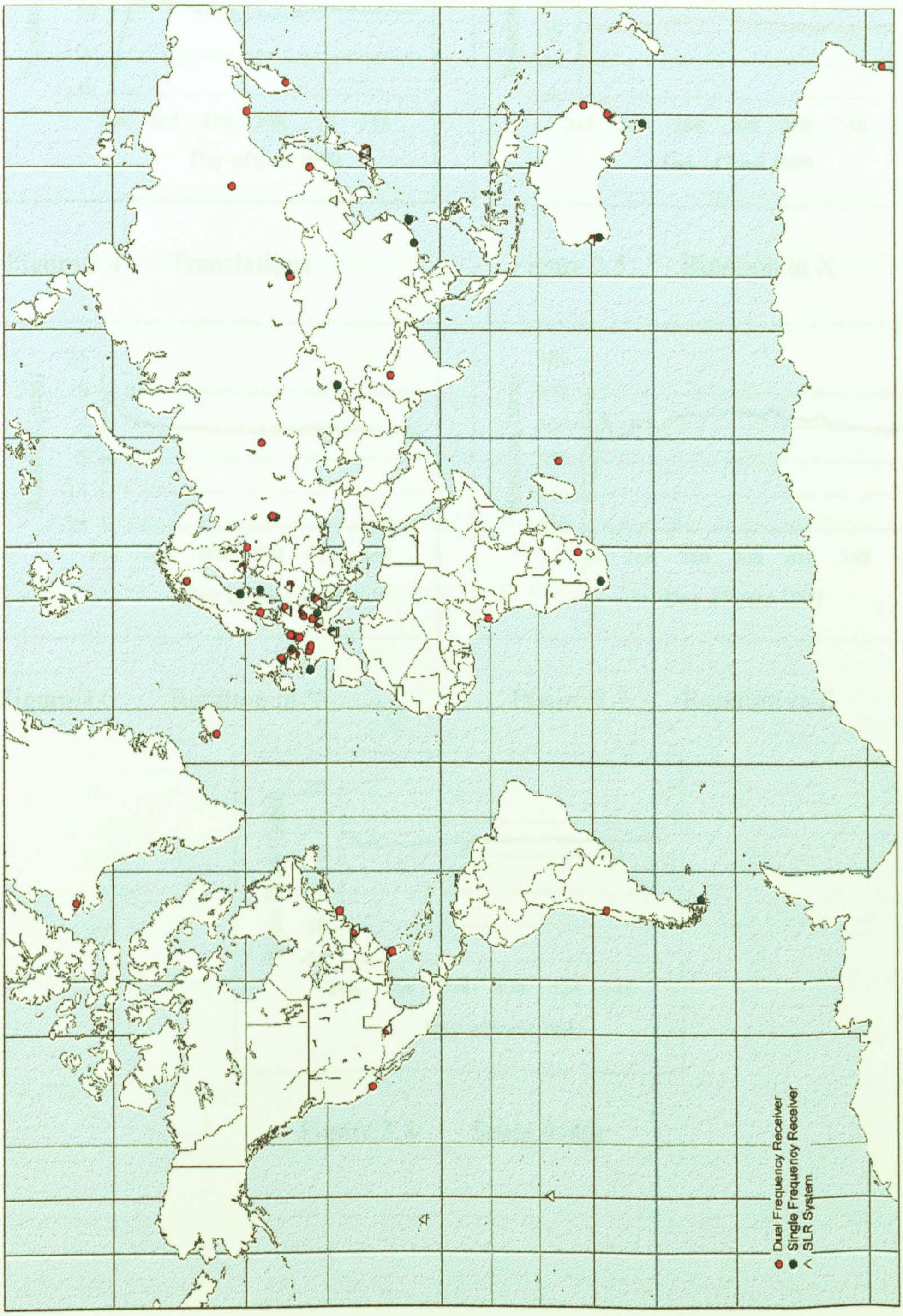

Figure 3.3 GLONASS receiver stations and SLR observatories that participated in IGEX-98. Sourced from Slater et al [1999].

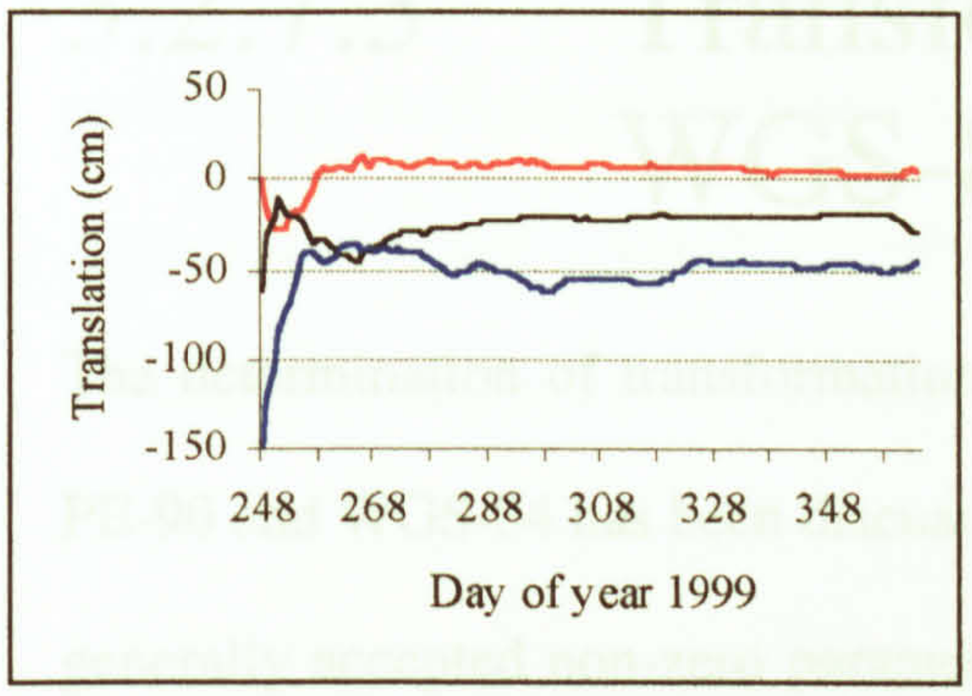

Figure 3.4 Translations

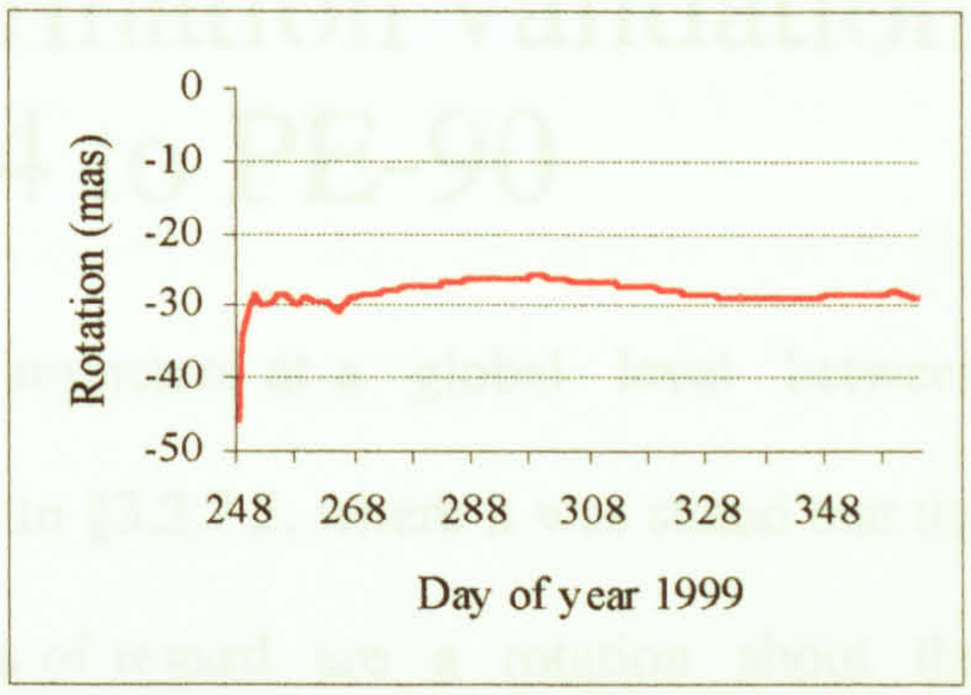

Figure 3.5 Rotation in X

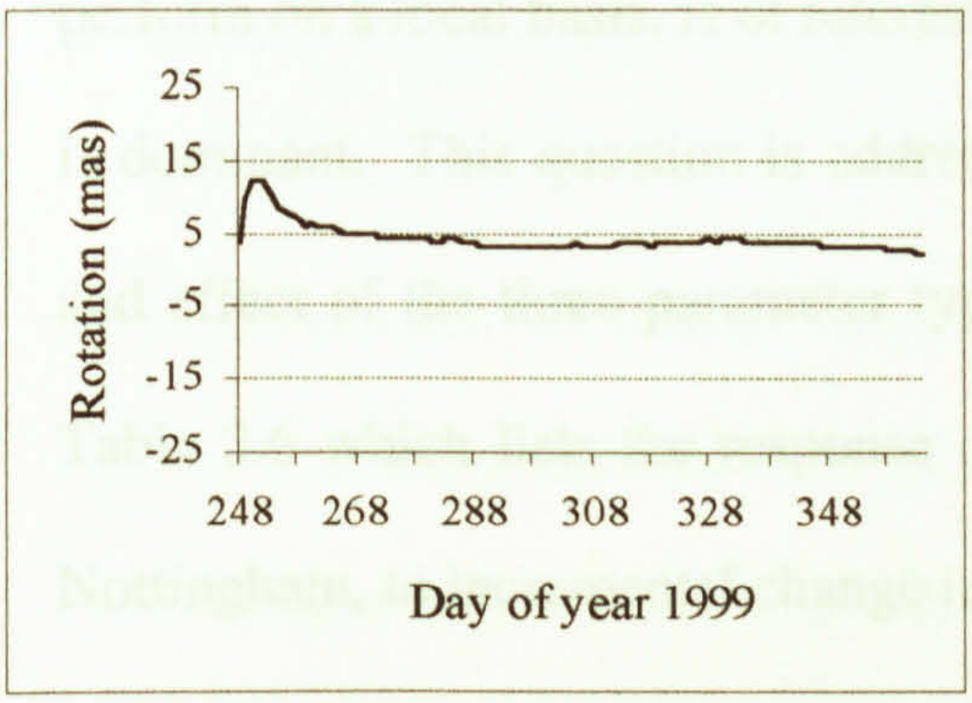

Figure 3.6 Rotation in Y

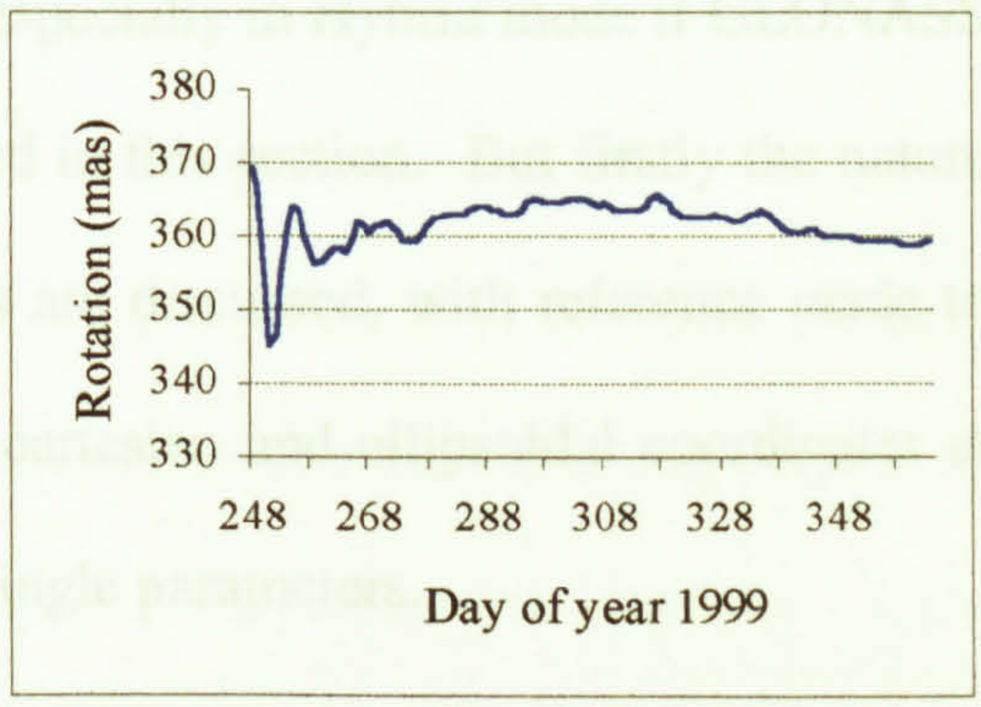

Figure 3.7 Rotation in Z

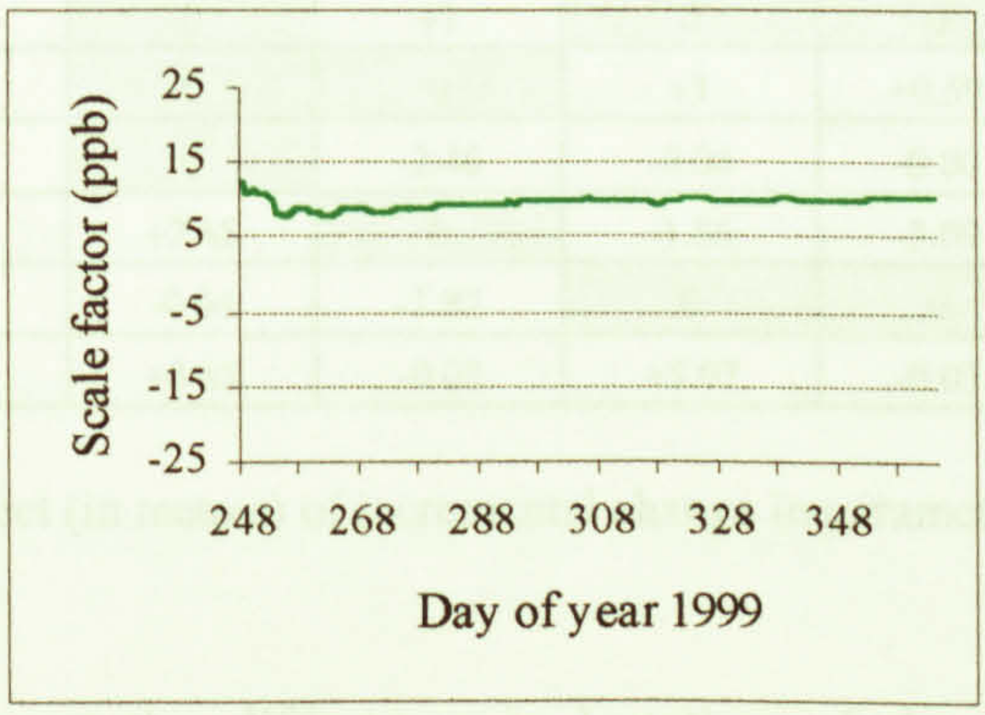

Figure 3.8 Scale factor

3.2.7.3 Transformation validation WGS-84 to PE-90

The determination of transformation parameters at a global level between PE-90 and WGS-84 has been discussed in §3.2.7.2, where it was stated that the generally accepted non-zero parameters of regard are a rotation about the Z-axis and a translation along the Y-axis. But how these global parameters perform on a local basis, is of interest, especially in Hybrid mode if GLONASS is dominant. This question is addressed in this section. But firstly the nature and effect of the three parameter types are discussed, with reference made to Table 3.6 which lists the response of cartesian and ellipsoidal coordinates at Nottingham, to incremental change in single parameters.

Change in parameter | Effect	Cartesian X	Cartesian Y	Cartesian Z	Latitude	Longitude	Height
dX +1 m	+1	0	0	-0.80	+0.02	-0.40
dY + 1 m	0	+1	0	0	+0.99	-0.01
dZ + 1 m	0	0	+1	+0.59	0	-0.20
rX + 0.1 arcsec	0	-2.46	-0.04	-0.06	-2.47	0
rY + 0.1 arcsec	+2.45	0	-1.86	-3.09	+0.06	-0.01
rZ + 0.1 arcsec	-0.04	-1.87	0	0	+1.87	0
SF + 1 ppm	+3.85	-0.08	+5.07	-0.03	0	+6.36

Table 3.6 The effect (in metres) of incremental change in parameter (PE-90 to WGS-84)

Translations represent the difference in location of the fixed origins of two cartesian coordinate reference frames. In order to determine this set of parameters, *absolute* positions of points in both reference frames are required. The effect of translations, dX, dY and dZ, on ellipsoidal coordinates is shown in Table 3.6.

But what is an absolute position, or for that matter a relative position? Relative positioning involves measurement of the 3-D vector between a known and unknown location. Absolute positioning on the other hand involves direct measurements made at a single position to a set of satellites.

Rotations depend on the relative orientations of baseline vectors, and so are independent of absolute coordinates. Their effect on cartesian and ellipsoidal coordinates is again shown in Table 3.6.

Scale factor can be visualised as inflation (scale factor > 1) or deflation (scale factor < 1) of a sphere, with points on the surface either separating or contracting respectively. The effect of multiplying a baseline length by a scale factor is identical to scaling of the two sets of endpoint cartesian coordinates, so scale factor can be determined from either baseline lengths or 3-D cartesian coordinates [Rizos, 1997], and its determination is therefore independent of absolute position. Table 3.6 shows that for ellipsoidal coordinates it is only the height component that is significantly affected by scale factor, with a change of 1 ppm introducing a height change of over 6 metres.

The investigation into the transformation between PE-90 and WGS-84 now starts with an analysis covering the UK from 50°N 4°E to 62°N 8°W, of its theoretical effect on position, as predicted through the application of the generally accepted transformation. This is a rotation about the Z-axis of 0.3919 arc second and a translation along the Y-axis of 2.5 metres.

The effect of this transformation has been split into cartesian and geographical components, and contoured to give Figures 3.9 to 3.13. A plot for change in Z-cartesian does not appear since it is insensitive to both Y-translation and Z-rotation, and remains at zero (Table 3.6), and the major variation as expected is in components of change in Y-cartesian and longitude.

The second stage of the investigation concerns the attempted realisation of the transformation between PE-90 and WGS-84, through the practical observation of a UK network in both coordinate reference frames, and the subsequent derivation of sets of transformation parameters, using the IESSG program *trancoda*. This part of the investigation relied on provision of some or all of the following IGEX by-products:

- Raw GLONASS observations in RINEX format.
- Precise GLONASS ephemerides on PE-90 (or the Russian B.E.).
- UK IGEX observing site coordinates on PE-90.

The intention was to locate a minimum of two selected stations, IESSG-2 and one other, relative to observing IGEX sites in the UK, at Leeds, Great Yarmouth, and the National Physical Laboratory, (the PE-90 coordinates of which would be available later), and then extend this network. Only single frequency Hybrid receivers were available to the IESSG, so only the shortest baselines to UK IGEX sites were considered. These and other IGEX sites operating within Europe used dual frequency Hybrid or GLONASS receivers. As a contingency, considering the parlous state of the GLONASS

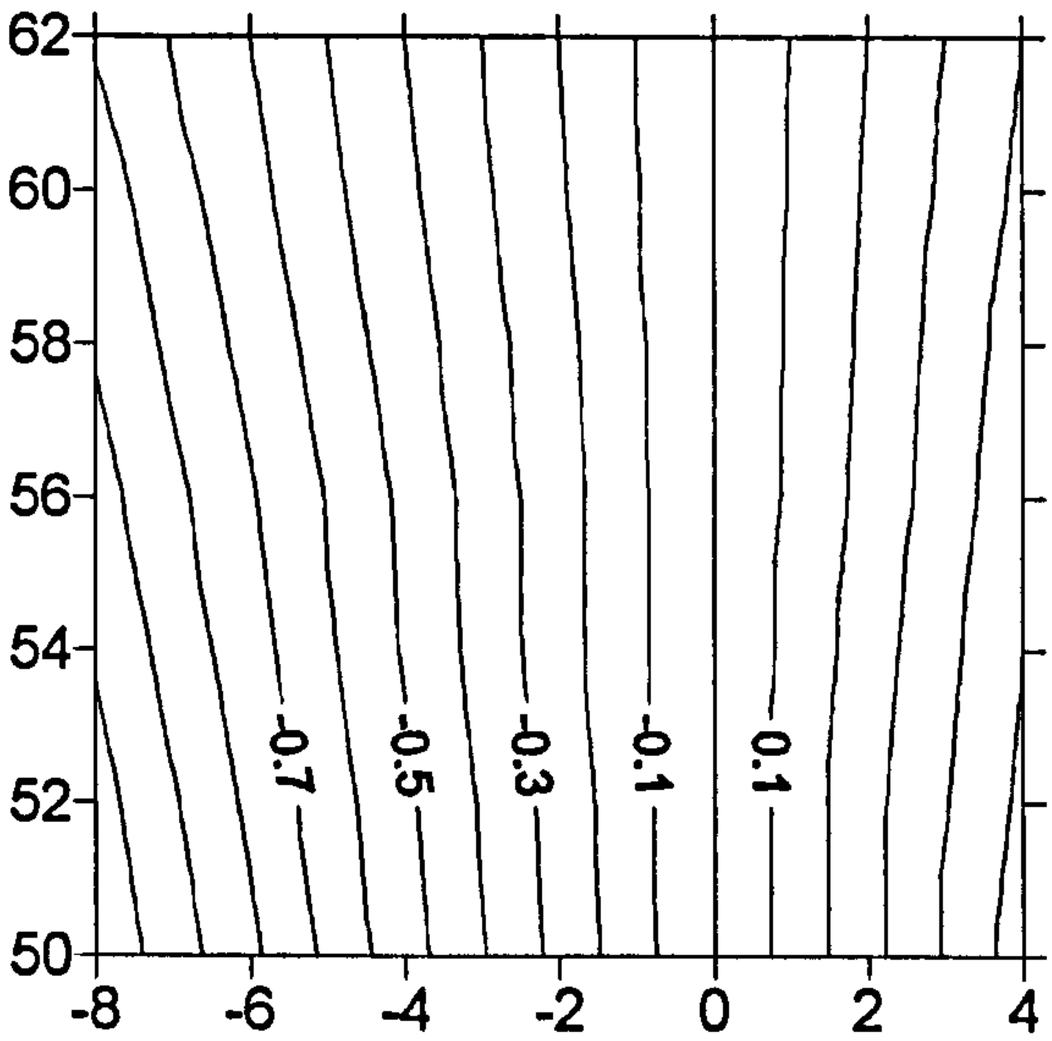

Figure 3.9 Change in X-cartesian (m)

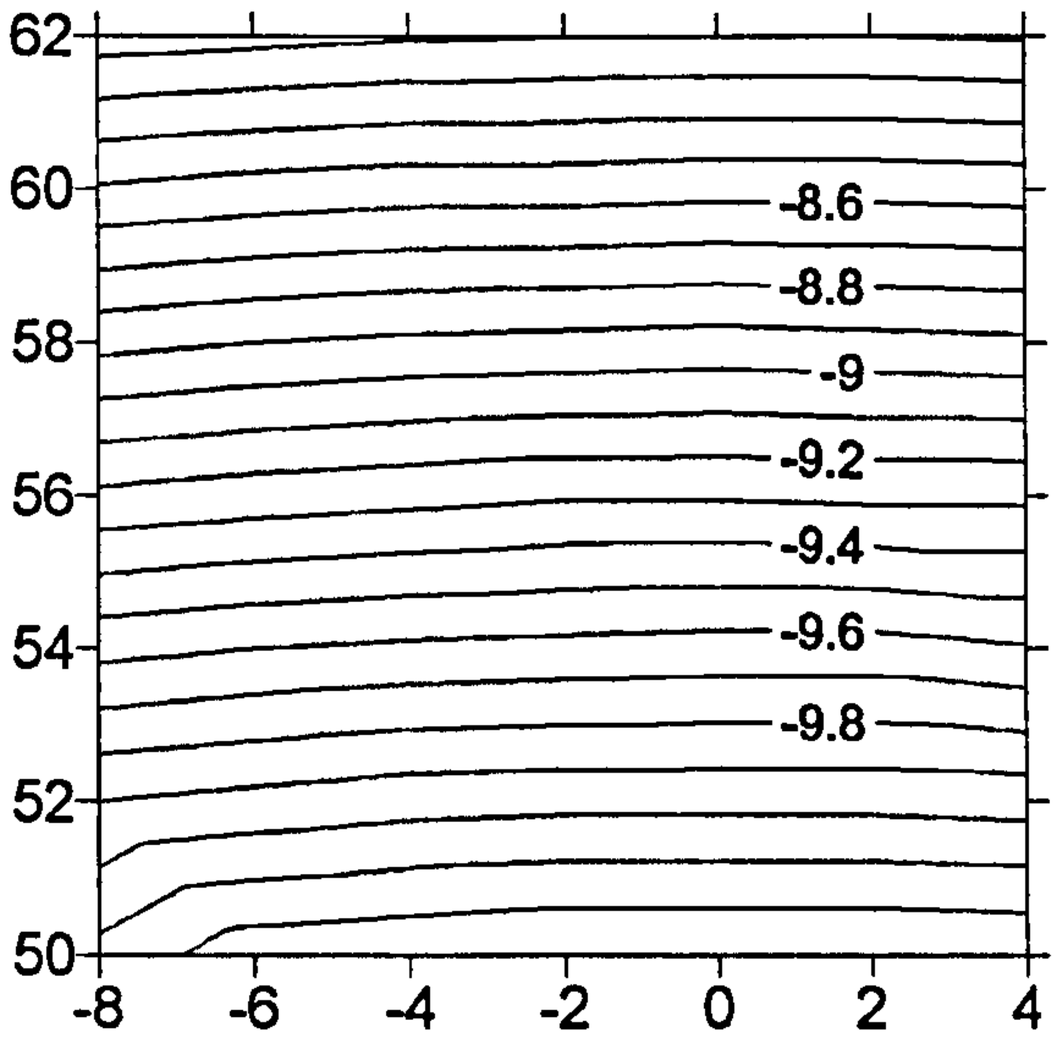

Figure 3.10 Change in Y-cartesian (m)

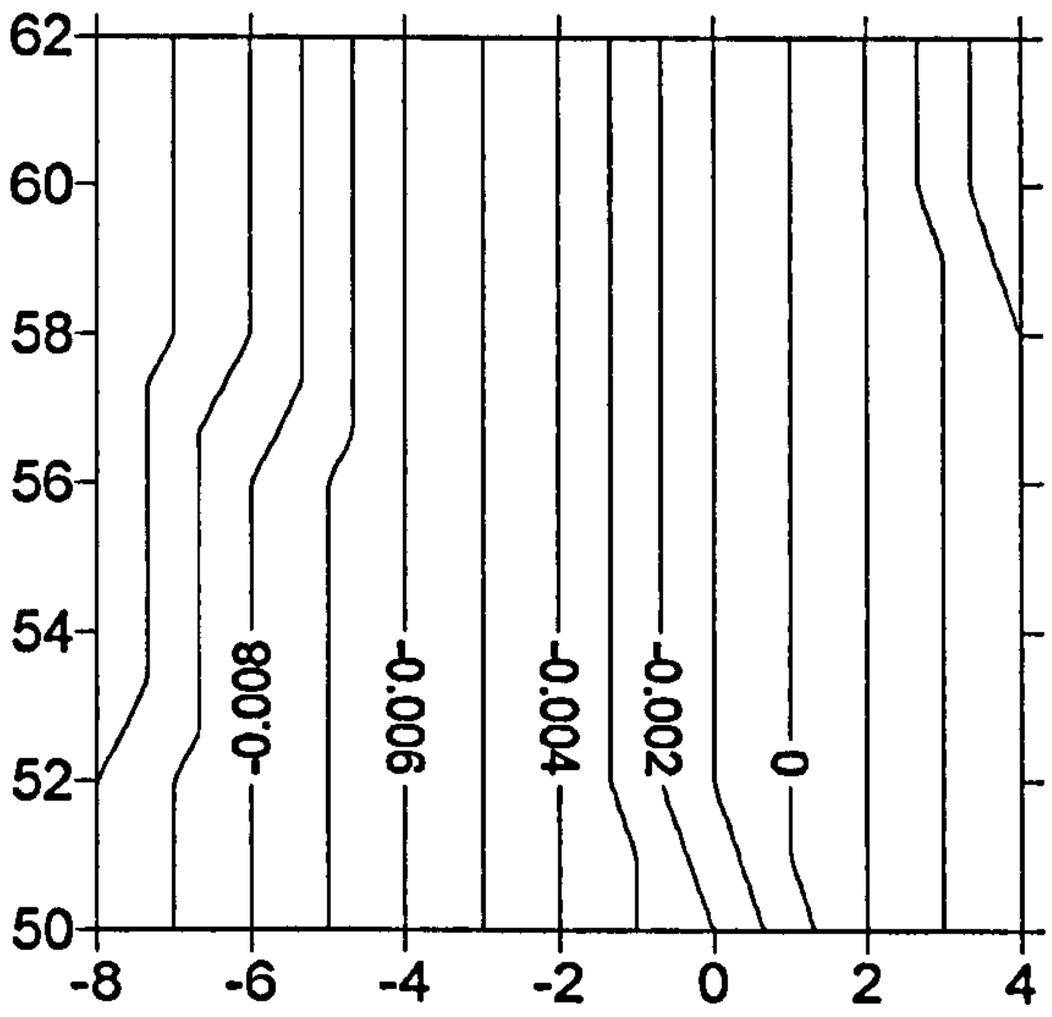

Figure 3.11 Change in latitude (sec)

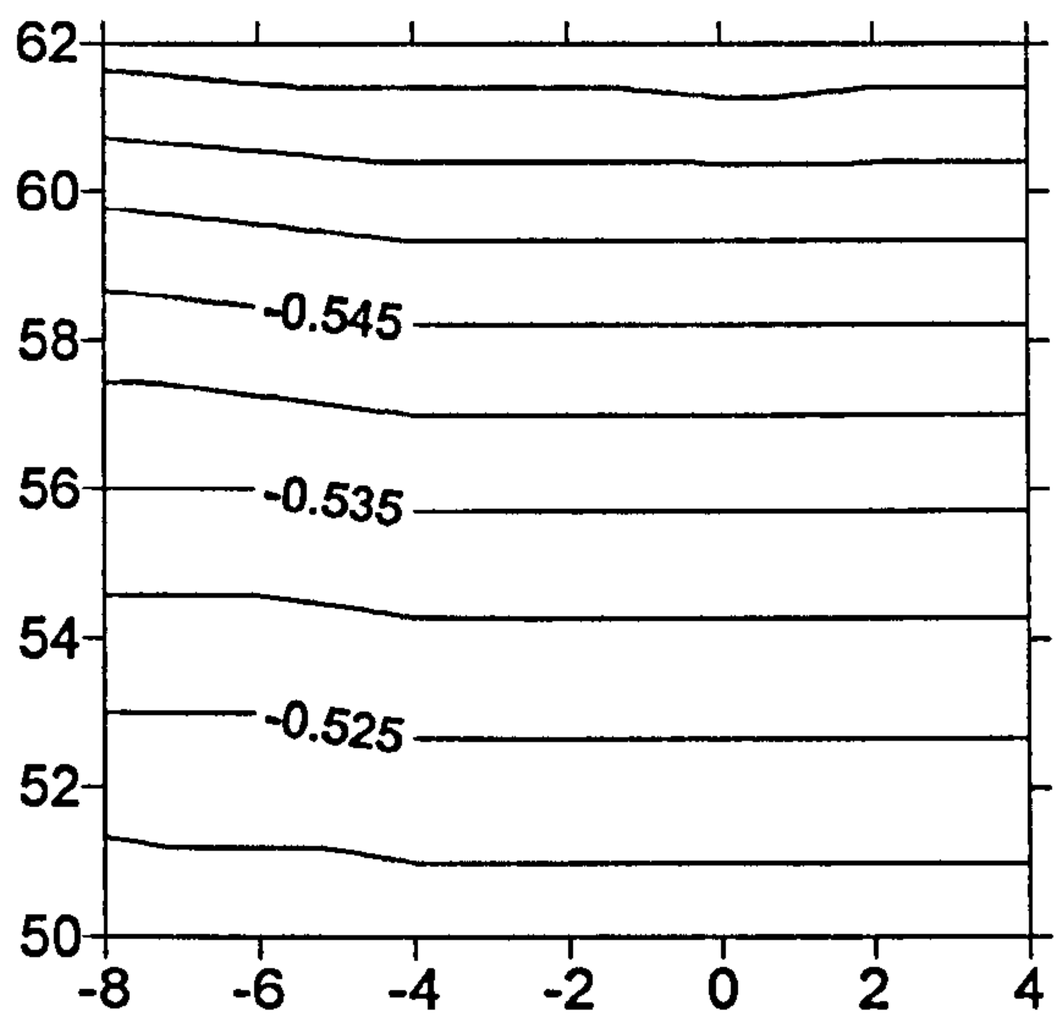

Figure 3.12 Change in longitude (sec)

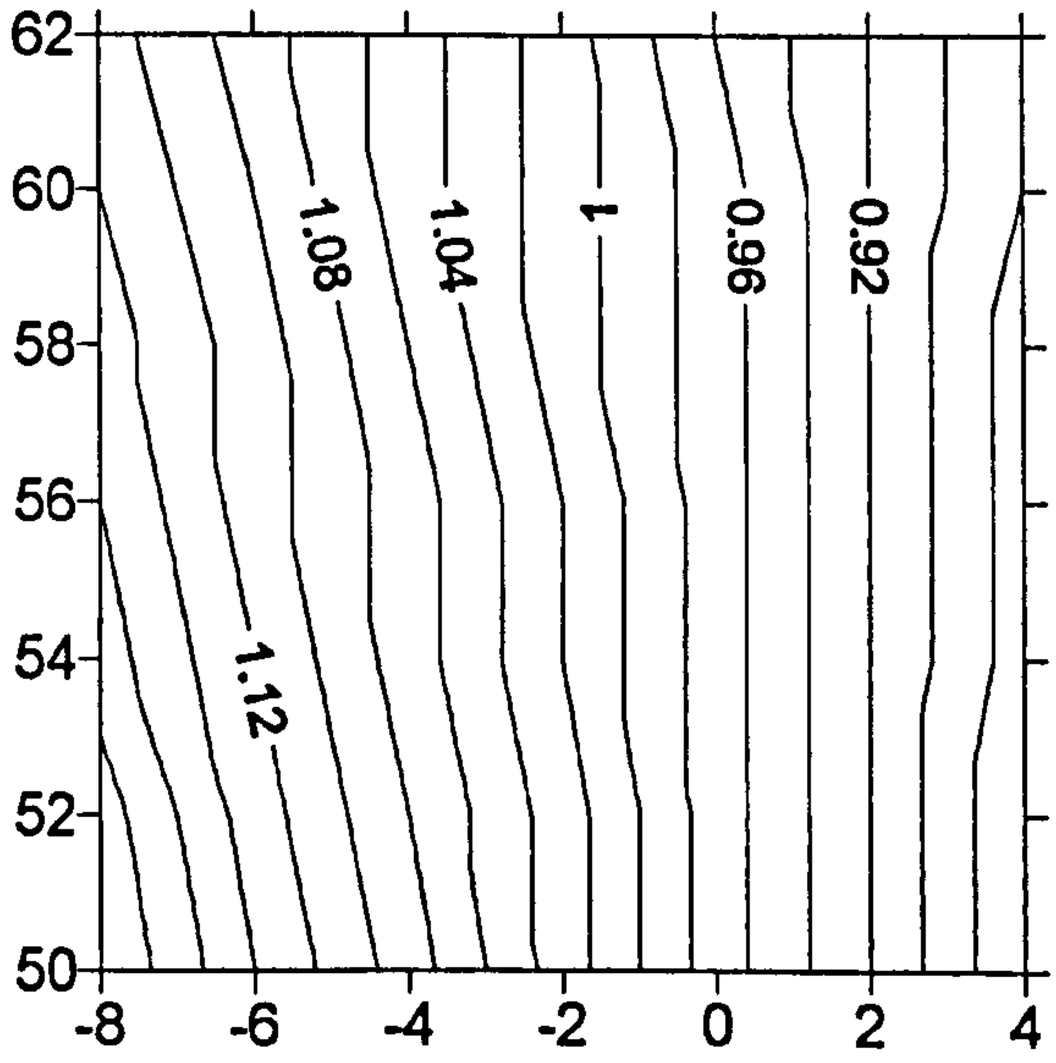

Note

Latitude 1 sec ≈ 30.9 m
Longitude 1 sec ≈ 18.7 m

Figure 3.13
Change in height (m)

constellation, and before IGEX results were available, extended observation sessions were logged and processed in GLONASS L1 stand-alone mode, to accumulate a single PE-90 location for IESSG-2. Owing to logistical and security issues this was in fact, the only site that could be so located.

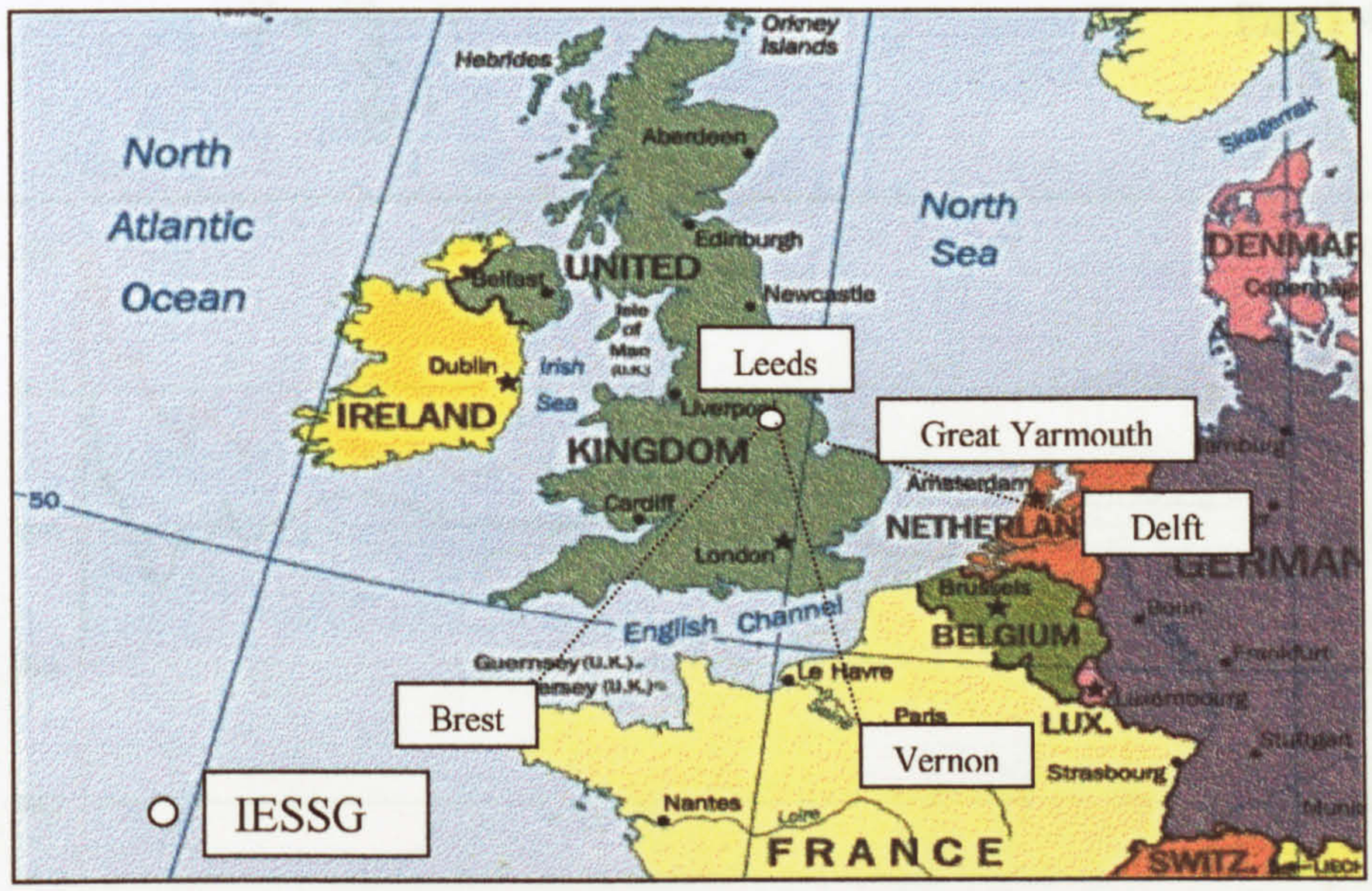

Figure 3.14 North European IGEX sites
(Map source: University of Texas map collection, Europe)

The coordinate accumulations at IESSG-2 were the result of observations made over three one-week periods between mid-September and mid-October 1999, and are shown graphically in Figures 3.15 to 3.17 (latitude coded red). In an effort to derive the best coordinate estimates, a minimum constellation gate of six satellites was applied together with a 3.5 PDOP gate, which allowed the inclusion of over 95% of positions. These results, aggregated with those from GAS processing of earlier data from 1998, are summarised in Table 3.7. It was only possible to gate output from GAS by minimum constellation, however the relatively small number of samples, coupled with a low probability of outliers (as suggested by the three one-week sessions), justified inclusion in the final accumulation. The five sets of results spanning a total of twenty-eight days,

were combined in a weighted mean (Equation 3.4), $\overline{X}$, based on sample size, where x_i is the sample mean, r_i is the number of records comprising that sample, and $n = 5$.

$$\overline{X} = \frac{\sum_{i=1}^{n} r_i x_i}{\sum_{i=1}^{n} r_i} \qquad \text{Eqn.3.4}$$

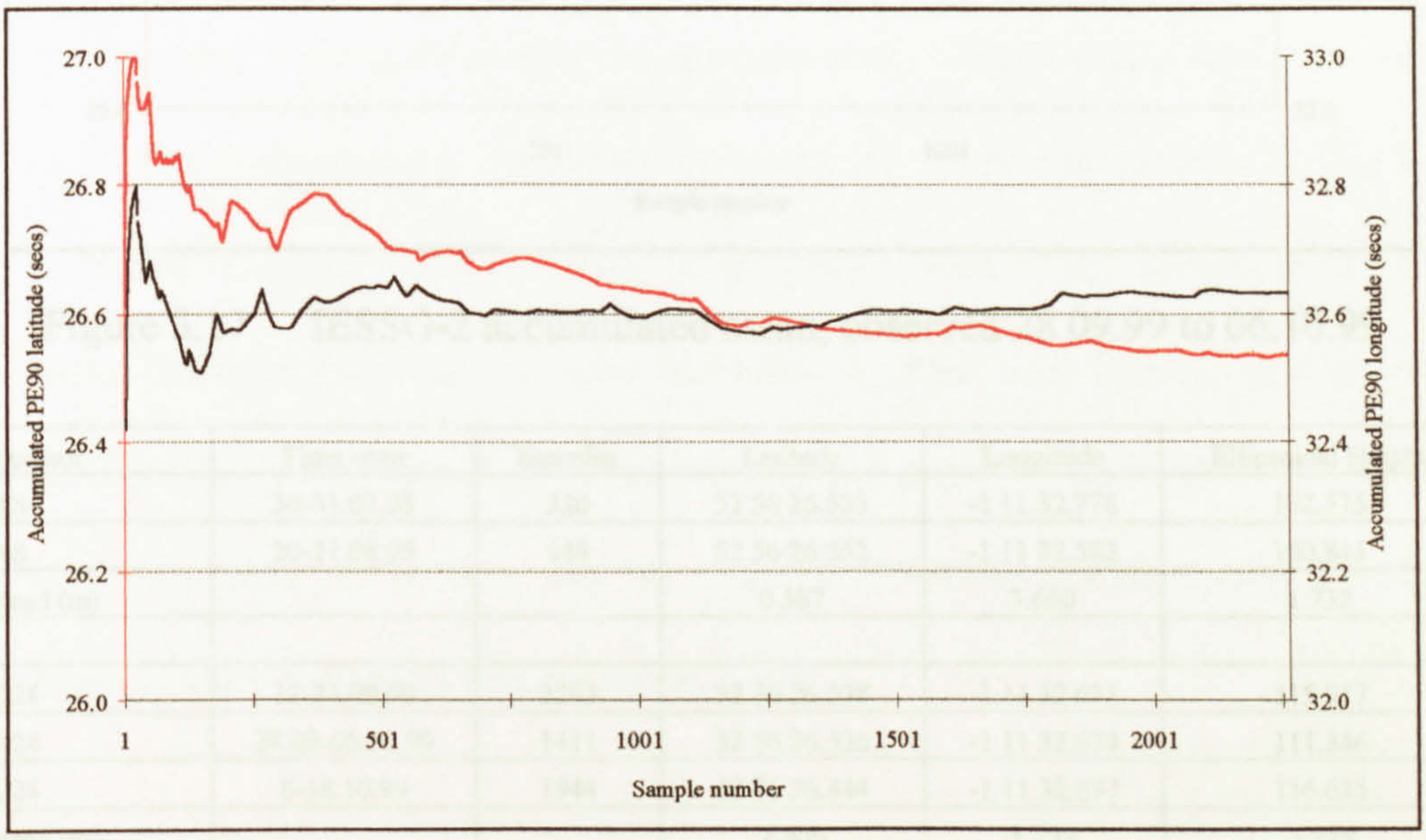

Figure 3.15 IESSG-2 accumulated mean, observed 13.09.99 to 21.09.99

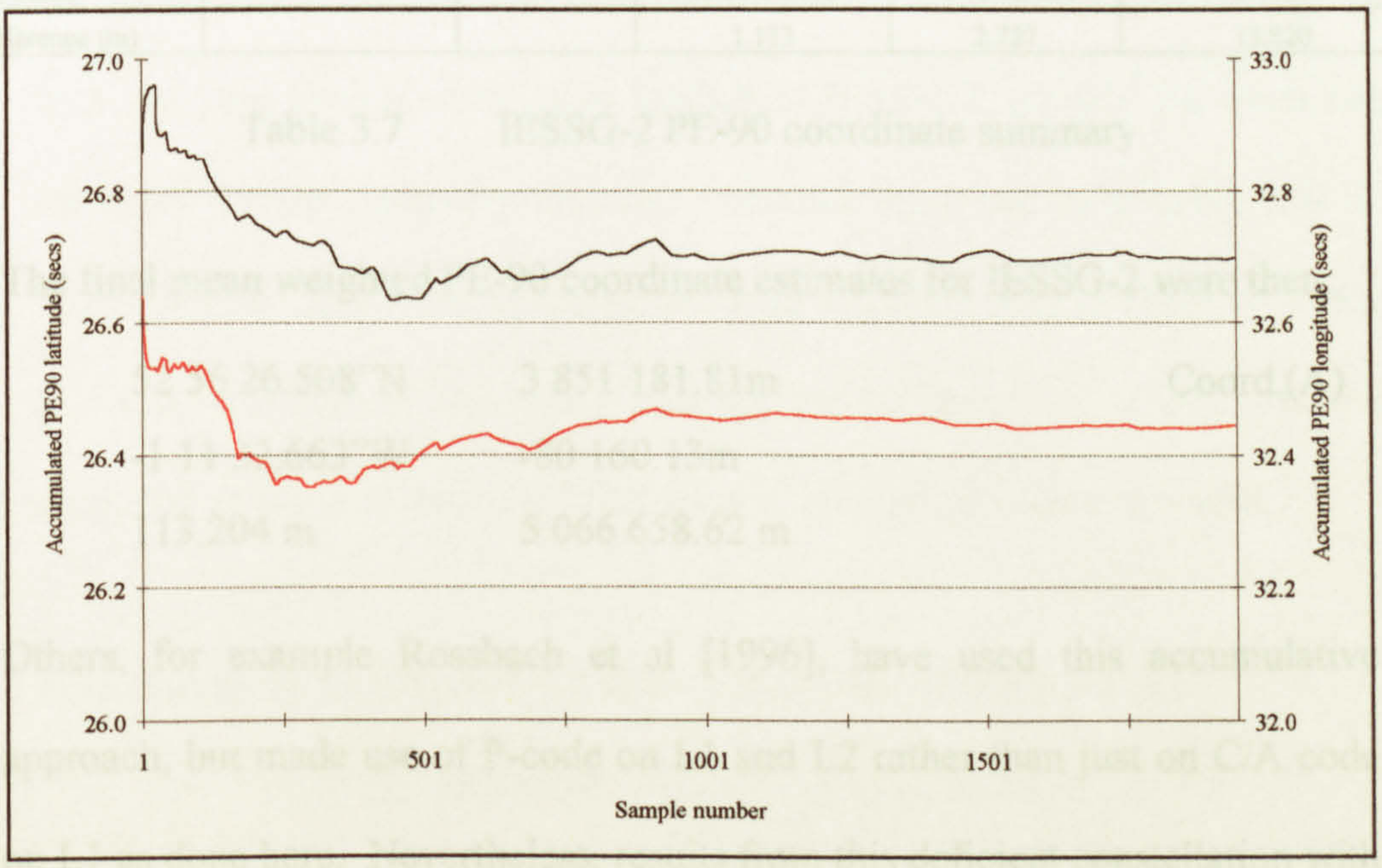

Figure 3.16 IESSG-2 accumulated mean, observed 08.10.99 to 18.10.99

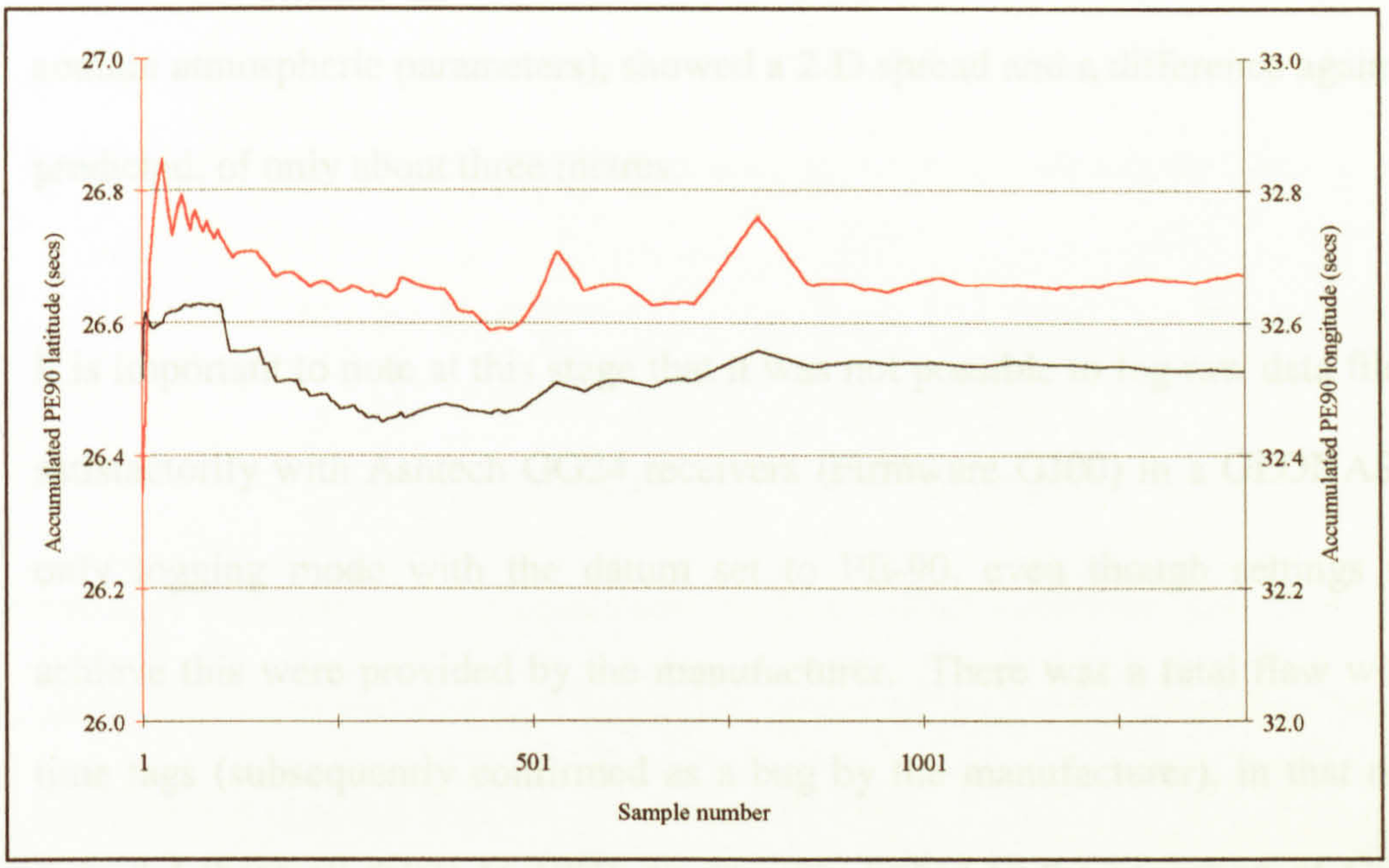

Figure 3.17 IESSG-2 accumulated mean, observed 28.09.99 to 06.10.99

Processor	Time span	Samples	Latitude	Longitude	Ellipsoidal Height
GAS	30-31.07.98	320	52 56 26.533	-1 11 32.778	102.575
GAS	20-21.08.98	548	52 56 26.552	-1 11 32.582	100.843
Spread (m)			0.587	3.660	1.732
GG24	13-21.09.99	2265	52 56 26.538	-1 11 32.631	115.917
GG24	28.09-06.10.99	1411	52 56 26.526	-1 11 32.674	111.346
GG24	8-18.10.99	1944	52 56 26.444	-1 11 32.697	116.625
Spread (m)			2.906	1.233	5.279
Weighted mean	-	Σ 6488	52 56 26.508	-1 11 32.663	113.204
Predicted			52 56 26.472	-1 11 32.809	99.384
Difference (m)			1.113	2.727	13.820

Table 3.7 IESSG-2 PE-90 coordinate summary

The final mean weighted PE-90 coordinate estimates for IESSG-2 were then:

52 56 26.508"N	3 851 181.81m	Coord.(A)
-1 11 32.663"W	-80 160.13m	
113.204 m	5 066 658.62 m	

Others, for example Rossbach et al [1996], have used this accumulative approach, but made use of P-code on L1 and L2 rather than just on C/A code on L1 as done here. Nevertheless, results from this deficient constellation with no atmospheric models applied (the GLONASS navigation message does not

contain atmospheric parameters), showed a 2-D spread and a difference against predicted, of only about three metres.

It is important to note at this stage that it was not possible to log raw data files satisfactorily with Ashtech GG24 receivers (Firmware GJ00) in a GLONASS only logging mode with the datum set to PE-90, even though settings to achieve this were provided by the manufacturer. There was a fatal flaw with time tags (subsequently confirmed as a bug by the manufacturer), in that not only did these all relate to 1980, so possibly linked to the inception of GPS time, but time ordering was also inconsistent, with both forward and reverse time jumps within the files. This bug did not apply to on-receiver generated positions sent to a PC, nor to raw GLONASS PE-90 ephemeris and observations logged in Hybrid mode.

The option to accumulate short term L1 GLONASS pseudorange positions was not considered at the network extension stations, in light of experience gained with the long term accumulation spreads at IESSG-2, notably the overt need for much longer observing periods. Another important note here, was that IGEX precise GLONASS ephemerides were available only in ITRF 96.0 terms (for use with Hybrid solutions), and not PE-90 [Ineichen, 2000], and were moreover in a non-standard RINEX format, precluding their use herein.

Considering the well-known WGS-84 coordinates of IESSG-2 to be:

52° 56' 26.47439" N	3 851 174.48 m
1° 11' 32.28313" W	-80 152.88 m
98.38290 m	5 066 646.9 m,

and if the generally accepted transform between WGS-84 and PE-90 is applied as per above and Ashtech [1997], then the equivalent PE-90 coordinates are:

52° 56' 26.47157" N	3 851 174.31 m	Coord.(B)
1° 11' 32.80887" W	-80 162.70 m	
99.3841 m	5 066 646.92 m	

which is different to the accumulated weighted mean longitude, Coord.(A) by about 3.0 metres and in height by almost 14 metres, and if the translation along the Y-axis is ignored, then the coordinates become:

52° 56' 26.47291" N	3 851 174.32 m
1° 11' 32.67503" W	-80 160.19 m
99.3527 m	5 066 646.92 m,

which is again different to the accumulated weighted mean longitude, Coord.(A), but by the lesser value of 0.5 metres, with no improvement in height.

At this stage, IGEX site PE-90 coordinates were unavailable, and so could not have been used, together with their raw data, in the network. So the (approximated) absolute coordinates of just one network station, IESSG-2, were known on both WGS-84 and PE-90. This meant that the network could be instrumental in extracting just rotational and change in scale parameters. Why? – because such a network though well defined in shape and scaling, is free to rotate about the single known point. Furthermore, even with more than one set of absolute coordinates, the position of the UK, straddling the zero meridian and cartesian coordinate reference frame X-axis, would result in correlation between parameters that would preclude the extraction of 7

parameters i.e. dX and dZ are highly correlated with scale factor, and dY is highly correlated with rZ.

IESSG-2 could then be assigned 2 sets of provisional PE-90 coordinates, Coord.(A) based on accumulated stand-alone mode, and Coord.(B) based on use of the existing transformation. This allowed two processing threads to be established to determine PE-90 network coordinates relative to IESSG-2, and thus two realisations of the transformation parameters between PE-90 and WGS-84.

The next stage required the establishment of a sparse network of extension stations to cover the geographical extent of mainland UK. This went ahead whilst awaiting IGEX site coordinates, with four baselines observed between IESSG-2 and Avonmouth, Immingham, Newhaven, and Stornoway (Figure 3.18).

Figure 3.18

UKGAUGE and transformation network

These stations were selected from the UKGAUGE project which was being run concurrently. UKGAUGE had operated for a number of years regularly re-coordinating points on ITRF94/97 (with which WGS-84 is now in close alignment) using high precision GPS techniques.

Time constraints dictated that the primary UKGAUGE points could not be occupied for this work, so offset stations were first established close-by using Ashtech Z-12s in single-frequency mode for several hours (a maximum of 20 metres station separation), and simultaneously in dual-frequency mode on long baselines relative to IESSG-2. The offset stations were then observed on PE-90 relative to IESSG-2 (Coord.B), using single-frequency Ashtech GG-24s, for up to five days of twelve hours per day. All data processing was by WinPrism version 2. Results, all single-frequency, are given in Tables 3.8 to 3.12.

WGS-84 Obs. (1)	WGS-84 Obs.	PE-90 Obs. (2)	PE-90 Obs.	Predicted PE-90 (3)	(3) – (2)
51 30 22.48640	3 973 681.12	51 30 22.47873	3 973 680.64	51 30 22.48190	0.098 m
-2 42 48.25888	-188 325.83	-2 42 48.75350	-188 335.36	-2 42 48.78026	-0.500 m
58.899	4 968 841.13	59.600	4 968 840.81	59.943	0.343 m

Table 3.8 Baseline from IESSG-2 to Avonmouth

WGS-84 Obs. (1)	WGS-84 Obs.	PE-90 Obs. (2)	PE-90 Obs.	Predicted PE-90 (3)	(3) – (2)
53 37 50.87419	3 790 391.54	53 37 50.93453	3 790 389.64	53 37 50.87251	-1.917 m
-0 11 17.35508	-12 447.35	-0 11 17.88149	-12 457.01	-0 11 17.88302	-0.029 m
51.001	5 112 524.26	51.443	5 112 524.98	51.976	0.533 m

Table 3.9 Baseline from IESSG-2 to Immingham

WGS-84 Obs. (1)	WGS-84 Obs.	PE-90 Obs. (2)	PE-90 Obs.	Predicted PE-90 (3)	(3) – (2)
50 46 53.74465	4 040 913.58	50 46 53.73585	4 040 914.21	50 46 53.74320	0.227 m
00 03 17.03284	3 860.06	00 03 16.51497	3 849.91	00 03 16.51333	-0.031 m
50.480	4 918 257.41	52.160	4 918 257.82	51.450	-0.710 m

Table 3.10 Baseline from IESSG-2 to Newhaven

WGS-84 Obs. (1)	WGS-84 Obs.	PE-90 Obs. (2)	PE-90 Obs.	Predicted PE-90 (3)	(3) – (2)
58 12 11.65175	3 348 043.93	58 12 11.65207	3 348 042.21	58 12 11.64275	-0.288 m
-6 22 31.13066	-374 082.72	-6 22 31.65201	-374 091.09	-6 22 31.67468	-0.423 m
60.952	5 397 750.91	60.510	5 397 749.74	62.064	1.554 m

Table 3.11 Baseline from IESSG-2 to Stornoway

The determination of positions using L1 data over a long baseline will be of a much lower accuracy than a determination using a dual frequency receiver, which can virtually eliminate ionospheric effects. However because of the demand for dual frequency Hybrid and GLONASS receivers by the IGEX program, such units were unavailable to the IESSG.

Considering night and daytime baseline results over two days, single frequency GLONASS baseline length was found to vary by on average 1.5 metres, being shorter by this value in daytime. This agrees with for example Beutler et al [1989] referred to in Rizos [1997], who quoted a shortening scale error of 0.4 to 3 ppm for L1 only baselines with ionospheric delay neglected. Averaged baseline lengths for single frequency GLONASS and dual frequency GPS are given in Table 3.12.

A possible solution to this would be to derive dual-frequency corrections using the GPS data logged simultaneously between IESSG-1 (< 1 metre from IESSG-2) and the relevant UKGAUGE station, and apply them to the raw L1 GLONASS data before processing.

Baseline IESSG-2 to	Dual frequency GPS	Single frequency GLONASS
Avonmouth	n/a	190 460.38
Immingham	101 898.64	101 900.12
Newhaven	255 105.11	255 105.20
Stornoway	670 197.64	670 197.67

Table 3.12 Observed baseline lengths

Unfortunately the PE-90 coordinates of IGEX sites did not, in the end, materialise: IGEX had requested participants in the IGEX program to provide observed accumulated PE-90 stand-alone dual-frequency site coordinates, but either these data were not provided to IGEX, or were unavailable to the IESSG.

In view of this disappointment, the network was tied to the IESSG-2 reference point, using Coord.(B), giving results as detailed above. The alternative PE-90 coordinates for IESSG-2 were Coord.(A), the single frequency accumulated position. If this is used as the PE-90 network origin, then alternative network PE-90 coordinates are arrived at by simply adding the vector difference between Coord.(A) and Coord.(B) to the observed PE-90 cartesian coordinates in Tables 3.8 to 3.11. The vector difference was, in metres:

$$\begin{bmatrix} -7.50 \\ -2.57 \\ -11.70 \end{bmatrix} \qquad \text{Vector (A)}$$

The next step was to derive transformations between the PE-90 and WGS-84 network coordinates. As mentioned above, the location of the UK, straddling the X-axes of the WGS-84 and PE-90 cartesian coordinate reference frames poses a special case for transformations, in that several special cases of parameter correlation occur. It can be seen that a rotation about the Z-axis is correlated with, and inseparable from, a translation along the Y-axis, and scale

factor is similarly inseparable from translations along the X and Z-axes. It makes sense therefore, when determining sets of transformation parameters, to solve for just one of each of these pairs of parameters in addition to those that are uncorrelated.

In this case, as argued above, with a relative network of stations, only rotations and scale factor would be meaningful. The two sets of PE-90 network coordinates were used in turn with the single set of WGS-84 coordinates, to derive sets of transformation parameters using the IESSG software *trancoda*. The vector difference, Vector (A), between the two PE-90 coordinate sets was identified exactly by *trancoda* as translations in X, Y and Z, this can be seen by comparison of row 5 in Tables 3.13 and 3.14, which show solutions to various combinations of parameters. Other points to note from comparison of these two tables are:

- Change in scale factor rows 1 and 2, from 0.06 ppm to 2.11 ppm, caused by the introduction of height error intrinsic to the accumulated GLONASS L1 pseudorange solutions. This amounted to about 14 metres, which agrees with the prediction (Table 3.6) of about 2.2 ppm.

- If the shift in network location by Vector (A) is accounted for by solving for 7 parameters, then the solutions for rotations and scale factor are identical, see rows 5 of Tables 3.13 and 3.14, reflecting the statement made before that rotations and scale factor are independent of absolute position. This statement refers to the location of the networks anywhere in space, but they must remain fixed relative to one another.

dX (m)	dY	dZ	rX (arc sec)	rY	rZ	SF (ppm)	RMS residual
			0.08 (0.14)	-0.02 (0.01)	-0.41 (0.19)	0.06 (0.06)	0.674
					-0.51 (0.02)	0.06 (0.06)	0.724
					-0.51 (0.02)		0.755
			0.08 (0.14)	-0.02 (0.01)	-0.41 (0.19)		0.708
-7.88 (11.1)	-7.08 (27.9)	7.25 (10.1)	0.26 (0.76)	-0.36 (0.42)	-0.55 (0.54)	-0.14 (1.16)	0.542

Table 3.13 PE90 to WGS-84 parameters with Coord.B

dX (m)	dY	dZ	rX (arc sec)	rY	rZ	SF (ppm)	RMS residual
			0.00 (0.17)	-0.05 (0.02)	-0.36 (0.22)	-2.11 (0.08)	0.793
					-0.36 (0.03)	-2.11 (0.10)	1.148
					-0.36 (0.22)		7.825
			0.00 (1.53)	-0.05 (0.16)	-0.36 (2.06)		7.781
-15.38 (11.1)	-9.65 (27.9)	-4.45 (10.1)	0.26 (0.76)	-0.36 (0.42)	-0.55 (0.54)	-0.14 (1.16)	0.542

Table 3.14 PE90 to WGS-84 parameters with Coord.A

A test routine was also run to verify the operation of *trancoda*. This involved firstly the transformation of WGS-84 coordinates to PE-90 using the generally accepted 7-parameter transformation, and secondly these two coordinate sets were input to *trancoda* to derive the originating transformation. Efficient recovery resulted, row 2 of Table 3.15. Uncertainty in coordinate height is dominant in satellite positioning, especially when considering the single frequency long baseline work done here with GLONASS. So, to further test, for the UK region, the transformation sensitivity to height error in input coordinates, Z and X translations equivalent to 5 and 10 metre height errors were introduced to the PE-90 coordinate set. Whilst these systematic height errors were efficiently recovered when solving for 7 parameters (rows 2 and 3), when a reduced number of parameters were solved for, height error propagated into an enlarged but less certain Z-rotation and emergent scale factor.

Such propagation of height error into scale factor was realised in the practical work done here, as referred to in the bullet point above. In practice with more than one absolute position known in the network of stations, and if single frequency baselines are observed, then any un-modelled differential ionospheric effects will introduce uncertainty, which will be manifest in the appearance of a scale factor parameter.

Case / parameter	dX (m)	dY	dZ	rX (arcsec)	rY	rZ	SF (ppm)
Gen. accepted	0	-2.5	0	0	0	0.392	0
Feedback (rms res. 0.003m)	0.025 (0.066)	-2.579 (0.164)	-0.003 (0.060)	0.002 (0.005)	0.001 (0..03)	0.391 (0.003)	-0.002 (0.007)
5m height error (rms res. 0.003m)	3.025 (0.066)	-2.579 (0.164)	3.997 (0.060)	0.002 (0.005)	0.001 (0.002)	0.391 (0.003)	-0.002 (0.007)
10m height error (rms res. 0.003)	6.025 (0.066)	-2.579 (0.164)	7.997 (0.060)	0.002 (0.005)	0.001 (0.002)	0.391 (0.003)	-0.002 (0.007)
10m height error (rms res. 0.335)				-0.060 (0.069)	-0.002 (0.007)	0.435 (0.093)	1.577 (0.032)
10m height error (rms res. 0.354)						0.515 (0.011)	1.577 (0.031)

Table 3.15 Testing *trancoda*

In conclusion, problems with or absence of IGEX products, compounded by the use of single frequency receivers, precluded the incisive verification of the transformation between PE-90 and WGS-84. However if these deficiencies were to be resolved at some later time, then this work may serve as the basis for deriving a better understanding of the transformation on a regional scale.

3.2.7.4 Transformations and digital mapping

A 1:1250 digital mapping framework was used to evaluate kinematic vehicle tracking in Nottingham, discussed in Chapter 9. This section attempts to answer the question: how accurate is the datum transformation between WGS-84 and the mapping datum OSGB36, that allows the integration of the former with the latter, and how can this be tested using kinematic positioning techniques?

To investigate this, both GPS and Hybrid were used to test the veracity of the Ordnance Survey 20-centimetre accuracy transformation between WGS-84 and OSGB-36, and further the veracity of the generally accepted transformation between PE-90 and WGS-84.

These examinations were not based on the usual method of observations made at accurately coordinated points such as trig. pillars, but rather took a novel approach. The trig. pillar method was adopted by Pattinson [1998] at seven sites in the Nottingham area, and the claimed 20-centimetre accuracy transformation from WGS-84 proved. The novel approach taken in this work was to delineate amenable regular shaped features between such well coordinated points by the post-process kinematic method, using the road wheel mounted antenna used in prior exercises. Roundabouts were selected as the best example features, not only because of their finite size, but also because their usually circular nature when imported to digital mapping, would readily

indicate any systematic mismatch in overall location as an overlap. Whilst feature mapping may be at a lesser accuracy than GPS reference points at trig. pillars, this method should indicate whether non-trivial systematic bias exists in the two transformations.

Three roundabouts were examined, two to the West of the University, *University SW* and *Priory*, and one at the Northern edge of the city centre, *Hyson*. In GPS mode, transformed to OSGB36, all three indicated a systematic vector error of about half of one metre to the East i.e. OSGB36 digital mapping was to the East of GPS indications. In Hybrid mode a further bias of up to 2.5 metres was found, though this was not systematic across the three roundabouts. Figure 3.19 shows *University SW* by GPS and Hybrid, with a zoomed segment in Figure 3.20 The systematic shift of Hybrid (red) to the west of GPS (black) can be seen in both Figures.

Figure 3.19

University SW
GPS and Hybrid (I)

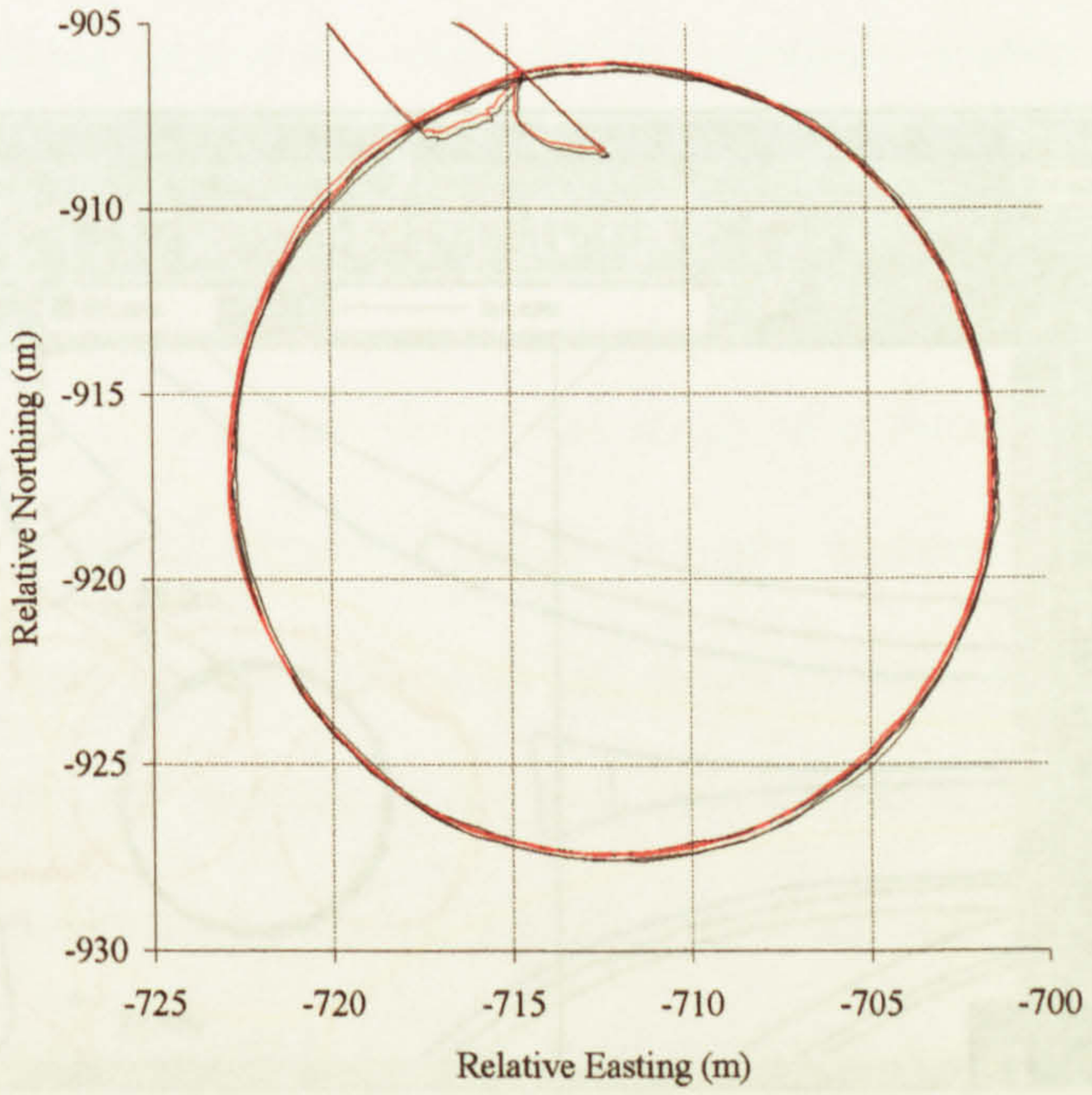

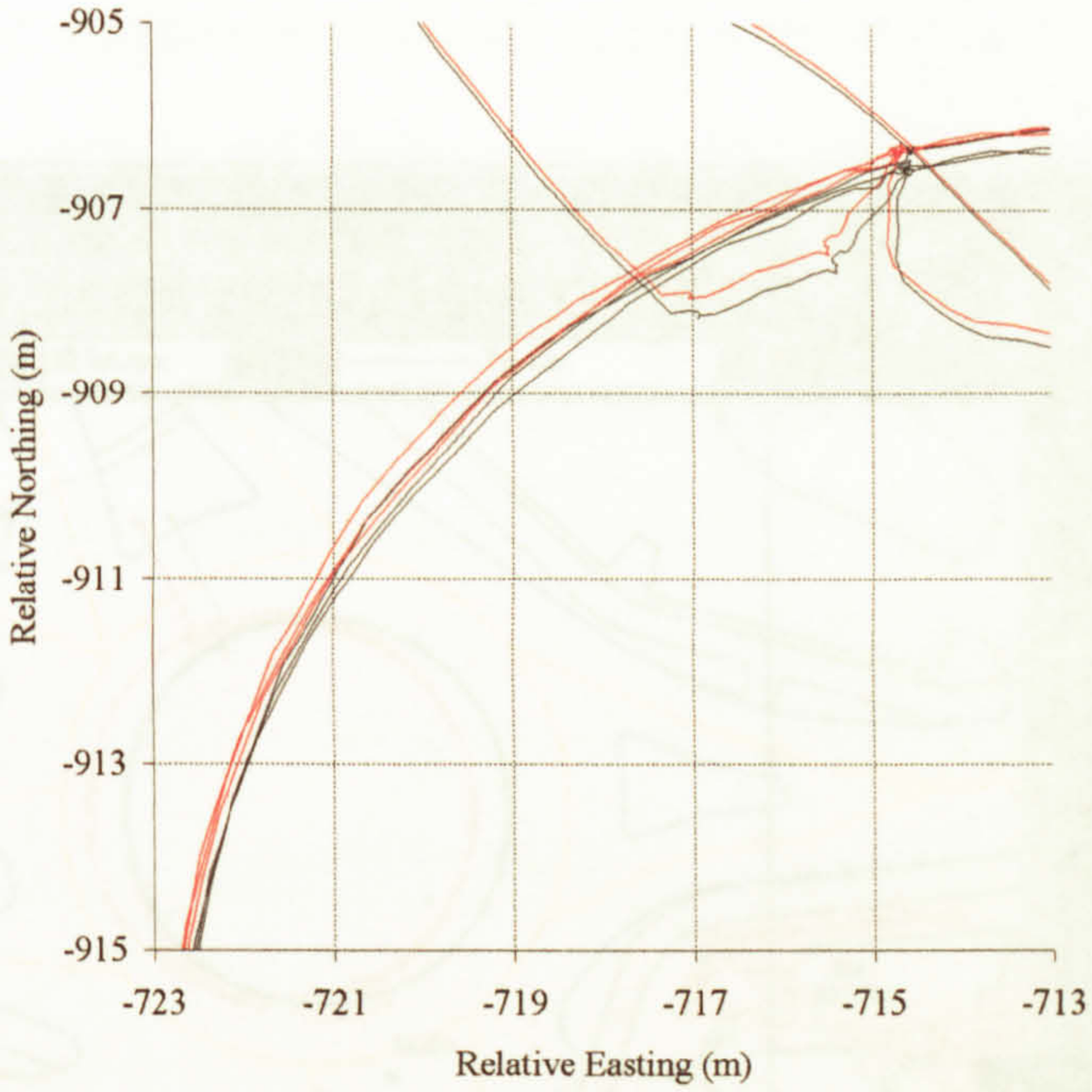

Figure 3.20

University SW, GPS and Hybrid (II)

Figure 3.21 shows the above GPS trace superimposed on digital mapping, in *black*. The convoluted *red* trace is Hybrid using the broadcast ephemerides from the Russian navigation message for the two GLONASS satellites, the IGEX version was substituted to give the more reasonable Hybrid trace in Figure 3.20. The same situation occurred at *Hyson*.

Figure 3.21 *University SW* with Hybrid using Russian GLONASS ephemerides

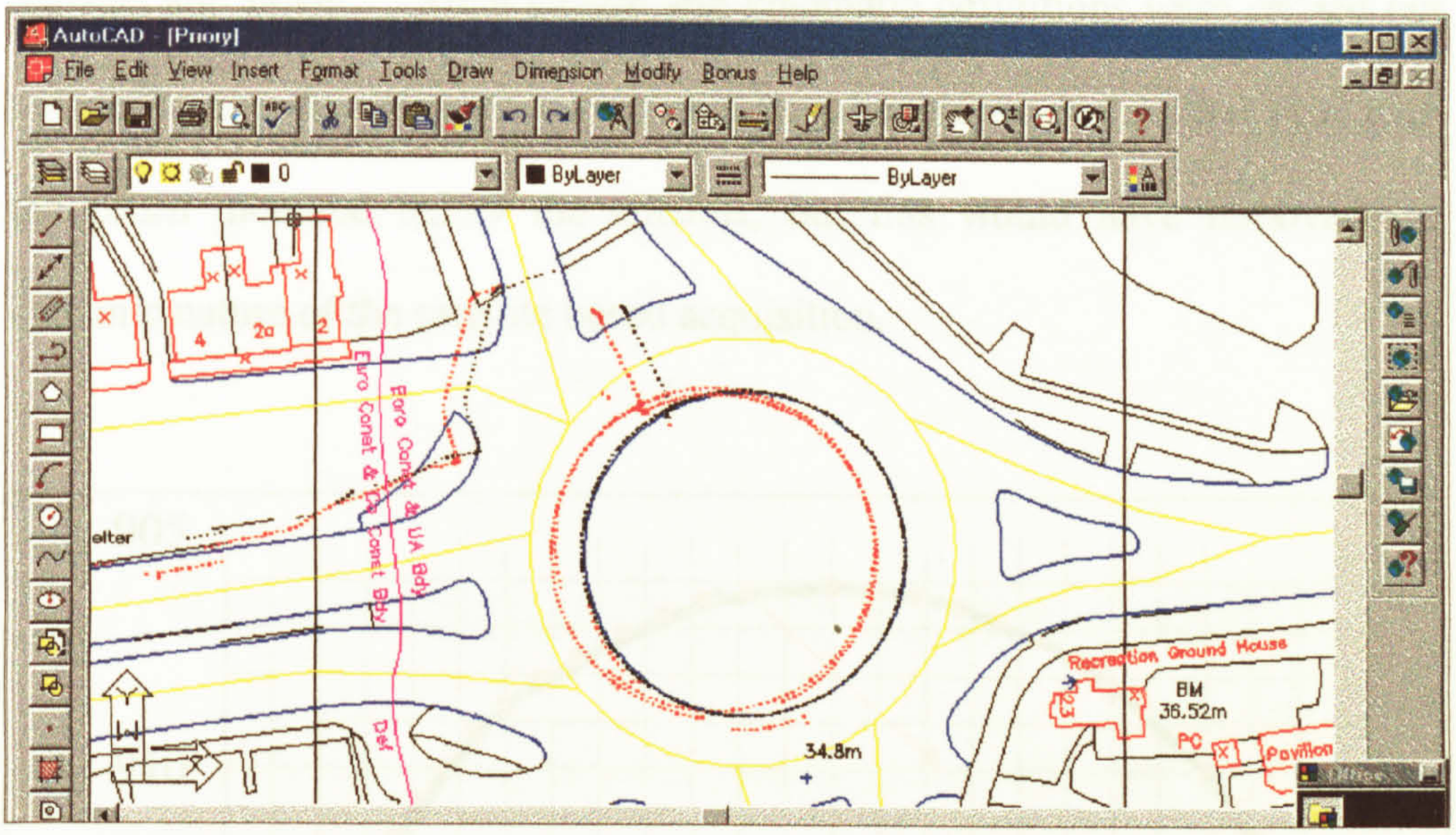

Figure 3.22 *Priory* by GPS and Hybrid

Interestingly *Priory*, Figure 3.22, which was traced in the morning session (17th December 1999), did not suffer from a defective GLONASS navigation message, owing to a correctly updated and uploaded navigation message occurring between the morning session at *Priory*, and the afternoon session at *Hyson* and *University SW*.

The ability of the technique to accurately define the shape of a feature was qualified by comparison with observations made by total station. The University SW site was used for the tests, with definition by total station, Ashtech Z-12 GPS receiver, and Ashtech GG24 in GPS and Hybrid modes. Kinematic tracking was incrementally shifted until the optimum match with total station positioning was achieved, results suggest similar capabilities across the receivers and modes of positioning. Those for the Z-12 are presented in Figure 3.23, where a match of no worse than 20 centimetres was

found, which is within the variation of verticality of the pole supporting the antenna and prism. Total station and kinematic definitions were carried out independently. In retrospect these could have been done at the same time with the prism mounted below the antenna, but this would have removed the dynamic nature of the satellite based acquisition.

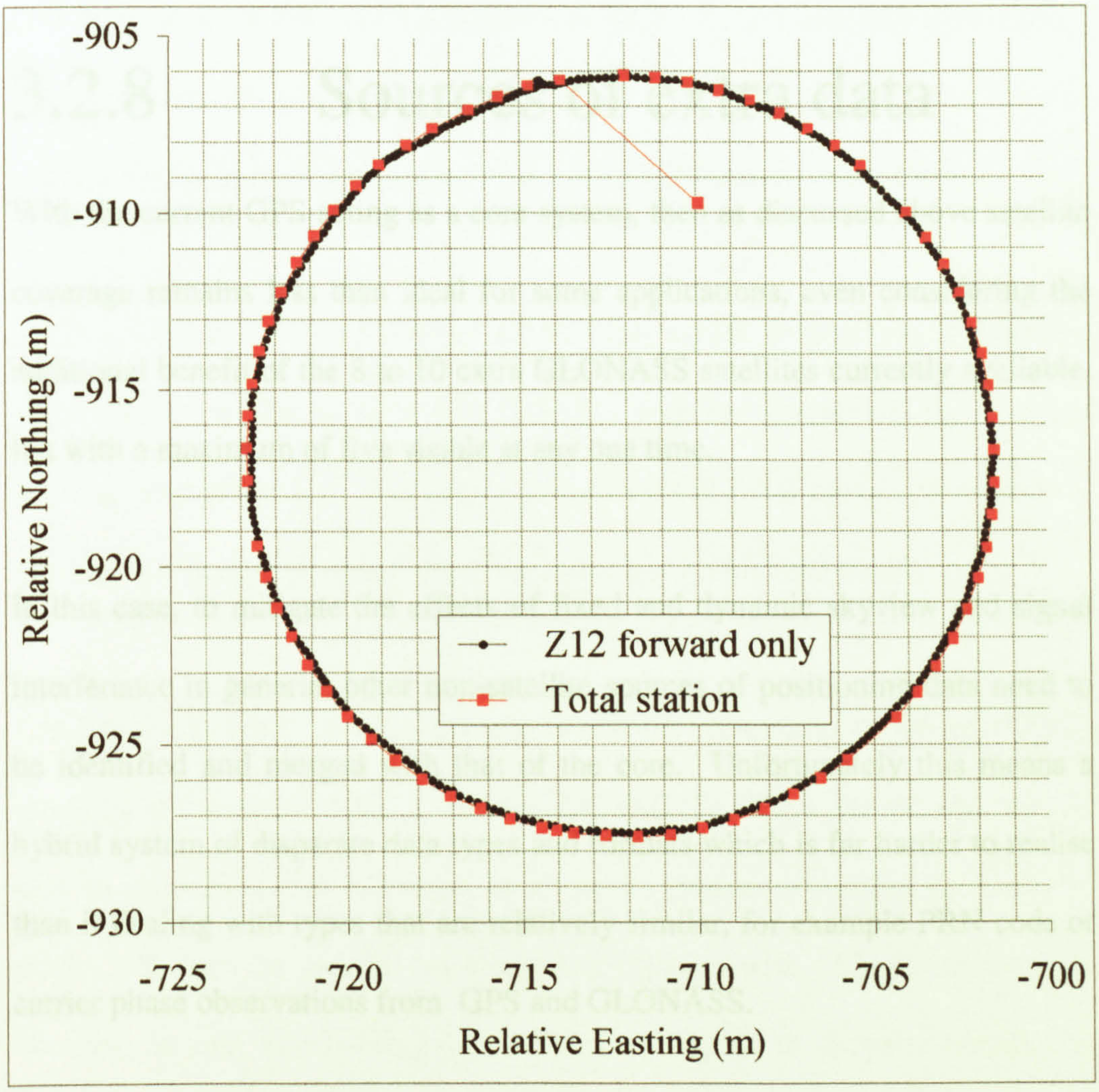

Figure 3.23 Shape definition by kinematic methods

Summarising, in contrast to trig. pillar positioning by static GPS, features such as roundabouts when coordinated using kinematic GPS, and then transformed to OSGB36 using the OS 20-centimetre parameters, appeared to agree at the

half-metre level, for the sample tested. Furthermore the inclusion of GLONASS in a Hybrid solution may degrade achievable accuracy further. Nevertheless, Hybrid will undoubtedly perform better than GPS in a poor reception environment, and results suggest that this technology and acquisition arrangement may be used to update existing mapping.

3.2.8 Sources of extra data

With the current GPS acting as a core system, then as discussed above satellite coverage remains less than ideal for some applications, even considering the additional benefit of the 8 to 10 extra GLONASS satellites currently available, but with a maximum of five visible at any one time.

In this case, to mitigate the effects of fixed and dynamic skyview and signal interference in general, other non-satellite sources of positioning data need to be identified and merged with that of the core. Unfortunately this means a hybrid system of disparate data types and formats which is far harder to realise than if dealing with types that are relatively similar, for example PRN code or carrier phase observations from GPS and GLONASS.

Example candidate systems are now examined from terrestrial and space origins.

3.2.8.1 Terrestrial

Eurofix

The existing Loran C and Chayka (Russian Loran C equivalent) systems can be used to benefit a GNSS as a source of additional observations in the urban environment. The Loran C signals can also be modulated to enable broadcasting of DGPS correction data (see §4.3.1.2) and integrity information, other sub-channels could be allocated to DGLONASS messages. The Eurofix concept was proposed by the Delft University [Offermans et al, 1999].

Loran C operates in the LF band at 100 kHz, signal propagation is therefore very different to that of GPS / GLONASS, with far less sensitivity to signal blockage and reflection. But with a wavelength of 3000 metres measurement resolution is not good, especially if the system is poorly calibrated.

The use of a Loran C channel to broadcast DGPS corrections results in a GNSS accuracy at the metre level. Differential GNSS (DGNSS) can then be used in turn to calibrate Loran C ranges to a similar degree of accuracy. Loran C ranges can then be used in an integrated solution with DGNSS to improve integrity, as well as providing positioning coverage in times when insufficient GNSS satellites are available because of limited skyview and multipath interference.

The LF nature of Loran C could also be of benefit in supplying a differential service offshore when operating in a field controlled predominantly by

microwave radio links. These can completely drown conventional services provided by satellite downlinks such as SkyFix.

Dead Reckoning

A Dead Reckoning (DR) system establishes the position of a vehicle from an initial position, by integrating distance increments and directions of travel [Kealy et al, 1999]. Typically, gyro compasses and odometers are used. These are low grade sensors that limit high accuracy to short departures from the start point, being dependent on errors that accumulate from gyro drift, surface characteristics of granularity, and low frequency error caused by temperature dependent tyre pressure.

DR's short term capability may, in an integrated solution with for example GPS, complement GPS during short signal outages caused by restrictive skyview [Ramjattan et al, 1995]. Satellite positioning whenever available can be used to calibrate the DR sensors. However in some cases GPS integrated with DR does not provide a continuous solution, and resort is made to other location information e.g. in [Kealy et al, 1999] the use of integrated measurements from GPS, GLONASS and DR. Highlighted in this work was the need for an adaptive or *self-learning* Kalman Filter, to handle the high level of track convolution in city navigation. See also Moore et al, 1995.

Video / INS aiding

Another way to circumvent the performance of GPS under conditions of short term signal masking, is to integrate an INS with GPS. However the performance of an unaided INS, may, depending on the grade of the IN

sensors, degrade rapidly, when error growth is unbounded by GPS positioning. So input from another system may be needed.

Further integration with spatial data from a Geographical Information System (GIS) is an option [Brown et al, 1999], by way of point and feature recognition by video imagery. For example a GIS can provide source data for road matching, and a Digital Elevation Model (DEM) can provide skyline profiles.

A pure optical feature matching navigation system, that could be integrated with GPS, uses a holographic database is described by [Pu et al, 1997]. Here a CCD camera is used to record imagery along a vehicle's track. Still frames are extracted from the resultant video to be waypoints stored in a holographic database. A vehicle can subsequently reacquire the same track through image search and match routines.

3.2.8.2 Space based

EGNOS

For detail of this European initiative see §3.1.

WAAS and LAAS

The Federal Aviation Administration (FAA) plans to replace current terrestrial navigation systems with a GNSS. This would use GPS as the core, with a two tier augmentation system – the Wide Area Augmentation System (WAAS), and the Local Area Augmentation System (LAAS), providing extra data through a

combination of additional geostationary satellites and ground reference signals, in a similar arrangement to EGNOS.

These augmentations are needed to meet aviation requirements for service *accuracy, integrity, continuity,* and *availability*, which have been officially defined by the ICAO, [ICAO, 1998]:

- *Accuracy* The degree of conformance between the estimated, measured, or desired position and/or the velocity of a platform at a given time and its true position or velocity.

- *Integrity* The trust which can be placed in the correctness of the information supplied by the total system. Integrity includes the ability of a system to provide timely and valid warnings to the user when the system must not be used for the intended operation.

- *Continuity* The continuity of a system is the capability of the total system (comprising all elements necessary to maintain aircraft position within the defined airspace) to perform its function without non-scheduled interruptions during the intended operation. The continuity risk is the probability that the system will be unintentionally interrupted and not provide guidance information for the intended operation.

- *Availability* The availability of a navigation system is the percentage of time that the services of the system are within required performance limits. Availability is an indication of the ability of the system to provide useable service within the specified coverage area.

Together, WAAS and LAAS will provide seamless navigation coverage throughout the US National Airspace System (NAS). WAAS will provide en route and terminal guidance throughout the NAS and Category I landing guidance at most airports. LAAS will be used exclusively to provide landing guidance at more stringent levels of Category II and III, and Category I where it is not provided by WAAS.

MSAS

The Multi-functional transport Satellite Augmentation System (MSAS), is similar to the US WAAS in Japan. MSAS again uses GPS as the core, with two geostationary satellites providing additional signals. MSAS capable receivers are identical to those in use with WAAS.

Lockheed Martin Regional Positioning System (RPS)

In early 2000 [Galileo's World, 2000], Lockheed Martin announced the formation of a GPS Augmentation company. This will initially offer a local ground-based augmentation system, with eventual expansion into a satellite based wide-area augmentation, named the Regional Positioning System (RPS), based on a constellation of 12 geostationary satellites at 6 locations, to give 100% redundancy for safety critical navigation services. World-wide infra-structure is to be based on three regional subsidiaries – hence the term RPS.

3.3 GNSS-2

Concerns within the European Union (EU) on over-reliance on GPS, which though freely available, has no legal obligation to users for continuity or quality of service, led in the late 1990's to the idea of a European global positioning system, a completely new independent service, or GNSS-2, compatible with GPS, but owned, operated, and ostensibly controlled in the civilian domain. This is Galileo (not an acronym) project, currently the only significant GNSS-2 on the drawing board. It can also be said that the EU was very interested in the massive revenue flows and employment potential within the EU, that were hitherto of most benefit to the US.

In February 1999 the European Commission (EC) formalised the idea and prior discussions around a European alternative to, and competitor with, GPS and GLONASS, in a communication proposing the creation of a strategy to develop the Galileo satellite positioning system [Hofmann-Wellenhof, 2000]. Galileo is likely to be based on MEO and possibly Geostationary Earth Orbit (GEO) satellites, with ground based infrastructure similar to that of GPS.

The EU has been occupied in a long term dialogue with the Russians on incorporating GLONASS into GNSS-2. More recently European interest has focussed on access to the GLONASS spectrum allocation, and Proton launch vehicles. If this is realised, then two major entry barriers to the global positioning market will have been removed. However there were reports in March 2000 [GPS World, 2000c], that the Chinese might bid up to three times

the European's market valuation for GLONASS, to acquire the complete system including hardware and spectrum.

In 1999 the EC and ESA (European Space Agency) awarded contracts totalling EURO 80M towards the Galileo system definition phase, funding the following projects / aims:

- GALA (GALileo Architecture definition): Aim is to define the global architecture and system specifications, through research into world-wide user needs and market analysis.

- GAST (Galileo Architecture Support Team): Set up to provide technical guidance to the EC on the monitoring of the GALA project, and interaction between GALA and studies linked to Galileo system definition e.g. INTEG, SAGA, and others.

- GUST (Galileo User Support Transport). Aim is to support the EC in the area of Galileo receivers, with regard to early standardisation, receiver certification and compatibility with GPS and GLONASS.

- GEMINUS (Galileo European Multimodal Integrated Navigation User Service): Aim is to define the essential features of Galileo necessary to meet the needs of subscribers. This uses output from GALA in validation exercises aimed at six key markets: Road corporate, Road consumer (mass market), Rail, Maritime, Aviation, Science, and Timing.

- INTEG (INTegration of Egnos into Galileo): GNSS expertise has been built up based on experience with EGNOS. The aim of this program is to analyse a seamless transition from EGNOS to Galileo from technical, economical, operational, and institutional standpoints

- SAGA (Standardisation Activities for GAlileo): Has responsibility for standardisation activities, and interoperability between Galileo and other systems like GLONASS and GPS.

- SARGAL (study for Search And Rescue in GALileo): Aim to define technical specifications for SAR-dedicated antenna to be installed on Galileo MEOs, analysis of enhanced and new SAR services.

- GalileoSat (Galileo space segment and related ground segment): Aim is to define the space and ground segments.

Even though Galileo is still at the conceptual stage, it has provoked some important reactions from the US. Firstly Galileo has met with a cool response, with an unwillingness on their part, to enter into constructive dialogue on the technical imperative of interoperability between systems. This is necessary for the seamless use of multiple constellations identified by Slater in §3.2.7. Meanwhile they have been busy rescheduling the GPS modernisation program. It is perhaps a cynical viewpoint to see lack of co-operation and acceleration of their own program as a means to stall Galileo in its early stages. However before Galileo was proposed, the US time schedule for modernisation was very laid back, with arguments over funding creating much delay. Since the funding of Galileo feasibility studies in 1999 and 2000, money for GPS improvement has started to materialise where none was available before, SA has been removed, and modernisation of Block IIR and IIF series brought forward significantly.

Problematic for both GPS and Galileo was spectrum allocation under review at the 1997 World Radio Conference (WRC), with pressure from Mobile Satellite Services (MSS) to share part of the GNSS band of 1559-1610 MHz. At the 2000 meeting, the MSS issue was resolved by its exclusion from future sharing studies, and a further band 1164-1215 MHz was allocated to GNSS type signals.

The definition stage of Galileo comprising the above listed projects, started in late 1999 for completion at the end of 2000. The decision to go ahead with development was made in April 2001, with an operational target date of 2008.

This (ambitious) timetable still allows the US a substantial time period in which to develop their modernisation program, undermining all the time the advantages that an independent system such as Galileo would offer. How committed the EU is to remain to Galileo, depends to a large extent on the Public Private Partnership (PPP) level of funding. If this evaporates under the influence of low predictions of service uptake as users favour an enhanced GPS, then Galileo may only survive as a military system funded by the EU states, if at all.

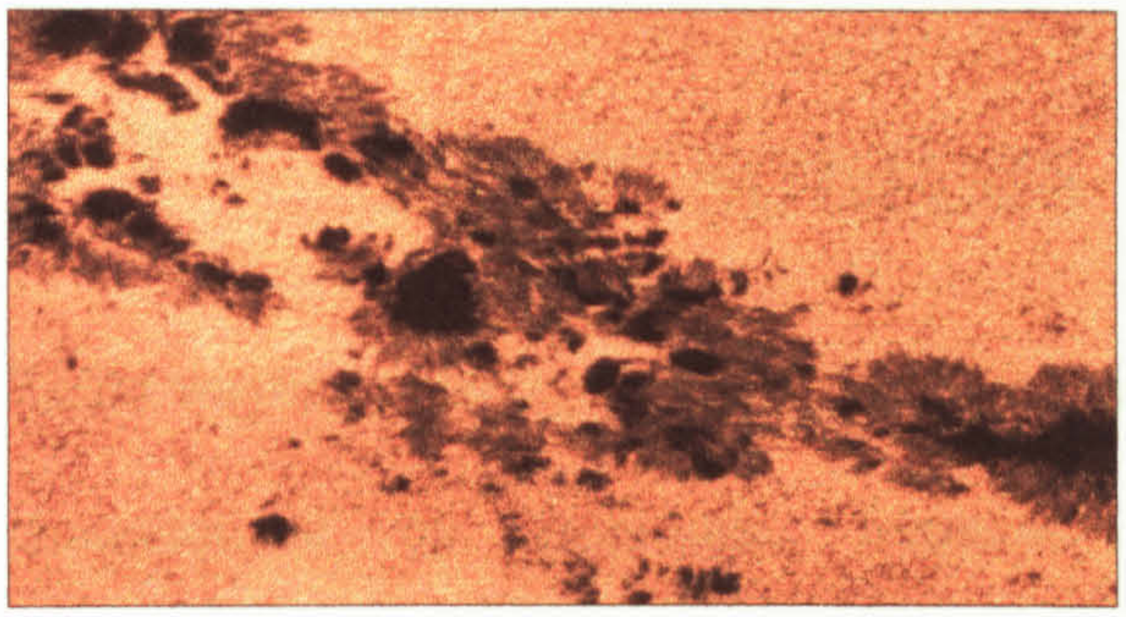

Chapter 4

Positioning Techniques

4.1 Introduction

The purpose of this chapter is to introduce the standard positioning techniques that have been developed for use with GPS, to consider their applicability to GLONASS and Hybrid, and finally to discuss the various approaches adopted to deal with the multi-frequency nature of GLONASS. These techniques can be classified according to the two modes of operation: either *absolute* mode, by which is meant a single receiver operating in isolation; or *relative* mode, involving the positioning of one receiver relative to at least one other. Variants of either mode may use pseudorange, carrier phase, or a combination of these *observables,* in both static and dynamic applications.

These techniques have been developed to address, with varying levels of efficiency according to accuracy needs, the various error sources that can impact on the observables. It is appropriate therefore, before considering positioning techniques, to firstly identify these sources of error, describe their cause and nature, and quantify the possible range of their effect.

4.2 Error sources

Radio waves or *electro-magnetic radiation* (EMR) propagating through space can be characterised by amplitude, frequency, phase, and polarisation. During propagation, signals may be affected by spatial, temporal, and physical factors, which give rise to signal fading, delays, phase shifts, and polarisation changes in the nominal signal [Wells, 1987]. For GPS type satellite transmissions, these changes can occur in all phases of signal propagation: at the satellite, in transit through the atmosphere, and finally at the receiver. Specific error sources are now discussed under these headings.

4.2.1 Satellite and atmosphere

4.2.1.1 At the satellite

At the satellite there are four relevant error sources: satellite clock, ephemeris, signal multipath, and the potential for SA. Satellites use high stability atomic clocks to maintain both frequency and time standards. Both rubidium and caesium units are in use, with a typical daily drifts of 1 part in 10^{12} and 1 part in 10^{13} respectively. Thus the derivative time is of very high stability too. However frequency drift and hence clock drift are inevitable *(all clocks drift)*. Satellite clock drift is forcibly corrected by the system controllers when it approaches one millisecond, which is equivalent to a range error of about 300 kilometres. In the intervening period GPS satellite clocks are not explicitly aligned with GPS system time, rather they are allowed to drift slowly, and their behaviour monitored and modelled as the coefficients of a second order polynomial (Equation 4.1). These coefficients are provided to users in the

navigation message, which when applied, give equivalent range accuracy from this cause of between 2.6 to 5.2 metres. The equivalent GLONASS model consists of offset and rate terms (Equation 4.2). GLONASS clocks are kept within 1 millisecond of UTC(SU).

$$dt = a_0 + a_1(t - t_0) + a_2(t - t_0)^2 \qquad (4.1)$$

where

t_0 some reference epoch
a_0 satellite clock offset
a_1 fractional frequency offset
a_2 fractional frequency drift

$$dt = a_0 + r_1(t - t_0) \qquad (4.2)$$

where

t_0 some reference epoch
a_0 satellite clock offset
r_1 error rate in seconds per second

Positioning relative to a satellite requires the satellite's ephemeris or *orbital parameters* to be known. Any uncertainty in these parameters propagates into positioning error. Ephemeris rms error associated with GPS and GLONASS BEs is at about 5 and 20 metres respectively, the difference being attributable to relatively less well known GLONASS satellite force models. Ephemeris error is therefore a significant component of the absolute positioning error budget. The IGS provides post-processed GPS ephemerides with centimetre accuracy, and IGEX delivers similar for GLONASS with sub-metre level accuracy, with a three month lead-time, but in the ITRF, not PE-90.

Signal *multipath* is the generation of one or more spurious signals, in addition to the direct signal, through reflection from surfaces local to the satellite antenna. Multipath signals are delayed relative to the true signal, and have a lower signal to noise ratio. The occurrence of multipath depends on the local environment, large flat vertical surfaces are the best reflectors. The size of error is signal wavelength dependent. The maximum theoretical multipath error in a code observable is one chip length (about 290 metres for GPS L1 C/A code), but in practice five to ten metres is typical. For carrier phase the maximum figure is about one-quarter cycle or about 5 centimetres. Young et al [1985] computed theoretical baseline length dependent range errors of up to 2.5 centimetres for P-code, and 0.25 millimetre for carrier phase, for a reflector-antenna (at the satellite) separation of one metre, for a baseline of 300 kilometres. So satellite multipath is likely to be important for longer baselines.

GPS and GLONASS carrier phase wavelengths are similar, and so too are the size of multipath error. On the other hand, GLONASS code error should be twice that of GPS, since the GLONASS code chip length is twice that of GPS. But in practice code multipath is also similar, since short multipath delay predominates.

There is no general mathematical model to determine or predict the effect of multipath on a position solution [Rizos, 1997]. However its effect may be monitored at the observable level, by examining the behaviour of least squares residuals over time. Sinusoidal signatures present in such time series are indicative of strong multipath.

SA was switched off in May 2000. Prior to this it was the major error source in absolute positioning mode. With SA turned off, accuracy improved by an order of magnitude, the ionosphere then becoming the dominant error source. See §2.2.4 for details of SA.

4.2.1.2 Transiting the atmosphere

The orbital heights of GPS and GLONASS (hereafter GPS for brevity) satellites mean that their signals must transit two main atmospheric regions, the ionosphere and the troposphere. Both regions, which are now discussed in turn, interfere with these signals.

The ionosphere is an electrically active layered region extending from about 50 to 1000 kilometres above the Earth's surface, with an effect on EMR that peaks at about 350 kilometres altitude. Within this region, solar ultra-violet and x-ray radiation impinge on atoms and molecules, freeing electrons, in a process named *ionisation*. These free electrons affect the propagation of radio waves. As the sun is the cause of ionisation, variation in ionisation with time has an underlying diurnal dependence. A measure of the density of these free electrons is the *total electron content* (TEC). The TEC characterises the level of ionospheric activity, and is defined as the number of free electrons in a column stretching through the ionosphere with a cross sectional area of one square metre from the observer to the satellite.

The free electrons interfere with signals transiting the region, to a degree that is dependent on the TEC, and inversely dependent on the frequency of the signal. So a

relatively high signal frequency can translate into a relatively low level of interference. For GPS this interference causes errors, which are manifest as an advanced carrier phase and delayed pseudorange observables, which can be approximated by Equations 4.1 and 4.2 respectively.

$$\Delta_{phase}^{iono} = -\sec z\left(\frac{40.3}{frequency^2}\right)*TEC \qquad (4.1)$$

where

Δ = the delay in metres, for a satellite at the zenith
z = is the zenith angle of the satellite at the observer

$$\Delta_{code}^{iono} = \sec z\left(\frac{40.3}{frequency^2}\right)*TEC \qquad (4.2)$$

TEC predictability at GPS frequencies can be spatially classified according to equatorial, mid-latitude, and polar regions of the Earth. At mid-latitudes, TEC levels are the most predictable, whilst polar regions have a susceptibility to disturbances in the TEC that are highly correlated with geomagnetic activity. Coronal mass ejections (CMEs) are huge bubbles of gas threaded with magnetic field lines ejected from the sun [Langley, 2000], and if these are directed towards the Earth then world-wide disturbances to the geomagnetic field, called geomagnetic storms are caused. Storms give rise to disturbances in the TEC known as *scintillations*, which cause change to signal speed and direction of propagation, together with temporal fluctuations in the amplitude and phase of the signal at the receiver. Amplitude variation can cause signal fading, and ultimately, loss of receiver lock.

The highest TEC values (causing up to 100 metres pseudorange and carrier phase bias for low elevation satellites), the strongest large-scale TEC gradients, and the worst scintillations, all occur in the equatorial region, within about ± 30° of the geomagnetic equator. Peak TEC activity is directly correlated with the eleven-year cycle of sunspot activity (Figure 4.1). The picture at the chapter heading shows a close-up of a group of sunspots, individual spots are about the same size as the Earth. Scintillations occur in general between sunset and midnight, and there is also a seasonal dependence: in the band of longitude from the Americas to India effects are strongest between September and March. In the Pacific the situation is reversed.

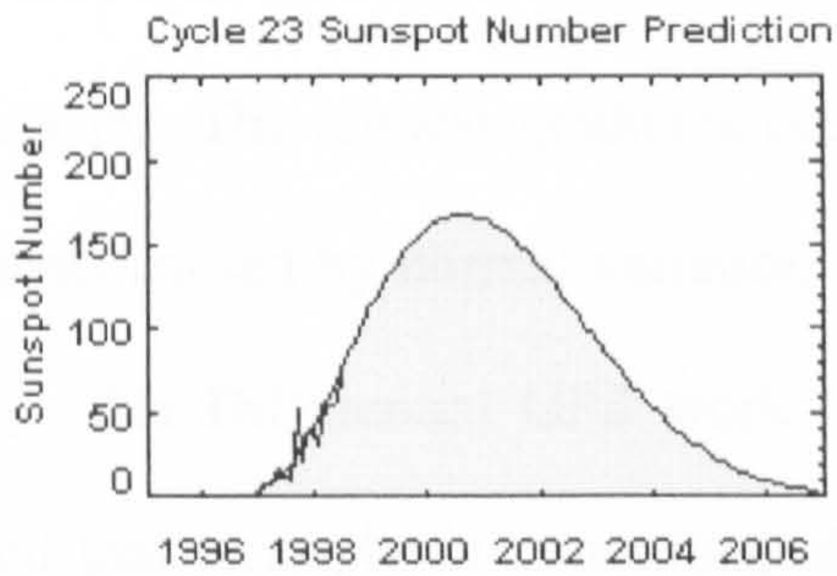

Figure 4.1 Predicted solar activity
(sourced from NOAA website)

Single frequency receivers

Single frequency GPS users working in absolute mode in mid-latitudes, may partially correct for the effect of the ionosphere, using the set of eight forecast ionospheric coefficients broadcast in the navigation message. Their form is based on the global ionospheric model developed by Klobuchar [1986], and when combined with receiver and satellite position and UTC time of day, generally remove better than 50 percent of the error [Rizos, 1997]. For example at a mid-latitude site, Nottingham, in January 1999, the accumulated average height error for nineteen hours of GPS

data was 3.4 metres with the Klobuchar model enabled, and 14.6 metres without. Wanninger [1993] quotes for the mid latitude case, C/A range errors of 20-30 metres daytime, and 3-6 metres at night.

The Klobuchar model is based on a single daily peak in ionospheric activity at 14:00 hours, however in equatorial regions there are often two maxima, one around noon and another in the evening. The second maximum can exceed the first and extremely large day-to-day TEC variability can occur at these times. Under these conditions the use of forecast ionospheric activity is unlikely to be of great value.

In relative positioning mode it is not the value of the TEC, but rather its horizontal gradients that are most important. The highest gradients occur in the North-South direction, whilst minor gradients caused by diurnal variation occur in the East-West direction [Wanninger, 1993]. For Differential GPS work (see §4.3.1.2) on short baselines, it may be assumed that ionospheric conditions above the two sites are similar. In that case differential corrections computed at a reference station and applied at a remote station will include the error due to the ionosphere. For the mid-latitude case [Wanninger, 1993] a baseline error of up to 3 ppm is quoted. The accuracy of DGPS is reduced in the presence of large-scale horizontal TEC gradients, as only part of the ionospheric error at the remote is included in the correction at the reference station. For example, in Brazil, a horizontal gradient equivalent to an L1 differential range error of at least five metres per 100 kilometres (dependent on satellite elevation) was experienced after sunset in March 1992. Hence the efficacy of DGPS in equatorial regions is often poorer than that achievable in mid-latitudes.

Single frequency carrier phase relative positioning is similarly affected. For example processing a ten-kilometre baseline, again in Brazil, in one-hour segments, showed coordinate errors of one centimetre before sunrise, up to five centimetres during the day, and more than thirty centimetres from early evening until after midnight. Clearly, in equatorial regions, around the peak of solar activity, precise GPS surveying may not be achievable with single-frequency units.

Dual frequency receivers

In absolute mode, with dual frequency receivers, the dispersive nature of the ionosphere can be used to minimise its effect, through the linear combinations of observables. This addresses first order effects, but not the higher order terms which include effects of the geomagnetic field and ray-path bending. During periods of high ionospheric activity the higher order effects can be several tens of centimetres of range error, and at quiescent times be at the centimetre level or less [Klobuchar, 1996]. For pseudorange observables on L1 and L2, the expression, for the first order ionospheric delay, is:

$$\Delta_{P_1}^{iono} = \frac{f_2^2}{f_2^2 - f_1^2}[P_1 - P_2] \qquad (4.3)$$

where

Δ = the absolute ionospheric delay in metres

f_1 = the L1 carrier frequency

P_1 = the L1 P-code pseudorange measurement

A similar expression exists for carrier phase:

$$\Delta_{L_1}^{iono} = \frac{f_2^2}{f_2^2 - f_1^2}\left[(\lambda_1 N_1 - \lambda_2 N_2) - (\Phi_1 - \Phi_2)\right] \quad (4.4)$$

where

Δ = relative ionospheric delay in metres

N_1 = L1 carrier cycle ambiguity

Φ_1 = L1 carrier phase measurement in metres.

λ_1 = L1 carrier wavelength in metres.

In carrier phase mode the cycle ambiguity terms, *N* (to be explained in §4.3.2), are unknown, however providing there are no cycle slips, they will take the form of constants, and so the expression can be used to compute variation in ionospheric delay over time.

The GLONASS navigation message does not contain forecast ionospheric parameters, but there are several possible options to follow to overcome this shortcoming: firstly use a dual-frequency GLONASS or Hybrid receiver, or secondly in the case of a single frequency Hybrid receiver, apply the broadcast GPS model to GPS and GLONASS observables alike, or finally run a dual frequency GPS receiver concurrently with the single frequency Hybrid receiver and use data from the former to correct the latter.

In conclusion, GPS and GLONASS users need to be aware of the large global variability in the nature of the ionosphere and its effect on observables, taking account especially in equatorial areas, of ionospheric activity in terms of diurnal, seasonal, and solar cycles.

The troposphere consists of dry gases and water vapour, occupying the lower atmosphere from ground level up to about 30 kms altitude. At the pole the height extends to about 9 kilometres, and at the equator exceeds 16 kilometres. It is an electrically neutral region, therefore delays to signals in this region are frequency independent, and so GPS code and carrier delays are identical at all frequencies. The nature of the delay is that it changes both the speed and direction of signal propagation. Total delays can be as high as 50 metres at low satellite elevation, and typically 3 metres at the zenith. Tropospheric delay is a function of receiver altitude and satellite elevation.

Signal delay can be divided into wet and dry components. About 90% of tropospheric delay arises from the dry component, and the rest from the wet. The dry component is proportional to pressure and inversely proportional to temperature, and various models using surface *met* observations have been developed to deal with this quite effectively. The wet delay is harder to handle since it is directly proportional to water vapour content. Water vapour generally exists below twelve kilometres altitude above sea level, and most water vapour below four kilometres.

One of the primary contributors to horizontal positioning error is, according to Spilker [1996], decorrelation of the troposheric wet component for satellites at low elevation angle errors at widely different azimuths. Also, significant changes may occur over tens of kilometres or just a few hours, as exemplified by weather variability in the UK. However, it is possible to measure water vapour content of the atmosphere directly, using water vapour radiometry, and thereby mitigate the wet

delay. But this is a costly sophisticated solution and so not generally available, see Dodson et al [1993].

Neglecting error due to the troposphere causes a scale error in relative mode. For example a one-metre zenith delay translates into a 0.4 ppm scale error, that is baselines appear longer. Uncertainty in modelling the tropospheric delay mostly degrades the height component of a positioning solution. There is a cause and effect ratio of thumb of 1 : 3, that is a one-millimetre differential tropospheric delay, causes a relative height error of about three millimetres [Rizos, 1997].

4.2.2 At the receiver

Contributions common to the GPS and GLONASS error budgets include: the receiver clock, local multipath, on-receiver noise, cycle slips, and antenna phase centre variation. Additionally with GLONASS and Hybrid receivers such as the Ashtech GG-24, GLONASS measurements have the potential to be contaminated by inter-channel biases or ICBs (see Chapter 3). These sources are now discussed in turn.

Downward pressure on unit costs means that receivers for general usage are fitted with quartz technology clocks. These are of a much lesser quality than those carried by the satellites, and drift relatively quickly. The frequency-determining component of a clock is the oscillator, and a main determinant of clock performance is oscillator stability, or how well the oscillator stays on frequency (Table 4.1).

Signal multipath (see also §4.2.1.1) may also occur at the receiver's antenna, with local fixed and dynamic reflective sources such as buildings and traffic, respectively. The optimum method to deal with multipath on the ground, is to avoid as far as possible sites that could favour its occurrence. Multipath mitigation has been the subject of innovative developments in receiver design, many details of which are proprietary, for example Trimble 4000 SSi and Leica 500 series.

Type of clock	Oscillation frequency	Stability 1 part in	Time to lose one second	Cost
Digital watch crystal oscillator	32 kHz	10^5	1 day	$0.35
Oven quartz crystal oscillator	1-50 MHz	10^9	30 years	$30.00
Rubidium	6.8 GHz	10^{12}	30,000 years	$4,000
Caesium	9.2 GHz	10^{13}	300,000 years	$55,000
Hydrogen maser	1.4 GHz	10^{16}	300,000,000 years	Very expensive

Table 4.1 Clock cost and quality
[Sourced and adapted from IBM GIS web site]

On-receiver measurement noise affects both code and carrier phase, it is a random error, with typical code and carrier phase figures in high quality receivers, of less than 0.5 metre, and sub-millimetre level, respectively. But note that the GLONASS code wavelength is twice that of GPS, so in theory GLONASS code noise could be at the metre level.

Code noise can be reduced by either averaging, or filtering, typically using carrier phase smoothing [Hatch, 1982]. Carrier phase noise can also be mitigated using an averaging process. The FDMA nature of GLONASS giving rise to ICBs was introduced briefly in Chapter 3, and is covered comprehensively in §4.3.2 At this point however it is worth pointing out that ICBs cause a diminution in precision in both absolute and relative positioning modes.

The phase centre of an antenna is the apparent point to which measurements are referenced. Phase centre variation is caused by non-spherical reception properties of the antenna, so that the measured phase of the same signal received from different directions is different [Schupler et al , 1991]. The error can reach several centimetres, is not the same for different antenna types, nor for L1 and L2. The effect can be mitigated by using a common antenna type, commonly orientated, typically to magnetic North.

The predicted ranging accuracy obtainable with a specific satellite, is supplied in the navigation message as User Range Error (URE) values. Note that URE does not include error estimates due to inaccuracies of the single-frequency ionospheric delay model. UREs are supplied as rms values, σ_{URE}, which when factored by DOP variants, give a rough indication of expected precision, in terms of distance root mean square error (DRMS). The probabilities associated with DRMS are dependent on the geometry of the solution [Rizos, 1997]. 2.DRMS is normally quoted, and the probabilities associated with the circle of radius 2.DRMS have been found to range from 95.4% to 98.2% [Bowditch, 1977]. For the various DOPs the expressions for 2.DRMS are:

$$2 . DRMS_{Vert} = 2 . VDOP . \sigma_{URE}$$

$$2 . DRMS2_{2\text{-}D} = 2 . HDOP . \sigma_{URE}$$

$$2 . DRMS_{3\text{-}D} = 2 . PDOP . \sigma_{URE}$$

Typical URE figures have already been quoted in Chapter 2 §2.2, in the context of GPS in comparison with GLONASS.

4.3 Observables and methods

The nature of a particular positioning task, together with accuracy linked with cost constraints will determine which satellite types of measurements are used, code or carrier phase, and also what observation strategy and processing techniques are to be applied. Code and carrier phase observables and their measurement are now examined, together with the processing techniques associated with them. Explanations in this section use GPS as the example, but the descriptions and development of equations are applicable to both GPS and, with some restrictions, GLONASS, see §4.3.2.

4.3.1 Pseudorange

The initial design of GPS was intended to provide a single observable only, the *pseudorange*, and it was only later that access to and the utility of the underlying carrier phase was realised. The latter is dealt with in §4.3.2.

A receiver contains knowledge of the pseudorange codes transmitted by all satellites. When a signal arrives at the receiver, a local copy of the code is generated, which is then shifted until the received and local codes are in alignment, lock is then said to have occurred. The amount of shift is a measure of the elapsed time, or time delay, Δt, between signal transmission by the satellite and reception (Figure 4.2). If this is factored by the speed of light then the equivalent metric range is obtained – or it would be were it not for the impact of an error budget, as described in the sections

above. These uncertainties give rise to the term pseudorange, the units of which are seconds.

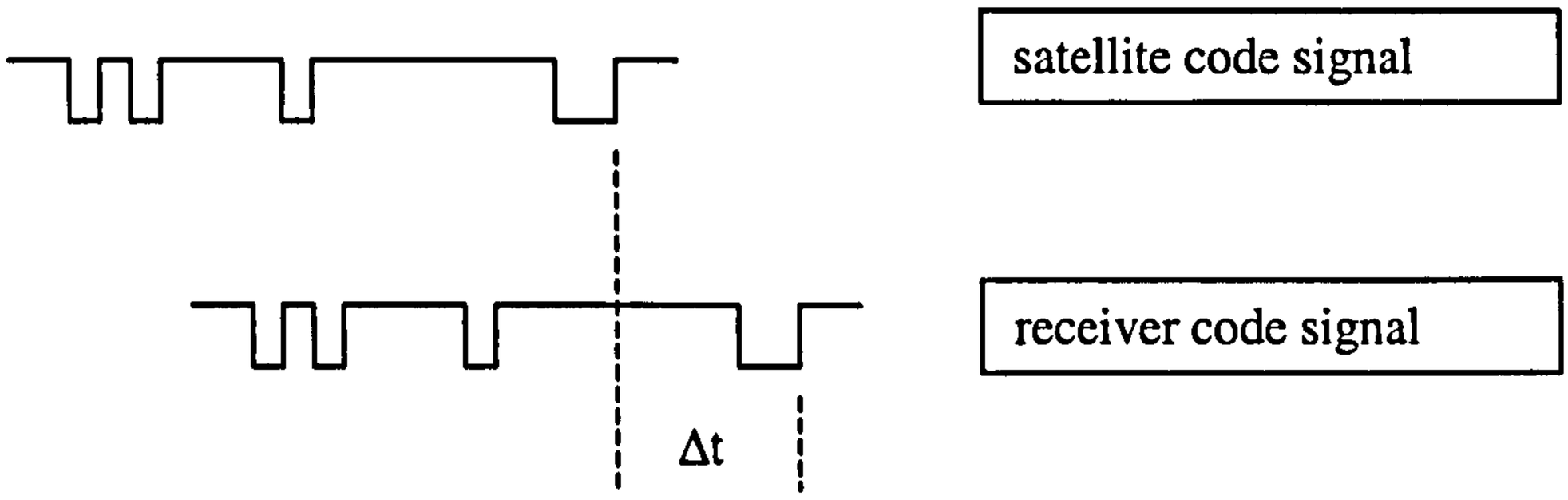

Figure 4.2 Code matching

The pseudorange equation is developed between satellite *i* and receiver *A*, in terms of time in seconds, according to Bingley [1993]:

$$\rho_A^i = T_A - T^i \tag{4.3}$$

where:

ρ_A^i = measured pseudorange between receiver A and satellite i, in the receiver time reference frame (secs)

T_A = time of signal reception in the receiver in the receiver reference time frame (secs)

T^i = time of signal transmission in the satellite reference time frame (secs)

Now $T_A = t_A + \delta t_A$ and $T^i = t^i + \delta t^i$, and substituting into Equation (4.3)

where:

t_A = time of signal reception in the GPS time frame (secs)

t_i = time of signal transmission in the GPS time frame(secs)

δt_A = a correction to bring receiver time into line with GPS time (secs)

δt^i = a correction to bring satellite time into line with GPS time (secs)

So that, Equation 4.3 now becomes:

$$\rho_A^i = (t_A + \delta t_A) - (t^i + \delta t^i) \tag{4.4}$$

Rearranging gives

$$\rho_A^i = (t_A - t^i) - (\delta t^i - \delta t_A) \tag{4.5}$$

If the pseudorange is assumed error free then it equates to the true geometric range, *GR*, which in metres is expressed as:

$$GR_A^i = c(t_A - t^i) \tag{4.6}$$

where:

c = speed of light ($m.s^{-1}$)

GR_A^i = geometric range between receiver A and satellite i. This is obtained by taking the difference between the time that the signal was emitted at the satellite and the time of arrival at the receiver, all in the true GPS time reference frame, and multiplying by the speed of light (m)

GR_A^i is also $\{(x_A - x^i)^2 + (y_A - y^i)^2 + (z_A - z^i)^2\}^{0.5}$, which contains the 3D coordinates of the receiver, A, to be solved for, and the known satellite coordinates

Rearranging Equation (4.6):

$$\frac{GR_A^i}{c} = t_A - t^i \tag{4.7}$$

Substituting into Equation (4.5), and adding error terms

$$\rho_A^i = \frac{GR_A^i}{c} + \delta t_A - \delta t^i + dIONO_A^i + dTROPO_A^i + \varepsilon_A^i + e_A^i \tag{4.8}$$

where:

$dIONO\ _A^i$ = ionospheric delay (secs)

$dTROPO\ _A^i$ = tropospheric delay (secs)

ε_A^i = multipath, on-receiver noise (secs)

e_A^i = on-receiver delay (secs)

Equation (4.8) is frequency independent, and so is applicable as the *pseudorange equation* for both GPS and GLONASS code observables, and useable under various modes of receiver operation, as described next.

4.3.1.1 Absolute mode

In this mode all terms on the right hand side of Equation (4.8) must be estimated, eliminated by one means or another, or ignored – so affecting accuracy, see Table 4.2.

For the 3-dimensional estimation of a receiver's absolute location, solutions to 4 unknowns are needed, for each epoch. These are the X, Y, Z Cartesian coordinates, and the time offset between local (receiver) time and GPS time, δt_A. The receiver's unknown WGS-84 coordinates are embedded in the geometric range term, GR_A^j, of Equation (4.8), as is any ephemeris error, which cannot be modelled in an absolute situation.

Error	Typical value	Remedy
Ephemeris	5 m	None
Satellite clock	5 m	Use broadcast clock parameters, but residual error exists
Satellite multipath	cms	None – assumed below measurement noise level
SA (epsilon and dither)	0 m (May 2000)	None when active
Ionospheric delay	20 m	Single frequency uses Klobuchar model Dual frequency eliminates it
Tropospheric delay	10 m	None
Receiver multipath / imaging	5-10 m	Avoid by properly siting antenna
Receiver clock	300 $km.ms^{-1}$	A 4^{th} unknown in the basic position solution
Receiver noise	metres	Carrier phase smoothing

Table 4.2 Stand-alone pseudorange error sensitivity and remedy

The effect of ephemeris error on position when in absolute mode can be estimated using the rule of thumb [Rizos, 1997]:

$$\textit{Position error} = \textit{PDOP} * \textit{Ephemeris error} \text{ (m)}$$

The situation is complicated since ephemeris error is different for each satellite.

If GLONASS measurements are used to supplement those of GPS, then a fifth unknown appears, this is the difference between GPS time and UTC(SU). Since a new Equation (4.8) is needed for each satellite pseudorange simultaneously observed, and the 4 (or 5) unknowns are common to each of these equations, then a minimum of 4 (or 5) satellites and hence 4 (or 5) equations are needed for a non-redundant solution. This set of equations is easily solved, but provides no cross-check between observations i.e. zero redundancy. It is preferable that at least six or seven satellites should be observed, for the following reasons:

- Extra satellites allow a least squares approach to be applied, this has benefits in terms of reliability and accuracy

- If one satellite fails to track for reasons of noise or blockage, then another is immediately available

The accuracy of this method when using GPS C/A code observables with SA on, at the 95% level, is better than about 80 metres horizontally and 100 metres vertically, see Chapter 2, Table 2.9. Since SA was switched off these figures have improved by an order of magnitude. Official figures for the *new* GPS were issued on 31st January 2001. Even though SA-like intentional degradation is not applied to GLONASS,

95% horizontal accuracy has been found by independent monitoring, to be about 25 metres horizontally, and 45 metres vertically, with a twelve satellite constellation [Benhallam et al, 1996]. The performance disparity between GPS with SA off, and GLONASS, may be attributable to: GLONASS chip length, which is twice that of GPS, and leads to poorer measurement resolution; a less accurate BE; and no ionospheric corrections.

The relative method of observation significantly improves performance over what is achievable in absolute mode, this is the subject of the next section.

4.3.1.2 Differencing observables

The algorithms presented here are based on Equation (4.8), but instead of working with a number of equations involving receiver-satellite relationships, equations involving multiple receivers and satellites are combined linearly, to eliminate common error terms.

The workhorse of the relative mode of positioning is the Double-Difference (D-D) linear combination of simultaneous measurements from two receivers to two satellites. It is a progression from the less efficient Single-Difference (S-D), of simultaneous measurements from one receiver to two satellites or from two receivers to one satellite, which for demonstrative purposes is included here. The advantage of D-D over S-D is that more error sources are cancelled in a D-D.

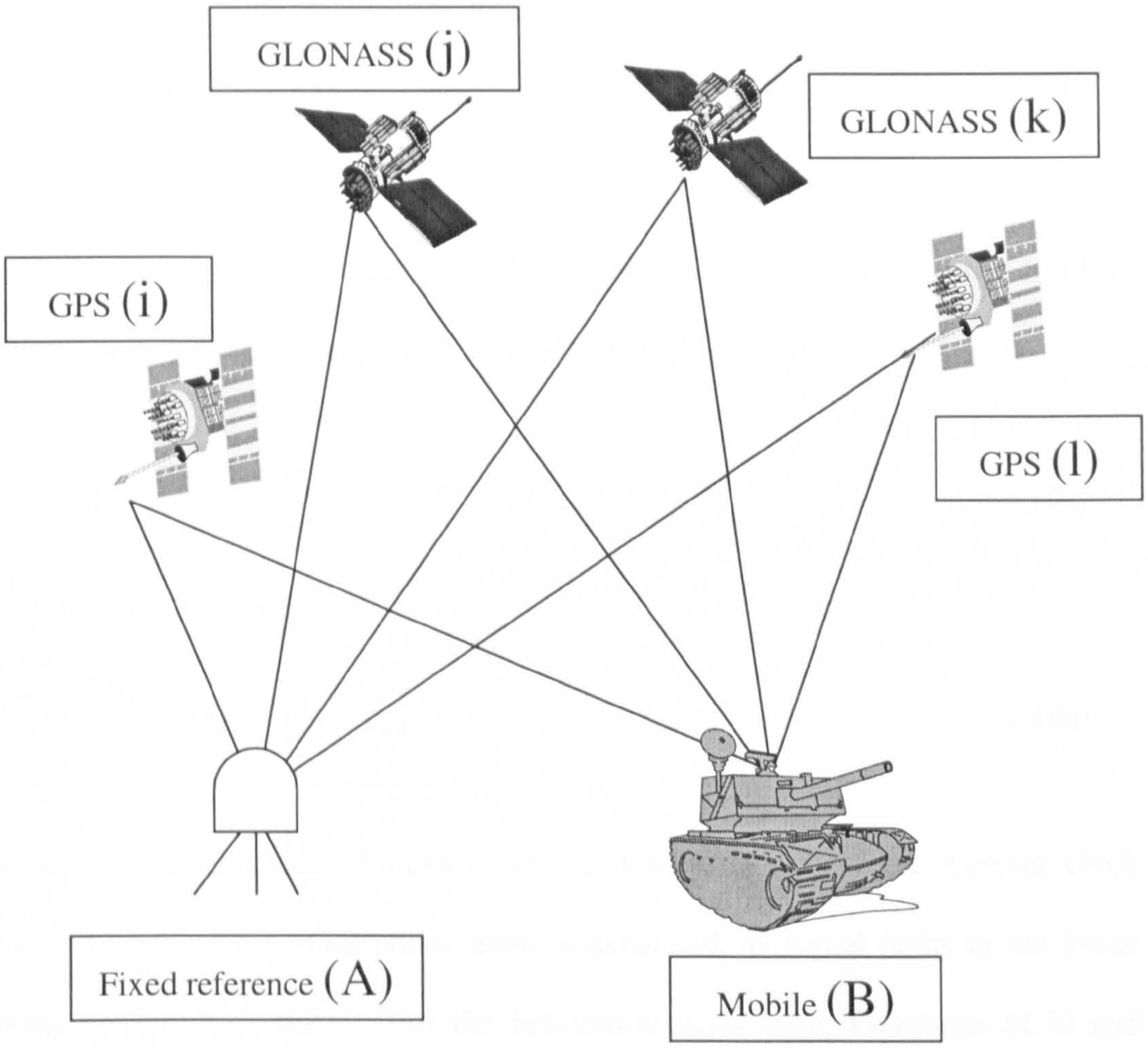

Figure 4.3 Relative positioning network and measurements

Single difference

Referring to Figure (4.3), the two options for forming the S-D equations of the form Equation (4.8) are: *between-satellites* involving measurements from just receiver *A* to satellites *i* and *j*, *j* and *k*, and *k* and *l* and so on (this can be used as an enhanced form

of stand-alone positioning, since several receiver-common error sources will cancel), see Equation (4.9).

$$PR_A^i - PR_A^j = \frac{GR_A^i}{c} - \frac{GR_A^j}{c} - \delta t^i + \delta t^j + \varepsilon_A^i - \varepsilon_A^j + e_A^i - e_A^j \qquad (4.9)$$

Which may be written as

$$PR_A^{ij} = \frac{GR_A^{ij}}{c} - \delta t^{ij} + \varepsilon_A^{ij} + e_A^{ij} \qquad (4.9a)$$

The alternative is *between-receivers,* using measurements from receivers *A* and *B* to satellite *i*, then *j*, *k*, and so on, which in mathematical form is:

$$PR_A^i - PR_B^i = \frac{GR_A^i}{c} - \frac{GR_B^i}{c} + \delta t_A - \delta t_B + \varepsilon_A^i - \varepsilon_B^i + e_A^i - e_B^i \qquad (4.10)$$

Which may be written as

$$PR_{AB}^i = \frac{GR_{AB}^i}{c} + \delta t_{AB} + \varepsilon_{AB}^i + e_{AB}^i \qquad (4.10a)$$

The between-satellite case, Equations (4.9 and 4.9a) is free of the receiver clock term, and some of the atmospheric error is cancelled, as signal paths in the lower atmosphere will be similar. For the between-receiver case, Equations (4.10 and 4.10a), the satellite clock term has cancelled, SA and residual ephemeris error eliminated, and for short baselines (SBL) most of the atmospheric error is cancelled, since signal paths are very similar over their complete length. In either case a minimum of four satellites is required to solve for the mobile position, and receiver clock offset.

Double difference

Further error cancellation can be achieved by simultaneously differencing between receivers and satellites. D-D equations can be formed by differencing pairs of either Equations (4.9) or (4.10), the result is the same, in Equation (4.10b), as satellite clock or receiver clock errors are eliminated respectively, to leave just the three coordinate unknowns of the mobile receiver, a noise term, and the GLONASS frequency dependent ICB term which can be included in the noise term.

$$PR_{AB}^{ij} = \frac{GR_{AB}^{ij}}{c} + \varepsilon_{AB}^{ij} + e_{AB}^{ij} \qquad (4.10b)$$

As with any positioning solution, adding more data increases both precision and reliability, this is the case with the D-D relative to the S-D.

4.3.1.3 Differential corrections

Since the early days of GPS *differential* methods have been used to reduce errors for vehicle navigation. Currently the horizontal accuracy of differentially corrected GPS (DGPS), is normally better than five metres. Systems operating in this mode are typically used in real-time navigation applications, in for example marine and land seismic acquisition.

Differential code methods rely on the basic assumption that observation errors are approximately the same at two spatially separated receivers. In its simplest form, a reference station is established over a known point, coordinated to a higher accuracy than that required for subsequent vehicle navigation. Pseudorange measurements at

the reference station are compared with known ranges, PseudoRange Corrections (PRCs) are then computed and relayed to the *remote*, where they are applied, and the accuracy of its location thereby improved.

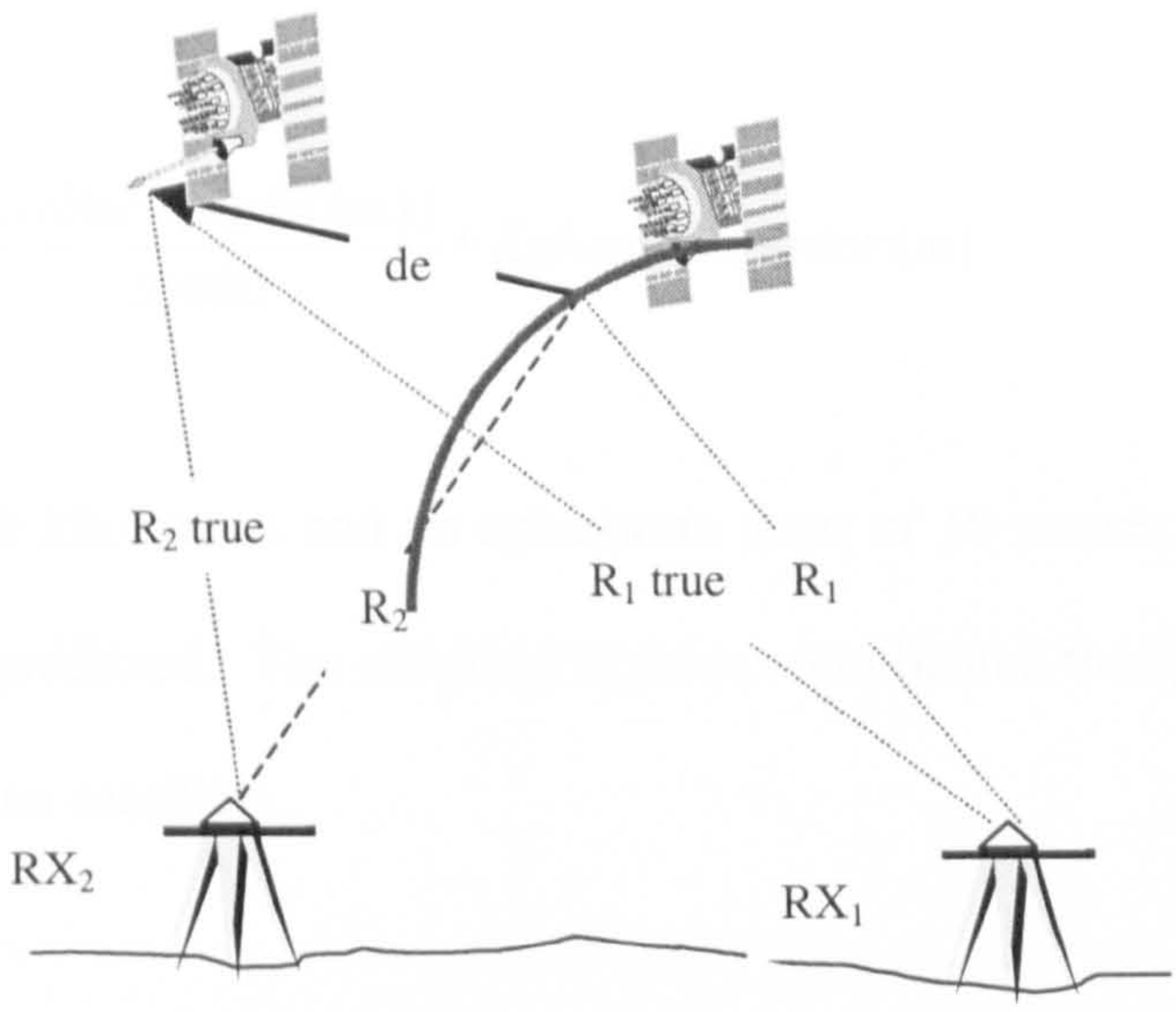

Figure 4.4 Decorrelating ephemeris error over long baselines
(Adapted from Abousalem, 1997)

The PRCs can be applied at post-process, but are generally used in real-time, with relay to the remote via some form of terrestrial or satellite radio link. The effectiveness of the differential method depends on several factors: spatial decorrelation of the atmosphere, PRC age, latency and update rate. As spatial separation between reference and remote increases firstly atmospheric error decorrelates, followed at about 1000 kms by ephemeris error. Figure 4.4 demonstrates how this error, *de*, develops with a large receiver separation. In this example, pseudorange measurements made at receiver 2, would be free of ephemeris error since the vector *de* is orthogonal to the range vector between satellite and receivers. This is also the case when two receivers are close together. On long

baselines however receivers see *de* from a different aspect and this can give rise to pseudorange errors, expressed in the figure as the radial difference, (R_1 true – R_1).

Baseline error due to ephemeris error can be estimated using a rule of thumb [Rizos, 1997]:

$$Baseline\ error\,(m) = \frac{baseline\ length(kms)}{20000} * Ephemeris\ error\,(m)$$

So with a baseline of 10 kilometres and an ephemeris error of 10 metres, a baseline error of 1 centimetre is predicted. The situation is more complicated though, because orbit error differs between satellites.

PRC age is defined as the total overhead to compute and deliver corrections to the remote, and latency reflects the delay in application at the remote (Figure 4.5). Another important factor is PRC update rate or how frequently PRCs are received. The sum of GPS PRC age and latency was quite crucial with SA active, since SA has a high frequency nature and so changes quite quickly. SA has been characterised e.g. van Graas et al [1996], as having a period on the order of 2 to 5 minutes, with an amplitude standard deviation of about 23 metres.

An old PRC degrades remote positioning accuracy. Figure 4.6 demonstrates this with the relative performance of DGLONASS and DGPS positioning before the removal of SA. These show that GLONASS PRCs age much more gracefully, since no equivalent to SA is applied with GLONASS. The accuracy of a DGLONASS solution deteriorates initially, then reaching a steady state at a relatively low error

level. However, with SA removed, performance of real time DGPS and DGLONASS is equalised.

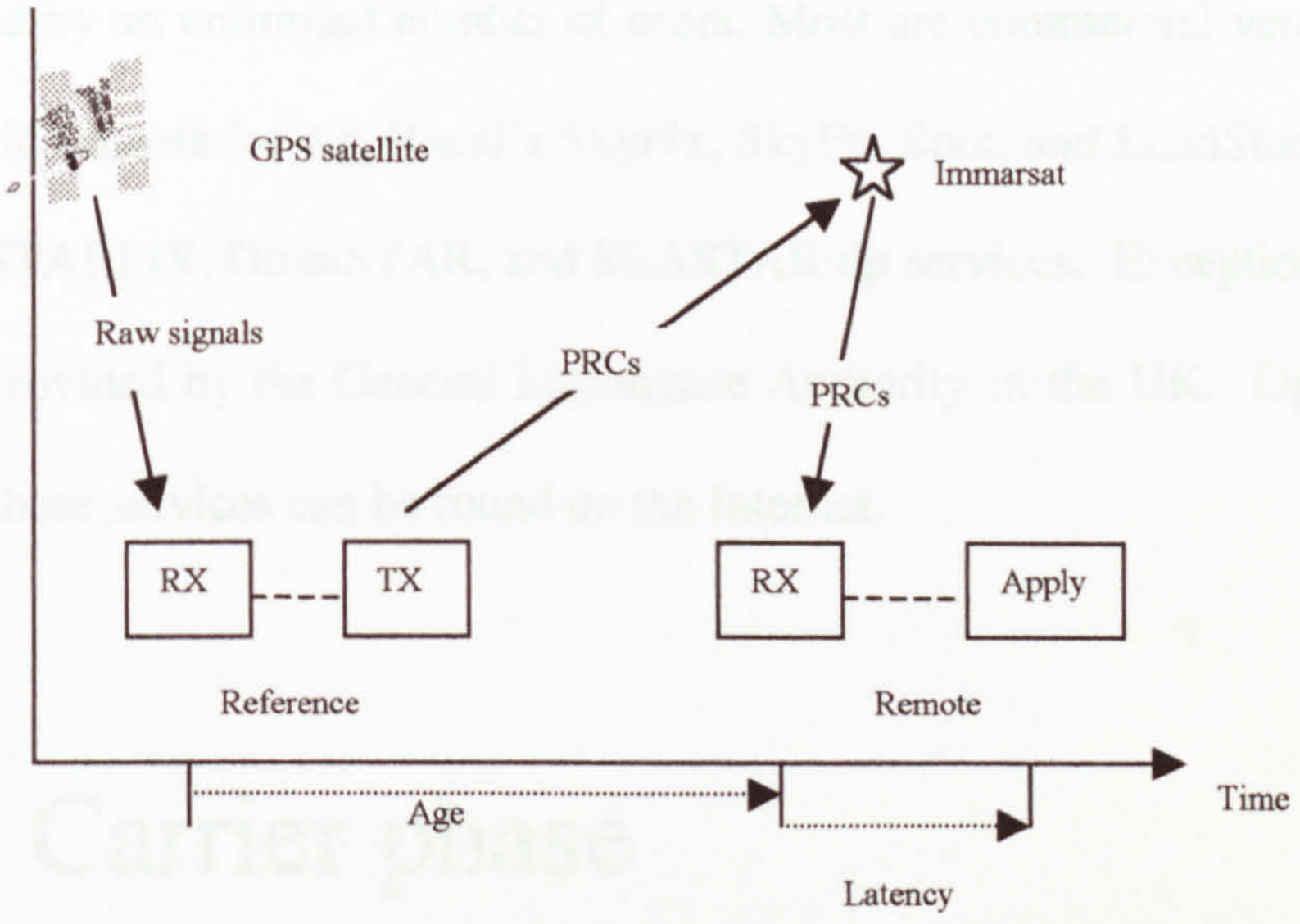

Figure 4.5 Pseudorange correction flow in time

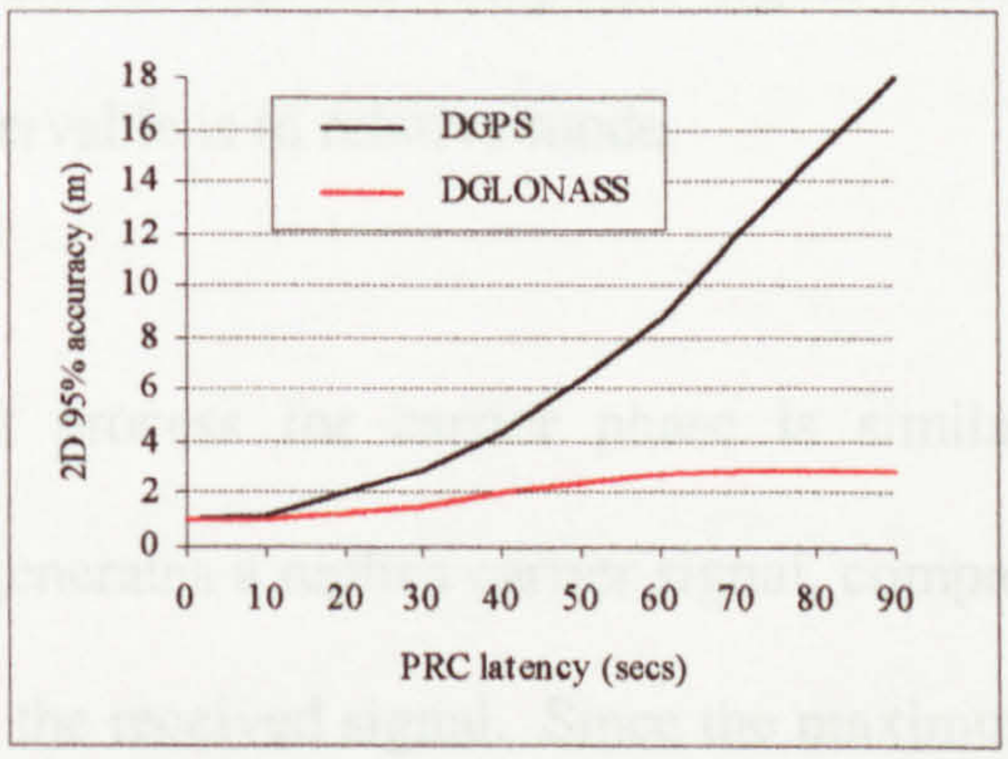

Figure 4.6 Position error as a function of update rate /age / latency
(Adapted from ASHTECH, 1997)

Basic differential methods aggregate all error sources into pseudorange and pseudorange rate corrections for each satellite. A more complex and efficient solution is to decompose the PRC into component errors, typically SA, atmospherics and ephemeris, and model them over some spatial extent of operation. But this involves a significant communications and control infrastructure, together with

multiple reference stations, for example Wide Area DGPS (WADGPS), see Abousalem, (1997) for details. Many providers of differential services exist, with geographical coverage ranging from local to global. They are passive services and so can be used by an unlimited number of users. Most are commercial ventures and require a service access fee e.g. Racal's SkyFix, SkyFix Spot, and LandStar services, and Fugro's STARFIX, OmniSTAR, and SEASTAR dp services. Exceptions are the free service provided by the General Lighthouse Authority in the UK. Operational details of all these services can be found on the Internet.

4.3.2 Carrier phase

The carrier phase is the fundamental signal remaining after codes and navigation message have been demodulated from the composite signal received. The standard use of the carrier phase observable is in relative mode.

The receiver measurement process for carrier phase is similar to that for the pseudorange: the receiver generates a replica carrier signal, compares and then shifts this to be in alignment with the received signal. Since the maximum shift is less than one wavelength, it is the fractional part of a wavelength that the receiver measures and reports. With modern high quality receivers the shift can be resolved to better than 1% of a wavelength, equivalent to a few millimetres for all GPS and GLONASS carrier phase observables. This is therefore the level of measurement noise. However, to realise these highly precise measurements as millimetre-level position accuracy, the fractional wavelength measurements must be added to the *true* number

of complete cycles to give an unambiguous observable. This then represents the total distance between the satellite and receiver.

The problem is that the integer cycle count output by the receiver for a specific satellite is based on an arbitrary number assigned when the receiver locks to that satellite. The receiver then keeps track of the relative change in fractional and thence whole cycles as the measured phase passes through 0° / 360°. But if the signal is noisy and lock is lost, then abrupt changes in the integer count can occur, known as cycle slips, which are discussed in §4.2.2. Establishing the true number of integer cycles is not a simple process.

The carrier phase observable, Equation (4.11) is analogous to that of the pseudorange in Equation (4.8), except that it is now defined in terms of cycles rather than time (by introducing frequency and inverse speed of light coefficients), and an integer cycle term is included [Bingley, 1993].

$$\Phi_A^i = \frac{f^i}{c} GR_A^i + f^i(\delta t_A - \delta t^i) + N_A^i + dIONO_A^i + dTROPO_A^i + \varepsilon_A^i + e_A^i \qquad (4.11)$$

where

Φ_A^i = the measured fractional part-wavelength of the range between receiver *A* and satellite *i*, plus the initial arbitrary cycle count summed with any change in whole cycles since receiver lock.

N_A^i = integer ambiguity, the unknown integer number of wavelengths that establishes the true cycle count between receiver A and satellite i, by correcting the at lock-on arbitrary receiver count on the LHS to the true value.

f^i = carrier signal frequency, L1 or L2, or GLONASS satellite specific at L1 or L2.

The unknowns are now the three coordinate unknowns, the relative receiver clock offset, and the geometrically correct integer count at receiver lock.

As with the pseudorange equation, the carrier phase observable can be linearly differenced to mitigate or eliminate components of the error budget.

Single difference

Using the between-receiver relative positioning case, Equation (4.11) is differenced for receivers at points *A* and *B*.

$$\Phi_A^i - \Phi_B^i = \frac{f^i}{c} GR_A^i - \frac{f^i}{c} GR_B^i + f^i(\delta t_A - \delta t^i) - f^i(\delta t_B - \delta t^i) + N_A^i - N_B^i + dIONO_A^i - dIONO_B^i + dTROPO_A^i - dTROPO_B^i + \varepsilon_A^i - \varepsilon_B^i + e_A^i - e_B^i \quad (4.12)$$

Which condenses to, on a short baseline

$$\Phi_{AB}^i = \frac{f^i}{c} GR_{AB}^i + f^i \delta t_{AB} + N_{AB}^i + \varepsilon_{AB}^i + e_{AB}^i \quad (4.13)$$

This is the between-receiver S-D carrier phase equation, which is frequency consistent i.e. each involves just one satellite and satellite frequency per equation, and can be used with either GPS or GLONASS observations. The unknowns of coordinate difference, relative receiver clock offset, and the geometrically correct integer count at receiver lock-on remain, but now atmospheric effects on short baselines are eliminated. Four satellites are required for a non-redundant position solution. The S-D is now developed to the D-D.

Double difference

Differencing between-receiver S-Ds between satellites cancels the clock offset term with GPS, but with GLONASS the situation is more complex. The full D-D equation is:

$$\Phi^{l}_{AB} - \Phi^{l}_{AB} = \frac{f^{l}}{c} GR^{i}_{AB} - \frac{f^{l}}{c} GR^{l}_{AB} + f^{i}\delta t_{AB} - f^{l}\delta t_{AB} + N^{l}_{AB} - N^{l}_{AB} + \varepsilon^{i}_{AB} - \varepsilon^{l}_{AB} + e^{i}_{AB} - e^{l}_{AB} \quad (4.12)$$

And with GPS, $f^{i} = f^{l}$, so Equation (4.12) collapses to

$$\Phi^{il}_{AB} = \frac{f^{i}}{c} GR^{il}_{AB} + N^{il}_{AB} + \varepsilon^{il}_{AB} \quad (4.13)$$

There remain the three coordinate difference unknowns, and an integer difference term for each satellite pair, requiring therefore a minimum of four satellites in three equations.

Success in determining the *N* terms is gauged by their proximity to integers, in association with a confidence level that is a function of measurement noise and constellation geometry. Good solutions are indicated by estimates of *N* that are very close to integers, this is the so-called *integer fixed*, *fixed*, or *fixed ambiguity* solution. Poor measurement noise levels and geometry are associated with poor confidence and estimates of *N* that are not close to integers, in this case the *N* terms are not declared as fixed, and remain as *floating point* numbers in a so-called *float* solution.

A further step can be taken by differencing double difference equations from two successive epochs, to give the *triple* difference. This adds to the benefits of a D-D by eliminating the integer ambiguity term, but leaves relatively few observations and a high noise level [Bingley, 1993]. A major benefit of the triple difference is its use in the identification of cycle slips.

For the GLONASS or Hybrid case $f^i \neq f^j$ (Figure 4.3), consequently the FDMA equivalent to Equation (4.13) is:

$$\Phi_A^i - \Phi_B^j = \frac{f^i}{c} GR_{AB}^i - \frac{f^j}{c} GR_{AB}^j + f^i \delta t_{AB} - f^j \delta t_{AB} + N_{AB}^i - N_{AB}^j + e_{AB}^{ij} \qquad (4.14)$$

Because of its multiple frequency nature this equation has no benefit relative to the S-D, since the receiver clock offset cannot be eliminated.

4.3.2.1 Cycle slips

The integer term, *N*, for a particular satellite, is a constant from epoch to epoch only whilst lock is uninterrupted. If the signal is interrupted then lock will be lost. Loss of lock can be caused for example by: microwave interference, multipath, severe ionospheric activity, large antenna acceleration, low SNR, or just plain signal blockage.

Equation (4.11), repeated below, can be used to demonstrate the mathematics of a cycle slip. Firstly Equation (4.11) is simplified by aggregating terms on the RHS, and separating the LHS into fractional carrier phase, θ, and the integer cycle count,

C, since lock, as per Equation (4.15). This represents the situation at epoch 1 prior to the occurrence of a cycle slip.

If lock is subsequently lost, and then reacquired at epoch 2, measurement of the fractional cycle resumes, but the integer cycle count will not have kept up with the change in relative position between the satellite and receiver, and so *N* must be assigned a new value, which is $N_A^i + S_A^i$, as in Equation (4.16). The *S* term is the cycle slip, also shown as $\phi_2 . \phi_1$, in Figure 4.7.

$$\Phi_A^i = \frac{f^i}{c} GR_A^i + f^i(\delta t_A - \delta t^i) + N_A^i + dIONO_A^i + dTROPO_A^i + \varepsilon_A^i + e_A^i \qquad (4.11)$$

At epoch 1 (pre-cycle slip)

$$C_A^i + \theta_A^i = Other\ terms + N_A^i \qquad (4.15)$$

At epoch 2 (post cycle slip)

$$C_A^i + \theta_A^i = Other\ terms + N_A^i + S_A^i \qquad (4.16)$$

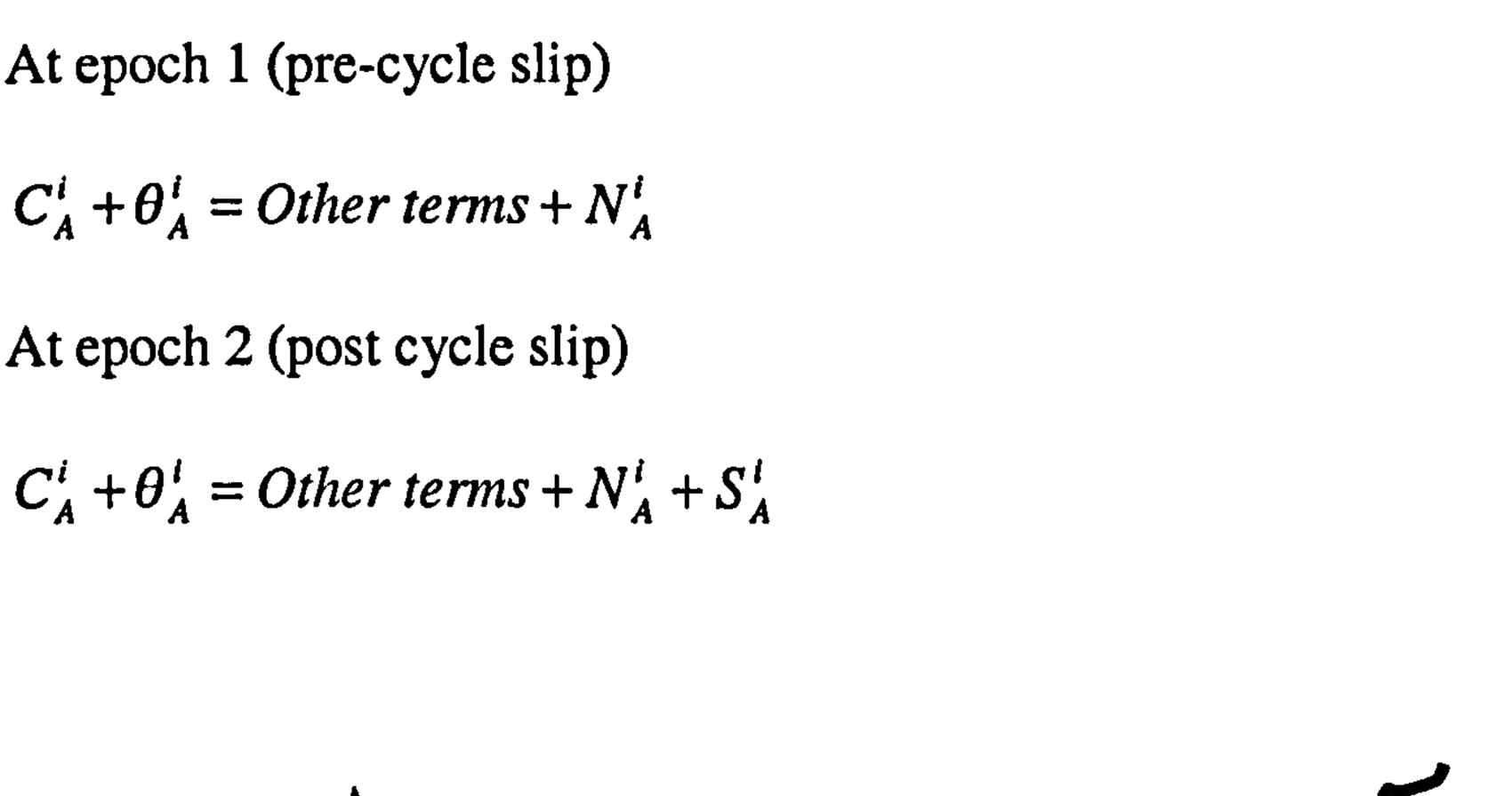

Figure 4.7 Cycle slippage

Cycle slip detection and thence correction, is based typically on the monitoring of measurement residuals output by the LSE, a slip being indicated by a spike in residuals time series.

After a cycle slip a delay can occur with reacquiring carrier phase positioning, especially in real time kinematic mode, since the ambiguous carrier cycle count must be re-established, and this may be difficult if noise levels remain elevated.

4.4 Accommodating GLONASS

Several approaches have been developed to deal with the non-cancelling receiver clock error term introduced by the multiple frequency nature of GLONASS into Equation (4.14), when using GLONASS or Hybrid observables. The most popular ploy is frequency manipulation to some common value, with all but one solution, from the receiver manufacturer Trimble, being third party software solutions.

The Trimble approach related by Povalyaev et al [1996] was hardware based in L1 Hybrid and dual frequency GLONASS-only receiver models, involving on-receiver conversion of disparate GLONASS signal frequencies to GPS L1, or GPS L1 and L2. This would seem to circumvent the problems of inter-channel bias and differential frequency. Practical evaluation on a 900 metre baseline gave measurement residuals of better than 1.5 centimetres. Both receivers have received little attention, as they are not on the open market, rather on loan for scientific purposes only [Ackroyd, 1998], for example to IGEX, see Chapter 3.

Rossbach et al [1996], ostensibly preserved the integer nature of the ambiguity terms by scaling the equations to an *auxiliary* frequency. This is the smallest common multiple of the frequencies of the satellite pair, ambiguity terms are then at a common but very small wavelength. For a pair of GLONASS satellites at the opposite ends of the L1 bandwidth, the auxiliary frequency is about 65μm, and for a Hybrid D-D the range is between 880-890 nm i.e. akin to infra-red light. For L2 the respective wavelengths are about 84μm and 2.4 nm respectively. These wavelengths are several orders of magnitude lower than achievable carrier phase resolution, it is therefore impossible to fix the ambiguities at integer values. Rather, ambiguity fixing to the nearest 1000 may be acceptable for GLONASS, or fixing to 100000s for Hybrid. An alternative is to constrain rather than restrict ambiguities. Whichever option is chosen, the resultant solution is essentially of a float rather than fixed ambiguity nature.

The auxiliary carrier frequency is determined as follows

$$\lambda^{aux} = \frac{\lambda^i}{k^i} = \frac{\lambda^j}{k^j} = \frac{c}{f^i k^i} = \frac{c}{f^j k^j} \qquad (4.15)$$

where

$\lambda^{aux,\,i,\,j}$ = auxiliary, satellite i, and satellite j signal wavelengths

$k^{i,\,j}$ = satellite specific constants

c = speed of light

For GLONASS

$$f_{L1}^i = 1602 + (n^i * 0.5625)\,MHz \qquad (4.16)$$

where

f_{L1}^i = frequency of satellite *i* on L1

n^i = *ith* GLONASS channel number

Rearranging Equation (4.16)

$$= (2848 + n^i)0.5625 \tag{4.17}$$

$$= (2848 + n^i)\Delta f_{L1} \tag{4.18}$$

and

$$= (2848 + n^i)\Delta f_{L2} \tag{4.19}$$

where

$\Delta f_{L1} = 0.5625$

$\Delta f_{L2} = 0.4375$

Taking the case with two GLONASS satellites i and j, on L1

$$\lambda^{aux} = \frac{c}{k^i(2848 + n^i)\Delta f_{L1}} = \frac{c}{k^j(2848 + n^j)\Delta f_{L1}} \tag{4.20}$$

Equality is achieved between the two RHS terms if $k^i = (2848 + n^j)$ and $k^j = (2848 + n^i)$. So, using the i satellite term as an example, gives the expression for the auxiliary wavelength and thence frequency:

$$\lambda^{aux} = \frac{c}{\Delta f_{L1}(2848 + n^i)(2848 + n^j)} \tag{4.21}$$

For the Hybrid case Equation (4.20) becomes

$$\lambda^{aux} = \frac{c}{k^i f_{L1,GPS}} = \frac{c}{k^j(2848 + n^j)\Delta f_{L1,GLN}} \tag{4.22}$$

Equality is achieved between the two RHS terms if $k^i = (2848 + n^j)\Delta f_{L1,GLN}$ and $k^j = f_{L1,GPS}$, so

$$\lambda^{aux} = \frac{c}{\Delta f_{L1,GLN}(2848 + n^i) f_{L1,GPS}} \tag{4.23}$$

A common frequency approach was also used at Nottingham by Swann [1999]. But in this case all equation components were scaled to GPS L1 frequency (only an L1 Hybrid was available). Since the *N* terms were also scaled, they lost their integer nature, and a float solution ensued.

Researchers at the University of Leeds [Walsh et al, 1996] considered the use of a GPS-only solution fixed ambiguity solution, to firstly determine *calibration* terms to GLONASS observables, then secondly including these in a Hybrid solution with GPS. Providing lock was kept on sufficient GPS satellites, then the calibration terms could be updated. If as in the case of a cluttered skyview, the number of GPS satellites fell below the minimum with sufficient geometry for some short period of time, then use of the most recent calibration values could be continued in a GLONASS dominated Hybrid solution.

A further alternative was adopted by Landau et al [1996], using GLONASS in Hybrid float mode, to reduce the time taken to arrive at a GPS-only ambiguity fixed solution. Test results on a 10 metre baseline with GPS-alone, gave the first fixed ambiguity solution after 2000 seconds, and when supported by GLONASS as above, after only 600 seconds. This provides a more cost-effective positioning solution.

Other approaches included: Pratt et al [1997] who used pre-processing at the S-D stage, by way of differential code based estimates clock error, but such estimates will however be contaminated by code level multipath and measurement noise [Swann,

1999]; and Leick et al [1995] who used a mean-frequency technique, rather than auxiliary frequency.

4.5 GLONASS Inter-channel bias

Modern receivers are predominantly digital in nature, with analogue components limited to roles of signal amplification and filtering at the receiver *front end*, prior to the digitisation stage. It is these analogue RF components that are sensitive to the variation in signal frequency intrinsic to GLONASS. This sensitivity is manifest as differential measurement delay through the receiver, the *ICBs* introduced in Chapter 3. The size of ICBs is frequency dependent, and varies with temperature. However, once the signals have left the analogue and entered the digital section of a receiver, any further delay is frequency and temperature independent. Post-digitisation on-receiver delays can be calibrated at manufacture.

ICB sensitive components exist in the antenna and receiver, as well as antenna cabling. This issue, which affects both code and carrier phase, can be dealt with through: system design to reduce sensitivity; calibration and removal; relative weighting in a Hybrid solution; or acceptance with a resultant degradation in accuracy. In a noisy urban environment however, the effects of ICBs will be swamped by the effects of multipath.

GPS avoids ICBs through the use of common and highly stable L1 and L2 frequencies across the constellation, simplifying receiver and antenna construction. Also at manufacture the receiver component specification is repeatable to a very high

degree. A high level of frequency commonality means that any frequency dependent delays are a common bias at a receiver installation, and cancel in a standard between-satellite S-D.

On the other hand GLONASS' use of FDMA leads to different delays for each satellite signal as it passes through each component of a receiver installation, which can be compounded by change in temperature, and the quality of certain receivers' components.

GLONASS measurement bias can for the Ashtech GG24, reach significant levels e.g. Gourevitch et al [1996] reported average carrier phase ICBs on a ZBL at the one to two millimetre level, for up to 5 MHz satellite signal separation, and at about the metre level for pseudorange. Calibration trials by Raby et al [1993] showed that for a pair of CAA ISN (Civil Aviation Authority Institute of Satellite Navigation) receivers plus cables and antennas at the same temperature, relative calibration values varied across the GLONASS bandwidth by about 0.2 cycles or 40 mm, with a standard deviation of about 2 millicycles or 0.4 mm. Pratt et al [1997b] found code bias of several metres, and no detectable antenna phase centre variation with frequency. And finally Blighton [1998] of Ashtech UK, quoted code and carrier ICBs as typically less than 1 metre and 8 mm respectively.

If a change in receiver operating temperature occurs, then the ICBs will change over time. Walsh et al [1996], found trends in ICB for receiver plus cable and antenna, that followed thermal change. Raby et al [1993] tested the response of a complete CAA ISN receiver installation to a temperature change of 8°C. A variation in the

total carrier phase delay of about eight millicycles (1.8 millimetres) was found, with a change of 100° C corresponding to a phase delay of about two centimetres. In response to thermal change, the antenna and cabling were found to introduce more variation in delay than the receiver components. [Dodson et al, 1999] developed this work in carrier phase relative positioning mode on a ZBL, where a between-receiver thermal offset of 25°C gave rise to a virtual baseline of up to 20 mm for the Hybrid case, and up to 30 mm for GLONASS alone, see Chapter 5 for details.

To summarise so far, it has been found that ICBs can be responsible for significant measurement and thence positioning errors. To deal with this, efforts have been made to laboratory and otherwise calibrate GLONASS capable receivers. Cooper et al [1997] suggested the use of a locally generated reference signal, as a means to internally calibrate GLONASS ICBs. This involved the injection of a locally generated carrier signal at GLONASS channel frequencies, into the RF chain and very close to the antenna. This signal would propagate through the hardware and be detected by an interference mitigation element, and the receiver would lock to the signal. The phase of this signal was then compared by a micro-processor against the known input phase, hence the delay incurred by hardware processing up to that point was determined, and could be applied as a correction to the live carrier phase. A similar type of hardware scheme has been proposed by Riley et al [1995], using a dedicated receiver channel to track a locally generated L1/L2 signal which would be switched through the set of GLONASS channels. This would allow not only real time ICB calibration, but also measurement of relative L1/L2 receiver delay variation.

Finally the use of temperature controlled components is suggested, using oven technology to maintain receivers, antennas and cables at say a constant 45°C. A complete installation calibration at the factory could then be done at one temperature. Considerations of component ageing may mean that repeat calibrations is necessary. Values could be set into an EPROM for real-time application. Meanwhile 3S Navigation [1996] have developed a temperature stabilised Hybrid L1 and L2 antenna, with 0.5°C stability, as a way to mitigate thermally induced signal delay variation.

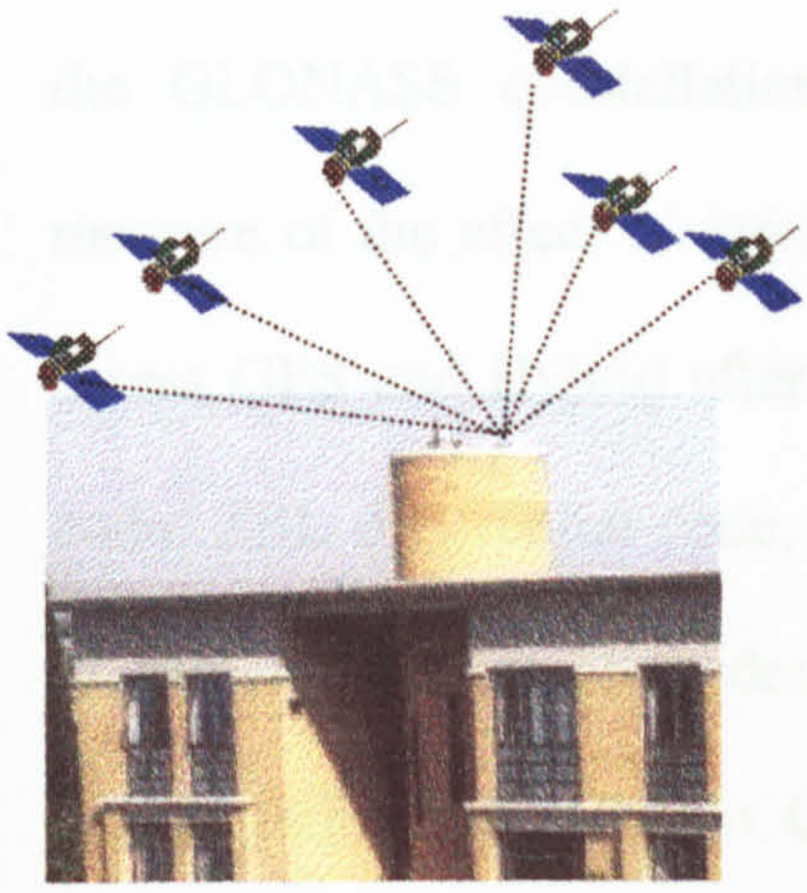

Chapter 5

Practical Static

5.1 Introduction

This chapter is concerned with the practical work of evaluating the capabilities of GPS, GLONASS and Hybrid, in static mode. *Static* is used in the sense of an immobile receiver, covering single receiver operation giving *absolute* or *stand-alone* positioning, and various modes of relative positioning on a zero baseline (ZBL).

The main purpose here is to quantify the result of propagation of error into the position domain, rather than considering individual error budget components. Absolute and ZBL modes of operation are used to characterise performance, with observations made by Ashtech GG-24 and Ashtech Z-12 receivers, from an IESSG tower point, in a clean multipath environment. This point was designated IESSG-2.

The benefit of the set of tests detailed below, carried out in Nottingham between 1997 and 2000, was to update the results of prior examinations when

the GLONASS constellation was more complete, to provide a practical measure of the effect of receiver temperature on positioning accuracy, and to assess GPS and Hybrid after SA was switched off. Analyses of stand-alone code, ZBL differential code, and ZBL relative carrier phase cases have been examined for the three modes of operation: GPS, Hybrid and, when supported by a sufficient constellation, GLONASS.

In this chapter, ZBL error components are often displayed individually in graphics, or sometimes together on a single plot. In both cases RGB (Red, Green, Blue) colour coding has been adopted. Thence Red, Green, Blue correspond to Northing, Easting and Height errors.

5.2 Stand-alone C/A code

The effects of errors such as GPS's SA and the ionosphere, on measurements made by a single receiver, may be reduced through a long term observation campaign. Test results discussed here are mostly based on 24 hour continuous logging sessions with Ashtech GG-24 receivers. There are two types of result, either the receiver's own instantaneous solution, referred to as *autonomous positioning,* or *post-process,* computed using raw data with offline software after the event.

Both types of result are termed the Observation, or simply O, and the known point coordinates as the Truth or simply T. Wherever a positioning component

error is quoted below, it should be taken to mean *Truth* minus *Observation*, or $T - O$, as defined above.

Three methods were used to process the data.

- On-receiver *autonomous* position output to a logging PC.
- Raw pseudorange *post-processing* by AOSS (Ashtech Office Suite for Survey).
- Raw pseudorange *post-processing* by GAS (GPS Analysis Software).

Results were analysed with respect to recoverability of the known station coordinates. Findings in two-dimensional positioning were in general agreement with prior investigations using Ashtech GG-24s e.g. Hall et al [1997] and with contemporaneous GG-24 data supplied on a daily basis, by for example the Lincoln Laboratory at the MIT (Massachusetts Institute of Technology) web site. Positions and errors at MIT were computed using independent software. The IESSG and MIT results shared an anomalous height behaviour, this is discussed in §5.2.1.

Table 5.1 provides an initial overview of *autonomous* performance, over 24 hours, at a 15-second logging interval, with at least four satellites. The default receiver settings were used, which meant that ionospheric corrections were not applied. The same results with a maximum PDOP of 2 applied are in Table 5.1a, this allows performance to be compared on the basis of fix geometry of a common quality. *Number epochs* indicates the number of epochs for which position solutions existed. Mean error values for these populations are followed by standard deviation in brackets.

The geometry-limited epoch counts in Table 5.1a, for GLONASS, highlights the run down state of the constellation, showing a capability almost three times worse than GPS. Also GLONASS plan position estimates (Table 5.1a) are less accurate than either GPS or Hybrid, but accumulation precision is comparable with Hybrid and much improved over that of GPS. This superiority is attributed to SA not being used by the Russians. As previously noted, SA was switched off in May 2000, affecting the performance of GPS (§5.2.1) and Hybrid (§5.2.2). Comparison of performance before SA removal, Table 5.1, and after, Table 5.2, shows improvements in error spread by factors of about 10 and 4, for GPS and Hybrid respectively.

Mode	Day of month	Max sats	Number epochs	Max PDOP	East error (m)	North error (m)	Height error (m)
GPS	05	11	5833	3.0	-0.4 (15.7)	-1.9 (20.4)	-23.5 (34.3)
Hybrid	02	18	5777	2.6	1.8 (11.5)	-0.7 (11.5)	-19.1 (21.9)
GLONASS	10	7	5013	39.3	13.8 (47.3)	10.2 (73.0)	-11.3 (35.7)

Table 5.1 Autonomous C/A error July 1998 with SA on, no ionospheric corrections applied (24.3 hours at 15 sec. epoch)

Mode	Day of month	Max sats	Number epochs	Max PDOP	East error (m)	North error (m)	Height error (m)
GPS	05	11	4751	2	-0.4 (15.3)	-2.0 (18.8)	-23.8 (31.1)
Hybrid	02	18	5586	2	1.5 (10.9)	-0.6 (11.2)	-19.5 (20.9)
GLONASS	10	7	1724	2	3.5 (11.5)	-4.5 (9.7)	-25.3 (28.8)

Table 5.1a Autonomous C/A error July 1998 with SA on, PDOP ≤ 2, no ionospheric corrections applied (24.3 hours at 15 sec. epoch)

Mode	Day of month	Max sats	Number epochs	Max PDOP	East error (m)	North error (m)	Height error (m)
GPS	16	11	1376	3.6	-0.1 (1.5)	-1.1 (2.2)	-19.4 (5.1)
GPS	19	12	1440	3.1	0.0 (1.7)	-0.9 (2.6)	-20.9 (4.7)
Hybrid	17	17	1440	3.1	1.2 (3.3)	-0.9 (3.8)	-19.8 (10.1)
Hybrid	20	17	1440	2.9	0.8 (4.9)	-2.1 (8.3)	-19.0 (11.4)

Table 5.2 Autonomous C/A error May 2000 with SA off, no ionospheric corrections applied (24 hours at 60 sec. epoch)

Performance of autonomous GPS, Hybrid, and GLONASS mode are now discussed further.

5.2.1 GPS

A graphic representation of GPS plan error, shown in Figure 5.5, for 5th July 1998, exemplifies the typical spiralling and looping trail of a stand-alone position under the influence of SA [Hein et al, 1997]. SA typically causes stand-alone positioning to wander at speeds of up to 10 $km.h^{-1}$, and on average at about 0.8 $km.h^{-1}$. This error is reflected in the sinusoidal character of the height error time series in Figure 5.3. Height accuracy is relatively weak, as it is less well determined than the plan dimension because all measurements are from above the horizon. Discontinuities can be seen in these time series, confirmed as caused by changes in constellation.

Figure 5.4 shows the accumulated mean plan error components converging towards zero over 24-hours, with plan coordinate recoverability at the one to two metre level for daily averaging under conditions of SA. Height error on the other hand, converged on average to about -18 metres i.e. the pseudoranges were apparently too short. This situation can also be seen in error frequency distributions in Figure 5.6, which shows that plan components are normally distributed, whereas the height element is skewed.

This sign of the height error does not agree with signal propagation theory, in that atmospheric delay should elongate pseudoranges, depressing the height

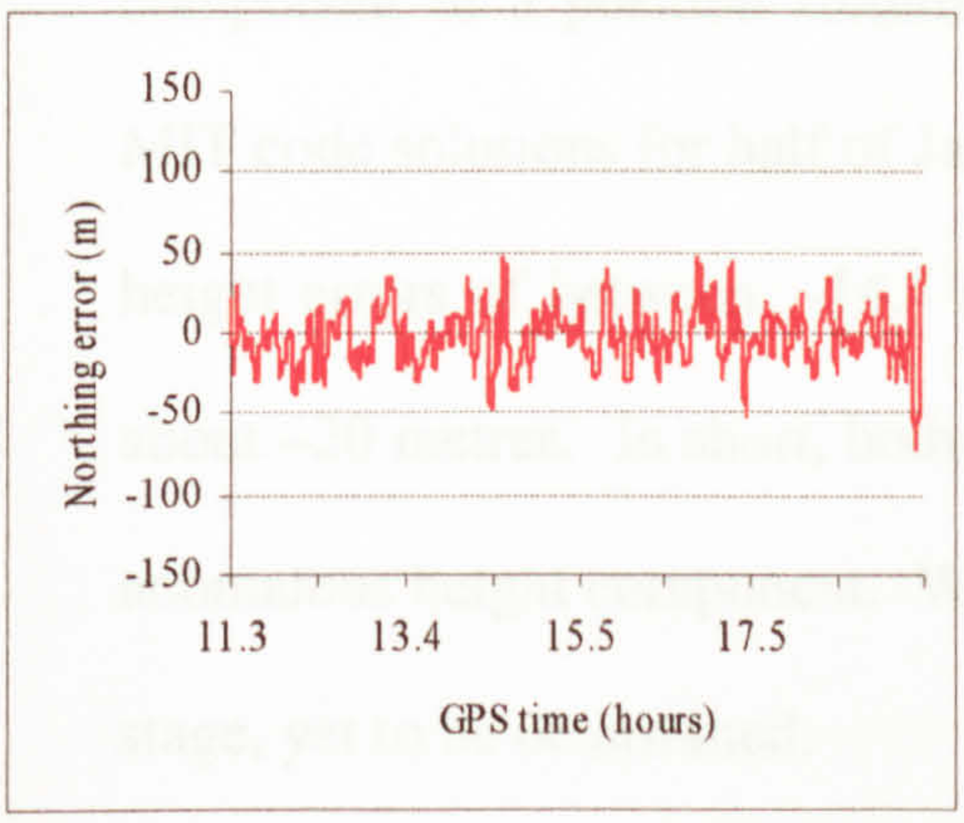

Figure 5.1
Stand-alone GPS Northing error

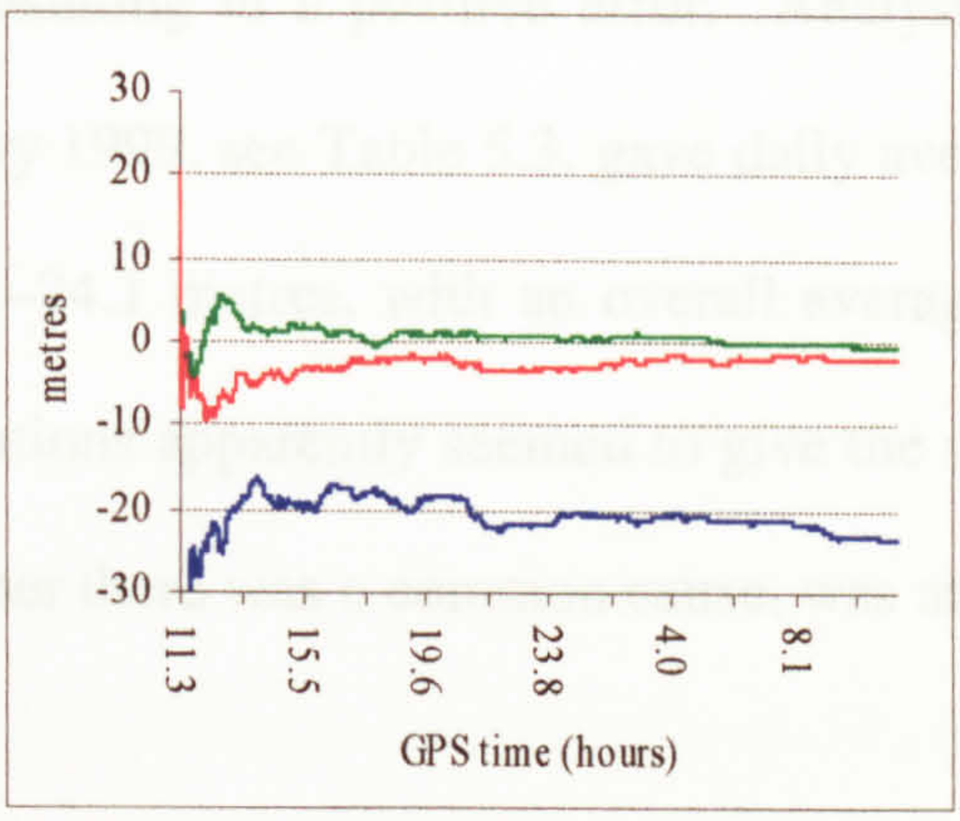

Figure 5.4
Cumulative average stand-alone GPS error components

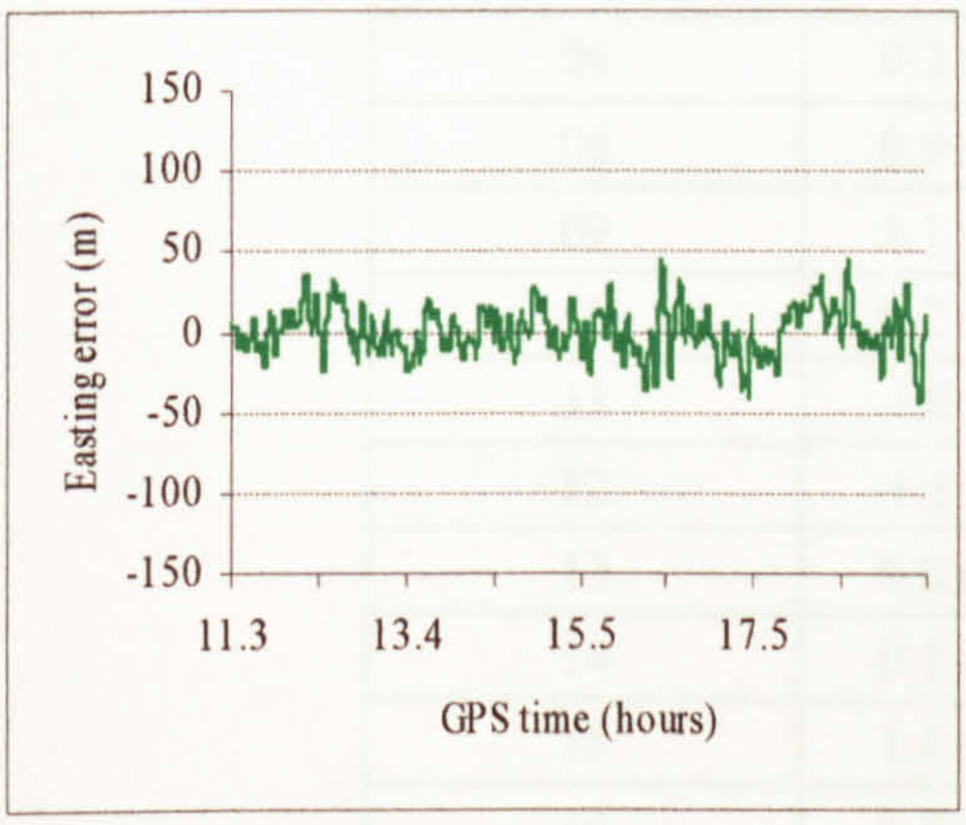

Figure 5.2
Stand-alone GPS Easting error

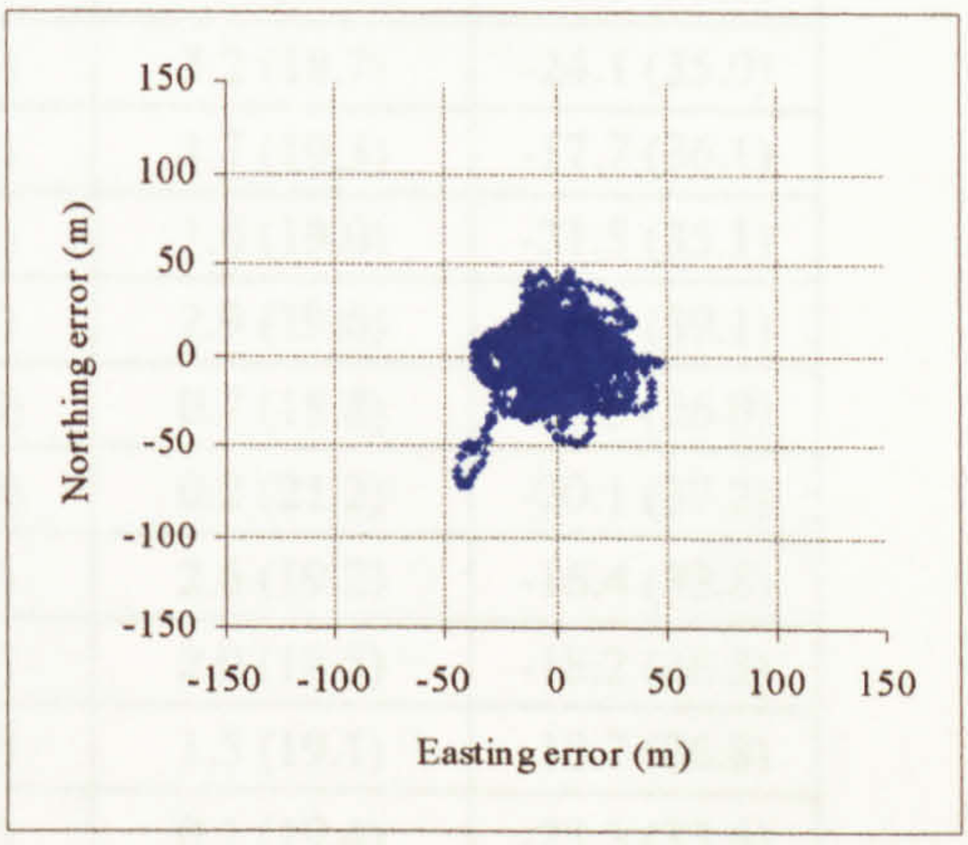

Figure 5.5
Stand-alone GPS plan error

Figure 5.3
Stand-alone GPS height error

Figure 5.6
Stand-alone GPS error frequency
(Five metre bin size)

component of a position solution, resulting in a positive error. Analysis of MIT code solutions for half of January 1999, see Table 5.3, gave daily average height errors of between -14.4 and –24.1 metres, with an overall average of about –20 metres. In short, both solutions apparently seemed to give the same anomalous height component. Whether there was a common cause, was at that stage, yet to be determined.

Day | Error	Easting (m)	Northing (m)	Height (m)
03	0.1 (14.3)	-0.4 (19.0)	-21.7 (36.0)
04	0.3 (14.2)	3.2 (18.7)	-24.1 (35.0)
06	0.9 (15.2)	1.7 (19.3)	-17.7 (36.1)
09	1.1 (14.6)	1.6 (19.0)	-21.5 (35.1)
10	0.2 (14.8)	2.9 (19.6)	-14.4 (39.1)
11	-1.8 (15.0)	0.7 (18.8)	-20.5 (36.0)
12	-1.1 (17.5)	0.2 (21.2)	-20.1 (37.2)
13	0.6 (14.7)	2.6 (19.2)	-16.4 (33.8)
14	0.1 (14.6)	2.0 (18.5)	-18.2 (36.3)
15	1.4 (14.8)	1.5 (19.1)	-18.7 (36.8)
16	0.8 (14.4)	0.1 (19.4)	-23.3 (33.6)
17	0.9 (15.3)	2.4 (20.2)	-22.0 (37.7)
Average	0.3	1.5	-19.9

Table 5.3 MIT stand-alone GPS C/A error January 1999

Whilst Ashtech and MIT were exploring this anomaly, further investigative work was done at the IESSG. Firstly the receiver was run for three further 24 hour sessions with the on-receiver Klobuchar-type ionospheric model enabled. Autonomous results, in Table 5.4, demonstrated that this option was quite effective and repeatable at mitigating the ionospheric delay, with mean height errors of less than 5 metres.

As part of the investigation, it was also considered important to establish whether the use of the on-receiver ionospheric model option had any effect on the raw measurement data. To this end a ZBL was observed, with one receiver operating with ionospheric modelling enabled and the other without. If subsequent processing of the two sets of raw code data gave the same height component results, then it could be said that that the ionospheric model option had no effect on raw data. AOSS was used to accumulate single point code phase solutions for each receiver. Mean height errors with ionospheric modelling applied, were –1.4 and –2.4 metres, suggesting that the on-receiver model option had no effect outside that on autonomous operation.

Day | Error	Easting (m)	Northing (m)	Height (m)
13	-0.1 (14.6)	1.4 (19.1)	1.5 (34.9)
14	-0.1 (16.4)	-0.8 (19.4)	2.8 (35.0)
18	0.3 (14.8)	-3.5 (18.9)	3.4 (34.0)
Average	0.0	-1.0	2.6

Table 5.4 IESSG stand alone GPS C/A error January 1999, ionospheric corrections enabled

Finally, comparison was made between cumulative height estimates by GAS and AOSS processing of raw code data, for 18 hours of data from August 1998. The difference in accumulated height was 0.8 metres, with height estimates much closer to zero, typically between zero and – 10 metres, again suggesting the receiver autonomous height solution was erroneous.

MIT later confirmed that an error in their own processing software had caused atmospheric models to be applied twice, thus giving rise to the negative height

component errors at their web site. With this rectified cumulative height estimates were close to zero, see Burke [1999]. For example for the 7th February, the cumulative average Easting, Northing and Height errors were – 0.7, 2.3, and 0.3 metres respectively.

The anomalous height component output by the Ashtech GG-24 remained unresolved at the time of writing.

It has already been stated that SA was switched off in May 2000, on the 2nd at about 04:05 AM in fact. Evidence of stand-alone performance shows the dramatic change in accuracy at the transition point, see Table 5.4a and Figure 5.13.

2nd May 2000	95% error	
Time span	Plan (m)	Height (m)
00:00 – 04:05	66	109
04:05 – 08:10	5.2	12

Table 5.4a Autonomous GPS C/A code error at the SA on/off transition
(adapted from GIM International Vol.14, No.6)

A post-SA autonomous 24 hour logging session at the IESSG produced results depicted in Figures 5.7 to 5.12. Whilst taking note of the change in scale between sets of figures, compare these with results under SA in Figures 5.1 to 5.6, all position error components are severely damped, and accumulations become close to steady state relatively quickly. Standalone accuracy is now dominated by atmospheric and multipath induced errors, both of which vary with time and place.

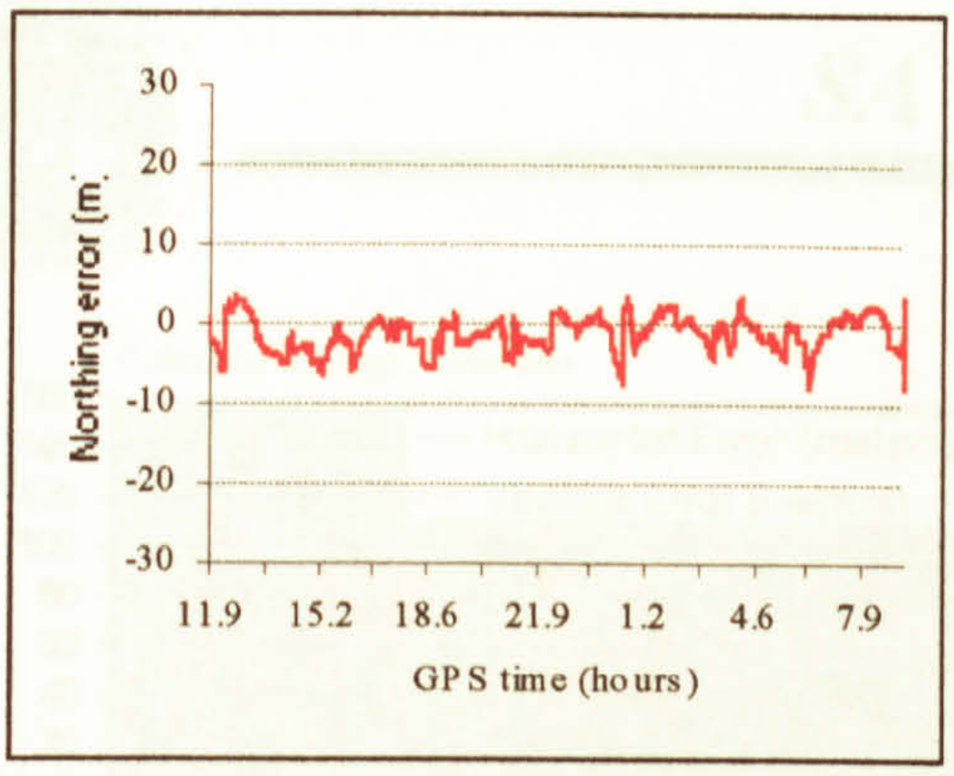

Figure 5.7
Stand-alone GPS Northing error, post-SA

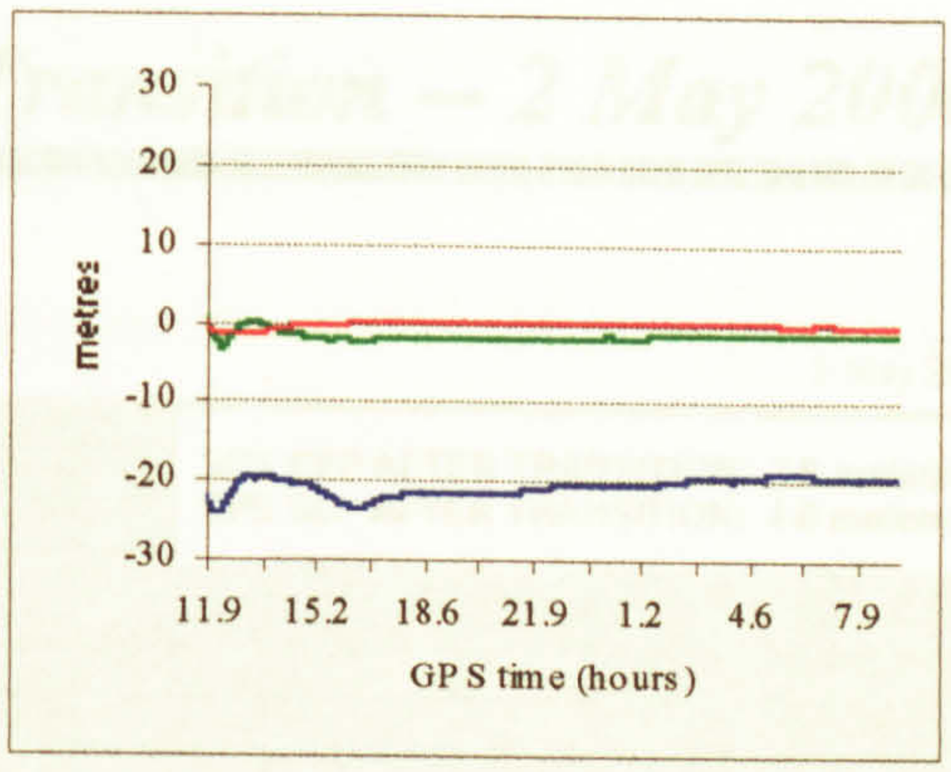

Figure 5.10
Cumulative stand-alone GPS error components, post-SA

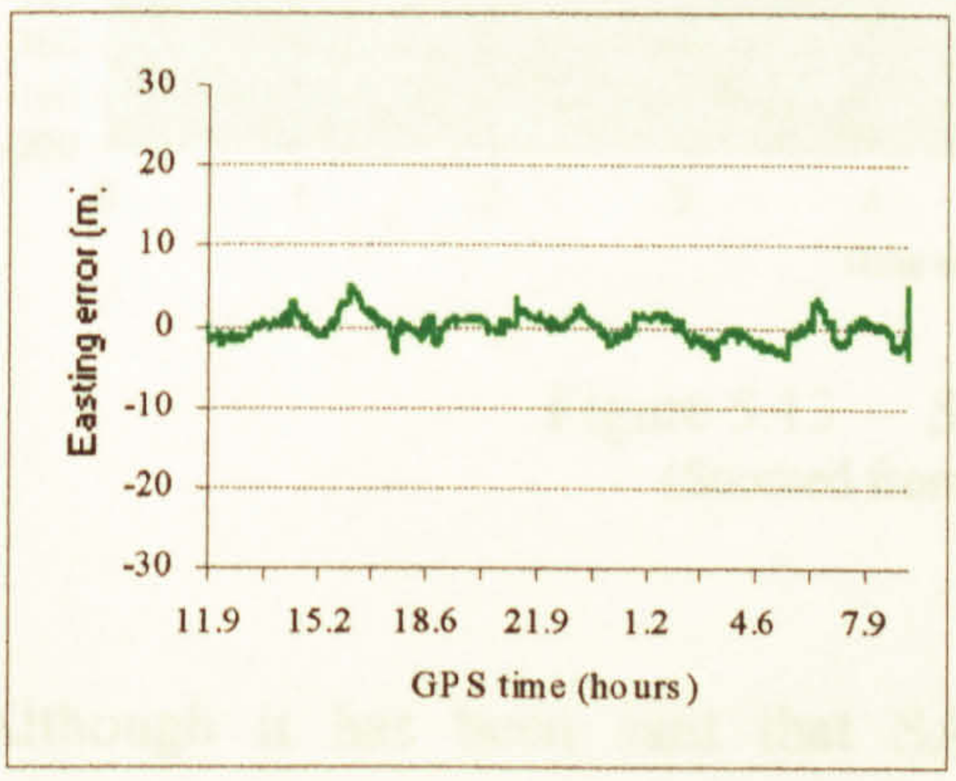

Figure 5.8
Stand-alone GPS Easting error, post-SA

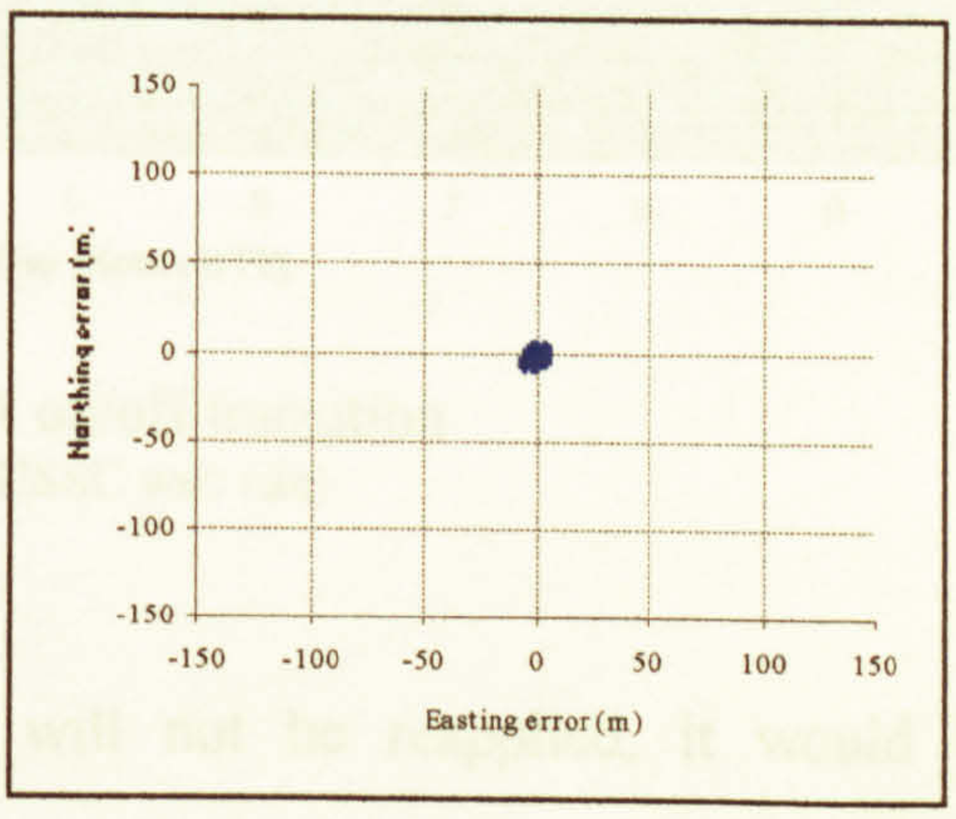

Figure 5.11
Stand-alone GPS plan error, post-SA

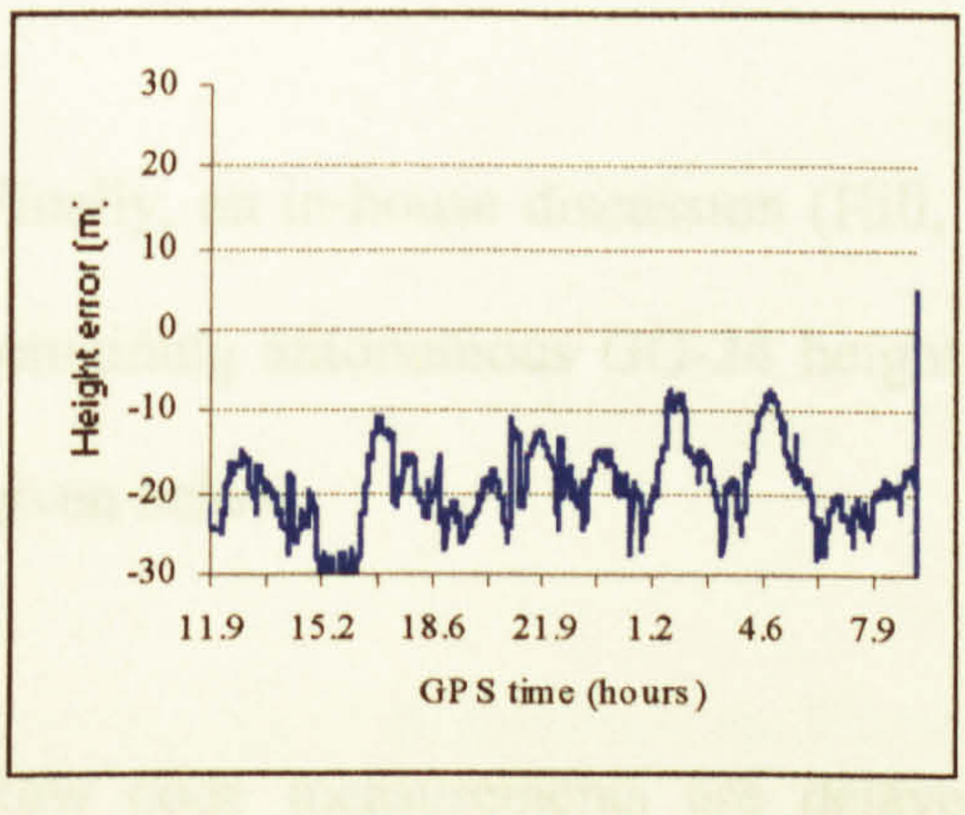

Figure 5.9
Stand-alone GPS Height error, post-SA

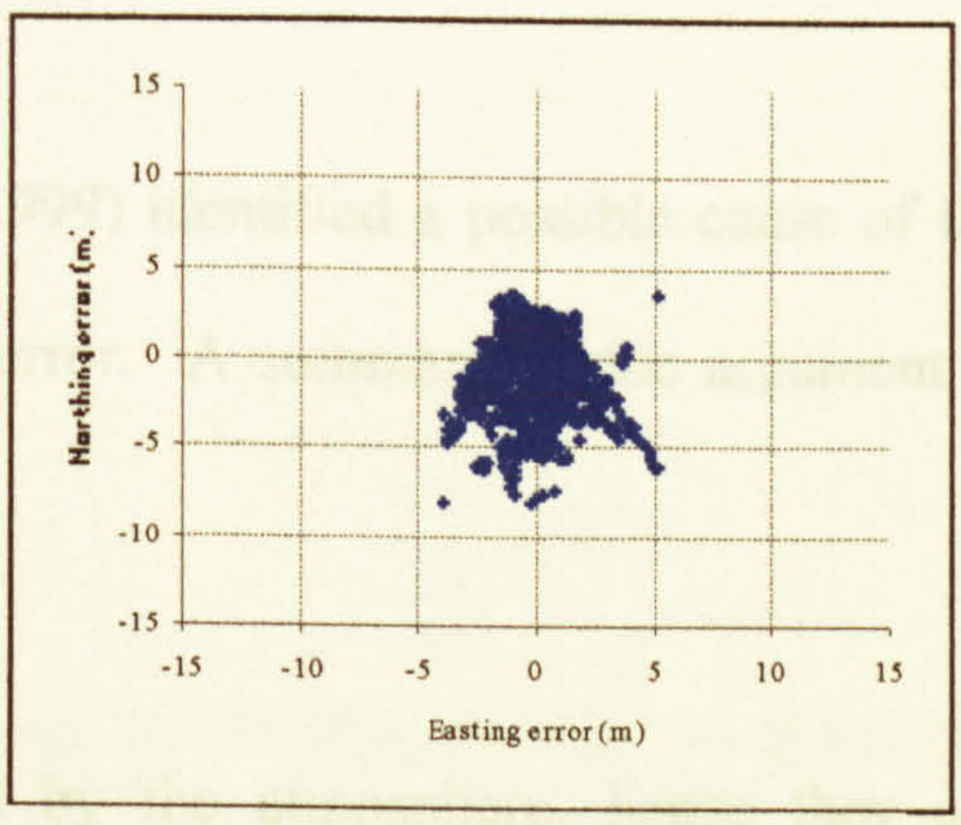

Figure 5.12
Stand-alone GPS plan error, post-SA (Large scale view of Figure 5.11).

SA Transition -- 2 May 2000

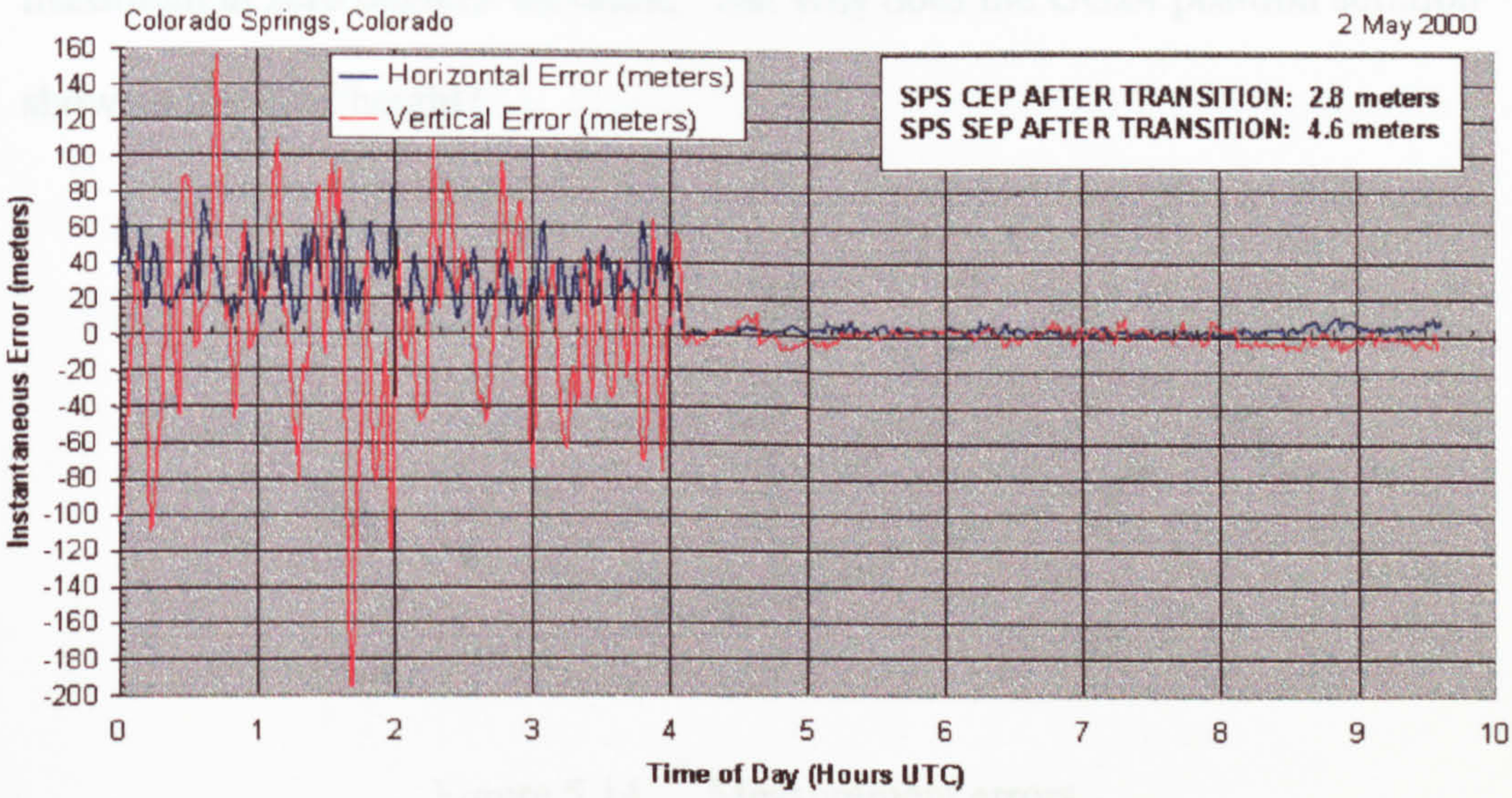

Figure 5.13 SA on/off transition
(Sourced from USSC web site)

Although it has been said that SA will not be reapplied, it would be circumspect to remain prepared for its effects, as GPS remains a military controlled system.

Finally, an in-house discussion (Hill, 1999) identified a possible cause of the remaining autonomous GG-24 height error. A summary of the argument is given below.

Raw code measurements are delayed by the atmosphere, hence they are elongated, and it might be expected that the height element of a resultant solution would be depressed. The magnitude of this delay is elevation dependent i.e. in the direction of the observer's or antenna's zenith the minimum signal path and hence delay through the atmosphere occurs.

However as the line of sight to a satellite approaches the local horizon then the proportion of the signal path passing through the atmosphere increases to a maximum at zero degrees elevation. But why does the GG24 position solution show an elevated height?

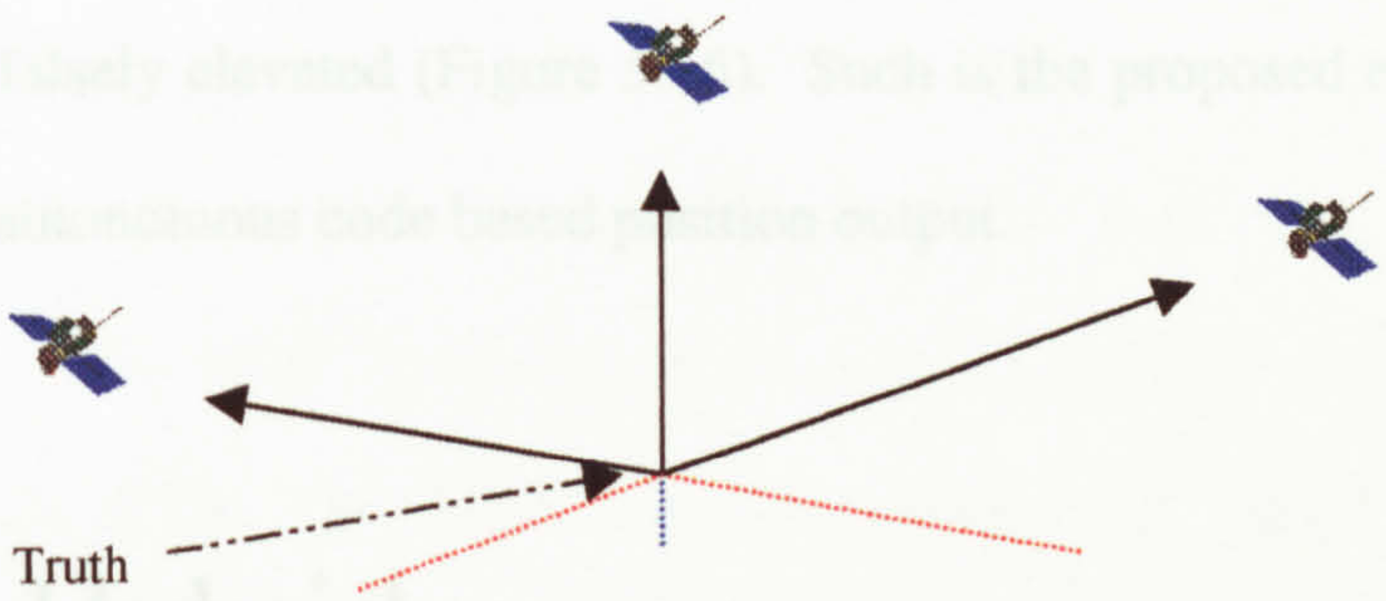

Figure 5.14 Measurement errors

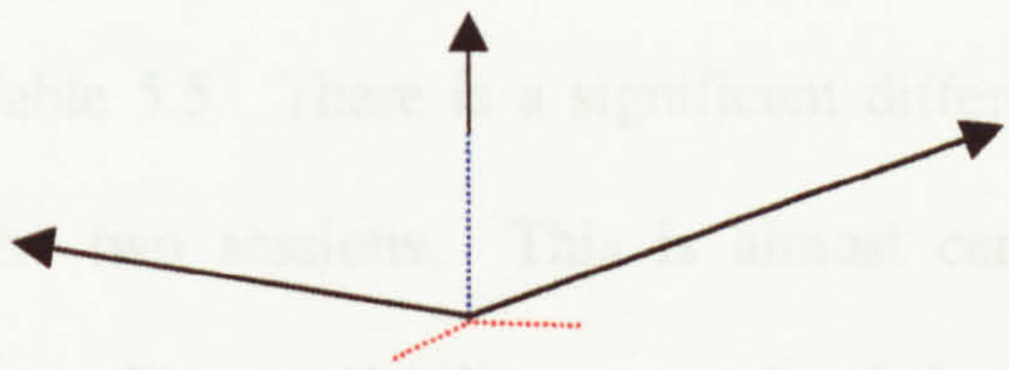

Figure 5.15 Measurements corrected for mean apparent clock error

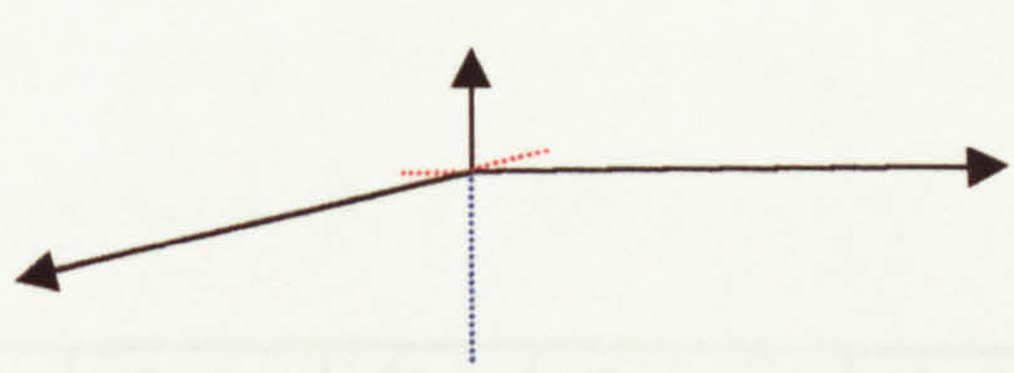

Figure 5.16 The effect on height

If no corrective atmospheric models are applied then the measurements will not fit together well (Figure 5.14) and the receiver will see the mean delay (or residual) as a clock error and apply this to all observations. With normal geometry the residuals are dominated by the larger atmospheric delays at low elevation (Figure 5.14), so when the receiver computes the clock error this will

also be dominated by large (mean) delays. Applying such a mean clock error pushes back all measurements by the same amount (Figure 5.15). Under conditions of generally acceptable geometry quality, the 2-D position is affected relatively little as it slides up and down the direction line from antenna to the constellation centroid, however height is affected to a much higher degree and is falsely elevated (Figure 5.16). Such is the proposed explanation of the GG-24 autonomous code based position output.

5.2.2 Hybrid

Two autonomous SA contaminated Hybrid sessions were logged in July 1998, results are given in Table 5.5. There is a significant difference in the mean plan error between the two sessions. This is almost certainly caused by changing GLONASS satellite availability across its 8-day repeat geometry cycle. Error spreads remain similar over time, under the dominant influence of SA.

Mode	Day	Max sats	Number epochs	Max PDOP	East error (m)	North error (m)	Height error (m)
Hybrid	02	18	5777	2.6	1.8 (11.5)	-0.7 (11.5)	-19.1 (21.9)
Hybrid	17	15	5760	3.0	2.6 (10.4)	-4.6 (10.6)	-20.0 (17.6)

Table 5.5 Autonomous C/A code error July 1998 with SA on (24 hours at 15 sec. epoch)

Hall et al [1997] quote 2D 95% error for GPS and Hybrid of 44 and 16 metres respectively. However the latter figure was derived with a GLONASS constellation of twenty one satellites. Compare this with a GLONASS

constellation of 14 satellites as in Table 5.5, with a 2D 95% error of about 32 metres for the Hybrid case. So a lesser GLONASS content equates to a lesser accuracy. Hall et al [1997] also quote 95% 2D velocity error, of 0.4m.s^{-1} for GPS and 0.07m.s^{-1} for Hybrid.

Continuing with the practical Hybrid case, Hybrid dispersion about the known point, see Figure 5.21, is much improved relative to the GPS case, though it is evident even at this small scale that inclusion of GLONASS serves only to damp the effects of SA. The Hybrid error time series for 2nd July, Figures 5.17 to 5.19, also show a relatively amplitude-damped nature, with evidence of some longer wavelength error components materialising above the noise, particularly noticeable in Figure 5.17. The latter could be caused by failure to fully address ionospheric effects.

Comparison of cumulative error components for GPS in Figure 5.4 with Hybrid in Figure 5.20, reveals likely GLONASS-specific effects, such as ephemeris, satellite clock, and poorer measurement resolution, propagating into the Hybrid solution. As a result, convergence to a steady state takes significantly longer time than in the GPS case.

Considering fix dispersion, Hybrid provides at mid-1998, a factor of improvement over GPS of about 2 with an unlimited PDOP, see Table 5.1, which is shown graphically in a comparison between Figures 5.6 and 5.22. In earlier days, when the GLONASS constellation was more complete, an improvement factor of about five was found, see e.g. Hall et al [1997] and

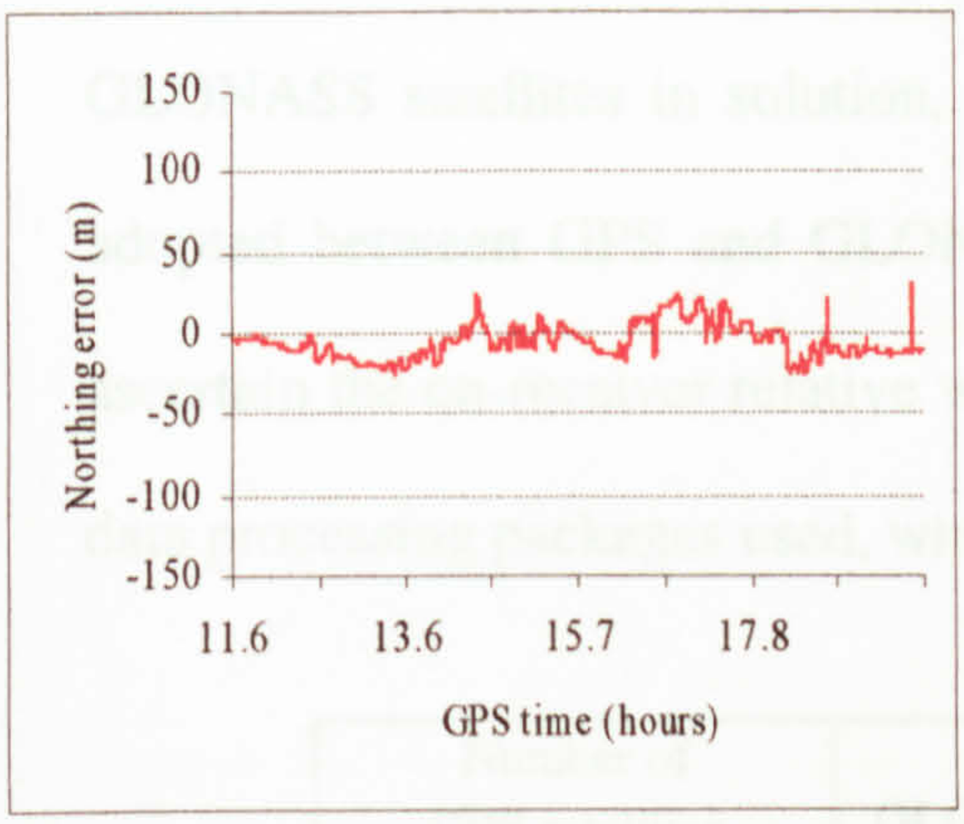

Figure 5.17
Stand-alone Hybrid Northing error

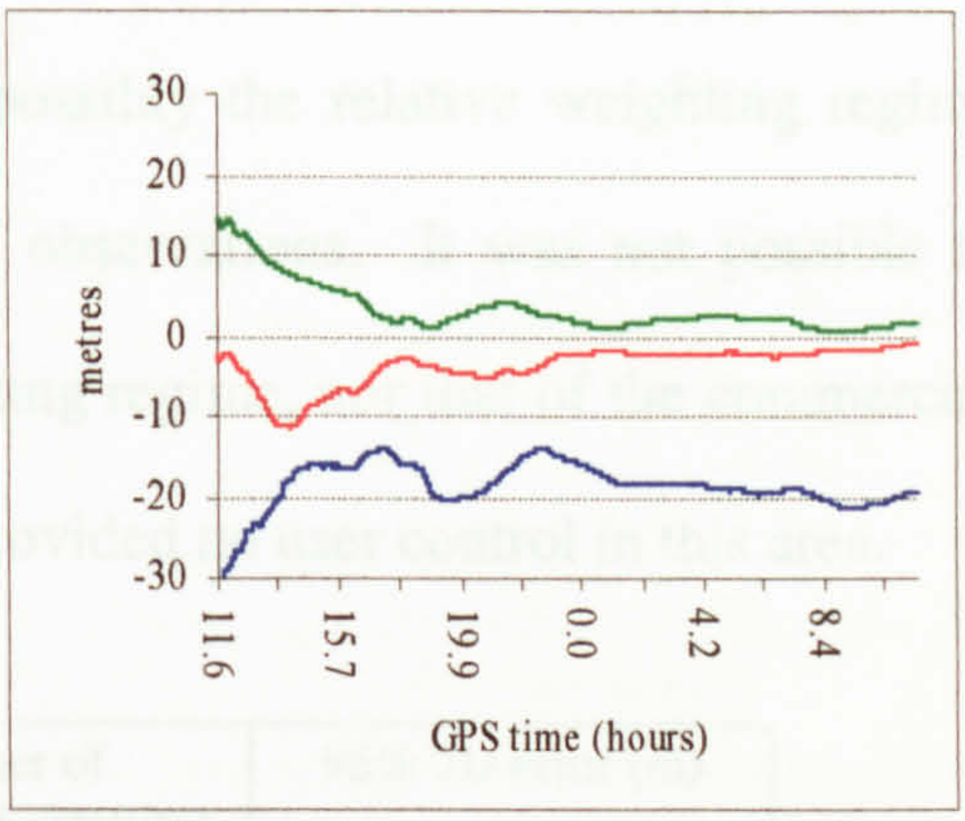

Figure 5.20
Cumulative average stand-alone Hybrid error components

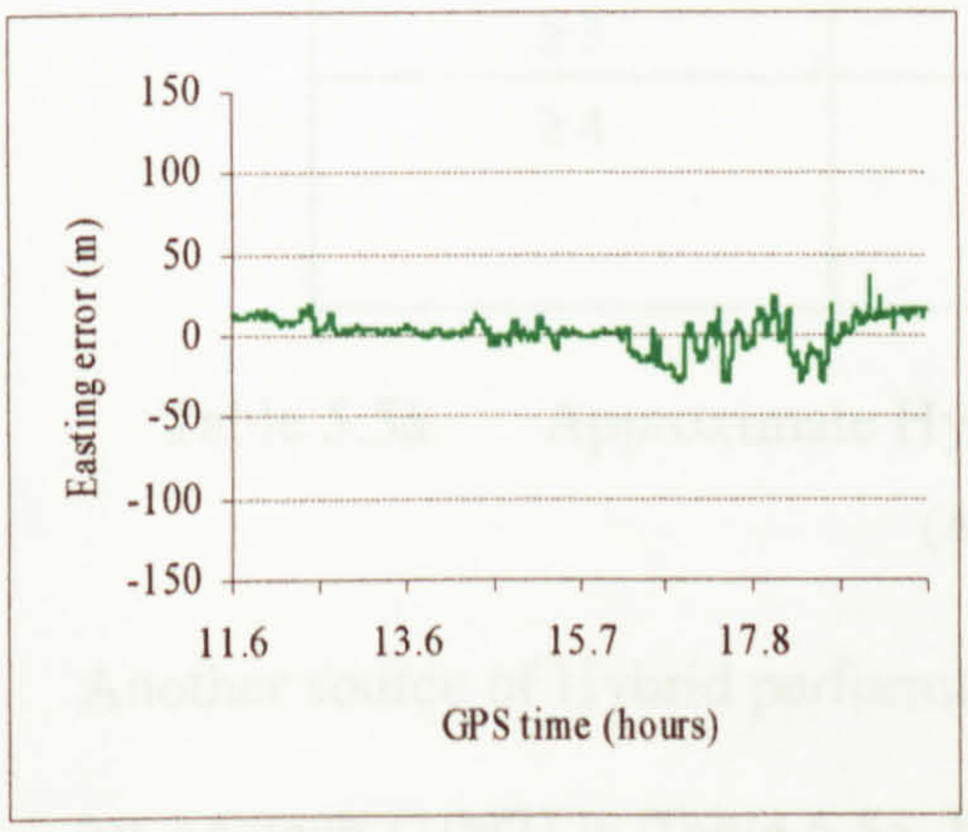

Figure 5.18
Stand-alone Hybrid Easting error

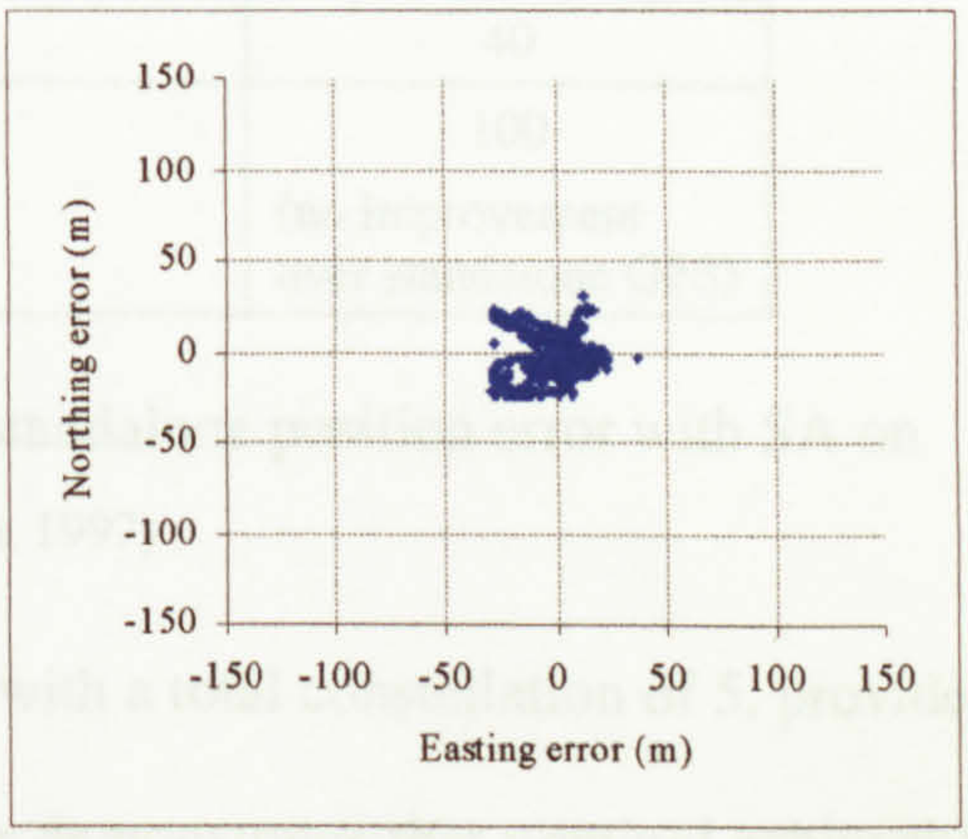

Figure 5.21
Stand-alone Hybrid plan error

Figure 5.19
Stand-alone Hybrid height error

Figure 5.22
Stand-alone Hybrid error frequency
(Five metre bin size)

Misra et al [1996b]. The factor of improvement is a function of the number of GLONASS satellites in solution, and possibly the relative weighting regime adopted between GPS and GLONASS observations. It was not possible to ascertain the on-receiver relative weighting regime, nor that of the commercial data processing packages used, which provided no user control in this area.

Number of GPS satellites	Number of GLONASS satellites	95% 2D error (m)
≥ 0	≥ 5	16
≥ 1	4	20
≥ 2	3	30
≥ 3	2	40
≥ 4	1	100 (no improvement over standalone GPS)

Table 5.5a Approximate Hybrid standalone position error with SA on (Ashtech, 1997)

Another source of Hybrid performance, with a total constellation of 5, provided by Ashtech [1997] in Table 5.5a, further demonstrates that *nominal* achievable Hybrid accuracy is improved with an increasing number of healthy GLONASS satellites in solution, given here with an HDOP close to unity.

Finally, actual Hybrid performance achieved with SA off, together with that for GPS for reference, is listed in Table 5.2 (repeated below) and shown in Figures 5.23 to 5.28. It can be seen that long term average Hybrid and GPS errors are similar, in plan ranging from 0.9 to 2.2 metres, but the Hybrid standard deviation for all dimensions is greater by a factor of two over GPS, the reverse of the SA case. Scatter plots (note the change in scale) for GPS in Figure

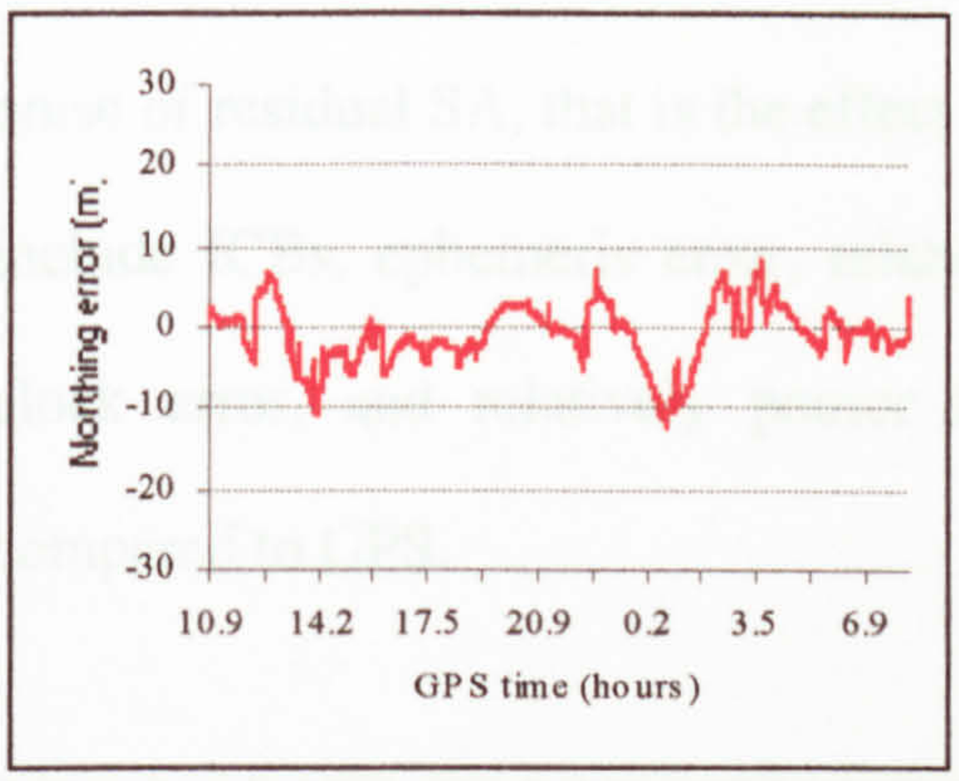

Figure 5.23
Stand-alone Hybrid Northing error (post-SA)

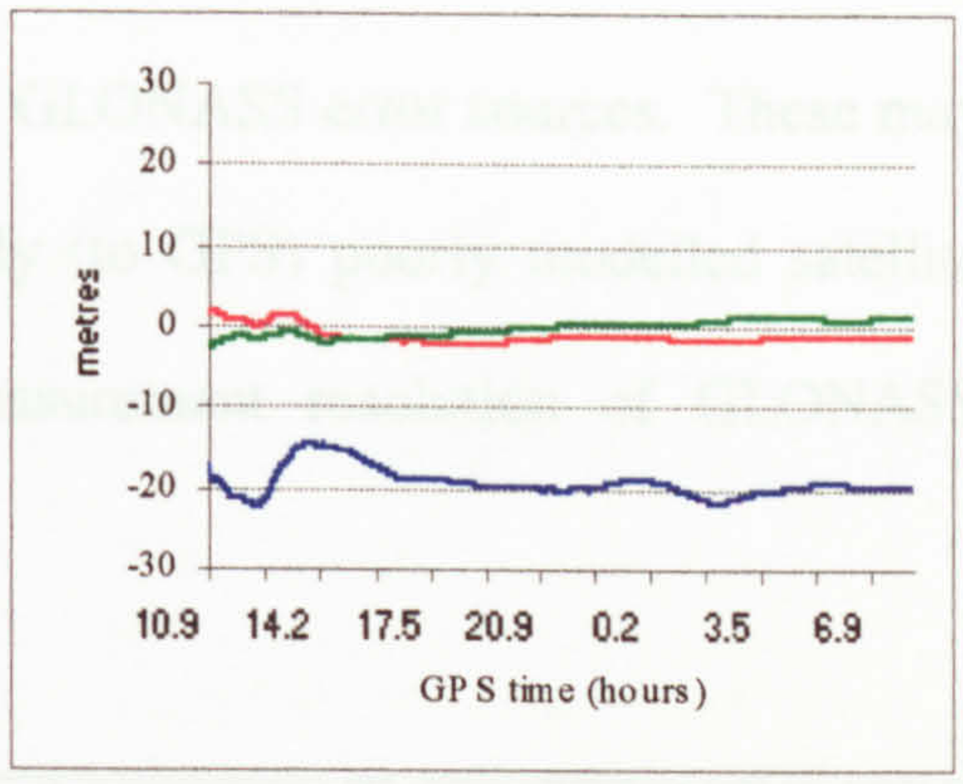

Figure 5.26
Cumulative stand-alone Hybrid error components (post-SA)

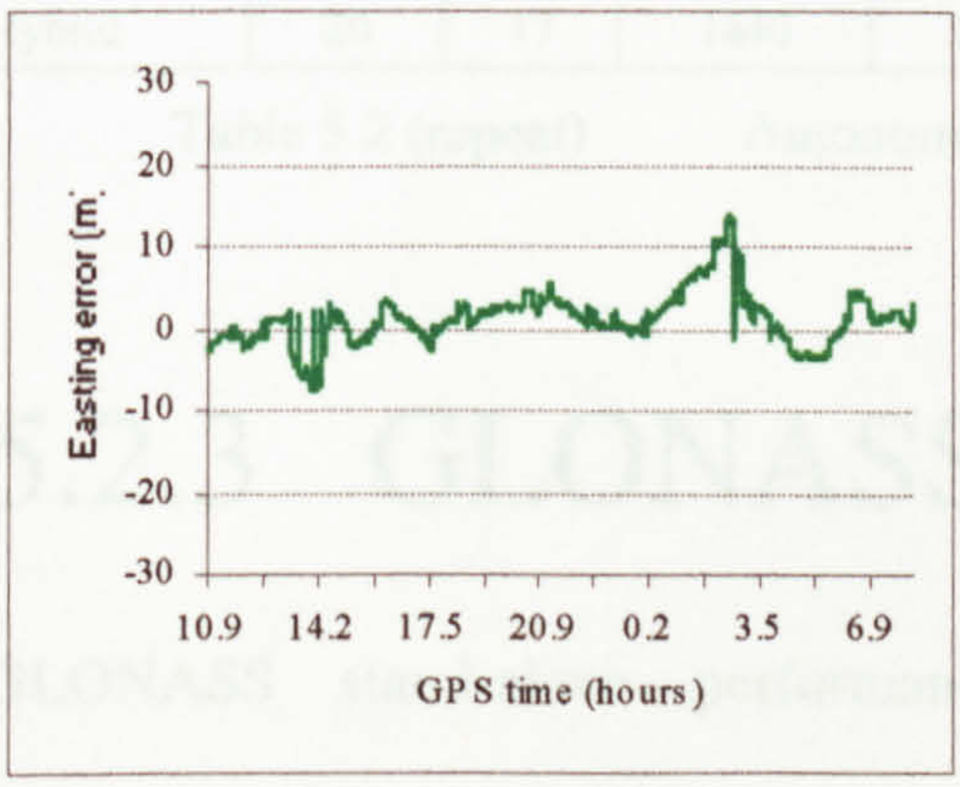

Figure 5.24
Stand-alone Hybrid Easting error (post-SA)

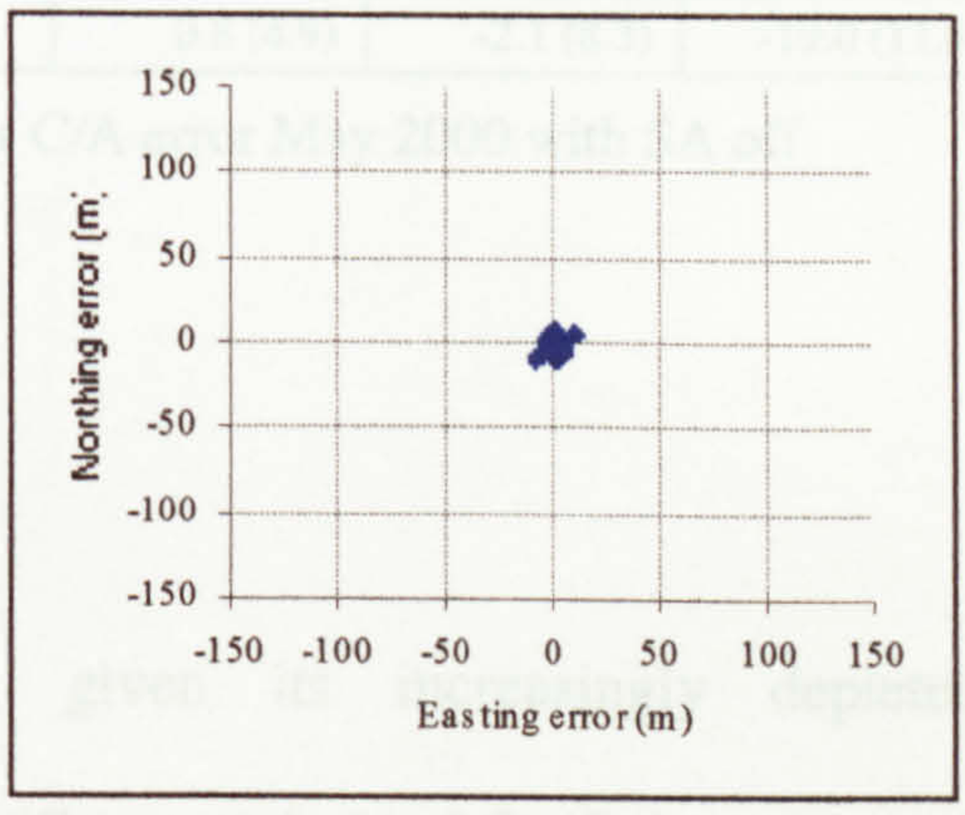

Figure 5.27
Stand-alone Hybrid plan error (post-SA)

Figure 5.25
Stand-alone Hybrid Height error (post-SA)

Figure 5.28
Stand-alone Hybrid plan error (post-SA). (Large scale view of Figure 5.27).

5.12, and Hybrid in Figure 5.28, reveal what was hitherto hidden beneath the noise of residual SA, that is the effect of GLONASS error sources. These may include ICBs, ephemeris error, relatively (to GPS) poorly modelled satellite clock error, and relatively poorer measurement resolution of GLONASS compared to GPS.

Mode	Day of month	Max sats	Number epochs	Max PDOP	East error (m)	North error (m)	Height error (m)
GPS	16	11	1376	3.6	-0.1 (1.5)	-1.1 (2.2)	-19.4 (5.1)
GPS	19	12	1440	3.1	0.0 (1.7)	-0.9 (2.6)	-20.9 (4.7)
Hybrid	17	17	1440	3.1	1.2 (3.3)	-0.9 (3.8)	-19.8 (10.1)
Hybrid	20	17	1440	2.9	0.8 (4.9)	-2.1 (8.3)	-19.0 (11.4)

Table 5.2 (repeat) Autonomous C/A error May 2000 with SA off

5.2.3 GLONASS

GLONASS stand-alone performance, given its increasingly depleted constellation, is predictably poor for significant periods of the 8-day geometry repeat cycle, with major changes in availability from day to day, and within each day. This is confirmed by autonomous results from 10th July 1998, presented in Figures 5.29 to 5.34. These GLONASS data were acquired with the same geometry as the Hybrid case, in Figures 5.17 to 5.22.

The GLONASS time series contain six intervals, varying from 7 to 86 minutes when no solution was generated, and for an unknown reason one interval of 14 minutes no satellite signals were received at all. These outages were caused either by the PDOP limit being exceeded (> 40) and/or less than 4 satellites

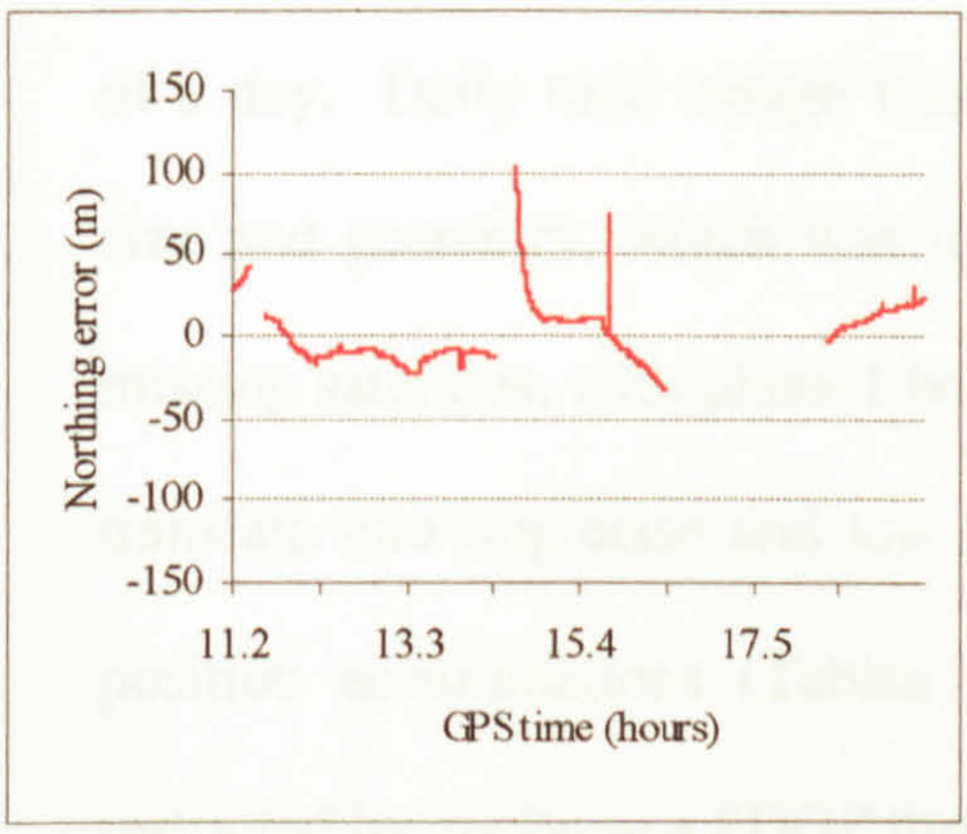

Figure 5.29
Stand-alone GLONASS Northing error

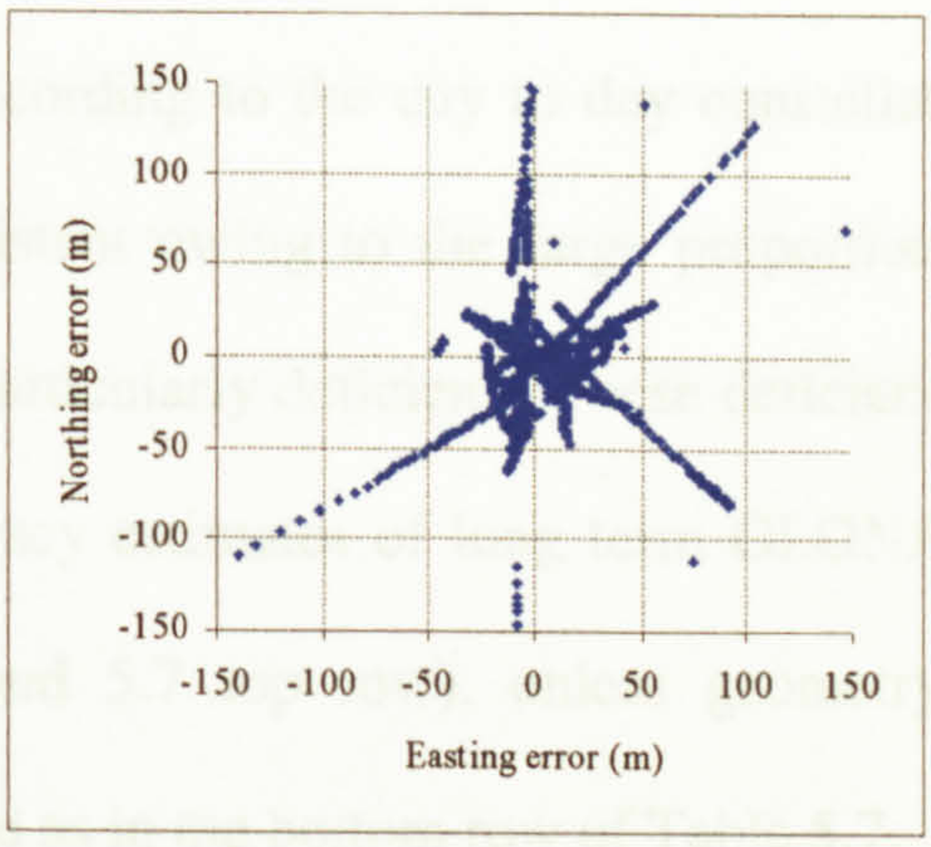

Figure 5.32
Stand-alone GLONASS plan error

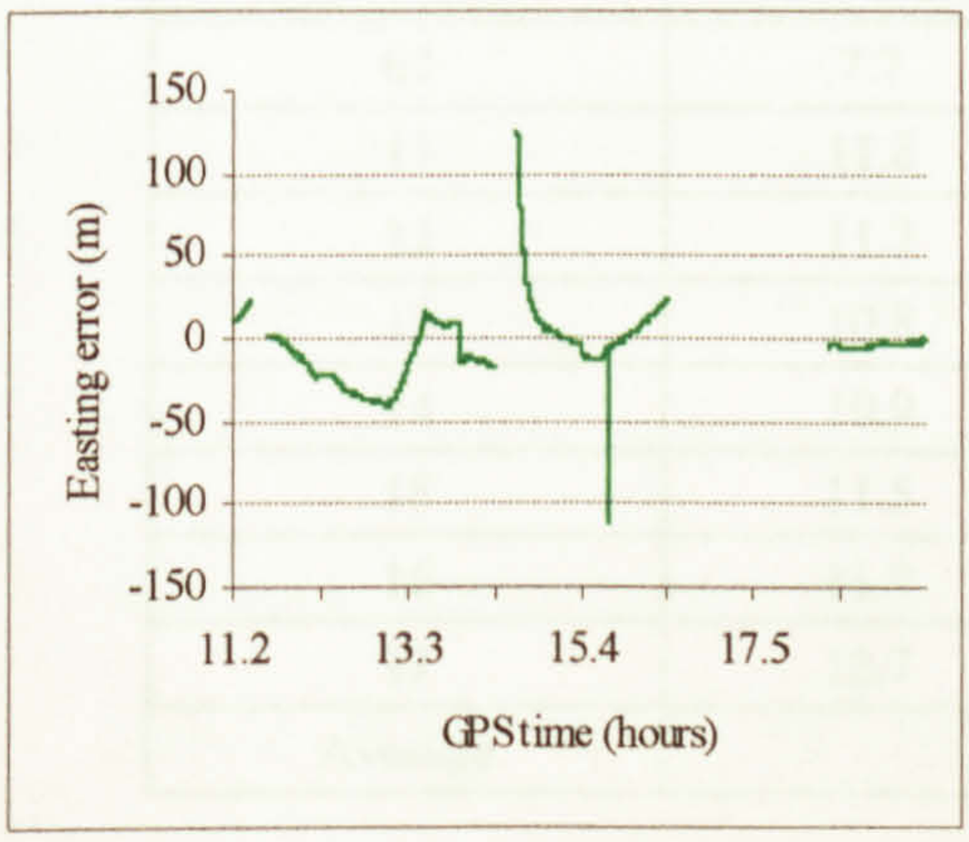

Figure 5.30
Stand-alone GLONASS Easting error

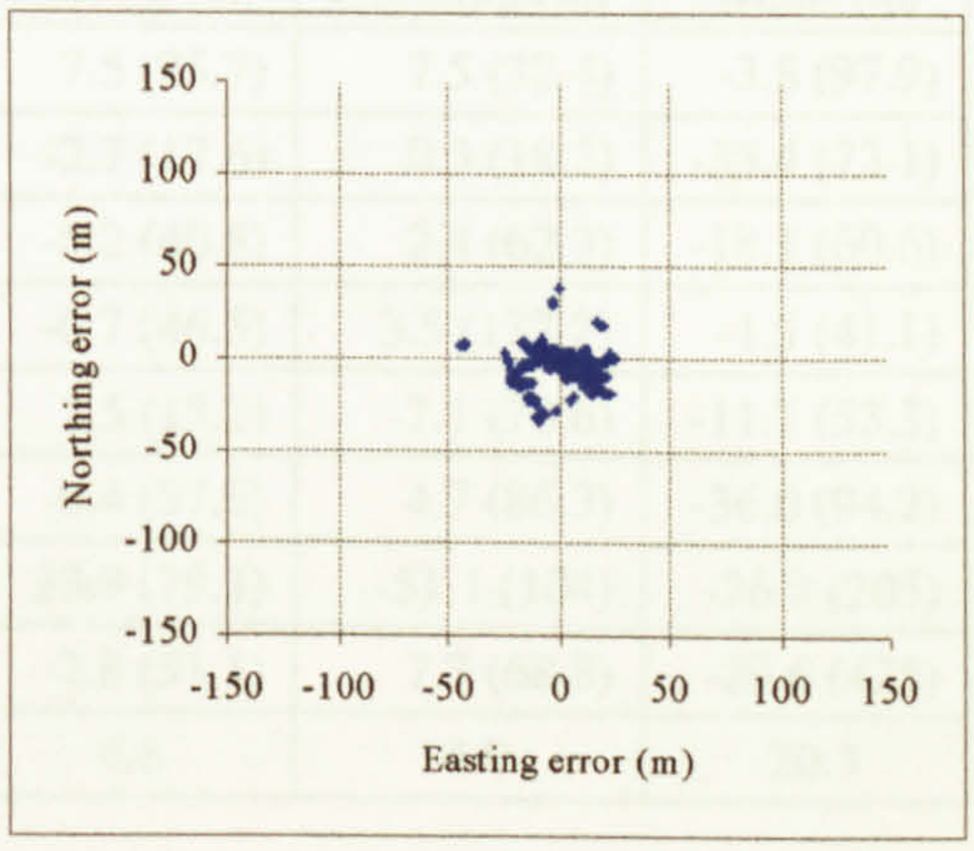

Figure 5.33
Stand-alone GLONASS plan error
PDOP ≤ 2

Figure 5.31
Stand-alone GLONASS Height error

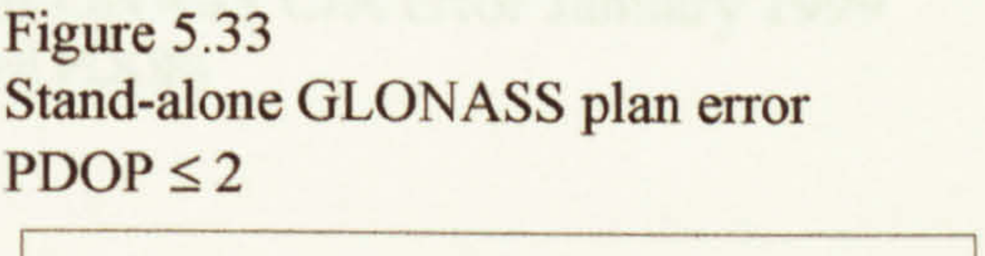

Figure 5.34
Number of GLONASS satellites in solution

being visible above the 5° mask. The total outage was about 3.4 hours or 14% of a day. Daily total outage varies according to the day to day constellation size and geometry, which was inconsistent owing to the large proportion of missing satellites, with plane-1 being particularly deficient. These deficiencies translate into imprecise and low accuracy estimates of long term GLONASS position accumulations (Tables 5.6 and 5.7 top row), unless geometry is restricted by applying a PDOP threshold as in the bottom row of Table 5.7.

Day of month	Hours @ 1 min	Easting (m)	Northing (m)	Height (m)
03	7.7	7.5 (25.7)	7.5 (32.4)	-3.8 (97.9)
11	11.8	-2.7 (17.6)	0.3 (18.2)	-35.4 (73.1)
12	11.2	-5.2 (40.8)	2.4 (62.3)	-18.1 (60.6)
13	10.8	-0.7 (46.5)	3.5 (137.2)	-1.5 (41.1)
14	10.9	1.5 (15.2)	-7.1 (70.6)	-11.7 (53.3)
15	11.5	-0.4 (57.6)	4.7 (86.3)	-36.0 (94.2)
16	11.9	39.9 (79.3)	-51.1 (104)	-26.2 (205)
17	12.7	-2.8 (51.1)	7.7 (68.8)	-29.6 (425)
Average		4.6	-4.0	-20.3

Table 5.6 MIT stand-alone GLONASS C/A error January 1999
(unlimited PDOP)

Day of month	Max PDOP	Easting (m)	Northing (m)	Height (m)
10	39.3	13.8 (47.3)	10.2 (73.0)	-11.3 (35.7)
10	2	3.5 (11.5)	-4.5 (9.7)	-25.3 (28.8)

Table 5.7 IESSG stand-alone GLONASS C/A error 10-11 July 1998
(results extracted from Table 5.1)

Position error in plan with at least 4 satellites in the solution, is given for the unlimited PDOP case in Figure 5.32, and with a PDOP of 2 applied in Figure 5.33, in common with GPS (Table 5.1a). This allows a more valid comparison with GPS on the basis of a common level of geometry. However, when a PDOP threshold of 2 is applied to GLONASS, the number of GLONASS

solutions is reduced by 63%. The remaining solutions were relatively stable in plan since there was no intentional degradation such as that caused by SA. Position error components also lacked the high frequency character of the GPS error traces, and results were in general agreement with other analyses e.g. Maurer et al [1997].

5.3 Differential C/A code

The principles of differential code operation have been explained in §4.3.1.2.

In this section the performance of differential GPS, Hybrid, and GLONASS are examined. All data were acquired with a pair of Ashtech GG-24 receivers, on a ZBL, thus eliminating the effects of PRC age, along with SA, atmospheric, multipath, and ephemeris errors. On the other hand, and this is the main purpose of this section, the effects on positioning accuracy of non-identical receiver components, and GLONASS ICBs, may then become apparent. Data processing was by AOSS.

The ZBL was observed at the IESSG, for 24 hours on two separate days, at the end of July and again in mid-August 1998. This gave two unique snapshots of GLONASS availability in its eight day repeat geometry cycle.

GPS and Hybrid solutions were available over the complete time span, however the depleted GLONASS constellation provided a much lesser capability in DGLONASS mode.

The statistics for baseline component errors are presented for both days, in Tables 5.8 and 5.9. Since these were quite similar, results are further given in graphical format for only the end of July session, in Figures 5.35 to 5.40 Results are in broad agreement with those of others who conducted tests with GG-24s, e.g. Hall et al [1997].

Although differential operation using the transmission of differential corrections in real time is not evaluated here, for completeness an idea of accuracy achievable under the influence of *latency* or *ageing is* appropriate, according to Ashtech [1997], as follows. The influence of GLONASS PRCs on plan accuracy reaches a steady state at a correction age of about sixty seconds, at about 2.5 metres 95%. On the other hand GPS PRCs take just 30 seconds to degrade to 2.5 metres 95%, under the dominant influence of SA, and 60 seconds to degrade to 9 metres 95%. Thus DGLONASS requires a less frequent PRC update rate than either DHybrid or DGPS, allowing, if desired, other information to be relayed to users, in the PRC data stream. With SA off, other differential errors dominate DGPS and DHybrid, including residual atmospheric and ephemeris error, and multipath. The latter should be significant only at the mobile receiver, as the reference station should be always sited with multipath minimisation in mind.

5.3.1 DGPS

On the ZBL, DGPS provided the most accurate and consistent results over time, which is reflected in a mean 3D error of less than 5 cm, with standard

deviations at 0.1 metre or less, see Tables 5.8 and 5.9. The maximum excursion was to about 0.5 metre, see Figure 5.38. The only reasonable explanation for this, may have been intermittent differing signal impedance of the different antenna cable inter-connectors either side of the signal splitter, which fed the signals to the two receivers from the single antenna.

Mode | mean error	Northing (m)	Easting (m)	Height (m)	max PDOP	% epochs with a solution
DGPS	0.0 (0.0)	0.0 (0.0)	0.0 (0.1)	4.0	100
DHybrid	-0.6 (0.6)	-0.1 (0.6)	0.2 (1.3)	2.9	100
DGLONASS	0.1 (1.5)	-0.2 (1.3)	1.0 (3.3)	7.0 gate	49
DGLONASS	0.0 (1.2)	-0.2 (1.2)	0.7 (3.0)	4.0 gate	37
DGLONASS	0.2 (1.2)	-0.1 (1.0)	-0.2 (2.8)	2.9 gate	15

Table 5.8 Zero latency differential code 30th July 1998
(24 hours at 15 sec. epoch)

Mode | mean error	Northing (m)	Easting (m)	Height (m)	max PDOP	% epochs with a solution
DGPS	0.0 (0.0)	0.0 (0.0)	0.0 (0.0)	7.0	100
DHybrid	0.0 (0.3)	-0.1 (0.3)	-0.1 (0.8)	3.8	100
DGLONASS	0.1 (1.4)	0.3 (1.3)	-1.3 (2.7)	7.0 gate	35
DGLONASS	0.2 (1.3)	0.4 (1.2)	-1.4 (2.5)	3.8 gate	27

Table 5.9 Zero latency differential code 20th August 1998
(24 hours at 15 sec. epoch)

5.3.2 DHybrid

Differential Hybrid displays a significant deterioration in accuracy relative to DGPS, this can be seen by comparing the error distribution for DHybrid in Figure 5.35 with that for DGPS in Figure 5.37. This inferiority can be attributed to GLONASS ICBs, both on-receiver and between-receiver. These are present whenever GLONASS is involved in differential mode, either in Hybrid or GLONASS-only cases. If the ICBs are not treated in some way,

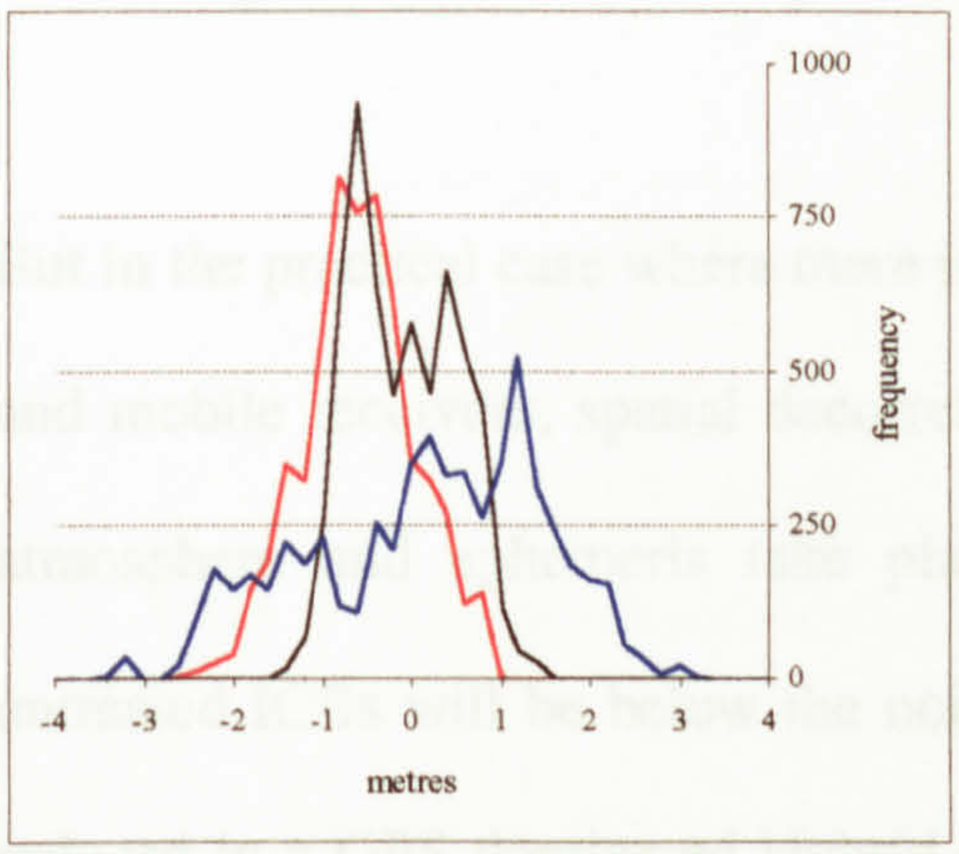

Figure 5.35

Plan error frequency
DHybrid max. PDOP 2.9
(0.2m bin size)

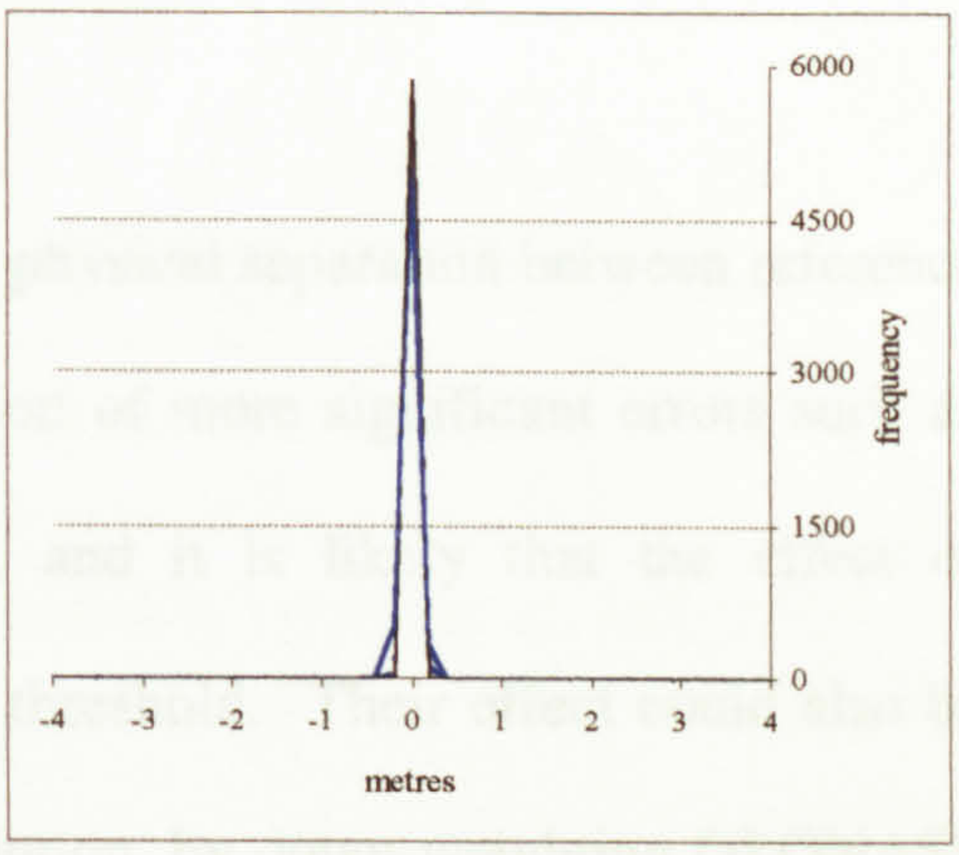

Figure 5.37

Plan error frequency
DGPS max. PDOP 4.0
(0.2m bin size)

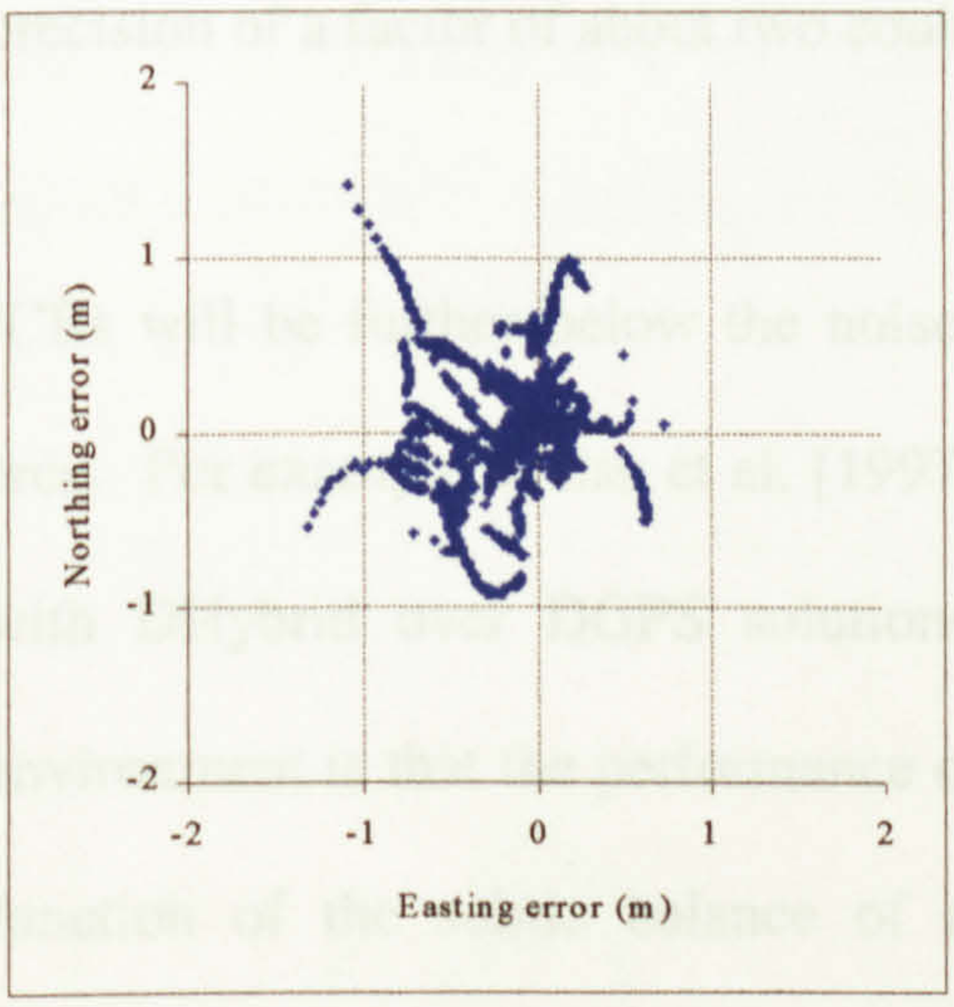

Figure 5.36

Plan error
DHybrid max. PDOP 2.9

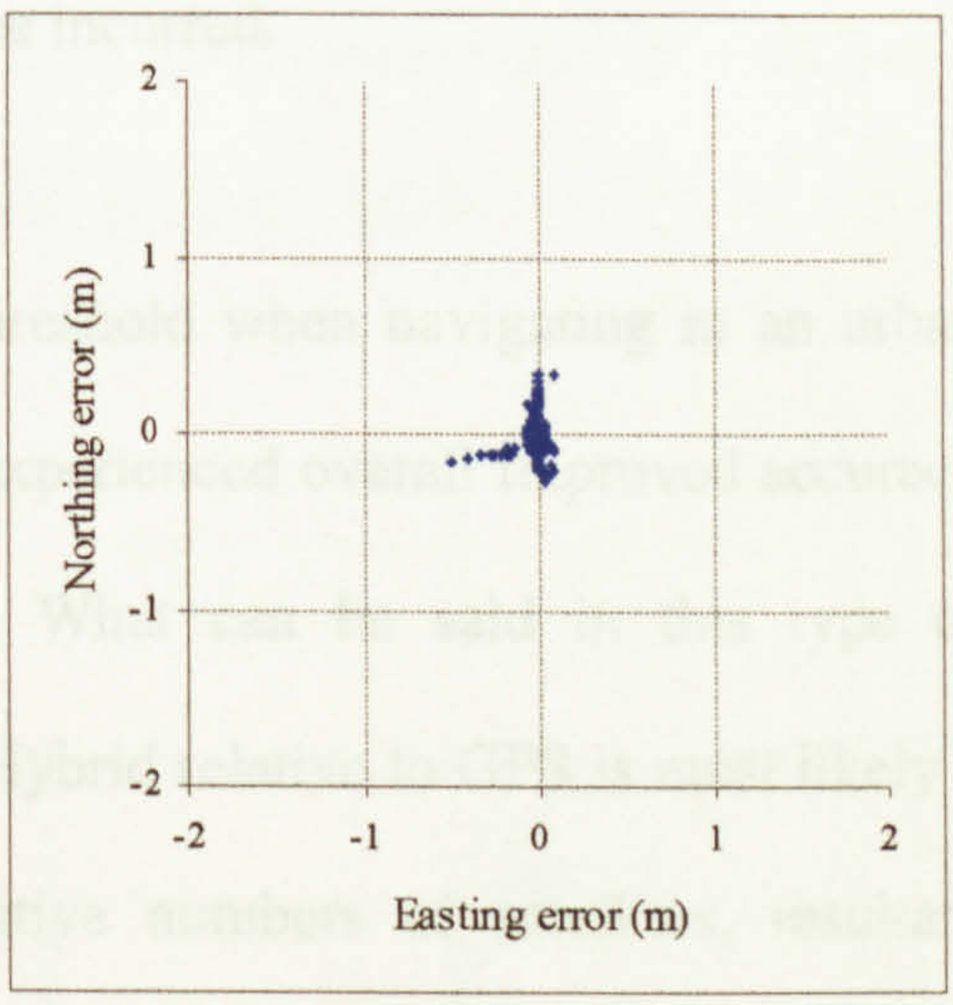

Figure 5.38

Plan error
DGPS max. PDOP 4.0

then as demonstrated here, they can propagate and degrade plan accuracy to the one to two metre level, and height accuracy to about two to four metres, thus countering what is achievable by DGPS alone.

But in the practical case where there is a physical separation between reference and mobile receivers, spatial decorrelation of more significant errors such as atmosphere and ephemeris take place, and it is likely that the effect of untreated ICBs will be below the noise threshold. Their effect could also be reduced in a GPS-dominated Hybrid solution, by down-weighting GLONASS observations. Note that detail of the weighting regime applied in AOSS was not made available. Hall et al [1997] reported on DHybrid performance on a 2 km baseline, demonstrating that with equal weighting a degradation in precision of a factor of about two could be incurred.

ICBs will be further below the noise threshold when navigating in an urban area. For example Walsh et al, [1997] experienced overall improved accuracy with DHybrid over DGPS solutions. What can be said in this type of environment is that the performance of Hybrid relative to GPS is most likely a function of the subtle balance of relative numbers of satellites, resultant geometry, and the relative weighting regime. Another researcher at Nottingham, [Swann, 1999], agreed with these findings.

Also, in any work environment, if the PRC transmission link becomes intermittent or is lost due to interference or blockage, and PRC age rises, then the graceful ageing of GLONASS PRCs can be used in Hybrid mode to control

the deterioration in accuracy caused by rapidly degrading GPS PRCs. Some figures for mixed modes, from Ashtech [1997], are given in Table 5.10.

Mode	Plan accuracy (95%) metres
D(GPS+GLONASS)	0.75
GPS + DGLONASS	1
DGPS + GLONASS	0.90

Table 5.10 Typical accuracy as a function of constellation and mode

(Adapted from Ashtech, 1997)

5.3.3 DGLONASS

By comparing DHybrid with DGLONASS with similar geometry, in Tables 5.8 and 5.9, and Figures 5.36 with 5.39 to 5.40, it is evident that in a DHybrid solution GLONASS ICBs may be controlled to some degree by GPS.

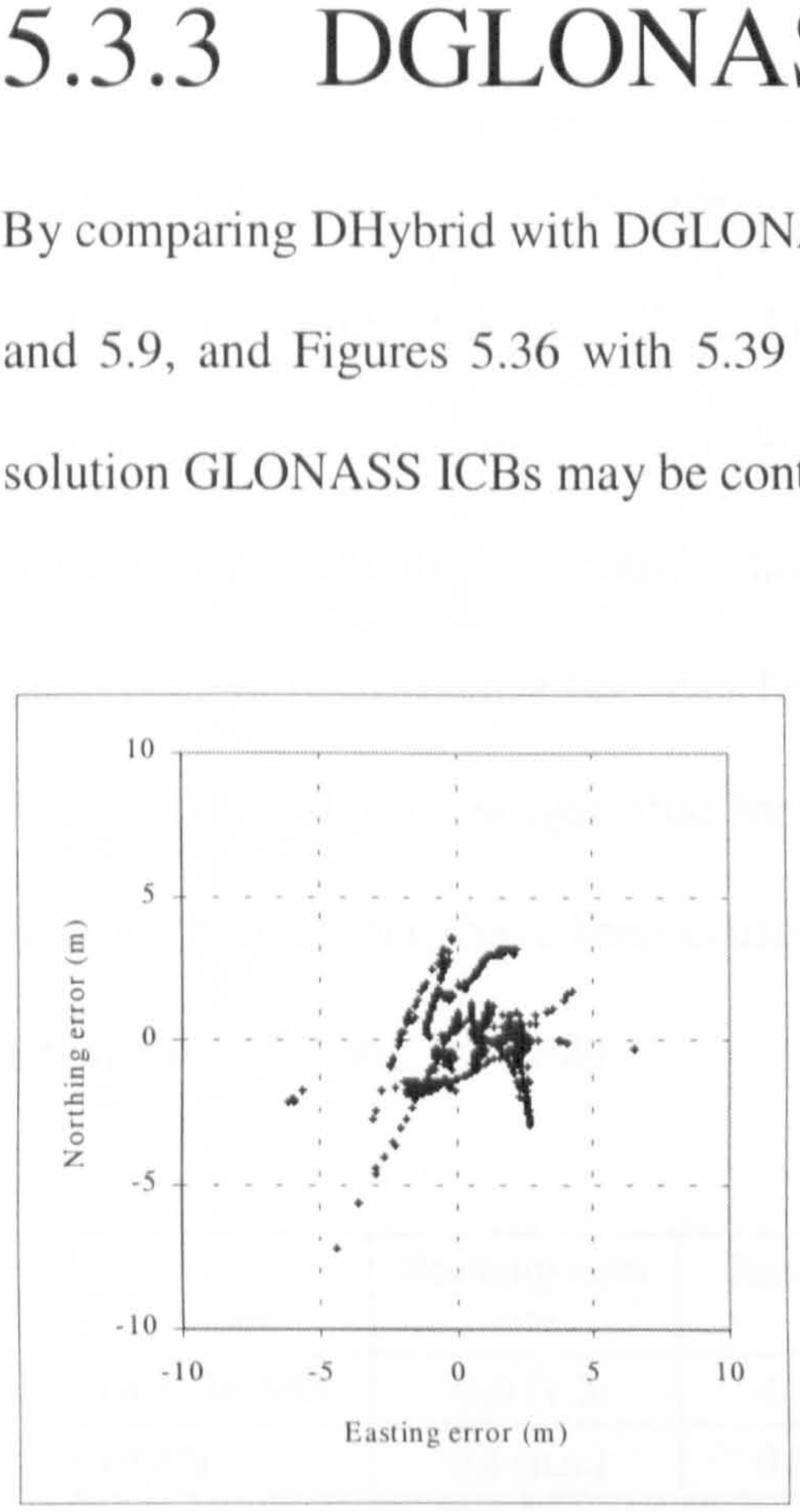

Figure 5.39 DGLONASS plan error, maximum PDOP 7

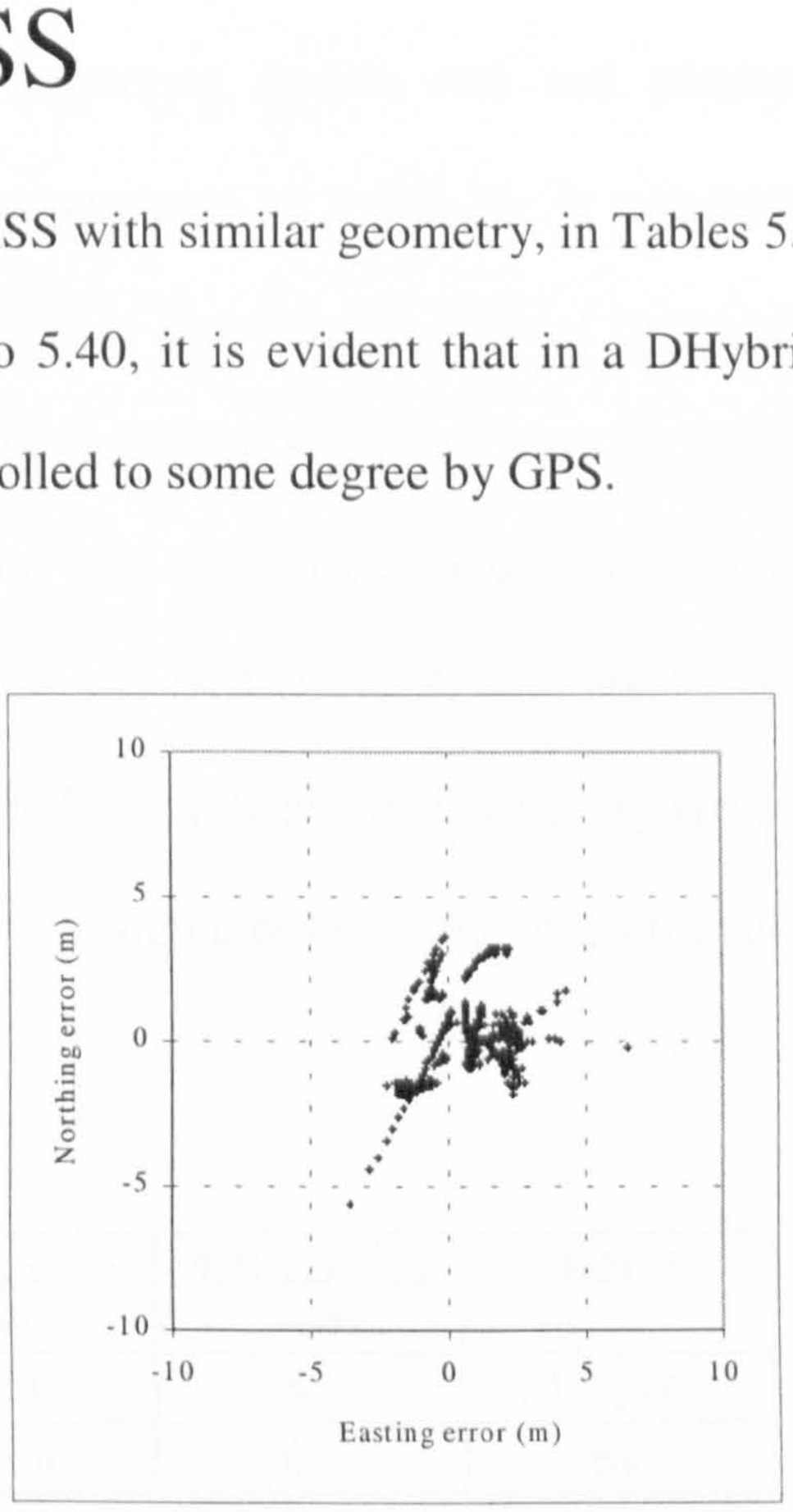

Figure 5.40 DGLONASS plan error, maximum PDOP 4

The tabulated results show that DGLONASS standard deviations in all components are at least twice their DHybrid counterparts. Currently, if DGLONASS is selected, then daily coverage with a PDOP of better than 7 is less than 12 hours, and if a stricter geometry threshold is applied, even less.

Another researcher, Ørpen et al [1997], worked with DGLONASS on a ZBL, with a similar number of satellites (14). Coordinate component standard deviations were at about the half-metre level for an average 1.2 HDOP. The only overt difference between the experiments was in receiver firmware, GE00, as opposed to GJ00 used in this research work. Tests were also done to check the relationship between differential correction update rate and resultant DGLONASS accuracy, with corrections generated by a GG-24. It was found that a 60 second update rate allowed errors to grow to just above 1 metre as a new message was received. A single reference station operating on an LBL at a range of 1100 km over eight hours, was also used to demonstrate the difference in performance between DGPS and DGLONASS, with results as in Table 5.11. It was thought that the DGLONASS average Northing error of nearly 3 metres, may have been caused by residual errors in the transformation between PE-90 and WGS-84.

Mode	Northing error (m)	Easting error (m)	95% 2D error (m)	HDOP
DGLONASS	-2.9 (1.2)	-0.4 (0.8)	4.8	1.3 (0.3)
DGPS	0.4 (n.a.)	0.0 (n.a.)	0.8	n.a.

Table 5.11 GG-24 LBL C/A code error components on a 1100 km baseline

5.4 Carrier phase

In this section the performance of GPS, Hybrid, and GLONASS are examined in carrier phase mode, again on a ZBL, using Ashtech GG24s. If observations are made on a ZBL, then the effect of between receiver delays such as GLONASS ICBs, on baseline determination, may be isolated and analysed. It is known [Raby et al, 1993], that the magnitude of these biases is temperature dependent, so further development of the standard ZBL apparatus was made to allow a between-receiver difference in operating temperature to be applied. This recreates in the laboratory the very real case where a reference station receiver may be in a quite different thermal environment to that of the remote receiver. For example the reference could be in an air-conditioned room, whilst the remote could be operating in an air temperature of 45° C, as recently (July 2000) experienced in Greece, giving a between-receiver thermal offset of many degrees.

ICBs and between receiver temperature offset have implications for the accuracy of both GLONASS and Hybrid mode positioning, as the effect of ICBs is magnified by increasing temperature for cases of both between-receivers and single receiver. The latter is not dealt with here, however others, for example Raby et al [1993] quote a total delay for a CAA ISN receiver plus antenna and cabling of 2mm for a 7°C thermal change, but figures are not quoted for resultant transfer into the position domain.

It is demonstrated here that with receivers operating at a common temperature, hybridisation can still result in a radial baseline error up to about 8 mm (§5.4.1), and if a thermal offset is introduced between-receivers (§5.4.2) then a virtual baseline of nearly 20 mm can arise. The data used in this experiment were logged in July 1998. Processing of a second set of data from August 1998 gave almost identical results, owing to slightly different GLONASS content. Data processing was by AOSS.

The experiments outlined in this section and results are now discussed in more detail.

5.4.1 Common temperature

Results from processing of data recorded by a pair of receivers operating on a ZBL at a common temperature for GPS, are given in Figures 5.41 to 5.46, and for Hybrid in Figures 5.47 to 5.52. The gaps in these time series were caused by the intermittent connection of an antenna cable inter-connector. Results are summarised, together with those of Hybrid in Table 5.12.

Mode | Error	Northing	Easting	Height	Vector	PDOP	Max sats
GPS	0.0 (1.3)	0.4 (1.0)	0.1 (2.3)	0.0 (1.6)	2.1 (0.8)	11
Hybrid	0.1 (1.7)	0.2 (1.1)	1.2 (3.4)	1.1 (2.3)	1.9 (0.7)	15

Table 5.12 ZBL error components, common temperature (mm)

Analysis of the baseline error component time series shows for GPS, as expected, that errors are random in nature. The error distribution in Figure 5.45 indicates a close to zero mean radial offset, which is also reflected in

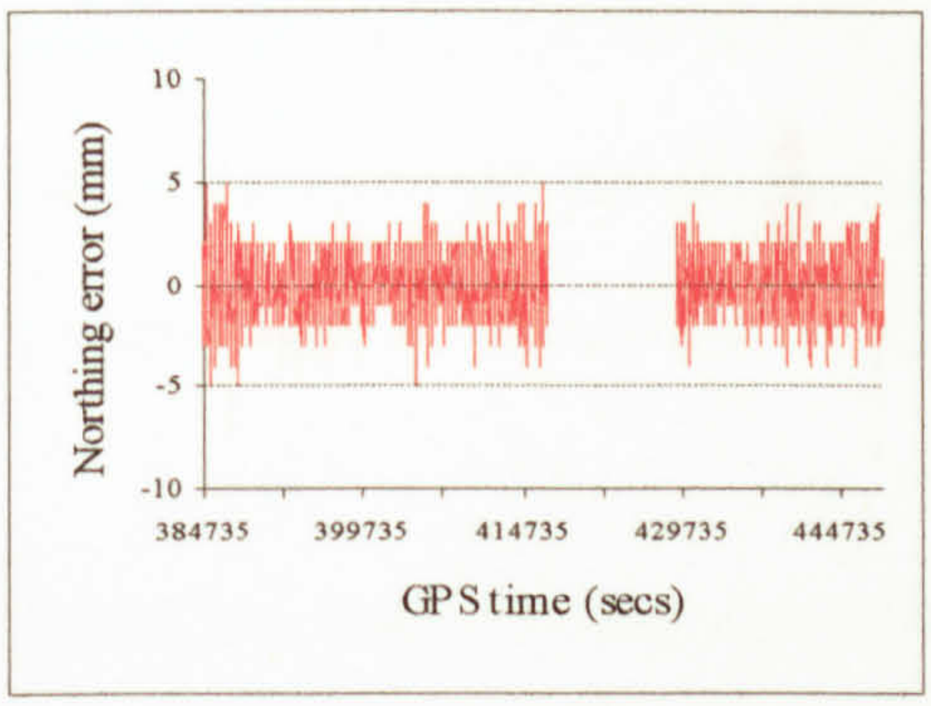

Figure 5.41 GPS Northing error

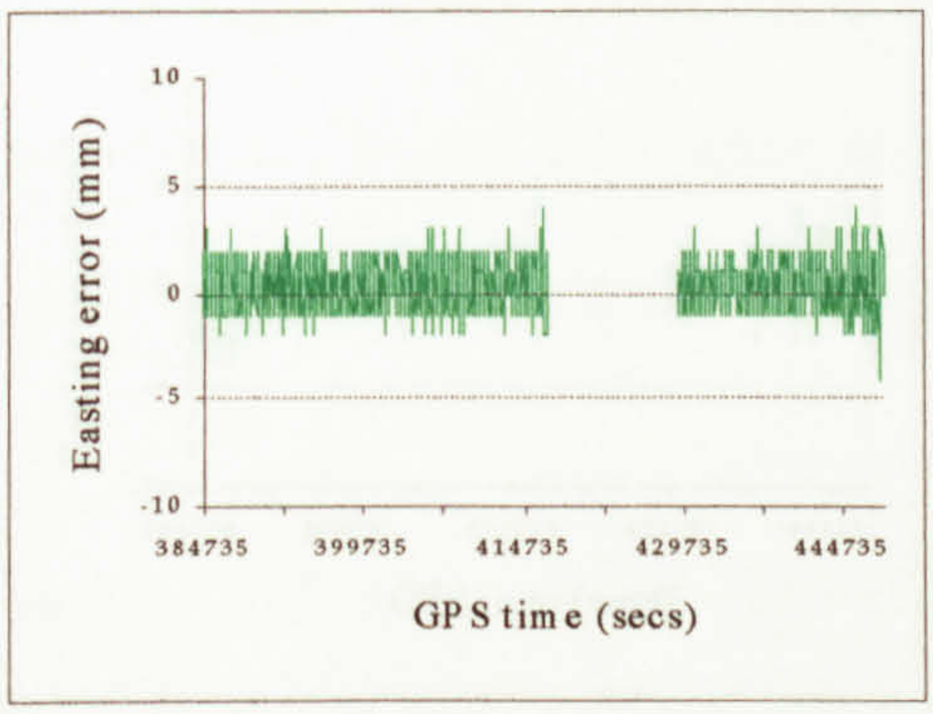

Figure 5.42 GPS Easting error

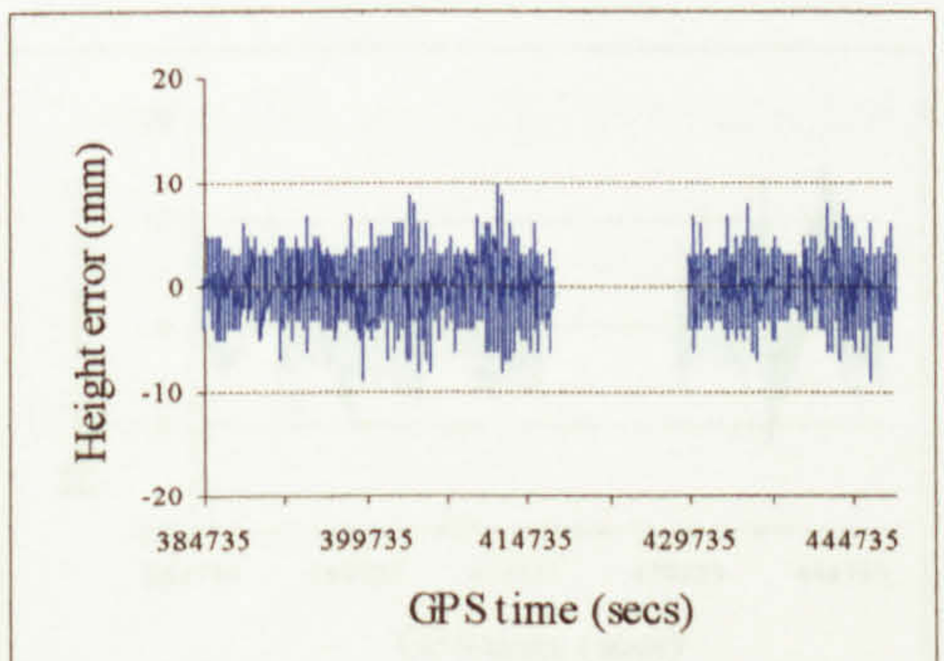

Figure 5.43 GPS Height error

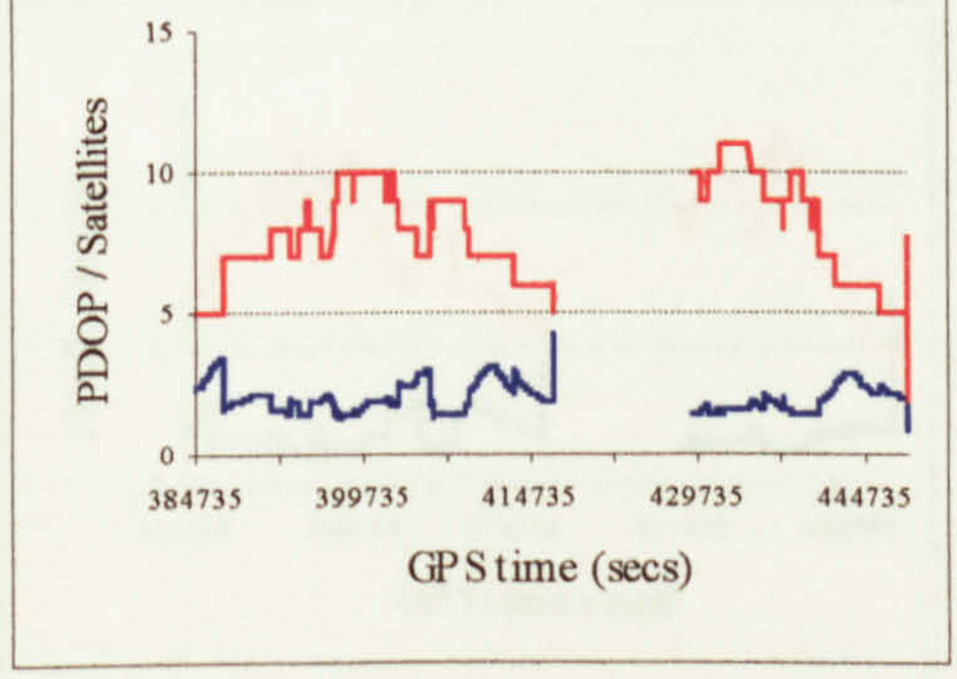

Figure 5.44 GPS PDOP and number of satellites

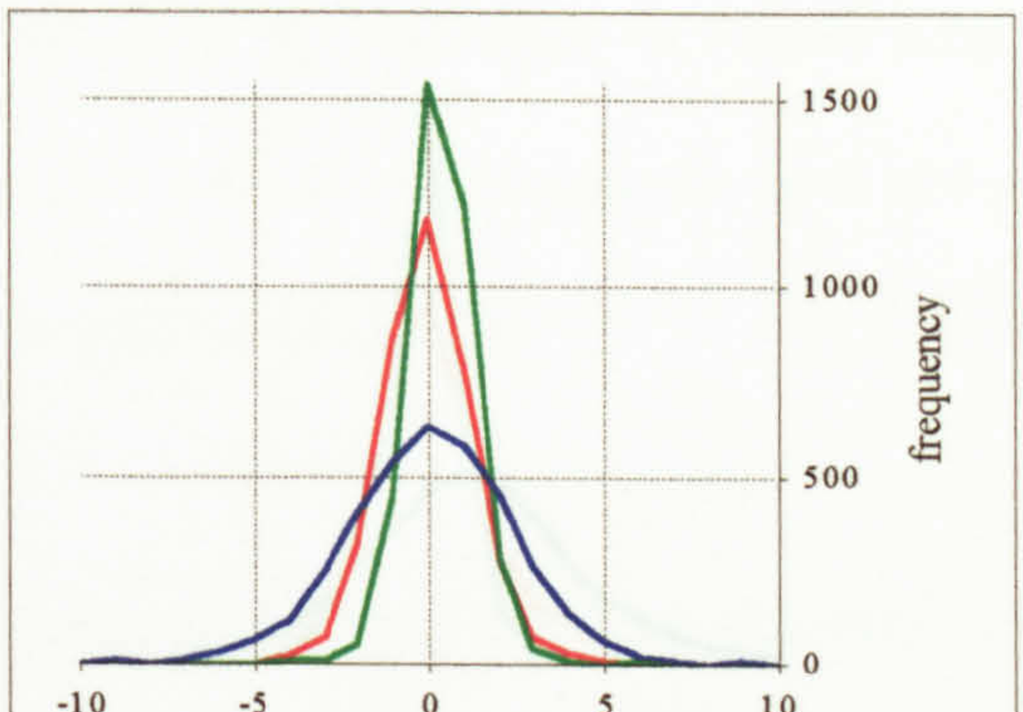

Figure 5.45 GPS error frequency

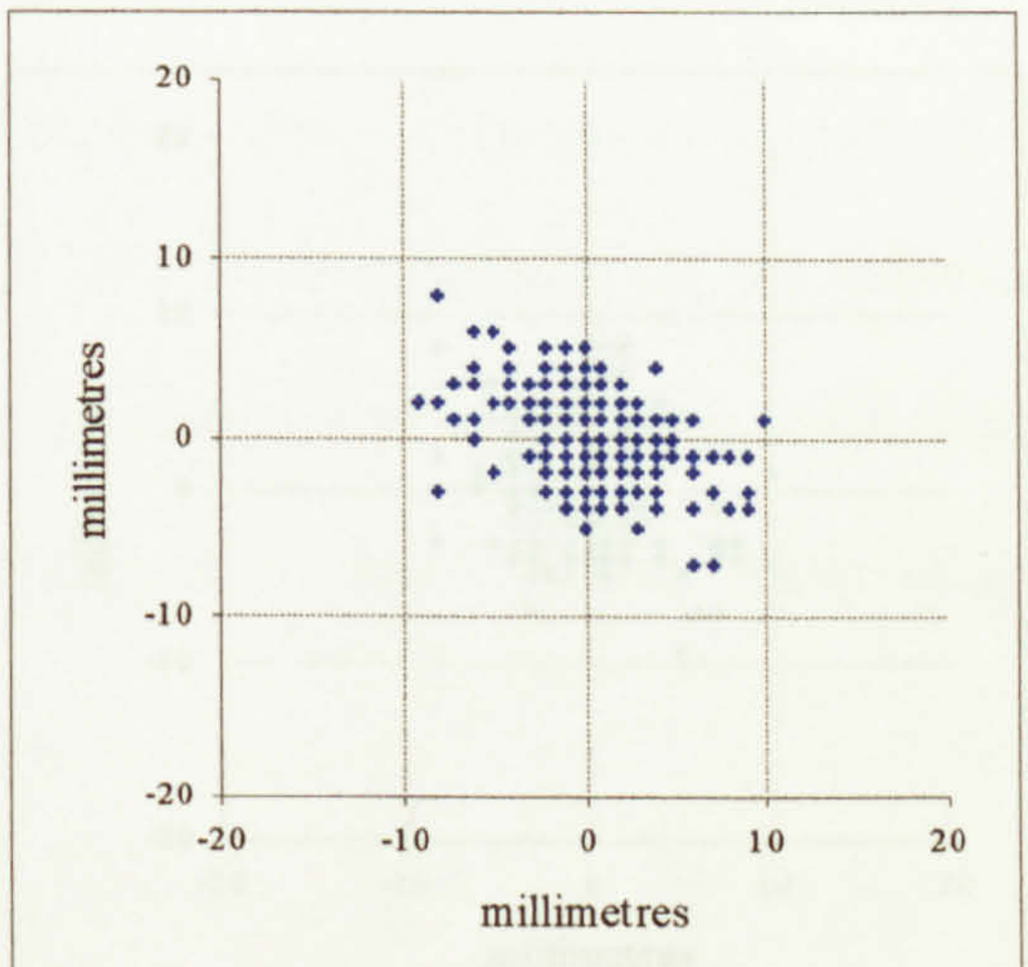

Figure 5.46 GPS Plan error

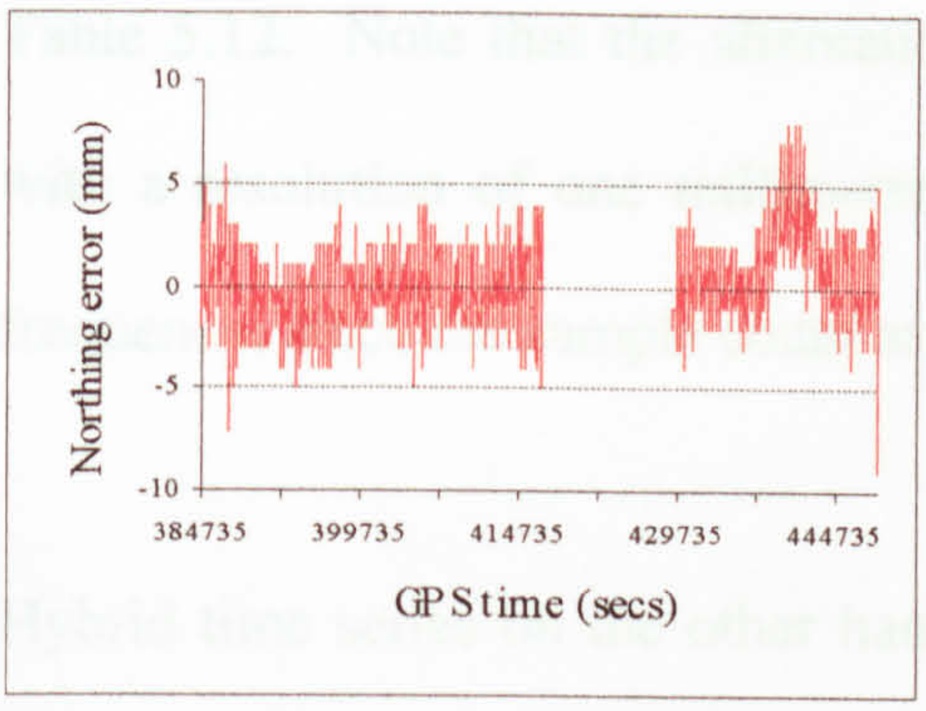

Figure 5.47 Hybrid Northing error

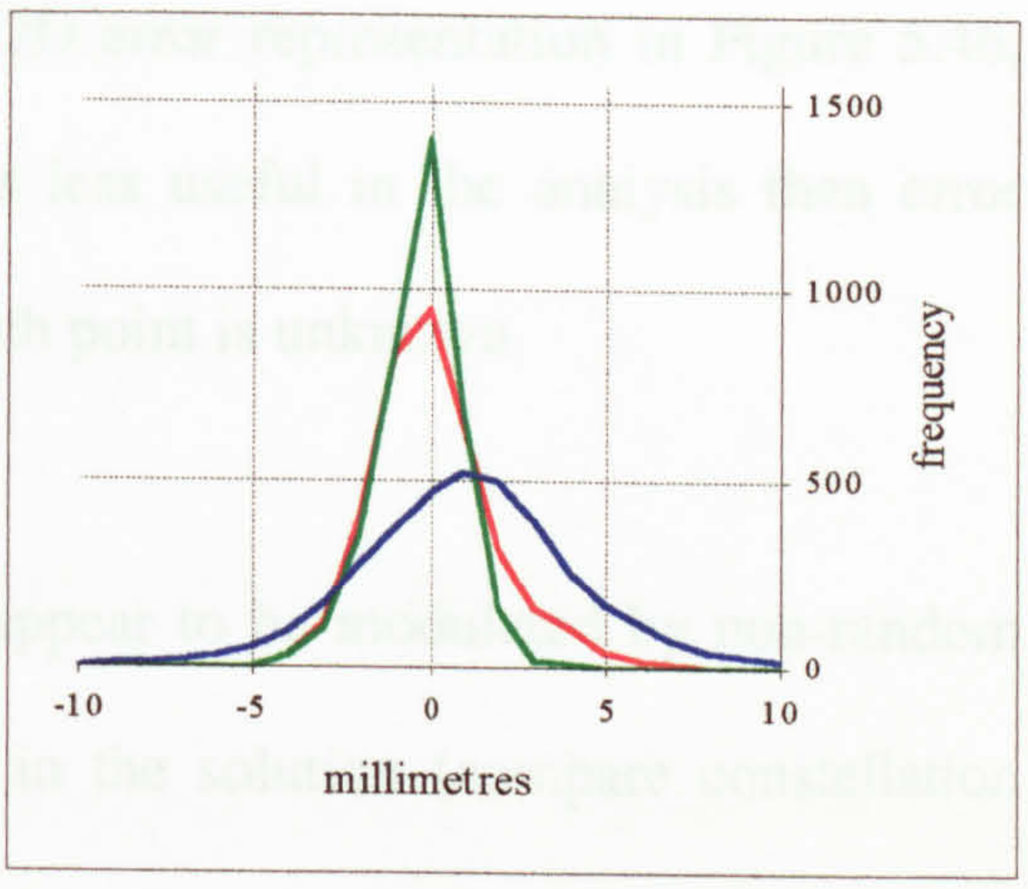

Figure 5.51 Hybrid error frequency

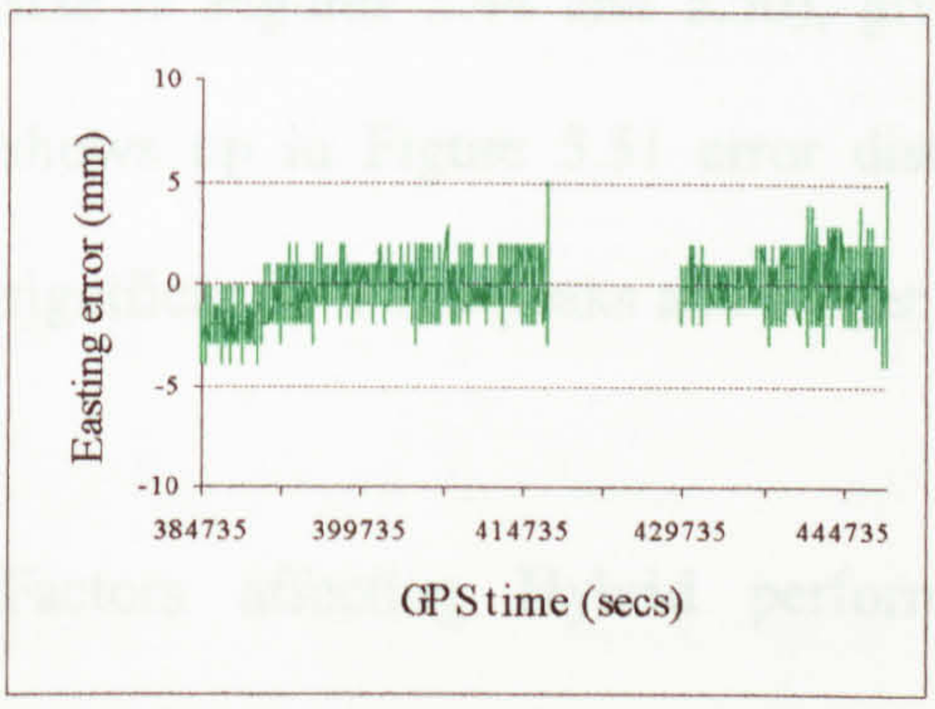

Figure 5.48 Hybrid Easting error

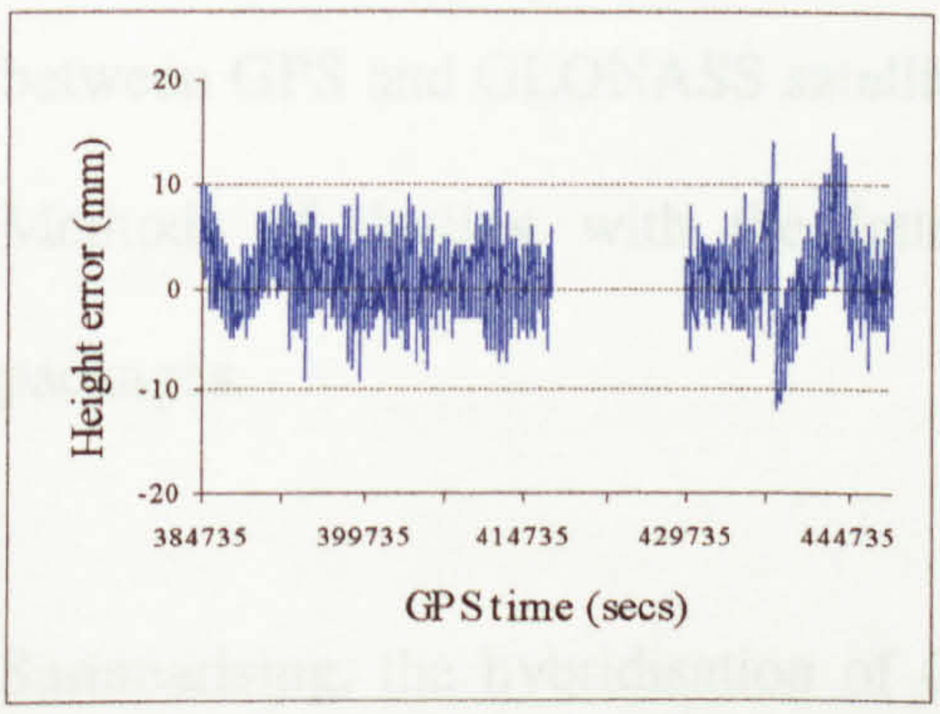

Figure 5.49 Hybrid Height error

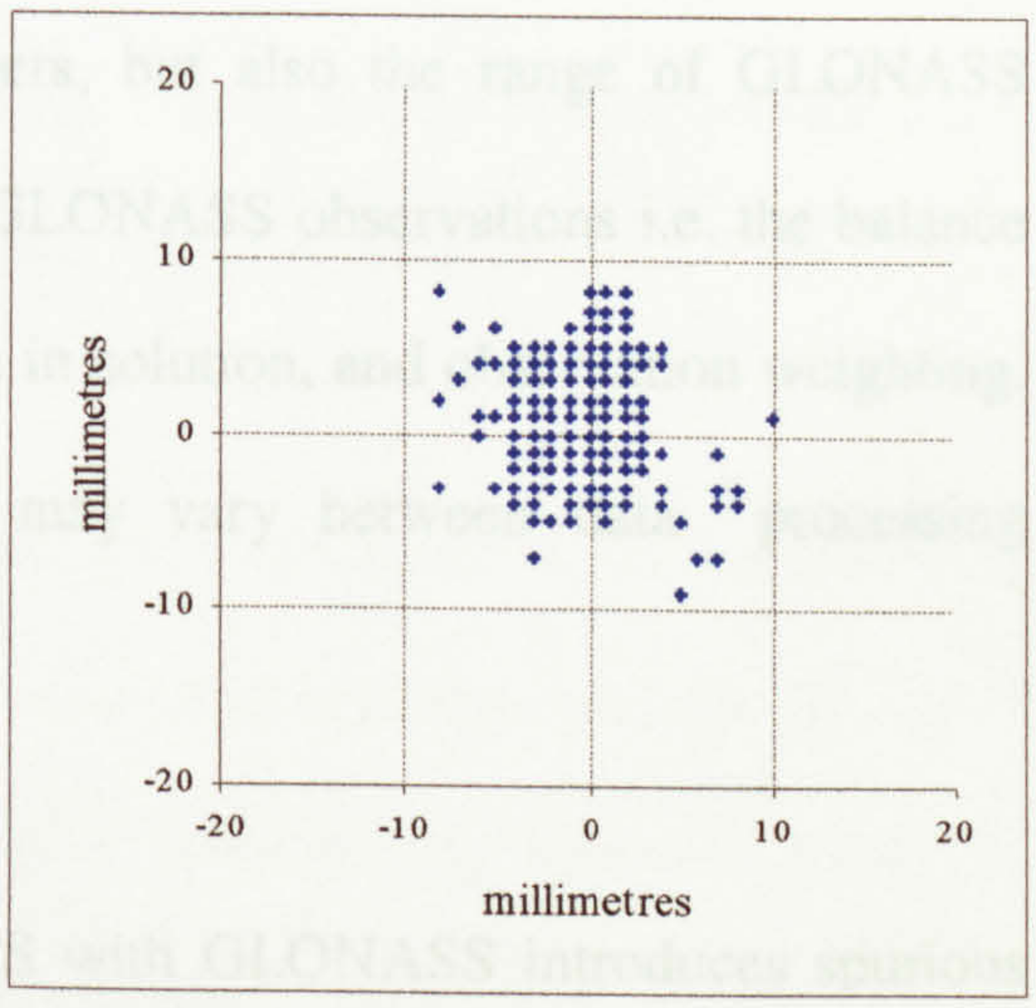

Figure 5.52 Hybrid Plan error

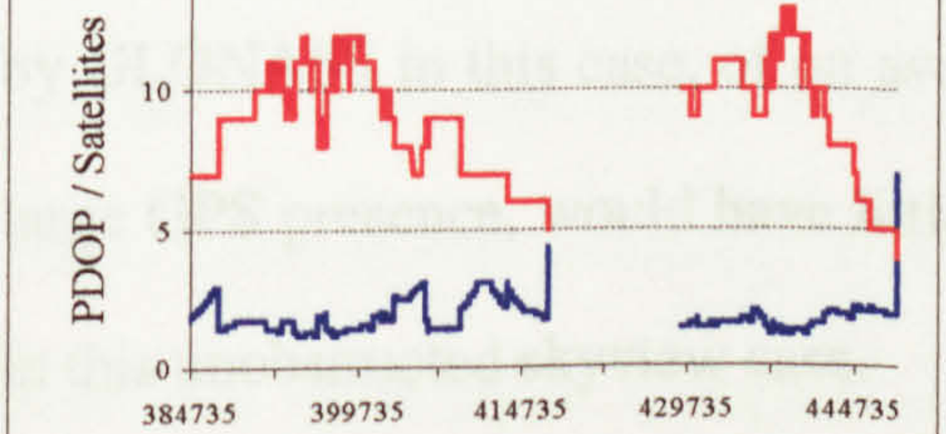

Figure 5.50 Hybrid PDOP and number of satellites

Table 5.12. Note that the alternative 2D error representation in Figure 5.46, with a resolution of one millimetre, is less useful in the analysis than error frequency, since the sample count at each point is unknown.

Hybrid time series on the other hand appear to be modulated by non-random error signals whenever GLONASS is in the solution (compare constellation size in Figures 5.44 and 5.50), giving a non-zero mean radial offset. This shows up in Figure 5.51 error distributions, which compared to GPS have significantly lower peaks and longer and fuller tails.

Factors affecting Hybrid performance include not only the available constellation in terms of sheer numbers, but also the range of GLONASS satellite frequencies in use, uptake of GLONASS observations i.e. the balance between GPS and GLONASS satellites in solution, and observation weighting. Methods of dealing with the latter may vary between data processing packages.

Summarising, the hybridisation of GPS with GLONASS introduces spurious measurements, which unless controlled, lead to a relatively poor baseline determination. It can therefore be said that the increased redundancy offered by GLONASS in this case, of on average 2, and at best 4 observations, with a large GPS presence, would have little effect in terms of solution improvement, in this unobstructed skyview case.

The focus now shifts to the case where receivers are operating at significantly different temperatures.

5.4.2 Different temperature

The sensitivity of positioning to a difference between receiver operating temperatures on a ZBL is now investigated.

In the initial test a between-receiver temperature difference was introduced by applying an air fan heater to just one receiver. Then after gaining some experience with the experimental rig, and in order to increase the thermal differential between receivers, one receiver was heated as before, and the other chilled by packing around the receiver case with freezer blocks.

Reiterating but expanding on what has been said in Chapter 4, for the following reasons GPS measurements both on-receiver and between-receivers (if a D-D is used) are unaffected by differential temperature, however those of GLONASS and by extension Hybrid are affected.

GPS is impervious owing to its CDMA nature, which allows all satellites to use identical transmission frequencies, furthermore these frequencies are highly stable across the constellation. This means that, no matter what temperature a receiver is operating at, all signals at a single receiver experience the same on-receiver delay. This is indistinguishable from the receiver clock offset which is also common to all signals, and both can be eliminated simultaneously in a

between-satellite S-D. For a pair of receivers operating at different temperatures, a D-D approach will similarly eliminate each (dissimilar) on-receiver delay. But note that it is possible to introduce a physical differential delay on a ZBL by using different antenna cable lengths after the signal splitter.

When satellite frequencies are dissimilar, as is the case with GLONASS, with its FDMA basis, then each satellite signal experiences a different on-receiver delay, leading to the ICBs referred to earlier. Furthermore, the delay at each satellite frequency is temperature dependent. If a thermal offset occurs between a pair of receivers then it is likely that receiver and hence receiver-satellite specific measurement bias will be introduced. There are then measurement inconsistencies in both elements of a D-D observable: a between satellite S-D observable is confronted with signals of different frequency (the fundamental change in delay across the GLONASS bandwidth); and a between receiver S-D where each is at a different temperature, is contaminated by differential signal delay at a single frequency. To further compound the issue, delays even at a common temperature are receiver-unique, as seen in §5.4.1. This is caused by receiver RF components not being repeatable at the point of (Russian) manufacture [Daly, 1999].

The RF designs of Hybrid and GPS receivers are different in that a Hybrid receiver uses a greater receiver tracking bandwidth to track in the relatively (to GPS) wide GLONASS bandwidth. This allows a wider range of noise frequencies to contaminate the receiver RF chain and thence signal processing

sections, elevating noise levels overall. Relative noise levels were investigated on a ZBL using an Ashtech GG24 (GPS only mode) and Ashtech Z12 (GPS only receiver). The test lasted for 5 hours and results, given in Table 5.13, show a significant increase of between 20% and 50% in error component standard deviation of Hybrid over GPS, confirming the above.

Receiver | mean error	Northing (mm)	Easting (mm)	Height (mm)	Vector (mm)
Ashtech GG24 (8/98)	1.8	1.4	2.8	1.8
Ashtech Z12 (4/99)	1.5	0.9	2.2	1.2

Table 5.13 Receiver performance on a GPS (L1) ZBL, carrier phase, standard deviation

In Hybrid mode, with GLONASS down-weighted relative to GPS, then it can be supposed that any thermally induced bias in GLONASS measurements will be dissipated, relative to GLONASS-only, since in general the GPS constellation is in the majority. However, in the analysis below it is shown that differential temperature can further degrade the achievable accuracy of a Hybrid carrier phase solution relative to GPS alone. This, though not discernible in results here, because the code noise threshold is relatively high, could in theory affect differential code too.

In practice, how efficiently thermal contamination propagates into the position domain of a Hybrid baseline solution, will depend on some combination of:

- Whether channel calibration over a thermal range has been conducted, and observations corrected.
- Size of initial offset and thermal gradient over time.
- The range of GLONASS frequencies involved.

- Relative numbers of GPS and GLONASS satellites in the solution.
- Contribution of GLONASS satellites to overall geometry (PDOP) i.e. how sensitive is the GPS geometry.
- Relative weighting regime between GPS and GLONASS.

Thermal tests

Since satellites cannot be tracked below the horizon, then height difference is the least well determined of the three baseline components, by a factor of two or three in comparison with the other two. This is borne out by results from several GPS determined ZBLs, one of which was quoted in §5.4.1. Height standard error (output from AOSS as an internal measure of precision) also proved to be the most responsive variable to temperature, hence its use as an indicator in the tests that follow.

A series of repetitive tests was designed and carried out during 1998, with the aim of determining for the practical Hybrid case, what typical size of baseline error might be thermally induced. Test dates were 21st April, 13th May, 14th May and 28th August. To isolate such errors a ZBL was used. A between-receiver temperature difference of about 20°C was introduced. In this way each receiver would log a unique set of GLONASS measurements, which may be of sufficient disparity to allow a virtual baseline to rise above the background noise.

To summarise, any coherent signature visible in time series of ZBL components, is caused on the receiver side of the antenna splitter, by differential hardware delays between receivers, be it cabling or on-receiver in nature.

Several Hybrid receiver manufacturers were canvassed as to whether the potential of differential temperature had been evaluated as a positioning error source. Ashtech [de Salas, 1998] had not, others made no reply, whilst 3S Navigation had introduced a thermally stabilised antenna.

The introduction of a temperature differential between-receivers, was found, whenever GLONASS measurements were involved, to reduce precision characterised by elevated standard error, and introduce an erroneous baseline measurement. Test results (Table 5.14) at the IESSG showed that whilst differential temperature could be a relatively major error source in precise work, its effect would be of no great concern to many applications requiring decimetre or metre level accuracy.

Test	Temp. offset	Northing error (mm)	Easting error (mm)	Height error (mm)	Vector error (mm)
1	22.0	2.1	1.7	7.0	7.2
2	20.1	4.9	4.2	18.0	18.2
3	21.8	6.2	5.3	17.0	17.8
4	23.9	16.1	4.0	13.1	18.4

Table 5.14 Hybrid virtual baseline, maximum dimensions

In all cases comparison was made between baseline solutions using GPS, Hybrid, and also against GLONASS when geometry and satellite visibility were sufficient to generate a solution. Given that GPS is unaffected by between-receiver thermal offsets, as discussed above, then its performance can be used as a reference (Figures 5.53 to 5.58) against which to evaluate the Hybrid and GLONASS solutions. A reference Hybrid data set was also recorded at one end of the GLONASS 8-day repeat geometry cycle

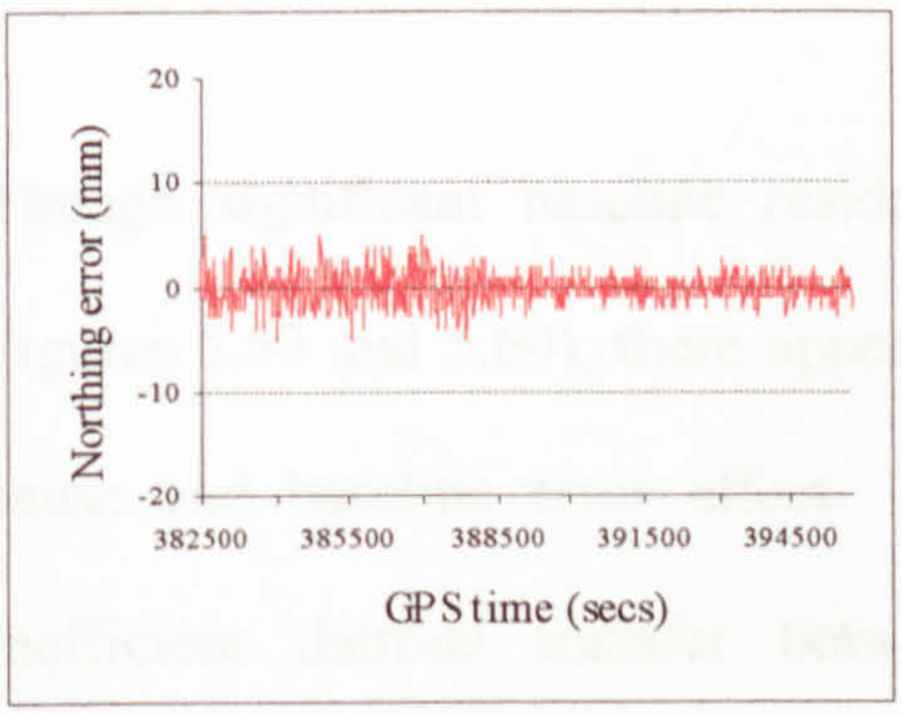

Figure 5.53 GPS reference ZBL, Northing error

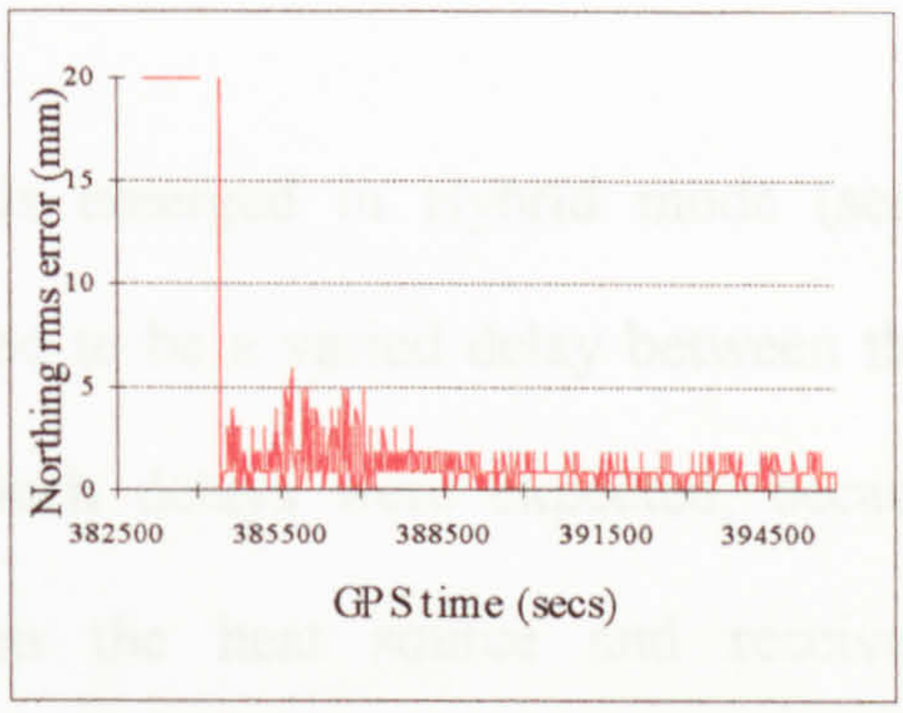

Figure 5.56 GPS reference ZBL, Northing standard error

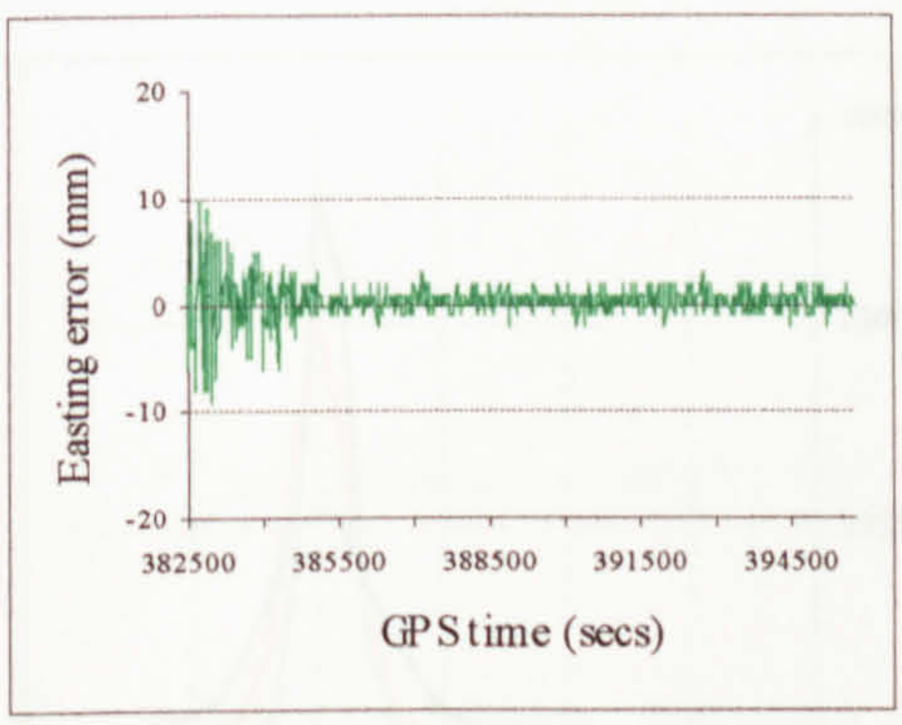

Figure 5.54 GPS reference ZBL, Easting error

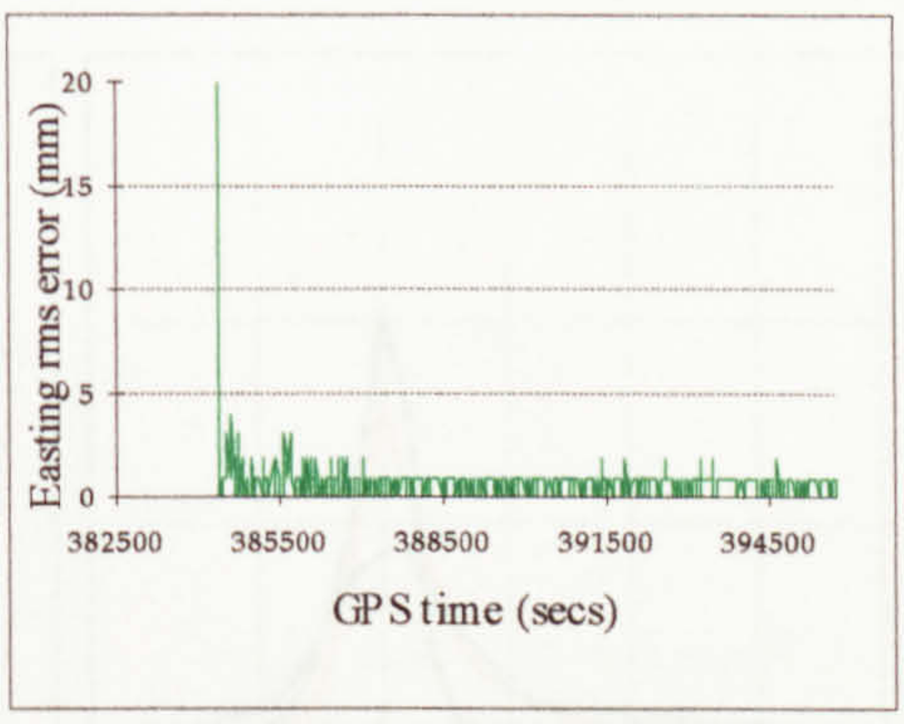

Figure 5.57 GPS reference ZBL, Easting standard error

Figure 5.55 GPS reference ZBL, Height error

Figure 5.58 GPS reference ZBL, Height standard error

(Figures 5.61 to 5.66), for comparison with the thermally contaminated Hybrid case, recorded 8 days later (Figures 5.67 to 5.72).

Though significant baseline residuals emerged in Hybrid mode (see also Figures 5.59 and 5.60), there appeared to be a varied delay between thermal cause and baseline error effect. Such delays were expected, because of inefficient thermal transfer between the heat source and receiver RF components. The delay varied between about 700 and 2000 seconds, for example see Figure 5.67.

Figure 5.59 GPS thermal ZBL error frequency

Figure 5.60 Hybrid thermal ZBL error frequency

The length of the delay could also be affected by the basic uptake of GLONASS satellites in the hybrid solution, as governed by algorithm criteria, and subtle changes in the balance between relative numbers of GPS and GLONASS satellites. This might be compounded by the frequency difference between the GLONASS reference satellite and its secondary satellites in a D-D, to give a more complex variation in both delay and error signal amplitude and frequency. Certainly thermal change should lead to increased levels of standard error.

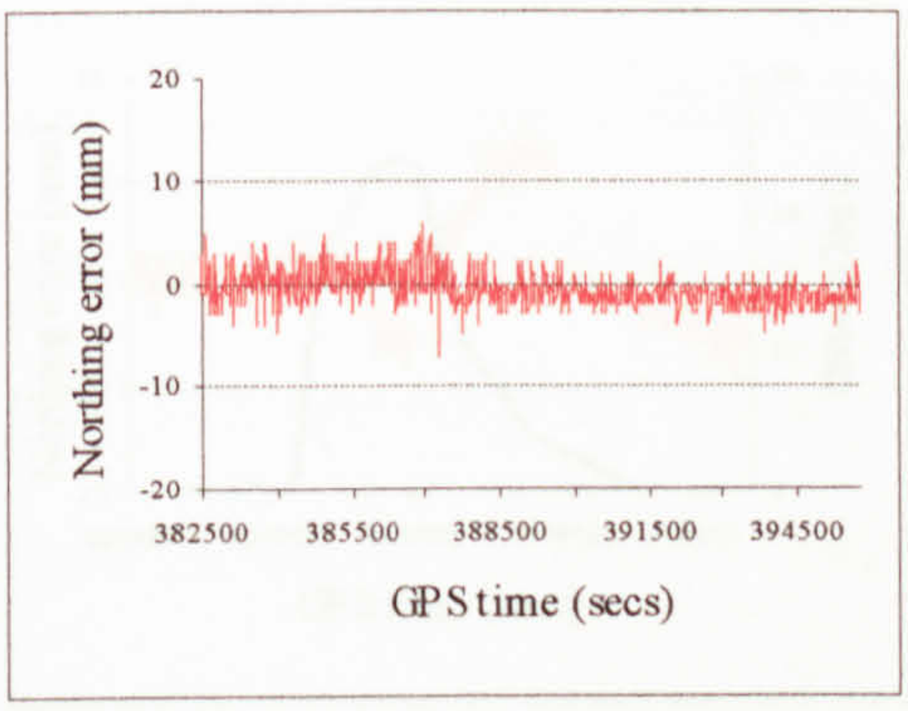

Figure 5.61 Hybrid reference ZBL, Northing error

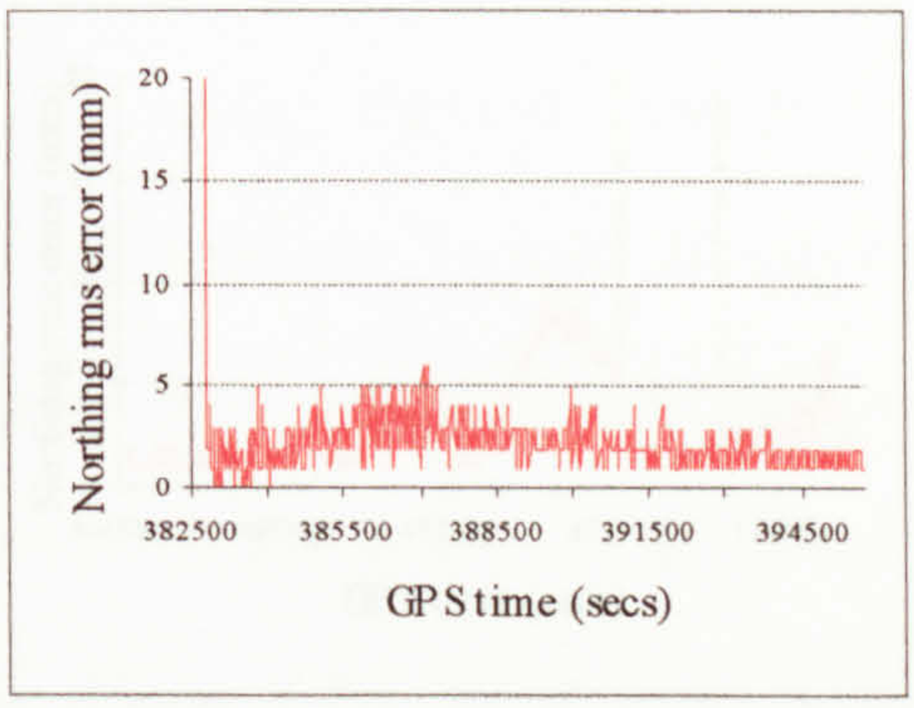

Figure 5.64 Hybrid reference ZBL, Northing standard error

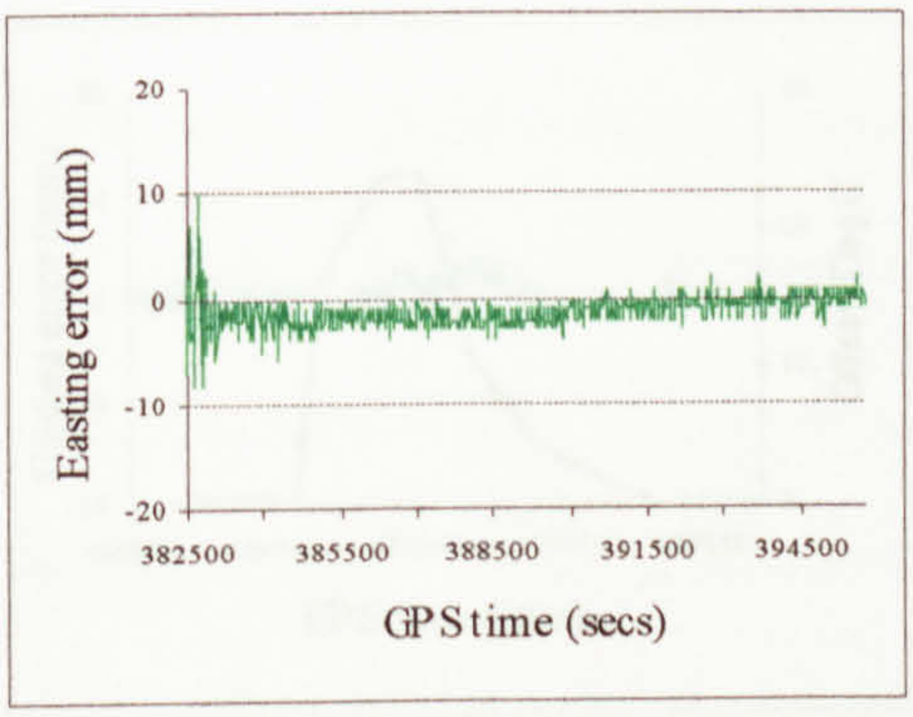

Figure 5.62 Hybrid reference ZBL, Easting error

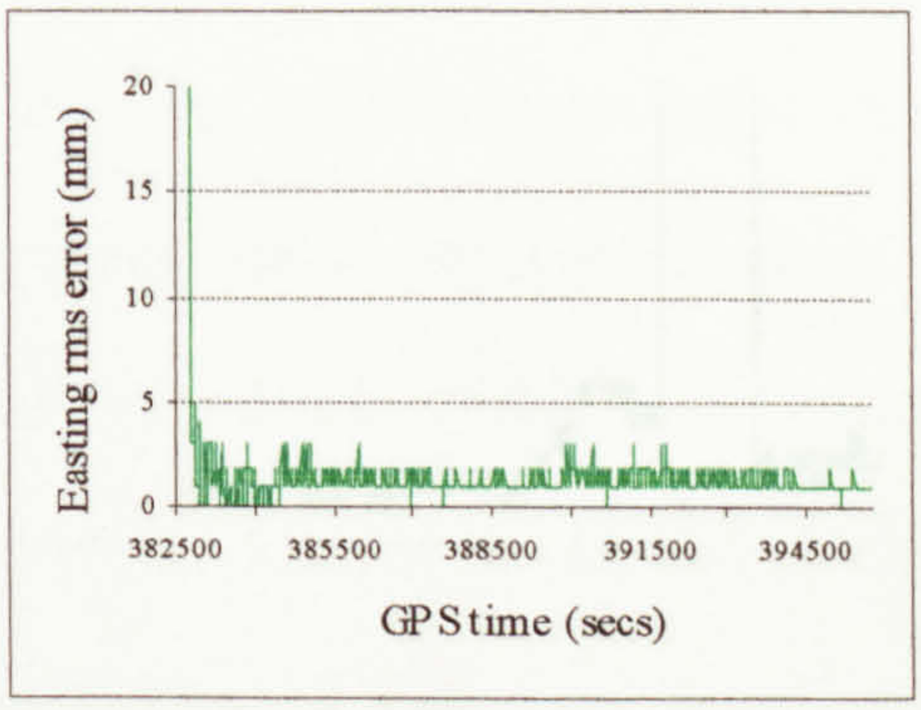

Figure 5.65 Hybrid reference ZBL, Easting standard error

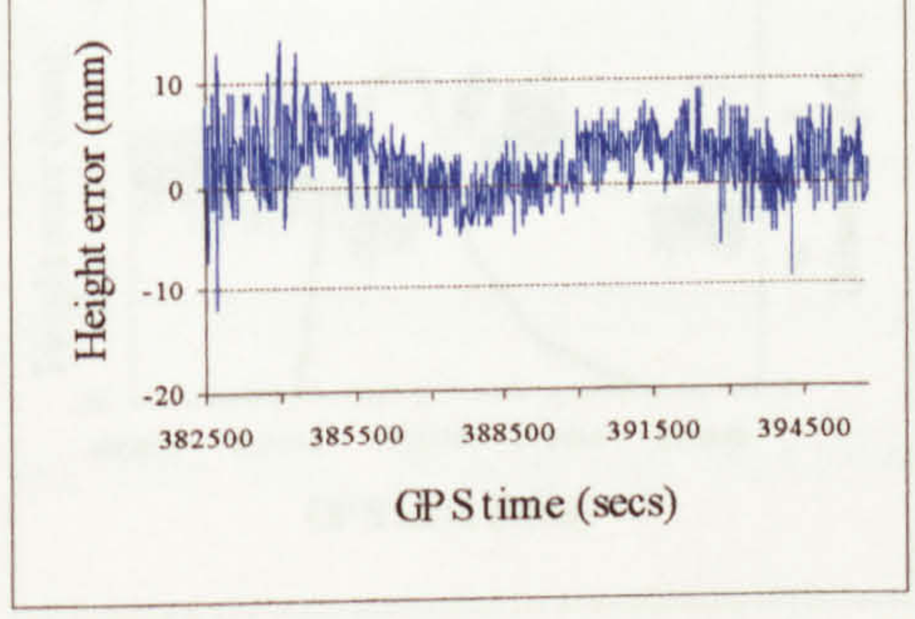

Figure 5.63 Hybrid reference ZBL, Height error

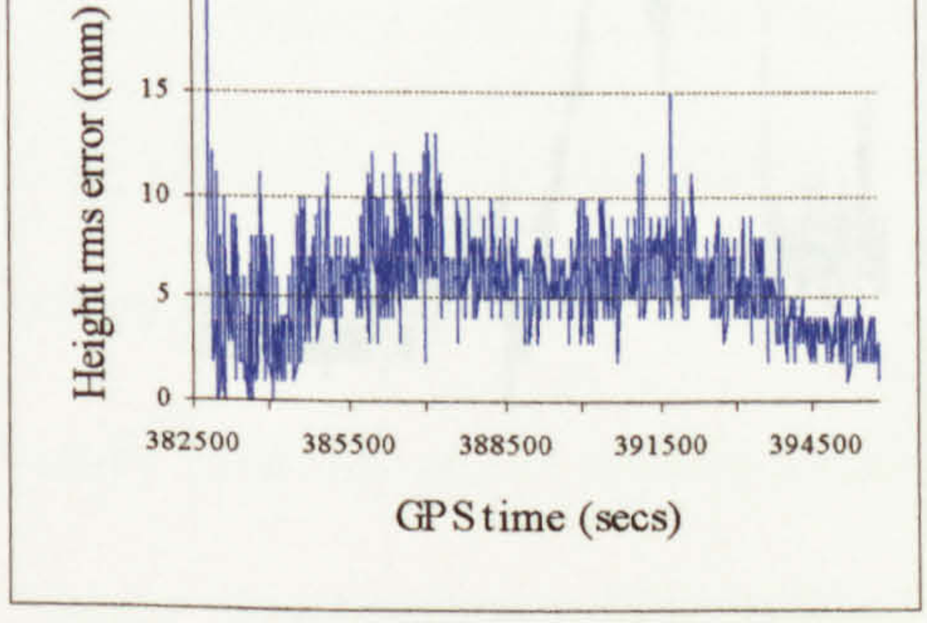

Figure 5.66 Hybrid reference ZBL, Height standard error

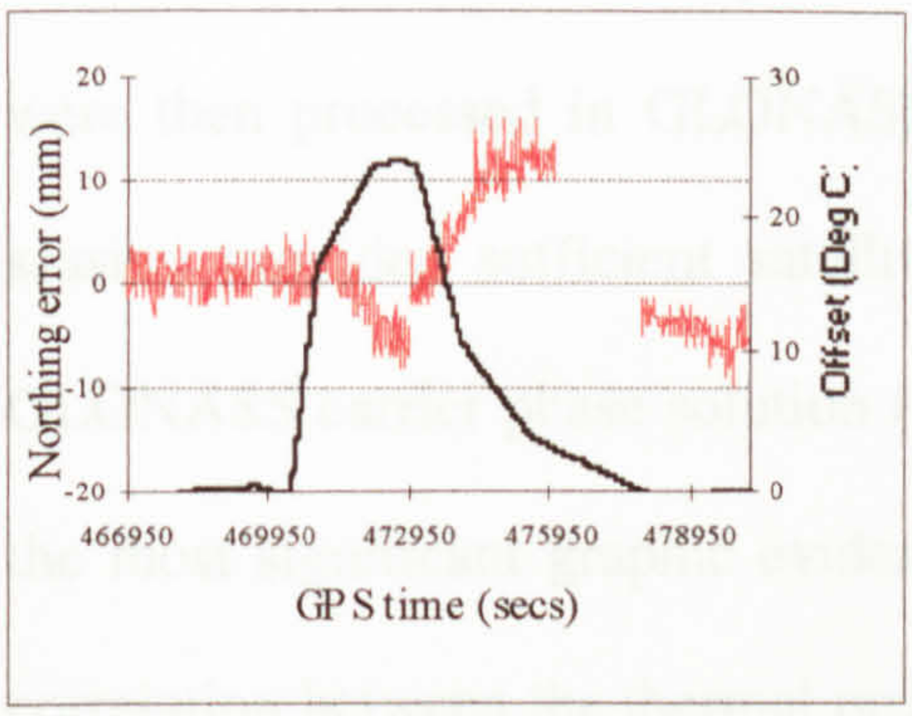

Figure 5.67 Hybrid thermal ZBL, Northing error

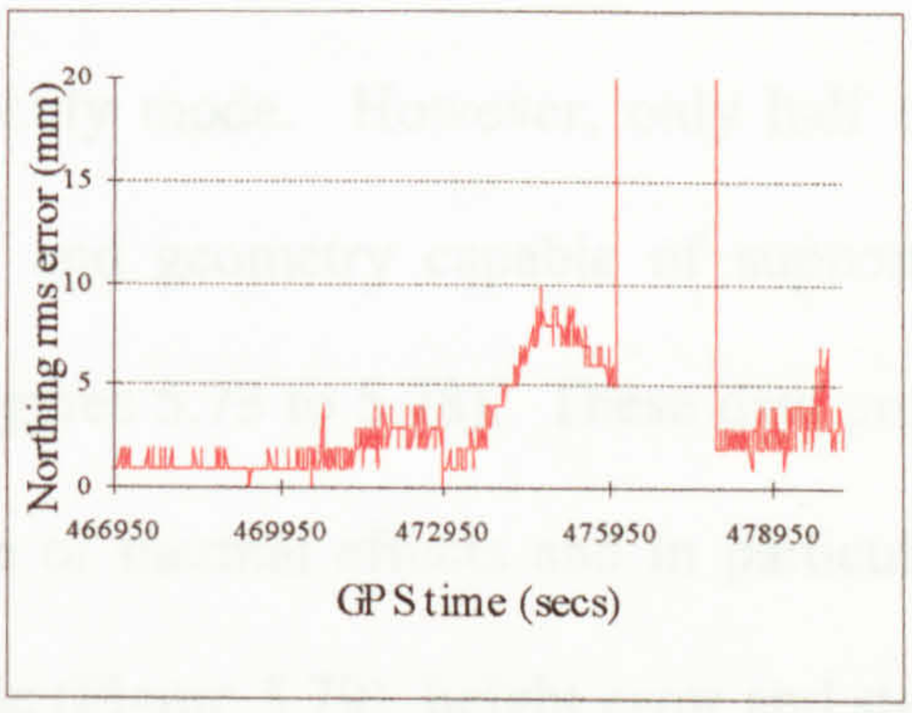

Figure 5.70 Hybrid thermal ZBL, Northing standard error

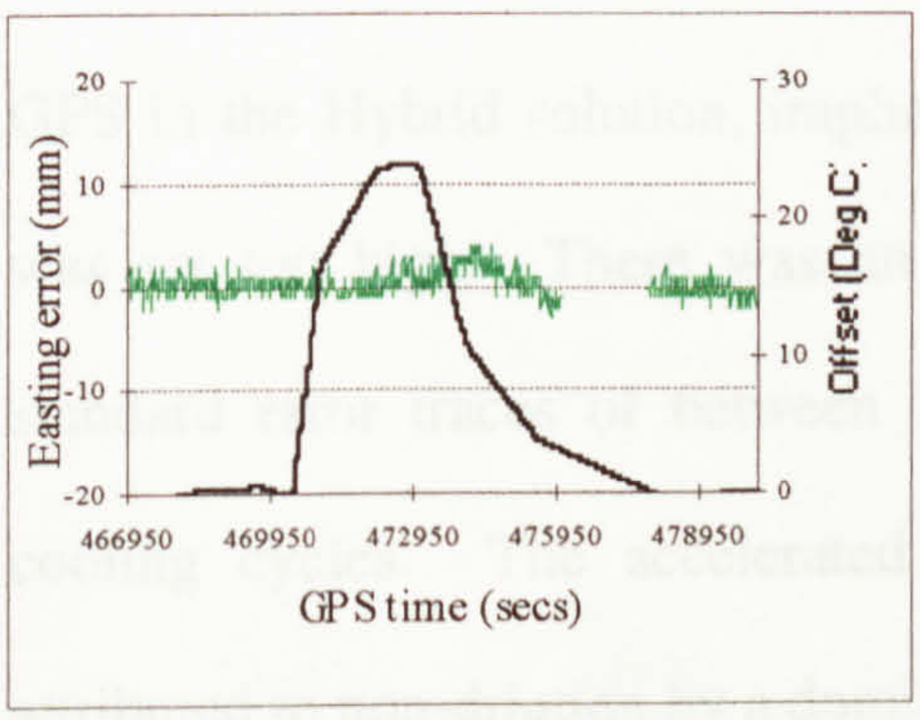

Figure 5.68 Hybrid thermal ZBL, Easting error

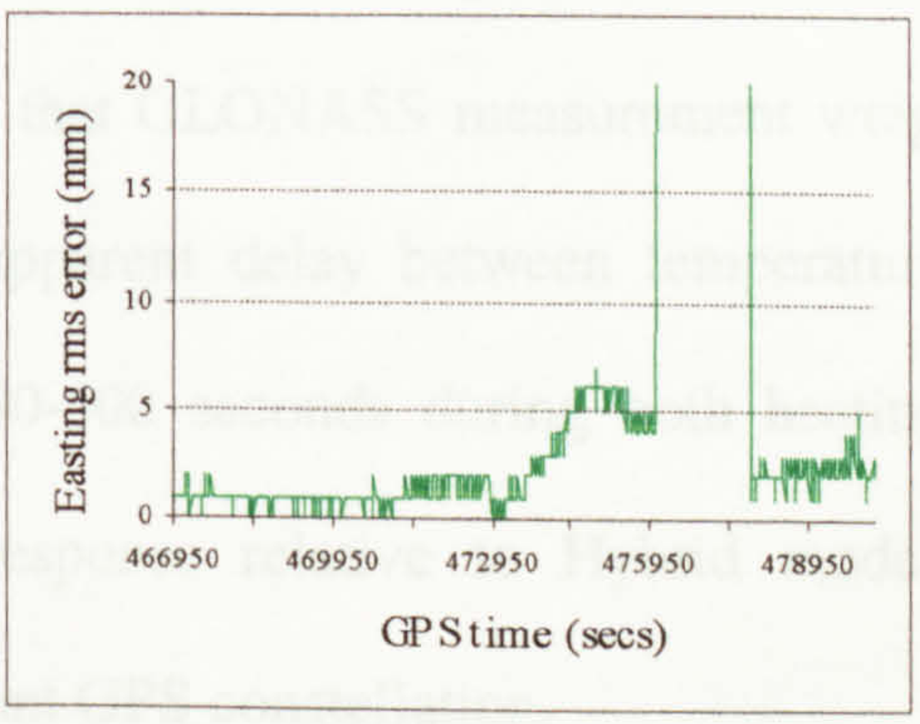

Figure 5.71 Hybrid thermal ZBL, Easting standard error

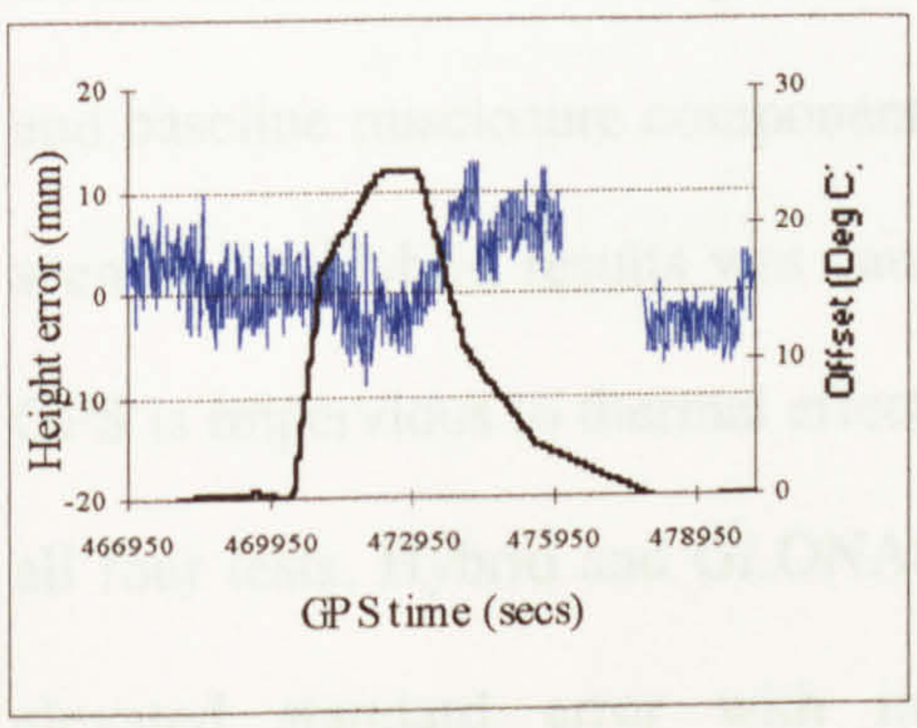

Figure 5.69 Hybrid thermal ZBL, Height error

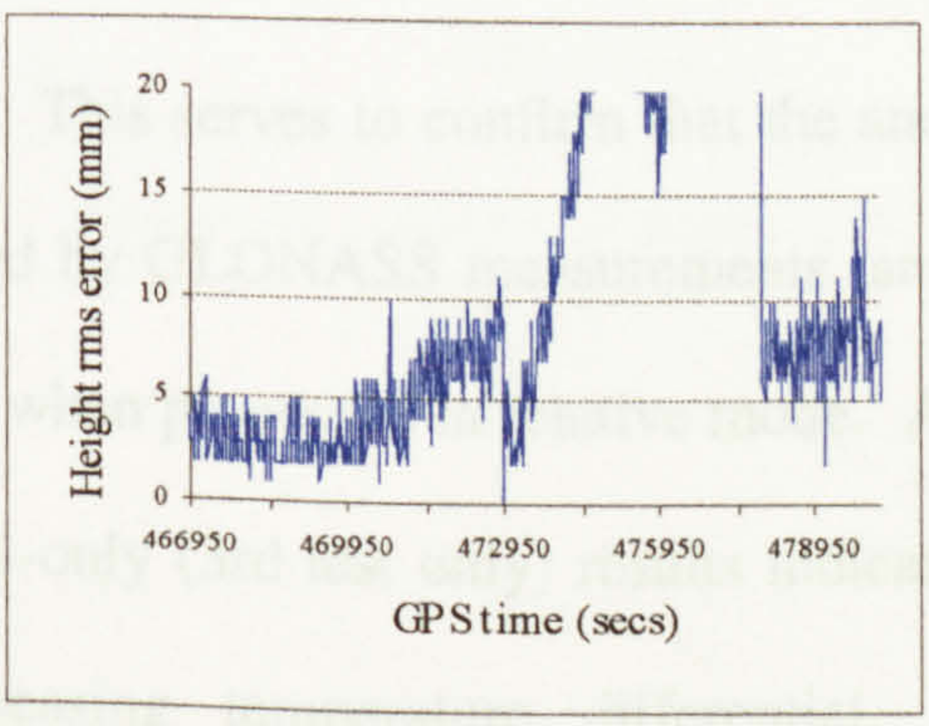

Figure 5.72 Hybrid thermal ZBL, Height standard error

as the GLONASS measurements fit less well together, within themselves and with those of GPS.

In order to isolate and clarify the nature of the induced bias, the four sessions were then processed in GLONASS only mode. However, only half of one session provided sufficient satellites and geometry capable of supporting a GLONASS carrier phase solution (Figures 5.73 to 5.78). These data provided the most significant graphic evidence of thermal effects and in particular the correlation between the thermal profile (Figure 5.79), height error and standard error, with a maximum induced height error of about 20 mm. This compares with 17 mm in Hybrid mode for the same test, which given the dominance of GPS in the Hybrid solution, implied that GLONASS measurement weighting was set too high. There was an apparent delay between temperature and standard error traces of between 300-500 seconds during both heating and cooling cycles. The accelerated response relative to Hybrid mode, was attributed to non-dilution by a dominant GPS constellation.

To summarise, in GPS-only mode, there was no modulation of standard error and baseline misclosure components. This serves to confirm that the anomaly seen in the Hybrid results was caused by GLONASS measurements, and that GPS is impervious to thermal effects when processed in relative mode. Across all four tests, Hybrid and GLONASS-only (3rd test only) results indicated an elevated standard error with increasing temperature differential. The magnitude was between 10 and 30 mm, for a thermal change of 20-25°C.

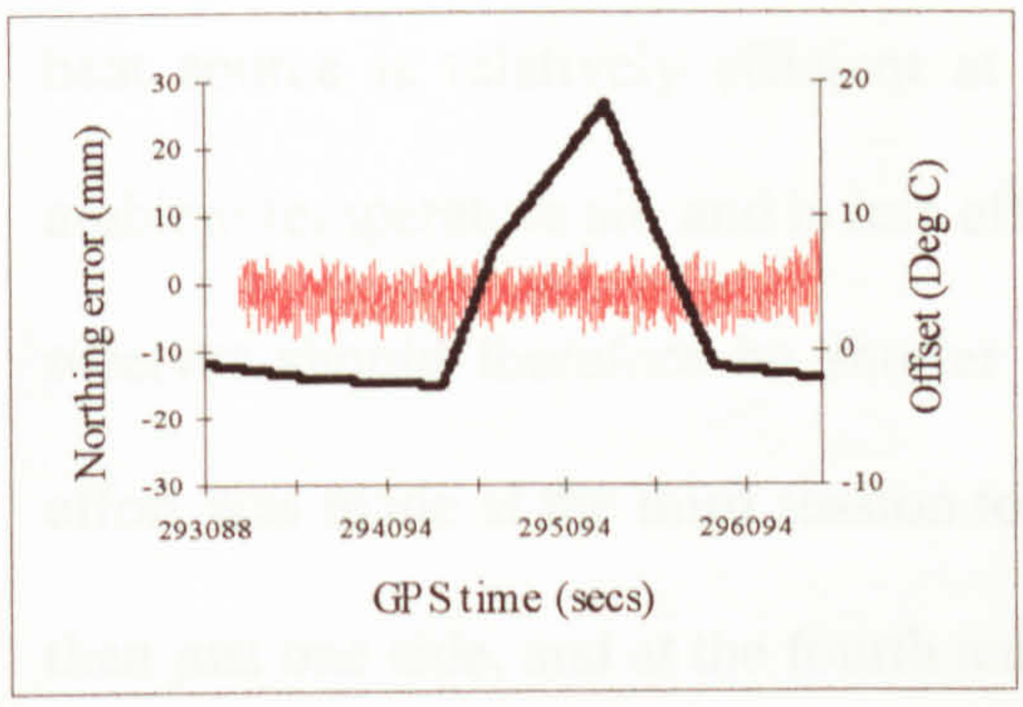

Figure 5.73 GLONASS thermal ZBL, Northing error

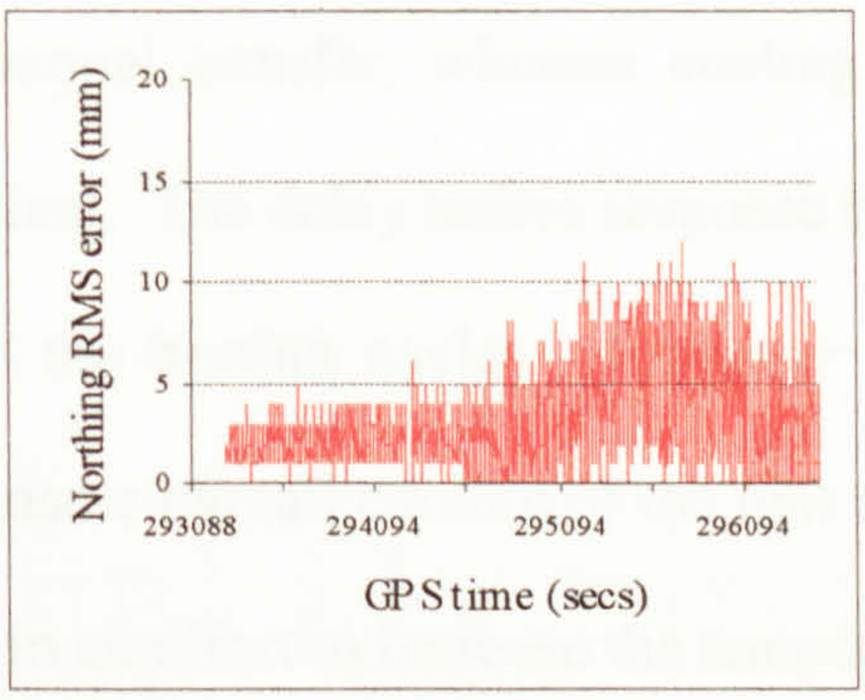

Figure 5.76 GLONASS thermal ZBL, Northing standard error

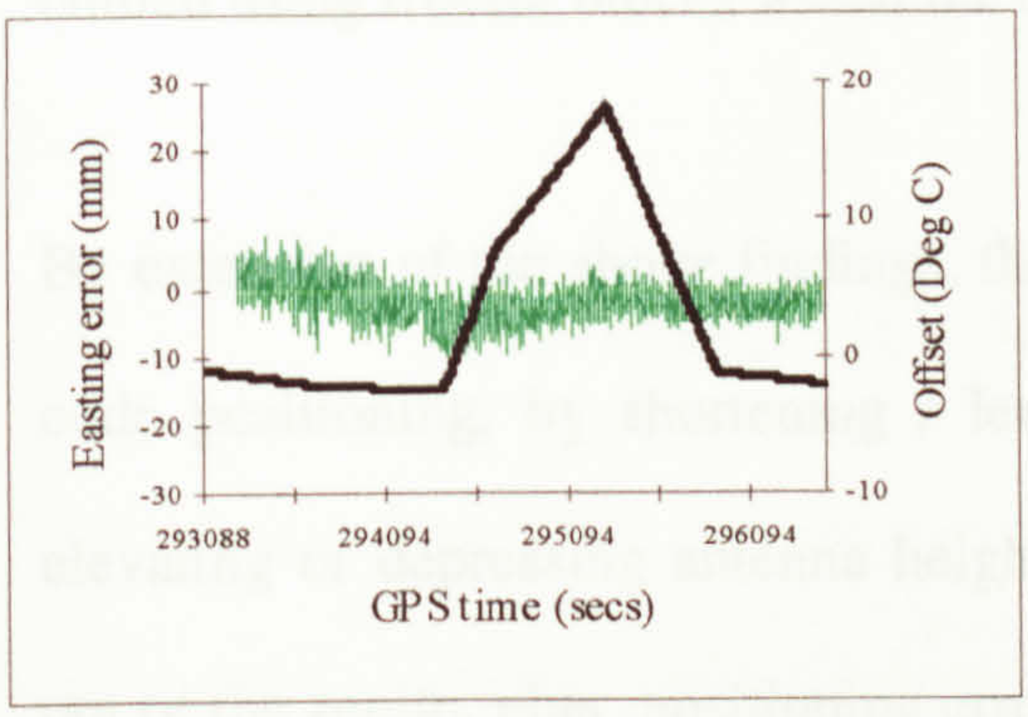

Figure 5.74 GLONASS thermal ZBL, Easting error

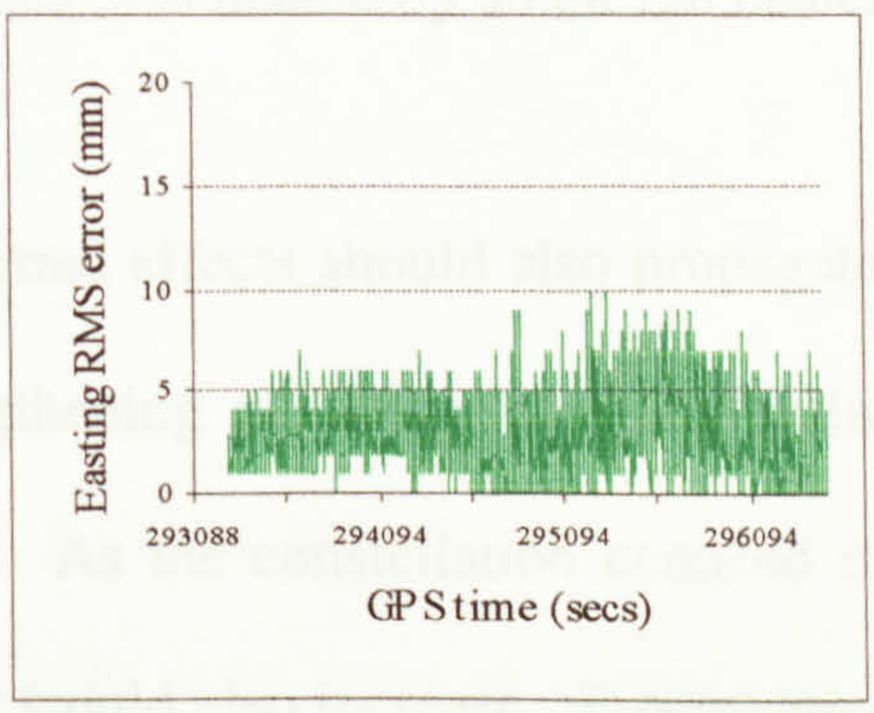

Figure 5.77 GLONASS thermal ZBL, Easting standard error

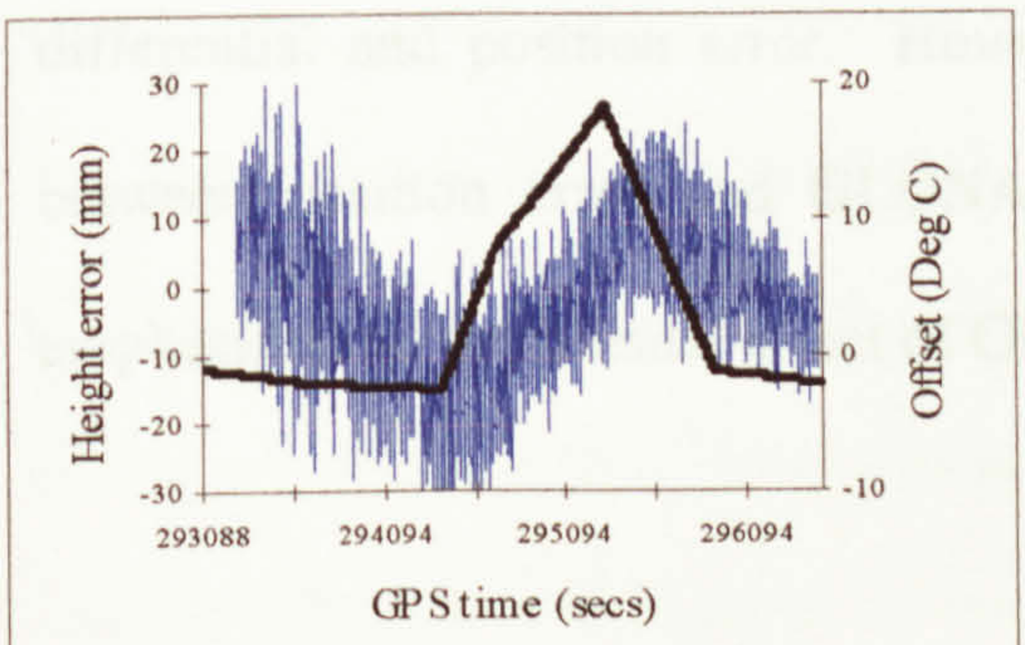

Figure 5.75 GLONASS thermal ZBL, Height error

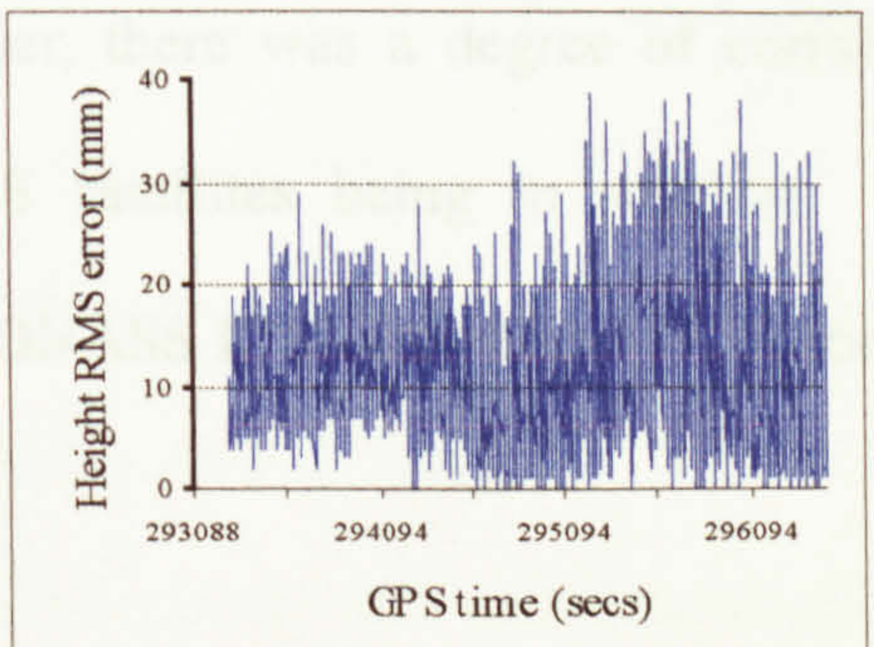

Figure 5.78 GLONASS thermal ZBL, Height standard error

Figure 5.79
Dual thermal cycle

What must be borne in mind with these trials, and their replication, is that the heat source is relatively efficient at thermal transfer, whereas cooling uses ambient temperature air, and is less efficient. The delay before response by the receiver should therefore be shorter in the heating cycles. However some effort was made at the third session to ensure overall cooling of the unit rather than just one side, and at the fourth test, in an effort to increase the temperature difference and magnify the thermal signature in the ZBL, one receiver was chilled using freezer blocks whilst the other was heated by an air fan heater.

By extension of the above findings, thermal effects should also propagate into code positioning, by shortening / lengthening pseudoranges, predominantly elevating or depressing antenna height. As the constellation centroid moves out of the zenith, plan positioning error would also increase. Processing of all data in DHybrid mode showed no discernible correlation between temperature differential and position error. However, there was a degree of correlation between position error and GLONASS satellites being in solution. This emphasises the detrimental effect of GLONASS ICBs on a Hybrid solution.

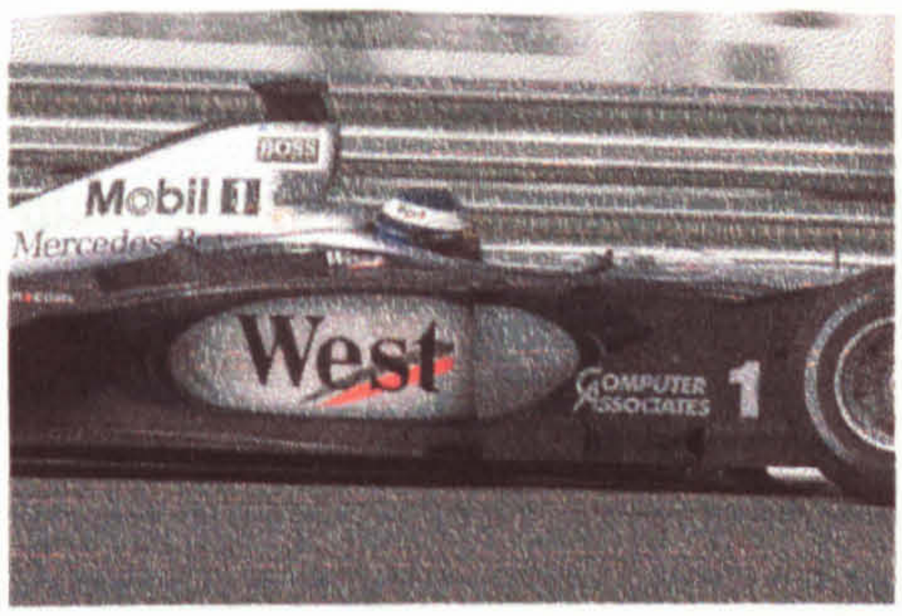

Chapter 6

Practical Dynamic

6.1 Introduction

This chapter considers the benefits of hybridisation as related to vehicle navigation. Vehicles rarely navigate under conditions of continuous ideal reception, rather there are typically both fixed and dynamic obstacles causing signal fading and blockage. Blocking or *masking* sources may be fixed as in roadside furniture and buildings, vary seasonally according to foliage cover, or vary within a daily cycle in terms of traffic type and density. The number of visible satellites is then reduced, and geometry may be less than optimum, both varying with time and location. If vehicle dynamics cause the antenna axis to point off-vertical, then a further variable mask is incurred.

More satellites equate to more chance of seeing a sufficient number of them with adequate geometry, to allow seamless navigation in difficult signal reception conditions. In this case, supplementation of a core GPS by any level of GLONASS availability can be of benefit. Just how much benefit there is,

and how best to describe this both qualitatively, and more usefully in quantitative terms, is one of the primary issues investigated here.

The dynamic positioning of vehicles of different types, with differing levels of antenna dynamics, is now evaluated on a relative basis between GPS and Hybrid. The following sections are laid out in an increasing level of positioning difficulty, until ultimately even augmented satellite positioning systems fail and other data types either alone or integrated are needed.

6.2 Buoy motion simulator

A test rig designed to simulate the semi-captive motion of a buoy mounted antenna, under wave action in a river, provided data with low level antenna dynamics and some off vertical pointing. A GG-24 was included in an array of simultaneously tested receivers and antennas. Only the GG-24 results are evaluated here. The test rig was set up about 20 metres from the IESSG, and 10 metres from a roadway with infrequent traffic. Hence there was likely to be fixed multipath caused by the rig structure and buildings, together with some contamination from dynamic multipath sources.

The rig shown in Figure 6.1, comprised a tripod from which a tethered platform was elastically suspended. This allowed three degrees of platform freedom. Receivers, power supplies and antennas were mounted on the platform.

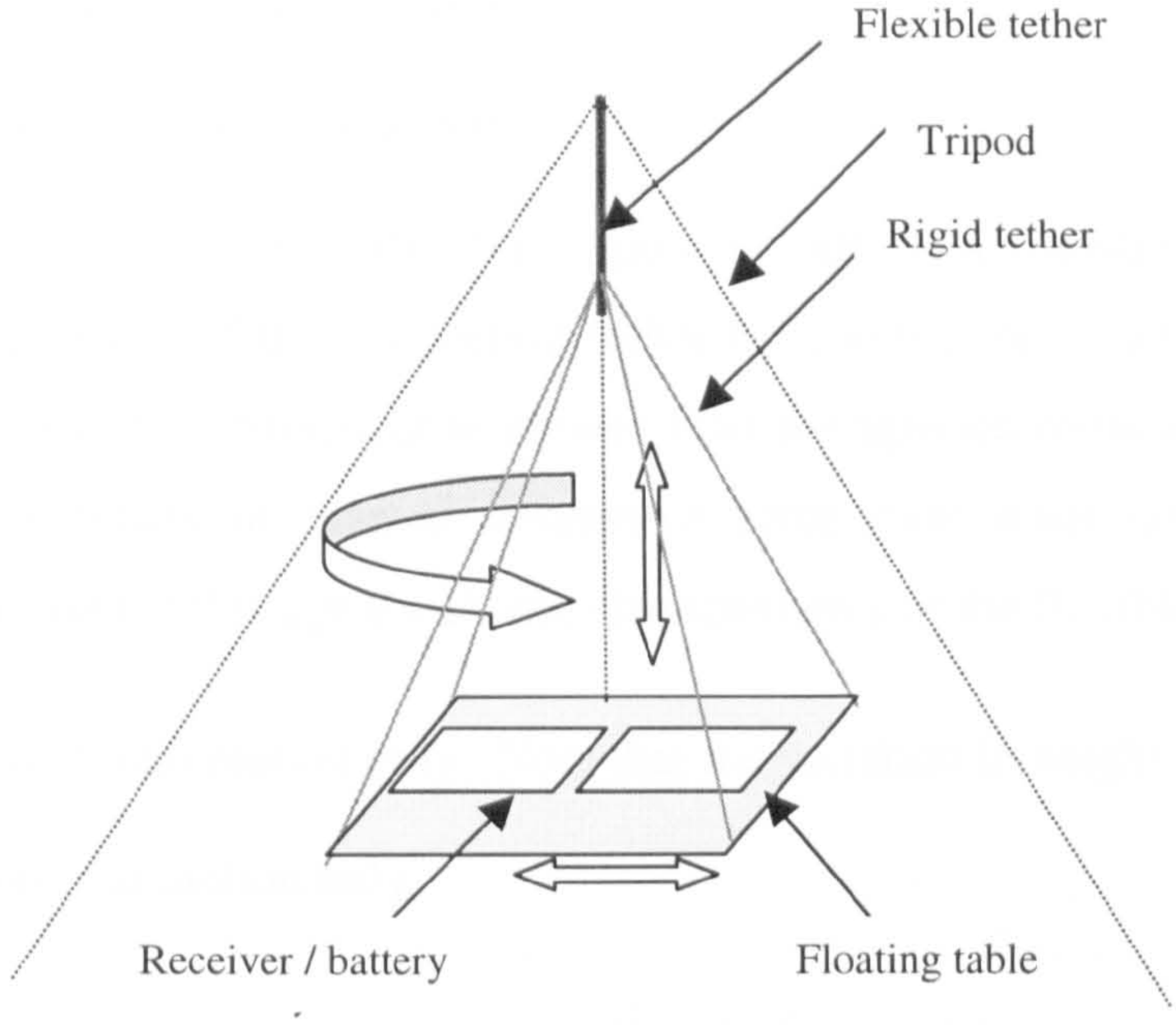

Figure 6.1 River buoy test arrangement

The baseline between reference and rig was about 40 metres, with GG-24 data recorded at 2 Hz for about 25 minutes. AOSS was used to generate the carrier phase fixed ambiguity GPS and Hybrid solutions. During the observation period there was a theoretical maximum of ten GPS and five GLONASS satellites available. The number of common satellites used in processing was eight GPS and three GLONASS satellites, numbers being reduced at the rig by a combination of signal blocking and dynamic antenna motion. GPS PDOP was about 2, whilst that for Hybrid was about 1.5 units.

Three types of platform motion were induced by hand: swinging in a NE / SW direction and rotational, both seen in Figure 6.2, and vertical only in Figure 6.3.

Five areas of coherent activity can be identified and labelled in the height component, corresponding to:

1 Swinging from NE to SW.

2 Swinging from NE to SW.

3 Vertical motion only, this region includes a unintentional permanent extension of the supporting tether by about 5 centimetres. Note the downward movement is greater than the upward movement, owing to the excess of manual depressive force over what height could be recovered through the elastic characteristics of the flexible tether.

4 Rotational motion only. Note that the variation in height is minimal.

5 Vertical motion only.

Between events the windy conditions on the day induced a level of noise and some few centimetres variation. The five centimetre change in height identified in (3) above was due to a partial failure in the vertical flexible suspension tethers.

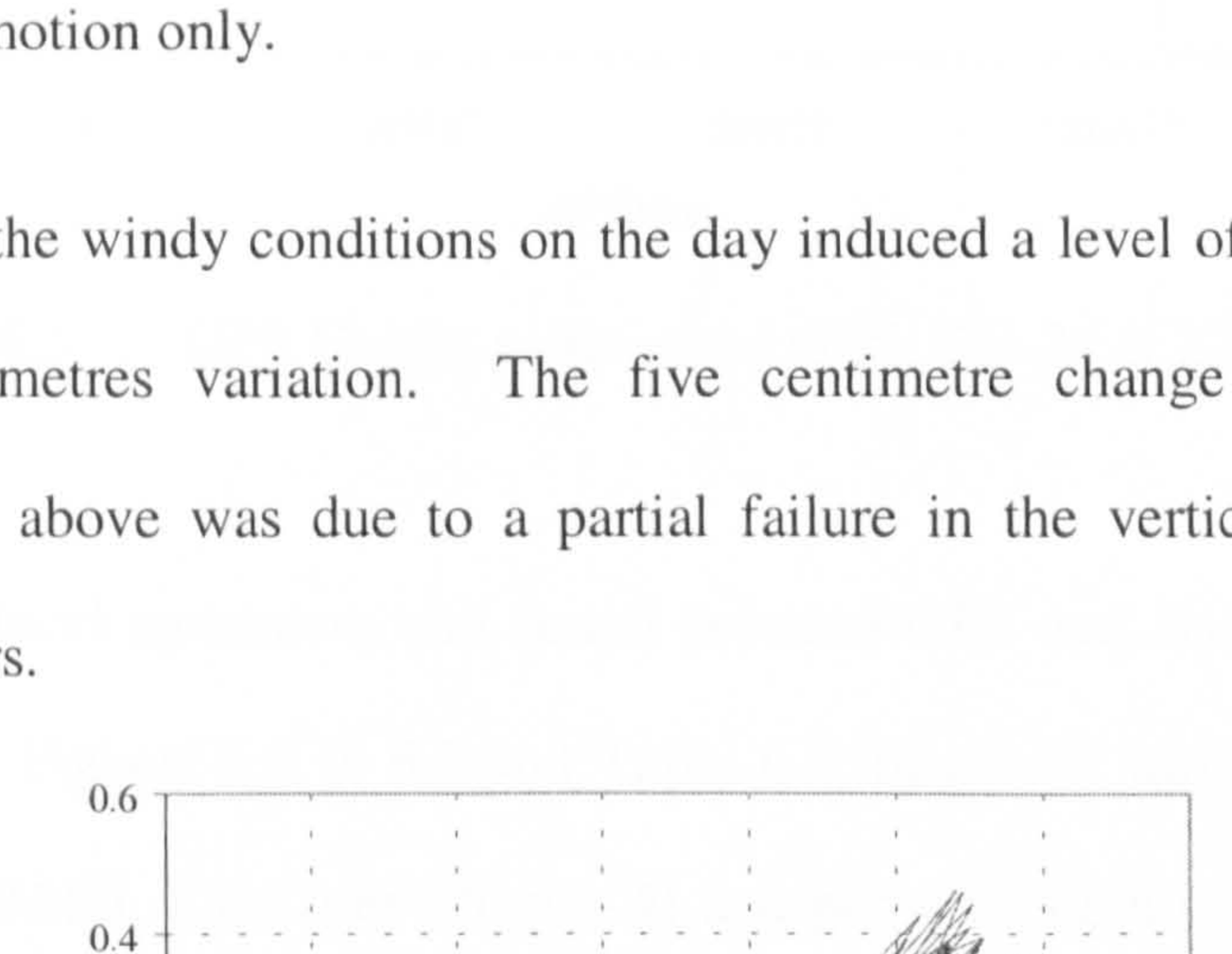

Figure 6.2 Plan trajectory by GPS, GG-24 at 2 Hz

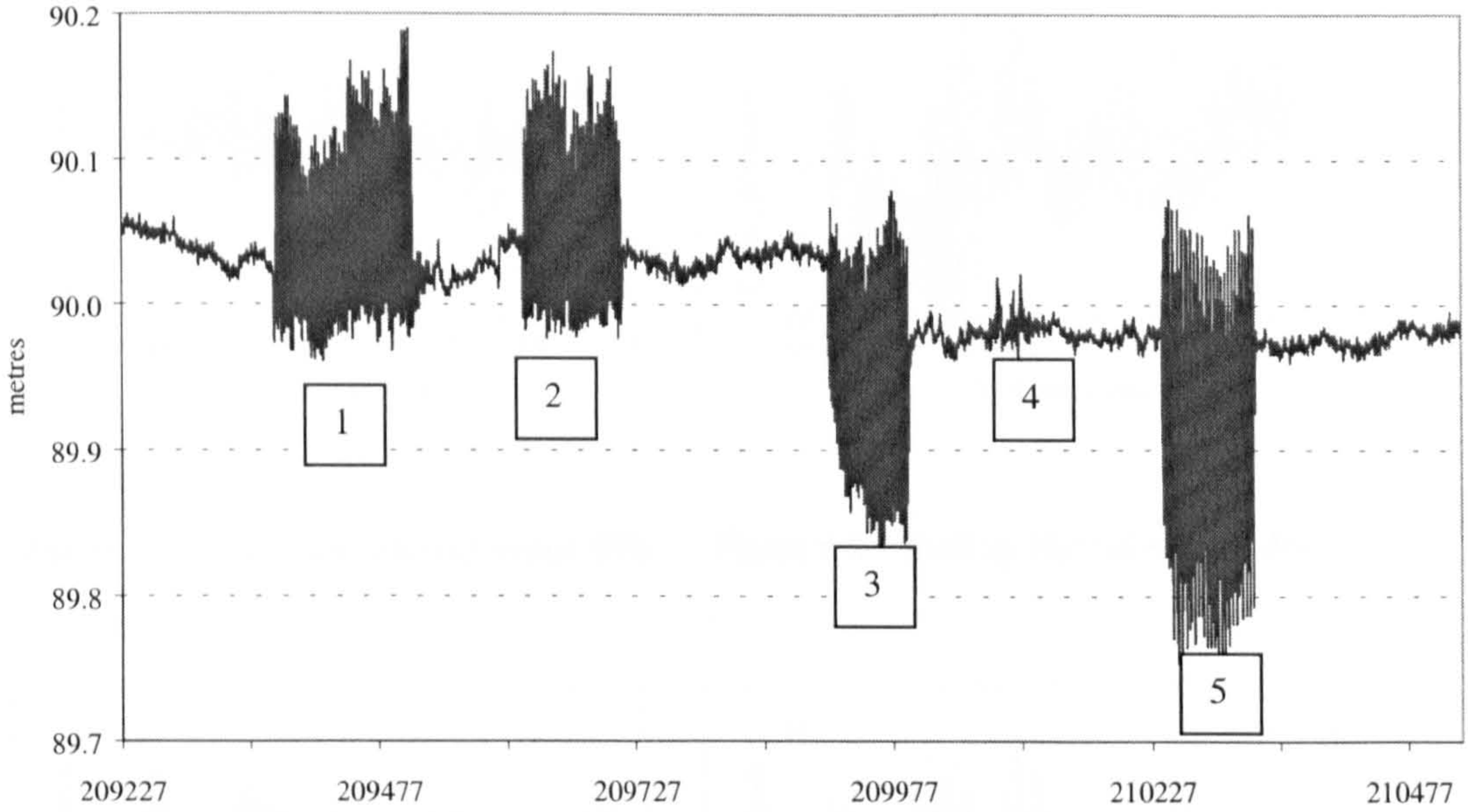

Figure 6.3 GPS Height variation by GPS, GG-24 at 2 Hz

Sub-centimetre level agreement was found between GPS and Hybrid modes. Differences, see Figures 6.4 to 6.7 and Table 6.1, might be attributed to the effects of GLONASS ICBs (see Chapter 4) and perhaps additional multipath contamination brought into the positioning solution. These results suggest that if Hybrid is to be beneficial in terms of accuracy, then the intrinsic noise level of GPS alone caused by multipath, should have a threshold level above or at least equal to that attributable to GLONASS ICBs. Figures 6.8 and 6.9 indicate the marginal improvement in constellation size and geometry of Hybrid over GPS.

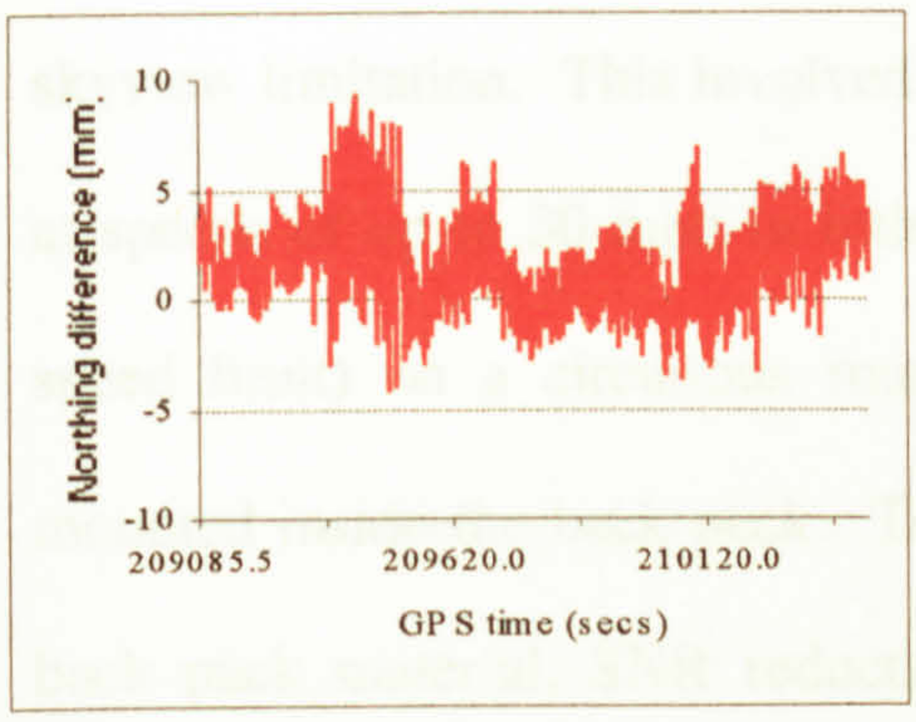

Figure 6.4 Northing: Hybrid minus GPS

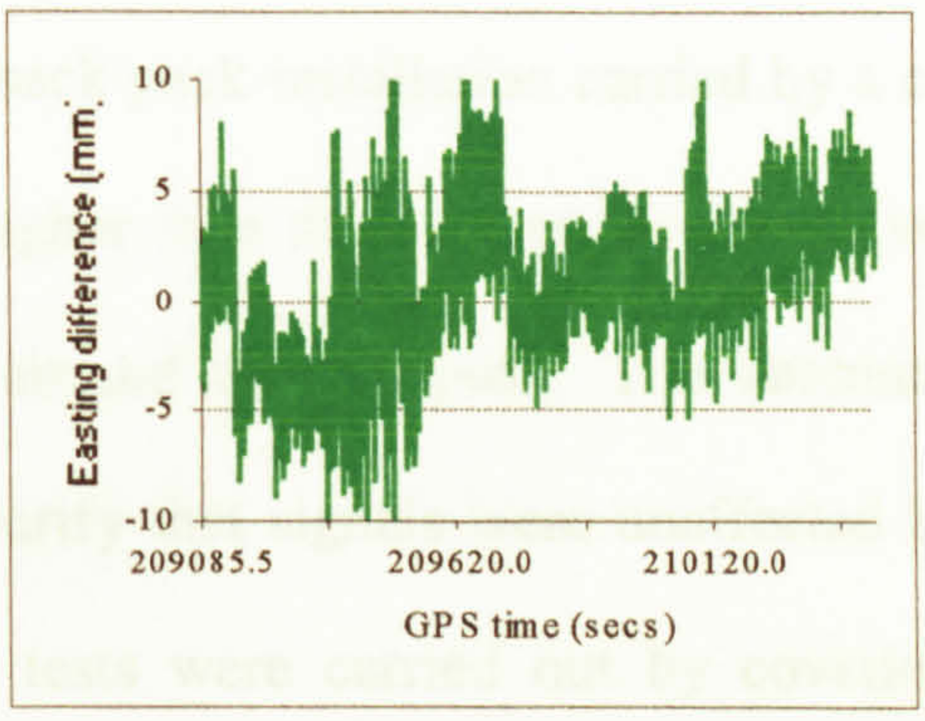

Figure 6.5 Easting: Hybrid minus GPS

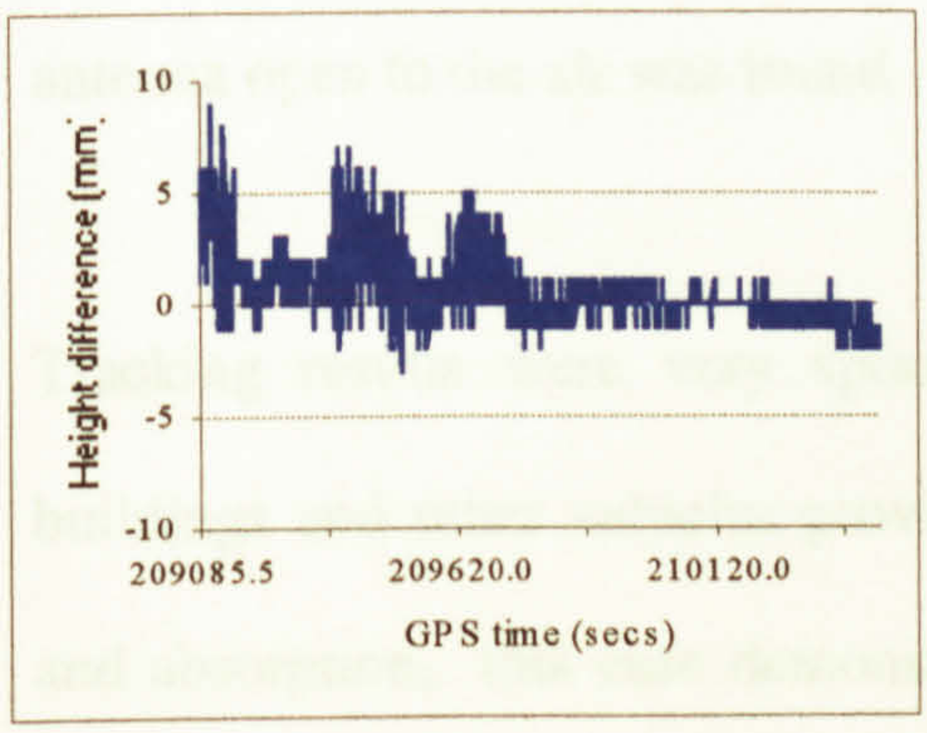

Figure 6.6 Height: Hybrid minus GPS

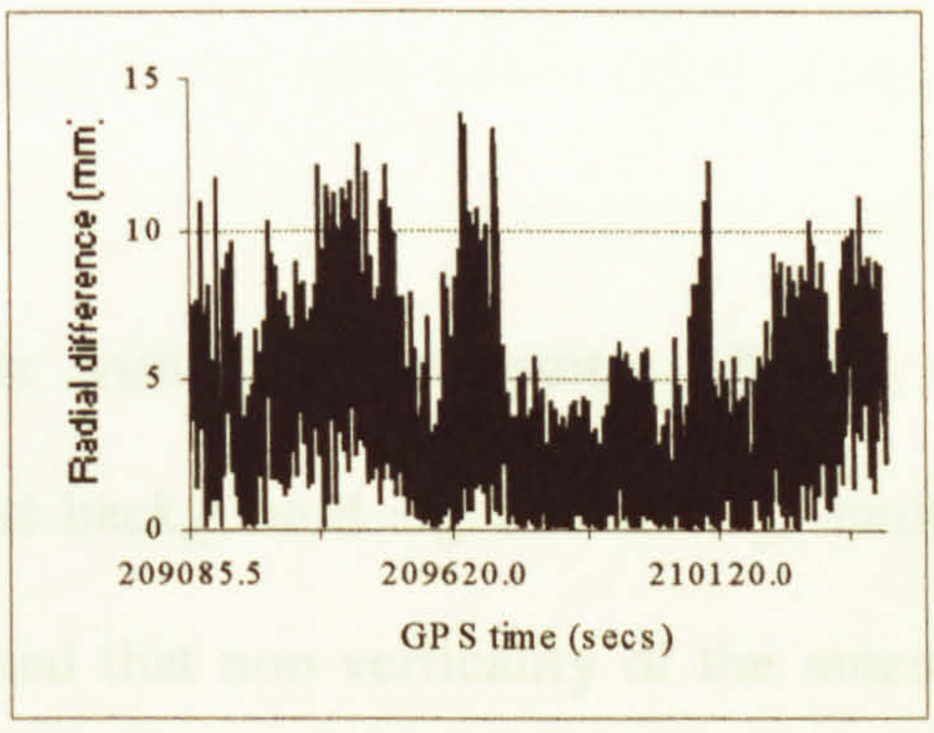

Figure 6.7 Radial: Hybrid minus GPS

Northing (mm)	Easting (mm)	Height (mm)	Radial (mm)
1.5 (1.9)	0.5 (3.3)	0.7 (1.4)	3.6 (2.5)

Table 6.1 Hybrid minus GPS, average values (mm)

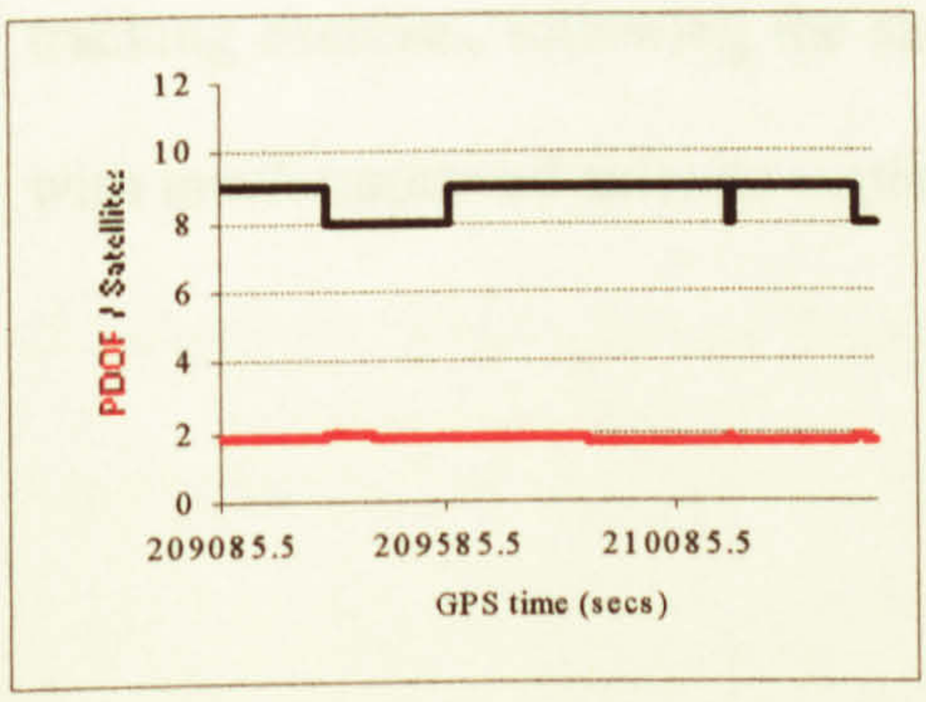

Figure 6.8 GPS constellation (Rig)

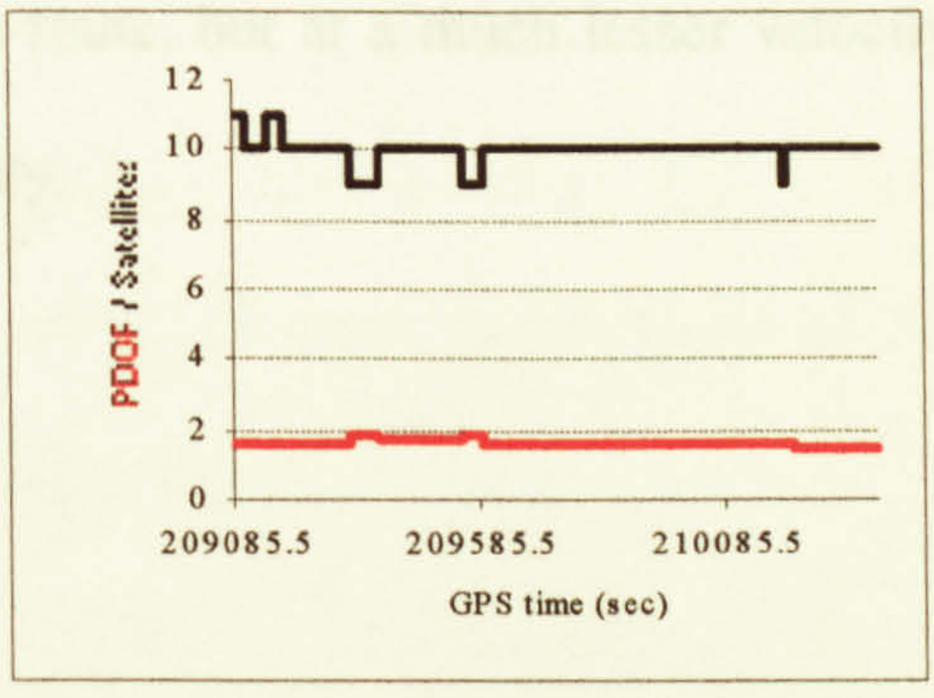

Figure 6.9 Hybrid constellation (Rig)

6.3 Cycle tracking

The next test was pitched at a higher level of difficulty in terms of dynamic skyview limitation. This involved a back pack installation carried by a cyclist at speeds of up to 30 mph (a little higher than the campus motorised vehicle speed limit) on a circuitous route around the campus. The antenna was mounted inside the back pack. To verify that signals were unaffected by the back pack material, SNR reduction tests were carried out by covering the antenna with single and multiple layers of various fabrics, together with double layers of the pack material itself. No change in SNR relative to that with the antenna open to the air was found.

Tracking results were very sporadic with little continuity. Whilst trees, buildings and other vehicles provided background signal masking, multipath and absorption, this case demonstrated that non-verticality of the antenna in combination with signal blocking by skull and brain matter were the major issues in positioning for this type of sport application.

The next test took a step backwards, in a dynamic sense, from the cycle tracking exercise, following the same route, but at a much lesser velocity and with much improved antenna verticality.

6.4 Track tracing – low velocity (1)

The vehicle in this case was a distance measuring wheel, as typically used by highways departments. The antenna was elevated above head height at about two metres, to avoid signal masking/absorption by the body, but still retaining sources of fixed and dynamic multipath and signal masking. Speed of advance was a brisk walking pace at about 7 kph. The equipment was used to define the joint between kerb and road metal, i.e. where the vertical kerb edge meets the horizontal road surface. This profile was selected as large segments appeared with good contrast in geo-referenced aerial photography of the campus (previously digitised by IESSG staff), with which it was compared. The objective was to look for weak areas of profile definition by each method, suggest an explanation, decide whether one system could be augmented by the other, under what circumstances, and compare areas where both systems were likely to operate well.

The photography had been flown some few years earlier at a scale of 1:10000, and processed at the time with an SD2000 analytical plotter, with an estimated final coordinate accuracy, by the operator, of around one metre.

The satellite positioning solution was Hybrid carrier phase by AOSS, and with the exception of the area to the East of 454300 metres and North of 338400 metres, see Figure 6.13, was of float ambiguity.

Representative sections of the satellite positioned route are shown as the continuous blue trace in Figures 6.10 to 6.13, and the equivalent trace from aerial photography followed the road side yellow line, here shown as the red trace.

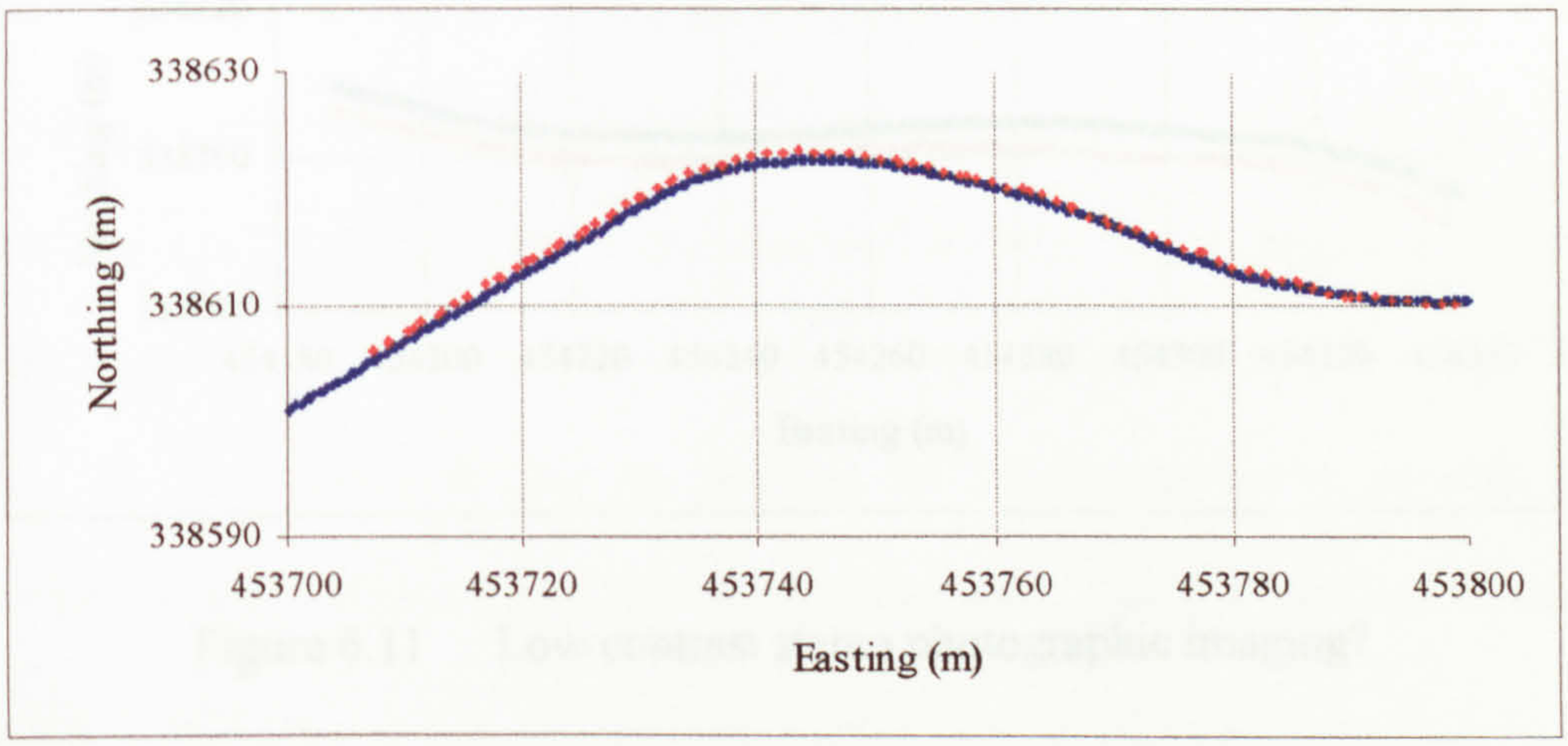

Figure 6.10 Positioning under clear skyview conditions

Figure 6.10 demonstrates the high level of agreement between the two methods, at a metre or better, in an area of clear skyview and good ground feature contrast. A region of poor agreement is shown in Figure 6.11 where cast shadows may have interfered with photo point picking, the trend follows that of the kinematic track, however it is offset, suggesting that the margin between grass and walkway may have been extracted rather than the yellow line. Park [1999], using the same digitised data set came to similar conclusions, in that correct edges were sometimes difficult to follow on the analytical plotter. Finally, Figure 6.12 has a clear skyview with good colour contrast, in this case kinematic tracking was run down one side of the road, and

the analytical plotter down the other. Resultant road width was found to be on average about nine metres, whilst that measured by tape was about 6.5 metres. Without the benefit of road definition on both sides by both methods it was not possible to determine which method was, if at all, inferior.

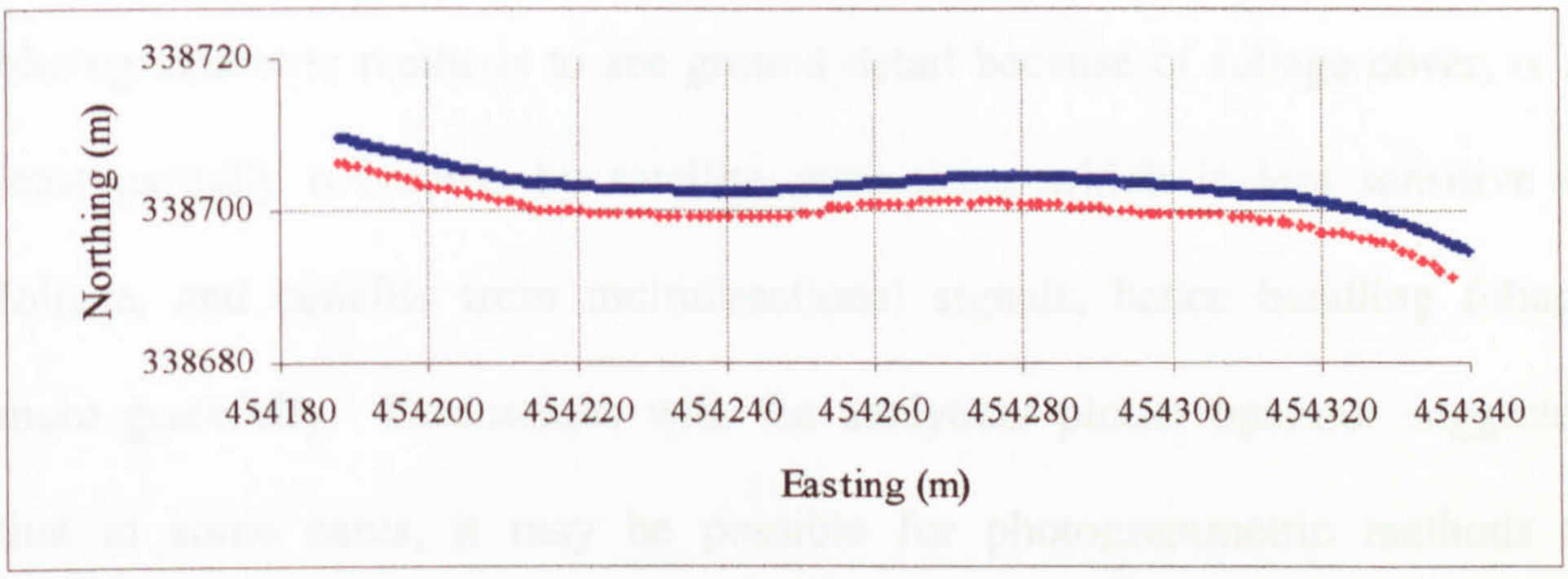

Figure 6.11 Low contrast stereo photographic imaging?

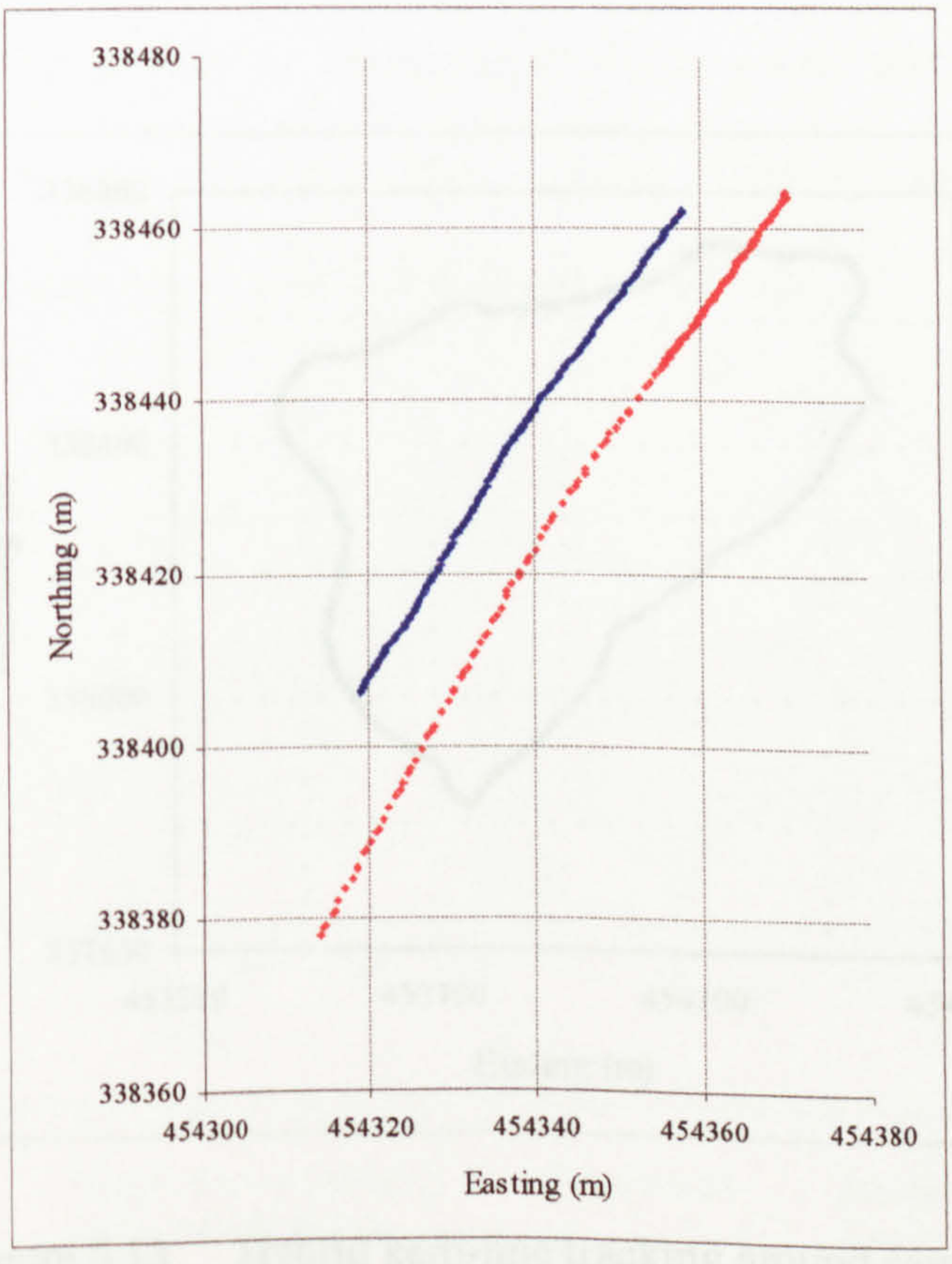

Figure 6.12 Positioning alternate kerblines under clear skyview conditions

An idea of overall relative capability is demonstrated in Figures 6.13 and 6.14. The south-east section of these figures should be ignored, as different routes were followed (unaware at the time of positioning by satellite means). It can be seen that for this particular route and environment, satellite methods have a positioning capability of about 50% more than aerial photography. Inability of photogrammetric methods to see ground detail because of foliage cover, is at least partially overcome by satellite positioning which is less sensitive to foliage, and benefits from multidirectional signals, hence handling foliage more gracefully. Discussions with the analytical plotter operator suggested that in some cases, it may be possible for photogrammetric methods to overcome these effects by using oblique view, rather than the standard vertical photography.

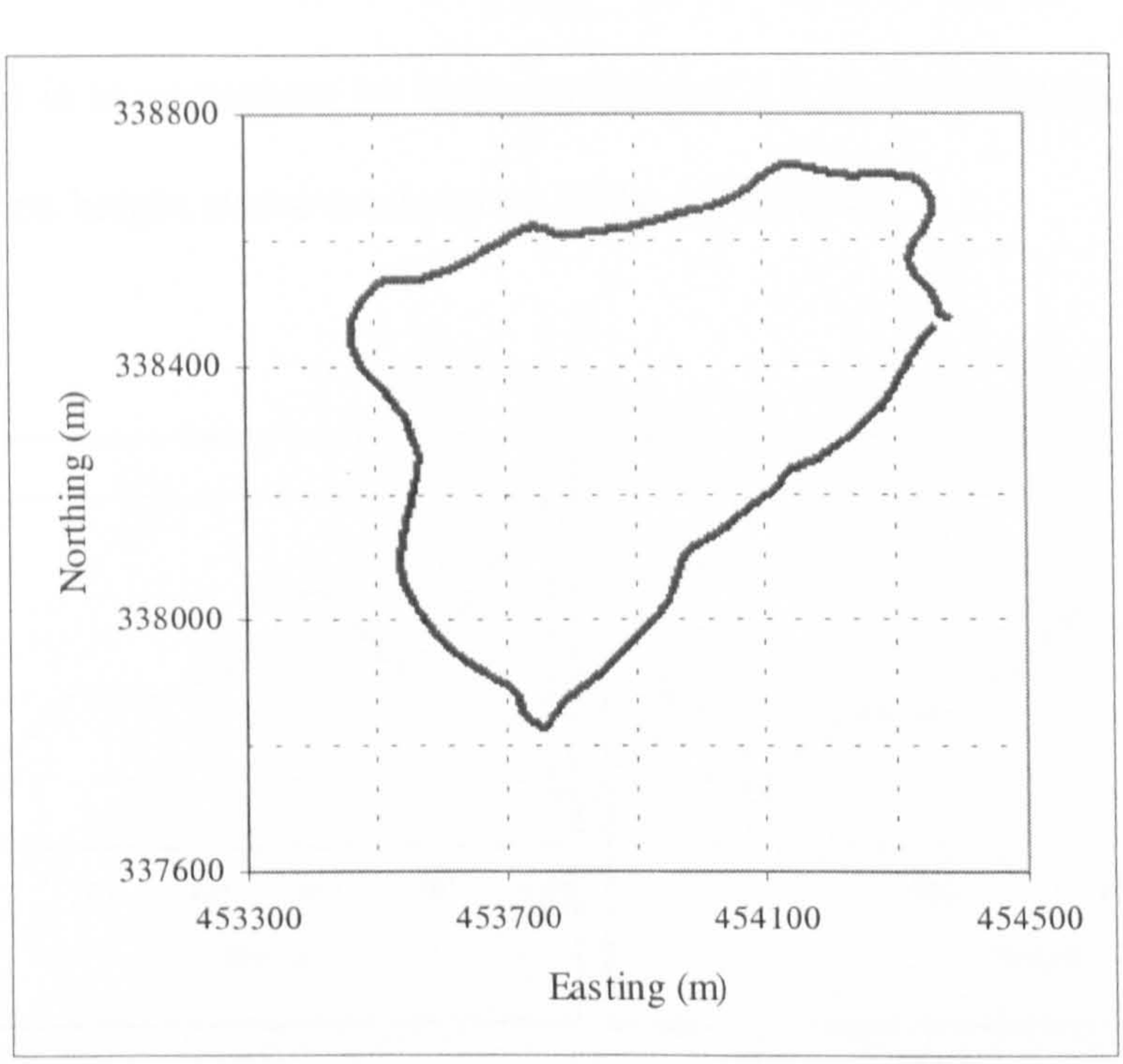

Figure 6.13 Hybrid kerb-line tracking around campus

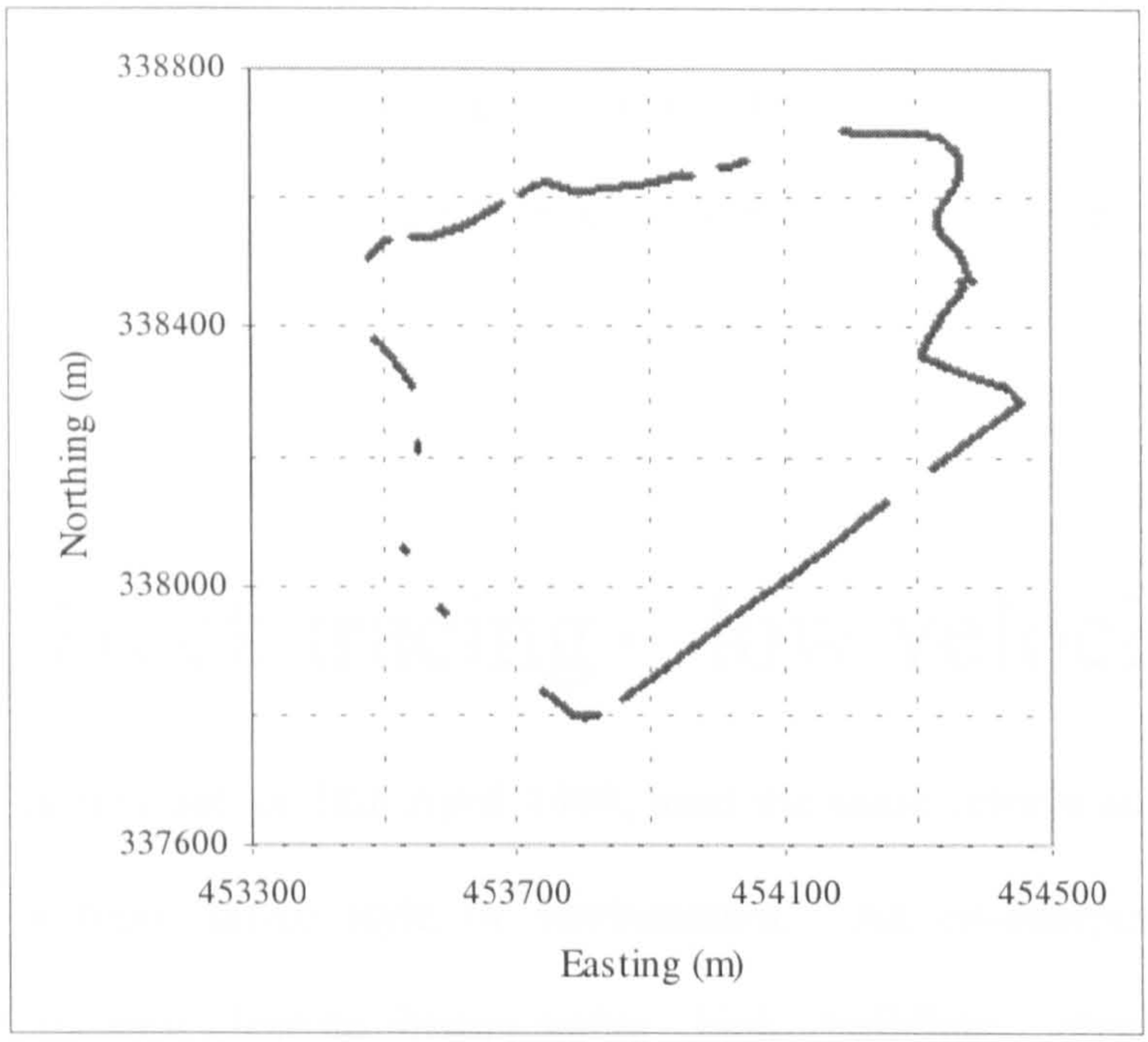

Figure 6.14 Analytical plotter / aerial photography kerb-line tracking around campus

Height determination for an interesting segment by each method (Figures 6.15 and 6.16) is in agreement by between 1.9 and 2.6 metres, taking into account the antenna height above roadway of about 1.8 metres.

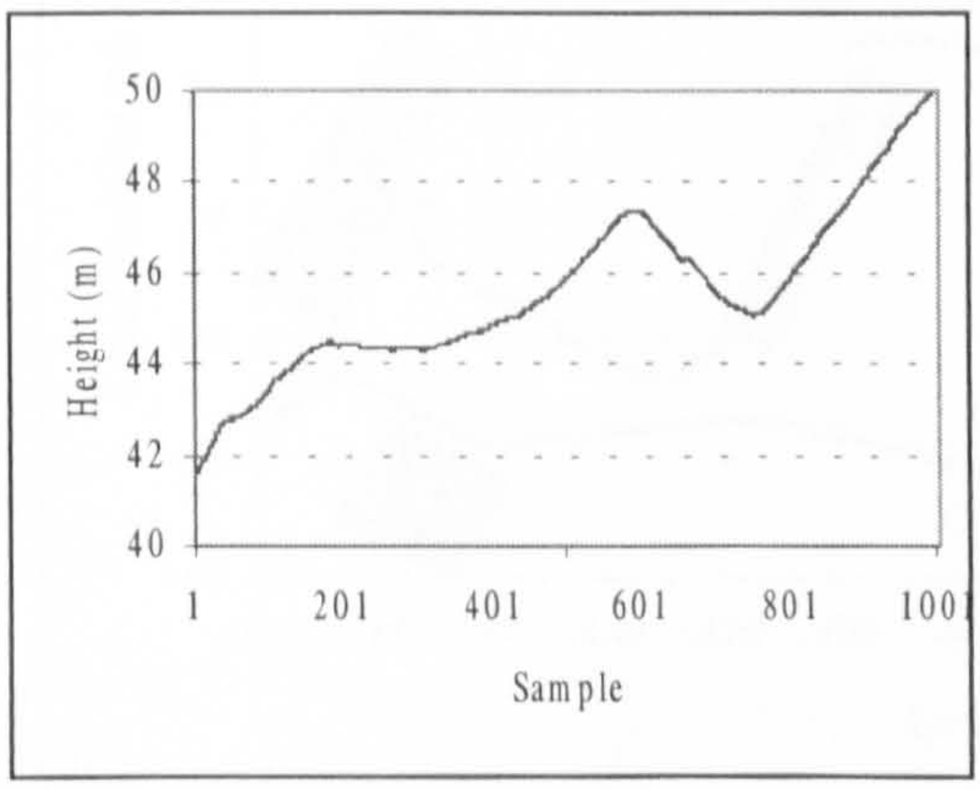

Figure 6.15 Height determination of kerb-line by satellite positioning

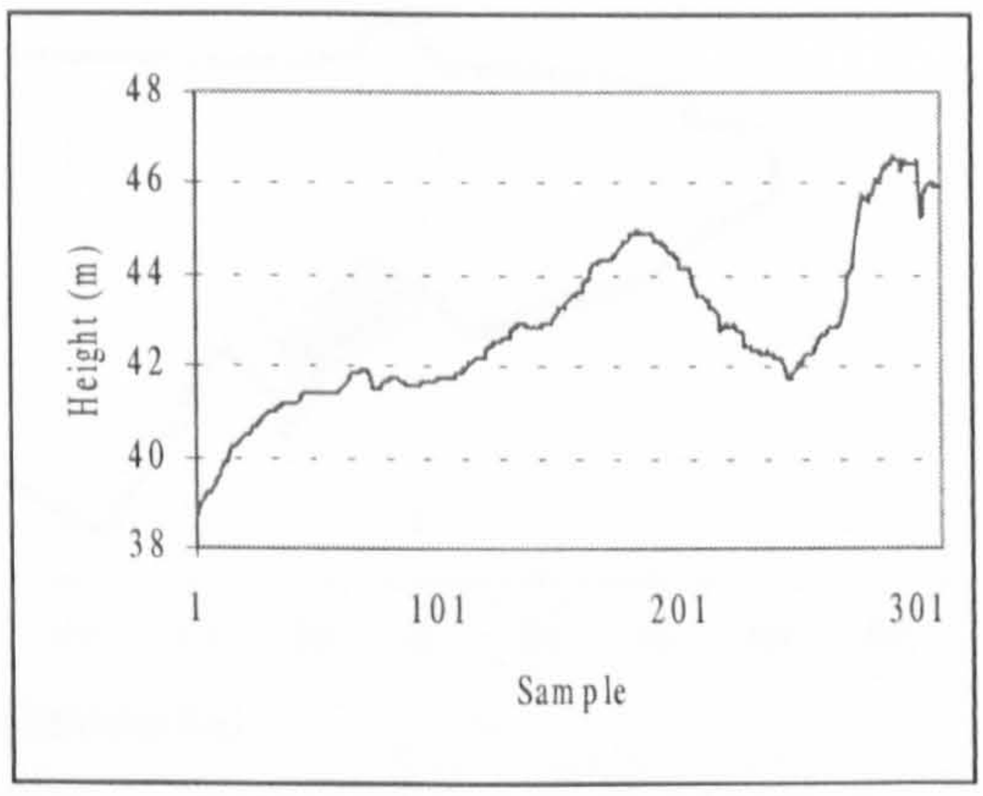

Figure 6.16 Height determination of kerb-line by analytical plotter / aerial photography

In summary, satellite methods could supplement vertical photography where foliage occurs, conversely photography could assist satellite positioning where environmental noise levels are high e.g. from fixed and dynamic multipath sources.

6.5 Track tracing – low velocity (2)

This test carried out on 28th April 1998, used the same vehicle as in §6.4, but involved a more urban style of environment. An on-campus route was followed, passing close to fifteen metre high buildings, shaded red in Figure 6.17, up and down smooth and stepped inclinations, and close to a wall of dense twenty metre high trees (shaded green). Speed of advance was at a slow walking pace, with data logging at 1 Hz.

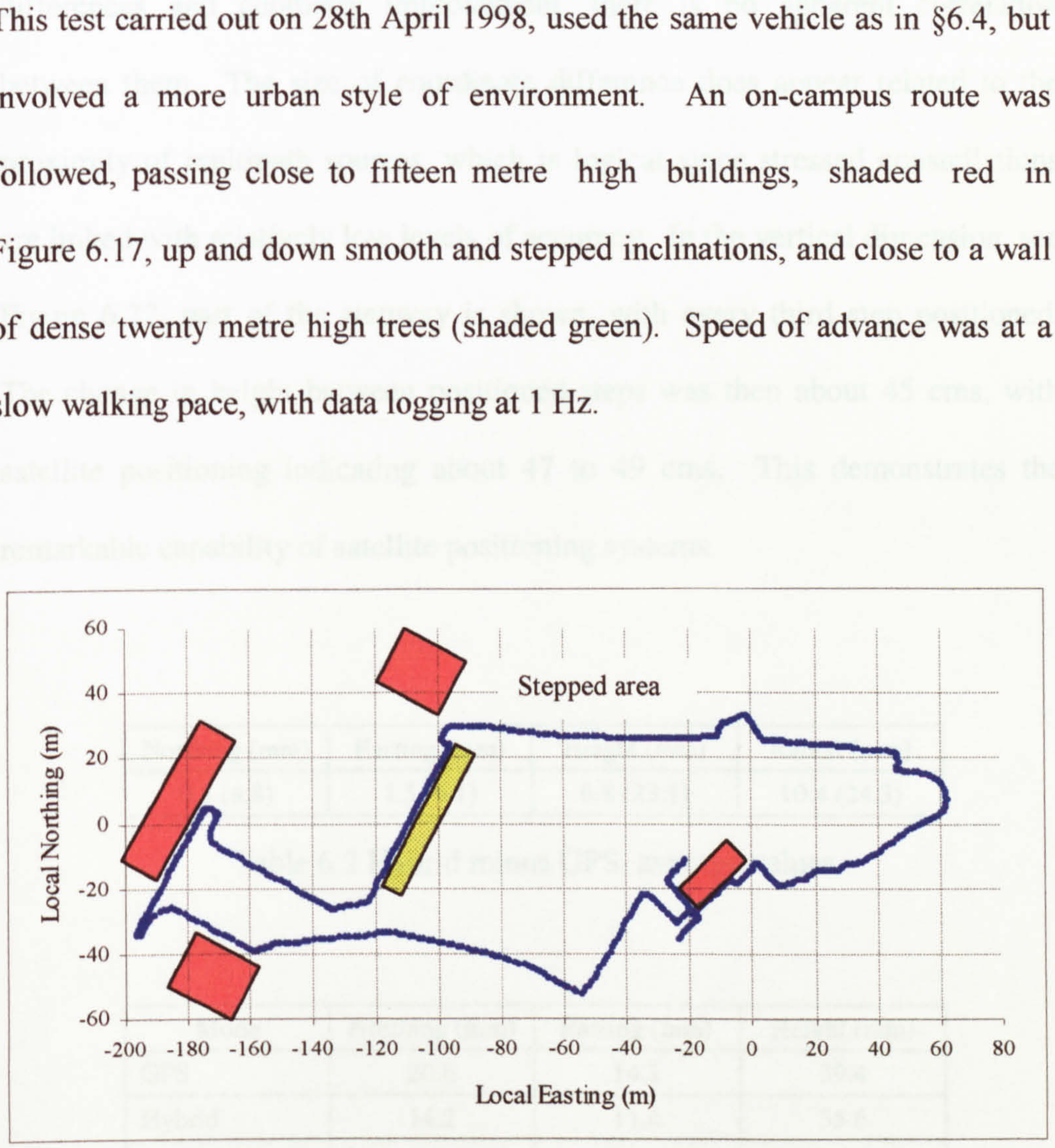

Figure 6.17 Hybrid tracking

AOSS carrier phase solution differences, shown in Table 6.2 are as before, probably an indication of included GLONASS specific errors of ICBs and additional multipath. The benefits of hybridisation are expressed in Tables 6.3 to 6.4, which demonstrate a reduced solution RMS level, and improvements in geometry. The improvement in geometry for a zero increase in constellation, is explained, if a more suitable GLONASS satellite takes the place of a GPS satellite. Figures 6.18 to 6.21 provide an alternate view of coordinate differences and geometry improvement, there is no apparent correlation between them. The size of coordinate difference does appear related to the proximity of multipath sources, which is logical since stressed constellations are linked with relatively low levels of accuracy. In the vertical dimension, see Figure 6.22, part of the stepway is shown, with every third step positioned. The change in height between positioned steps was then about 45 cms, with satellite positioning indicating about 47 to 49 cms. This demonstrates the remarkable capability of satellite positioning systems.

Northing (mm)	Easting (mm)	Height (mm)	Radial (mm)
0.8 (8.8)	1.5 (6.1)	6.8 (23.1)	10.4 (24.3)

Table 6.2 Hybrid minus GPS, average values

Mode	Northing (mm)	Easting (mm)	Height (mm)
GPS	20.6	14.1	39.4
Hybrid	14.2	11.4	35.6
Change	31.0 %	19.1 %	9.6 %

Table 6.3 Solution RMS, average values

Change in ..	Average	Best	Worst
PDOP	-0.5	-3.9	-0.1
# satellites	2.8	4	0

Table 6.4 Hybrid constellation improvement over GPS alone

Improvement in absolute accuracy was impossible to gauge, since again there was no mapping truth. The only other way to overcome this, would be to use a previously and independently coordinated track on which the positioning equipment could be run repeatedly. A model railway track found at holiday complexes would have been suitable, but this was not followed up, and a roller coaster was also considered but abandoned because of safety considerations.

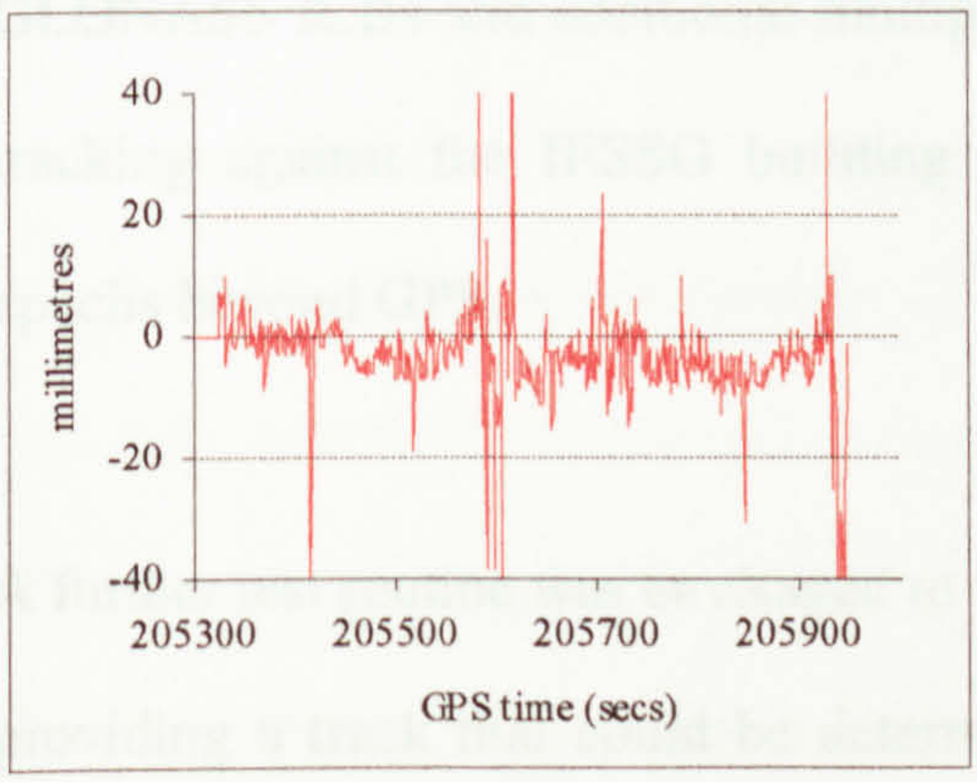

Figure 6.18 Northing: Hybrid minus GPS

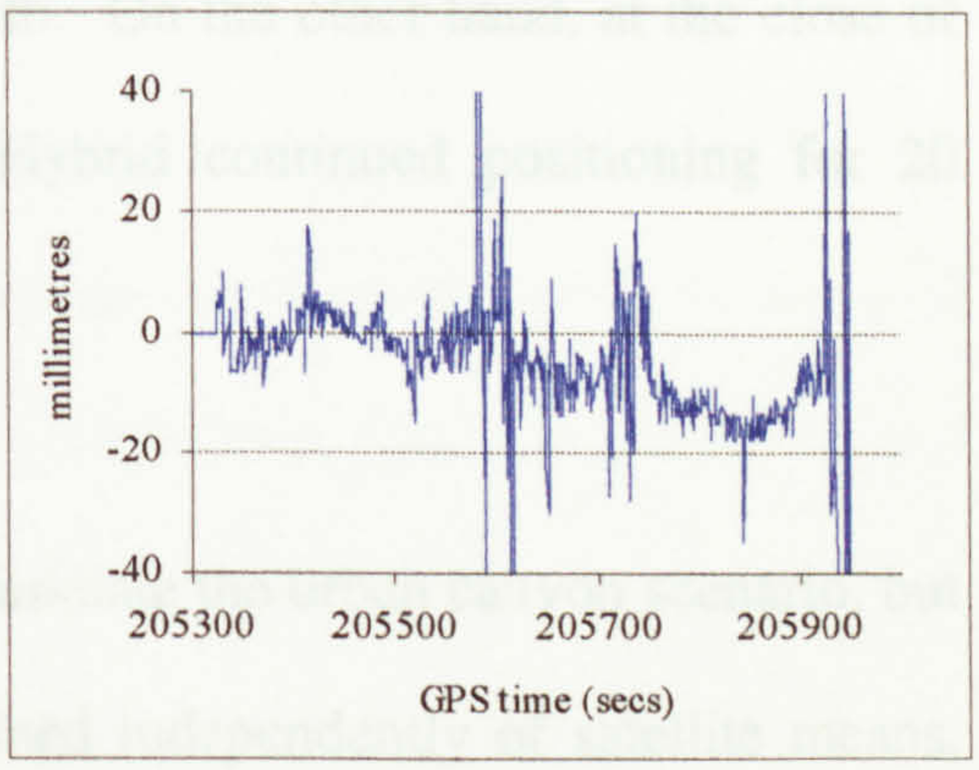

Figure 6.20 Height: Hybrid minus GPS

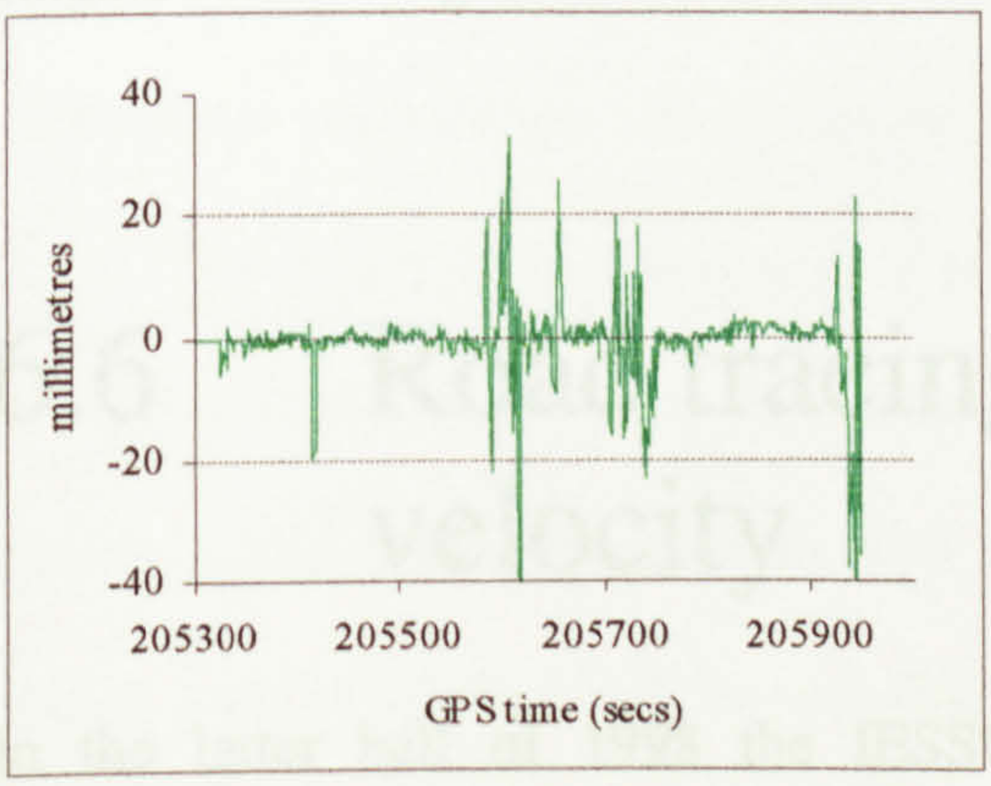

Figure 6.19 Easting: Hybrid minus GPS

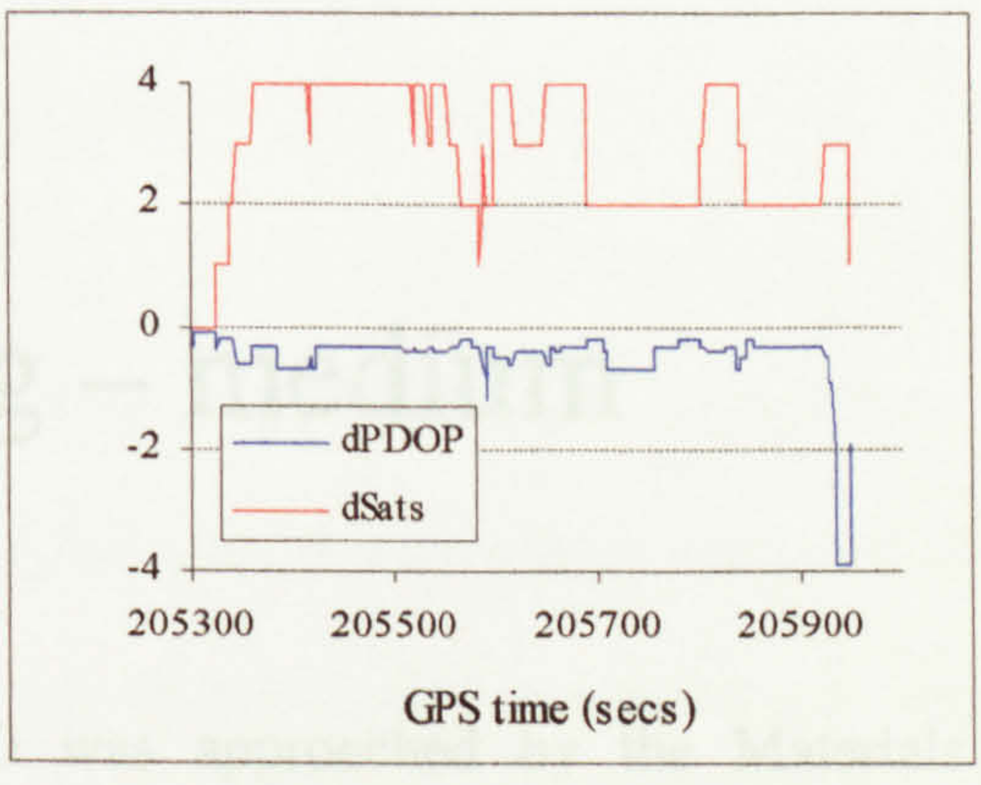

Figure 6.21 PDOP / satellites: Hybrid minus GPS

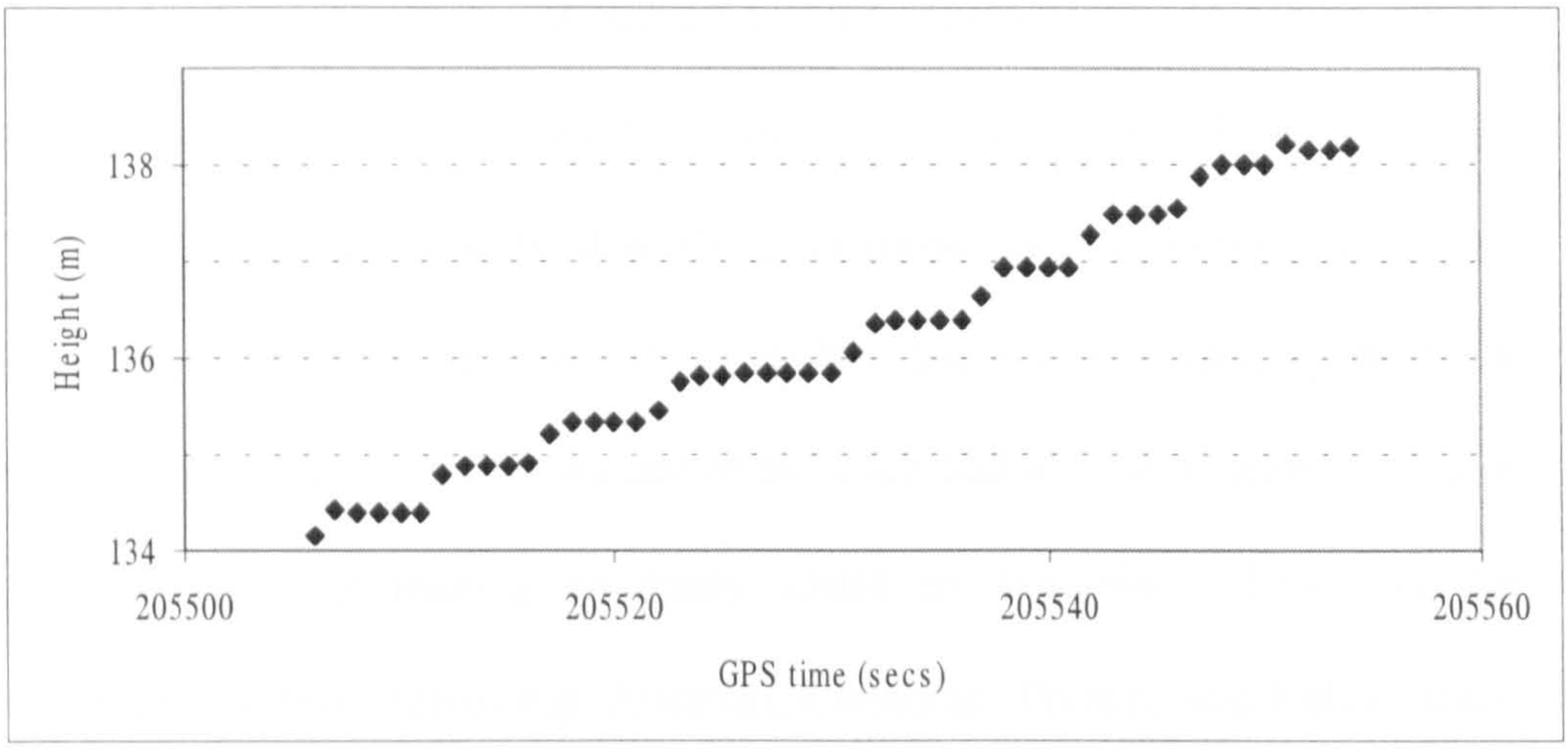

Figure 6.22 Hybrid step definition

Finally, it was notable that the GPS solution initialised 31 epochs (at 1Hz) earlier than Hybrid, again this may have been caused by the effects of GLONASS ICBs and additional multipath. On the other hand, at the close of tracking against the IESSG building, Hybrid continued positioning for 20 epochs beyond GPS.

A further test routine was envisaged to simulate the urban canyon scenario, but providing a track that could be determined independently of satellite means. The idea was to follow car park bay markings, with the antenna at various heights below the general car roof level.

6.6 Road tracing – medium velocity

In the latter half of 1998 the IESSG was approached by the Materials Engineering and Materials Design department with a demanding vehicle

tracking application. This was related to their development of a sled for the bob skeleton winter sport (funded by British Aerospace, now BAE Systems). Whilst mathematical models describing intrinsic sled dynamics had been established, little or no information on track shape was provided by the track operators. This meant that the nature of the track had to be determined through practical usage, by making as many slides as possible. This was not problematic for most teams e.g. Austrian, Canadian, French, and Italian, since each had their own facility, and could practice for three months every year. On the other hand there is no track in the UK, so the UK team was relatively inexperienced in terms of time on the ice.

If three dimensional track models could be determined, then the sled model could be integrated with this to assess performance and racing strategy. In this way the UK team's competitive disadvantage could be lessened. In terms of accuracy, the highest level using carrier phase was desirable, however, any level was regarded as useful, to augment the little information existing before. The complete remit for a positioning system was to provide, referenced to a down-track distance index: track location in three dimensions, sled location in three dimensions; sled velocity and acceleration; track gradient; track convolution parameters; and a heading indicator.

It was intended to attempt this project some time in the next competition season, which started two months later. After some deliberation it was decided that a satellite based positioning package was the only contender, as the equipment and processing software were already available, as opposed to an

Inertial Navigation System (INS), which would require hardware purchase and software to be written. The requirement for the IESSG, was then to develop a positioning package to be mounted either within the sled, or for attachment to the slider.

Package development details are given in Chapter 7, which is dedicated to field work at a track in the French Alps, and subsequent data processing.

The anticipated difficulty with sled positioning was threefold. Firstly, antenna pointing would be extremely dynamic as the sled lifted onto the vertical wall of the track when cornering, secondly skyview would be limited dramatically in the corners relative to a straight, and thirdly ground topography would present its own skyview limitation. Add to this a poor multipath environment, then it can be seen that satellite based positioning would be operating at the limit of its capabilities, hence the need for more satellites and the proposed use of the Ashtech GG-24 receiver in Hybrid mode.

This section reports on the testing of the developed package, as driven on a circuit around and through Nottingham City Centre on a minibus roof mounting. Test design was intended as a precursor to sled tracking, and was therefore intended to be much more demanding in terms of skyview limitations and noise, than tests discussed in earlier sections of this chapter.

It was soon found that repetitive vehicle tracking on a semi-captured track i.e. the vehicle was constrained by following the same traffic lane in so far as

possible, was a necessary feature of track definition in difficult signal reception environments, see Figures 6.23 to 6.26. These diagrams show a closed circuit from the University at bottom left through the City centre at top right and back. A particularly difficult area is a square feature at top right, this is bounded on all sides by large buildings, and is a popular meeting place for buses. Figures 6.23 and 6.24 show a single circuit by GPS and Hybrid respectively. Theoretically between 21 and 23 satellites were available above a zero degree mask over the observation period (Figure 6.28), but in practice because of limited skyview, only seven GLONASS satellites were combined with GPS, but this still almost doubled the core GPS constellation, to give a total of up to sixteen satellites. The obstructive nature of an urban environment is exemplified in Figure 6.29, which shows discontinuous raw data availability. The GPS constellation in this figure, coded G*nn*, shows very poor reception at the start of logging, improving only slightly with time. GLONASS (code R*nn*) and hence Hybrid satellite reception, was better in a relative sense, owing to three satellites starting from above sixty degrees elevation (Figure 6.31). Review of the GPS sky plot (Figure 6.30), explains the poor reception in GPS only mode, as caused by low elevation susceptibility to environmental masking. For one GPS only circuit this caused the number of satellites to fall below four, which when associated with poor resultant geometry, caused a hiatus in positioning of about forty percent of the circuit.

Overlaying the first GPS circuit by a second (Figure 6.25), gives a major improvement in GPS coverage, particularly in the south-west corner. On the

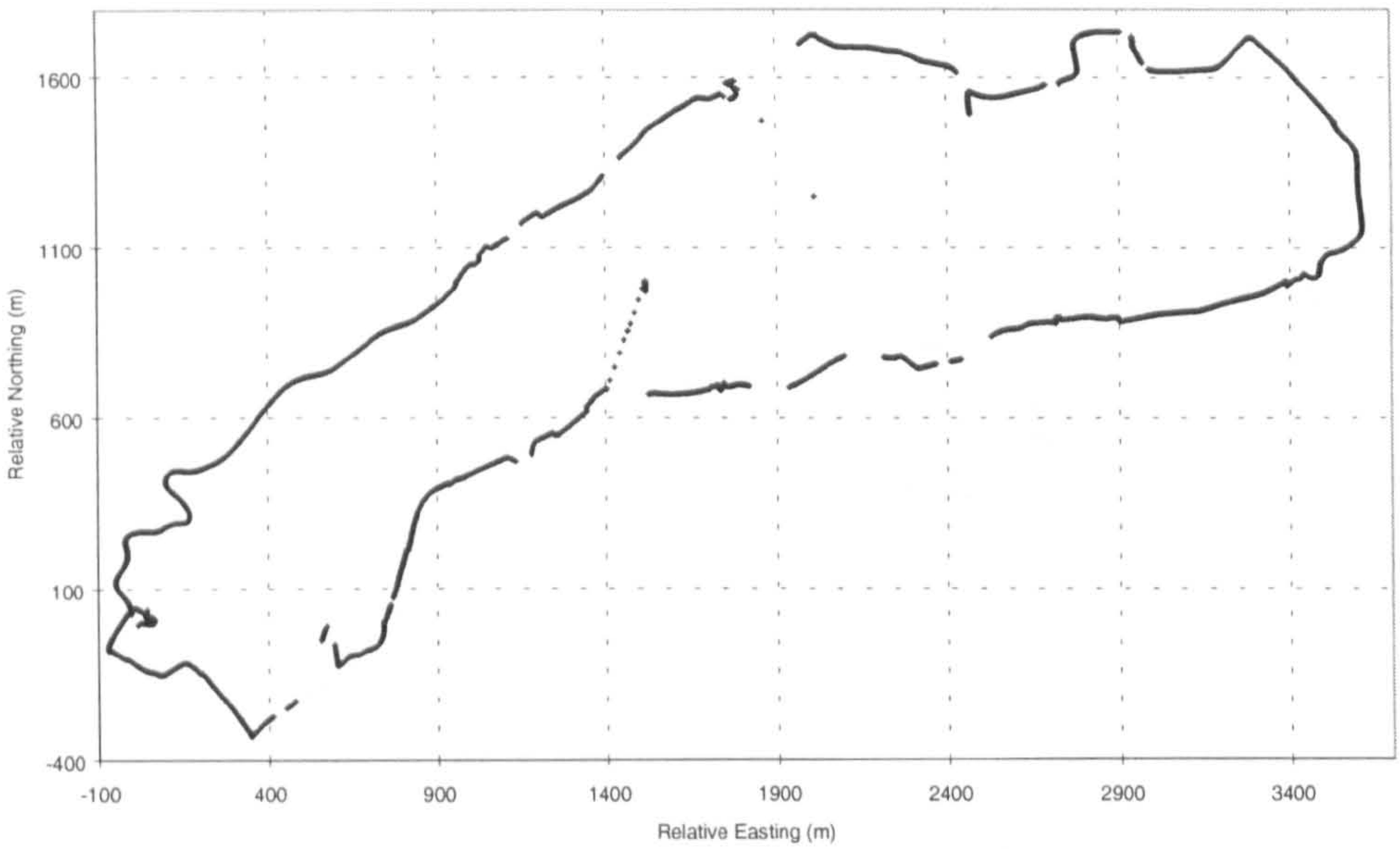

Figure 6.23 GPS: Minibus Circuit 1

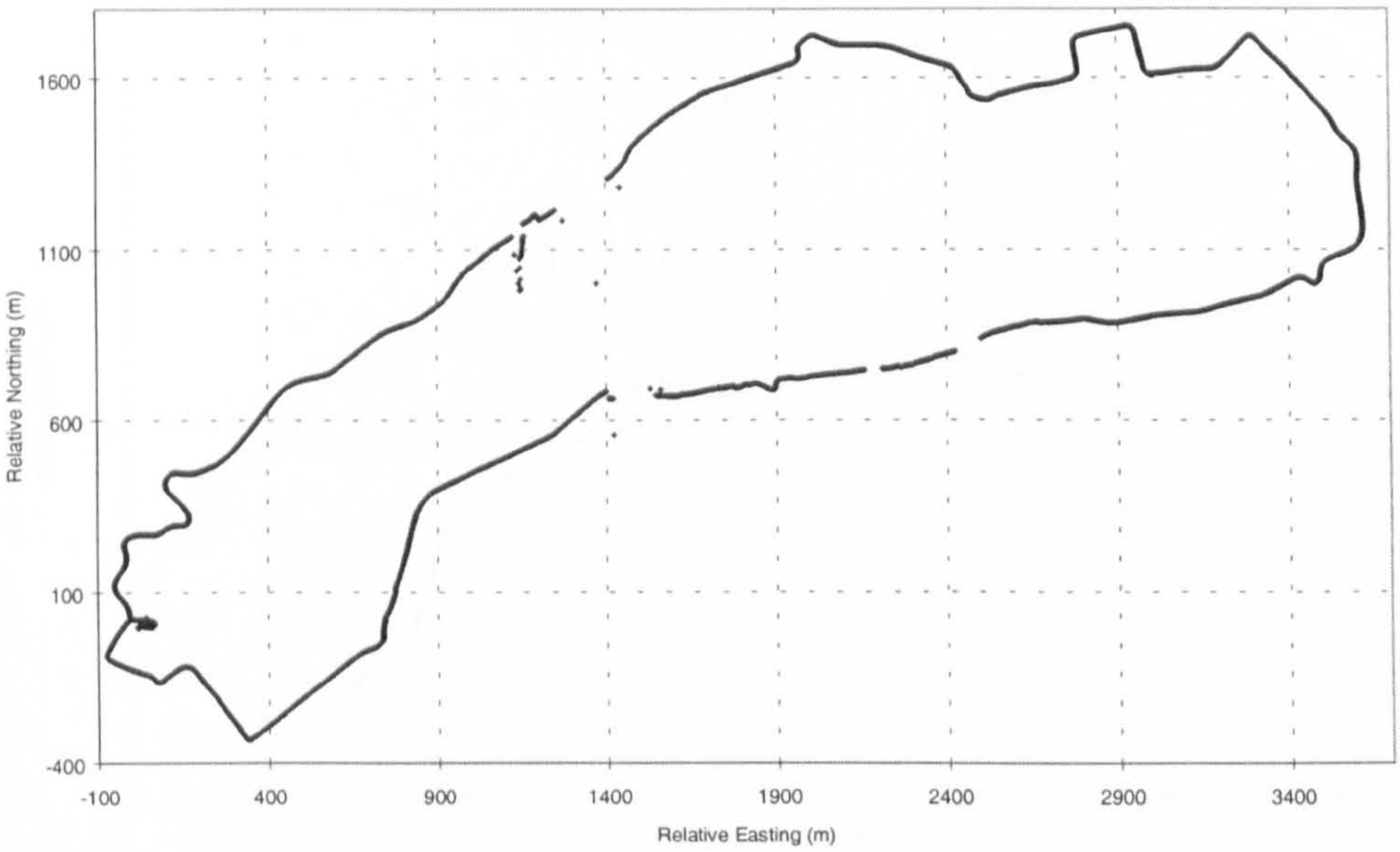

Figure 6.24 Hybrid: Minibus Circuit 1

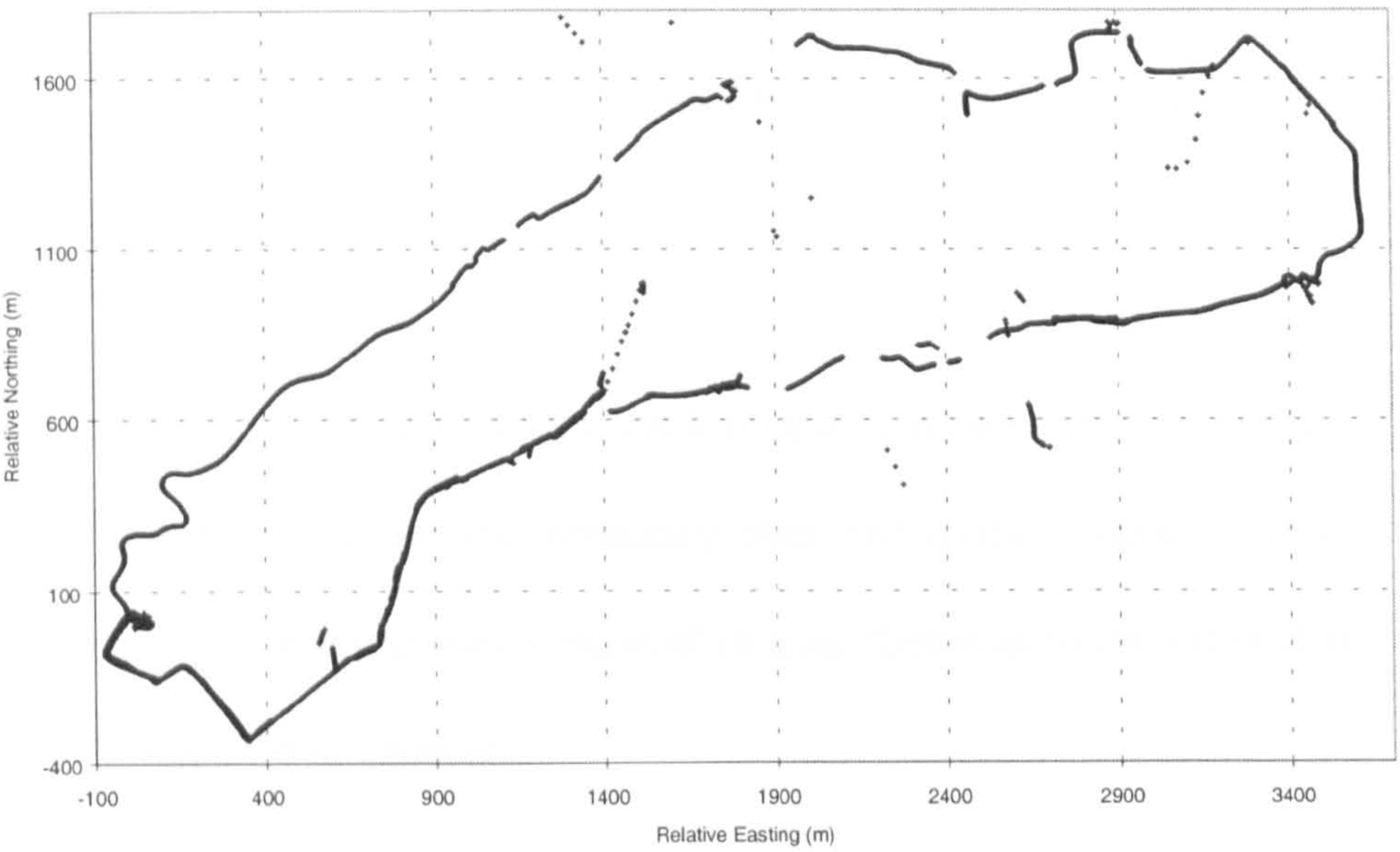

Figure 6.25 GPS: Minibus Circuits 1 and 2 together

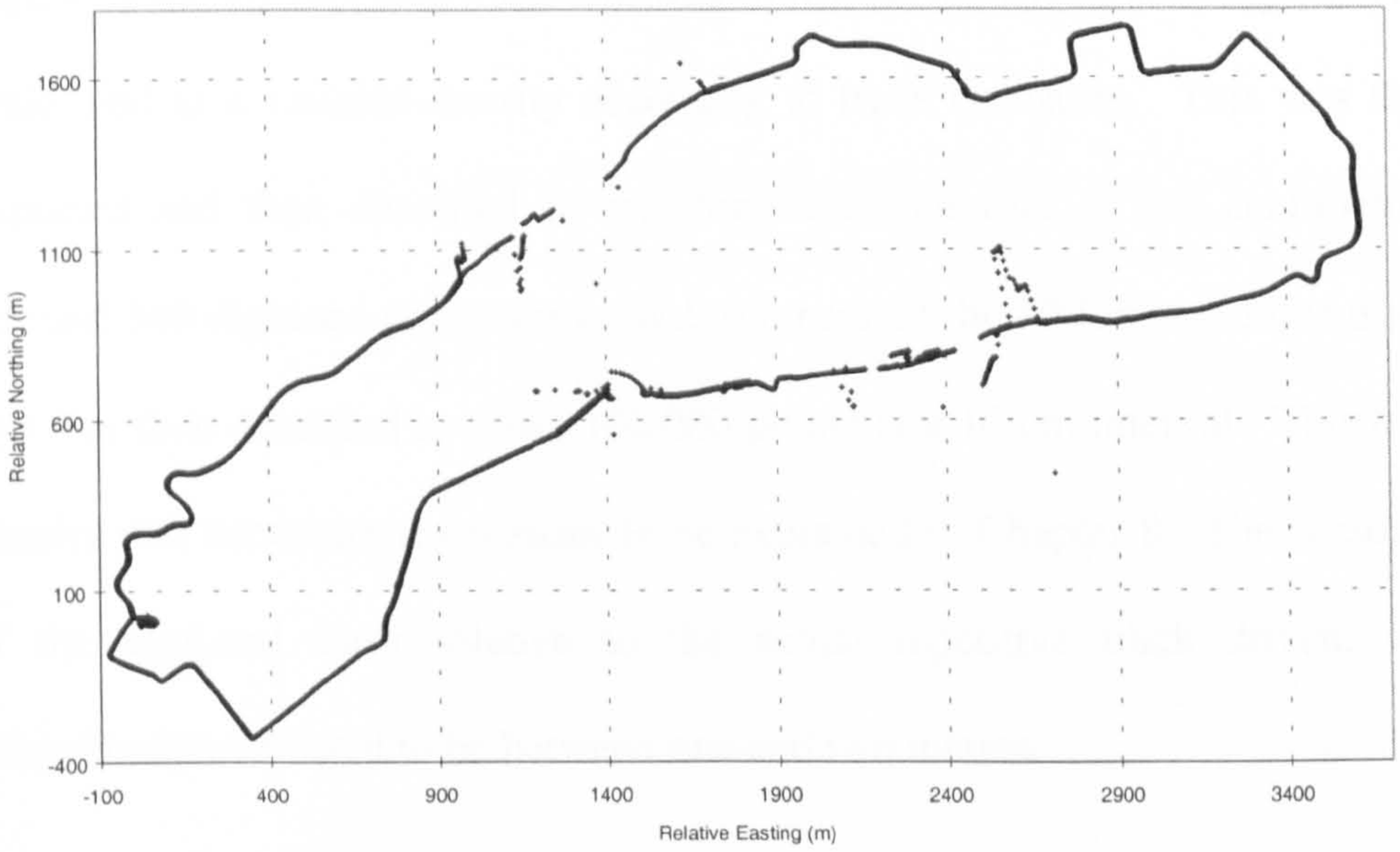

Figure 6.26 Hybrid: Minibus Circuits 1 and 2 together

other hand there is little to be gained by overlaying two Hybrid circuits (Figure 6.26), in this case, individually they were superior to the GPS only case.

This incremental building up of a track profile was facilitated by the change in constellation availability and geometry over just thirty minutes. It was this approach of multiple passes separated in time that was to be adopted for bob skeleton tracking in Chapter 7.

A form of *truth* (Figure 6.27) against which to evaluate the various circuits made, was derived using digital mapping of Nottingham at a 1:1250 scale, kindly provided by the Ordnance Survey of Great Britain. This was done by digitising the oft repeated track that was followed, on-screen at a large display scale, and at a variable density according to track curvature. This was then exported and then densified to an along-track interval of ten centimetres. Around 340 digitised points were used to represent the 10 km circuitous track, this was then densified to about 100,000 points at a 10 cm interval. This high density was necessary for reasons to be explained in Chapter 8. The accuracy of the digitised track relative to the actual repetitive track driven, was subjectively estimated to be between one and two metres.

In this chapter a practical review of satellite positioning capabilities for various vehicles has been made. It has been demonstrated that a high level of antenna dynamics in a low multipath environment can still support a GPS fixed ambiguity solution, whereas similar dynamics in a typical urban setting

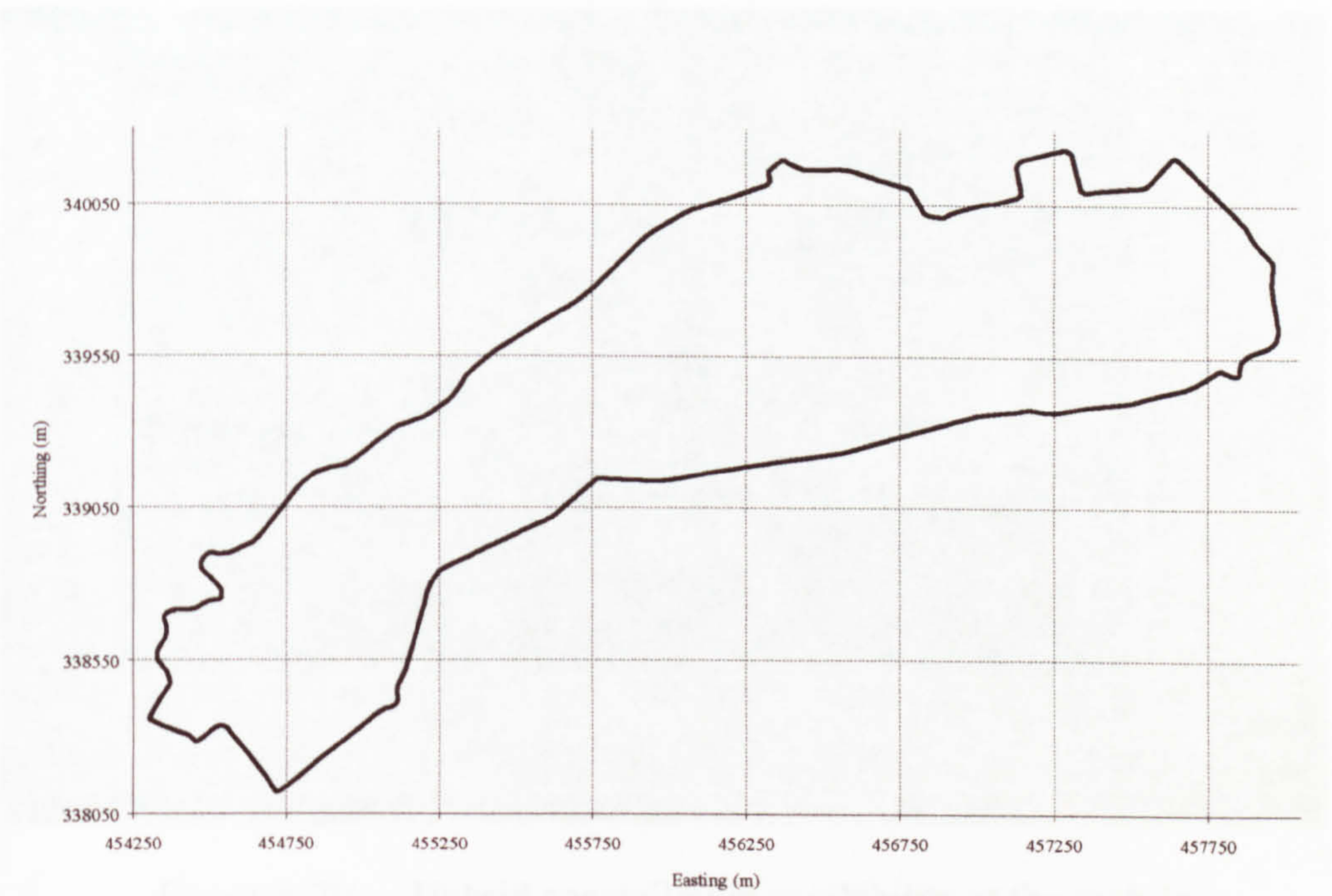

Figure 6.27 TRUTH: Based on estimated track in large scale digital mapping

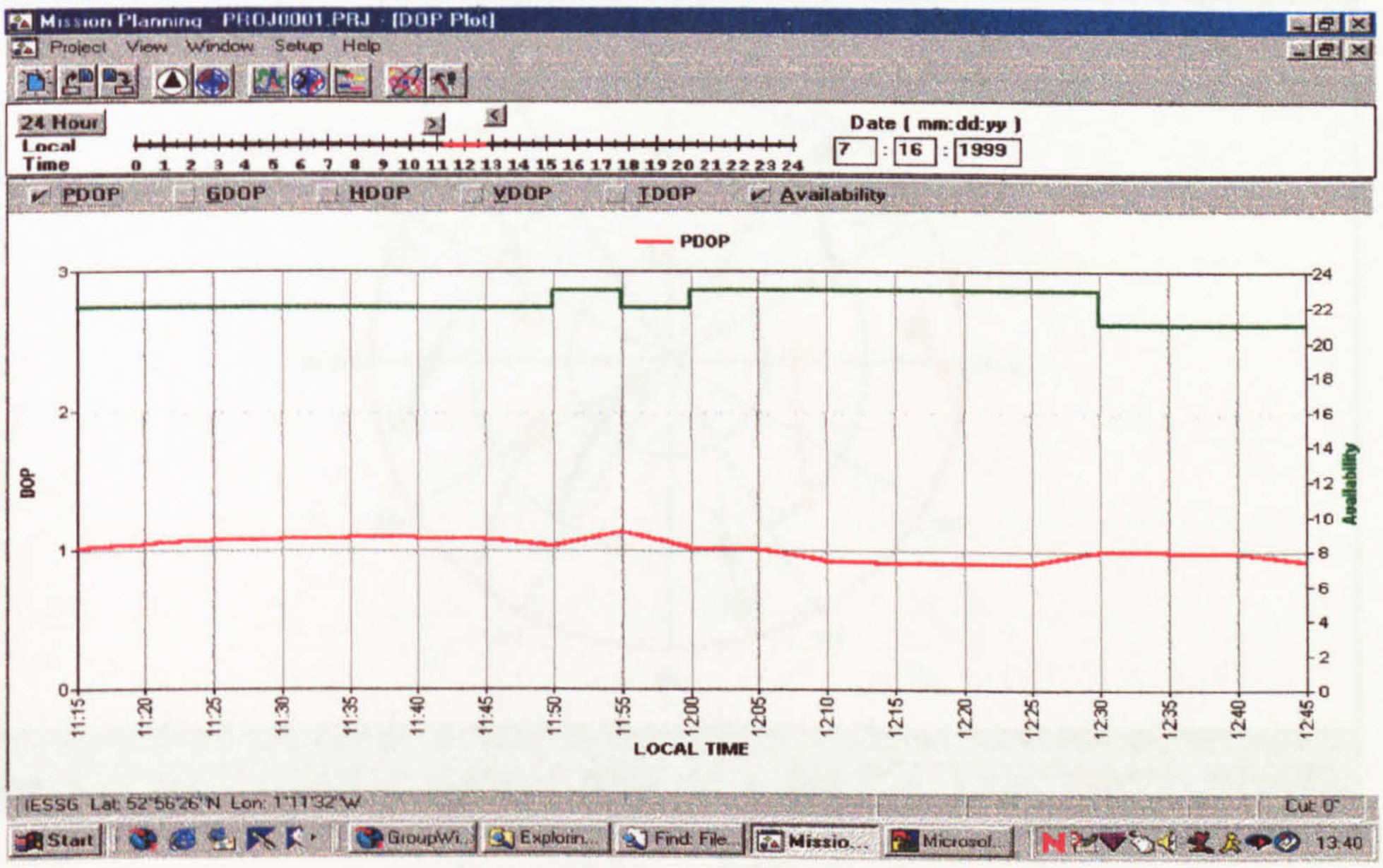

Figure 6.28: Theoretical Hybrid constellation availability

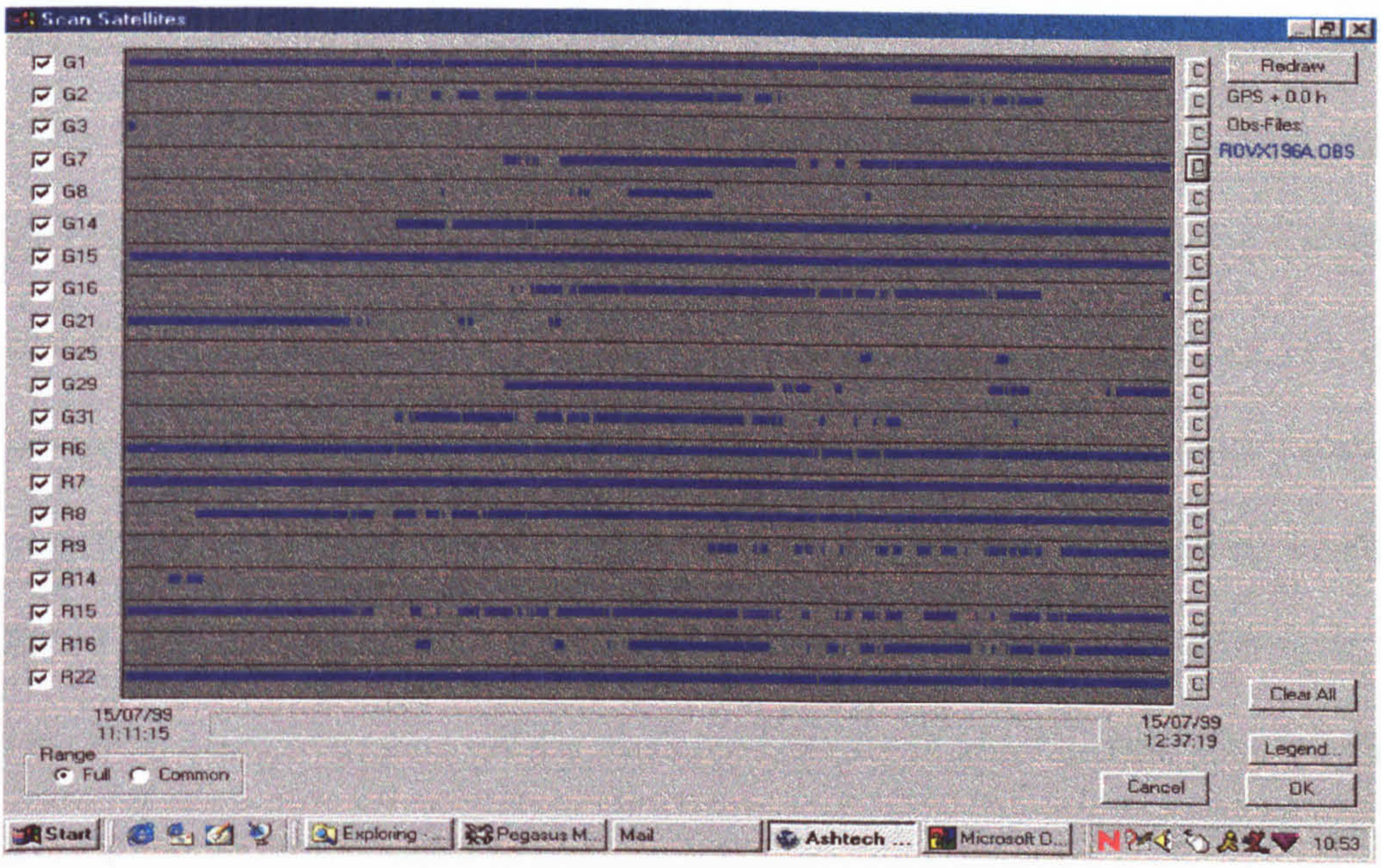

Figure 6.29 Hybrid constellation availability at the mobile

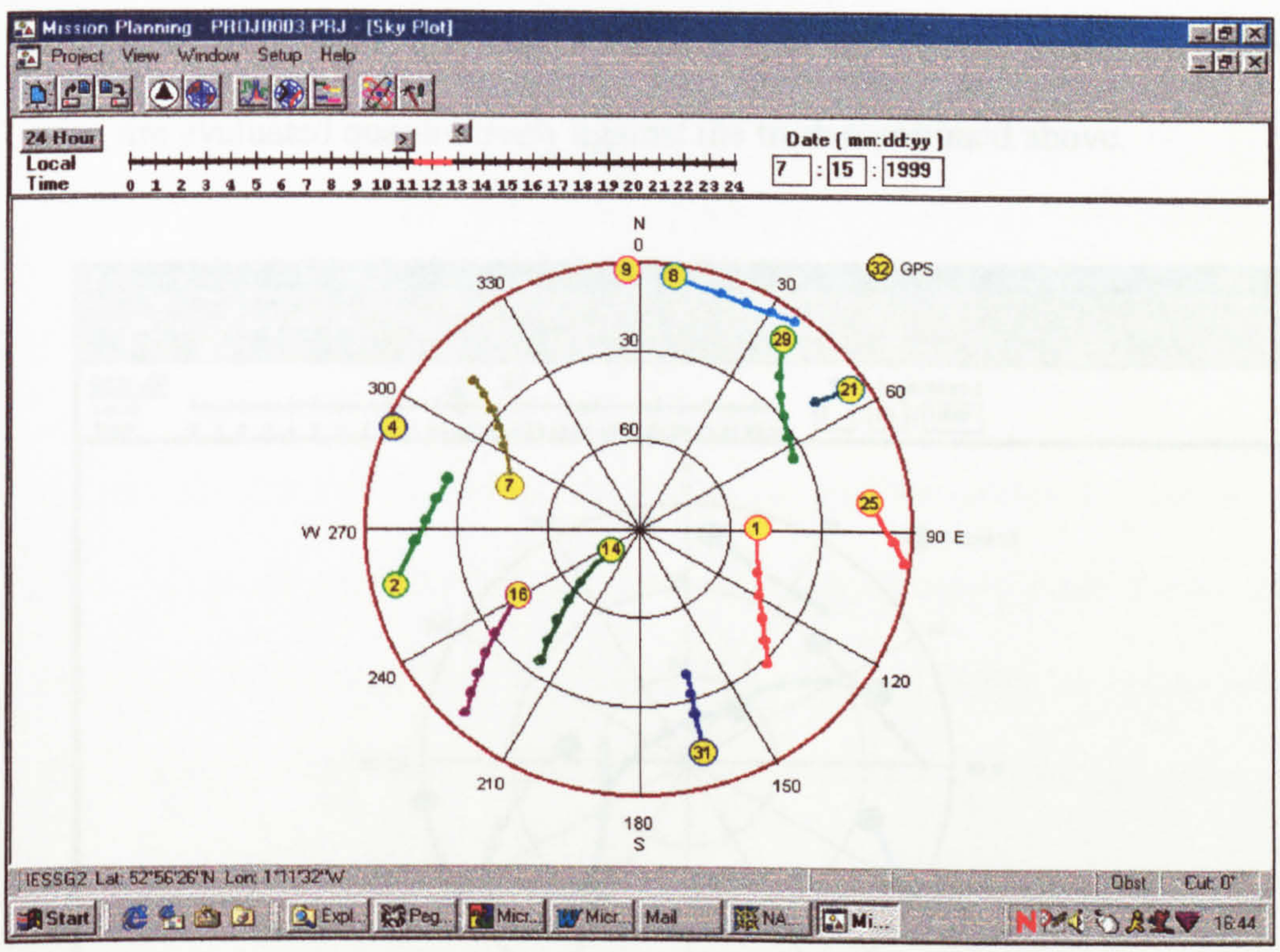

Figure 6.30 GPS sky plot

struggles not only to produce a fixed ambiguity solution but under extreme cases, even with Hybrid capability or Kalman filter forward and backward processing, can fail to position for extensive intervals. Comparison of satellite positioning with photogrammetric methods has shown that accuracy can be comparable, and that the technologies can be complementary under certain conditions. Also for satellite positioning in the urban environment, it was found that multiple circuits were both necessary and capable of building up a complete knowledge of a vehicle track, which may in turn be used to define the track parameters themselves.

Finally, in this section, a purely qualitative approach has been used to describe the relative capabilities of GPS and GLONASS. This is developed further in Chapter 9, where these and similar tracking data observed at a different time of year, are evaluated quantitatively against the truth mentioned above.

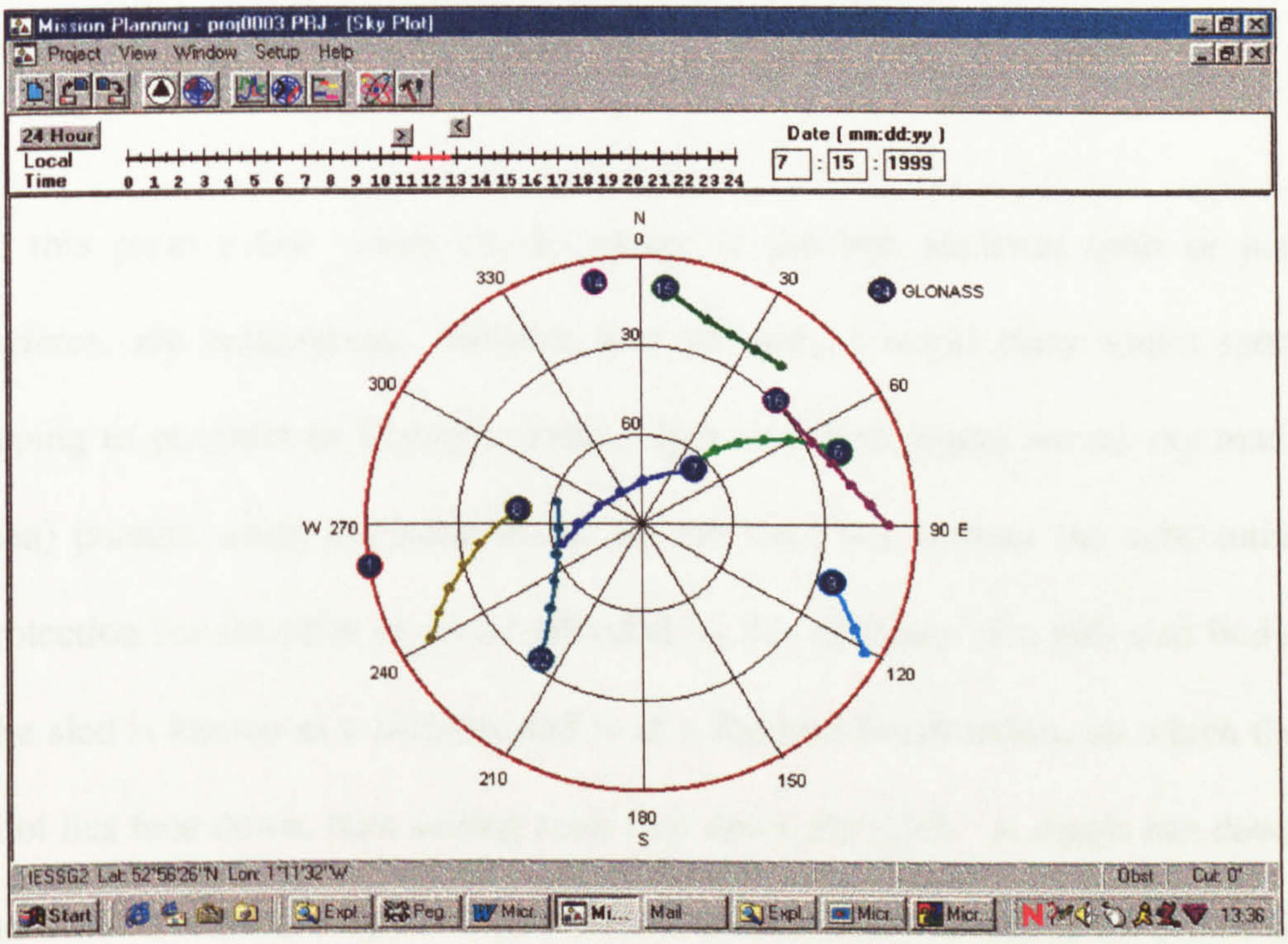

Figure 6.31 GLONASS sky plot

Chapter 7

Bob Skeleton

7.1 Introduction

This chapter covers all phases of the project to determine the bob skeleton remit introduced in §6.6. The following are covered: design considerations and fabrication of the positioning pack; logistics, planning, and execution of the field work; satellite data processing; extraction of defining track parameters; and finally ideas for improvements to the positioning instrumentation.

At this point a few words on the nature of the bob skeleton sport or just *skeleton,* are appropriate. Skeleton is a currently a world class winter sport hoping to progress to Olympic status. It is one-man (some would say mad-man) pursuit, using the same tracks as bob sled, but without the substantial protection for the pilot or *slider* afforded by the structure of a bob sled body. The sled is known as a *skeleton* and is of a flat-bed construction, on which the pilot lies face down, then sliding head first down the track. A single run down the track is termed a *slide*. There are no brakes, and steering is by means of subtle shifts in body weight, with torso and leg movements providing the main

steering control. Speeds of up to 145 kph are achievable, with up to 6g when cornering at the most demanding tracks. The sleds are packed with lead ballast of between 45 to 55 kgs weight. Fortunately capsizing or coming adrift of the sled is rare, and although severe bruising from contact with the ice walls is common, fatal accidents have yet to occur.

The tracks themselves are major engineering feats, using either natural and/or artificial topography. The test track at La Plagne in the French Alps, about 100 kms due south of Lausanne on the Massif de la Vanoise, exemplified the use of natural features, being sited facing north close to the top of a steep valley, at an elevation of about 1600 metres, and introducing skyview limitations to the south. La Plagne is one of the most demanding tracks in terms of achievable speed, radius of curvature, and hence g-force.

All tracks are constructed of concrete, with an integrated refrigeration system. The ice surface is constructed by spraying water on to the chilled concrete, this is then shaped by machine to remove short wavelength imperfections.

7.2 Positioning pack design

Slider safety in the event of a capsize dictated that there be no physical link forming a tether between the slider and the sled. The available Hybrid antenna, even though relatively small and lightweight, was too large to mount on the sled itself as it would have impeded the necessary steerage movements of the slider. So the antenna would have to be carried on the slider's back, ruling out

mounting a receiver card in the sled void space, next to the lead ballast. The solution was to collect the complete installation, receiver, antenna, cables and power pack, all together, in a single back-pack or rucksack. Having decided on a back-pack container, protection for the slider, from it and its contents, in the event of a spill on the track was paramount. Associate issues were minimisation of weight and dimension, and lowest profile to avoid artificial steerage effects when travelling at high speed.

Choice of receiver was limited by availability to the Ashtech GG-24, a relatively small unit measuring (10.3 x 6.8 x 5.5) cms. To minimise space needs, the antenna had to sit on top of the receiver, so together they determined the overall height of the installation at about 17 cms.

Containment and padding of the installation was decided after consultation with the slider, and comprised a special foam rubber, with features of rigidity, comfort and give. This material was cut to form layers about two centimetres thick, which were then hot air welded to form a single containment. At the same time overall dimensions were limited to provide a snug fit within a specially selected lightweight rucksack, whilst maintaining a low profile and low centre of gravity. The rucksack design was chosen for characteristics of moulding to the body shape, ability to keep position when in motion, aerodynamic shape and low profile, featherweight, and quick release buckles.

Figure 7.1 Unpacked

Figure 7.2 Stage 2

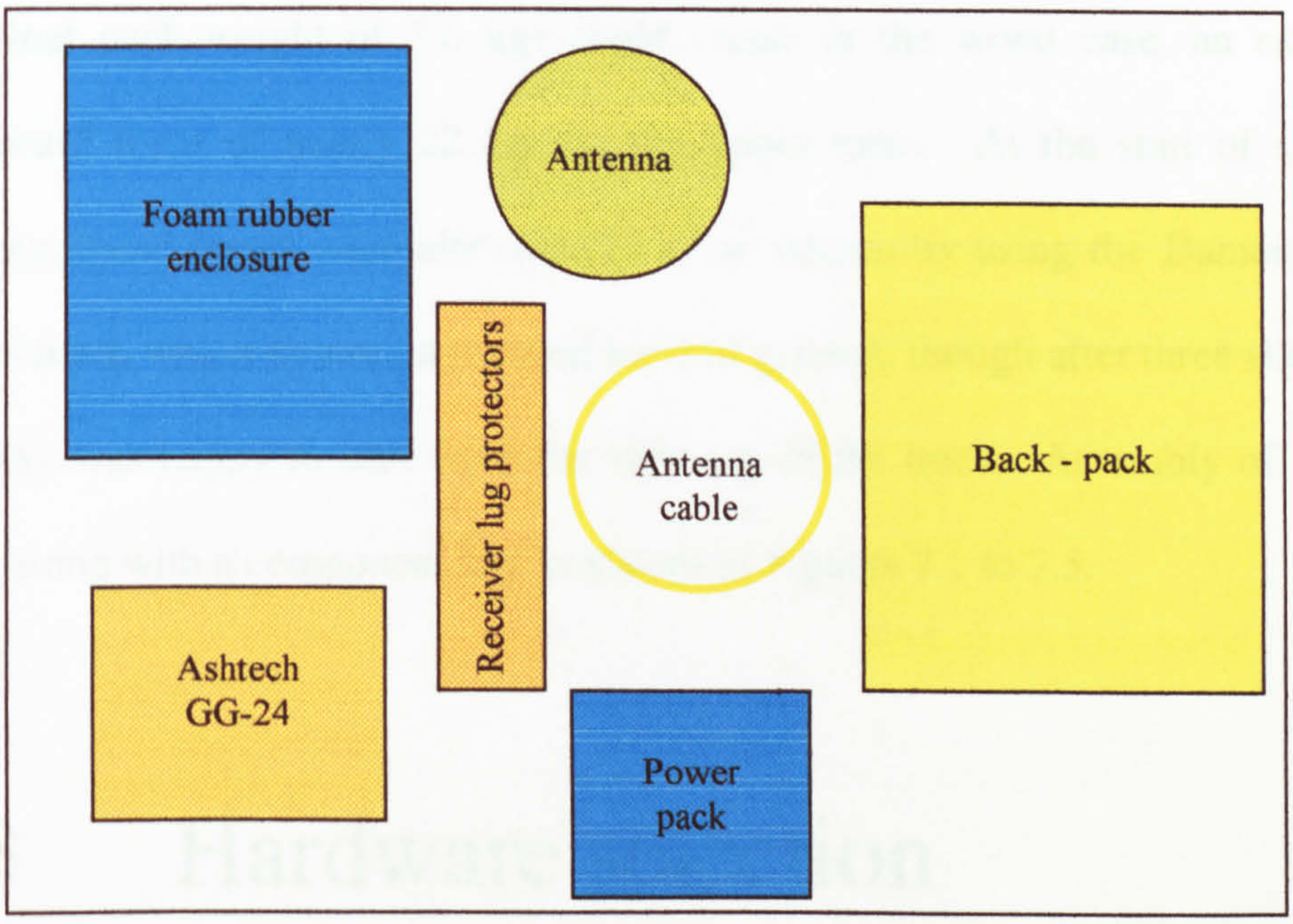

Figure 7.3 Key

Figure 7.4 Stage 3

Figure 7.5 Packed

Lowest centre of gravity was essential to minimise the overturning moment when entering and exiting a curve. Lowest weight was stipulated, because a maximum of about 6g could be experienced when cornering, and any extra weight carried by the slider increases dramatically in a turn. Overall weight was reduced by 175 gms by replacing one cable with a lighter one, reducing cornering weight by about one kilo.

The final pack weight of 3.6 kgs could create in the worst case, an extra downward force of nearly 22 kgs on the upper torso. At the start of sled tracking, these forces were alleviated to some degree by using the Damen or Ladies Start, which ensured a reduced level of g-force, though after three slides the pilot was happy to start from the very top of the track. Assembly of the pack, along with a component key, is shown in Figures 7.1 to 7.5.

7.3 Hardware selection

Baseline length between a local reference station to be set up at the track, and all parts of the track itself, was estimated to be at most a few hundred metres. So an L1 receiver was adequate, but the difficult signal reception conditions meant that Hybrid capability was essential. Dual frequency Hybrid receivers would have been preferred, as they are superior to single frequency units in difficult signal conditions. However, all units were taking part in IGEX (see §3.2.7) at the time. Dual frequency has the benefit of a faster convergence to a fixed ambiguity solution than single frequency receivers, see Figures 7.6 and 7.7, which were based on data collected with a clear skyview at Nottingham

[Russell, 2000]. Accelerated convergence is enabled through access to the P codes which provide a more accurate estimation of an ambiguity search start point and a smaller search volume, together with the widelane observable. The widelane observable with a wavelength of 86 cms enables a rapid coarse search of the search volume, narrowing the volume to be searched at L1. This altogether shorter lead time from switch on to ambiguity fixed solution is of major benefit when there is little time before the start of dynamic vehicle positioning. This would inevitably be the case in sled tracking, as there would be high risk of signal interruption when fitting the pack to the prone slider on the track. With an L1 only receiver, forward and backward post-processing can mitigate this, but this relies on the static occupation of a point at the end (and before the start) of dynamic tracking, under good conditions of signal reception – in reality this may not be possible.

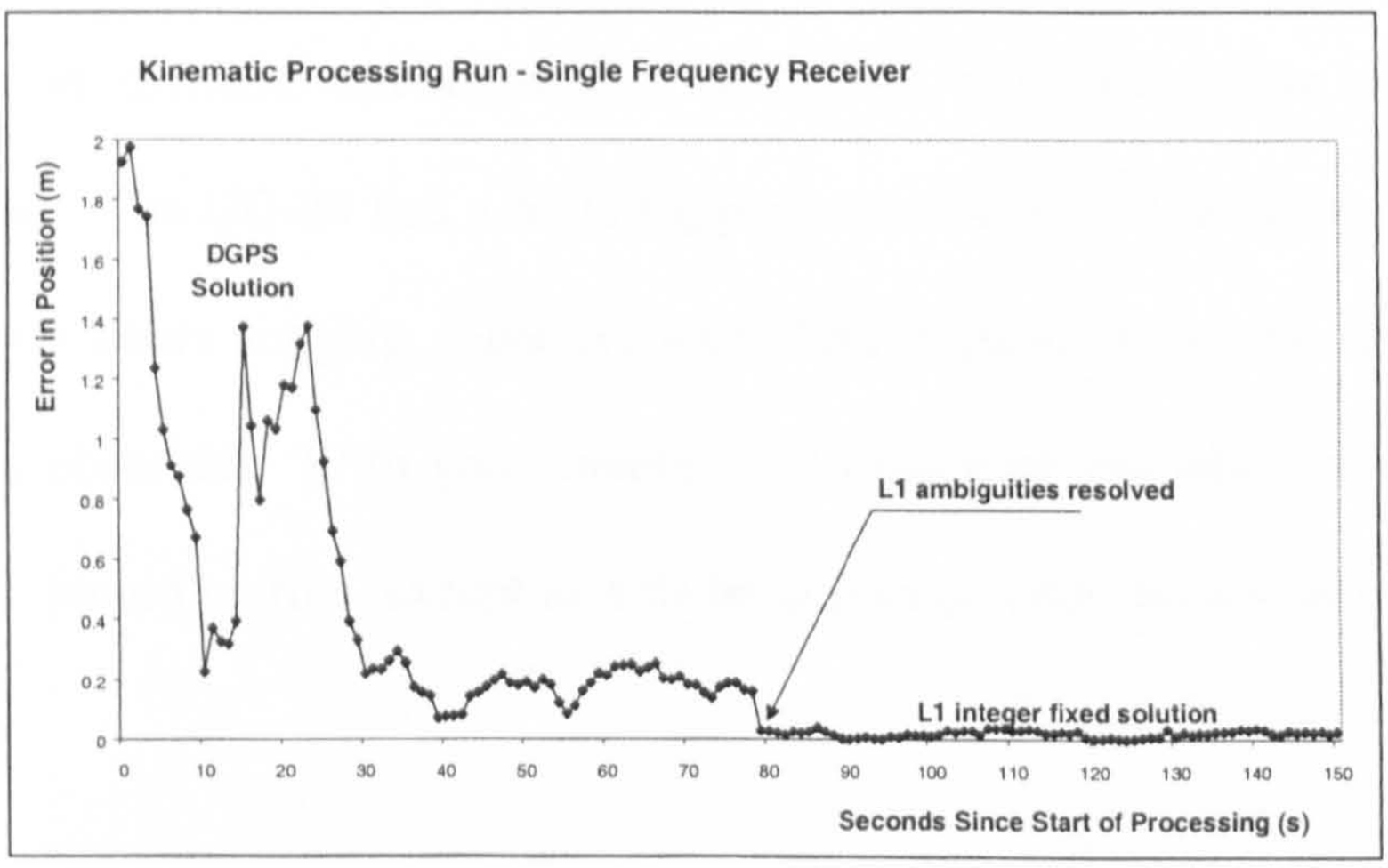

Figure 7.6 Single frequency ambiguity resolution [Russell, 2000].

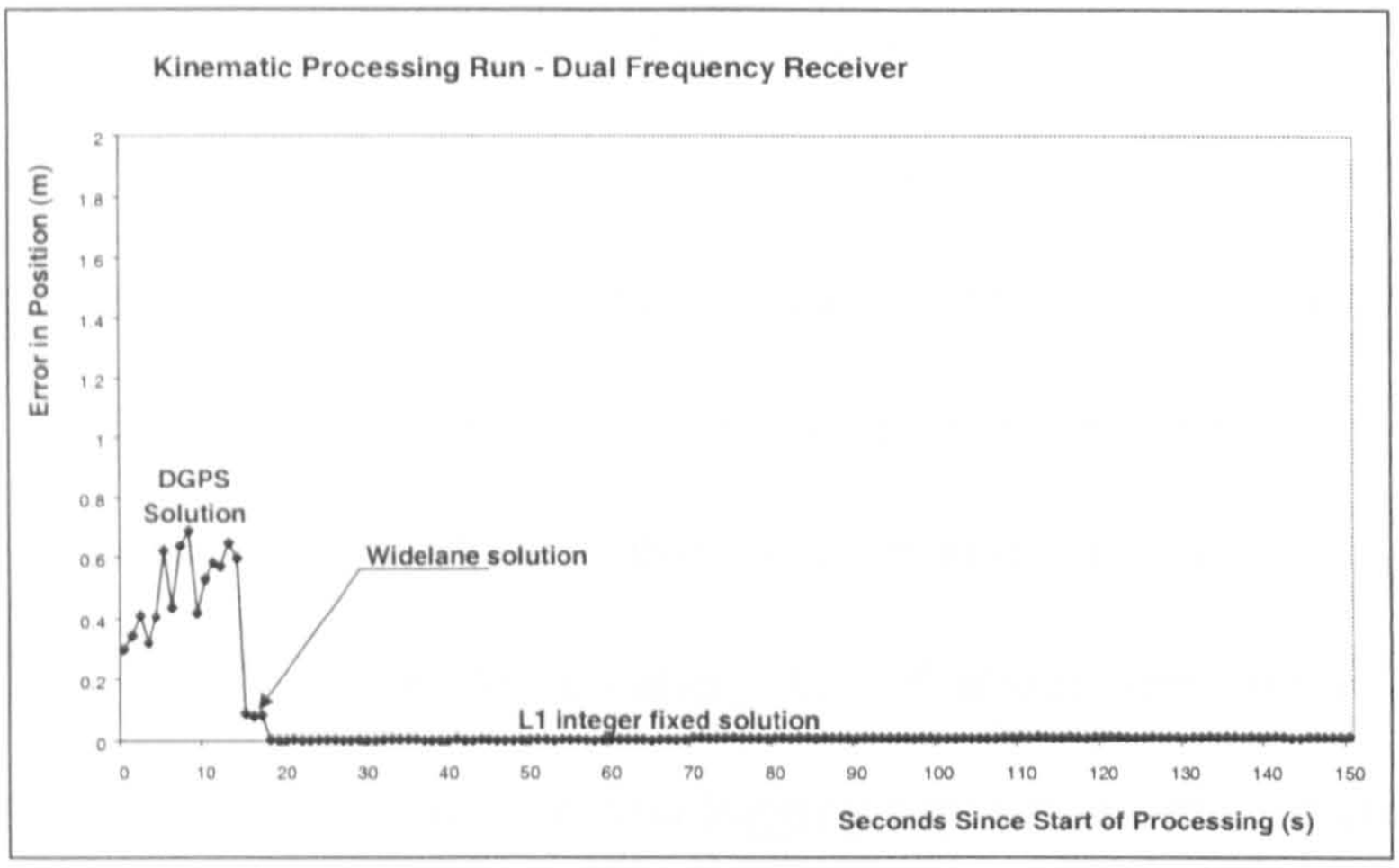

Figure 7.7 Dual frequency ambiguity resolution [Russell, 2000].

The typical length of a bob sled track is about 1500 metres, and transit time of a skeleton about 60 seconds. Such high speeds around highly convoluted tracks require the shortest data logging interval of any positioning system. This assists not only in definition of short wavelength features but also provides more epochs of data, and hence more opportunities to obtain a position in difficult environments. Even so, multiple passes were still envisaged. The GG-24 had a 5 Hz logging rate and a 20 Mb memory, giving about two hours logging capacity, ultimately dependent on the number of satellites observed. With good planning and track access when desired, this capacity would be fine, except as will be explained later, access was less than optimal.

The next issue was how to provide the 3W power needs of this receiver. Three watts equates to 0.25A.h, theoretically then, a battery pack capacity of 1A.h should provide up to four hours of power. Additional battery requirements included light weight, airline safety compliance if travelling by air, operation at

below zero temperatures, and fast charge capability. An exhaustive search, not only for a compliant battery but also for definitive battery performance specifications and an appropriate charger, culminated in the selection of a fast charge AA size Nickel-Cadmium unit to be used in ten cell battery carriers. Tests with these batteries showed that, when running the receiver at a 5 Hz logging rate in Hybrid mode, a battery life of about three hours could be expected, more than matching the data logging capacity mentioned above.

7.4 Logistics and planning

Three tracks were identified as possible venues for the tests. The track manager had to be sympathetic to the project, without being given explicit details, and since a competitive advantage was the target, the less inquisitive bystanders the better, so timing relative to track usage for practice runs by other teams was fairly crucial. Preliminary work was done for Altenberg in Austria, and Calgary in Canada, before finally settling on La Plagne, which was rescheduled twice before eventually proceeding in February 1999.

Project planning and identification of logistical issues were based on scanty knowledge of the La Plagne track, gleaned from anecdotal evidence, web based material (Figure 7.8), the largest scale maps available, and predicted weather conditions. Published parameters were: vertical drop of 124.5 metres, maximum gradient of 14.5%, average gradient of 8.29%, and total competition length of 1507.5 metres.

Difficulties were anticipated in all aspects of the work, and so a high level of contingency was required.

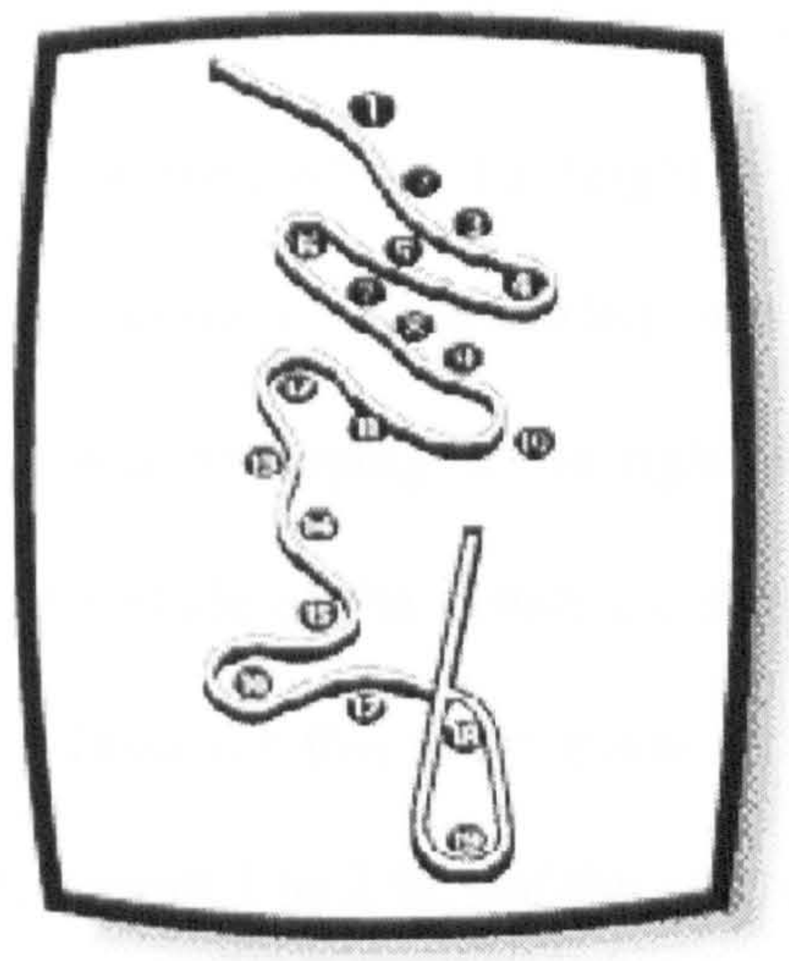

Figure 7.8 La Plagne bob sled track
(sourced from web site of the Fédération Internationale de Bobsleigh et de Toboganning – FIBT)

The main area of difficulty was identified as the sled tracking itself, with dynamic variation in skyview limitation and off-vertical antenna pointing. Even given the Hybrid constellation of over forty satellites, a pessimistic approach still had to be taken, and alternative methods of defining the track considered and set up. To assist ambiguity resolution, two initialisation stations were to be set up, one at the top and one at the bottom of the track.

It was estimated that the best positioning outcome would result from the aggregation of discontinuous tracking results from multiple slides, with various constellation availability and geometry, to build up an overall shape of the

track. As an initial test of the technology, anything more than this would be regarded as a bonus. However track time could not be guaranteed to allow a large number of slides.

So an alternative, using the road wheel from §6.4 was developed. The proposal was to run an antenna on the road wheel at a height of about three metres above the track (to reach above the track which curled over into a roof in a corner), and hard against the left wall swapping to the right wall when in a right hand corner. Use could also be made of the distance counter, if slippage on the ice surface was low level. Tests for this were made at the Nottingham ice rink, and slippage estimated at about 1 to 2 %, but this was on the flat rather than the downhill gradient at a bob sled track. If road wheel definition of the track was successful, then it would provide a continuous 3D reference line for any sled positioning.

The planned slide schedule was based on a coarse map of the track available at the facility's web site, together with anecdotal evidence from the slider who was to pilot the sled for us. Satellite coverage was evaluated over an horizon divided into octants, (Figure 7.9), on the basis of the skyview seen looking out from the centre of a curve, with no reference made to local topographic masking as this was uncertain. Hence it was considered that up to eight runs down the track would be required to define it.

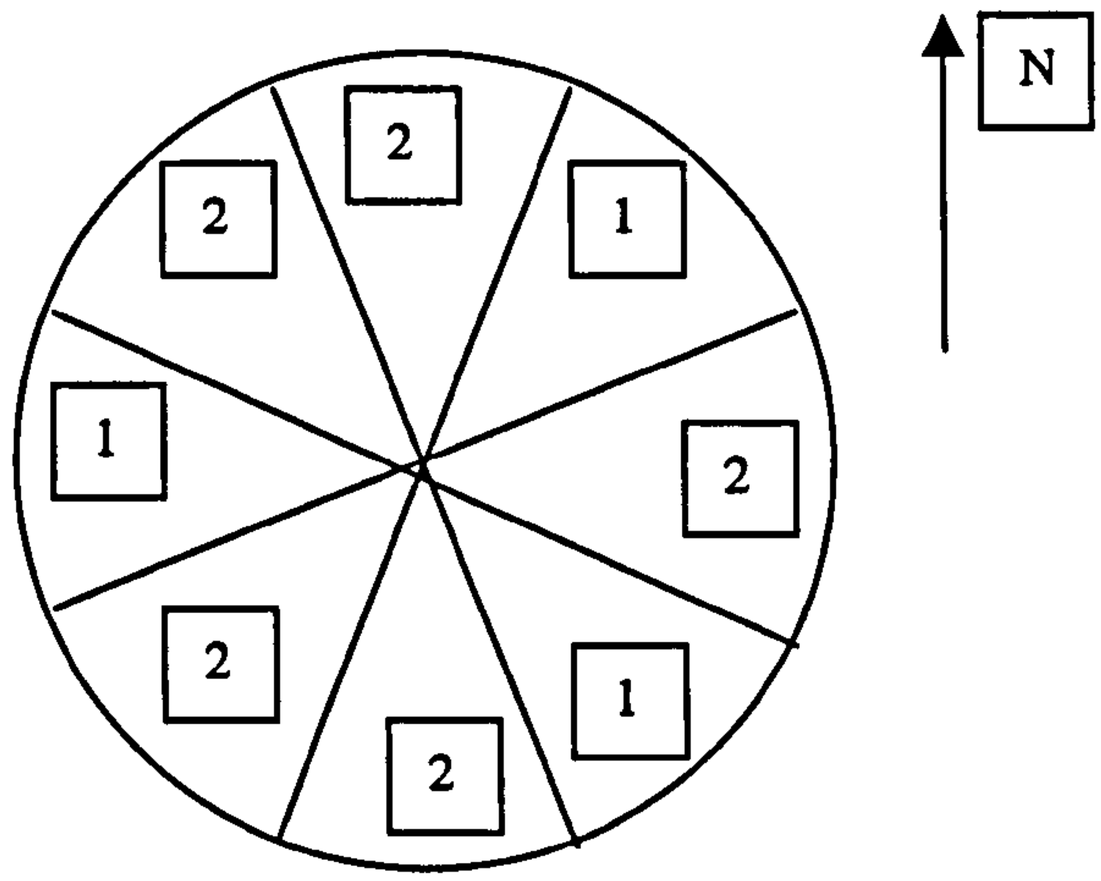

Figure 7.9 Curve directional outlook frequency at La Plagne

Predictions were made using mission planning software, as to the best timing to cover these individual segments. Such intervals were spread over several days and throughout the twenty-four hour period. Given limited track access and window of opportunity in the track schedule, acquisition by sled therefore, was forecast to be less than optimum.

7.5 Field work

Very heavy snow falls had been experienced in the French Alps for weeks before our arrival, with more expected during the project. This raised issues of station marking and recoverability when no soil or pavement could be reached, tripod settlement, and general work in up to blizzard conditions. Tripod settlement was to be dealt with by checking centring before each slide, and repeated measurement of the antenna height above a hilti-nail driven into a wooden ground marker, which was in turn embedded in the ice well below surface level.

Fortunately, the weather system had changed completely by the time of arrival, with icy conditions on the first day, no new snow at all, and a thaw on the subsequent two days, with clear skies and a bright sun. The track was also being used by the French national team bob sled team for trials, and for commercial bob sled runs of varying ferocity for the public, so as a non-paying user our priority was nil. Furthermore we were limited to sliding after 14:00 one day and after 16:00 the next. This meant that we had to be in a state of constant readiness for the three slides per day that we were allowed – amounting to three minutes (three slides) of track time per day! This caused problems related to limited receiver storage and battery life, as the receiver had to be switched on at the slightest hint of a window.

Inspection of the track prior to setting up confirmed the difficulties with limited skyview, with up to 50% limited skyview in most curves. However what had not been envisaged was the use of screens on all major corners (Figure 7.11) to keep the sun off the track, this would handicap the use of the road wheel, as elevation would have to be reduced below roof level. (Figure 7.11 is annotated with the skeleton route at about one metre up on the ice wall, and an outline indicating the ice surface). Also the need to keep the backpack to a low profile with low centre of gravity meant that the antenna was about ten centimetres below the level of the track walls in a straight. Given the track width of about 1.2 metres then a natural elevation mask of about nine degrees was imposed on the straight segments.

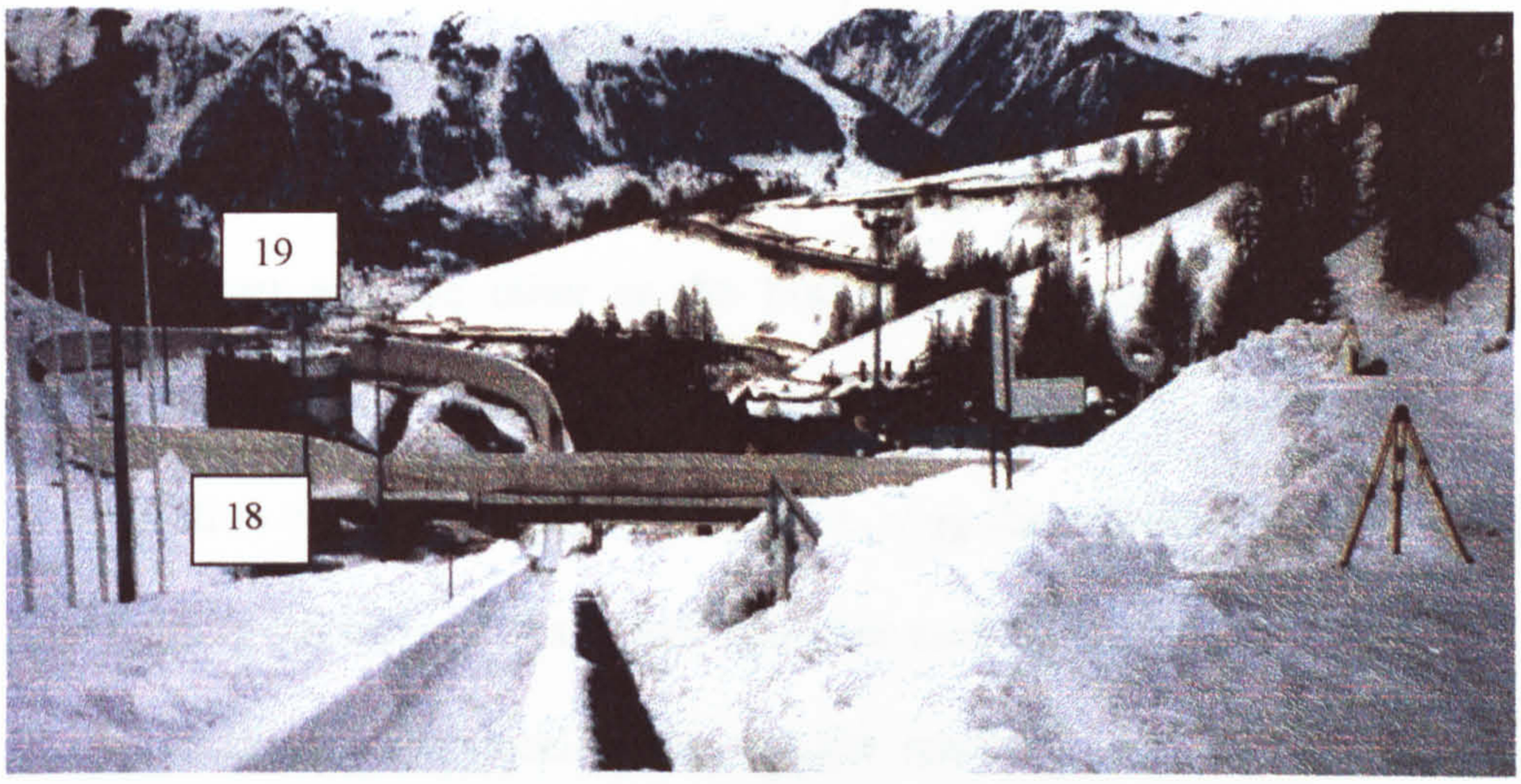

Figure 7.10 Curves 18, 19, and the deceleration slope

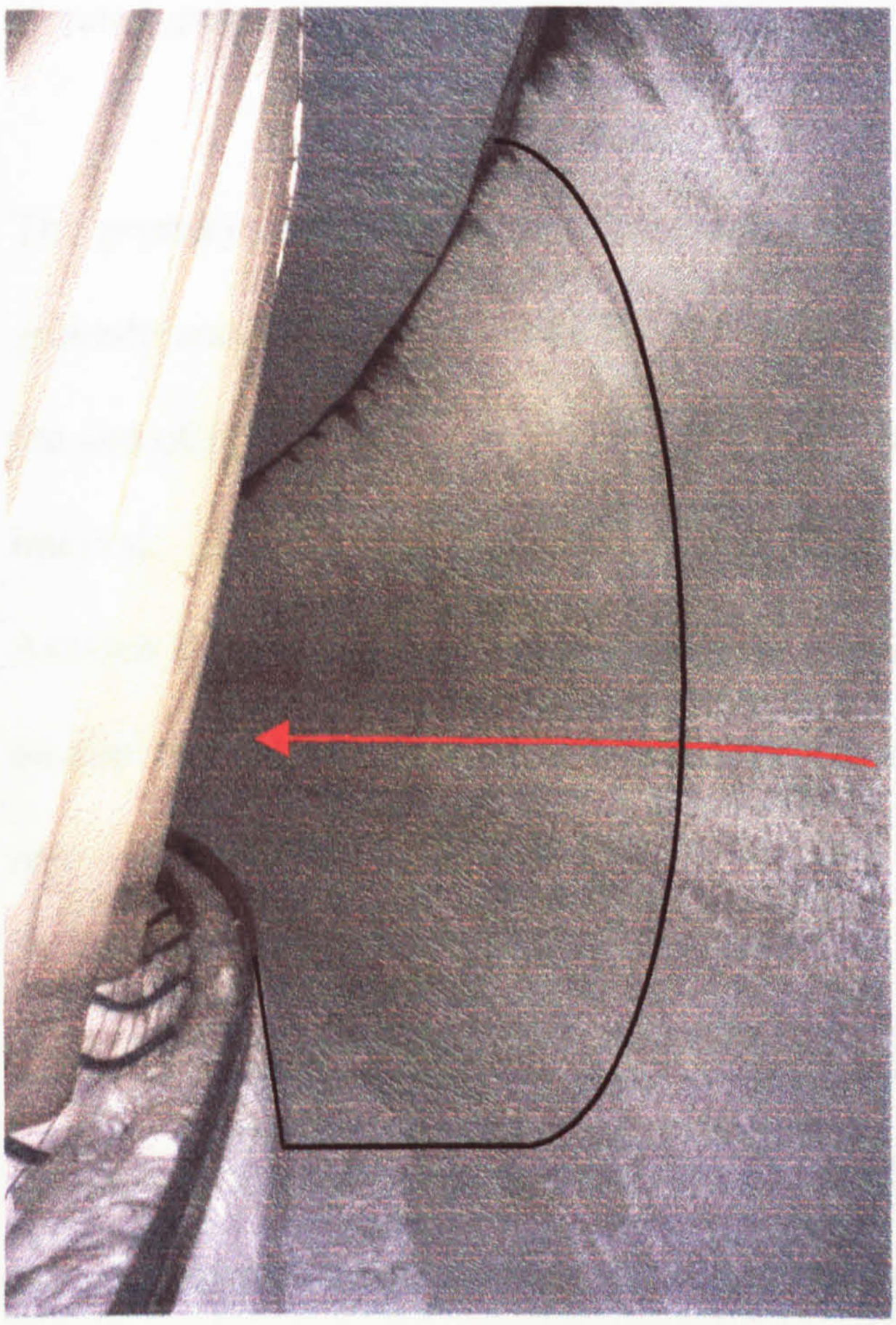

Figure 7.11

Midway through curve 16

Three local reference stations were established, one primary, and two secondary initialisation stations. One initialisation station was set up at the Damen Start and the other at the bottom of the track, at the top of the deceleration slope. These stations were close enough to the track to allow initialisation of the back pack unit, by removing the antenna from the rucksack and logging for ten minutes before and after each slide. Figure 7.10 shows the final two curves, the deceleration straight reaching into the foreground, the lower initialisation station (foreground), and primary reference station in the background at the right. The sled was to be positioned relative to the primary station, which had the best skyview. Figure 7.12 shows just how steeply situated and enclosed the track is.

The primary station was initially occupied by an Ashtech Z12 receiver with groundplane. This observed at 15 second epoch intervals for five hours, with the aim of positioning relative to the IGS network, which logged at a 30 second interval. At the same time the two initialisation stations were occupied by Ashtech GG-24 receivers logging at the same interval. The higher logging rate on-site was intended to be a defence against the less than optimum signal reception conditions.

The plan to carry out sled tracking during periods of optimum constellation availability was upset when it was found that all track work had to fit in with the official track schedule outlined above, which was strict and also prone to sudden change. The maximum Hybrid constellation available above a zero

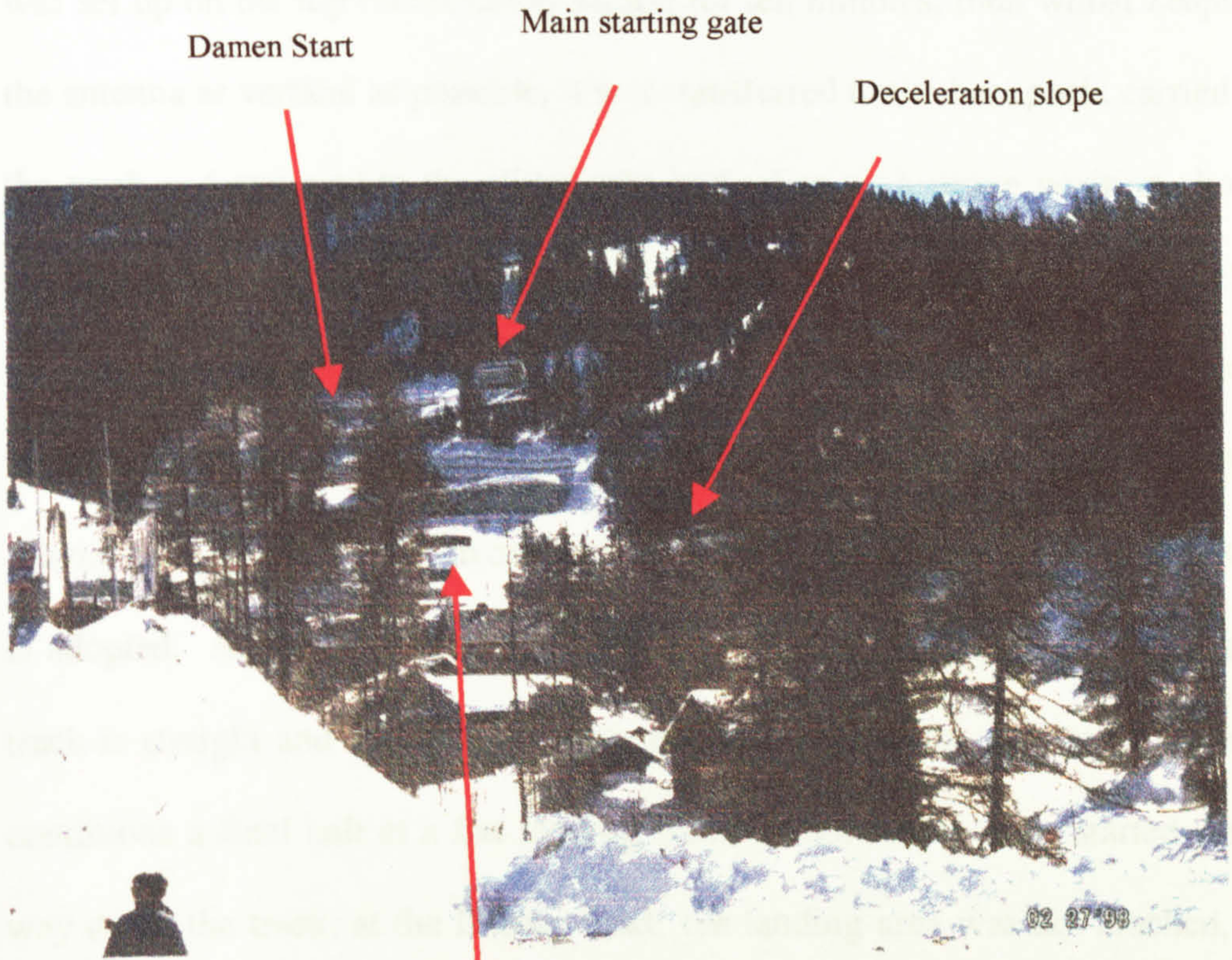

Figure 7.12 View from below the track

degree mask for the track time allocated over the two days available, was between 17 and 21, and 19 and 23 satellites.

The procedure adopted for each slide was as follows. The rucksack antenna was set up on the top initialisation station for ten minutes, then whilst keeping the antenna as vertical as possible, it was transferred to the backpack, carried to the track and strapped to the slider who had taken up a prone position above the sled (Figure 7.13). This was a difficult manoeuvre with steps and obstacles to negotiate, also the position of the track access point meant skyview was impaired and multipath level increased. The slide then took place with a gravity start (Figure 7.14). In competition a sprinting start pushing the skeleton is adopted. At the bottom end of the track, after the finish post is passed, the track is straight and inclined to allow natural deceleration, and under normal conditions a final halt at a flat landing area. Because the slide started some way down the track, at the Damen Start, the landing area was not reached, so the backpack was removed at some point on the inclined part. The backpack antenna was then transferred to the bottom initialisation station for a further ten minutes before being returned to the start point in readiness for the next slide.

A total of four slides were made with the backpack, one on the first and three on the second day. A track walk with the antenna mounted on the road wheel was also run on the second day. We found that rubber soled walking boots stuck to the track very well when walking it (Figure 7.15), as long as there were no loose ice fragments remaining from the previous run – the track was swept using a compressed air hose before each of the French team trials.

Figure 7.13 Donning the pack

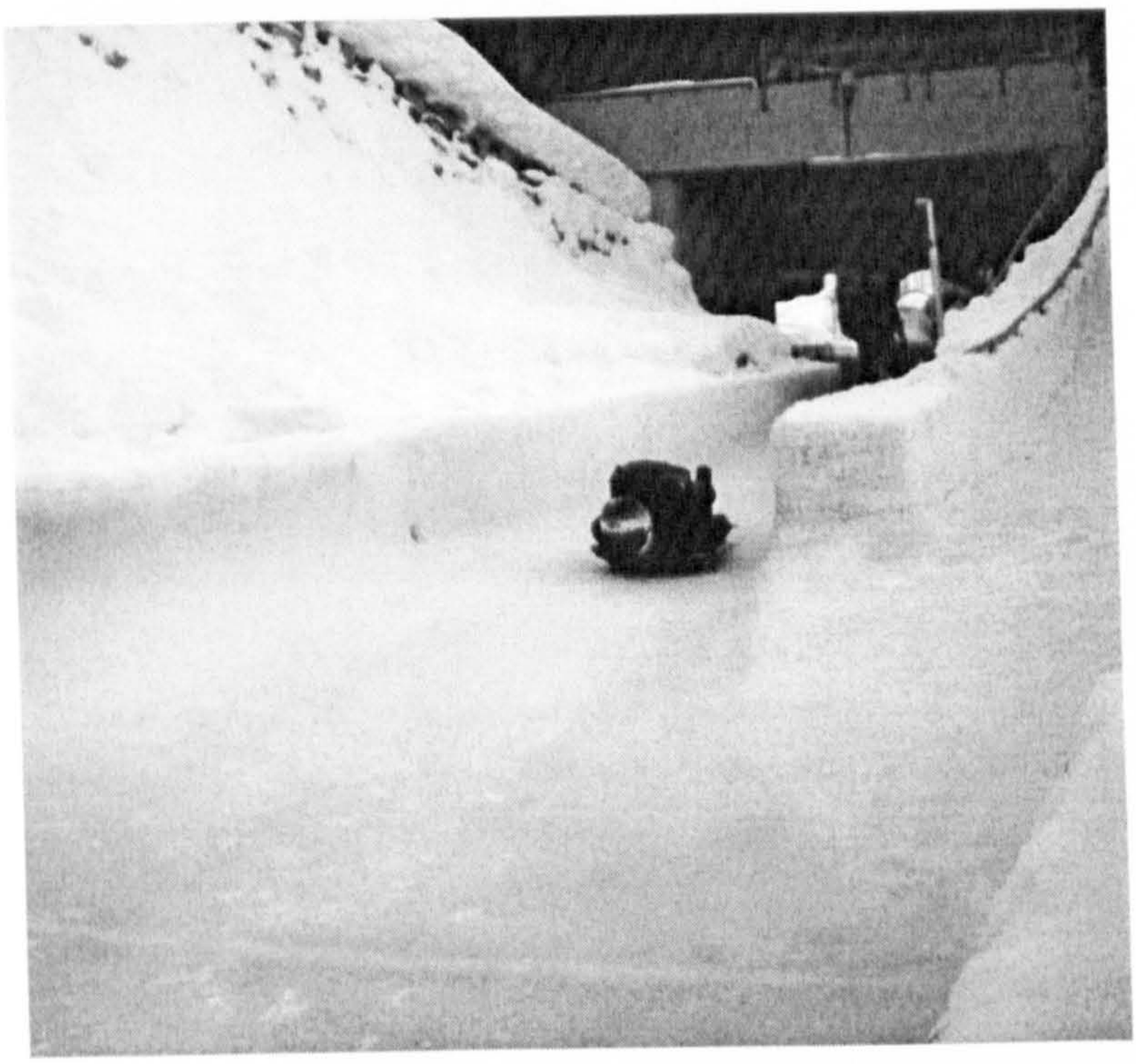

Figure 7.14 Partez! (Start!)

Figure 7.15 Road wheel in a corner

7.5.1 Raw sled results

Data recorded at the sled during each slide are summarised in Table 7.1. The satellite codes are (G)PS and GLONASS (R). This table confirms the difficult signal reception conditions forecast for this track, with intermittent signals dominating. From this it can be seen that slide 1 on the 28th provided the best potential for producing a core sled trajectory.

Satellites	Slide 1/27th	Slide 1/28th	Slide 2/28th	Slide 3/28th
G3				Very int.
G6		Int.	Very int.	Very int.
G17	Int.	Int.	Very int.	Very int.
G22	Int.	Int.	Very int.	Very int.
G25		Int.		
G30		Int.		
R1	Very int.	Int.		
R3				Very int.
R9		Final 60% int.		Very int.
R16	Very int.	Int.	Very int.	Very int.
R17	Very int.	Int.	Very int.	Very int.
R18		Int.	Very int.	Very int.

Int. = Intermittent

Table 7.1 Satellite visibility at the sled

Closer inspection revealed however that, before even considering the standard of geometry, the minimum requirement of four satellites was available mainly at the very start and end of the track when in the best skyview and with low vehicle dynamics, and only fleetingly during the slide, between 50760 to 50820 seconds (Figure 7.16).

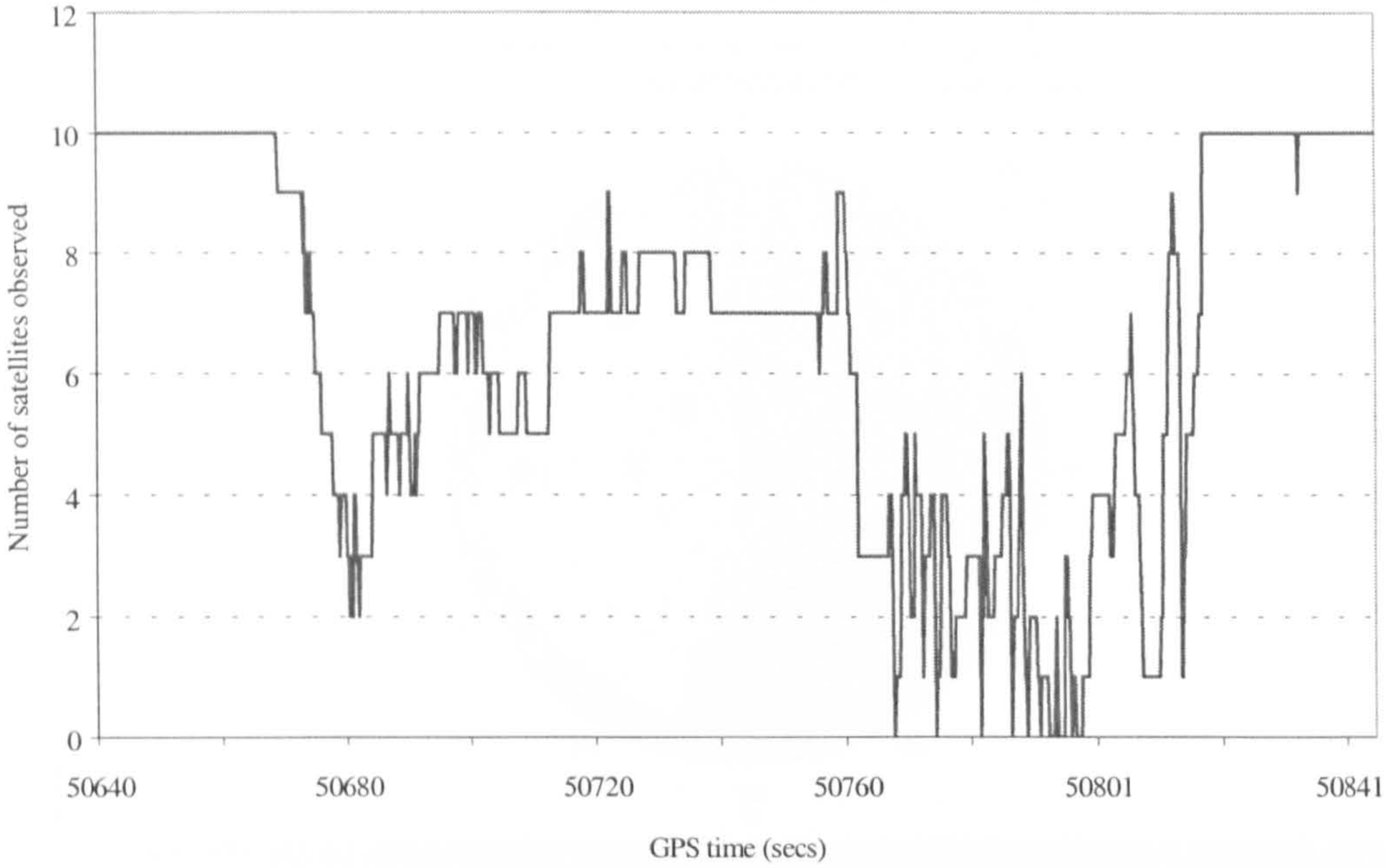

Figure 7.16 Satellite count

Satellites	% epochs
0	9.4
1	18.5
2	15.3
3	23.8
4	19.4
5	6.9
>5	6.8

Table 7.2 Constellation size as a percentage of slide epochs

Table 7.2 shows about one third of epochs at a constellation size of four or more, but this does not help if geometry is as per Figure 7.17, which is the prediction for an east facing curve on the day and time. Finally a small constellation, with poor geometry, is compounded by signal multipath.

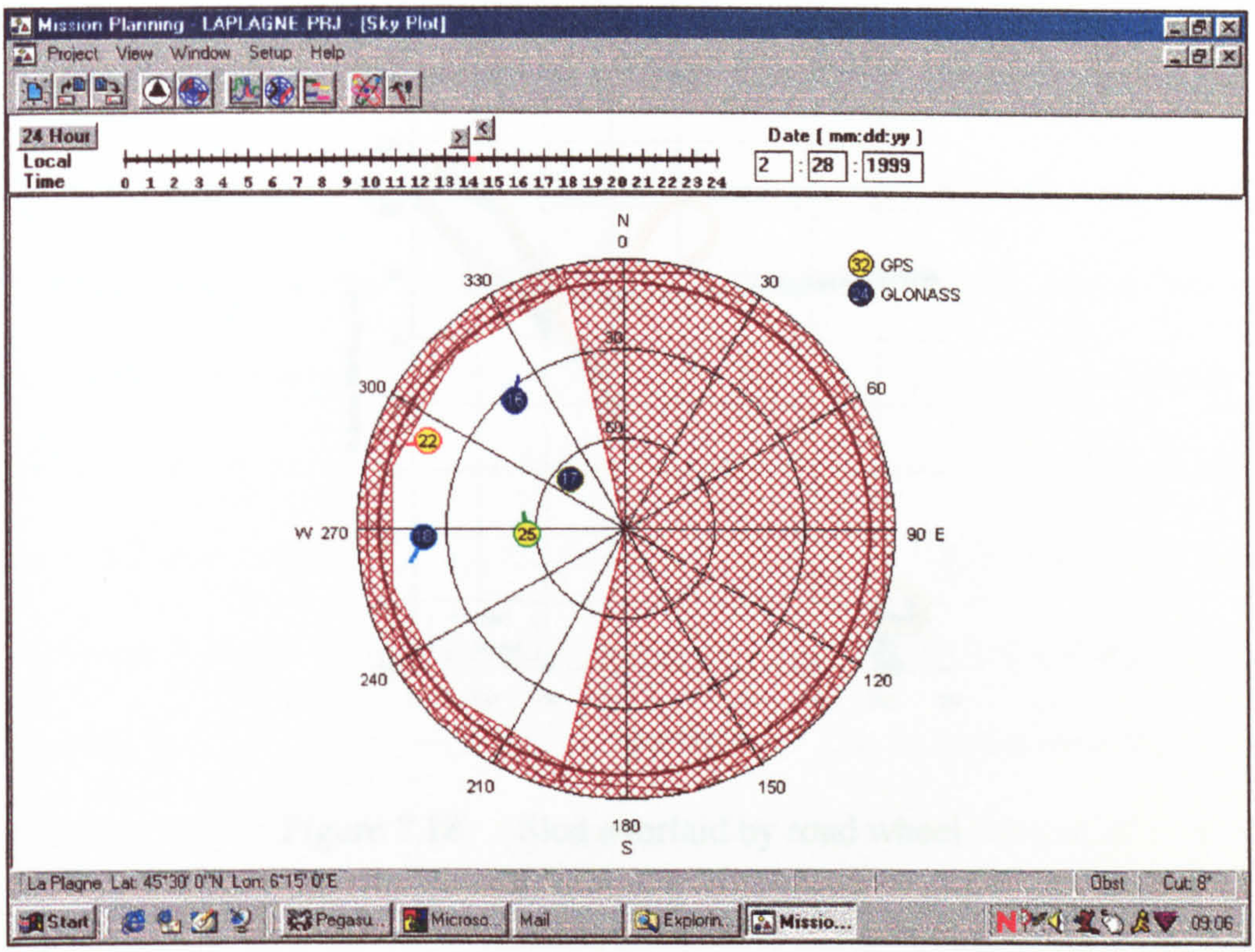

Figure 7.17 Constellation prediction for the sled in an east facing curve

Attempts were made to process the combined raw pseudorange and carrier phase data using all the available data processing packages: GAS, AOSS, and WinPrism. The *best* results were obtained using WinPrism, and these were limited to the start and end segments of the track. WinPrism had the advantage of a Kalman filter option. The coherent tracking segments are reproduced with the final track by road wheel overlaid (Figure 7.18), and magnified in Figures 7.19 and 7.20. Whilst the sled did produce a small amount of tracking that agreed with the wheel, this comparison shows it to very unreliable as a single source for track convolution determination. The curious deformation of the sled relative to wheel track, was most likely caused by defective geometry and Kalman filter effects, in association with multipath interference.

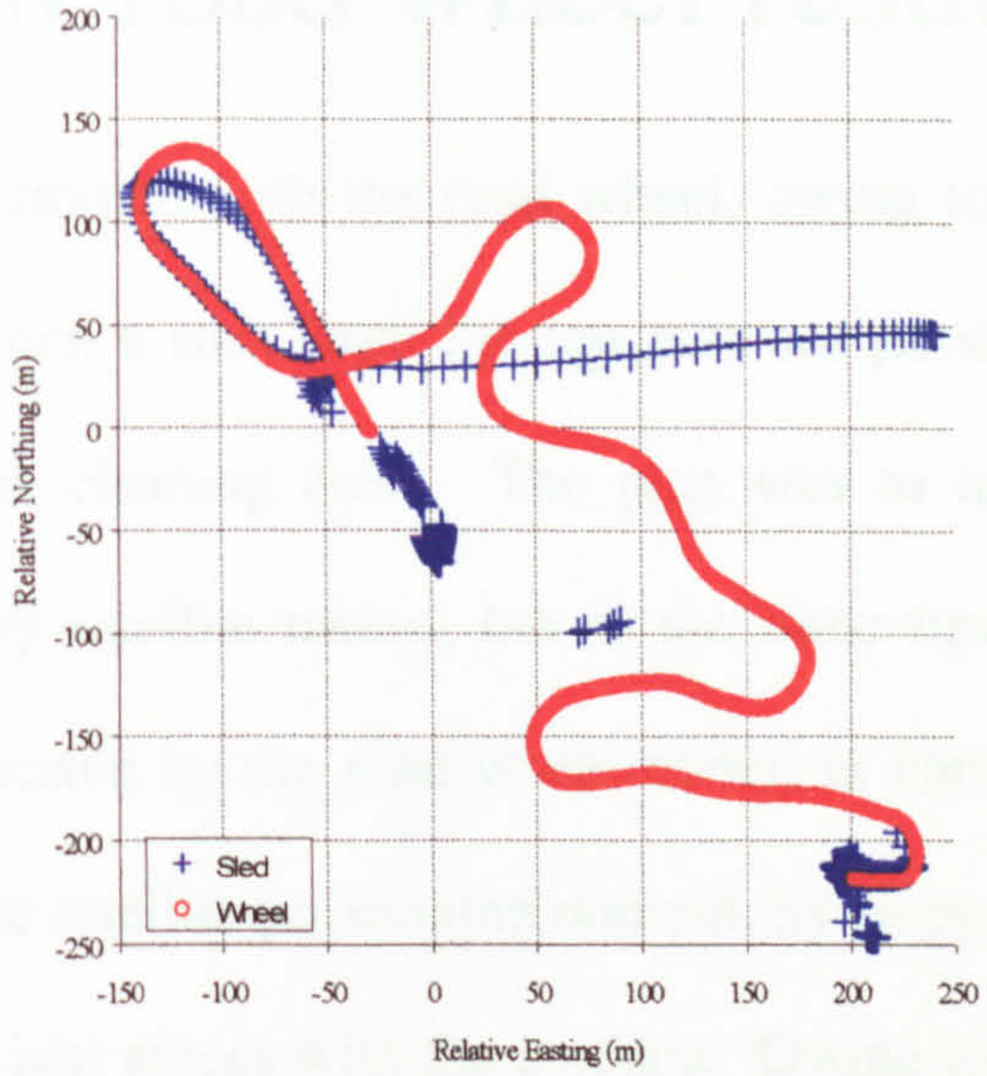

Figure 7.18 Sled overlaid by road wheel

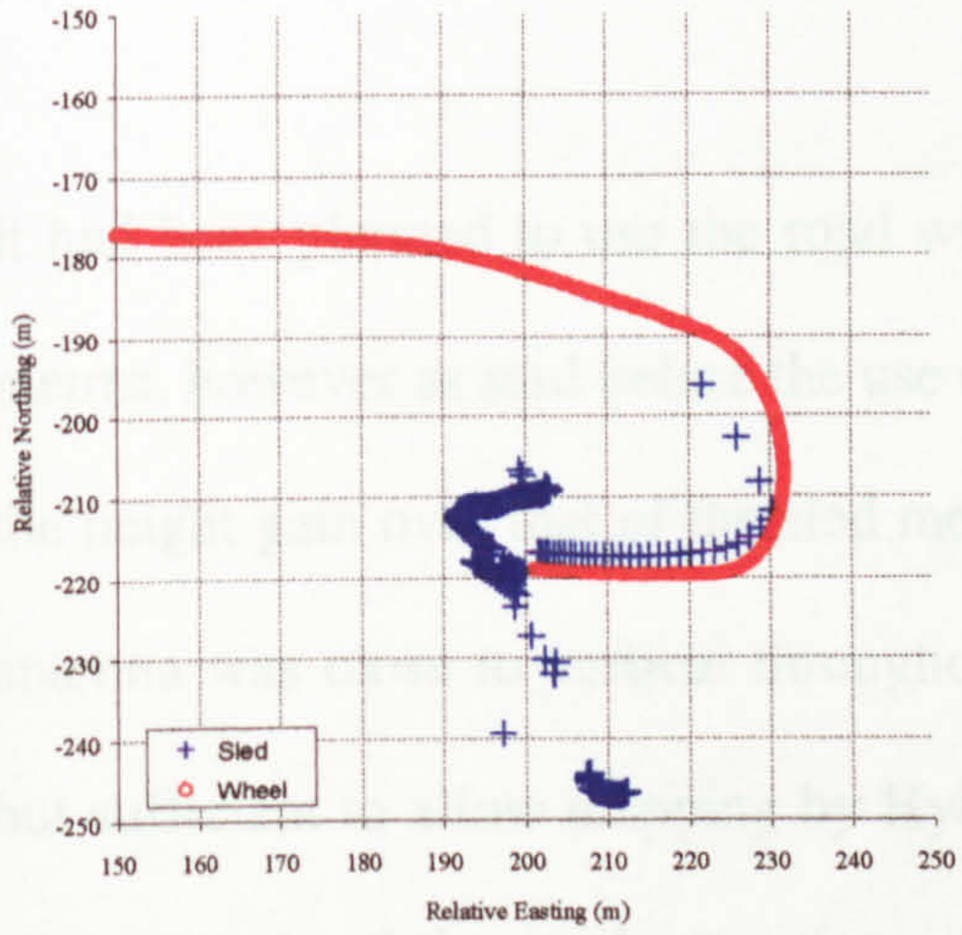

Figure 7.19 Sled overlaid by road wheel – start of slide

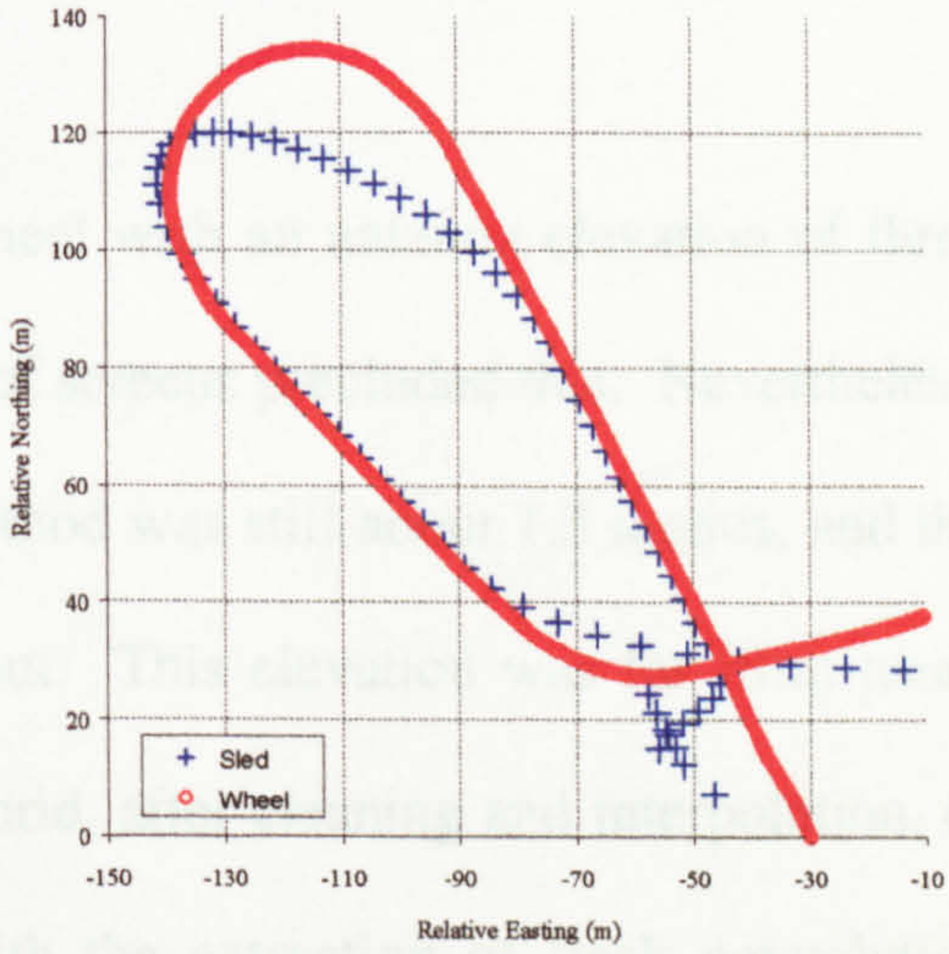

Figure 7.20 Sled overlaid by road wheel – end of slide

7.5.2 Raw road wheel results

Only one run was permitted with the road wheel, owing to track operational pressures, and even then a start from the top was not possible, as we had to keep ahead of a track cleaning crew. The plan was to make a continuous profile of the track by satellite means, but at the same time correlate along-track distance as indicated by the road wheel meter, at named waypoints and then mark them, in the satellite positioning domain, by stopping and repeatedly crossing the track at right angles with the antenna. Owing to pressure from the track cleaning crew, the latter was not possible, and correlation could only be made between distance indicated down-track and entry/exit from the numbered corners, at repeatable features. This meant that the correlation between wheel and satellite indicated distances was less reliable.

It had been planned to use the road wheel with an antenna elevation of three metres, however as said before the use of screens precluded this. Nevertheless, the height gain over that of the sled method was still about 1.3 metres, and the antenna was close to vertical throughout. This elevation was far from ideal, but sufficient to allow mapping by Hybrid, after cleaning and interpolation, of all segments of the track, together with the extraction of track convolution parameters and vertical gradient.

The Hybrid track (Figure 7.22) is far superior in terms of track definition, to that obtained by GPS alone (Figure 7.21). This validates the larger constellation argument for this application. It was unfortunate that only one

pass was allowed, precluding the aggregation approach, and necessitating a higher level of intervention in the construction of the final plan and vertical profiles.

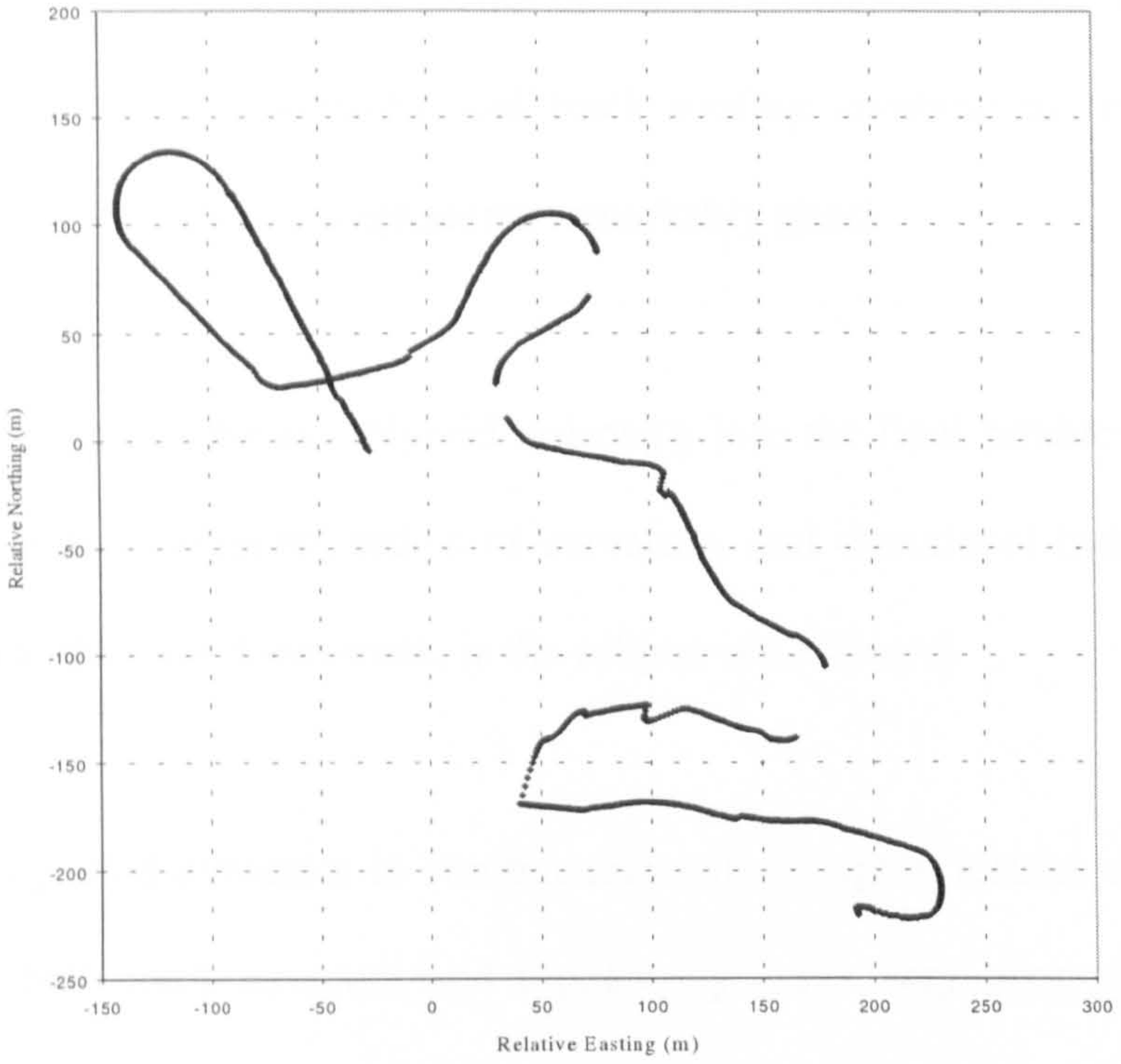

Figure 7.21 Road wheel by GPS

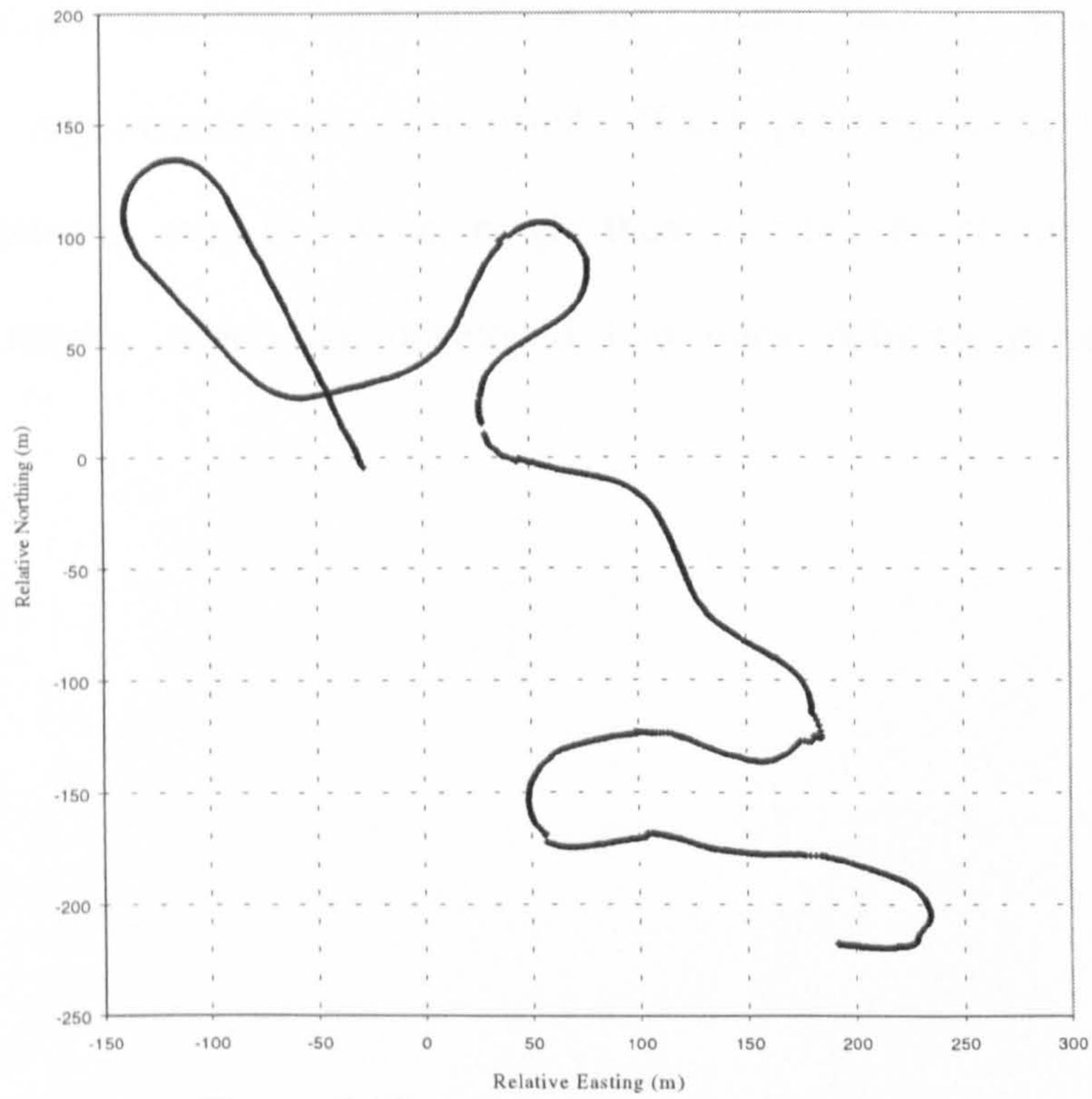

Figure 7.22 Road wheel by Hybrid

Figures 7.23 and 7.24 illustrate Hybrid availability and geometry colour coded on a background of the final edited trajectory, where code red corresponds to less than five satellites and a PDOP of more than 5. Considering the major curves 6, 10, 12, 15, and 16, the higher up the valley (further south) the poorer the constellation, as topography and track roofing combine to restrict the skyview, otherwise the coverage seems remarkably good.

The development of the raw Hybrid trajectory into the final products of plan trajectory, vertical gradient, radius of curvature, and directional indicator, all referenced to distance down-track, is the subject of Chapter 8.

Summarising, sled dynamics in combination with a highly restricted skyview caused by both track structure and topography, gave very poor positioning results by satellite positioning technology. In a more benign environment with less topographic masking, for example at the Calgary track in Canada, then a significant improvement was anticipated. Track profiling using the wheel mounted antenna, even at a lesser height than intended, by comparison gave excellent results, which are developed into track defining parameters in Chapter 8.

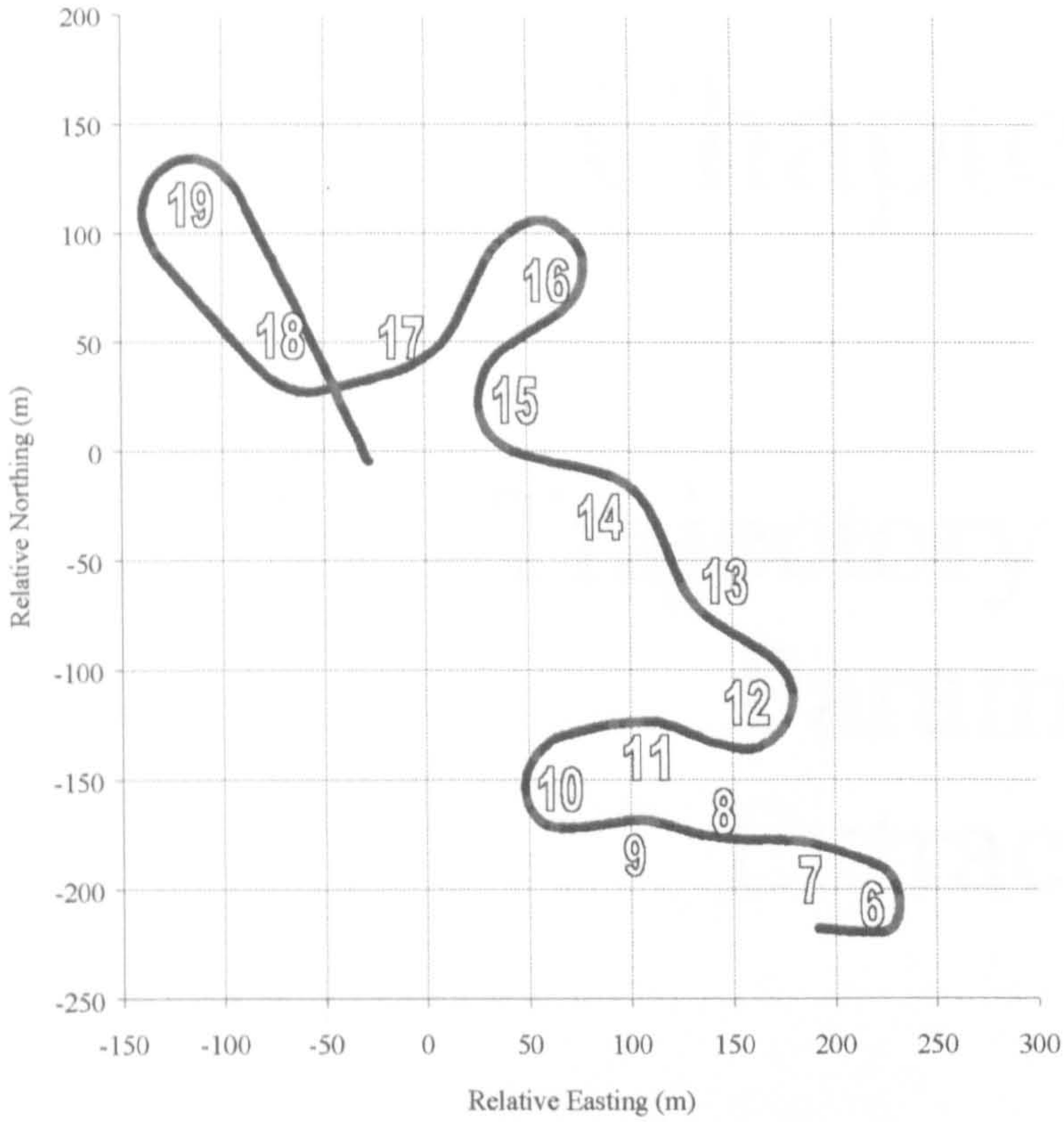

Figure 7.23 Hybrid: constellation ≤ 5

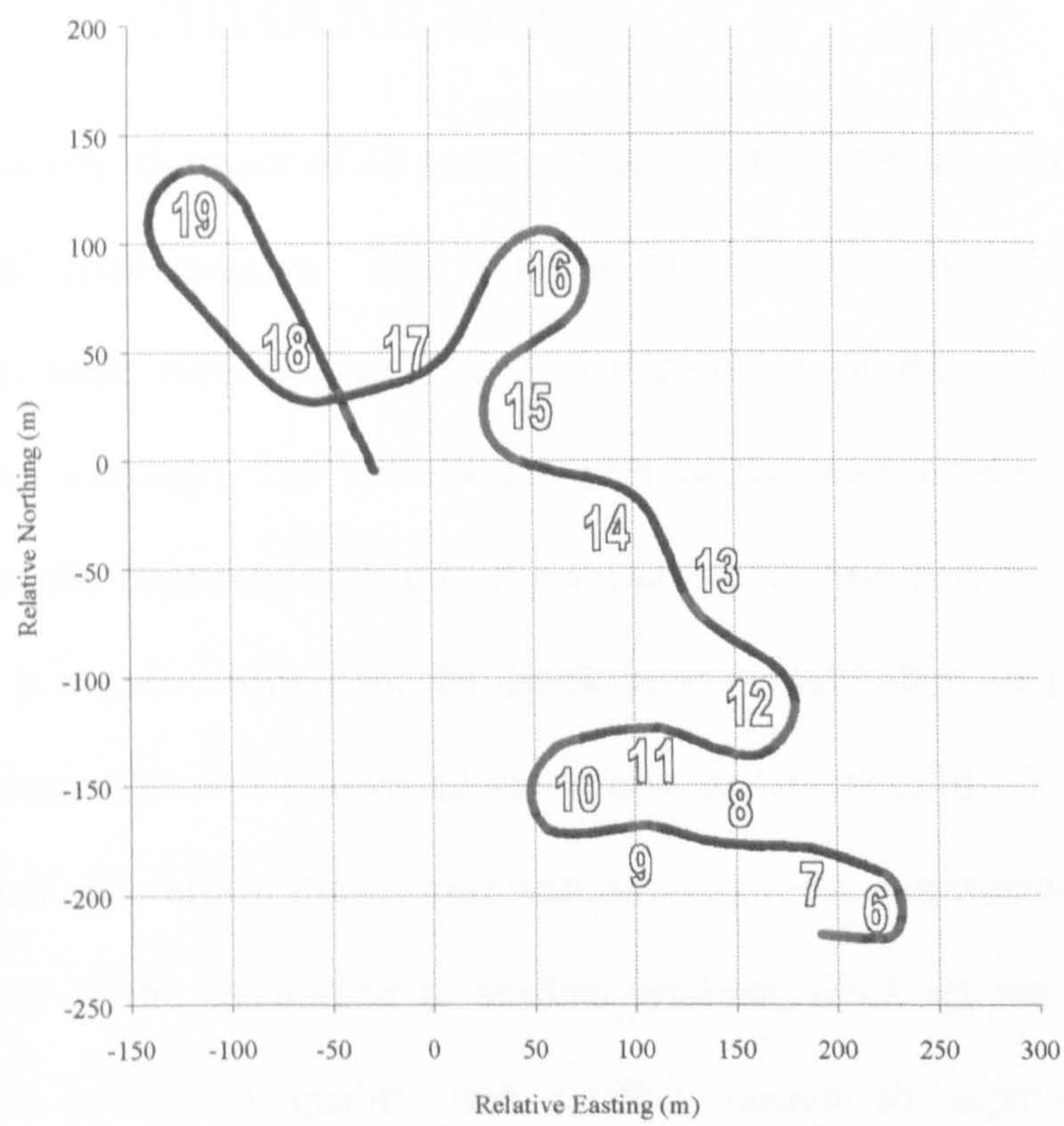

Figure 7.24 Hybrid: PDOP > 5

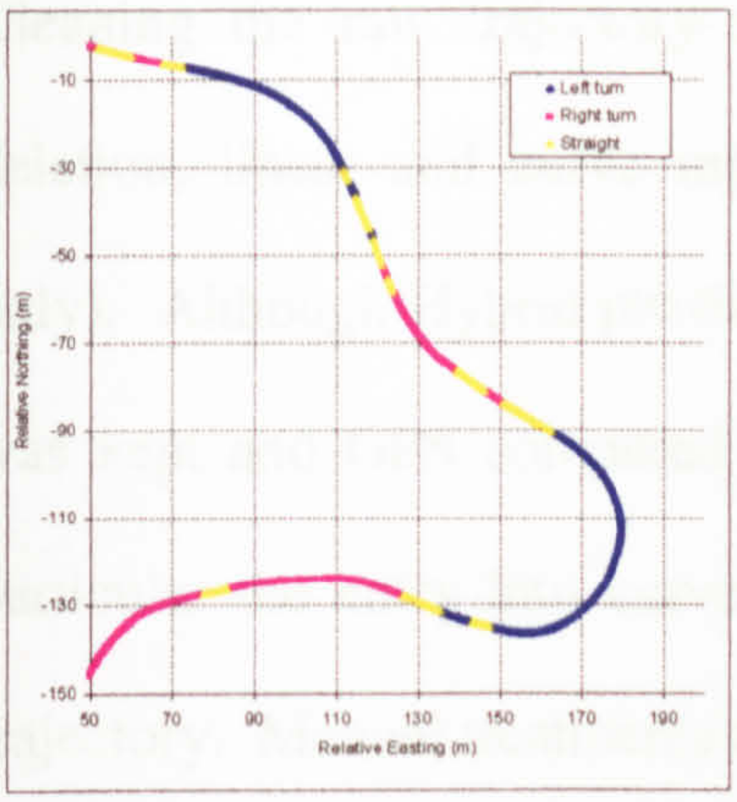

Chapter 8

Trajectory and Parameter Extraction

8.1 Introduction

The necessary character of all bobsled tracks is that they have no vertical or horizontal discontinuities. This is not to say there are no rapid changes in direction, there certainly are, and it is negotiation of these that determine competitor ranking. The smooth character of the track allows filtering and editing of the trajectory with a high level of confidence, and the fact that the gradient is negative except for the deceleration straight after the finish line, is also a bonus. The ability to visualise and edit the trajectory in 3D did not exist, hence plan and vertical dimensions were initially treated in isolation, reuniting again only in the calculation of vertical gradient, cross referenced by time. Disparate coordinate quality was another reason to separate the two dimensions.

Cleaning the raw trajectory required several manual treatments, including deletion, linear and curve interpolation, and block shift and rotation (plan only). Although Hybrid provided the majority of the trajectory, an open mind was kept and GPS compared / overlaid, since there were odd occasions, in particular the entry into curve 6, where GPS alone provide a more coherent trajectory. Manual treatments are covered in §8.2.

After manual intervention, the coarsely edited trajectory was subjected to various filter routines, with the aim of preserving the underlying features, whilst removing high frequency noise. Also in preparation for parameter extraction, the down-track position interval needed regulation to a common value. Automated treatments are the subject of §8.3.

Finally §8.4 covers the automated extraction of track defining parameters.

8.2 Manual treatments

The raw Hybrid plan trajectory contained anomalies that were not sympathetic to automated treatment, for example see the trace defects in Figures 8.1 to 8.3. Manual intervention was needed to handle these abnormalities. Manual in this case, meant editing individual points within small track segments on very large scale Excel displays. Obvious outlying points were eliminated, Kalman filter based aberrations e.g. (Figure 8.3) were either deleted based mainly on agreement with adjoining coherent segments (Figure 8.3a), but with reference to geometry and solution noise levels too, or adjusted with reference to the

GPS solution if available and plausible e.g. (Figure 8.1) edited to give Figure 8.1a. Interpolation based either on a curved fit or straight line as appropriate was imposed where necessary. Figure 8.2 shows an apparent discontinuity, this is in fact real and it merely indicates a shift of the wheel from one side of the track to the other, to keep against the side wall, as the track rose up to form the entrance to a curve. Such segments were shifted and rotated slightly to match the adjoining segments, see for example Figure 8.2a. By its very nature, artistic licence is intrinsic to manual processes, and non-repeatable to some degree. However, feedback provided by the slider on the veracity of the final edited version was very positive, with especial agreement on curve 6 (Figure 8.2) which had been the subject of some deliberation.

The vertical dimension was no less problematic than that described above for plan. Figure 8.4 shows the full raw profile overlaid by the final version. The raw profile is disturbed by obvious aberrations, however there are three segments that appear coherent but offset from the adjoining profile. These are probably caused by change in constellation, unfortunately only the number of satellites in solution at an epoch rather than satellite identities is reported by the processing software, precluding deeper analysis of the cause. Manual intervention consisted of block shifting the offset segments (see Figure 8.4a), and eliminating and then interpolating across aberrations. The highest uncertainty at this stage concerned the interval between 610 to 720 metres down-track. Investigation of data response to non-zero elevation masks, resulted in altered positioning of the offset segments, but also brought in a

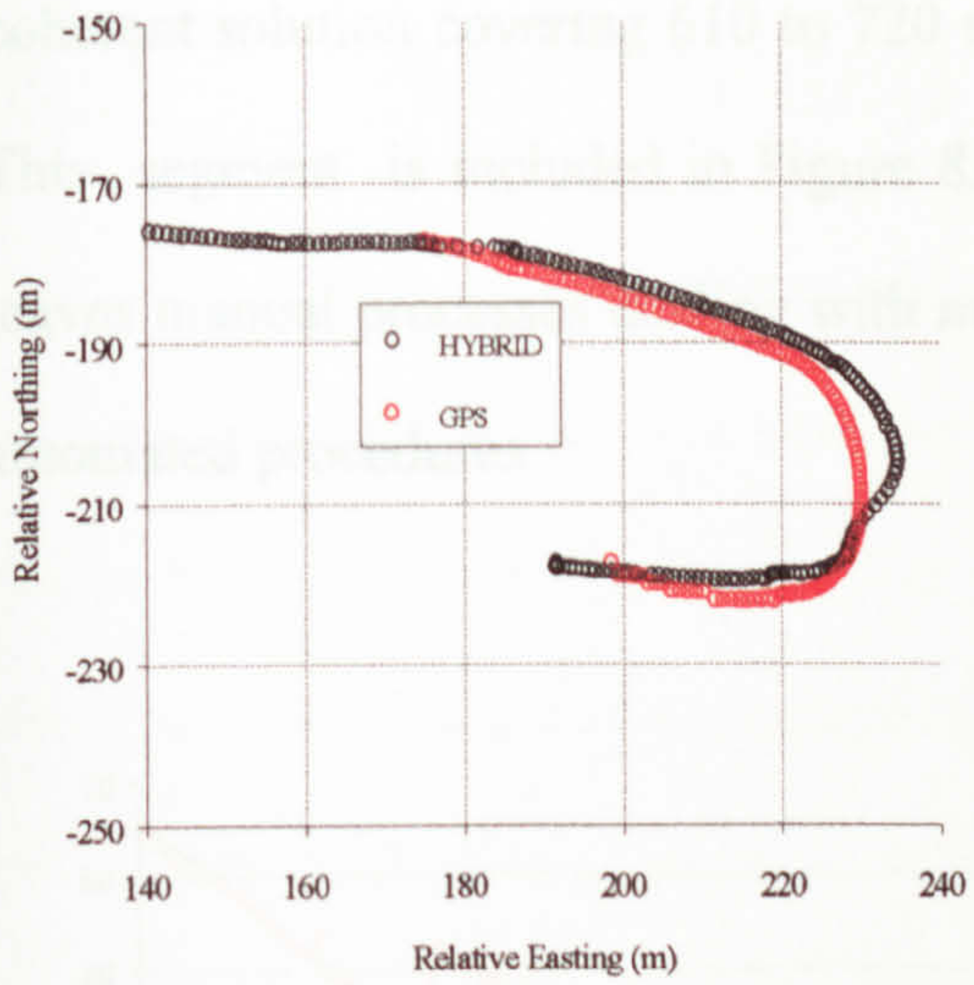

Figure 8.1 Curve 6 (raw)

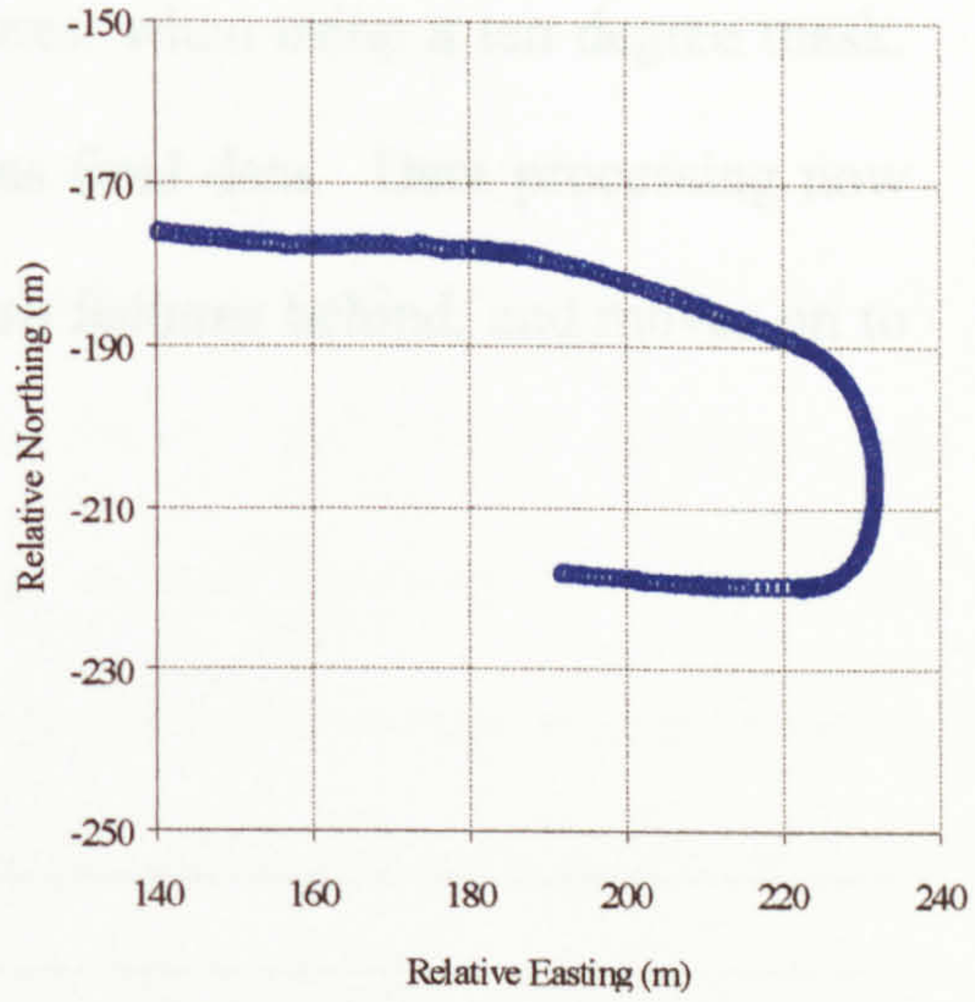

Figure 8.1a Post-manual processing

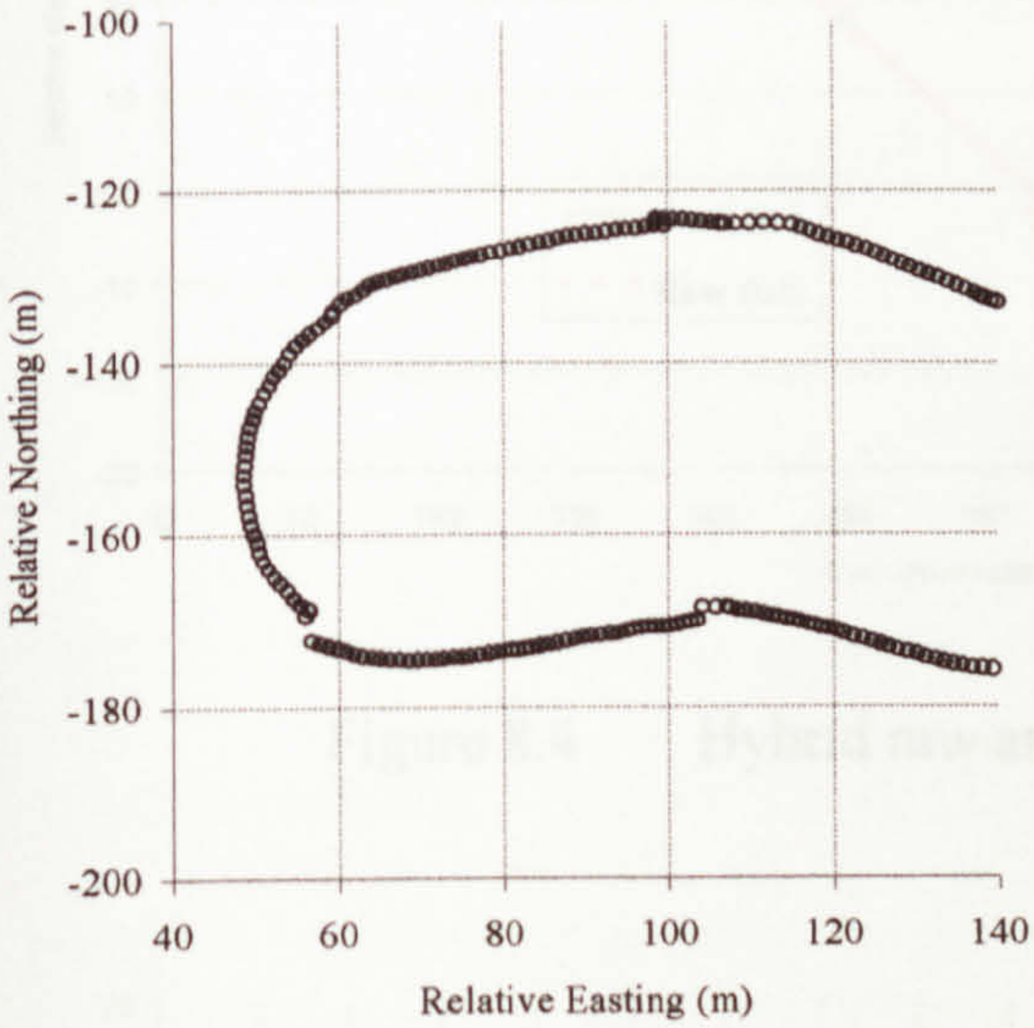

Figure 8.2 Hybrid curve 9 (raw)

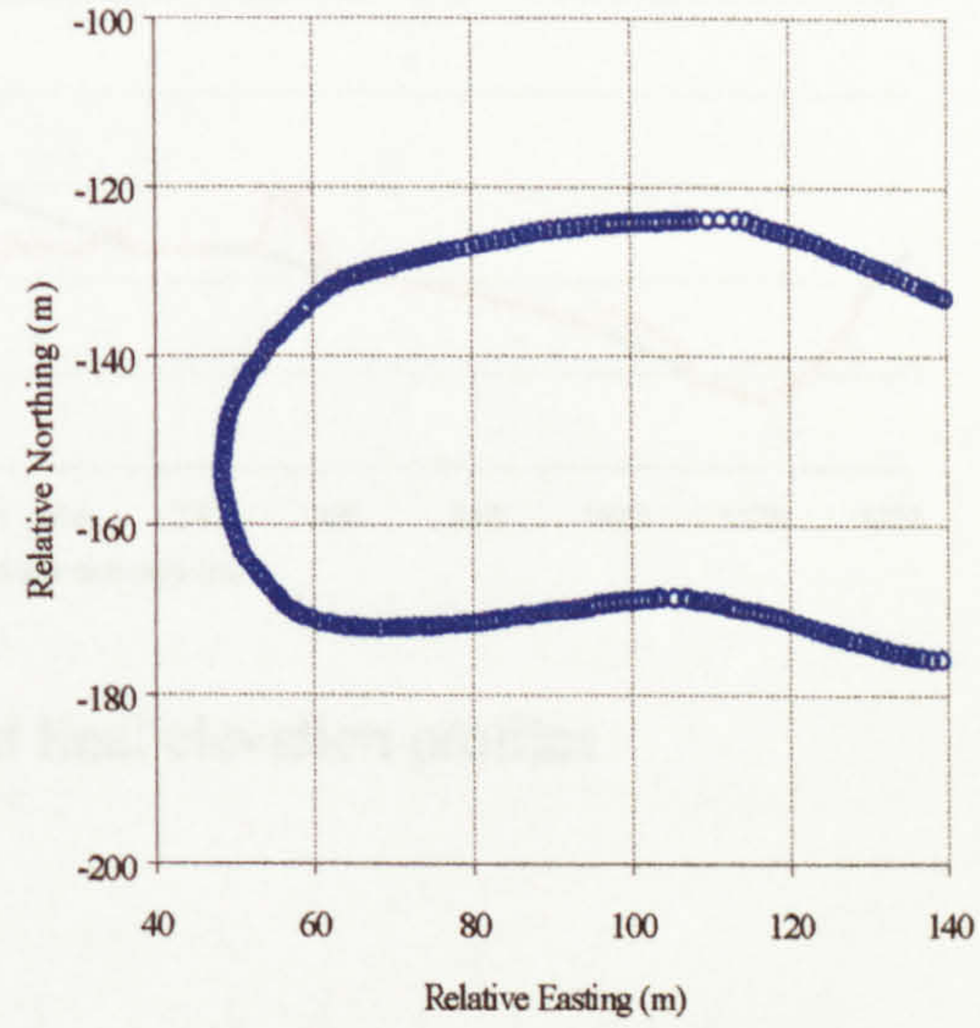

Figure 8.2a Post-manual processing

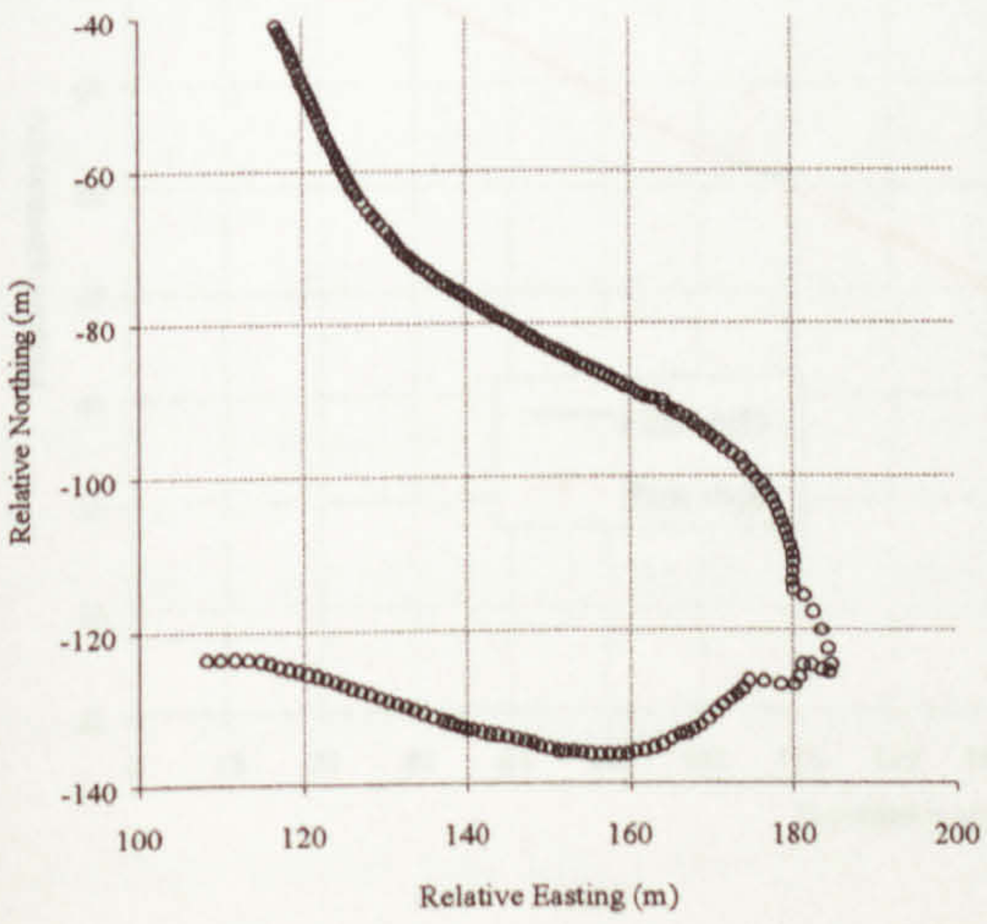

Figure 8.3 Hybrid curve 12 (raw)

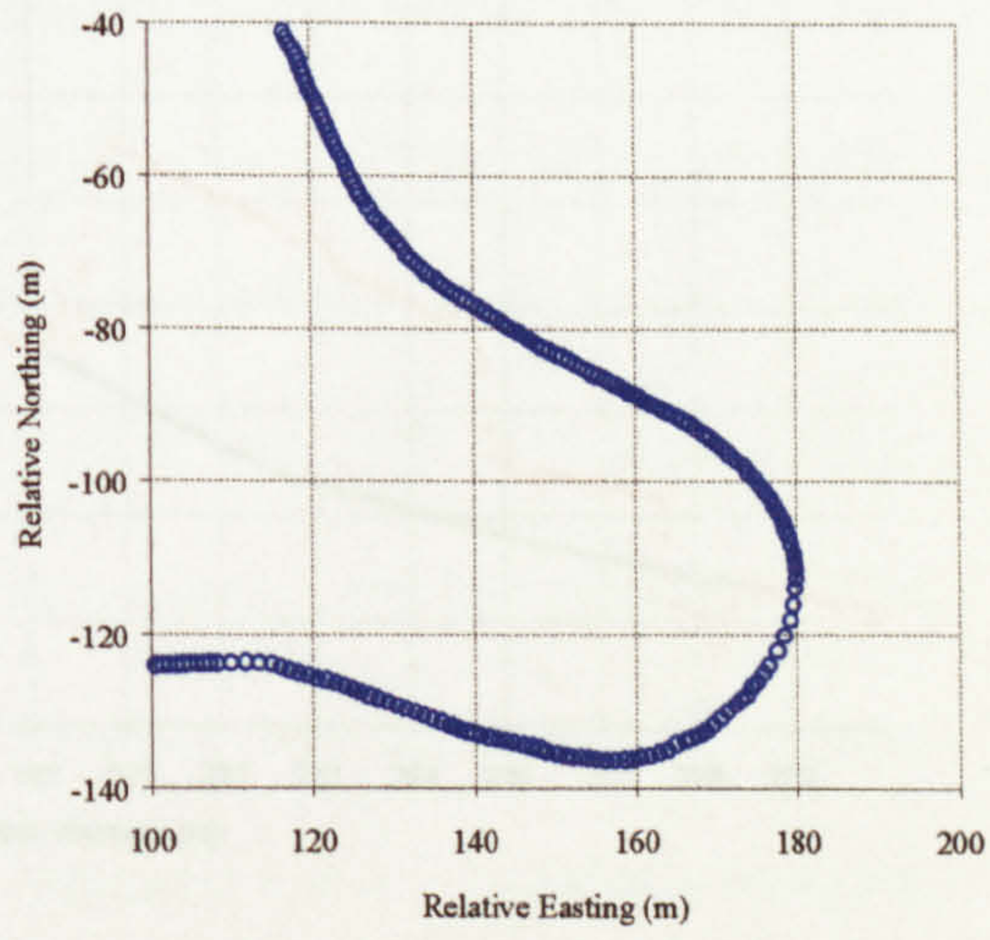

Figure 8.3a Post-manual processing

coherent solution covering 610 to 720 metres, when using a ten degree mask. This segment is included in Figure 8.4 as final data. Data processing now leaves manual processes dealing with macro features behind, and moves on to automated procedures.

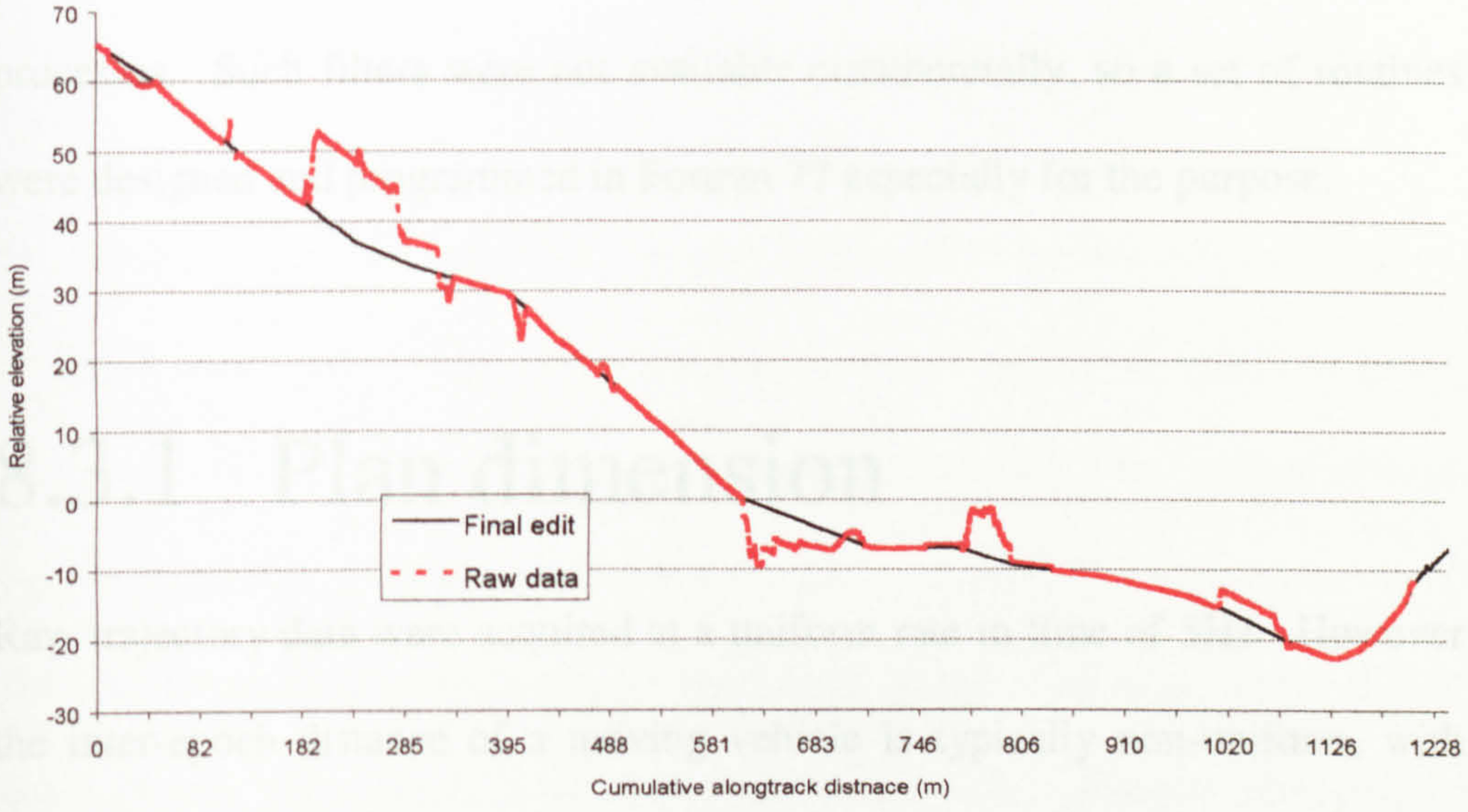

Figure 8.4 Hybrid raw and final elevation profiles

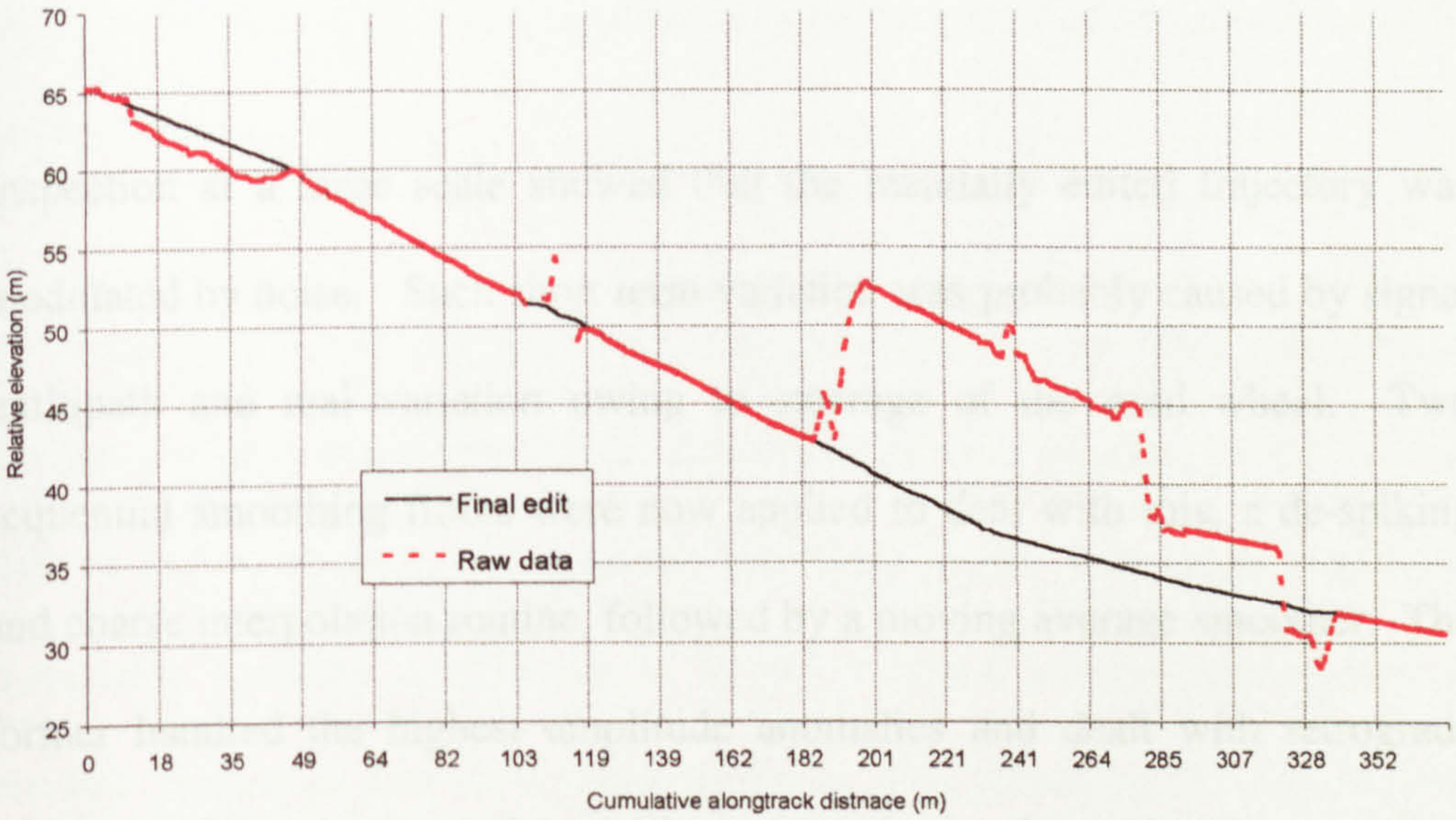

Figure 8.4a Part profile detail

8.3 Automated treatments

The need for a comprehensive editing suite was avoided through the use of localised manual editing of macro features, as set out in §8.2. However, all filters beyond the manual intervention stage were of necessity automated, with the aim of producing uniform trajectory characteristics, to supply to subsequent processes. Such filters were not available commercially, so a set of routines were designed and programmed in Fortran 77 especially for the purpose.

8.3.1 Plan dimension

Raw trajectory data were acquired at a uniform rate in time of 5Hz. However the inter-epoch distance of a moving vehicle is typically non-uniform, with periods of positive, zero and negative acceleration, all compounded by change in vehicle heading. This section details the processes developed and applied to provide a standardised down-track distance interval.

Inspection at a large scale showed that the manually edited trajectory was modulated by noise. Such short term variation was probably caused by signal multipath and real variation owing to steerage of the road wheel. Two sequential smoothing filters were now applied to deal with this, a de-spiking and coarse interpolation routine, followed by a moving average smoother. The former handled the highest amplitude anomalies and dealt with retrograde tracking, whilst the latter damped high frequency noise. Various averaging

filter lengths were applied and the optimum selected, in terms of noise damping, whilst honouring the input trajectory to a high degree.

Interval	Length (m)
Minimum	0.08
Maximum	3.05
Average	0.95
Standard deviation	0.31

Table 8.1 Coordinate interval summary (post hand edit)

The relatively smooth trajectory was then delivered to an interpolation routine, designed to regulate the sampling interval of an irregularly sampled (in space) source file. Table 8.1 summarises the road wheel interval after manual editing. The interpolation routine searched for the shortest interval in the file, then to simplify programming and preserve the nature of the input data, either this or some shorter value could be used to resample the file. Shorter interpolation distances preserved the source data more highly, and in this case 2 cms was chosen. The level of detail in the output file was then finally controlled by a decimation routine, so that a coordinate could be output at any multiple of the interpolation distance.

To obtain the smoothest trajectory, the interpolated data were then fed, at various decimation multiples, to a cubic spline routine [Burger, 1989]. In this filter a series of splines (or curves) are fitted to the data (Figure 8.5), by computing function coefficients in x and y across successive overlapping window lengths of four data points (or *knots*, here joined by chords), moving through the data with an increment of one data point. These coefficients are then used to derive the coordinates of a number of intermediate points between

knots, as required. A major advantage of the cubic spline is that the original data are preserved.

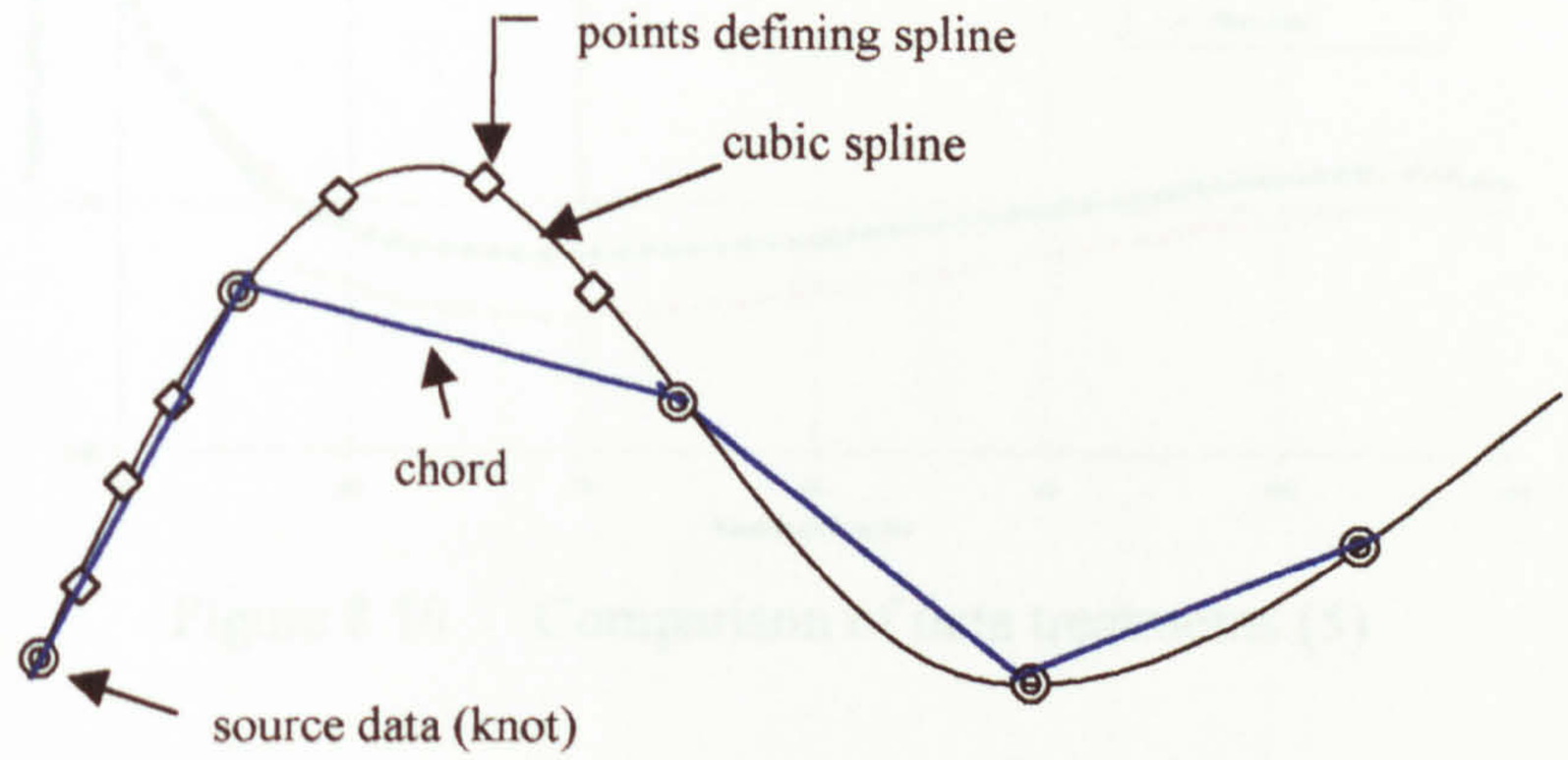

Figure 8.5 Cubic spline (exaggerated)

It is possible to fit a cubic spline to irregularly spaced data, by varying the number of points between knots, in this case however, it is of no benefit since radius of curvature computations require a regular spacing.

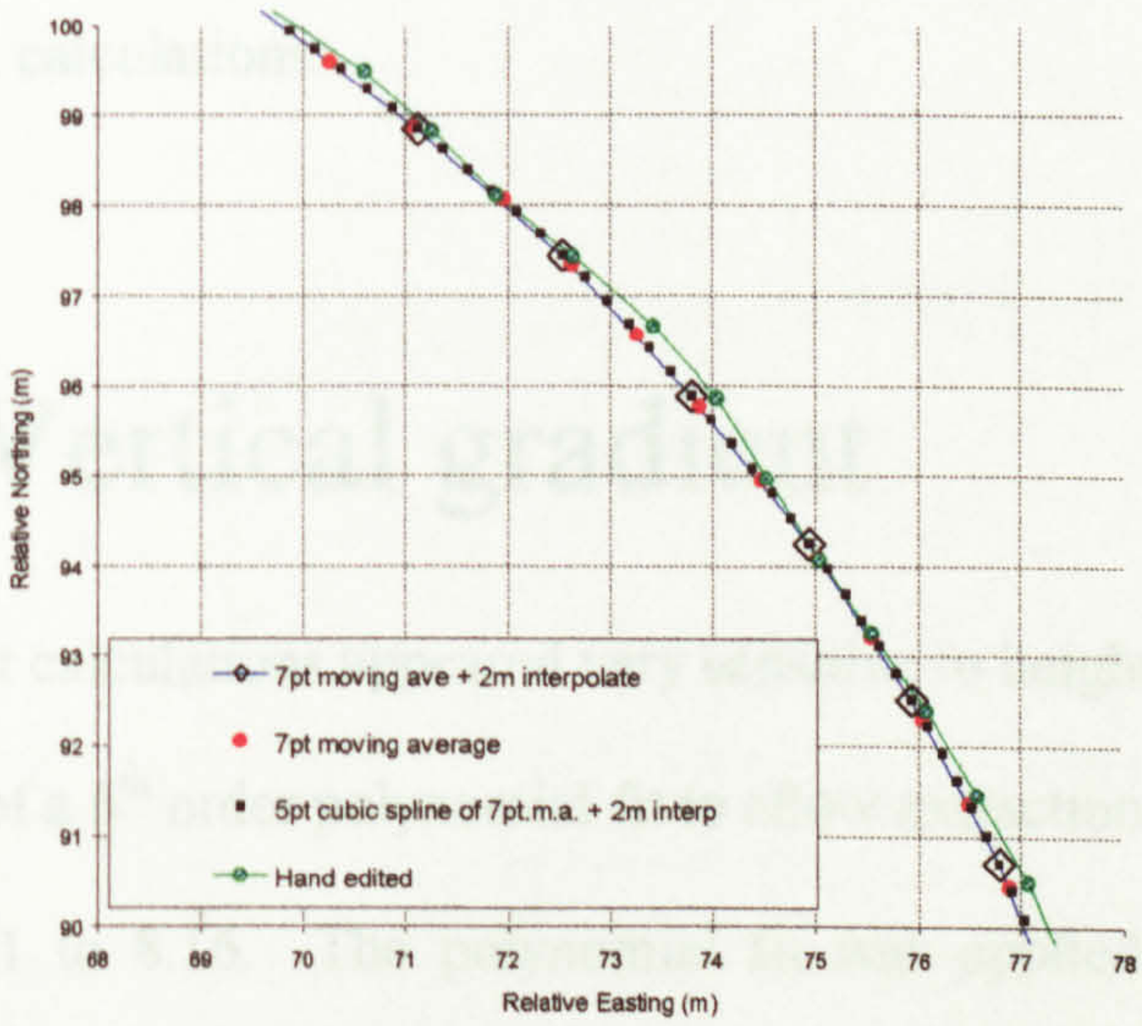

Figure 8.6 Comparison of data treatments (1)

Output from a four-points-between-knots cubic spline appeared fairly insensitive to the source file interval, with no discernible difference whether a

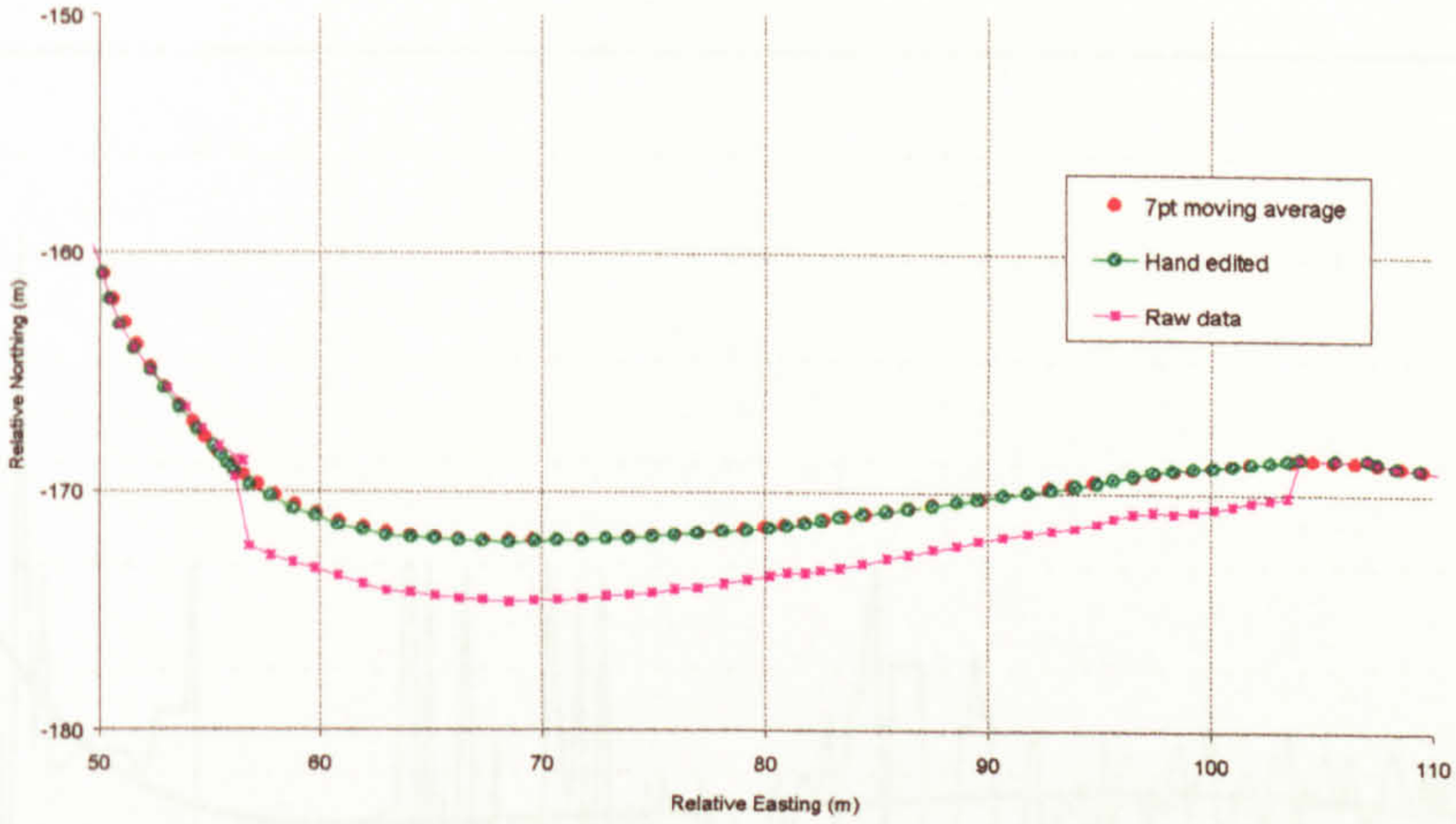

Figure 8.10 Comparison of data treatments (5)

8.3.2 Vertical dimension

The final height profile has already been provided in Figures 8.4 and 8.5. The profile remained relatively noisy after the manual edit stage, so a moving average filter was applied to damp high frequency content, before inclusion in vertical gradient calculations.

8.4 Vertical gradient

Vertical gradient calculations appeared very sensitive to height error, requiring the application of a 6^{th} order polynomial fit to allow extraction of useful values, see Figures 8.11 to 8.16. The polynomial fit was applied in Excel, using segments about 200 metres in length, with a fifty percent overlap with adjoining segments to mitigate filter artefacts at the ends of data.

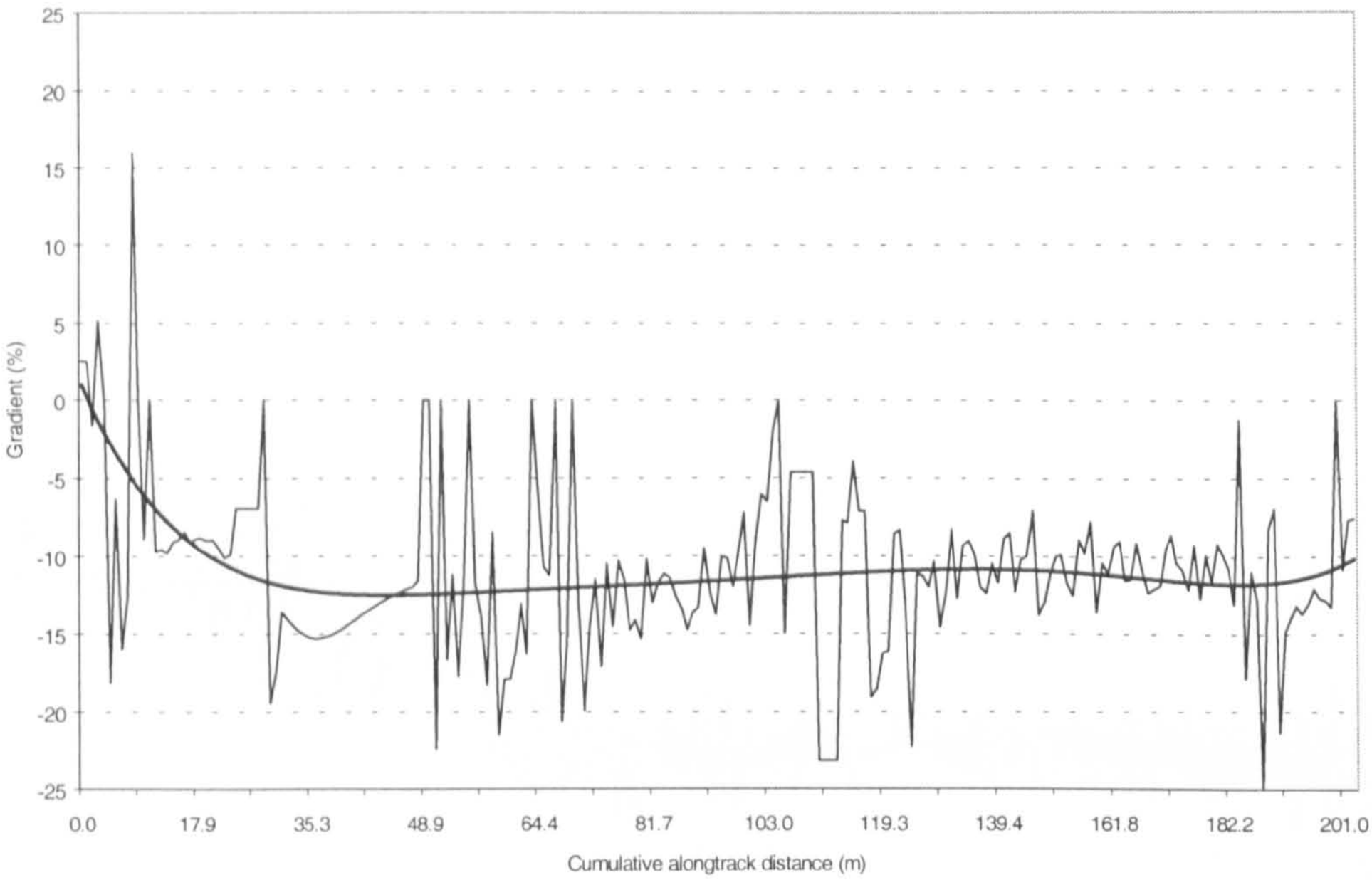

Figure 8.11 Approximate gradient profile – Curve 6

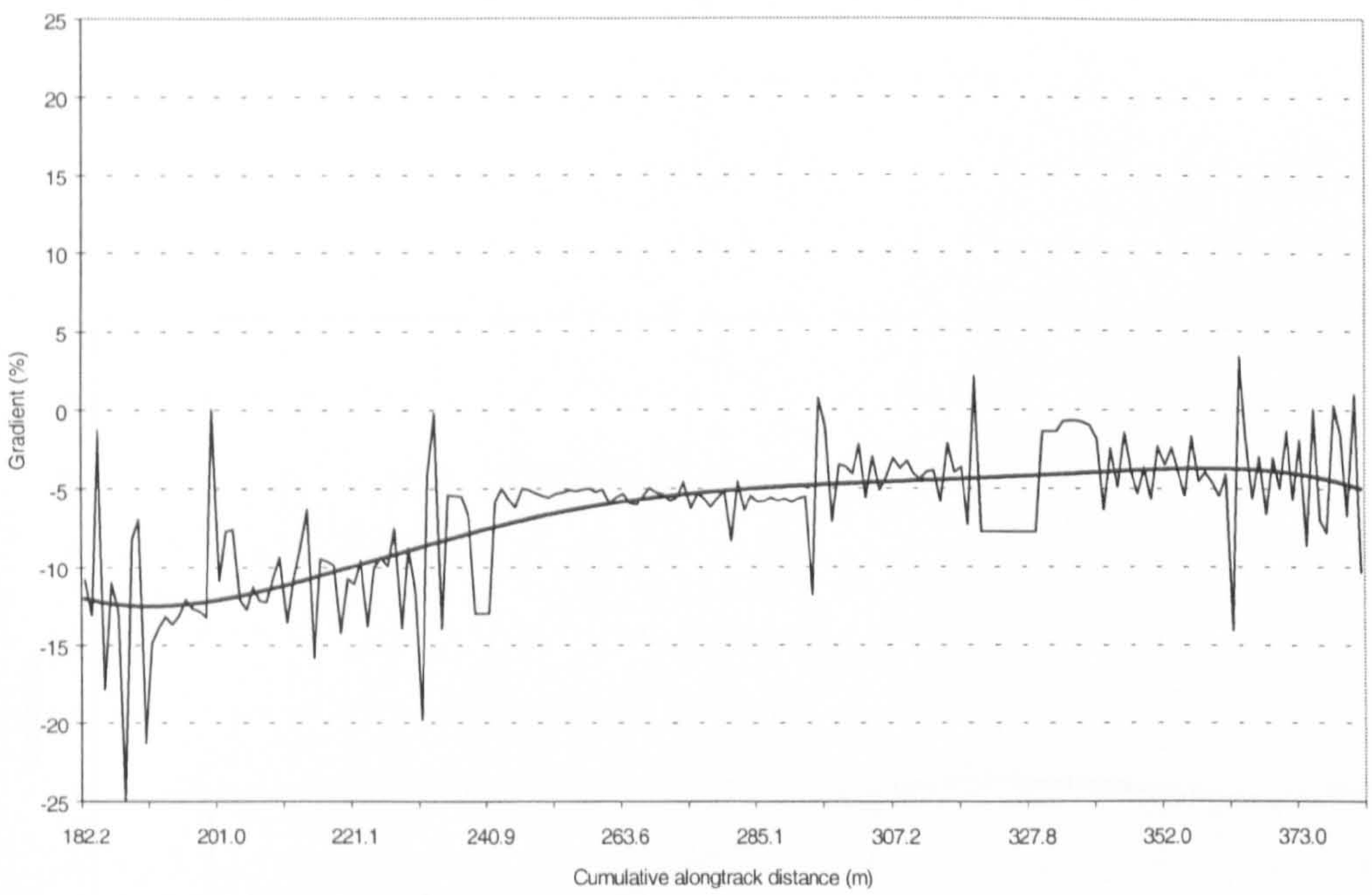

Figure 8.12 Approximate gradient profile – Curve 9

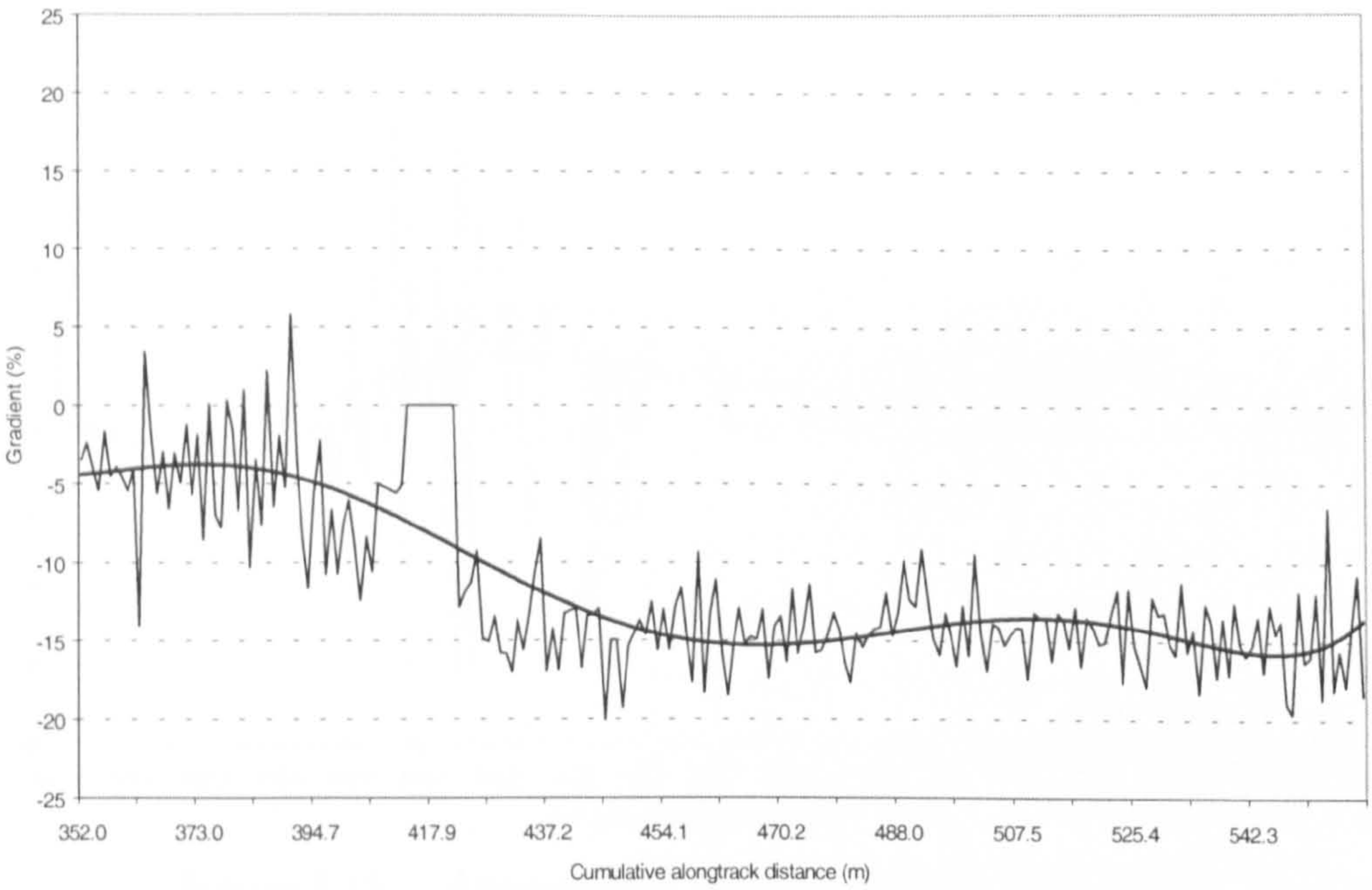

Figure 8.13 Approximate gradient profile – Curve 11

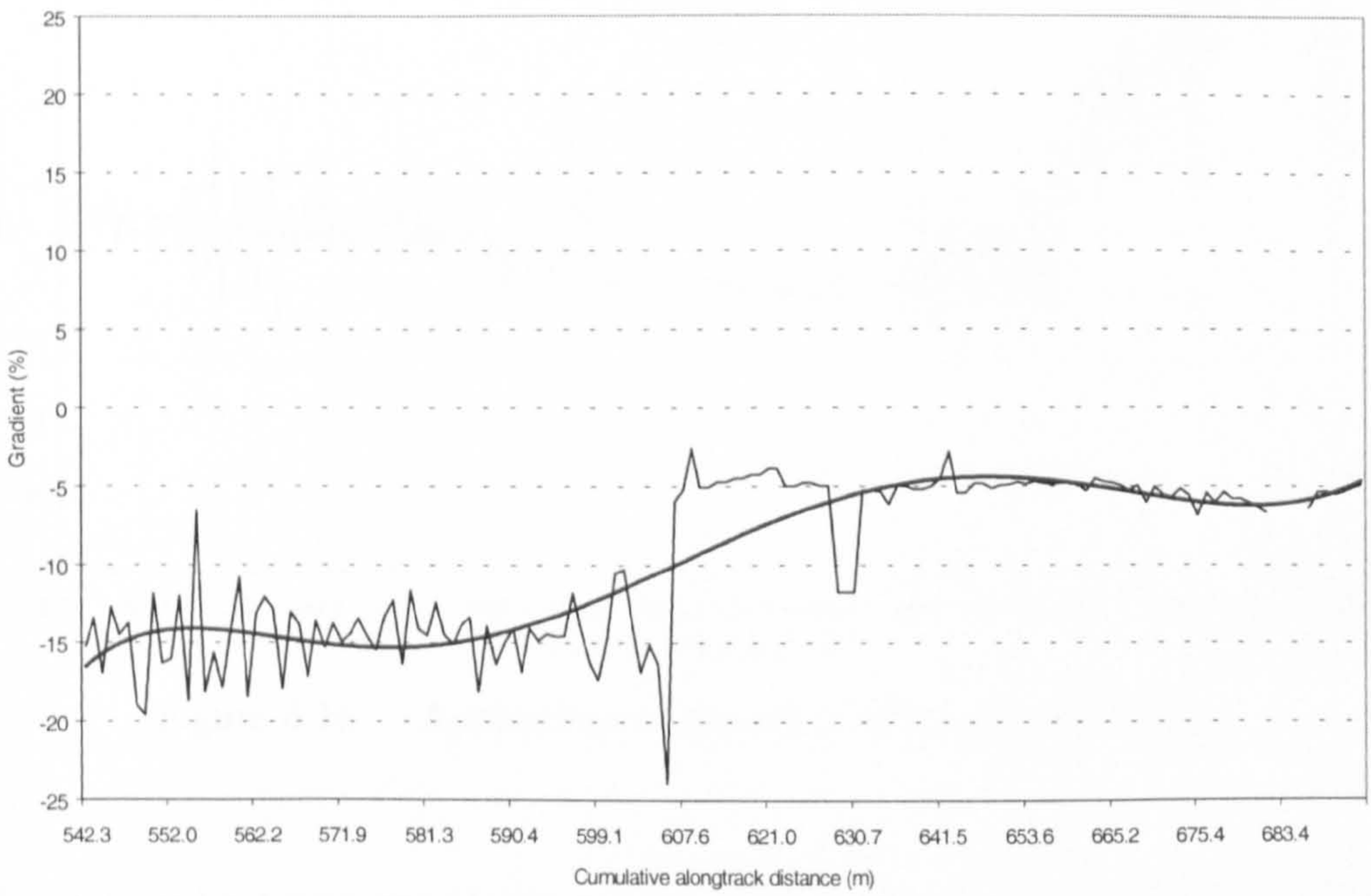

Figure 8.14 Approximate gradient profile – Curve 13/14

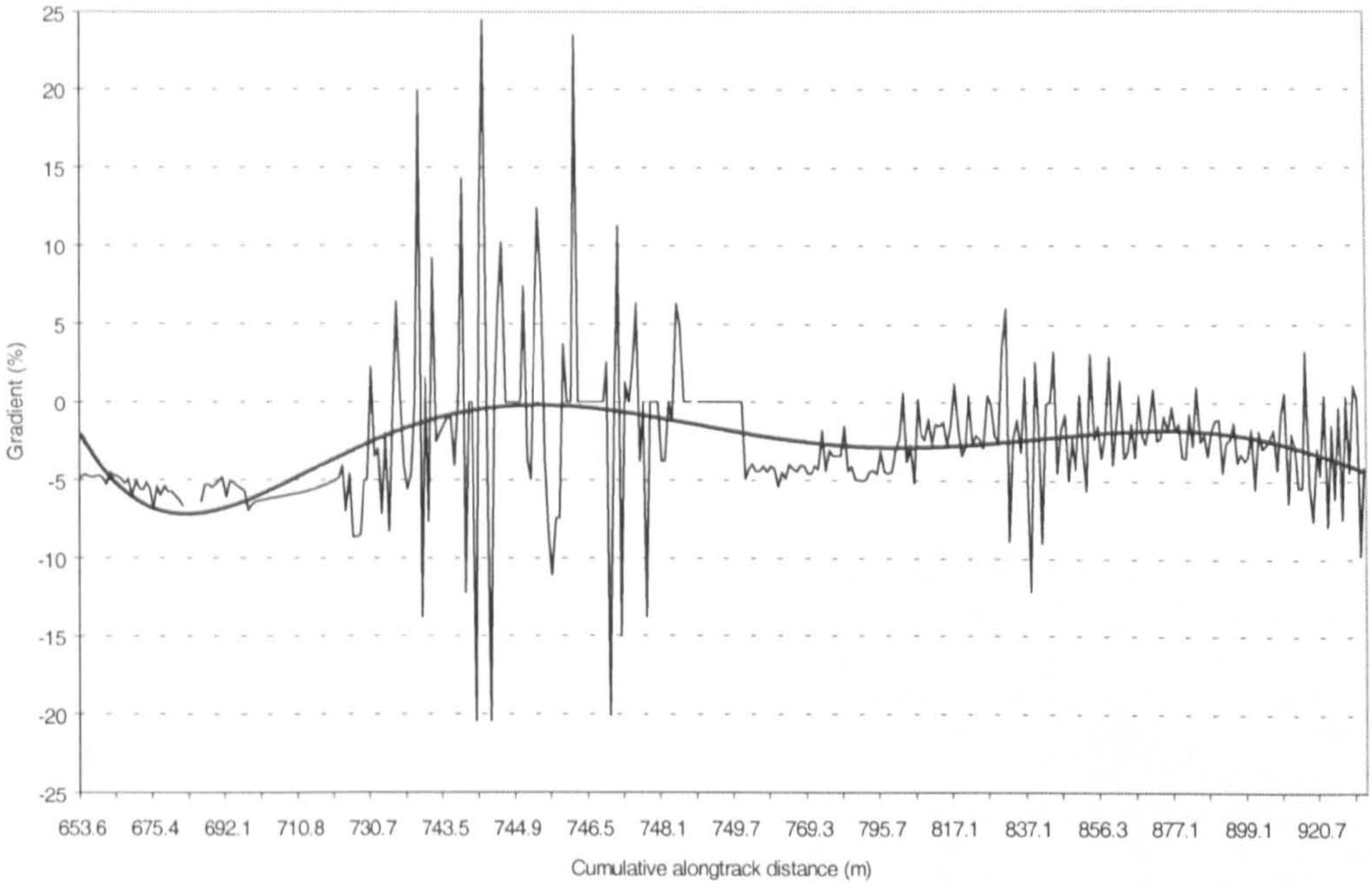

Figure 8.15 Approximate gradient profile – Curve 16

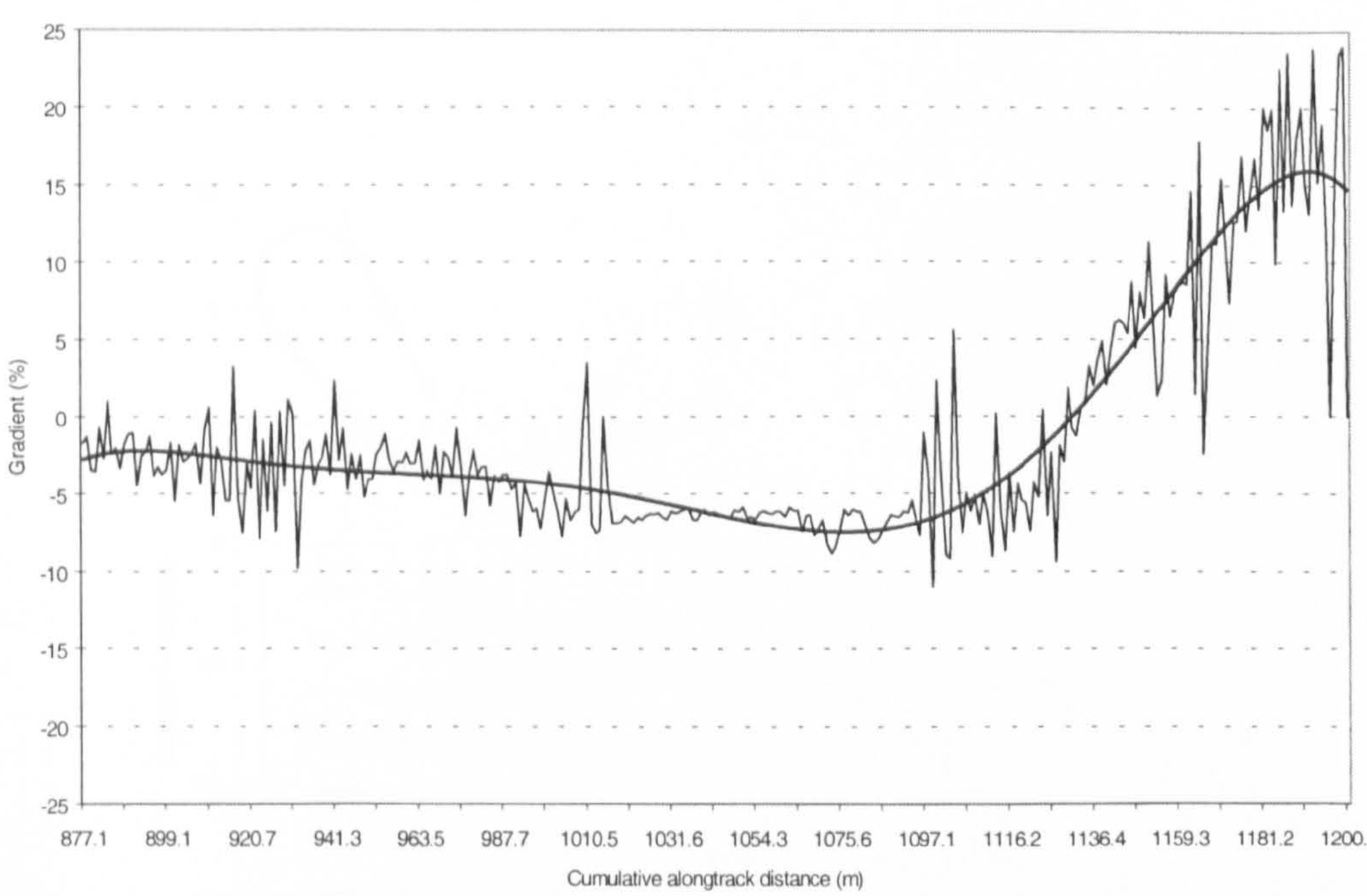

Figure 8.16 Approximate gradient profile – Curve 18/19

Vertical gradient was one element of the final deliverable for this project, and in Figures 8.17 and 8.18 it is used to coarsely colour code the final plan trajectory.

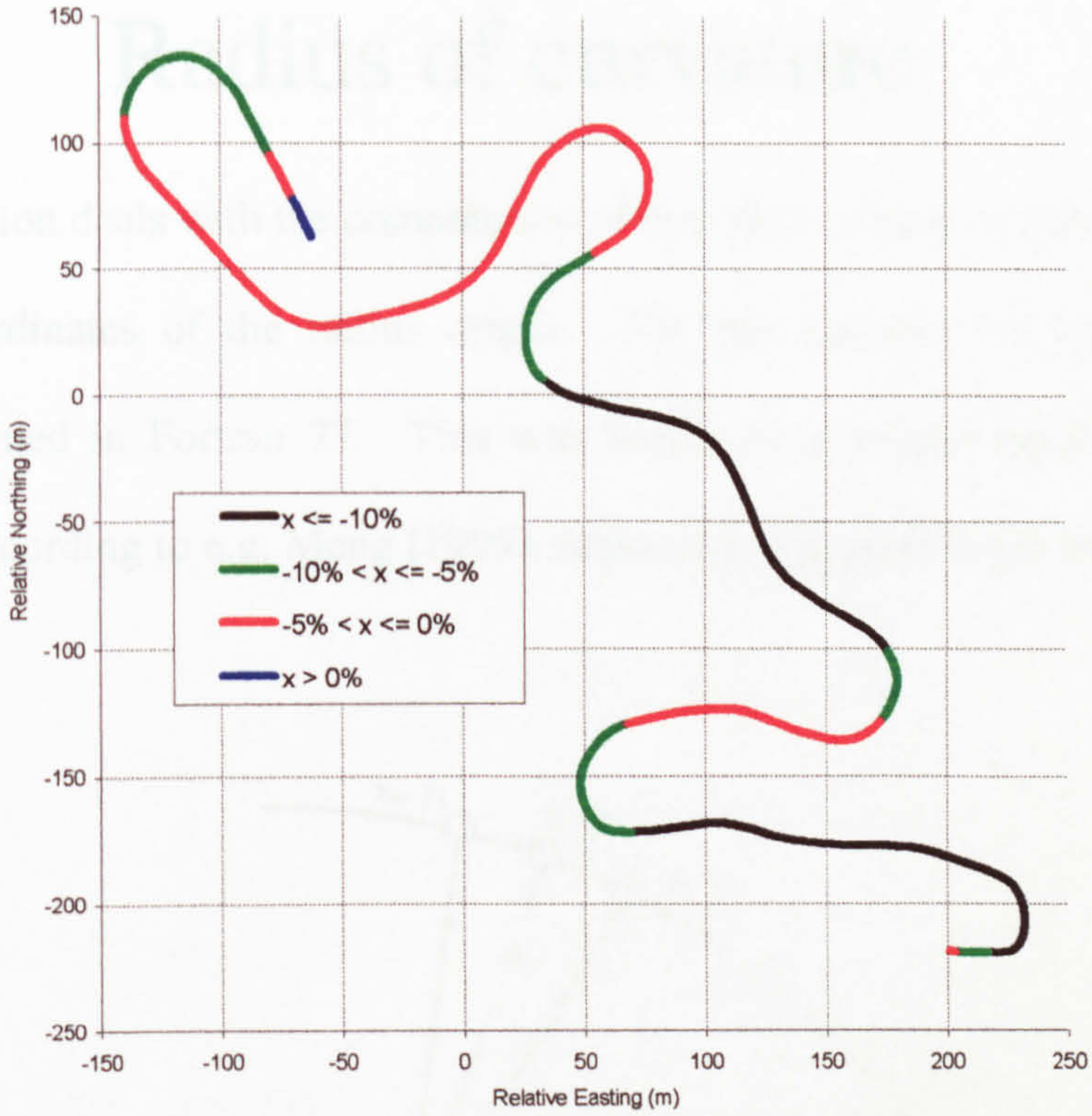

Figure 8.17 Plan trajectory, coarse colour coded by vertical gradient

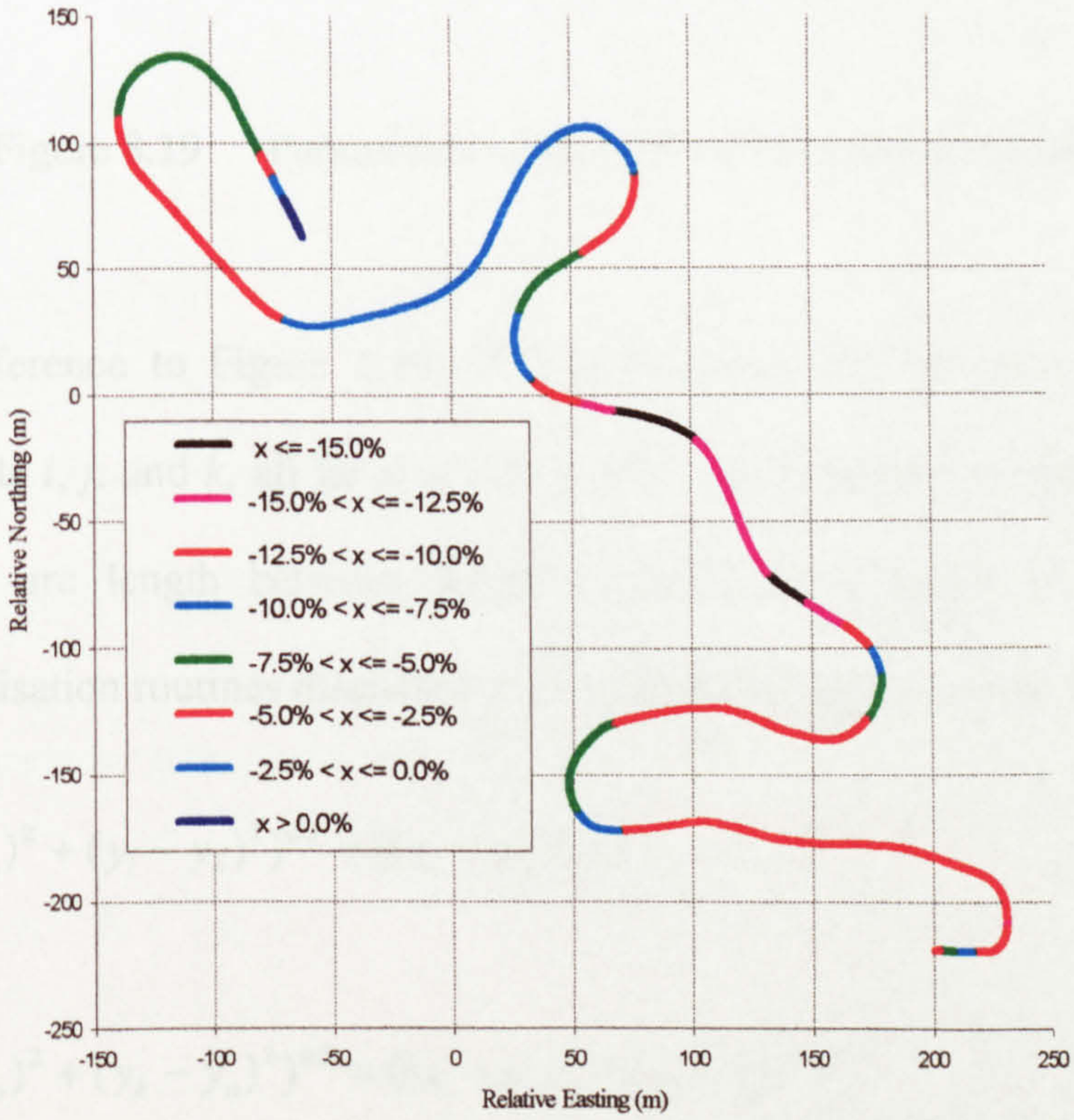

Figure 8.18 Plan trajectory, finely colour coded by vertical gradient

8.5 Radius of curvature

This section deals with the computation of two-dimensional radius of curvature and coordinates of the radius origin. For this purpose an algorithm was programmed in Fortran 77. This was based on a simple equation in three points according to e.g. Meng [1999], expanded in greater detail and illustrated below.

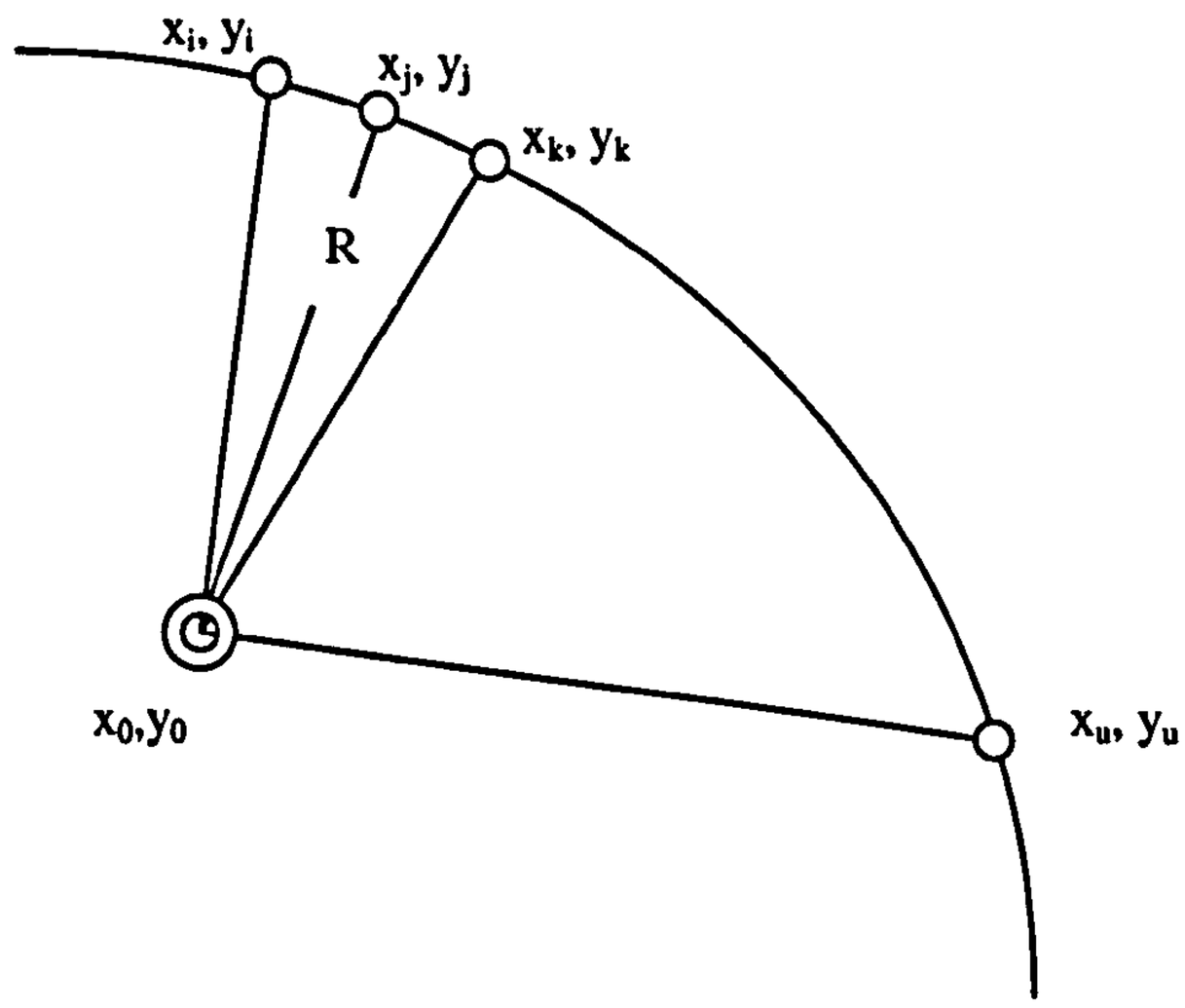

Figure 8.19 Parameters in the radius of curvature calculation

With reference to Figure 8.19, if it is assumed that the three points with subscripts *i*, *j*, and *k*, all lie at a radius of R metres from the origin at (x_o,y_o), and the arc length between points is equal (as a result of the interval standardisation routines discussed above), then two equations can be set up:

$$((x_i - x_o)^2 + (y_i - y_o)^2)^{0.5} = ((x_j - x_o)^2 + (y_j - y_o)^2)^{0.5} \quad (8.1)$$

and

$$((x_k - x_o)^2 + (y_k - y_o)^2)^{0.5} = ((x_i - x_o)^2 + (y_i - y_o)^2)^{0.5} \quad (8.2)$$

Multiplying out and rearranging, gives

$$2x_o x_j - 2x_o x_i + 2y_o y_j - 2y_o y_i = x_j^2 + y_j^2 - x_i^2 - y_i^2 \tag{8.3}$$

and

$$2x_o x_i - 2x_o x_k + 2y_o y_i - 2y_o y_k = x_i^2 + y_i^2 - x_k^2 - y_k^2 \tag{8.4}$$

and with further rearrangement

$$(x_j - x_i)x_o + (y_j - y_i)y_o = 0.5(x_j^2 + y_j^2 - x_i^2 - y_i^2) \tag{8.5}$$

and

$$(x_i - x_k)x_o + (y_i - y_k)y_o = 0.5(x_i^2 + y_i^2 - x_k^2 - y_k^2) \tag{8.6}$$

Which in matrix format is

$$\begin{bmatrix} a_1 & b_1 \\ a_2 & b_2 \end{bmatrix}\begin{bmatrix} x_o \\ y_o \end{bmatrix} = \begin{bmatrix} c_1 \\ c_2 \end{bmatrix} \tag{8.7}$$

where

$$a_1 = (x_j - x_i)$$

$$a_2 = (y_j - y_i)$$

$$b_1 = (x_i - x_k)$$

$$b_2 = (y_i - y_k)$$

$$c_1 = 0.5(x_j^2 + y_j^2 - x_i^2 - y_i^2)$$

$$c_2 = 0.5(x_i^2 + y_i^2 - x_k^2 - y_k^2)$$

The solution for the approximate radius of curvature origin coordinates is then

$$\begin{bmatrix} x_o \\ y_o \end{bmatrix} = \begin{bmatrix} a_1 & b_1 \\ a_2 & b_2 \end{bmatrix}^{-1}\begin{bmatrix} c_1 \\ c_2 \end{bmatrix} \tag{8.8}$$

and for the approximate radius of curvature, R, from Figure 8.19, is

$$R = ((x_i - x_o)^2 + (y_i - y_o)^2)^{0.5} \tag{8.9}$$

Obviously, if the three points are irregularly spaced, for example *i*, *j* and *u*, in Figure 8.19, then the assumption that each point is at a radius *R* from (x_0, y_0), breaks down, and erroneous results occur. Window length is also a major determinant in the accuracy of derived radius of curvature and coordinates. Too short a window causes numeric instability as the three points approach a straight line, too long a window means that the assumption that the three points are on a curve of constant radius breaks down, other than in the event that the points do in fact lie on the same circle.

Radius of curvature time series for window lengths of 2.5, 5, and 10 metres, are given in Figures 8.20 to 8.22. Off the scale readings are heading towards infinity indicating straight segments, whilst values of about 50 metres or less indicate curved segments. The choice of window length is an iterative process, too short and the interval will approach a fictitious straight line, and too long a window again eliminates detail. The time series demonstrate that long windows should be used to identify the major trajectory components, and short windows to identify onset and departure from such features. For instance around distance marker 660, the trajectory exits from a curve and enters a straight. The fact that the next component is a straight may be identified from Figure 8.22, and the onset of the straight may be critically assessed from Figure 8.20.

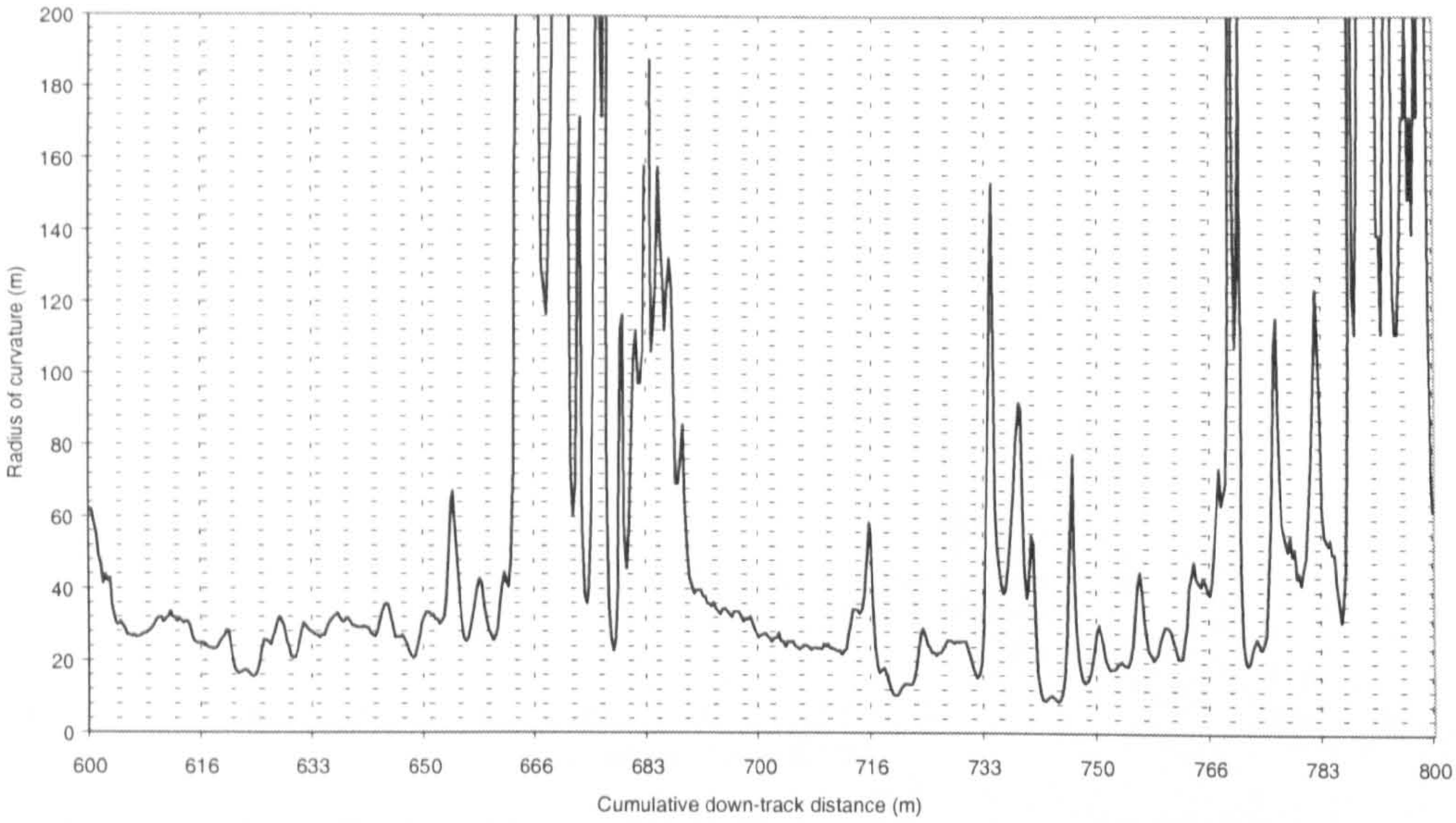

Figure 8.20 Radius of curvature using a 2.5 metre window length

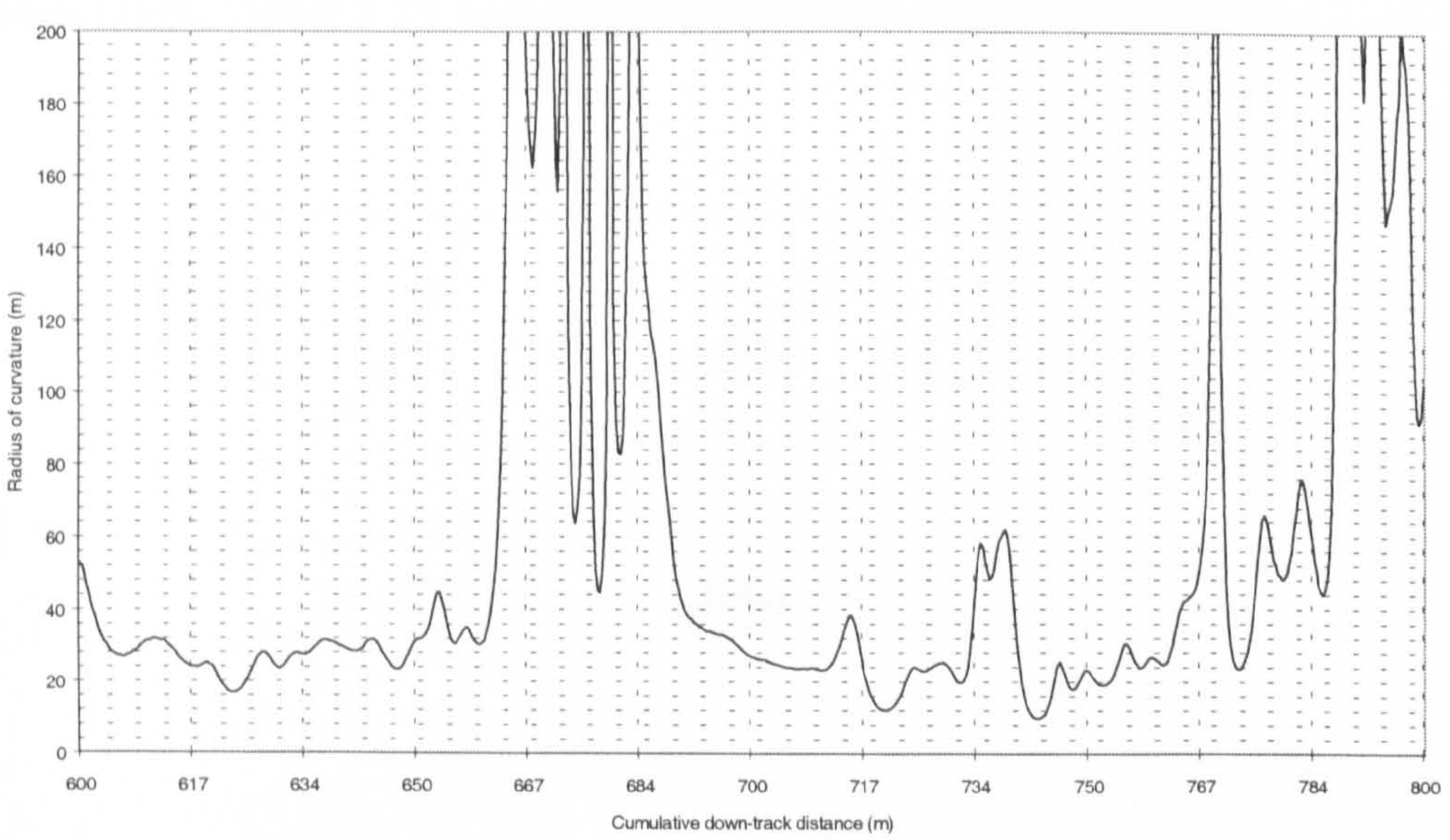

Figure 8.21 Radius of curvature using a 5 metre window length

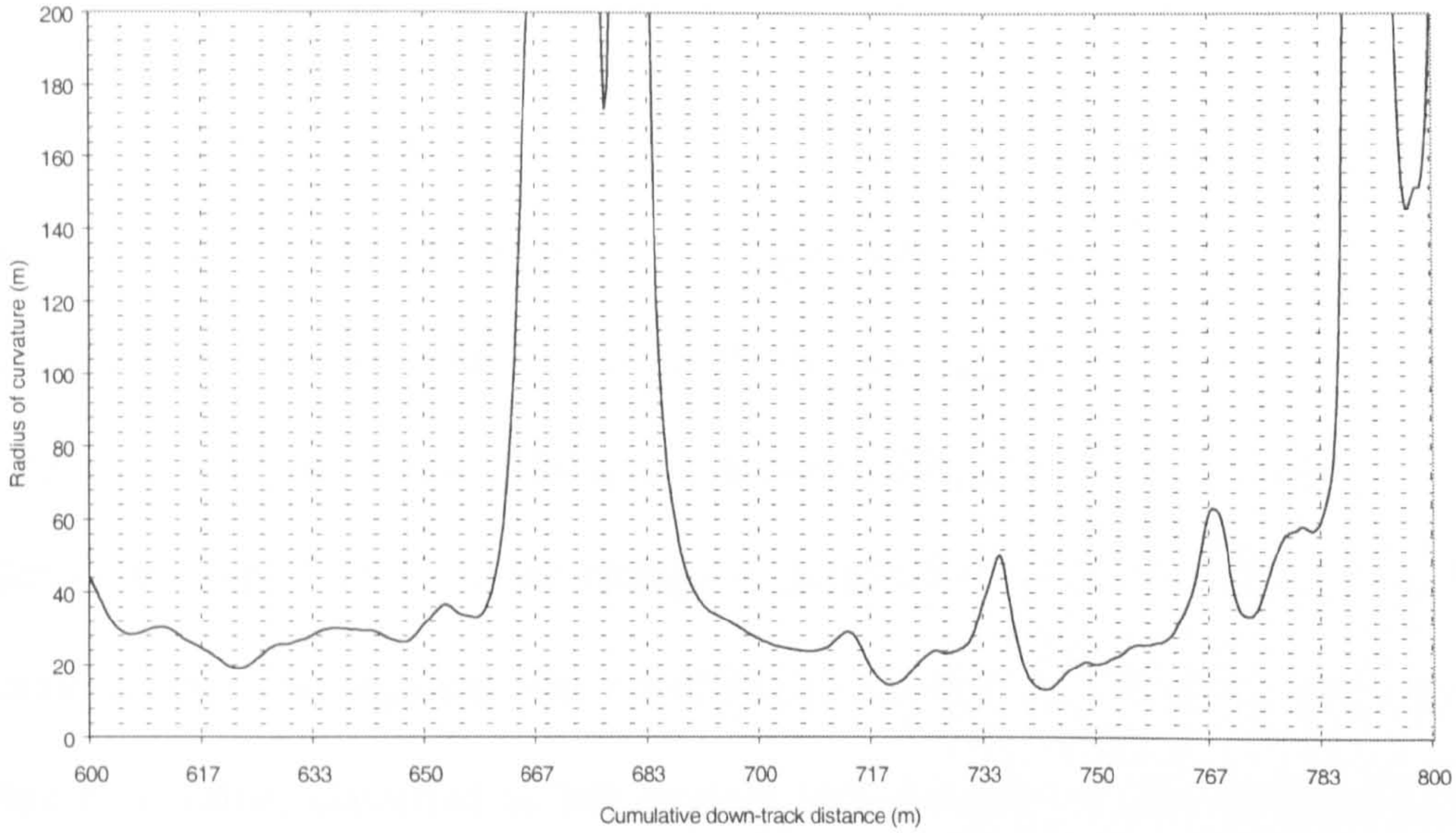

Figure 8.22 Radius of curvature using a 10 metre window length

Comparison of computed radius of curvature compared well with graphical assessment, Figure 8.23, agreeing to within a few tens of centimetres.

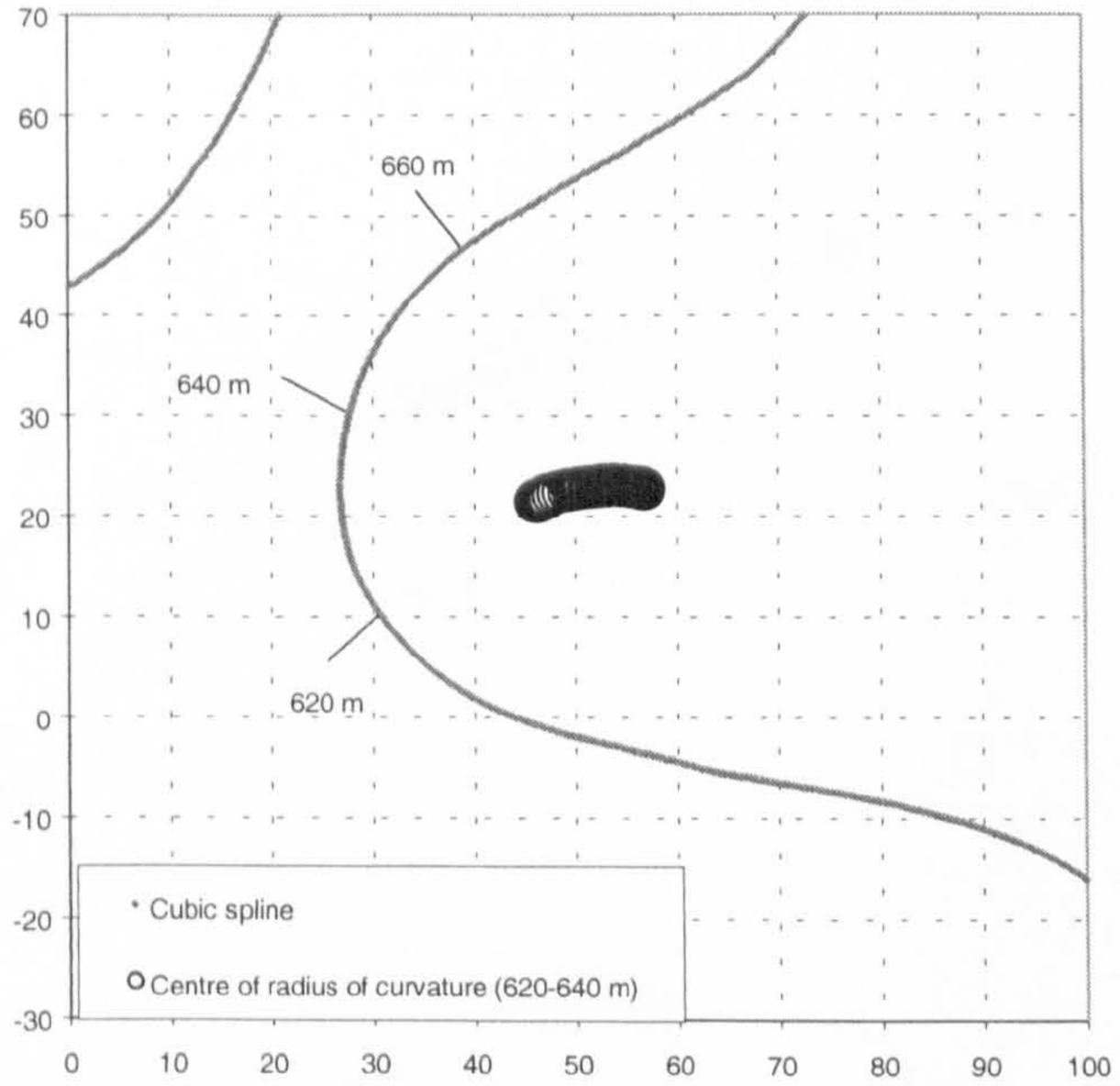

Figure 8.23 Radius of curvature detail – Curve 15

8.6 Directional classification

The need for trajectory classification according to a left / right / straight flag was addressed by the development of algorithms in Fortran 77. These were designed to monitor change in localised plan gradient, as follows with reference to Figure 8.23a. The gradient from point 2 to 3 was compared with that from point 1 to 2. If the change in gradient was less than the threshold value α, then the segment was classified as straight, and if greater than the threshold value, classified as left or right turn according to the mathematical sign.

The value of α was controlled by a percentage change in gradient or angular change in direction whichever was the greater.

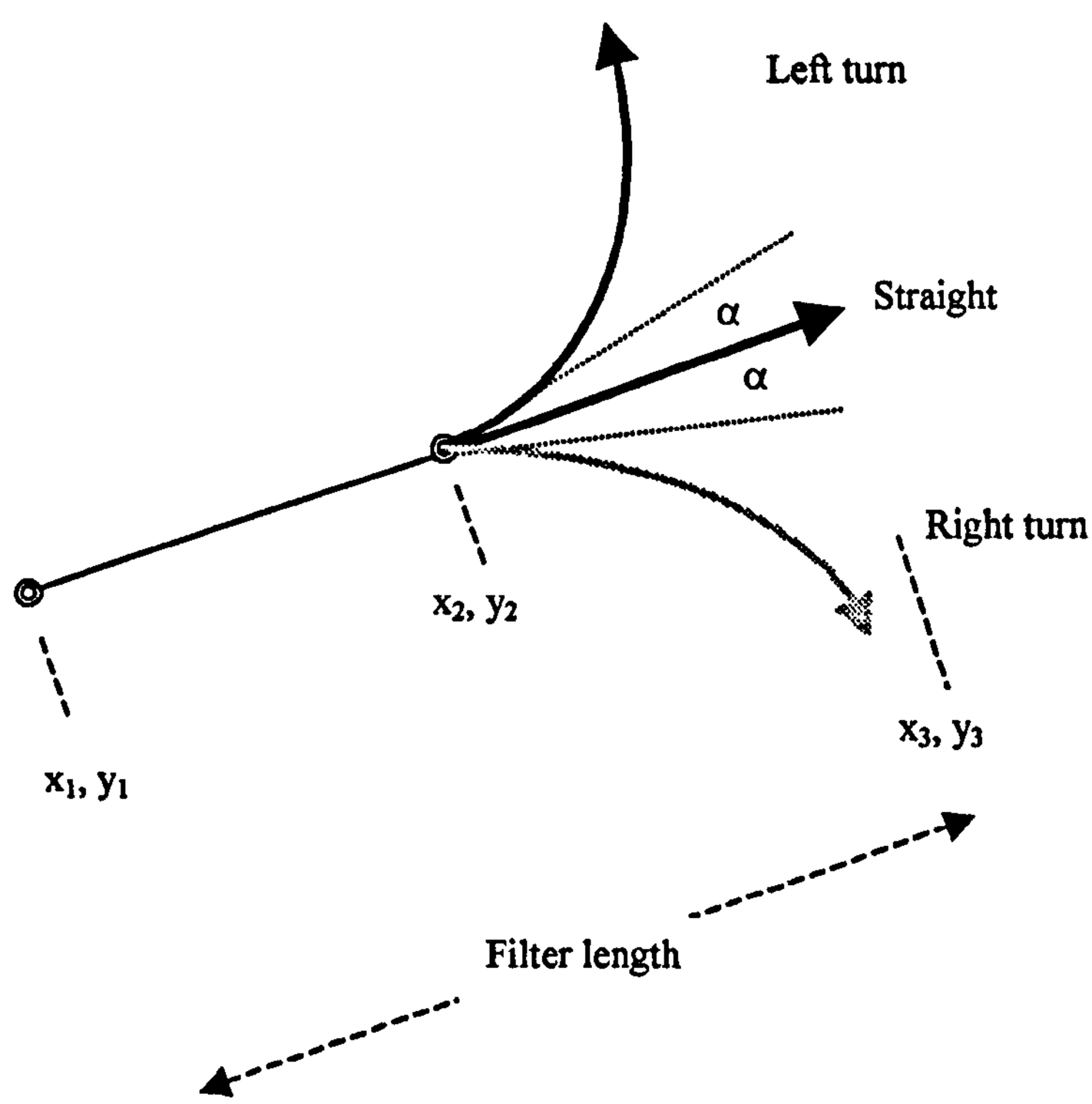

Figure 8.23a Segmentation filter

8.6 Directional classification

The need for trajectory classification according to a left / right / straight flag was addressed by the development of algorithms in Fortran 77. These were designed to monitor change in localised plan gradient, as follows with reference to Figure 8.23a. The gradient from point 2 to 3 was compared with that from point 1 to 2. If the change in gradient was less than the threshold value α, then the segment was classified as straight, and if greater than the threshold value, classified as left or right turn according to the mathematical sign.

The value of α was controlled by a percentage change in gradient or angular change in direction whichever was the greater.

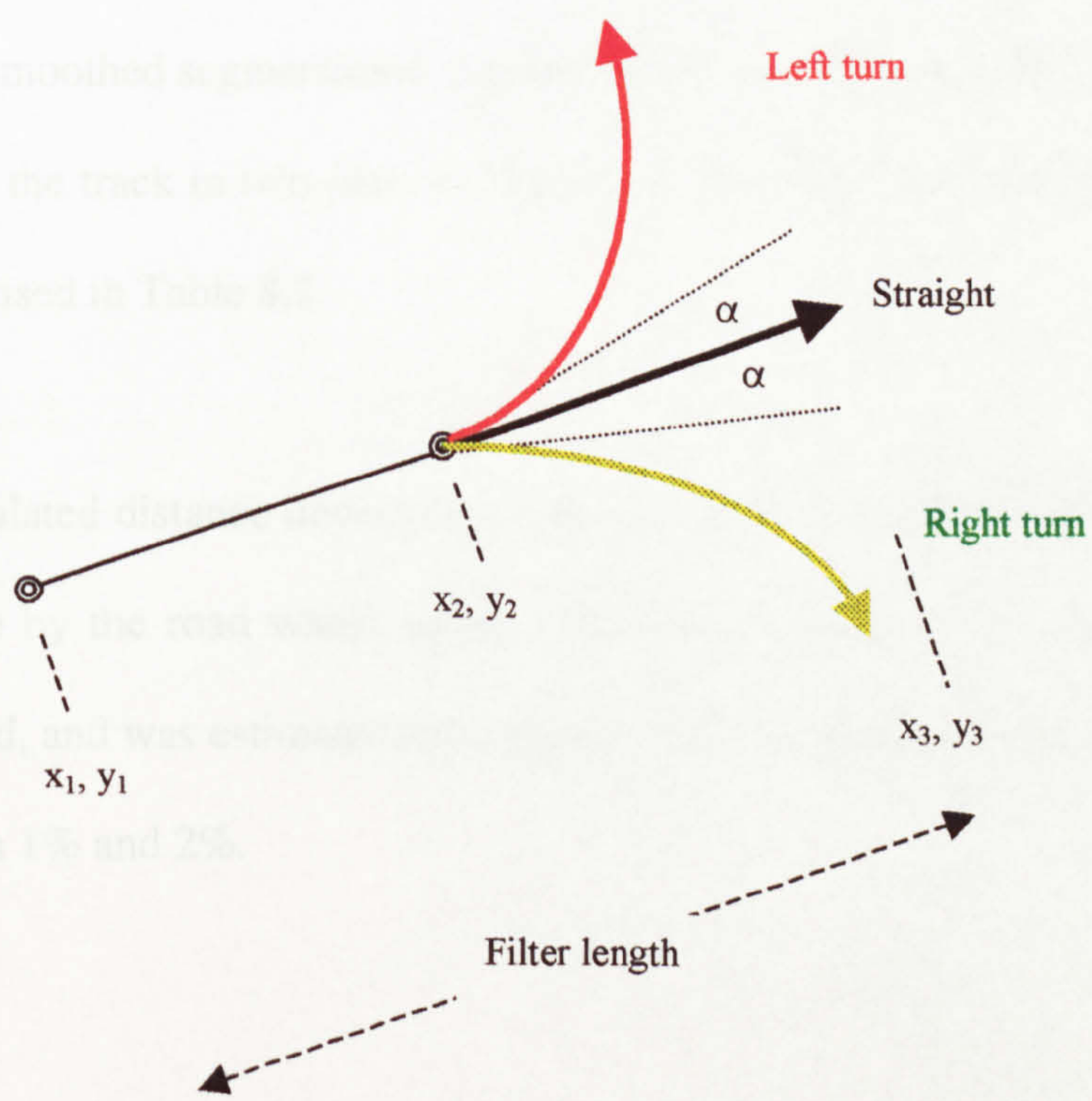

Figure 8.23a Segmentation filter

Optimum results were gained from the segmentation module using a total filter length of 10 metres and percentage gate of 10 percent. The term optimum is used in the sense of level of sensitivity of the data to the filter. If the filter is too short and narrow then segmentation is increased by a factor of two or three, providing a level of detail that was not required by the end user.

Comparing results in Figure 8.24 with Figure 8.25, results show that segment classification requires the application of a low level smoothing filter to eliminate short term directional sensitivity. These periods were typically a few samples or a metre or so in length, and were most likely caused by deviation of the physical track of the antenna from a track consistent with the track walls. Filter efficiency can be assessed by inspection of the trajectory at a large scale, and a priori knowledge of convolution details. Detail comparison of coarse versus smoothed segmentation is given in Figures 8.26 to 8.27a, and a zoomed view of the track in two parts in Figures 8.28 and 8.29. Smoothed results are summarised in Table 8.2.

Accumulated distance down-track was measured not only by satellite methods but also by the road wheel meter. Relative slippage of the road wheel was expected, and was estimated by comparison at the entry point to curve 18 to be between 1% and 2%.

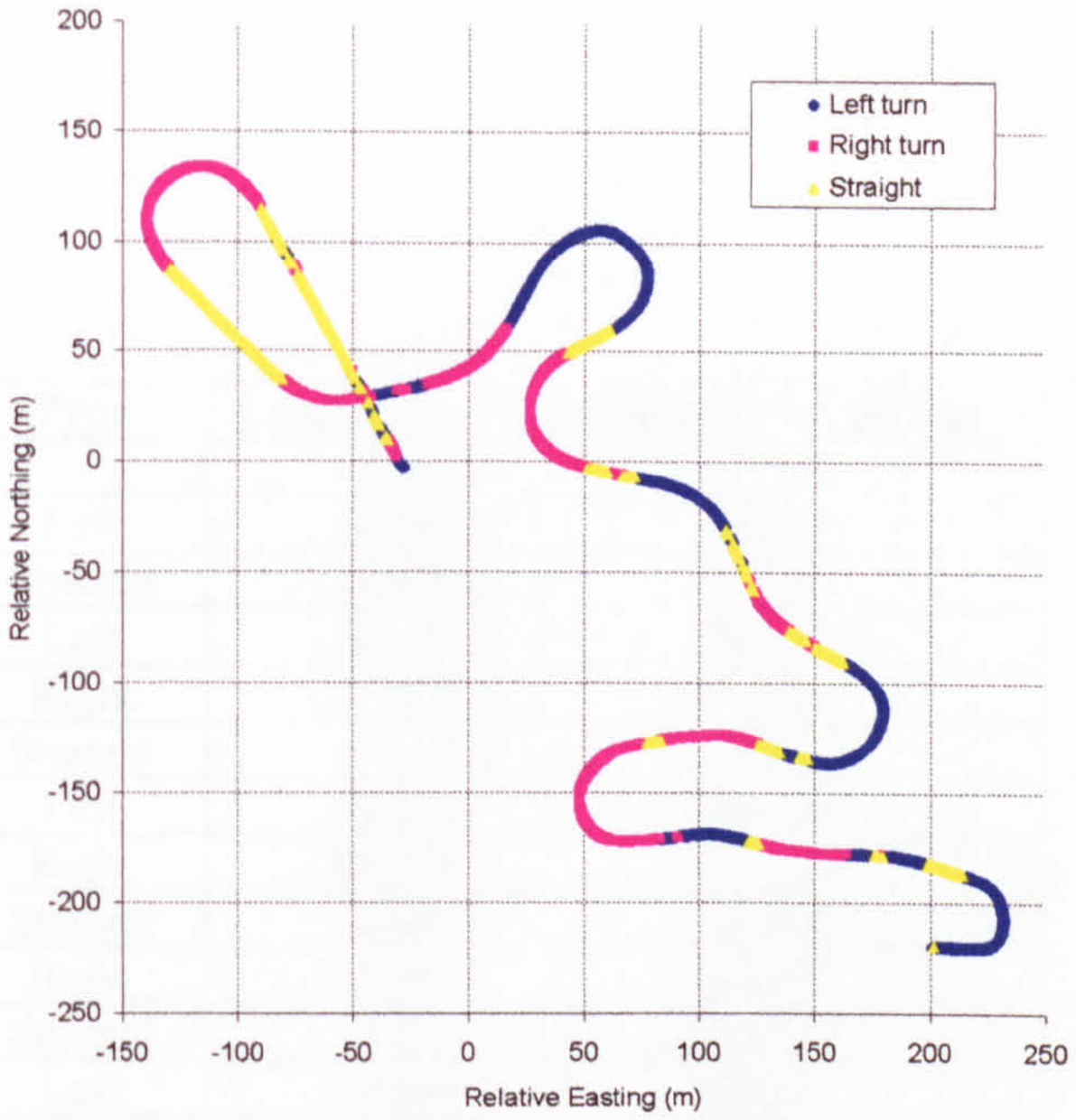

Figure 8.24

Coarse segmentation

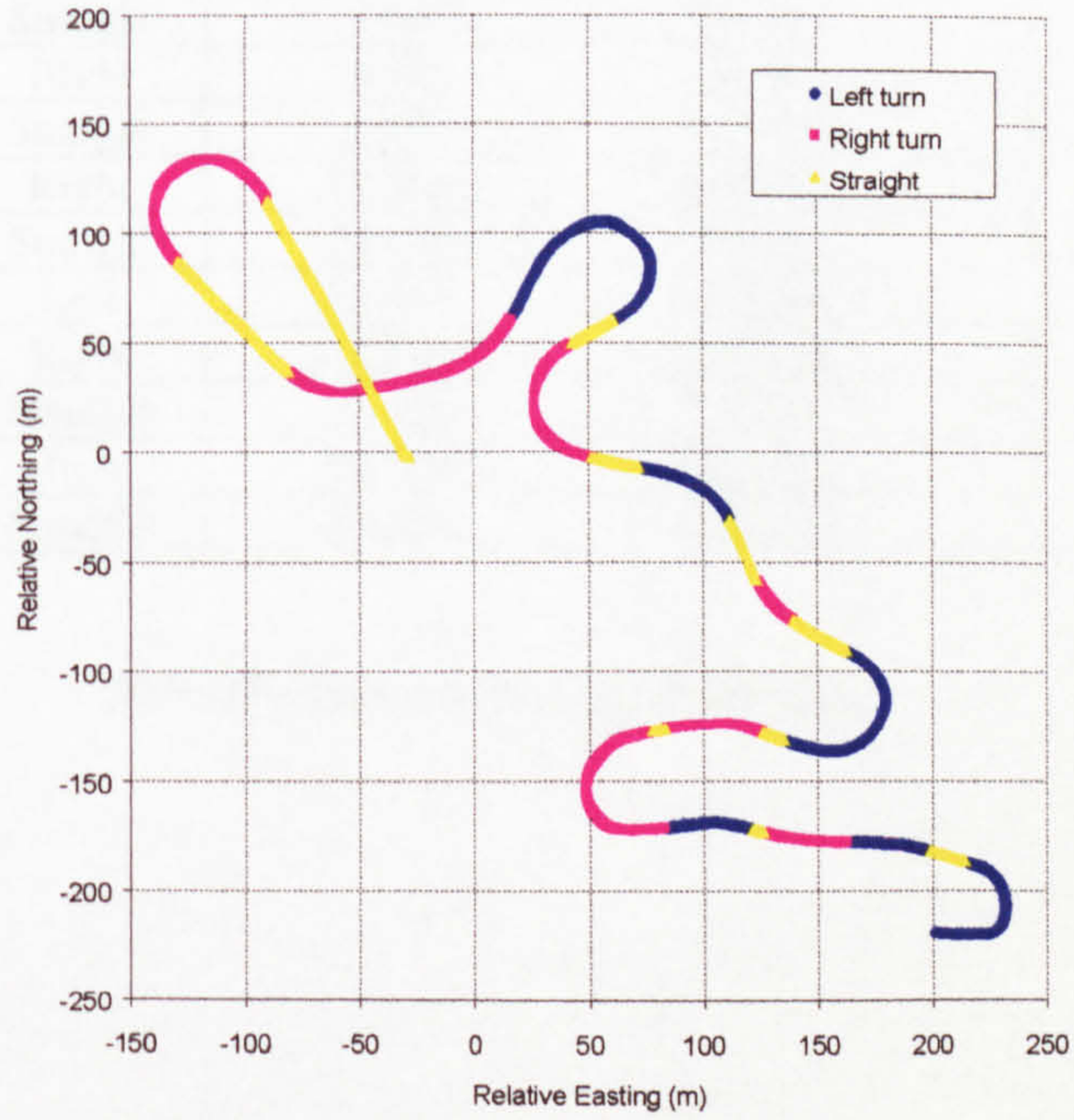

Figure 8.25

Smoothed segmentation

Segment No	Type	Length (m)	Cumulative length (m)
Filter ramp	-	5.167	5.167
1	Left	67.994	73.161
2	Straight	17.000	90.161
3	Left	36.000	126.159
4	Right	37.000	163.159
5	Straight	5.333	168.492
6	Left	38.332	206.824
7	Right	88.324	295.148
8	Straight	6.666	301.814
9	Right	42.999	344.812
10	Straight	10.333	355.145
11	Left	7.666	362.811
12	Straight	5.000	367.810
13	Left	73.990	441.800
14	Straight	27.999	469.799
15	Right	23.665	493.464
16	Straight	30.999	524.462
17	Left	47.332	571.795
18	Straight	5.667	577.462
19	Right	6.999	584.461
20	Straight	8.999	593.460
21	Right	71.325	664.785
22	Straight	21.666	686.451
23	Left	125.648	812.099
24	Right	110.666	922.765
25	Straight	70.336	993.101
26	Right	95.989	1089.090
27	Straight	133.036	1222.126

Table 8.2 Smoothed segmentation summary

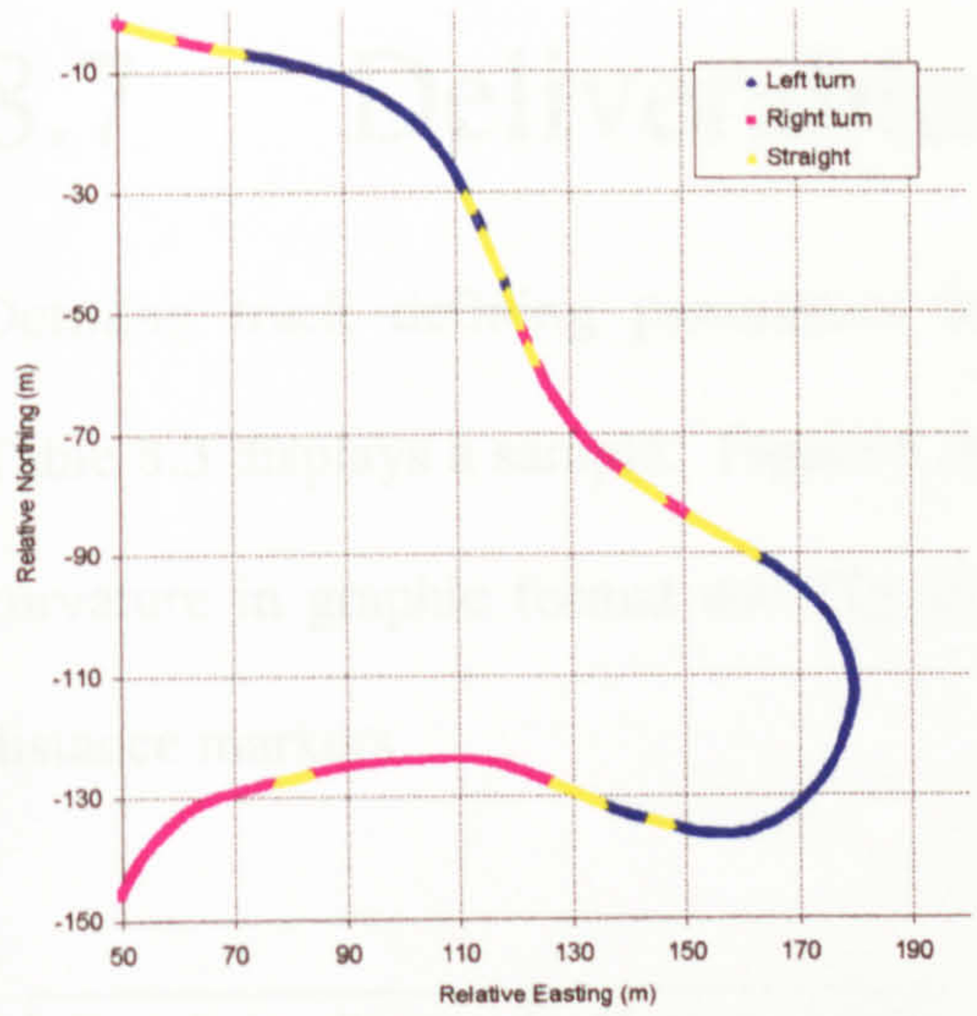

Figure 8.26 Coarse detail (I)

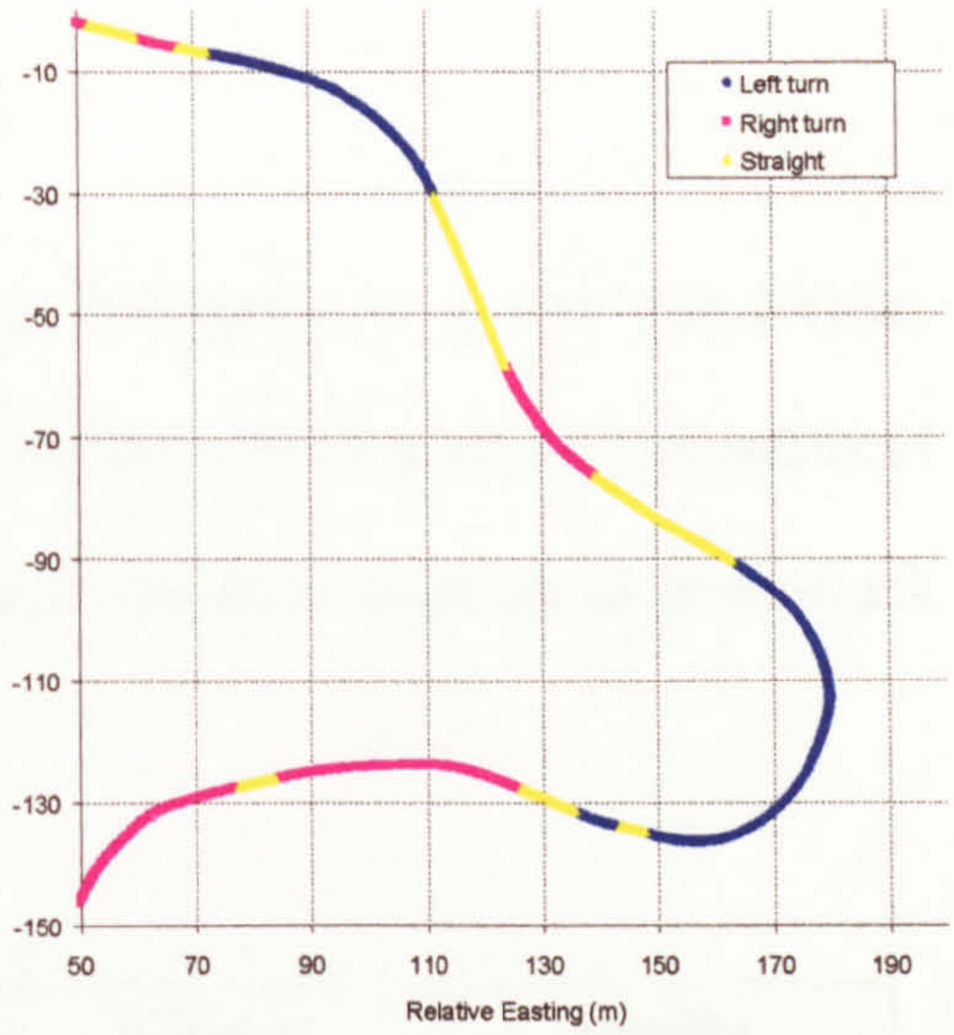

Figure 8.26a Smoothed detail (I)

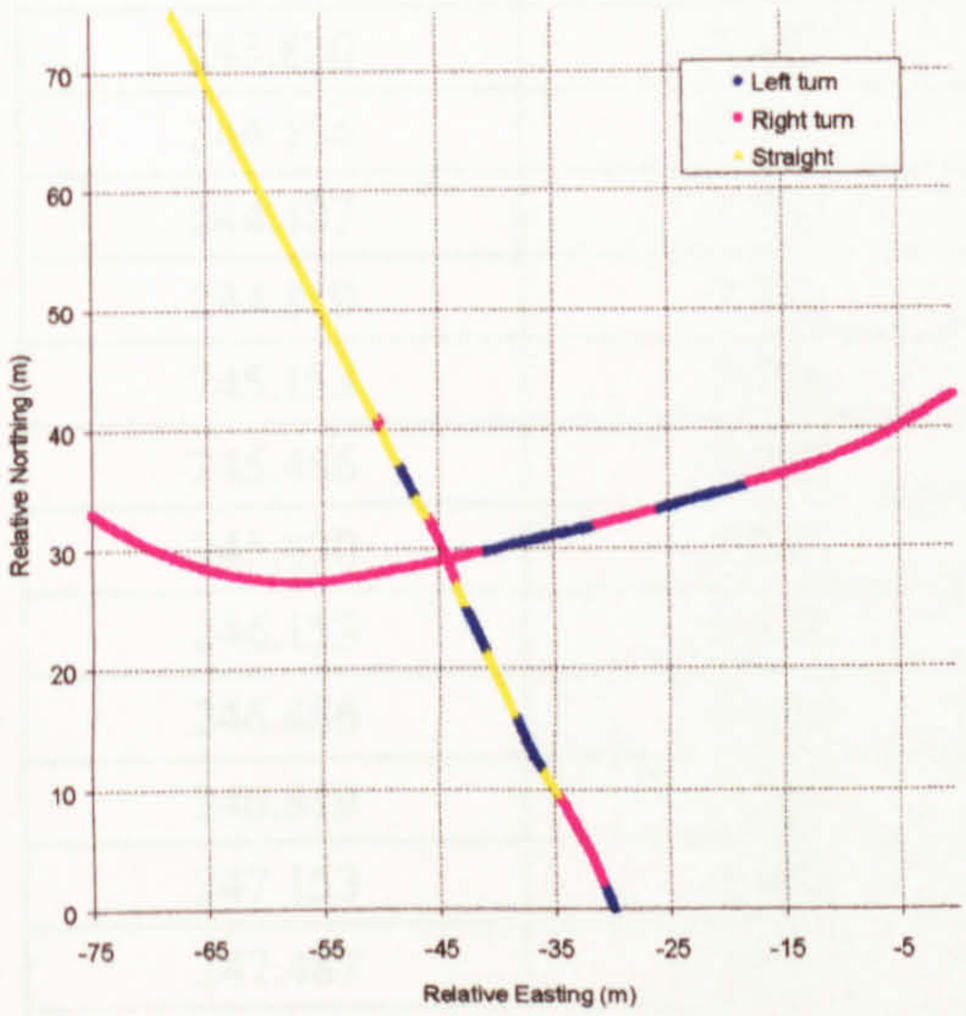

Figure 8.27 Coarse detail (II)

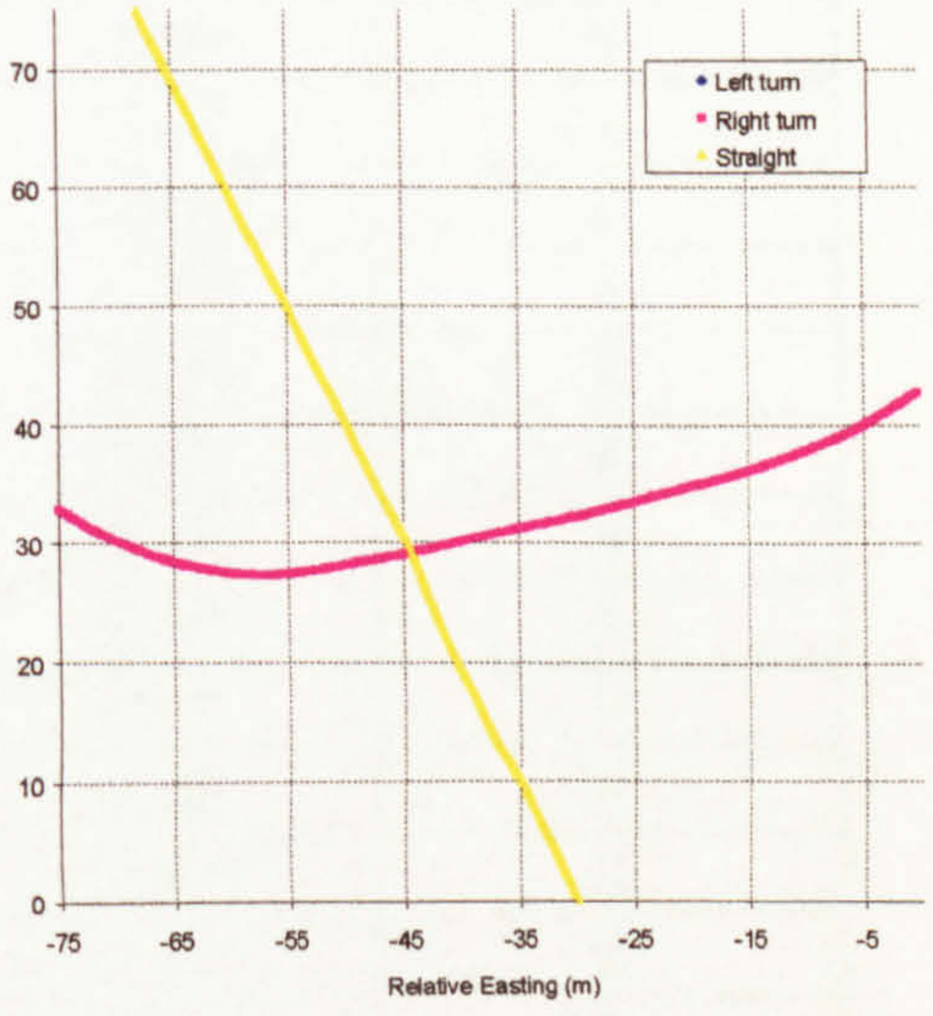

Figure 8.27a Smoothed detail (II)

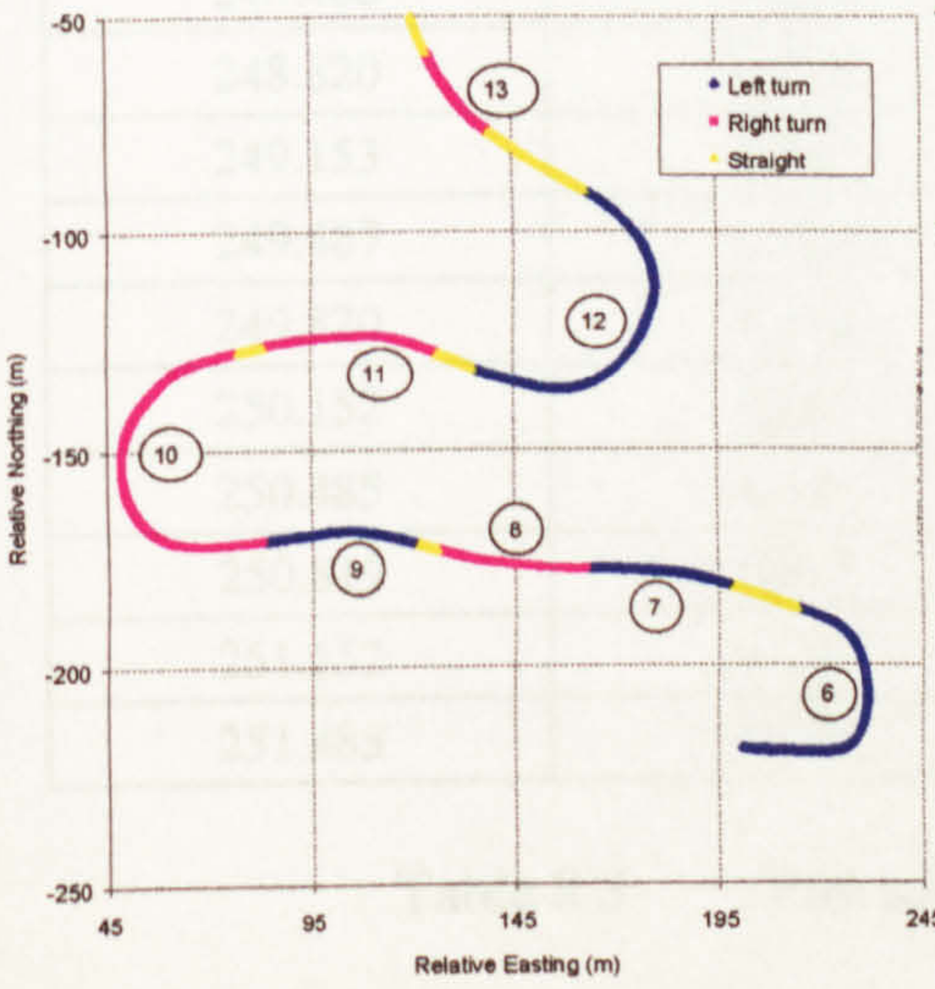

Figure 8.28 Smoothed north end

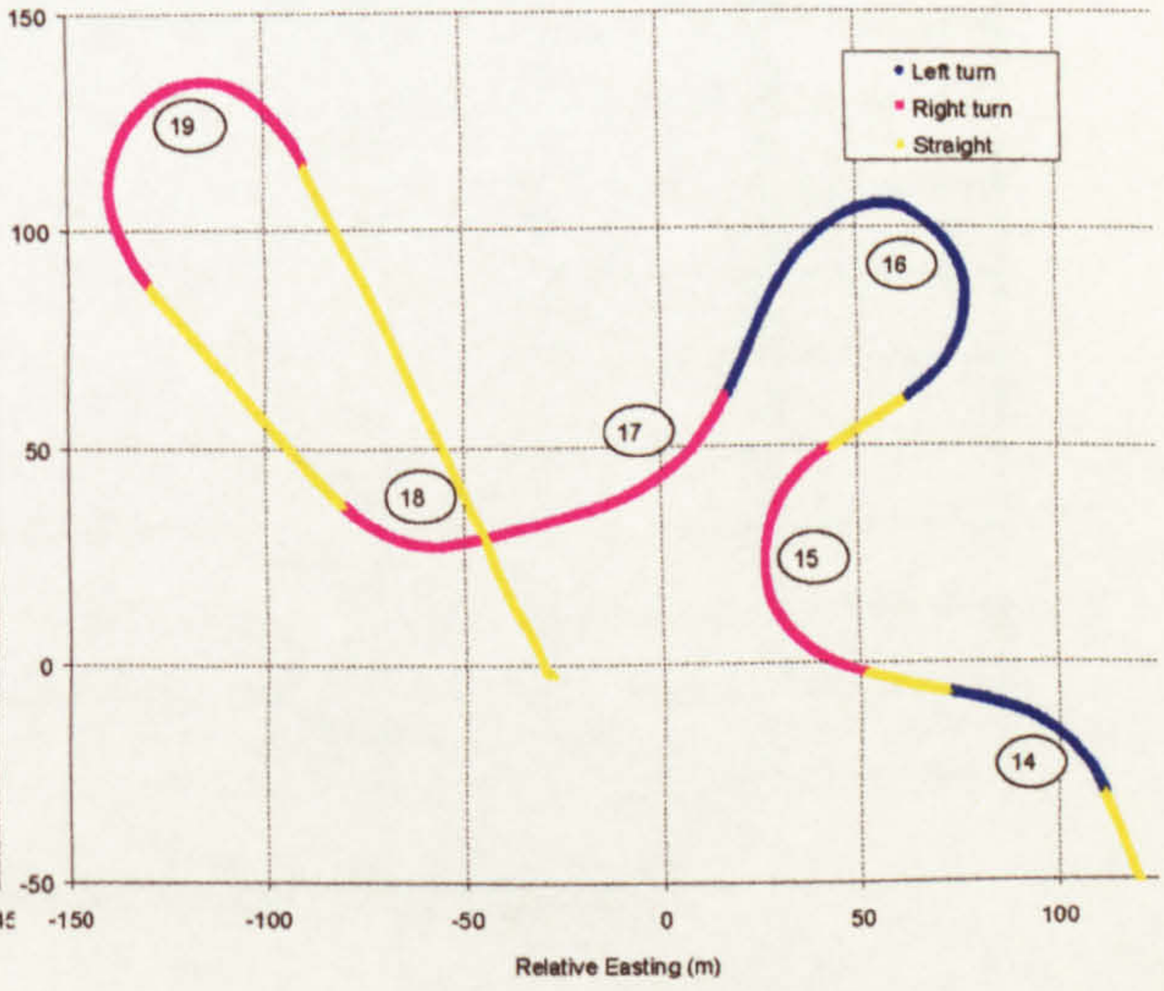

Figure 8.29 Smoothed south end

8.7 Deliverables

Defining track defining parameters were delivered in a text file format, Table 8.3 displays a sample. Figure 8.30 shows vertical gradient and radius of curvature in graphic format and Figure 8.31 the final position of down-track distance markers.

Cumulative distance down-track (m)	Vertical gradient (tan) %	Radius of curvature (m)	Heading Left/Right/Straight
243.154	-7.415	17.972	R
243.487	-7.388	17.637	R
243.820	-7.362	17.355	R
244.154	-7.335	17.141	R
244.487	-7.309	17.051	R
244.819	-7.282	17.070	R
245.153	-7.256	17.242	R
245.486	-7.229	17.560	R
245.820	-7.203	18.076	R
246.153	-7.176	18.708	R
246.486	-7.150	19.703	R
246.819	-7.124	20.895	R
247.153	-7.099	22.230	R
247.487	-7.073	23.629	R
247.820	-7.048	24.855	R
248.153	-7.022	25.421	R
248.486	-6.996	25.250	R
248.820	-6.971	24.557	R
249.153	-6.945	23.451	R
249.487	-6.920	22.482	R
249.820	-6.894	21.778	R
250.152	-6.869	21.289	R
250.485	-6.843	21.231	R
250.819	-6.817	21.705	R
251.152	-6.792	22.180	R
251.485	-6.766	22.858	R

Table 8.3 Part data set supplied to end-user

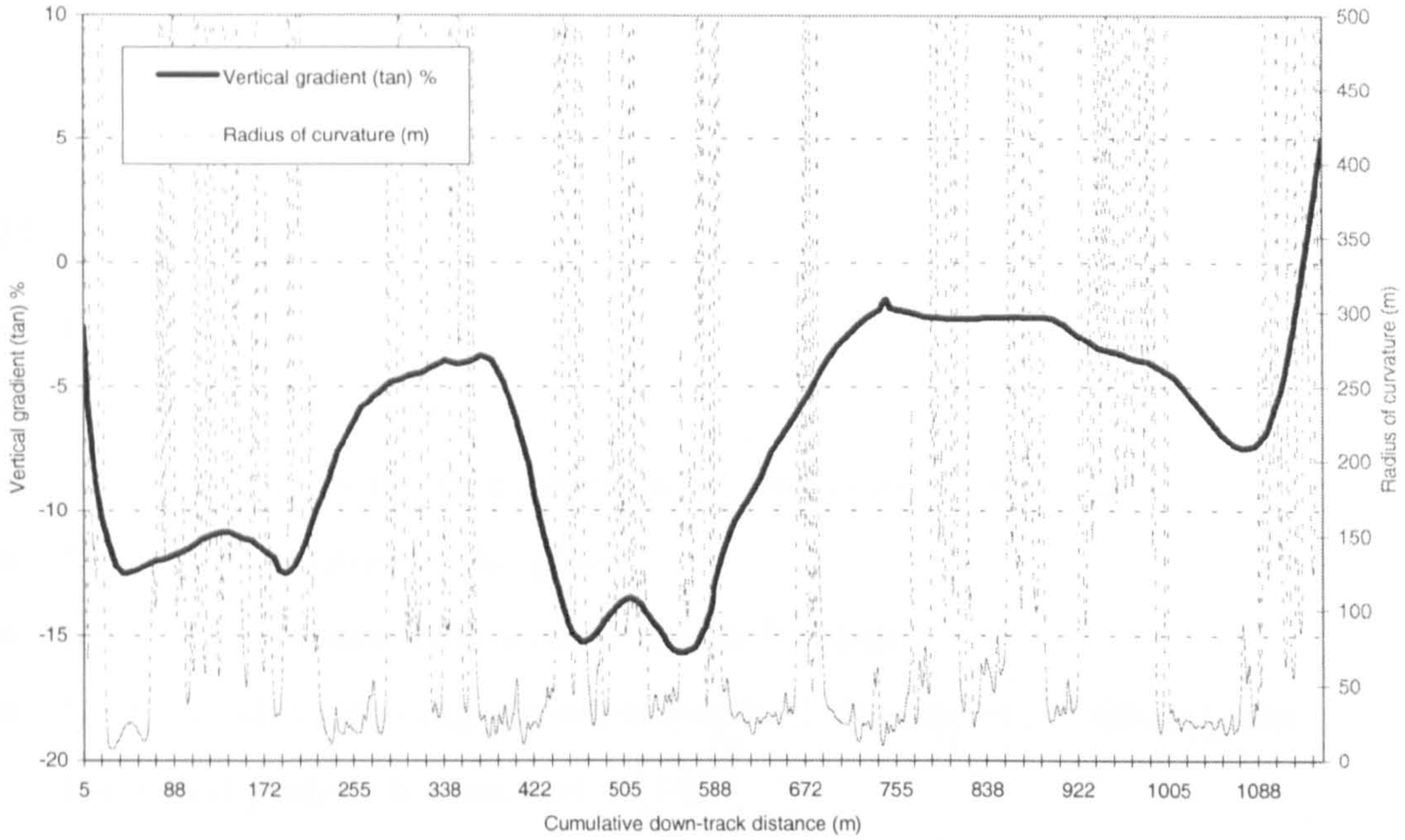

Figure 8.30 Vertical gradient and radius of curvature deliverables

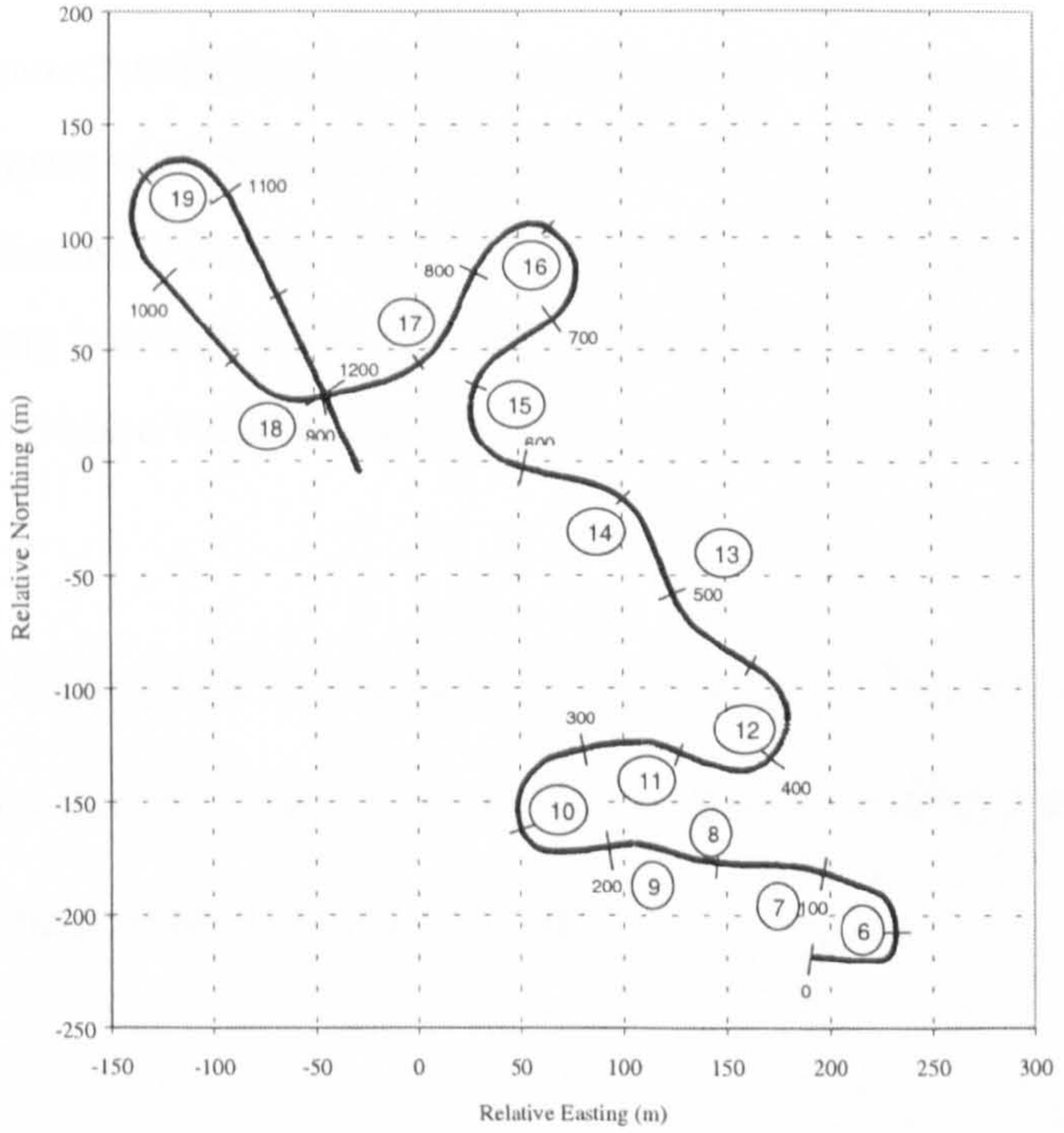

Figure 8.31 Curve numbering and final down-track distance markers

To summarise, the following processes were instrumental in arriving at these final products:

Plan coordinates

- Hand edit.
- 7 point moving average.
- 0.02 metre interpolation, exported at a 2 metre down-track interval.
- 5 point interpolating cubic spline.
- Radius of curvature, with window length 5 metres.
- Heading indicator, using a window length of 10 metres (± 5 metres), and horizontal gradient tolerance of ± 10%.

Vertical coordinate

- Hand edit.
- Gradient computed using hand edit plan and vertical coordinate.
- 6th order polynomial fit applied to gradient profile, using 50% overlapping segments in Microsoft Excel. Final values extracted at a large scale at intervals ranging between 2 and 10 metres depending on convolution, then densified to provide a value at one-third metre down-track interval.

These data could be supplied at any down-track interval, using some multiple of the fundamental results interval of one-third metre. Additionally, (x, y) coordinates could be provided for each record.

It is well known that GPS alone can perform poorly under conditions of severely restricted skyview. This was exemplified at the bob sled track when attempting to position a road wheel mounted antenna. Hybrid on the other hand, with 14 satellites supporting a core GPS constellation can be far more successful. Given the restricted antenna height, then Hybrid results were remarkable, providing the end-user with *very useful information* (even though the backup vehicle was used) where none were available before. However if the pointing of the antenna vertical axis is off vertical and changeable, then the skyview becomes so limited that even Hybrid mode fails, as in the case of attempted sled positioning. In that case data from other positioning sensors types are required, for example accelerometer technology, and gyros were suggested.

Whilst accelerometers are obviously not affected by skyview limitations and multipath that trouble satellite positioning, and in the short term are more accurate than satellite positioning, they do drift rapidly. This is where the integration of the two comes in, an accelerometer can be used for short term high accuracy location, and GPS to control the tendency for accelerometer drift.

Nevertheless, the information provided by the road wheel was instrumental in gaining a better understanding of track geometry, and is was worthy of note that in the first World Championship venue in the 1999/2000 season, at Calgary, Canada, that sliders using the BAE research funded sleds took gold,

0.5, 1, or 2 metre output was given. The final down-track interval was one third of a metre, giving a file size of about 4500 records. Figures 8.6 to 8.10 illustrate the non-invasive nature of the automated filters, demonstrating very little change between the hand edited version and intermediate or final product.

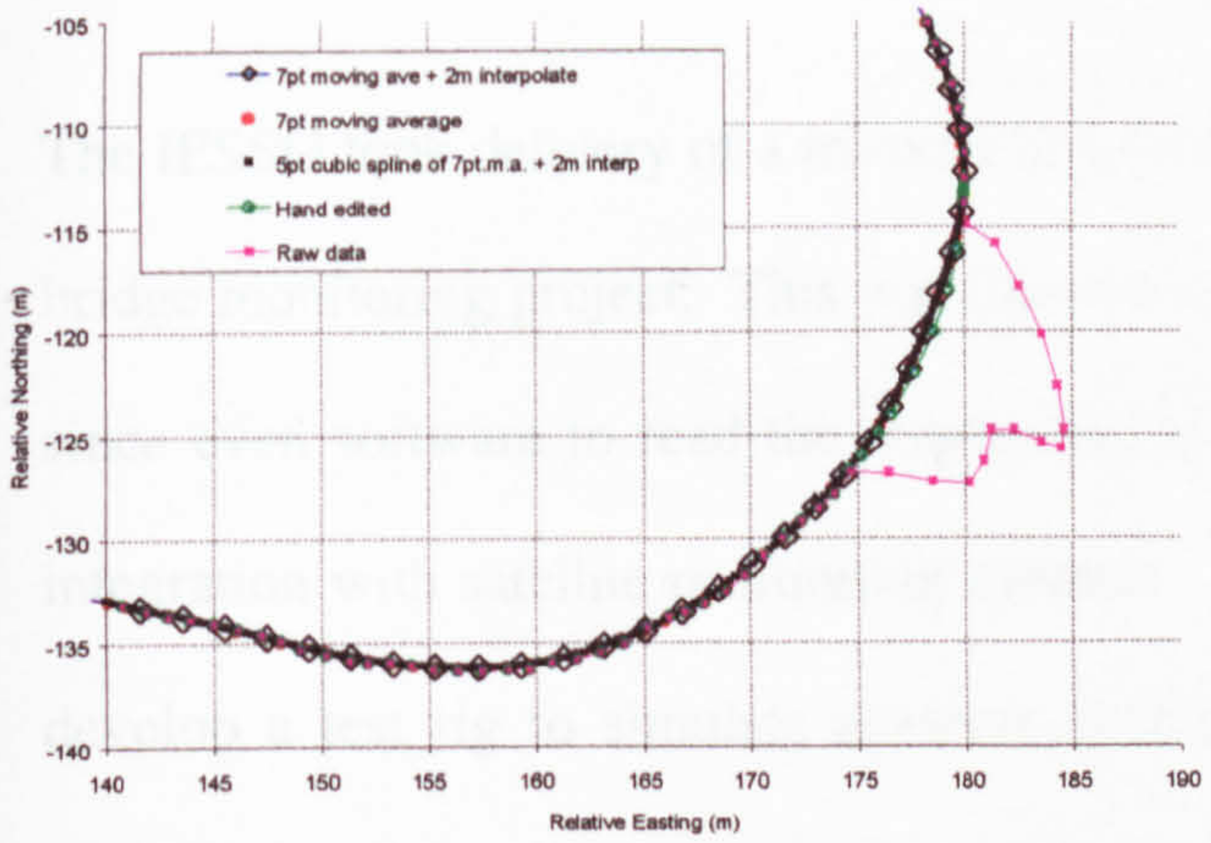

Figure 8.7

Comparison of data treatments (2)

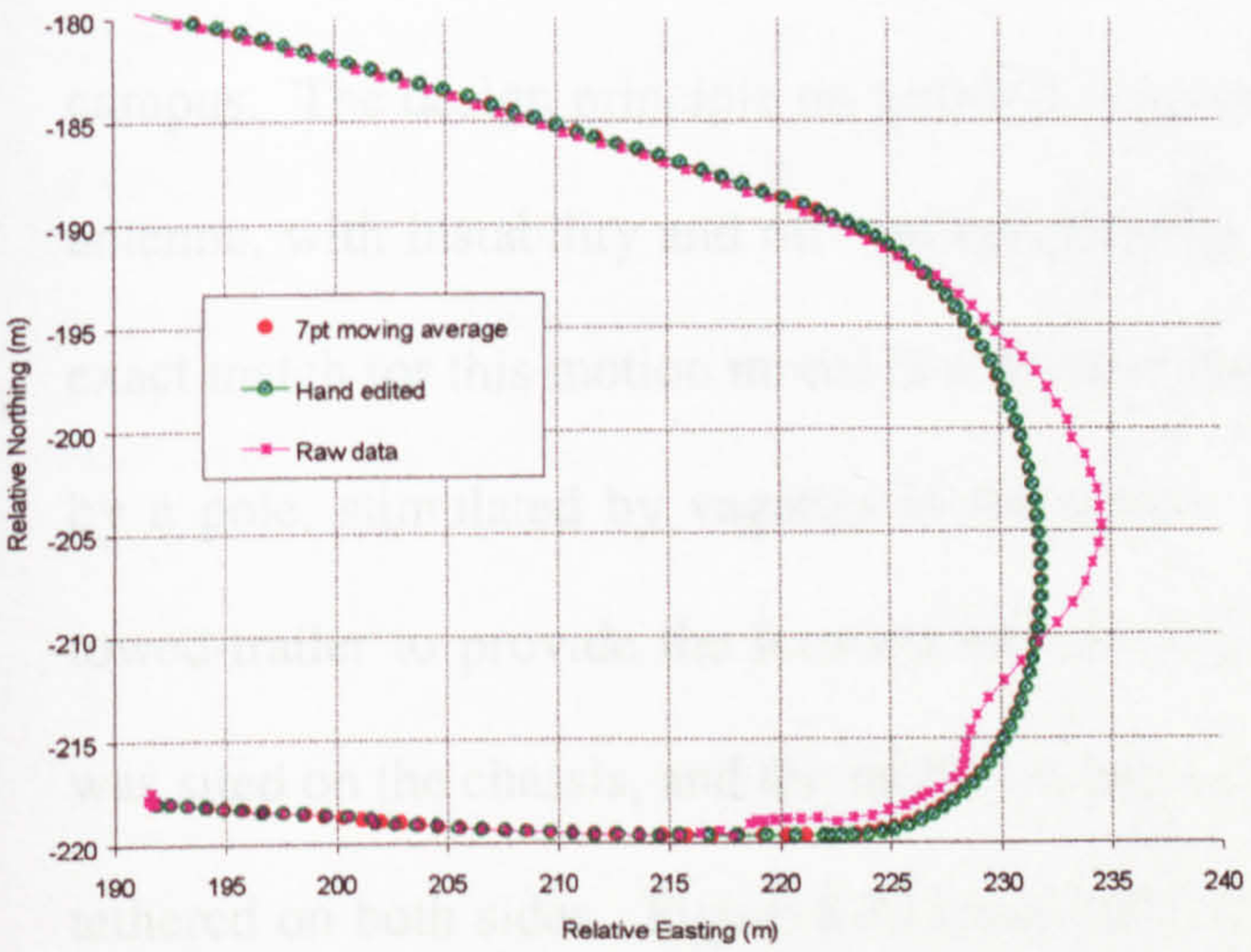

Figure 8.8

Comparison of data treatments (3)

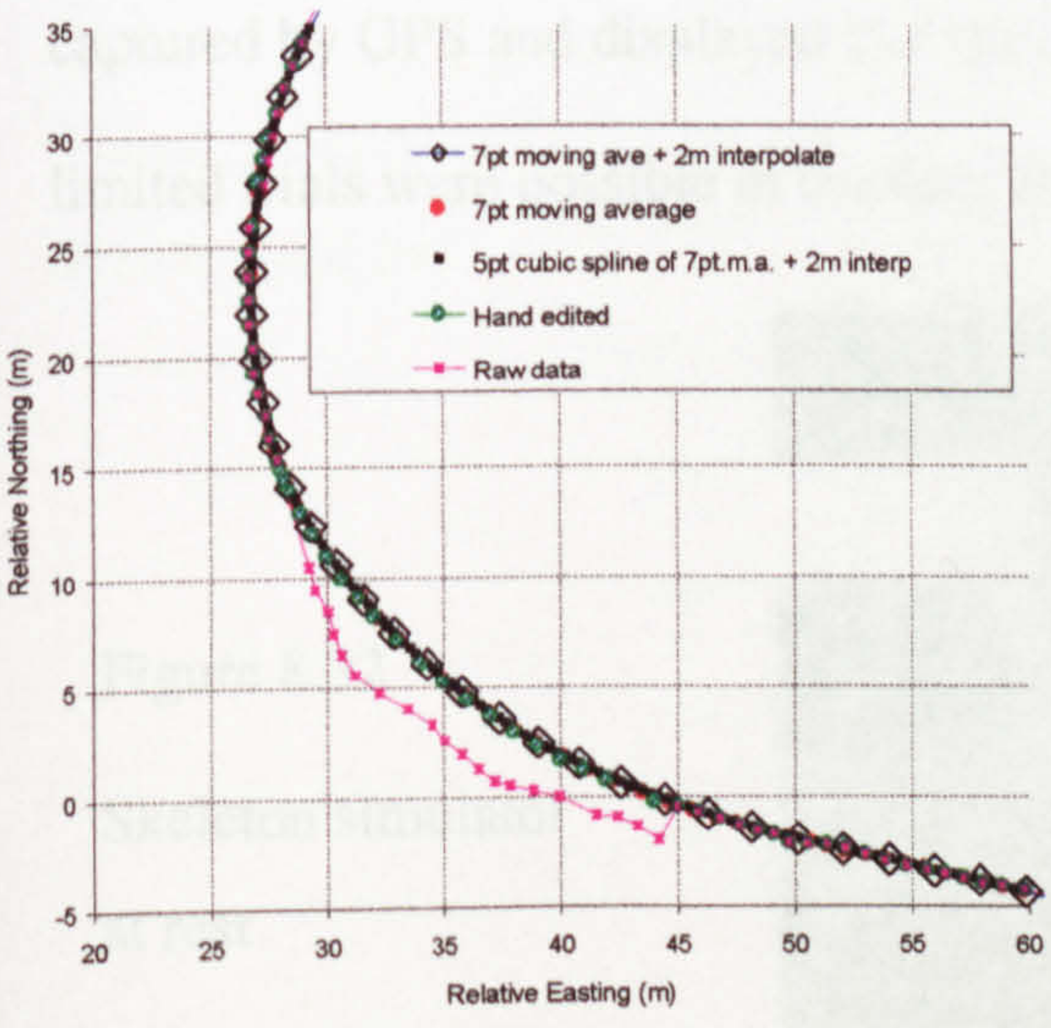

Figure 8.9

Comparison of data treatments (4)

winning for the very first time, and in both mens' and ladies' races. It was, in fact, our La Plagne slider who won the men's World Championship.

8.8 Further development

The IESSG took delivery of a tri-axial accelerometer later in 2000, for use in a bridge monitoring project. This was too late to be of use in Alpine field trials, since even software to read the output had to be developed first, never mind integration with satellite positioning systems. Nevertheless, it was possible to develop a test rig to simulate skeleton motion, for later use in comparative evaluation of satellite positioning and accelerometer based tracking, on campus. The design principle on a straight trajectory was a vertically pointing antenna, with instability and off-vertical pointing when cornering. An almost exact match for this motion model is a washing line supported at its mid-length by a pole, stimulated by vagaries in the wind. This idea was linked with a towed-trailer to provide the forward motion (Figure 8.32). A fixed antenna was sited on the chassis, and the mobile at the top of the unstable pole, flexibly tethered on both sides. Figure 8.33 shows the rig in a turn, and this motion is captured by GPS and displayed in Figure 8.34 as chassis and pole tracks. Only limited trials were possible in the time available.

Figure 8.32

Skeleton simulator at rest

Figure 8.33 Skeleton simulator in a turn

In mid-2000 BAE Systems, who continued funding of skeleton development, were also reported to be interested in an integrated accelerometer / satellite positioning package for skeleton positioning. No further news on developments and degree of success have been made available.

Figure 8.34 Simulated bob skeleton motion

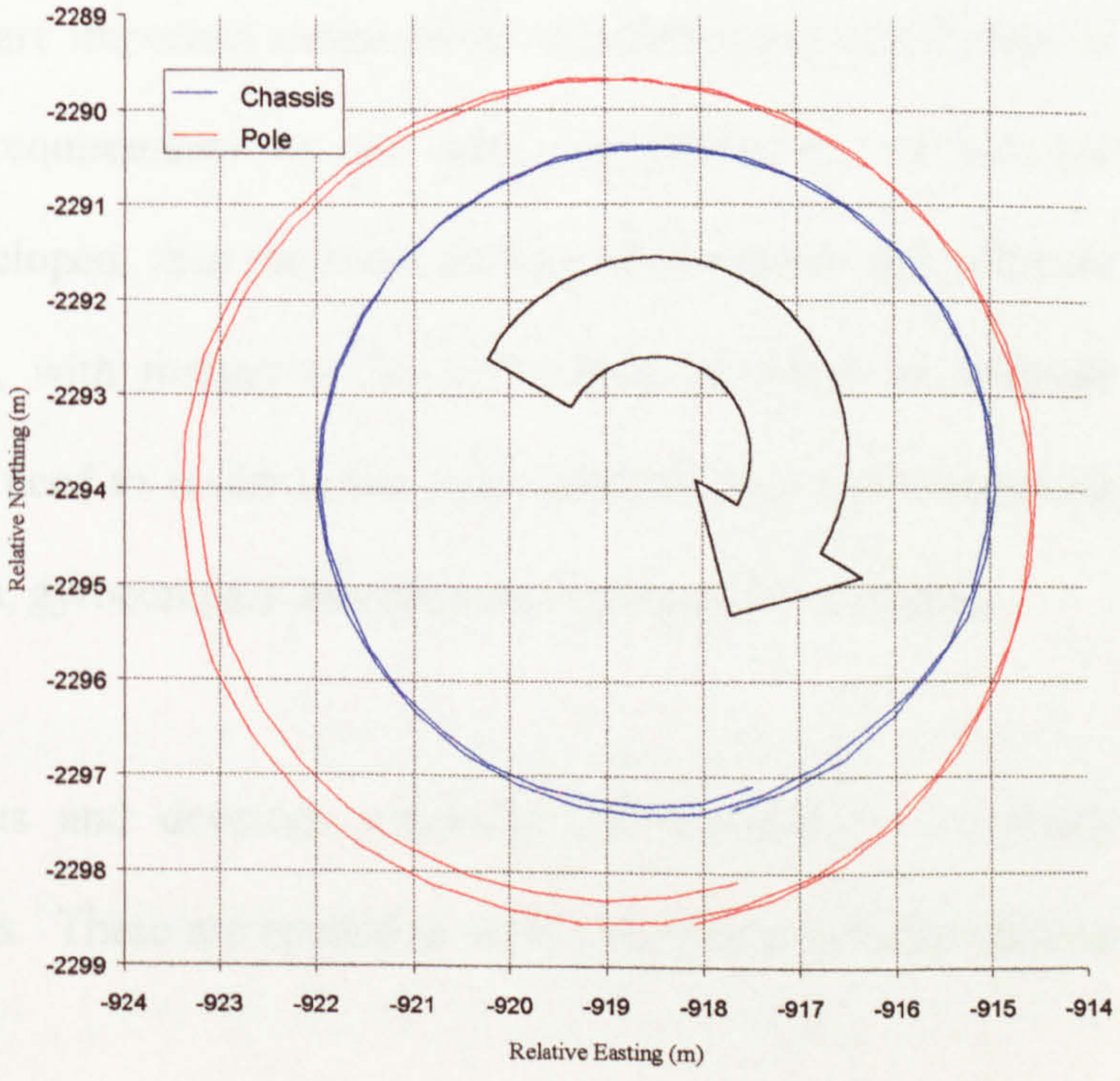

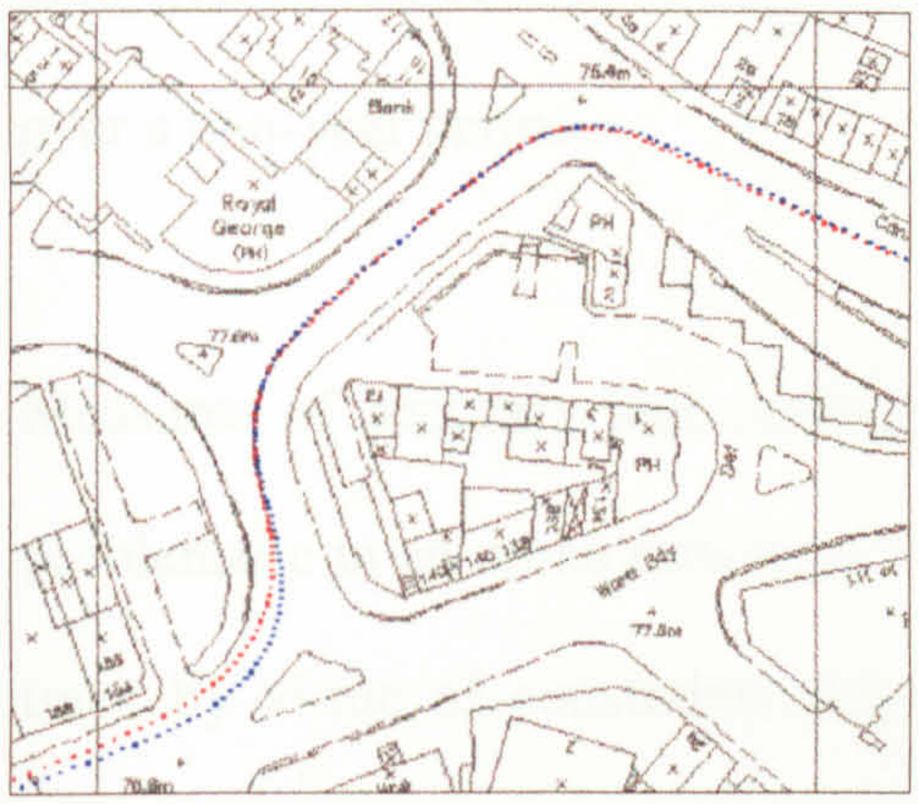

Chapter 9

Urban Tracking Performance Measures

9.1 Introduction

Characterising and quantifying the capabilities and limitations of satellite positioning systems, are important issues when considering the satisfaction of vehicle navigation requirements in the urban environment. If suitable measures can be developed, then informed choices on hardware and software needs may be made, with respect to the sufficiency of single or multiple constellations, or the need to resort to the more difficult option of integrating non-satellite type data, gyrocompass and odometer systems, for example.

This chapter suggests and develops *accuracy* and *continuity* as primary performance measures. These are applied to GPS and Hybrid vehicle tracking

data on a circuit between the University and Nottingham City centre, collected over a two-year period.

Measures of accuracy and continuity imply knowledge of a truth. This is problematic in an urban setting, as the vehicle can only follow a semi-captured track by virtue of constraints imposed by lane markings and road margins. Furthermore, positioning control by a more accurate system would be impractical. It is necessary therefore, to firstly consider ways to develop a *form* of truth, and then secondly to apply these in the evaluation of individual trajectories.

This chapter now continues with discussions on environmental factors affecting performance (§9.2), followed by performance measures (§9.3), and approaches taken to the determination of forms of truth (§9.4). Results from the Nottingham tests are then presented, followed by sample segments of GPS and Hybrid tracking data for open, medium, and severely limited skyview. The latter are supported by, and correlated with, photographic evidence. Finally the effect of macro level environmental factors on GPS and Hybrid performance – the seasons, is investigated for the northern summer and winter, using the same track around Nottingham

9.2 Factors affecting performance

Optimum positioning performance can only be achieved under conditions of ideal signal reception. *Ideal* corresponds to a fully open skyview with no

obstructions, and a zenith pointing antenna. Anything less than these conditions and performance will be impaired to some degree.

Obstructions have a two-fold effect. The first depends on permittivity of the local environment i.e. its transparency to microwave signals. This can range from nil with inorganic structures, to some reduction in the case of foliar cover (varying with leaf type and water content), which depending on tree type can be seasonal. Tests were made in winter and summer months to investigate this effect, see §9.7. *Inorganic* can be sub-divided into fixed and dynamic sources, though in a sense they are both dynamic when viewed from a moving vehicle. True dynamic is the more complex source, as it is variable in the short term, in as much as traffic density and type will depend on: day of the week (no lorries Sunday, and less buses), time of day (lorry deliveries in the early hours, higher bus density at peak times), and weather conditions (slower traffic speeds means a slowly changing skyview, with perhaps less positioning opportunities). In the medium to long term changes can occur in the inorganic backdrop of buildings as virgin building, and as demolition and re-building occur. The second effect of obstruction is multipath, this introduces additional spurious signals which can elevate noise levels, and introduce bias.

9.3 Performance measures

For generic vehicle navigation in an urban setting, the most important measurable variables are likely to be continuity (knowing where you are at some desired frequency), and accuracy or proximity to a truth (important when

deciding what exit to take, for example). Additionally integrity and availability can become very important in say construction, in particular where vertical excavation levels are crucial, but these are not developed as performance measures here.

In their assessment, continuity and accuracy are linked, in that if positioning classified as grossly inaccurate, or *outliers*, by comparison with a truth, is discarded, then measures of continuity may be affected. If the indicated track passes through buildings owing to Kalman filter lag, termed *ghosting*, then these data may contribute to continuity, if the basic shape of the trajectory is preserved. However there may be a trade-off against overall accuracy if such data are retained.

Accuracy can be classified according to deviation from the truth, and also according to the relative proportions of solution type – fixed ambiguity or float solution. Experience has shown though, that in a noisy skyview limited setting, float is likely to be the norm, and so solution type is of limited use when comparing performance.

Number of satellites is important not only from the viewpoint of a higher constellation density, but also in terms of geometric quality of a positioning fix, as expressed in DOP values. Poor geometry means not only poor precision but also an increased susceptibility to measurement bias. This was exemplified by the preference of GPS over Hybrid for one track segment at La Plagne, see Chapter 8, where the automatic selection of GLONASS satellites in preference

to GPS introduced what can only be assumed to be poorer measurements by way of multipath, whilst providing a marginal improvement in geometry.

Nevertheless geometry and number of visible satellites are useful indicators of constellation tolerance to difficult signal reception conditions, and are therefore used as performance indicators here, see §9.7.

9.4 Determination and use of a truth

Determination of a *truth,* that is what ground track did the antenna actually follow, is not easily achieved for urban vehicle navigation. For example the use of a more accurate land survey type system would be impractical given traffic levels at any time of day. On the other hand use of a captured track as suggested in §6.5 would not be realistic in terms of replicating the fixed and dynamic elements of the urban environment. Use of the everyday semi-captured track, by virtue of lane and road margins, must then be used, and there are then two possible ways to generate a truth.

Firstly, the truth could be accumulated through the agglomeration of several repetitive tracks, that follow as closely as possible the same route over the ground. (It is important here to have an awareness of where the antenna is located on the vehicle. Directly above the driver is a good idea). Although each circuit contributes a slightly different route, each also adds a slightly different positioning capability, owing to a changing dynamic skyview component, and constellation geometry and availability with time. These

capabilities when aggregated over time may be able to form a more complete trajectory. Individual tracks in GPS and Hybrid may then be assessed against such a truth. However this type of truth may contain positioning artefacts in particularly difficult areas. Moreover, this truth may be discontinuous, which is unhelpful, and leads to the second option.

If the route followed is highly repeatable through familiarity, and a digital mapping product is available at a large scale, say 1:1250 or better, then the (well) *known* track can be artificially created and exported, for use as an *artificial* truth. Export point density should vary widely, with the highest density at roundabouts, corners and junctions, requiring densification to some uniform interval before use as a truth.

Once sufficiently densified, the automated use of such a truth in a *comparative* process with individual or aggregate *test* tracks, is achieved by taking each point in turn, *A*, from the test file, and comparing it with every point, *B*, of the densified truth. A *match* is declared when *B* is found such that the distance *A* to *B* is the minimum for the whole truth file. This value or *residual*, denoted *j* in Figure 9.1, corresponds to the perpendicular distance between *A* and the truth, and it is these values that are used here to indicate the accuracy of a particular solution, by way of statistical measures.

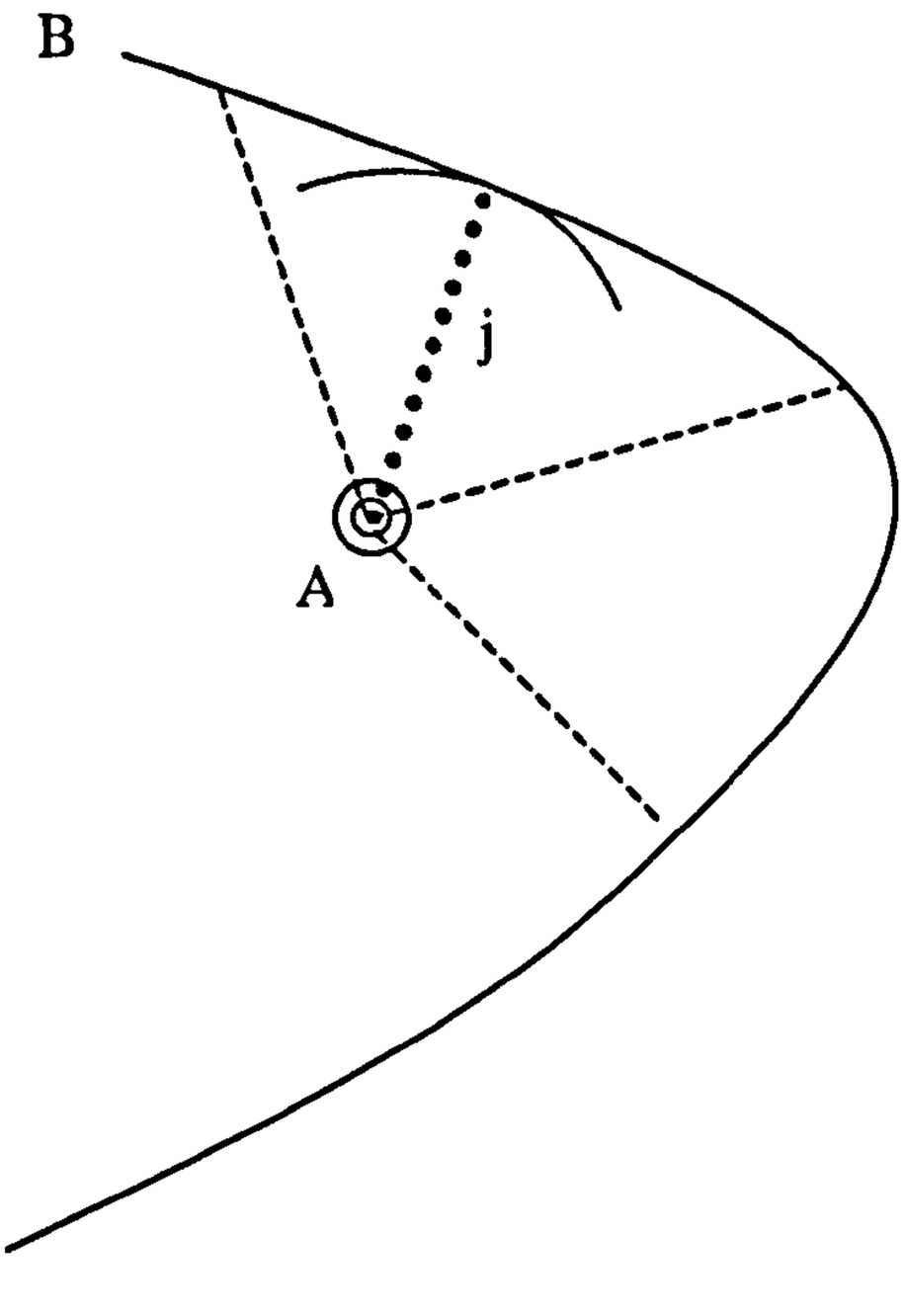

Figure 9.1 Accuracy variable *j*

Three statistical measures of fit were programmed in Fortran 77. These were the mean, RMS deviation (or standard deviation) and R95%, according to the following formulae, where n is the number of samples:

- $$Mean = \frac{\Sigma j}{n} = \bar{j} \qquad (9.1)$$

- $$RMS\ deviation = \left[\frac{\Sigma(j-\bar{j})^2}{n-1}\right]^{0.5} \qquad (9.2)$$

- R95 or Radius 95% = 95% of j values are less than this value.

These ideas are now realised through practical vehicle tracking exercise performed, in and around the city of Nottingham.

9.4.1 *Aggregate* truth

Experience has shown that a Kalman filter with forward-backward (F-B) or *bi-directional* processing capability, always performs better relative to uni-directional processing, in terms of accuracy and continuity of results. This is due not only to the weighted combination of the forward and backward results to give a single solution, but also that the need for a filter ramp (during which there is positioning) after a positioning hiatus, can be mitigated by working through the data from the opposite direction. Unfortunately the data processing suites available processed only GPS in F-B mode, and it can then only be predicted that a Hybrid F-B engine could provide the optimum result.

In GPS F-B mode a minimum of four circuits were required to completely define the route followed, on the other hand in some cases only two Hybrid circuits were needed to achieve the same coverage. From this perspective Hybrid is apparently a more cost effective solution.

The *aggregate truth* was achieved by mathematically averaging six GPS F-B circuits. No relative weighting was applied in its construction.

9.4.2 *Artificial* truth

An artificial truth was also created as described by the second option in §9.4. In this case OS (Ordnance Survey) 1:1250 *Land-Line* digital mapping of Nottingham was used. In all, 336 points were digitised to form the basis of a truth to cover the circuitous route of nearly 10 kilometres. These points were then fed to a Fortran 77 densification routine. A high level of densification was required if the most accurate performance figures were to be derived, so an interval of 10 centimetres was used, resulting in nearly 100,000 records. As a check on this routine, the digitised data and densified version were fed into the comparative routine, where average and RMS deviation values of 6.8 and 7.7 centimetres respectively were obtained, thus validating the process. The two truths, aggregate and artificial, were then compared, with R95 results of a little over 3 metres (Table 9.1), and R50 of just one metre, values which were around the expected level of agreement.

Input	Average (m)	RMS deviation (m)	R50 (m)	R95 (m)
Aggregate truth	1.3	1.1	1.0	3.2

Table 9.1 Aggregate versus artificial truth

With this validation, and after review against the digital mapping background, the artificial truth was used as the reference data set against which all other circuits were evaluated.

9.5 Performance evaluation

Three tracking exercises are examined, two from December 1998 and one from July 1999, covering winter and summer conditions. Analysis of particular circuits and sub-circuits is based on both comparison with the artificial truth, and comparison with each other, with reference to the various modes of position processing.

Vehicle positioning in these exercises was relative to the pre-established reference station at the IESSG. Starting with the on-the-fly (OTF) mode processed using AOSS, see Tables 9.2 and 9.5, these both show some improvement in most statistics of Hybrid over GPS, but this is not clear cut, and positioning gaps above ten metres are relatively high at between thirty and fifty percent overall.

Applying uni-directional Kalman filtering, processed using WinPrism software, reported in Tables 9.3 and 9.6, helps in theory to reduce these gaps, by way of modelling vehicle dynamics and making use of sparse observations, which in themselves would be insufficient to generate a position at an epoch. However, Kalman filtering by its nature can introduce erroneous tracking at the ends of blocks of data, as the quality of observations deteriorates. This may be reflected in the GPS R95% values which are larger than those for OTF positioning. Comparing within this mode, Hybrid can be seen to significantly outperform GPS in almost all statistics, which is an indication of the level of

GLONASS contribution, which is in turn a function of skyview limitation, and point in time within the GLONASS 8-day repeat geometry cycle.

Circuit	System	Process	Engine	Gap %		Residual (m)		
				> 5m	> 10m	Ave.	R95%	St.Dev.
1a	GPS	Epoch	-	36.2	29.1	5.4	10.9	3.3
1a	Hybrid	Epoch	-	34.3	28.7	5.4	10.3	3.4
1b	GPS	Epoch	-	34.9	30.0	6.1	12.7	4.1
1b	Hybrid	Epoch	-	32.9	27.3	4.9	10.8	3.8

Table 9.2 Circuit 1 : OTF positioning performance

Circuit	System	Process	Engine	Gap %		Residual (m)		
				> 5m	> 10m	Ave.	R95%	St.Dev.
1a	GPS	K filter	F	13.4	10.5	4.5	20.2	7.7
1a	Hybrid	K filter	F	6.9	5.1	2.5	8.8	4.3
1b	GPS	K filter	F	17.4	15.6	3.3	13.3	6.5
1b	Hybrid	K filter	F	6.8	4.5	2.2	5.8	3.1

Table 9.3 Circuit 1 : Forward Kalman filter positioning performance

Circuit	System	Process	Engine	Gap %		Residual (m)		
				> 5m	> 10m	Ave.	R95%	St.Dev.
1-a	GPS	K filter	F + B	13.2	12.0	2.0	5.1	3.4
1-a	Hybrid	K filter	F	6.9	5.1	2.5	8.8	4.3
1-b	GPS	K filter	F + B	1.8	1.5	1.9	5.1	1.8
1-b	Hybrid	K filter	F	6.8	4.5	2.2	5.8	3.1

Table 9.4 Circuit 1 : Bi-directional Kalman filter positioning performance

Kalman filtering can also be applied in bi-directional mode (Tables 9.4 and 9.7), resulting in the weighted combination of forward and backward solutions, as a single solution. This is recognised as the most beneficial Kalman filter, as it maximises the utility of the data before and after periods of loss of signal or protracted periods with too few satellites. Certainly when considering GPS residual statistics across all three circuits, there is an improvement of bi-directional over uni-directional processing. When considering relative gap management there is not always a clear advantage and

sometimes the situation deteriorates, compare GPS *Circuit 1a* Tables 9.3 with 9.4, and GPS *Circuit 3b* Tables 9.8 with 9.9.

Circuit	System	Process	Engine	Gap %		Residual		
				> 5m	> 10m	Ave.	R95%	St.Dev.
2-a	GPS	Epoch	-	37.8	31.7	2.2	6.2	3.4
2-a	Hybrid	Epoch	-	38.9	29.1	2.0	5.5	2.2
2-b	GPS	Epoch	-	54.4	49.2	2.7	8.2	3.5
2-b	Hybrid	Epoch	-	40.9	30.8	2.5	7.2	3.2

Table 9.5 Circuit 2 : OTF positioning performance

Circuit	System	Process	Engine	Gap %		Residual		
				> 5m	> 10m	Ave.	R95%	St.Dev.
2-a	GPS	K filter	F	17.2	16.2	2.8	10.1	4.2
2-a	Hybrid	K filter	F	5.4	5.3	1.8	4.4	2.1
2-b	GPS	K filter	F	36.9	36.2	5.0	19.5	12.6
2-b	Hybrid	K filter	F	6.5	4.7	2.2	7.1	2.6

Table 9.6 Circuit 2 : Forward Kalman filter positioning performance

Circuit	System	Process	Engine	Gap %		Residual		
				> 5m	> 10m	Ave.	R95%	St.Dev.
2-a	GPS	K filter	F + B	1.0	0.8	1.7	4.7	1.9
2-a	Hybrid	K filter	F	5.4	5.3	1.8	4.4	2.1
2-b	GPS	K filter	F + B	8.5	7.9	2.4	7.6	3.2
2-b	Hybrid	K filter	F	6.5	4.7	2.2	7.1	2.6

Table 9.7 Circuit 2 : Bi-directional Kalman filter positioning performance

Circuit	System	Process	Engine	Gap %		Residual		
				> 5m	> 10m	Ave.	R95%	St.Dev.
3b	GPS	K filter	F	15.9	15.0	5.1	12.1	4.5
3b	Hybrid	K filter	F	21.0	19.9	1.8	5.6	2.1

Table 9.8 Circuit 3 : Forward Kalman filter positioning performance

In summary, whilst residual based statistics appear to be fairly reliable, gap management appears inconsistent, and is therefore apparently not so useful, though it may be that analysis of the gap distribution would provide a better tool.

Circuit	System	Process	Engine	Gap %		Residual		
				> 5m	> 10m	Ave.	R95%	St.Dev.
3b	GPS	K filter	F + B	17.8	16.5	2.9	10.6	4.3
3b	Hybrid	K filter	F	21.0	19.9	1.8	5.6	2.1

Table 9.9 Circuit 3 : Bi-directional Kalman filter positioning performance

9.6 Photographic evidence

The statistics given in §9.5 relate the level of positioning difficulty in an abstract way, additional photographic and mapping evidence are helpful in linking these data to reality. Three skyview situations are provided, open (Figure 9.2), medium (Figure 9.3), and highly restricted (Figure 9.4). The mapping grid interval is 100 metre. In the open sky case (Figure 9.2), GPS in any mode and Hybrid have very similar performance, negotiating road margins and the roundabout with a high degree of veracity. The medium restricted case illustrated in Figure 9.3, gives rise to similar capabilities by GPS bi-directional and uni-directional processing, both being superior to Hybrid, with less sequential track separation, compare Figure 9.3a with 9.3c. It is only in the highly restricted case in Figure 9.4 that GPS-only in any mode fails, and Hybrid uni-directional provides the best solution. Summarising, the current GPS constellation even though larger than the design size, cannot handle the most difficult skyview conditions in our cities. This may not always be the case, for example on the Continent, where post-revolution boulevards are considerably wider than UK city roads.

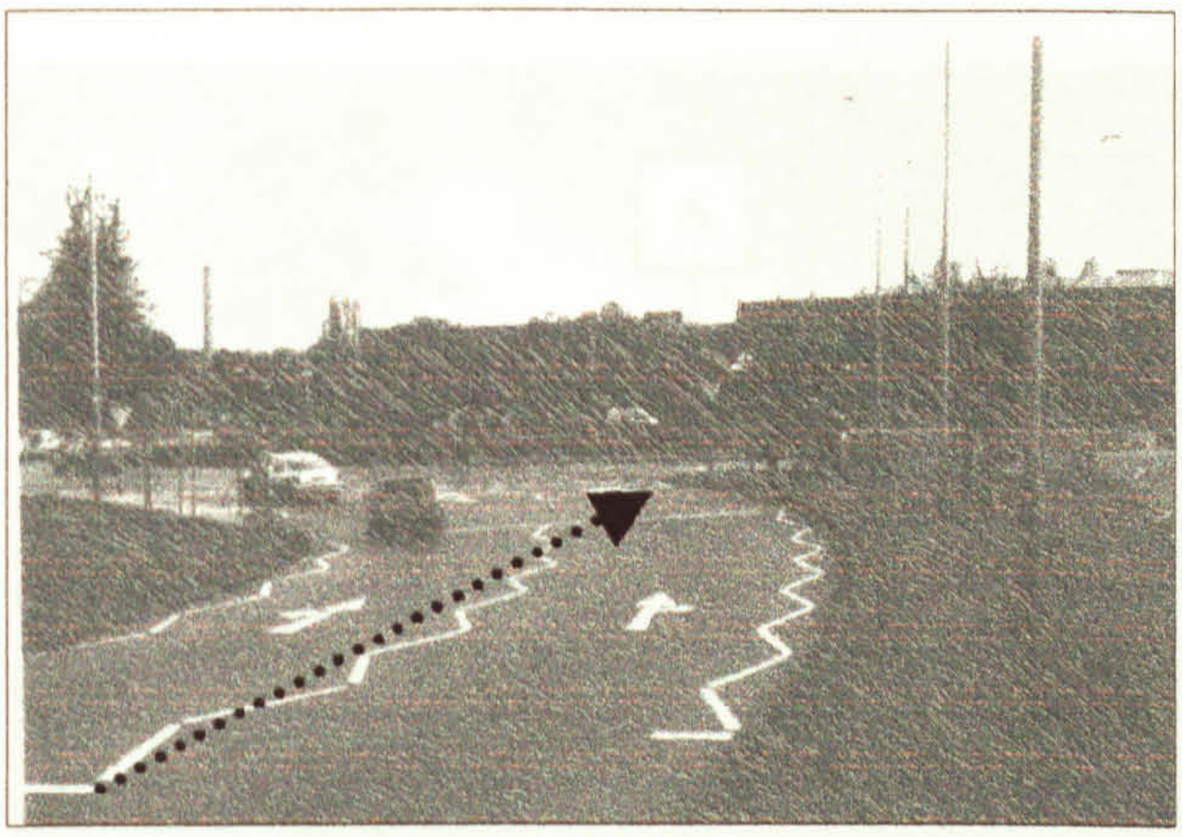

Figure 9.2
Open skyview
(Queen's Medical Centre)
07.12.98

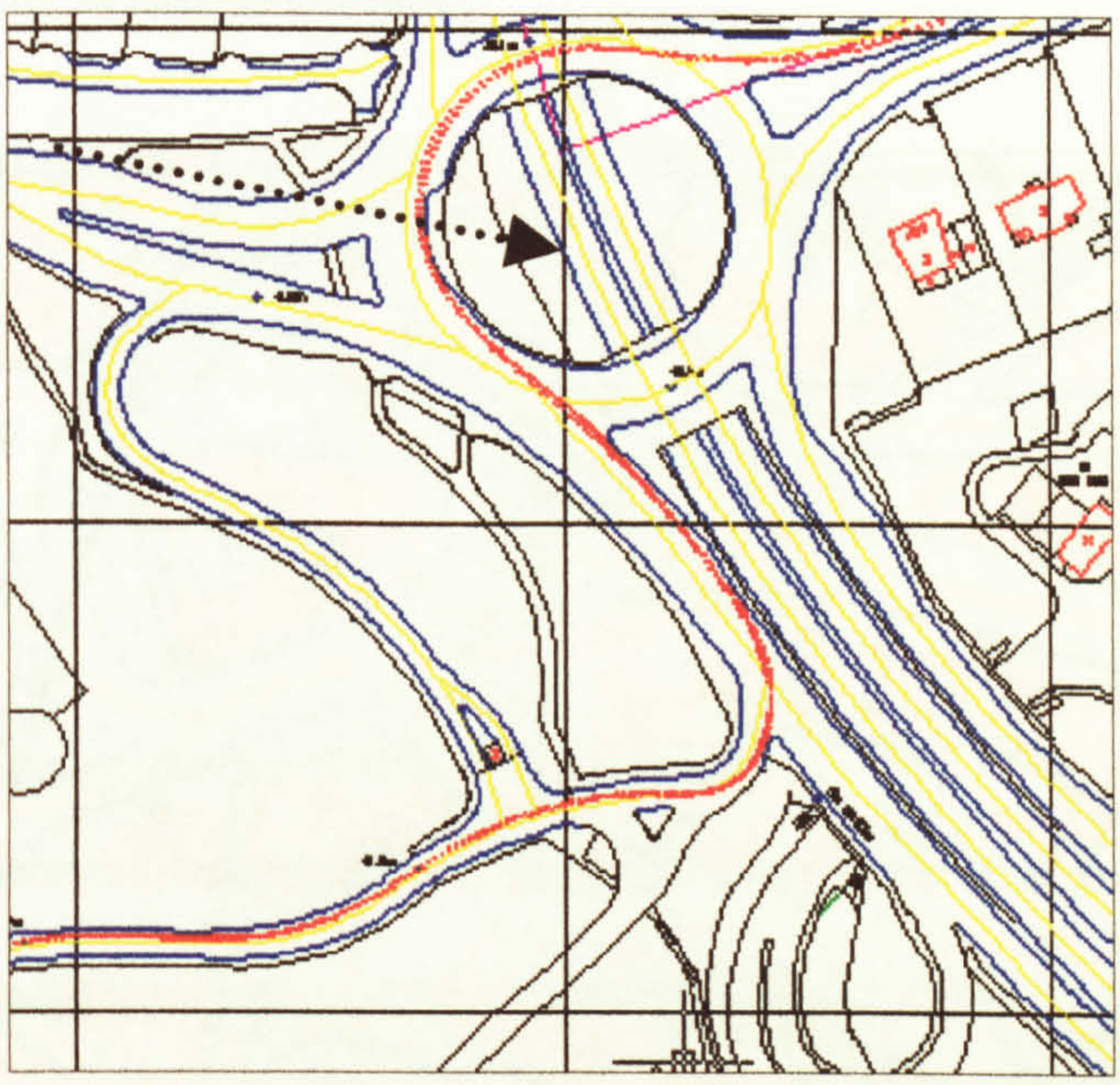

Figure 9.2a
GPS tracking

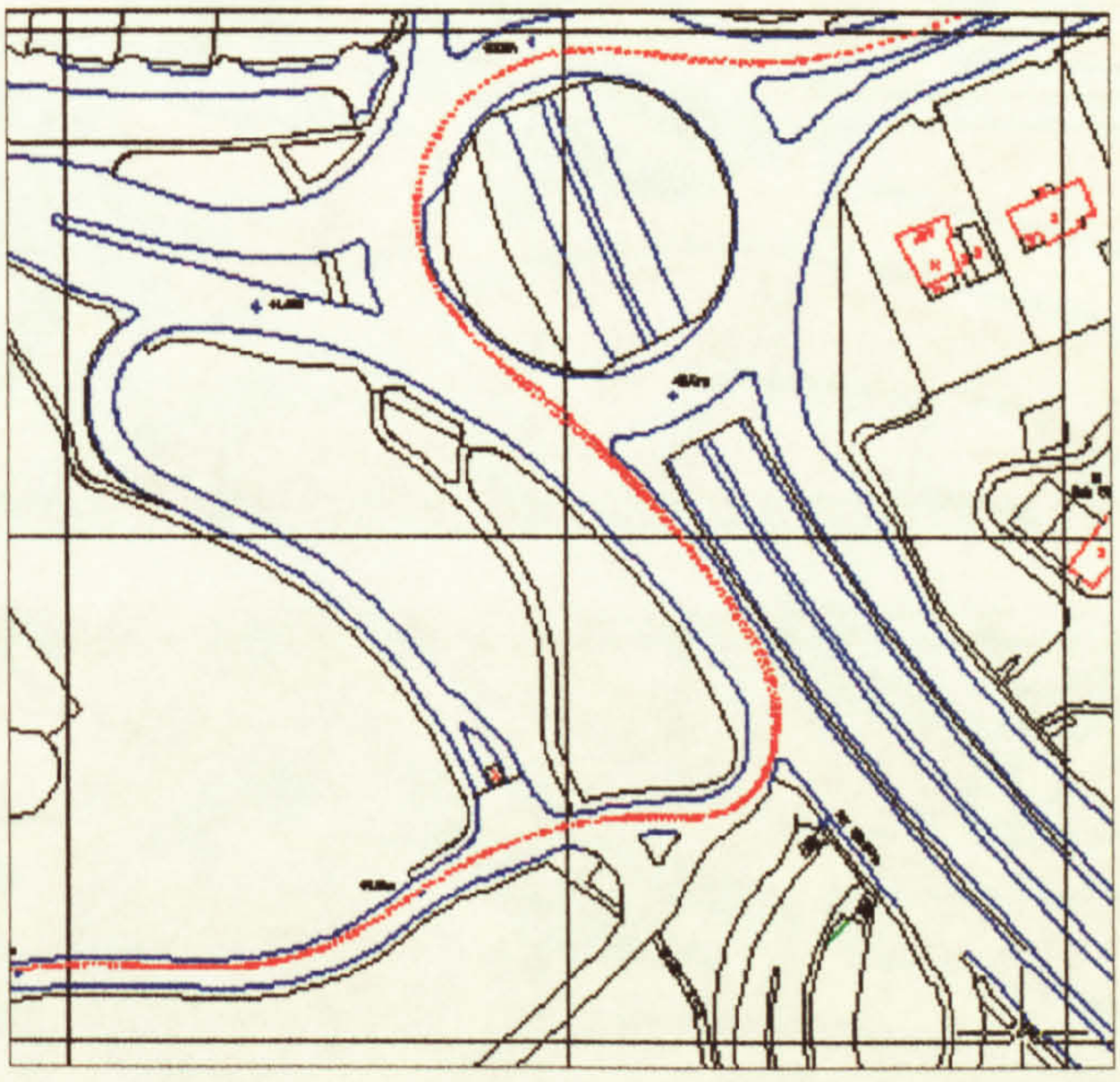

Figure 9.2b
Hybrid tracking

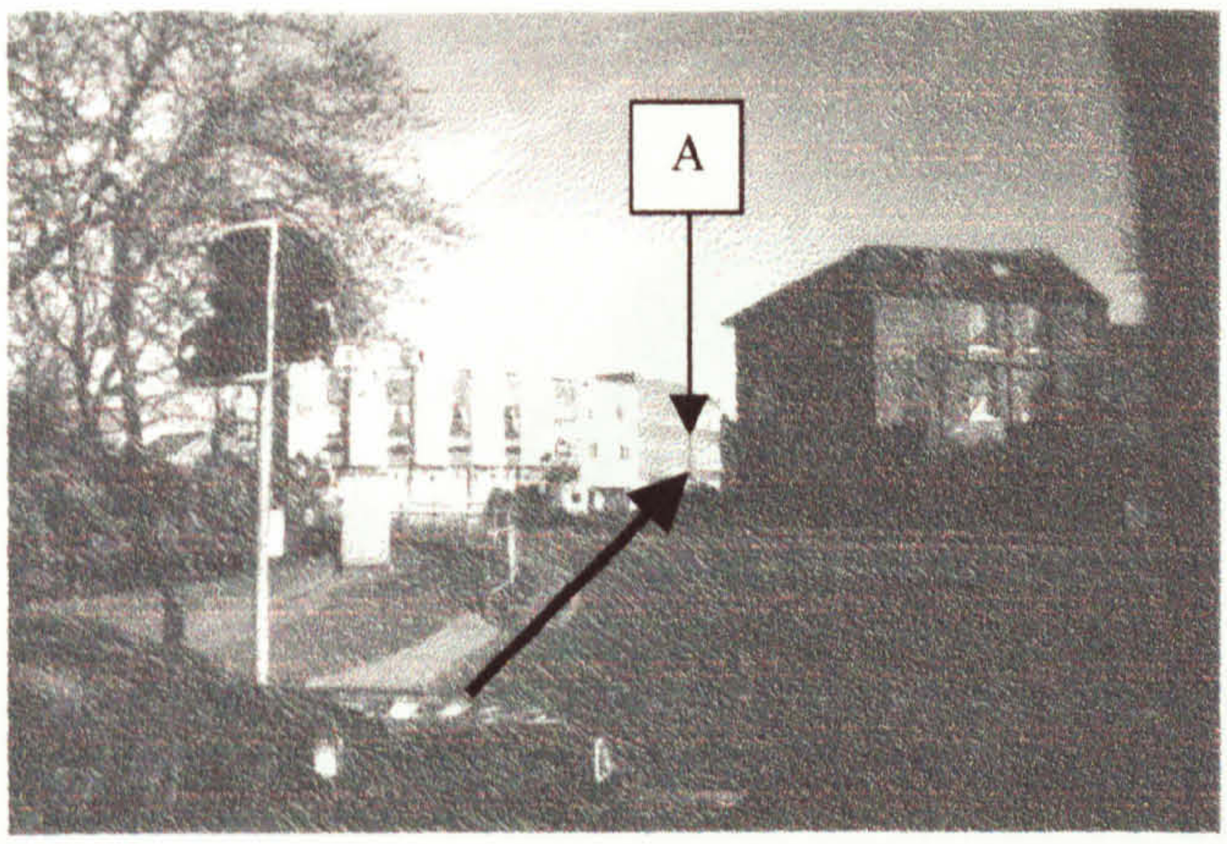

Figure 9.3
Medium restricted skyview
(Canning Circus)
12:09 UTC 07.12.98

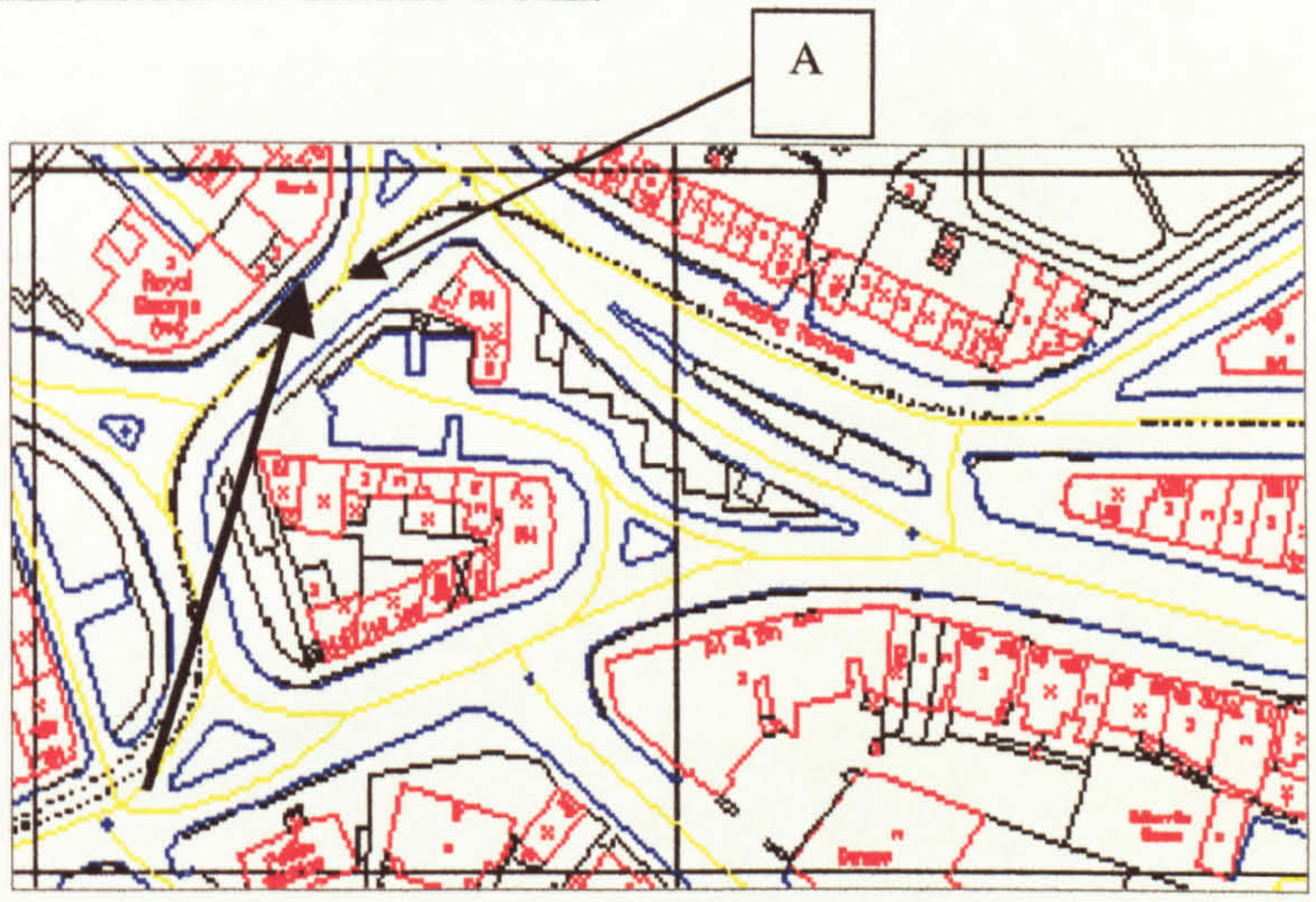

Figure 9.3a
GPS Forward and
Backward

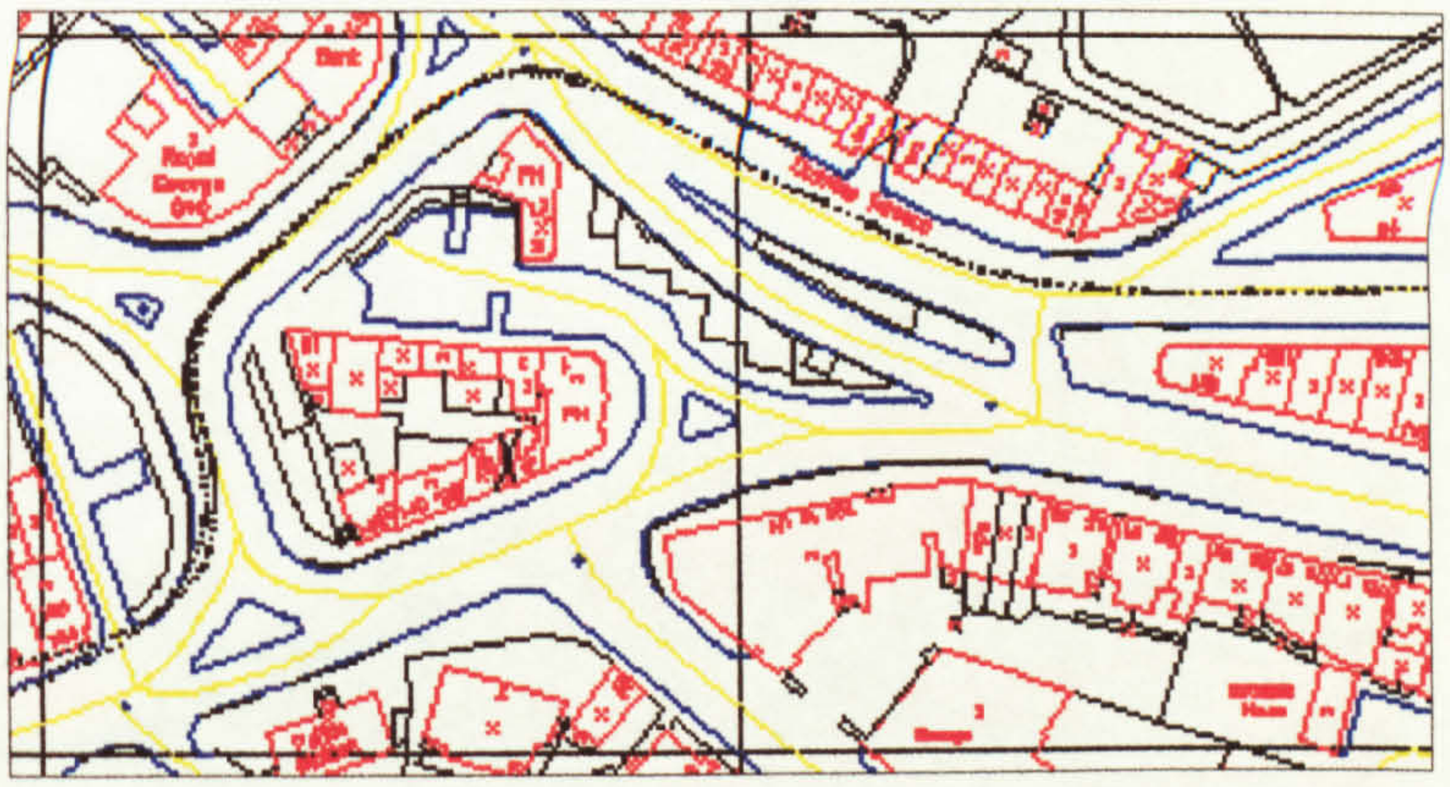

Figure 9.3b
GPS Forward

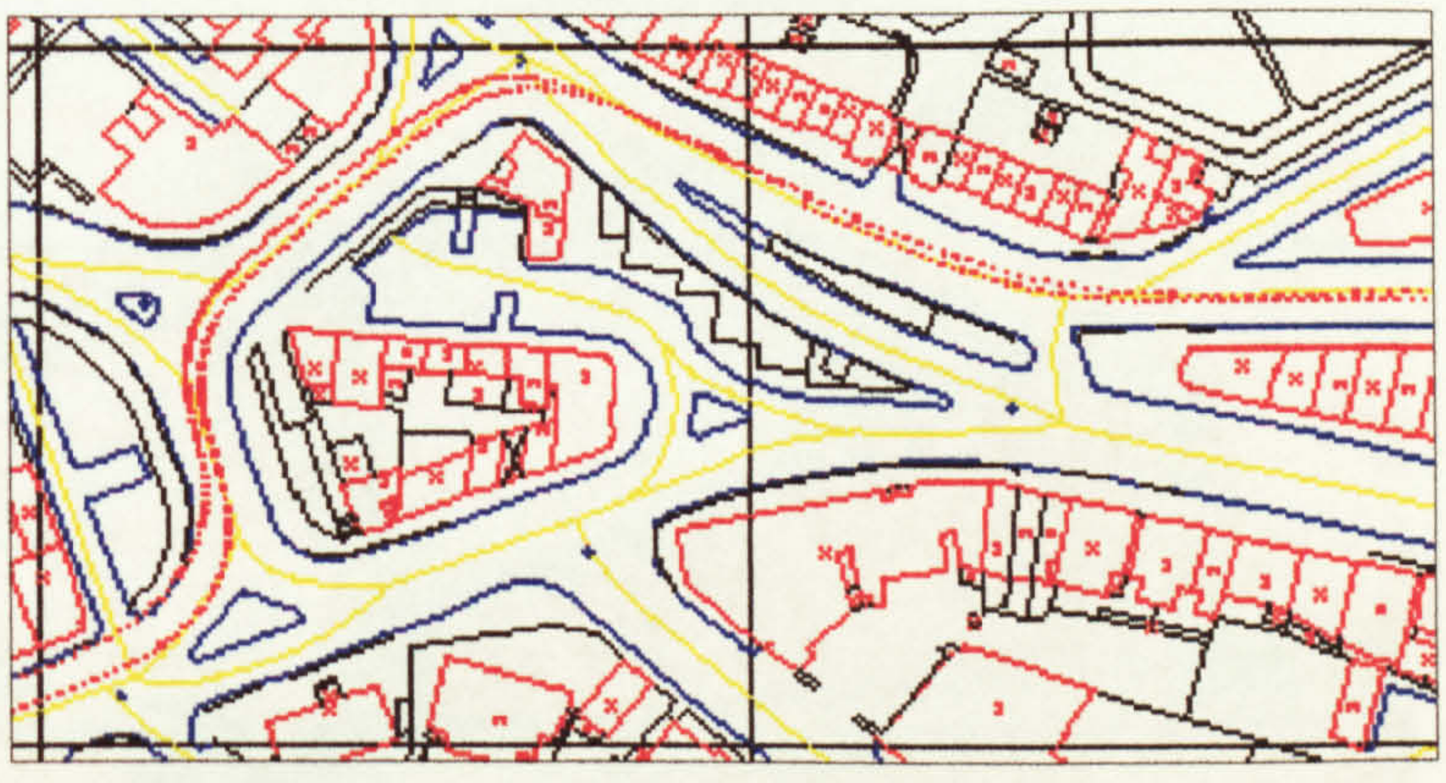

Figure 9.3c
Hybrid Forward

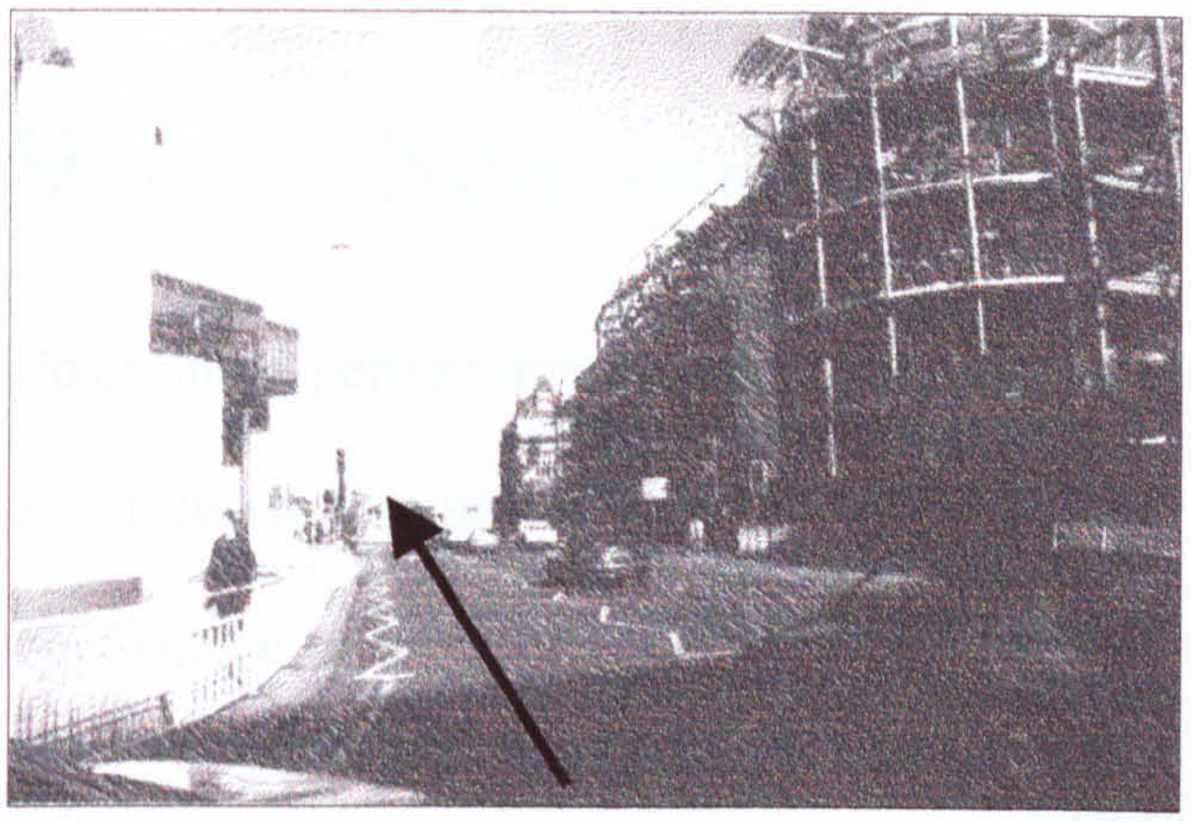

Figure 9.4
Highly restricted skyview
(Trinity Square)
12:12 UTC 07.12.98

Figure 9.4a
GPS Forward and
Backward

Figure 9.4b
GPS Forward

Figure 9.4c
Hybrid Forward

9.7 Seasonal effects

Positioning performance can be affected by changes in deciduous foliar cover according to the time of year. In summer some parts of the circuit took on the appearance of tunnels (Figures 9.5 and 9.6), refracting both light and satellite signals. Add to this GLONASS' widely varying contribution to Hybrid from day-to-day, meant that comparison of Hybrid over time was invalid, however GPS and Hybrid will be comparable if developed from the same data set, within each season, and GPS across seasons. Analysis of these cases is made here. Note that periods spent static for initialisation purposes have been eliminated from the data analysed here.

Considering constellation size, and comparing GPS to Hybrid in winter (Figure 9.7) or summer (Figure 9.8) exemplifies the advantage of hybridisation - the percentage of epochs with more than nine satellites is zero for GPS, and over fifty percent for Hybrid. The Hybrid constellation also appears less sensitive to seasonal effects. Comparing GPS across seasons, there is a clear improvement as the distribution shifts to the right from summer to winter. There was no increase in the GPS constellation over this period.

Considering geometry, in Figures 9.9 and 9.10, for winter and summer respectively, GPS geometry is clearly improved in winter, and again Hybrid appears more robust against foliar effects.

Figure 9.5 Foliage tunnel A

Figure 9.6 Foliage tunnel B

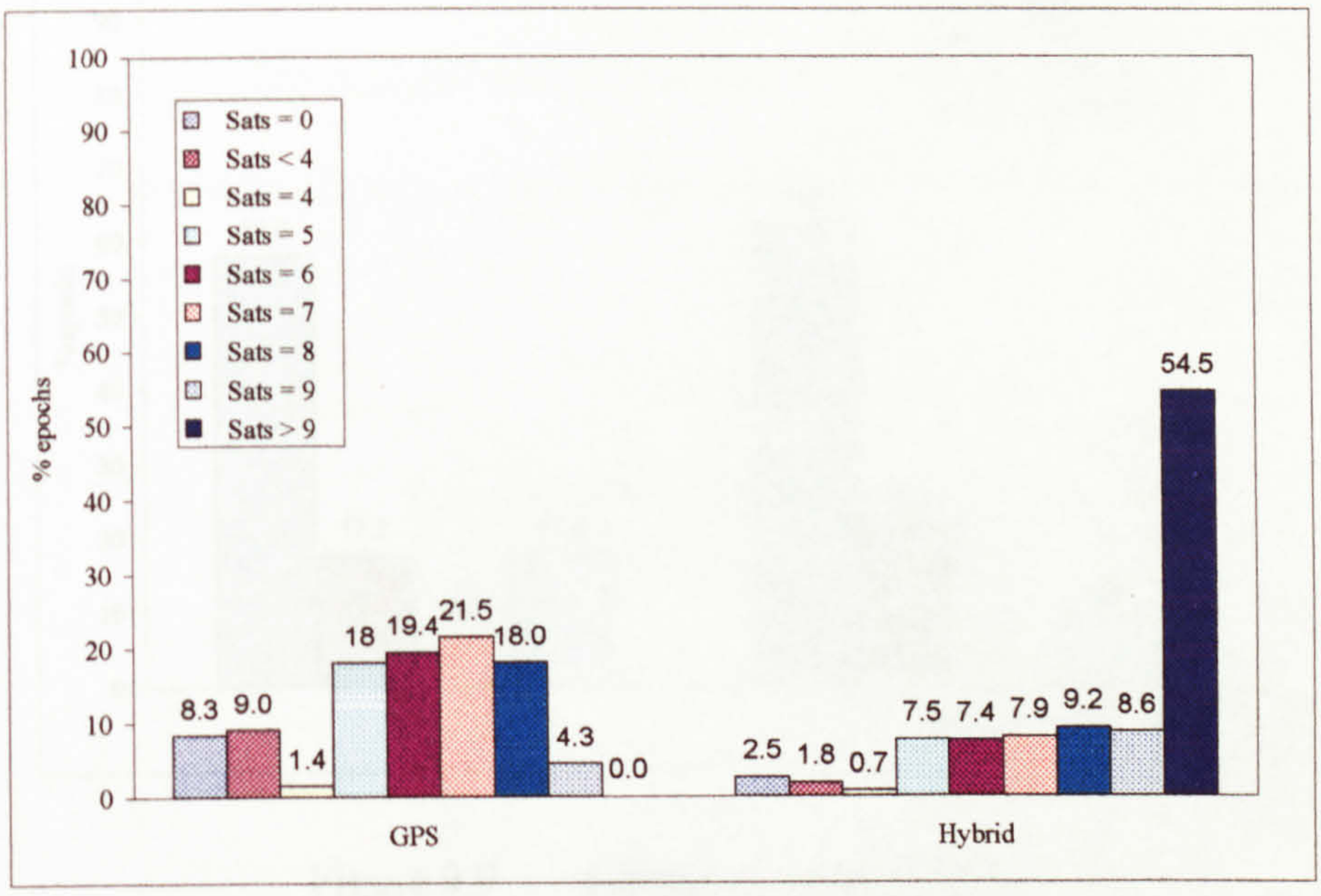

Figure 9.7 Constellation size, winter 1998

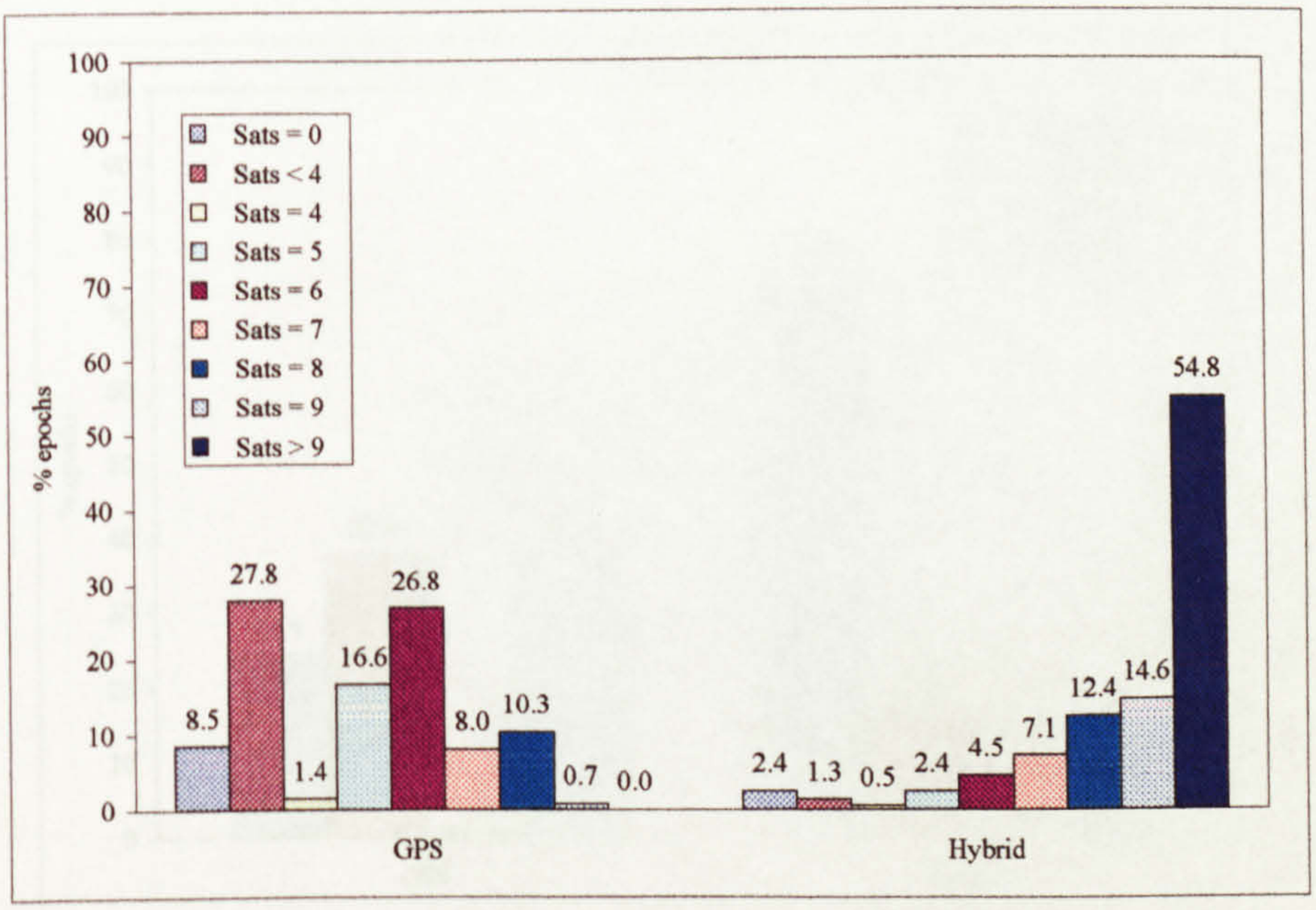

Figure 9.8 Constellation size summer 1999

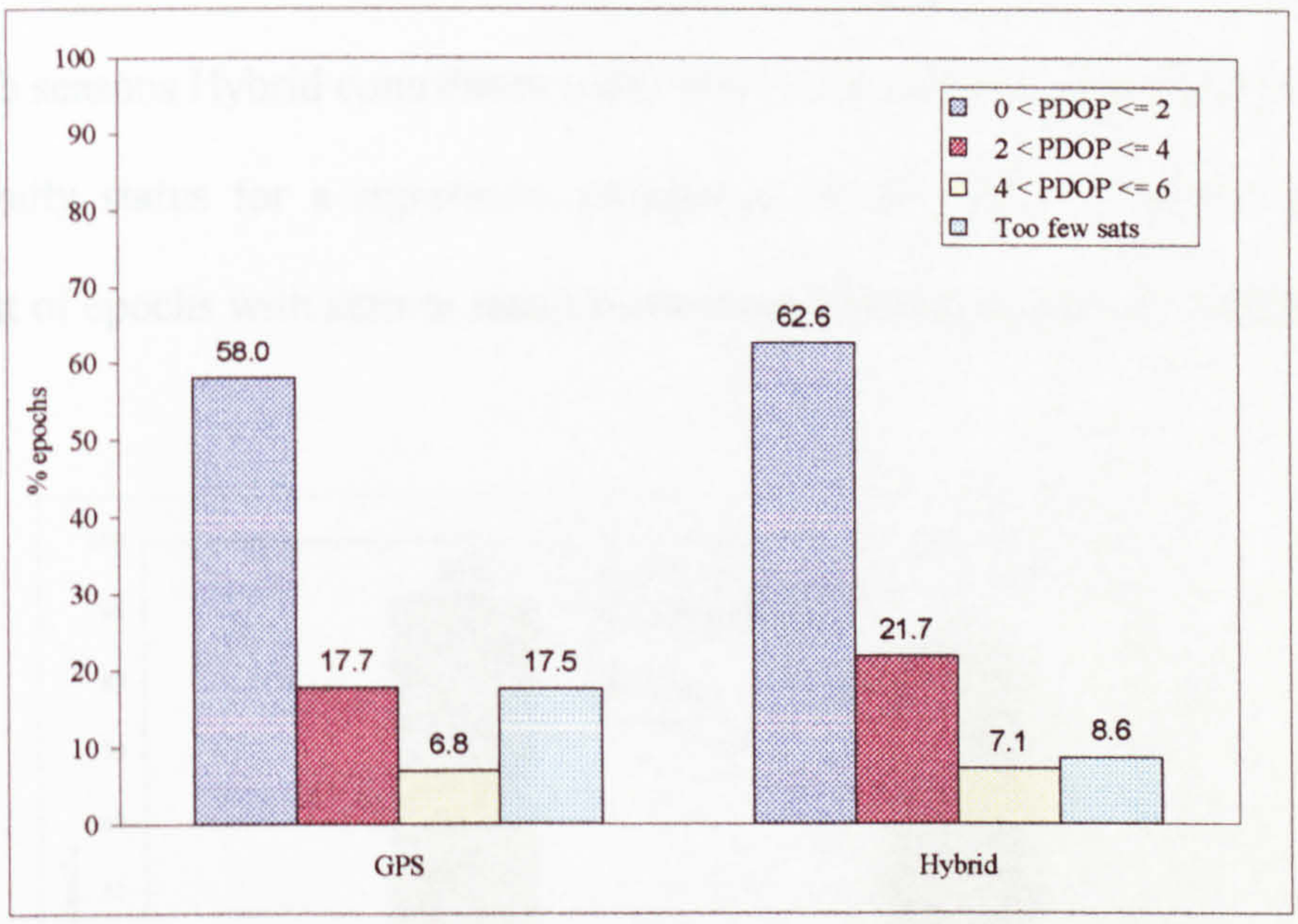

Figure 9.9 Geometry winter 1998

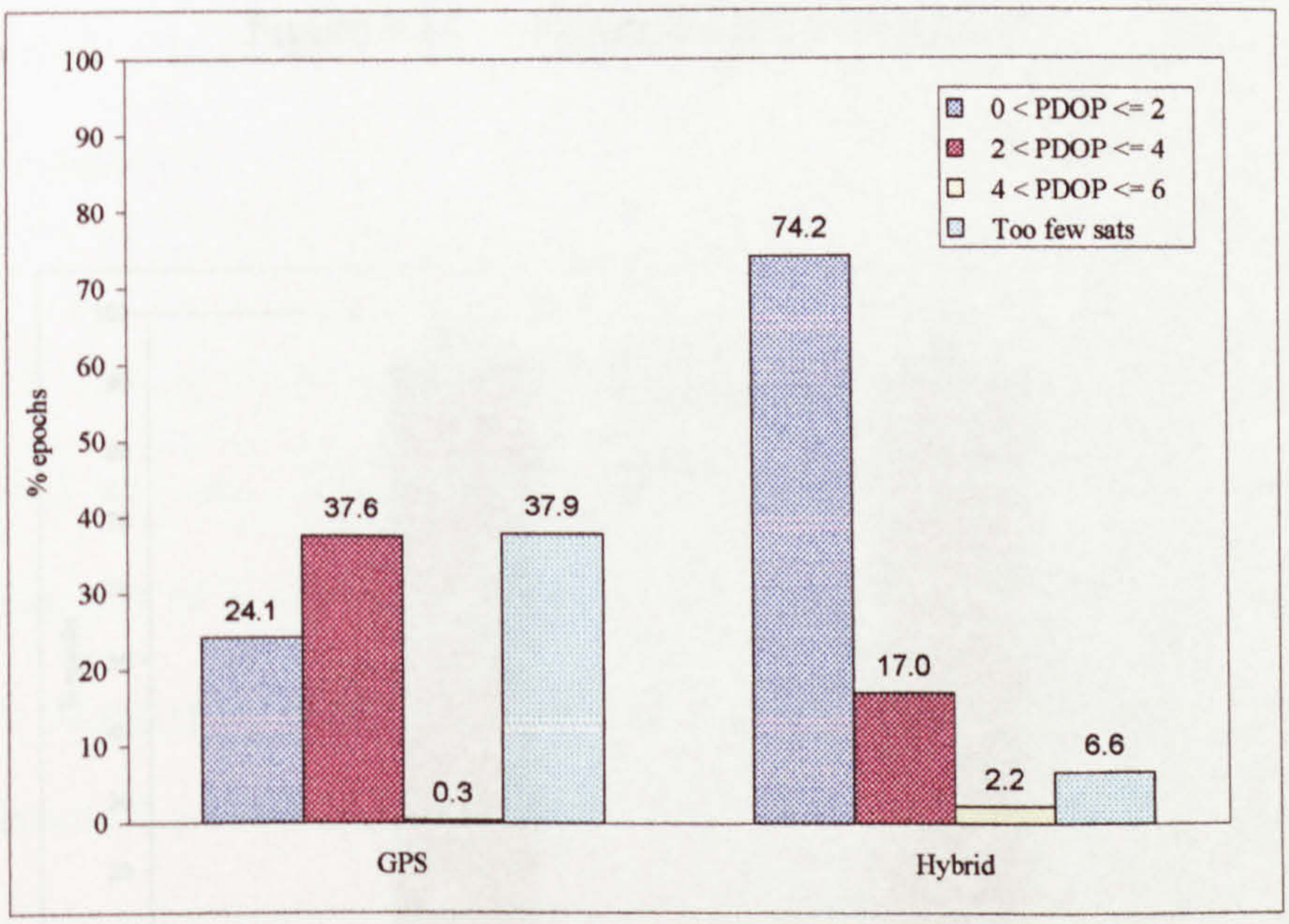

Figure 9.10 Geometry, summer 1999

Finally, considering solution type, in Figures 9.11 and 9.12, in the same way as geometry, GPS alone is unable to support an ambiguity fixed solution, however in both seasons Hybrid contributes sufficient observables to assist GPS to fixed ambiguity status for a significant proportion of the track. Missing epochs consist of epochs with zero or insufficient observables to support a solution.

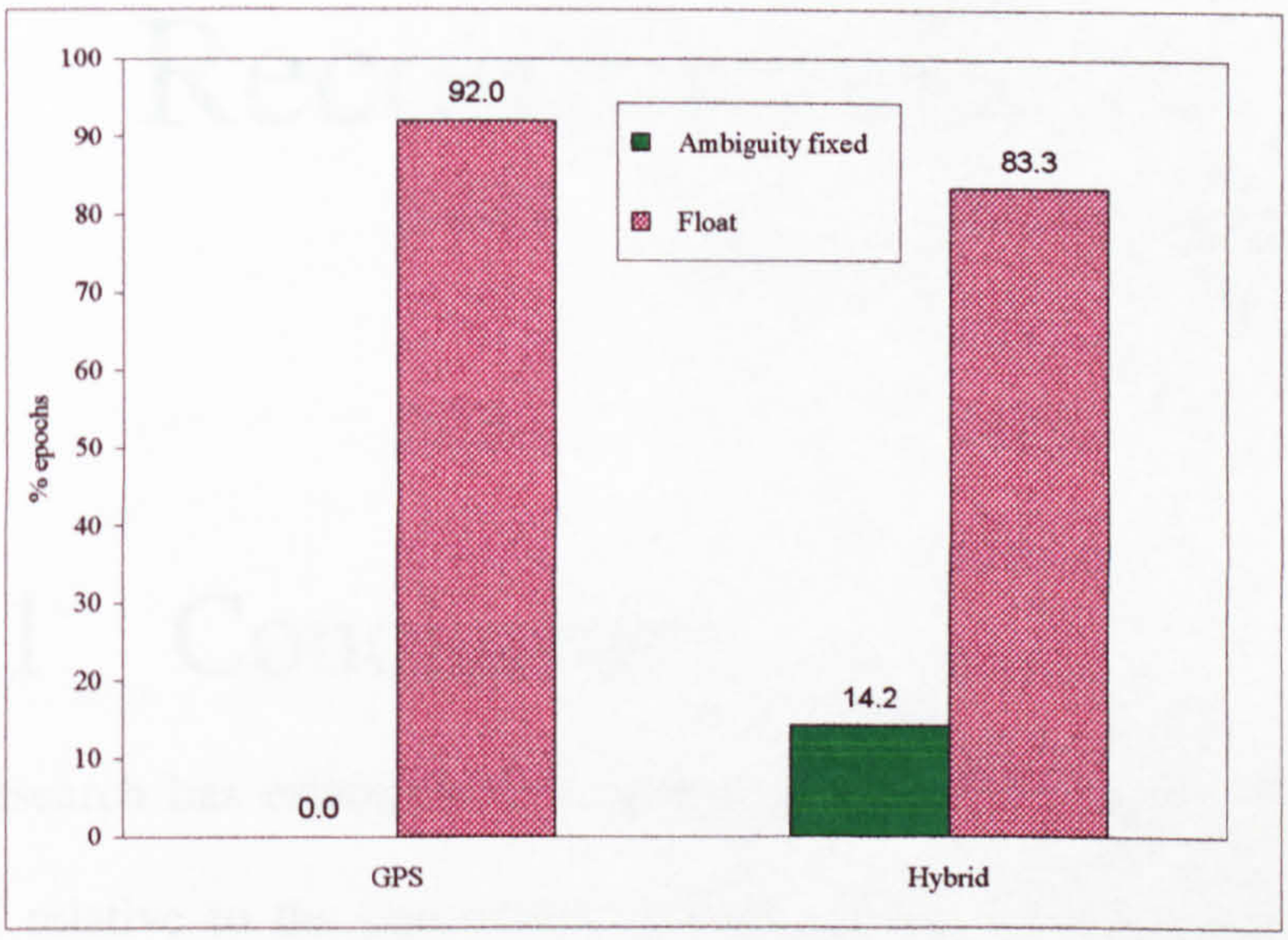

Figure 9.11 Solution type, winter 1998

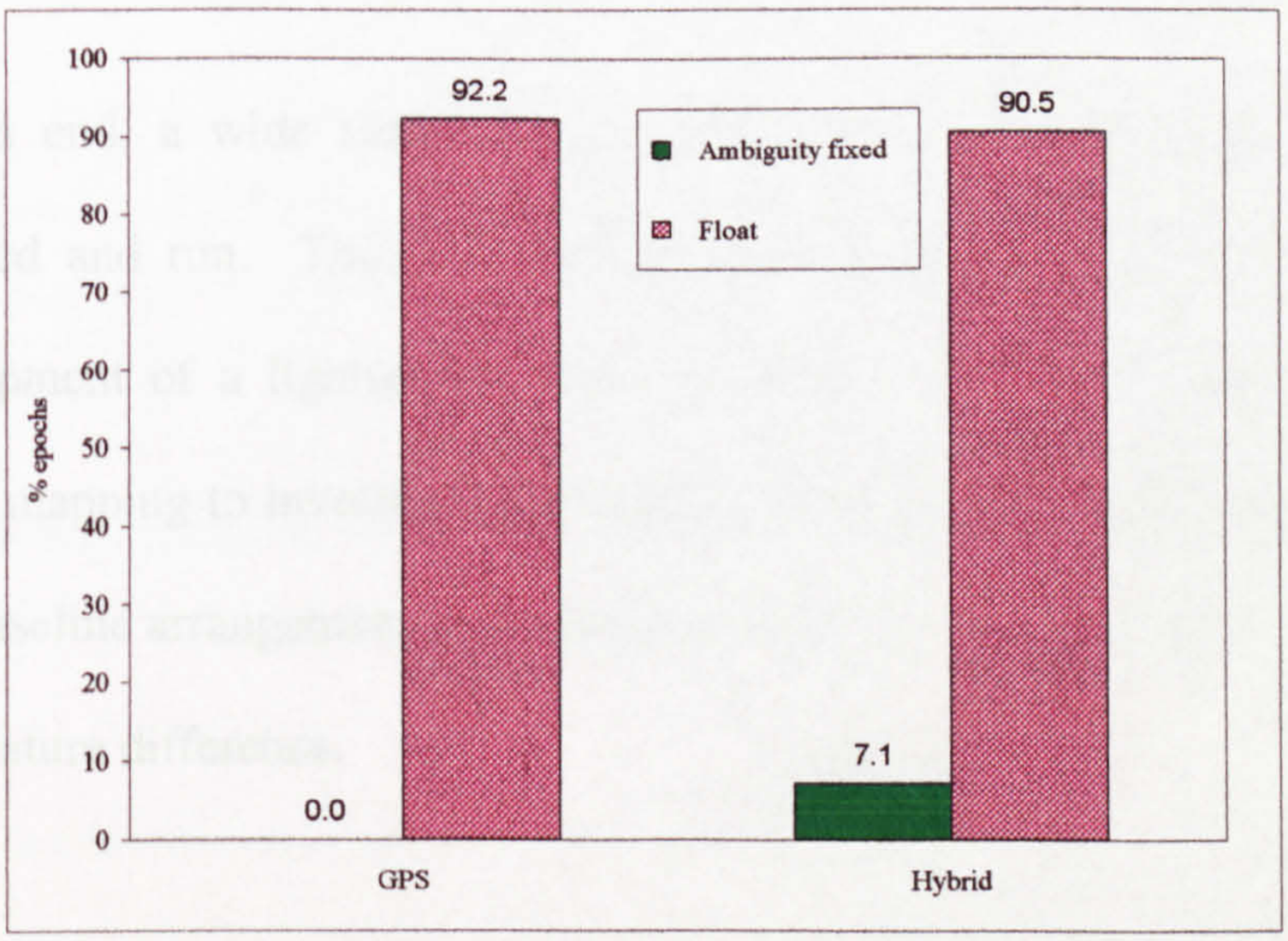

Figure 9.12 Solution type, summer 1999

Chapter 10

Conclusions and Recommendations for Further Work

10.1 Conclusions

This research has established the practical limitations and benefits of using Hybrid relative to the capabilities of GPS alone, for surveying and vehicle navigation applications. This will be of value to survey and navigation practitioners.

To this end, a wide range of field and laboratory experiments have been designed and run. This has involved innovative work in for example: the development of a lightweight package suitable for winter sport; the use of digital mapping to investigate the effect of system differences; and a modified zero baseline arrangement to obviate the effect of a between-receiver operating temperature difference.

The objectives of this research were to:

- Investigate the effects of between system difference and system peculiarities, to enable definitive figures on positioning accuracy to be derived.
- Assess the relative capabilities of GPS and Hybrid with respect to positioning accuracy and continuity.
- Establish the practical limitations of the Hybrid system.

The main achievements of this research were:

- The comprehensive investigation of effects of differences between GPS and GLONASS, and system peculiarities. This included: the validation on a local basis, of the transformation between the GPS and GLONASS coordinate reference systems, with limited success; the use of satellite positioning technology to delineate digitally mapped features, both as a way to update mapping but also as a tool to investigate the effect of possible transformation errors on a digital mapping background; the quantification of the effect of receiver operating temperature on Hybrid and GLONASS relative positioning; and an up-to-date quantitative evaluation of absolute positioning accuracy of GPS, Hybrid and GLONASS.
- The development of processes to give quantitative measures in order to analyse vehicle positioning performance by GPS and Hybrid with respect to accuracy and continuity, together with limited analysis of seasonal effects.
- The realisation of the practical limitations of GPS and Hybrid, using the bob skeleton application.

These achievements are now described in more detail, starting with the findings of research *into the static mode* of operation:

- In the absolute mode of operation long term GPS performance was, with reference to 2D scatter plots, on average over 50% worse than Hybrid. However when considering cumulative averaging over 24 hours, GPS is seen to stabilise more rapidly than Hybrid, with GPS taking 4 and Hybrid over 10 hours. This suggests that the Hybrid error distribution, and hence GLONASS error content, is greater than that of GPS.

- In absolute mode with SA switched off, the situation was similar to the case above, though with not such a marked difference, with GPS stabilising after about 2 and Hybrid after 5 hours.

- In order to characterise differential C/A code performance, a zero baseline approach was used. This eliminated all errors apart from those caused by GLONASS inter channel bias and non-identical receiver components. On average the DGPS baseline was zero length with a dispersion of 10 cms or less in all dimensions. DHybrid and DGLONASS baselines on the other hand were systematically offset from zero: DHybrid up to 0.6 m and DGLONASS up to 1.5 m, and both with an order of magnitude decrease in precision relative to DGPS. The deterioration incurred by hybridising GPS with GLONASS may be treatable by for example improvements in the relative weighting regime, or perhaps the transformation between PE-90 and WGS-84.

- Carrier phase was also examined on a zero baseline. Whilst the GPS baseline showed an average radial error of zero with a standard deviation of 1.6 mm, Hybrid incurred a systematic error above one millimetre, and a standard deviation 50% greater than GPS. It was also seen that the greater bandwidth necessary for a Hybrid (in GPS mode) relative to a GPS-only receiver, though giving equivalent mean baseline errors, resulted in Hybrid receiver standard deviations greater than GPS-only, by between 30 and 50%. GPS on

a zero baseline was as predicted, impervious to the introduction of a between-receiver thermal offset of up to 24°C. However Hybrid was affected, responding with the growth of a virtual baseline of nearly 20 mm.

- The above points suggest that Hybrid in its current realisation, through the use of commercial software, there is a trade-off between having an increased constellation but with a reduced precision and accuracy.

Dynamic applications were used to enquire into the gains achievable using Hybrid relative to GPS. Test environments, in terms of signal reception, varied intentionally, from benign to extremely arduous, including work at the La Plagne bob sled track in France. It had been hoped to work with Formula 1 racing, as contact had been established with McLaren, however the alternative bob skeleton application was interesting from several perspectives. The conclusions that can be drawn from the dynamic tracking research are summarised as follows:

- In a signal impaired environment with static and dynamic multipath and a dynamic skyview, GLONASS can make a major contribution to both continuity and accuracy as part of the Hybrid solution. This contribution is currently inconsistent over time, given the gaps in the GLONASS constellation, which cause a wide variety of utility over its 8-day geometry cycle. Any effects of GLONASS-specific biases are swamped by environmental noise.

- It was demonstrated that it is possible to generate a form of truth against which to evaluate individual circuits around a track, by aggregating multiple circuits. This approach was taken for a circuitous route between the University and Nottingham City

centre. For this route, accumulating circuits to give the complete route, required 4 GPS circuits, but only 2 Hybrid circuits to give equivalent complete coverage. Quantitative performance indicators of accuracy and continuity were developed. It was demonstrated in terms of accuracy using a standard Kalman filter solution, that an improvement of between 30 to 60% was achievable by hybridising, and positioning continuity was improved by between 50 and 70%. Moreover comparing the bi-directional Kalman filter GPS solution with the Hybrid standard Kalman filter solution, showed accuracy and continuity performance of on average similar capabilities.

- The benefit of hybridisation in an urban environment against a seasonal backdrop was impressive, for the days sampled. Hybrid figures indicated 55% of epochs with more than 9 satellites in view irrespective of the season. GPS was also consistent across seasons, at 0% of epochs with more than 9 satellites in view. Considering geometry, relative to GPS, Hybrid was instrumental in improving the number of epochs with PDOP better than 4 by 11% in winter, and 48% in summer. Regarding the number of epochs with too few satellites to provide a solution, Hybrid provided 55% less cases in winter than GPS, and similarly in summer 82% less. Finally, considering ambiguity fixed solutions, GPS was incapable, whilst under Hybrid between 7 and 10% of epochs achieved fixed ambiguity status.

- It was proposed to use the repetitive circuit approach to define the bob sled track, using a backpack positioning package carried by the slider. However, the topographic environment was, when combined with high antenna dynamics and a rapidly changing skyview as viewed from the vehicle, just too arduous. Hybrid capability had in this case been tested to the limit – and failed. The backup method of using a road-wheel mounted antenna to map the inner ice wall of the track, was successful, but required Hybrid, with GPS failing to

locate about 20% of the track. Not only this, but filters were needed to treat the trajectory, before such down-track distance referenced parameters of radius of curvature, and vertical gradient, could be extracted.

- It was intended to improve the skeleton positioning package for subsequent tracking trials. Fortunately a tri-axial accelerometer and flux gate compass had been supplied to the IESSG for an INS related project, so whilst communication and integration software was being written, a land-based skeleton simulator was developed and tested. Unfortunately the INS was not ready to be tested at the time of writing. However it was believed that the suggestion of an accelerometer based solution was being pursued by BAE, the sponsors of the skeleton engineering development.

- It was also demonstrated that both GPS and Hybrid tracking could be used to investigate possible systematic errors in digital mapping detail, through the innovative use of regular shapes such as roundabouts. GPS definition of sample roundabouts suggested a systematic directional bias of about 0.5 m. Such tracking could also be used to identify possible systematic errors between GPS and GLONASS, tests showed a directional bias of up to 2.5 m, but this was not consistent across the sample tested.

10.2 Recommendations for Further Work

This research has demonstrated that GLONASS, even in its current parlous state can be of significant use in a Hybrid solution. If funding does not materialise to repopulate the GLONASS constellation then its utility will fade further, making it difficult to justify further Hybrid receiver development.

However not all is in vain, as the test strategies developed here and the tests carried out would be suitable for any future hybridisation with GPS. Likely contenders may be the proposed Galileo, or perhaps the embryonic Chinese *Beidou Navigation System.*

It is suggested that the research done here could be widened and further developed in the following areas:

- To better understand the PE-90 to WGS-84 transformation in the UK
  - With a recently scaled down IGEX programme, dual frequency GLONASS receivers will become more readily available. These could be used to reoccupy the 5 points observed during this research, with the aim of providing absolute locations in the PE-90 coordinate reference frame, and thereby a (possibly) improved regional PE-90 to WGS-84 transformation.

- Regarding GLONASS inter channel bias
  - It is possible that this troublesome feature *could be handled at the point* of manufacture, through channel calibration at a range of temperatures, and the fitting of an on-receiver temperature sensor. Alternatively receivers could be maintained at a constant temperature of say 40°C using oven technology, and signal calibration factors developed and applied on-receiver.

  - The introduction of an operator controlled weighting regime within commercial software or otherwise, would allow a greater understanding

of the nature of individual biases and their propagation into the position domain, and what actions can be designed to mitigate them.

- Regarding dynamic tracking
  - The development of a relative weighting regime based on coordinate standard error, to improve the accuracy of the aggregate truth derived from repetitive circuits of the same track.

  - Testing of the technology at Formula 1 or 2 level, to see what satellite positioning can offer these applications. The effect of intense and complex vibration on the quartz clocks used by receivers, may prove interesting.

  - Testing of the land-based skeleton simulator once the INS currently under development at the IESSG reaches the operational stage.

Hybridisation of satellite positioning systems either between themselves, or with other sensors, is inevitable if positioning is to be highly continuous under all environmental conditions. For practical and commercial users there is a need to understand the subtle propagation of error into the position domain, that may originate in the process of integration of systems, and it is hoped that the ideas developed here, will provide other researchers with food for further thought in this field.

References

3S NAVIGATION (1997). *The Advantages of GNSS Receivers over GPS-only Receivers for Civilian Users*. Company paper, 3 pages.

3S NAVIGATION (1997). *TSA-100 Temperature Stabilised GPS/GLONASS/WAAS L1 + L2 Antenna System*. Marketing brochure.

ABOUSALEM M (1997). *Performance Overview of Two WADGPS Algorithms*. GPS World, May 1997, pp.48-58.

ACKROYD N (1998). Personal discussion with Trimble Europe's Technical Manager. October 1998.

AIR FORCE GUEST WEEKLY (1997). *Newsletter 66*, dated 6th October 1997.

ARMOR J (1997). *NAVSTAR Global Positioning System "Any Time, Any Place, Right Time, Right Place"*. Presentation slides, given at the Proceedings of ION GPS-97, 16-19 September, Kansas City, Missouri, USA.

ARMOR J (1999). Comments (not verbatim) at ION GPS-99.

ASHTECH INC (1997). *GG24C2 Surveyor GPS/GLONASS Receiver (Model 800205) Reference Manual*, 143 pages.

BAGLEY L (1992). *NAVSTAR Joint Program Office and a Status Report on the GPS program*. Proceedings of the 6th International Geodetic Symposium on Satellite Positioning, 17-20 March 1992.

BARNES J, CROSS P (1998). *Processing Models for Very High Accuracy GPS Positioning*. Journal of Navigation, V51, No.2, pp.180-193.

BASKER S, HOLMES D, TRETHEWEY ML (1997). *GLONASS: The System, Availability, and Issues*. Signal Computing Ltd., Guilford, UK, 11 pages.

BAZLOV Y, GALAZIN V, KAPLAN B, MAKSIMOV G, ROGOZIN V (1999). *GLONASS to GPS: A New Coordinate Transformation*. In Innovation, GPS World, January 1999, pp.54-58.

BENHALLAM A, ROSSO r (1996). *Performance comparisons between GPS and GLONASS transmission systems*. Proceedings of ION GPS-96, 17-20 September, Kansas City, Missouri, USA, pp.423-430.

BESER J, HAUNSCHILD M (1996). *Advantages of Integrated GPS / GLONASS Operations*. Geomatics Info Magazine (GIM International), Unknown month 1996, Volume 10.

BINGLEY R (1993). *GPS Data Processing*. Lecture given at the 6th Int. Seminar on the Global Positioning System, IESSG, University of Nottingham, April 1993, 18 pages.

BLIGHTON R (1998). Personal communication (Ashtech Europe). September 1998.

BLIGHTON R (1999). *GPS+GLONASS = better solutions*. Article in Surveying World journal, Issue No.2, Vol.7.

BOWDITCH (1977). *American Practical Navigator*, Vol.1. Published by the Defence Mapping Agency, Publication No.9.

BROWN A, SILVA R (1999). *Video-aided GPS/INS Positioning and Attitude Determination*. Proceedings of ION GPS-99, 14-17 September, Nashville, Tennessee, USA, pp.1961-1968.

BURGER P, GILLIES D (1989). *Interactive Computer Graphics – functional, procedural, and device level methods*, published by Addison-Wesley, 504 pages.

BURKE B (1999). Personal communication by email, 1st February 1999.

CAA-ISN, [2000]. CAA-ISN Approach Standards. Document published at the University of Leeds website, under Aviation.

CHERNOMYRDIN V (1995). Chairman of the Government of the Russian Federation, *The Decree 'On Executing Works in use of the GLONASS Global Navigation System for the Sake of Civil Users*. Decree No 237. URL http://mx.iki.rssi.ru/SFCSIC/decree.txt accessed at 8th June 1997.

COOPER J, DALY P (1997). *Pre-processing of GNSS Signals Subject to Interference*. Proceedings of ION GPS-97, 16-19 September, Kansas City, Missouri, USA, pp.1437-1446.

CSIC (1993). Document at Coordinational Scientific Information Centre of the Russian Military Space Forces. URL http://scsic@mx.iki.rssi.ru

CSIC (1995). *Coordinational Scientific Information Centre of the Russian Space Forces GLONASS Interface Control Document*. Presented as an Appendix to Working Paper 66 (GNSSP/2-WP/66), by V.Kuranov, at the 2nd Meeting of the Global Navigation Satellite System Panel (GNSSP) of the

ICAO (International Civil Aviation Authority), November 1995, Montreal, Canada. 43 pages.

CSIC (1998). *GLONASS Interface Control Document Version 4.0*, 45 pages. Accessed from URL http://www.rssi.ru/SFCSIC/

DALY M (1999). *Inter-channel biases.* Email communication.

DALY P (1993). *Navstar GPS and GLONASS: Global Satellite Navigation Systems.* Electronics and Communication Engineering Journal, December 1993, pp.349-357.

DANA P, PENROD B (1990). *The Role of GPS in Precise Time and Frequency Dissemination.* GPS World, July/August 1990, pp.38-43.

DE SALAS J (1998). *GG24 hardware delay.* Personal communication with Ashtech Europe Ltd, 13 May 1998.

DOD (1995). US Department of Defence. *Global Positioning System Standard Positioning Service Signal Specification.* 2nd Edition, June 2, 1995.

DODSON A, HILL C, SHARDLOW P (1993). *The effects of propagation on GPS measurements.* Sixth Int. Seminar on the GPS, IESSG, Nottingham, 22nd April 1993.

DODSON A, MOORE T, BAKER DF, SWANN J (1999). *Hybrid GPS + GLONASS.* GPS Solutions, Vol.3, No.1, Summer 1999pp.32-41.

DMA (1987). US Defence Mapping Agency. *Document Ref. DMA TR 8350.2 A: Supplement to the Department of Defence World Geodetic System 1984 Technical Report. Part 1 – Methods, Techniques, and Data used in WGS84 Development.*

ESA (1996). *European Space Agency GNSS Office publication: Global Navigation Satellite System.* 20 pages.

FOCUS FM (1999). *Differential GPS Services.* Promotional Literature.

FREI E, BEUTLER G (1990). *Rapid static positioning based on the fast ambiguity resolution approach "FARA": theory and first results.* Manuscripta Geodaetica (1990) Vol 15, pp325-356.

FROST & SULLIVAN (1998). *The Western European GPS Market*, report forecast, quoted in GPS World Showcase, August 1998, pp.58.

GALILEO'S WORLD (2000). Industry Dossier*: Lockheed forms GPS Augmentation Company*, Galileo's World Spring 2000, pp.47

GEORGIADOU Y, DOUCET K (1990). *The Issue of Selective Availability.* GPS World, September-October 1990, pp.53-56.

GHOUZHVA Y, KOUDRYAVTSEV V, KORNIYENKO V, PUSHKINA (1994). *GLONASS Receivers: An Outline.* GPS World, January 1994, pp.30-36.

GOUREVITCH S (1994). *Implications of "Z" Technology for Civilian Positioning.* Proceedings of ION GPS-94, 20-23 September, Salt Lake City, Utah, USA, pp.149-155.

GOUREVITCH S, SILA-NOVITSKY S, van DIGGELEN F (1996). *The GG24 Combined GPS+GLONASS Receiver.* Proceedings of ION GPS-96, 17-20 September, Kansas City, Missouri, USA, pp.141-145.

GPS WORLD (1994). *DoD implements AS.* Article in GPS World, March 1994, Vol.5, No.3, pp.21.

GPS WORLD (1997a). *Booster Rocket Failure Ruins First Block IIR Launch.* Article in GPS World, February 1997, p.20.

GPS WORLD (1998a). Editorial article entitled: *Donohue to resign FAA Post; WAAS Reports In.* GPS World, March 1998, p.20.

GPS WORLD (1999a). *Modernisation Cut: GPS Takes Hard Budget Hit.* Washington View editorial article. GPS World, September 1999, pp.14-16.

GPS WORLD (1999b). *Global View: Congress Shoots Down Modernisation Funds,* pp.18.

GPS WORLD (2000a). *Washington View: Budget Woes – Efforts to Save GPS Funding Come up Short*, Editorial article by Dee Ann Divis. GPS World, January 2000, pp14-18.

GPS WORLD (2000b). *Global View: GPS National Plan Takes Shape as Budget Battles Continue.* GPS World, February 2000, pp.16.

HALL T, BURKE B, PRATT M, MISRA P (1997). *Comparison of GPS and GPS+GLONASS Positioning Performance.* Proceedings of ION GPS-97, 16-19 September, Kansas City, Missouri, USA, pp.1543-1550.

HARTINGER H, BRUMMER F (1998). *Attainable Accuracy of GPS Measurements in Engineering Surveying.* FIG 98, Commission 6, Brighton, England, August 1998, pp.18-31.

HARVEY B (1995). *Practical Least Squares and Statistics for Surveyors.* Monograph 13, School of Geomatic Engineering, the University of New South Wales, NSW, Australia.

HATCH R (1982). *The Synergism of GPS Code and Carrier Measurements.* Proceedings of 3rd Int. Geodetic Symp. on Satellite Doppler Positioning, pp.1213-1232.

HEIN G, ROSSBACH U, EISSFELLER B (1997). *Advances in GPS/GLONASS Combined Solutions*. Proceedings of ION GPS-97, 16-19 September, Kansas City, Missouri, USA, pp.1533-1541.

HILL C (1997). In house personal discussion, IESSG, University of Nottingham.

HOFFMAN-WELLENHOF B, LICHTENEGGER H, COLLINS J (1994). *GPS Theory and Practice*. 3rd Edition, 355 pages, 4th Edition, Springer.

HOFMANN-WELLENHOF B (2000). *Understanding Galileo: On the Way to a New GNSS*. Article in Galileo's World, Spring 2000, pp.42-45.

ICAO (1998). International Civil Aviation Organisation (ICAO) Circular 267-AN/159. *Guidelines for the Introduction and Operational use of the Global Navigation satellite System (GNSS).*

IGS (1999). *International GPS Service for Geodynamics, 1998 Annual Report.* Published by IGS Central Bureau, Jet Propulsion Laboratory, Pasadena, California, USA.

IGS (2000). Internet web site of the International GPS Service for Geodynamics.

INEICHEN (2000). Personal communication, 28 June 2000.

KAZANTSEV V (1995). *The GLONASS and GLONASS-M Programs.* Proceedings of ION GPS-96, 17-20 September, Kansas City, Missouri, USA, pp.985-990.

KEALY A, TSAKIRI M, STEWART M (1999). *Land Vehicle navigation in the Urban Canyon – A Kalman Filter Solution using Integrated GPS, GLONASS, and Dead Reckoning*. Proceedings of ION GPS-99, 14-17 September, Nashville, Tennessee, pp.509-518.

KENNIE T, PETRIE G (1993). Engineering Surveying and Technology. 1st Edition, 485 pages, Blackie A & P.

KLOBUCHAR J A (1996). *Ionospheric effects on GPS*. Chapter 12 in Global Positioning System – Theory and Applications Vol.1, 3rd printing, AIAA.

LANDAU H, VOLLATH U (1996). *Carrier Phase Ambiguity Resolution using GPS and GLONASS signals*. Proceedings of ION GPS-96, 17-20 September, Kansas City, Missouri, USA, pp.917-923.

LANGLEY R (1991a). *The Orbits of GPS Satellites*. GPS World March 1991, pp.50-53.

LANGLEY R (1997). *GLONASS: Review and Update*. GPS World July 1997, pp.46-52.

LANGLEY R (1998). *The GPS End-of-WEEK Rollover.* Innovation, GPS World November 199, p.40.

LANGLEY R B (2000). *GPS, the Ionosphere, and the Solar Maximum.* GPS World, Vol.11, No.7, July 2000, pp.44-49.

LECHNER W (1997). *The Civil and Military Issues Facing GPS and GNSS – Panel Discussion.* Proceedings of ION GPS-97, 16-19 September, Kansas City, Missouri, USA, pp.3-20.

LEICK A, LI J, BESER J (1995). *Processing GLONASS Carrier Phase Observations - Theory and First Experience.* Proceedings of ION GPS-95, 12-15 September, Palm Springs, California, USA, pp.1041-1047.

LENNEN G R (1989). *The USSR's GLONASS P-Code – Determination and Initial Results.* Proceedings of ION GPS-89, September, Colorado Springs, Colorado, USA, pp.77-83.

LEWANDOWSKI W, DANAHER J, KLEPCZYNSKI W (1996). *Experiment using GPS/GLONASS Common-View Time Transfer between Europe and North America.* Proceedings of ION GPS-96, 17-20 September, Kansas City, Missouri, USA, pp.271-277.

MALYS S, SLATER J, SMITH R, KUNZ L, KENYON S (1997). *Refinements to the World Geodetic System 1984.* Proceedings of ION GPS-97, 16-19 September, Kansas City, Missouri, USA, 10 pages.

MAURER M, WINDL J, NIKLASCH N, RICHERT W, AUERNHAMMER H (1997). *Multi-Sensor-System for Landmobile Applications Using GPS/GLONASS and Additional Sensors.* Proceedings of ION GPS-97, 16-19 September, Kansas City, Missouri, USA, pp.831-838.

MENG X (1999). *Vehicle-borne Highway Geometric Alignment and Facilities Data capture by Using DGPS and GPS/GIS Integration.* Draft version.

MISRA PN, ABBOT RI (1994). *SGS85 – WGS84 transformation.* Manuscripta Geodaetica V19 No5, pp.300-308.

MISRA, P, PRATT M, MUCHNIK R, BURKE B, HALL T (1996a). *GLONASS Performance: Measurement Data Quality and System Upkeep.* Proceedings of ION GPS-96, 17-20 September, Kansas City, Missouri, USA, pp.261-270.

MISRA, P, ABBOTT R, GAPOSCHKIN E (1996b). *Integrated use of GPS and GLONASS: Transformation between WGS-84 and PZ-90.* Proceedings of ION GPS-96, 17-20 September, Kansas City, Missouri, USA, pp.307-314.

MISRA P, SLATER J (1998). *International Call for Participation (GLONASS IGEX-98 Campaign).* Document at: http://www.nima.mil/geospatial/products/GandG/ion/callpart.html, 12 pages.

MITRIKAS V, REVNIVYKH S, BYKHANOV E (1998). *WGS84/PZ90 Transformation Parameters Determination Based on Laser and Ephemeris Long-term GLONASS Orbital Data Processing.* Proceedings of ION GPS-98, 15-18 September, Nashville, Tennessee, USA, pp.1625-1636.

MOORE T (1994). *Coordinate Systems, Frames and Datums* - Lecture Notes, IESSG, University of Nottingham. 15 pages.

MOORE T, ASHKENAZI V, DUMVILLE M, LOWE D, TSAKIRI M (1995). *An Artificially Intelligent Vehicle Highway System.* Proceedings of ION GPS-95, 12-15 September, Palm Springs, California, USA, pp.1809-1818.

MOORE T (1997). *GLONASS Global'naya Navigatsionnaya Sputnikovaya Sistema* - Presentation material, IESSG, University of Nottingham. 7 pages.

MOORE T (1998). *GPS Modernisation.* Departmental lecture given at the IESSG, University of Nottingham, February.

MOORE T, HILL CJH (2000). Informal discussion, in house, on encryption and decryption.

MUELLER I (1985). *Reference Coordinate Systems and Frames: Concepts and Realization.* Bulletin Geodesique (59), pp.181-188.

NANU-001 (1997). NAVSTAR NANU Ref 062-97182 (1997). *What is a Leap Second?* US Coast Guard Navigation Centre website.

OFFERMANS G, HELWIG A, VAN WILLIGEN D (1999). *Eurofix System and its Developments.* Journal of Navigation, Vol.52, No.2, May 1999. pp.163-171.

ØRPEN O, HINSCH P (1997). *GLONASS for Offshore Applications.* Proceedings of ION GPS-97, 16-19 September, Kansas City, Missouri, USA, pp.989-994.

PANYUSHIN A, ZABOKRITSKY A, POSHECHENKOV A (1996). *Maintenance of GLONASS users with Precision A posteriori Data to improve Accuracy of Geodetic Attachment.* Int. Conference on Satellite Communications, ICSC Proceedings, September 1996, Moscow, Russia, pp.250-251.

PARK D W G (1999). *Using Linear Features for Absolute and Exterior Orientation*, PhD thesis, and verbal discussion of same, University of Nottingham.

PARKINSON BW, SPILKER JJ, AXELRAD P, ENGE P (1996). Editors of *Global Positioning System, Theory and Applications*, Volume 1, pp.17-18.

PATTINSON M (1998). *Datum Transformations in the UK.* Undergraduate thesis, University of Nottingham.

POVALYAEV A, KHVAL'KOV A, BELOUSOV R (1996). *Determination of Relative Coordinates from the Phase Shift Increments of GLONASS Carrier Signals.* Original reference: Radiotekhnika, 1997, No.4, pp.48-51. Translated from Izmeritel'naya Tekhnika, No.5, May 1996, pp.32-34. Root source: Measurement Techniques, Vol.39, No.5, 1996, pp.516-519.

PRATT M, BURKE B, MISRA P (1997). *Single-Epoch Integer Ambiguity Resolution with GPS L1-l2 Carrier Phase Measurements.* Proceedings of ION GPS-97, 16-19 September, Kansas City, Missouri, USA, pp.1737-1746.

PRATT M, BURKE B, MISRA P (1997b). *Single-Epoch Integer Ambiguity Resolution with GPS-GLONASS L1 Data.* Proceedings of 53rd ION National Technical Meeting, 1997, pp.691-703.

PU A, DENKEWALTER R, PSALTIS D (1997). *Real-time vehicle navigation using a holographic memory.* Optical Engineering, Vol.36, No.10, pp.2737-2746.

RABY P, DALY P (1993). *Using the GLONASS System for Geodetic Survey.* Proceedings of ION GPS-93, pp.1129-1138.

RAMJATTAN A, CROSS A (1995). *A Kalman Filter Model for an Integrated Land Vehicle Navigation System.* The Journal of Navigation, Vol.48, No.2, pp.293-302.

RILEY S, HOWARD N, AARDOOM E, DALY P, SILVESTRIN P (1995). *A Combined GPS/GLONASS High Precision Receiver for Space Applications.* Proceedings of ION GPS-95, 12-15 September, Palm Springs, California, USA, pp.835-844.

RIZOS C (1997). *Principles and Practice of GPS Surveying.* Monograph 17, published by the School of Geomatic Engineering, University of New South Wales, 555 pages.

ROONEY E, LAST A (1999). *GLONASS: As Good As It Should Be?* Proceedings of ION GPS-99, 14-17 September, Nashville, Tennessee, USA, pp.1363-1368.

ROONEY E (2000). Personal communication regarding the effects of non-resonant GLONASS orbits on the minimal requirements for daily tracking data.

ROSSBACH U, HABRICH H, ZARRAOA N (1996a). *Transformation Parameters Between PZ-90 and WGS-84*. Proceedings of ION GPS-96, 17-20 September, Kansas City, Missouri, USA, pp.279-285.

ROSSBACH U, HEIN W (1996b). *Treatment of Integer Ambiguities in DGPS/DGLONASS Double Difference Carrier Phase Solutions*. Proceedings of ION GPS-96, 17-20 September, Kansas City, Missouri, USA, pp.909-916.

RUSSELL D C (2000). *DEM Creation Using Satellite Positioning and Digital Photogrammetry for Application in Precision Agriculture*, PhD thesis in progress November 2000.

SCHUPLER B, CLARK A. *How different antennas affect the GPS observable*. GPS World, November/December 1991, pp.32-36.

SEEBER G (1993). *Satellite Geodesy: Foundations, Methods, and Applications*, 531 pages.

SENUS W, MISRA P (1996). *Report on the 1st Meeting of the GLONASS-GPS Interoperability Working Group*. Proceedings of ION GPS-96, 17-20 September, Kansas City, Missouri, USA, pp.1929-1930.

SERRA J J (1999). *Proton*. http://www.tbs-satellite.com/tse/online/ /lanc_proton.html. Web site accessed at 20th January 1999.

SHIENOK N (1999). Personal email from sfcsic@mx.iki.rssi.ru

SHAW M, TURNER D, SANDHOO K (2000). *GPS Modernisation*. GNSS 2000, May 4th 2000, Edinburgh, UK.

SLATER J, MALYS S (1997a). *WGS-84 – Past, Present and Future*. NIMA paper. The journal in which this was published was not known.

SLATER J, MISRA P (1997b). *A Report on the 2nd Meeting of the GLONASS-GPS Interoperability Working Group*. Proceedings of ION GPS-97, 16-19 September, Kansas City, Missouri, USA, pp.1893-1894.

SLATER J, WILLIS P, BEUTLER G, GURTNER W, LEWANDOWSKI W, NOLL C, WEBER R, NEILAN R, HEIN G (1999). *The International GLONASS Experiment (IGEX-98): Organisation, Preliminary Results and Future Plans*. Proceedings of ION GPS-99, 14-17 September, Nashville, Tennessee, USA, pp.2293-2302.

SPILKER J (1994). *GPS Signal Structure and Theoretical Performance*. In Global Positioing System (1996): Theory and Applications, Volume 1, Chapter 3.

SPILKER J (1997). Tropospheric Effects on GPS, Chapter 13 in Global Positioning System – Theory and Applications Vol.1.

STICH H, LECHNER W (1993). *Visit to GLONASS Centre is First for Outsiders*. Article in GPS World, September 1993, pp.16-17.

SWANN J (1999). *Advantages and Problems of Combining GPS with GLONASS*, PhD thesis, University of Nottingham.

TRIMBLE NAVIGATION (1996). *Improvements in Real-time GPS Surveying Performance Using Everest Multipath Rejection Technology*. Corporate paper,11 pages.

TRINITY HOUSE (2000). *Marine Differential GPS*. Information sourced from Trinity House Lighthouse Service website.

USDoT, USDoD (2000). *1999 Federal Radionavigation Plan*. Published and released by the US Departments of Transport and Defense, Washington DC, USA, on 18th February 2000.

USDoT (2000). US Department of Transport, Press Release: *New Radionavigation Plan Eyes Transition to Satellite-based Services in 21st Century*. Reference DOT 36-00. Released on 18th February 2000.

USCG (2000). Personal communication with US Coast Guard Navigation Centre.

VAN GRAAS, BRAASCH M (1996). *Selective Availability*, in Global Positioning System, Theory and Applications, Vol.1.

VIEWEG S, LECHNER W (1995). *Combination of NAVSTAR GPS and GLONASS for Civil Aviation –Pros and Cons-*. International Symposium on Precision Approach and Automatic Landing, ISPA-95, pp.409-416.

WALSH D, DALY P (1996). *GPS and GLONASS Carrier Phase Ambiguity Resolution*. Proceedings of ION GPS-96, 17-20 September, Kansas City, Missouri, USA, pp.899-907.

WALSH D, CAPACCIO S, DALY P, SHARDLOW P, JOHNSTON G (1997). *Real Time Differential GPS and GLONASS Vehicle Positioning in Urban Areas*. Proceedings of the IEEE Conference on Intelligent Transportation Systems, ITSC 1997, Piscataway, New Jersey, USA, pp.514-519.

WANNINGER L (1993). *Effects of the Equatorial Ionosphere on GPS*. GPS World, Vol.4, No.7, July 1993, pp.48-54.

WELLS D (1987). *Guide to GPS Positioning*, by Canadian GPS Associates, prepared under the Leadership of David Wells.

WILLIS P (1999). *IGEX campaign 3-month extension*. IGEX Electronic mail http://owner-igexmail@ensg.ign.fr or alternatively willis@ensg.ign.fr, 11th January 1999.

YOUNG L E, NEILAN R E, BLETZACKER F R (1985). *GPS Satellite Multipath: An Experimental Investigation*. Proceedings of 1st Int. Symp. on Precise Positioning with GPS, pp.423-432. page 4